

**Atlas of Phylogenetic Data for Entelegyne Spiders
(Araneae: Araneomorphae: Entelegynae)
with Comments on Their Phylogeny**

**Charles E. Griswold¹, Martín J. Ramírez²,
Jonathan A. Coddington³, and Norman I. Platnick⁴**

¹ *Department of Entomology, California Academy of Sciences, 875 Howard Street, San Francisco, CA 94103, USA; Email: cgriswold@calacademy.org;* ² *Museo argentino de Ciencias naturales “Bernardino Rivadavia,” Avenida Angel Gallardo 470, 1405 Buenos Aires, Argentina;* ³ *Systematic Biology – Entomology, Smithsonian Institution, P.O. Box 37012, NMNH E529, NHB-105, Washington, DC 20013-7012, USA;* ⁴ *Division of Invertebrate Zoology, American Museum of Natural History, Central Park West at 79th Street, New York, NY 10024, USA*

Table of Contents

Abstract	2
Introduction	2
Taxon choice	3
Conventions	5
Materials and methods	5
Specimen preparation	6
Acknowledgments	7
Results	8
The Entelegyne exemplars	8
Agelenidae	8
Amaurobiidae	9
Amphinectidae	12
Araneoidea	14
Archaeidae	14
Austrochilidae	15
Ctenidae	17
Deinopidae	18
Desidae	19
Dictynidae	21
Eresidae	24
Filistatidae	27
Gradungulidae, Huttoniidae	28
Hypochildae	29
Mimetidae	30
Neolanidae	31
Nicodamidae	32
Oecobiidae	33
Pararchaeidae	34
Phyxelididae	35
Psechridae	37
Segestriidae	39
Stiphidiidae	40
Tengellidae	41

Titanoecidae.....	42
Uloboridae.....	43
Zorocratidae.....	44
Zoropsidae.....	46
Characters.....	47
Discussion.....	70
Character systems and homoplasy levels.....	71
Groups.....	71
Conclusions.....	76
Literature cited.....	76
Appendices.....	83
Appendix 1. Taxa examined to provide exemplar data.....	85
Appendix 2. Data matrix.....	94
Appendix 3. Comments on data matrix.....	97
Illustrations.....	101
Index: Systematic and Geographic.....	319

We present a phylogenetic analysis of higher groups of entelegyne spiders, with representatives of all entelegyne families containing cribellate members and of Palpimanoidea. We examined 55 exemplar species of eresoids (Oecobiidae, Eresidae), Orbiculariae (Deinopidae, Uloboridae, Araneidae), Palpimanoidea (Archaeidae, Huttoniidae, Mimetidae, Pararchaeidae), titanocoids (Phyxelididae, Titanocidae), lycosoids and related groups (Ctenidae, Psechridae, Tengellidae, Zorocratidae, Zoropsidae), and several other entelegyne families of contentious relationships (Agelenidae, Amphinctidae, Desidae, Neolanidae, Stiphidiidae, Amaurobiidae, Dictynidae, Nicodamidae), plus representatives of the relatively basal araneomorph groups Palaeocribellatae (Hypochilidae), Austrochiloidea (Austrochilidae and Gradungulidae), and Haplogynae (Filistatidae, Segestriidae). We also included the enigmatic cribellate genera *Aebutina* (Dictynidae?) and *Poaka* (Psechridae? Amaurobiidae?). This selection of taxa covers much of the morphological diversity found through major groups of araneomorph spiders. The 154 characters in our dataset include all the classical character sources in higher level spider taxonomy. We present a large collection of labeled images to document character definitions and observations. The phylogenetic trees obtained with our dataset differ according to parameters of analysis (equal or implied weights), and diverge from previous results. We obtain a paraphyletic Araneoclada, excluding members of Haplogynae. At least some taxa previously assigned to Palpimanoidea appear to be nested within orb weavers. The outgroups to Orbiculariae remain an open question, and the monophyly of Nicodamidae, Amaurobiidae and Zorocratidae are questioned. We corroborated Austrochiloidea, Eresoidea, and the Divided Cribellum, Oval Calamistrum and RTA Clades.

The Entelegynae comprise the largest group of spiders with more than 38,000 described species (Platnick 2004). Ideas about entelegyne spider evolution were long dominated by the fauna of the northern hemisphere, especially Europe. This impoverished fauna includes distinct and distantly related taxa, most of which are ecribellate or colulate. Spiders with cribella, the remarkable spinning plate that works in conjunction with a comb on the fourth leg to make a “hackled band” capture thread, form a small subset of this northern fauna. For nearly a century the higher spiders were divided into two groups: those with cribella, and those without. All this changed in the late 20th century with global taxonomic studies of higher spiders (Lehtinen 1967), intense studies of the spiders of the southern hemisphere (Forster 1970; Forster and Wilton 1973), and application of Hennig’s cladistic principles to spider taxonomy (e.g., Platnick and Gertsch 1976; Platnick 1977).

The cribellum was reinterpreted as a primitive feature common to all higher spiders, albeit, for most, in greatly modified form. The cribellum is clearly more ancient than even the entelegyne condition, i.e., that of having separate copulatory and fertilization ducts.

Entelegynes have repeatedly been the subject of quantitative phylogenetic analysis. The earliest studies focused on clades of special interest, e.g., orb weavers (Coddington 1990a, 1990b; Griswold et al. 1998, Fig. 211), haplogynes (Platnick et al. 1991, Fig. 209), lycosoids (Griswold 1993, Fig. 213). The first attempt at a comprehensive entelegyne phylogeny was by Griswold et al. (1999), who chose and coded cribellate members from families across the araneomorph spectrum. Their approach was guided by the words of Lehtinen (1967:202) who declared, “because of the central position of the Cribellate groups in Araneomorphae, a detailed revision of them is a short cut to a rough classification of the whole suborder.” They chose exemplars from all cribellate families, reasoning that taxa retaining this plesiomorphic feature are more likely to straddle the basal nodes of the phylogeny of higher groups than are their relatives that have lost the cribellum: therefore they are most likely to reflect phylogenetic groundplans. Although phylogenetically ancient, the cribellum is a complex feature unlikely to have evolved more than once. Most major araneomorph clades have cribellate members (exceptions are Palpimanoidea and Dionycha). A phylogeny of these basal taxa should mirror the relationships of the large clades they exemplify. The provisional phylogeny of Griswold et al. (1999) tested many suprafamilial hypotheses of the last 30 years and was the first attempt to relate them using quantitative phylogenetic techniques. The cladogram confirmed some accepted groupings, refuted others, and several novel phylogenetic and nomenclatural changes were proposed (Fig. 212). Confirmed were the monophyly of Neocribellatae, Araneoclada, Entelegynae, and Orbiculariae. The Lycosoidea, Amaurobiidae and some included subfamilies, Dictynoidea, and Amaurobioidea (*sensu* Forster and Wilton 1973) appeared polyphyletic. Phyxelididae Lehtinen was raised to family level and Zorocratidae Dahl was revalidated. A group including all other entelegynes other than Eresoidea was weakly supported as the sister group of Orbiculariae and several new, informative, informal clades were proposed or redefined: the “Canoe Tapetum Clade,” “Divided Cribellum Clade,” the “Titanocoids,” the “RTA Clade,” the “Fused Paracribellar Clade,” the “Stiphidioids” and the “Agelenoids.” This slender paper (Griswold et al. 1999), constrained by publication in a congress volume, offered only the briefest outline of the data. Griswold and Wang (2001) presented a fuller account of the results, presenting character state trees for each of the 137 characters and figures depicting many of the character states.

In this study we will present and illustrate in detail the morphology and other characteristics of the exemplar taxa, explain the character coding, and discuss some implications of our trees for spider evolution. We hope that this paper, especially the new data presented herein, will provide a springboard to further, more detailed and more comprehensive analyses of araneomorph phylogeny.

This paper is dedicated to the memory of Ray Forster.

TAXON CHOICE

We chose exemplars from all cribellate families, reasoning that taxa retaining this plesiomorphic feature are more likely to straddle the basal nodes of the phylogeny of higher groups than are their relatives that have lost the cribellum: therefore they are most likely to reflect phylogenetic groundplans. We have also added 11 ecribellate representatives of clades that we believe are not adequately represented by their cribellate members only (e.g., Haplogynae, Nicodamidae), or where all their members lack cribella (Palpimanoidea, Araneoidea). Only the major group

TABLE 1. List of anatomical and institutional abbreviations used in the text and figures.

A	alveolus	ML	epigynal median sector or lobe
AC	aciniform gland spigot(s)	MJR	Martín J. Ramírez
AD	vulval afferent duct	MRAC	Musée Royal de l'Afrique Centrale, Tervuren
AER	anterior eye row	MS	modified PLS spigots (including pseudoflagelliform gland spigot)
AG	aggregate gland spigot(s)	MTP	membranous tegular process
ALE	anterior lateral eyes	MUSM	Museo de Historia Natural de La Universidad de San Marcos, Lima
ALS	anterior lateral spinneret	N	nubbin
AME	anterior median eyes	NMSA	Natal Museum, Pietermaritzburg
AMNH	American Museum of Natural History, New York	NS	non sticky silk
AN	anneli of subtegulum	OAL	ocular area length
AT	epigynal atrium	oL1	outside leg 1
AX	cribellate silk axial lines	oL4	outside leg 4
BH	basal haematodocha	OMD	Otago Museum, Dunedin
BMNH	The Natural History Museum, London	OQA	ocular quadrangle, anterior
C	conductor	OQP	ocular quadrangle, posterior
CB	cymbium	PC	paracribellar spigot(s)
CAS	California Academy of Sciences, San Francisco	PER	posterior eye row
CF	"cuticular finger" on PLS	PF	postepigastric fold
CG	Charles Griswold	PI	piriform gland spigot(s)
CO	copulatory opening	PLE	posterior lateral eyes
CM	cribellate silk mass	PLS	posterior lateral spinneret
CY	cylindrical gland spigot(s)	PME	posterior median eyes
DTA	tibial dorsal process	PMS	posterior median spinneret
E	embolus	PTA	tibial proapical process
EB	embolar base	PY	paracymbium
EF	epigastric furrow	QMB	Queensland Museum, South Brisbane
F	fundus	RMNH	Rijksmuseum van Natuurlijke Historie, Leiden
FD	fertilization duct	RTA	tibial retroapical process
FL	flagelliform gland spigot(s)	RW	cribellate silk reserve warp
FMNH	Field Museum of Natural History, Chicago	S	epigynal scape
FO	foundation line	SEM	scanning electron microscope
GV	groove	SR	sperm receptacle
HNU	Hunan Normal University, Changsha	SS	sticky silk
HS	spermathecal head	ST	subtegulum
iL1	inside leg 1	STC	superior tarsal claw
InBio	Instituto Nacional de Biodiversidad, San José	STP	sclerotized tegular process
ITC	inferior tarsal claw	T	tegulum
JC	Jonathan Coddington	TA	tegular apophysis
JGU	Johannes Gutenberg University, Mainz	TO	tarsal organ
LNZ	Landcare New Zealand, Wellington	TP	tartipore
LL	epigynal lateral lobe(s)	TR	terminal apophysis of embolic division
L3	leg 3	UE	uterus externus
L4	leg 4	USNM	National Museum of Natural History, Smithsonian Institution, Washington, D. C.
MA	median apophysis	VTA	tibial ventroapical process
MACN	Museo Argentino de Ciencias Naturales, Buenos Aires	ZMUC	Zoological Museum, University of Copenhagen
MAP	major ampullate gland spigot(s)		
mAP	minor ampullate gland spigot(s)		
MCZ	Museum of Comparative Zoology, Harvard		
MH	epigynal median hood		

Dionycha (*sensu* Coddington and Levi 1991) is not represented. The scope and placement of the Dionycha were tangentially addressed by Silva Dávila (2003; Fig. 214) and are currently under study (Ramírez, in prep.); we leave those problems to that study.

Our dataset comprises 55 exemplars (Appendix 1) from all of the 22 araneomorph families currently (Platnick 2004) with cribellate members. As outgroups we included HYPOCHILIDAE (*Hypochilus*), GRADUNGULIDAE (*Gradungula*), AUSTRORCHILIDAE (*Hickmania* and *Thaida*), FILISTATIDAE (*Filistata* and *Kukulcania*, Filistatinae), and SEGESTRIIDAE (*Ariadna*). In this group we included OECOBIIDAE (*Oecobius* and *Uroctea*) and ERESIDAE (*Eresus* and *Stegodyphus*) from the eresoids. From Orbiculariae we included DEINOPIDAE (*Deinopsis* and *Menneus*), ULOBORIDAE (*Octonoba* and *Uloborus*) and ARANEIDAE (*Araneus*). Recent phy-

logenetic study of Araneoidea (Griswold et al. 1998; Fig. 211) gives us confidence that *Araneus* accurately reflects the primitive conditions of characters treated herein for this superfamily. From the Palpimanoidea we included ARCHAEIDAE (*Archaea*), HUTTONIIDAE (*Huttonia*), MIMETIDAE (*Mimetus*), and PARARCHAEIDAE (*Pararchaea*). Our choice of exemplars for the Palpimanoidea included both haplogyne (*Archaea*, *Huttonia*) and entelegyne (*Mimetus*, *Pararchaea*) taxa. In particular, Mimetidae is the most contentious of the taxa placed in Palpimanoidea (Platnick et al. 1991, Fig. 209; Schütt 2002, Fig. 210). From the fused paracribellar clade (*sensu* Griswold et al. 1999; Fig. 212) we included AGELENIDAE (*Neoramia*), AMPHINECTIDAE (*Maniho* and *Metaltella*), DESIDAE (*Desis*, *Badumna*, *Matachia* and *Phryganoporus*, formerly *Matachiinae*), NEOLANIDAE (*Neolana*), and STIPHIDIIDAE (*Pillara* and *Stiphidion*). From the titanocoids (*sensu* Griswold et al. 1999; Fig. 212) we included PHYXELIDIDAE (*Phyxelida*, *Vyftutia*, and *Xevioso*) and TITANOECIDAE (*Goeldia* and *Titanoeca*). From lycosoids and related groups we included CTENIDAE (*Acanthoctenus*), PSECHRIDAE (*Psechrus* and *Poaka*), the latter genus recently transferred to the Amaurobiidae, TENGELLIDAE (*Tengella*), ZOROCRATIDAE (*Zorocrates*, *Raecius* and *Uduba*), and ZOROPSIDAE (*Zoropsis*). Other families represented are the AMAUROBIIDAE (*Amaurobius*) and *Callobius* (*Amaurobiinae*), *Macrobunus*, *Retiro*, and *Pimus* (*Macrobuninae*), DICTYNIDAE (*Dictyna* and *Nigma*, *Lathys*, and *Tricholathys* representing Dictyninae, Cicurinae, and Tricholathysinae, respectively, and the enigmatic *Aebutina*), and NICODAMIDAE (*Megadictyna* and *Nicodamus*). Voucher specimens for exemplars are listed in Appendix 1.

CONVENTIONS

Throughout the text, figures cited from previous papers are listed as “fig.”; those appearing in this paper as “Fig.” Abbreviations used in the text and figures are listed in Table 1. Exemplar localities in the text are represented by “Place, State, Country” except for those in Australia and the USA, which also include the State. All localities are listed completely in Appendix 1.

MATERIALS AND METHODS

Cladistic Analysis

Analyses were performed with TNT 1.0 (Goloboff et al. 2003, Goloboff et al. 2004) and Nona 2.0 (Goloboff 1993b). All characters in this dataset were treated unordered. Under equal weights, both programs find 96 optimal trees of 483 steps, using either collapsing rule 4 (TNT *collapse 4*) or “min length = 0” rule (TNT *collapse 2*, Nona *ambiguous-*) (Coddington and Scharff 1994). This set expands to 224 dichotomous trees (no collapsing; TNT *collapse 0*, Nona *poly=*). Using the parsimony ratchet (Nixon 1999) as heuristic search, TNT and Nona find the optimal trees in 100% of the replicates, each with 100 iterations keeping up to 5 trees per iteration, using tree bisection-reconnection (TBR) (TNT *ratchet: iter 100; mult = tbr replic 100 hold 5 ratchet*; Nona *hold/ 5 nixwts*100 100*). With so many hits it is likely the optimal tree was found.

We also analyzed the dataset under weighting regimes against homoplasy, using successive weighting (Farris 1969) and implied weighting (Goloboff 1993). The most recent method of implied weights was given priority over successive weighting because implied weights is not affected by starting points or ambiguities in weights from multiple trees. Successive weighting was calculated in Nona using the consistency index as a weighting function, using 100 random addition sequences followed by TBR swapping in each round (*run[swt mu*100]*). The searches stabilized in the second round, and the tree is very similar to the one found under implied weights; the minor

differences are shown in Figure 219. Analyses under implied weights were made with TNT, with integer values of the constant of concavity $K = 1$ to 6. Under this parameter, TNT finds the optimal tree under implied weights in 25% percent of the ratchet replicates. We present the unique, fully resolved optimal tree under a mild concavity with $K = 6$ (Fig. 217), and present the sensitivity to concavity changes in Figures 218 and 219. Ramírez (2003) found that mild concavity values produced higher topological congruence indices. The sensitivity of groups to changes in the analysis parameters also provides an insight to the support of groups (Giribet 2003).

We produced synapomorphy lists mapping the unambiguous changes (e.g., $0 \rightarrow 1$, but not $01 \rightarrow 1$; $01 \rightarrow 2$, but not $01 \rightarrow 12$; option *ambiguous*- of Nona, only option in TNT). Because synapomorphy lists for polytomies in consensus representations are dependent on the optimal resolutions, we calculated all optimal dichotomous trees and produced lists of synapomorphies that are common to all dichotomous trees (Fig. 216; command *apof* of TNT and Nona). Character indices (Fig. 220) were calculated exporting basic values (steps, minimum and maximum possible character lengths) from Nona to a spreadsheet. Under equal weights, only the best scores over the 224 dichotomous trees are reported in Figure 220.

Bremer support values were heuristically estimated by TBR swapping from the optimal trees, retaining suboptimal trees with increasing bounds, up to 50,000 (equal weights) or 30,000 trees (implied weights). Symmetric resampling frequencies ($p = 0.33$) are reported as GC values (GC = 100 is perfect support, GC = 0 is unsupported). The GC is the absolute frequency of a group, minus the frequency of the most frequent contradictory group, and has shown to be less biased than the traditional bootstrap or jackknifing estimations (Goloboff et al. 2003; Goloboff et al. 2004). We estimated the GC values with 1000 pseudoreplicates of five random sequence additions each followed by TBR swapping, keeping up to 10 trees, collapsing trees with a round of TBR

SPECIMEN PREPARATION

Male palpi were expanded for all taxa by immersing them overnight in a 10-15% solution of potassium hydroxide (KOH) and transferring them to distilled water where expansion continued. Palpi were transferred back and forth between KOH and distilled water until expansion stopped. Small structures were examined in temporary mounts following the procedure described in Coddington (1983), or in excavated slides with clearing medium. Spinneret preparations were obtained most reliably when animals were quick-killed by sudden immersion in boiling water. Extension of the spinnerets provided a clear view of all spigots. If live material was unavailable, clean museum material was chosen; the specimen was ultrasonically cleaned, the abdomen squeezed with forceps to extend and separate the spinnerets (Coddington 1989:73) if necessary, and the specimen passed through serial concentrations from 75% to 100% ethanol. Prior to scanning electron microscope examination palpi and spinnerets were critical-point dried; all other structures were air dried. Cribellate silk preparation and examination were done by Robin Carlson and Martín Ramírez. All drawings were made with a camera lucida attached to Olympus, Leitz, or Leica stereo or compound microscopes. Trichobothria bases were considered "smooth" if their sculpturing did not differ from the surrounding leg cuticle. Vulvae were cleaned by immersion in a trypsin solution for three to five days at room temperature or by digestion with contact lens cleaner overnight (Sierwald 1990), or cleared with clove oil or with Chlorox[®] bleach. The tracheal system was examined after digestion in KOH 10-20% in a double boiler. Specific methods are discussed under each character section. The preferred method of examining the tapetum was by microscopic examination of live or recently-dead specimens. The tapetum is a shiny reflective surface that, when present, occurs only in the ontogenetically lateral eyes, and not in the AME. It remains clearly visible for 24-48 hours after a spider's death (after this time the vitreous body usually becomes cloudy,

obscuring the details of the tapetum). When live material was not available, preserved specimens were prepared by removing the chelicerae and most of the musculature from the anterior part of the cephalothorax. The cephalothorax was immersed in lactic acid for 1–5 hours. Frequently the retina cleared and details of the tapetum became visible, though, for unknown reasons, this was not always successful.

ACKNOWLEDGMENTS

The following institutions and curators kindly lent essential specimens: Field Museum of Natural History (Petra Sierwald), Hunan Normal University (Changmin Yin), Instituto Nacional de Biodiversidad, Costa Rica, Johannes Gutenberg University (Peter Jäger), Landcare New Zealand (Grace Hall), Musée Royal de l’Afrique Centrale (Rudy Jocqué), Museo de Historia Natural de La Universidad de San Marcos (Diana Silva Dávila), Museum of Comparative Zoology (Herbert Levi and Laura Leibensperger), Natal Museum (Peter Croeser), The Natural History Museum, London (Paul Hillyard and Janet Beccaloni), Otago Museum, Dunedin (Ray Forster), Queensland Museum (Robert Raven), Rijksmuseum van Natuurlijke Historie (Christa Deeleman), and Zoological Museum University of Copenhagen (Nikolaj Scharff). Other specimens are from the American Museum of Natural History, California Academy of Sciences, Museo Argentino de Ciencias Naturales, and National Museum of Natural History (Smithsonian Institution).

Partial support for all authors came from NSF grant EAR-0228699 (Assembling the Tree of Life: Phylogeny of Spiders) (W. Wheeler P.I.). Griswold wishes to acknowledge financial support from National Science Foundation grants BSR-9020439 and DEB-9020439 (Systematics and Biogeography of Afrotropical Spiders), DEB-0072713: (Terrestrial Arthropod Inventory of Madagascar), the Exline-Frizzell and In-house Research Funds of the CAS, and post-doctoral fellowships from the Smithsonian Institution and the American Museum of Natural History. Coddington wishes to acknowledge financial support from National Science Foundation grants DEB-9712353 and DEB-9707744, and the Neotropical Lowlands Program and Biotic Surveys and Inventory Program from the Smithsonian Institution. Ramírez wishes to acknowledge financial support and post-doctoral fellowships from a Fessenden Research Fellowship from AMNH, a post-doctoral fellowship and grant PEI 6558 from CONICET, PICT03/14092 from FONCYT, and UBA research grant X019. Lucrecia Nieto shared new data on the internal anatomy of *Kukulcania*. Robin Carlson shared new data on the fine structure of cribellate silk; her research was enabled by the CAS Summer Systematics Institute, itself supported by NSF grant BIR-9531307.

Specimens and observations essential to the completion of this study were obtained through fieldwork in Australia, Cameroon, Madagascar, New Zealand, South Africa, Chile, and Tanzania. This fieldwork was made possible through permits issued by a variety of government bodies and traditional authorities. Permits to do research in Australia were made available from the Queensland National Parks and Wildlife Service, facilitated by Dr. R. Raven of the Queensland Museum. Permits to do research in Cameroon were made available from the Institute of Zootechnical Research, Ministry of Higher Education and Scientific Research of the Republic of Cameroon. Griswold especially thanks Dr. John T. Banser, Director of the Institute, and Dr. Chris Wanzie, for facilitating his research in Cameroon. Fieldwork in Cameroon was also made possible by the permission and assistance from the following traditional authorities: Their Royal Highnesses the chiefs of Batoke, Etome, and Mapanja, H.R.H. R.M. Ntoko, Paramount Chief of the Bakossi, Chiefs Jonas Achang, Albert Ekinde, and Peter Epie of Nyassosso, and H.R.H. the Fon of Oku. Permits to do research in and export specimens from Madagascar were obtained from the Association Nationale pour le Gestion des Aires Protégées (ANGAP) and Direction des Eaux et Forêts of the Ministre d’Etat a L’Agriculture et au Development Rural, under Accordes de

Collaboration of the Xerces Society (facilitated by Dr. C. Kremen, Mr. C. Ramlison, and Ms. B. Davies of that organization), and Institute for Conservation of Tropical Environments (ICTE) (facilitated by Drs. R. van Berkum and Benjamin Andriamihaja).

Permits to collect specimens in New Zealand protected areas were obtained from Te Papa Atawhai (Department of Conservation). We thank Lyn and the late Ray Forster and Brian Patrick for advice, help with logistics, and hospitality in New Zealand. Research in Tanzania was made possible through a Research Permit from the Tanzania Commission for Science and Technology (COSTECH) and Residence Permit Class C from the Tanzanian Department of Immigration, and export of specimens made possible by a CITES Exemption Certificate from the Wildlife Division of the United Republic of Tanzania, facilitated by Professor Kim M. Howell of the University of Dar-es-Salaam. Research in the East Usambaras (Tanzania) was made possible by accommodation at the East Usambara Conservation and Agricultural Development Project, Dr. J.K. Ningu, Project Manager, and facilitated by Mr. Massaba I.L. Katigula, East Usambara Catchment Forest Office, Tanga, and Mr. Bruno Samuel Mallya, Kwamkoro. Research in the West Usambaras (Tanzania) was made possible by Dr. S.A.O. Chamshama, Dean of Forestry, Sokoine University, Morogoro, and Mr. Modest S. Mrecha, Officer in Charge, Mazumbai Forest Reserve. Research in South Africa was made possible through a Research Permit from KwaZulu-Natal Nature Conservation Service. Research in Chile was made possible through a Research Permit from the Corporación Nacional Forestal (CONAF), and a grant-in-aid of research from Sigma-Xi to MJR.

Karin Schütt kindly supplied access to her thesis and manuscripts in press. We thank Leticia Avilés, Per de Place Bjørn, L. Joy Boutin, Fred Coyle, Crista Deeleman, Niall Doran, the late Ray Forster, Mark Harvey, Gustavo Hormiga, Andrew McLachlan, Lara Lopardo, the late Bill Peck, Barbara and the late Vincent Roth, Evert Schlinger, Diana Silva Dávila, Darrell Ubick and Carlos Viquez for providing crucial specimens. Roy Harimer assisted with digital photography of silk. Darrell Ubick (CAS), Susan Braden (NMNH), Angela Klaus and Kevin Frischmann (AMNH), and Fabián Tricárico (MACN) assisted with scanning electron microscopy. Cristian Grismado assisted with text editing. Photographs were kindly provided for reproduction by Rollin Coville, Pat Craig, Gustavo Hormiga, Joel Ledford, Teresa Meikle, Nikolaj Scharff, Lenny Vincent and Hannah Wood. Drafts of the manuscript were read and criticized by Robert Raven, Nikolaj Scharff, Petra Sierwald and Darrell Ubick, and the prepress version was proofed in its entirety by Dr. Michele L. Aldrich. We are grateful for their time, effort, and suggestions.

RESULTS

The results of this study are presented in two complementary forms. The first section, The Entelegyne Exemplars, contains a detailed description of the characters and their states in each of the exemplar taxa. The descriptions are organized in a consistent order: taxonomic details of the family, web and silk structures, eyes, chelicerae, legs (including setae, trichobothria and tarsal organ), spiracles and tracheae, spinneret and spigot data, with a description of male and female copulatory organs at the end of each family description. All stated characters are referenced by figures. The second section, Characters, contains a detailed discussion of all characters, references to figures and an explanation of the delineation of states.

THE ENTELEGYNE EXEMPLARS

Agelenidae C.L. Koch, 1837

The Agelenidae are a large, worldwide family of 39 genera and 487 species (Platnick 2004; Ramírez et al. 2004), particularly rich in Eurasia, Africa and North America. A few monotypic gen-

era occur in South America, and at least the synanthropic *Tegenaria domestica* appears to be cosmopolitan. Agelenids are widely known as funnel web spiders, building non-sticky sheets across which the spider runs quickly, hiding in a funnel shaped retreat at one end. Most are solitary but some African species are social. A bipartite colulus comprising two hairy patches (first noted by Lehtinen 1967:342) may be a synapomorphy for the ecribellate taxa. New Zealand is home to several endemic genera, including the only cribellate agelenids. We have chosen the New Zealand *Neoramia sana* as our exemplar. *Neoramia sana* were observed near Dunedin, New Zealand, where they live in a retreat surrounded by an appressed, radiating web upon which they move (Figs. 204H, I). The fine structure of *Neoramia* cribellate silk is unknown.

The eight eyes in two straight rows (Fig. 204I) have a canoe-shaped tapetum, the body is covered with plumose hairs, trichobothrial bases are smooth (Fig. 155H) and the capsulate tarsal organ has a teardrop- or keyhole-shaped orifice (Fig. 153F). The chelicerae have a large boss, teeth on the fang furrow and thickened setae near the fang base. We could not observe a chilum. Metatarsi III and IV of both sexes have apical preening combs of several setae. There are three claws but claw tufts, serrate accessory setae and scopulae are absent. Forster and Wilton (1973) recorded four simple tracheal tubes.

We describe *Neoramia* spinning organs here for the first time. The cribellum is divided into two fields of strobilate spigots (Fig. 82F). The anterolateral spinneret (ALS) has a wide, bare margin around the spinning field (Fig. 73B). The female ALS has two major ampullate spigots (MAP) clustered at the mesal margin, a large tartipore mesad of these and a piriform (PI) field of more than 30 spigots with rounded base margins interspersed with tartipores (Fig. 73B). Males retain only the anterior MAP, with the posterior one replaced by a nubbin (Figs. 74A–B). The female posterior median spinneret (PMS) (Fig. 73C) has two aciniform gland (AC) spigots along the anterior margin, a large mesal minor ampullate gland spigot (mAP) posterad of these, and two posterior cylindrical gland spigots (CY). The paracribellar spigots (PC) are remarkable: at midfield two thick bases each give rise to bundles of 10–12 strobilate PC shafts. The male PMS (Fig. 74C) lacks the CY, and only large nubbins remain of the PC, though one vestigial PC shaft remains in one male (Fig. 82B). The conical apical segment of the female posterolateral spinnerets (PLS) (Figs. 73D, 82A) has an apical modified spigot (MS) flanked by two slender nubbins, similar to those found in some phyxelidids (e.g., *Xevioso*), and are probably the bases of PC that have lost their shafts. There are 7–10 aciniform gland (AC) spigots interspersed by tartipores and three large CY spigots along the mesal margin (Fig. 73D) of the PLS. The apex of the male PLS retains only the nubbins of the MS and its two accompanying spigots (Fig. 74D). Males lack epiandrous spigots (Fig. 161F).

The male pedipalpus has a complex retrolateral tibial apophysis (RTA) consisting of a broad apical and three slender subapical processes (Figs. 179C, 189B). The bulb (Figs. 179A–B, 189B) has two processes in addition to the embolus: a sclerotized, cup-shaped conductor (C) that opposes the tip of the embolus and a flexibly attached, attenuate median apophysis (MA). The form of the tibia and bulb resembles many ecribellate agelenids, e.g., *Calilena* (Chamberlin and Ivie 1941) from California. The epigynum has teeth posteriad of the copulatory openings and the entelegyne vulva is simple.

Amaurobiidae Thorell, 1870

Amaurobiids are a large, worldwide family of 68 genera and 626 described species (Platnick 2004) including cribellates and ecribellates. Our exemplars are the cribellate *Amaurobius fenestralis* from Denmark, *Callobius bennetti* and *Callobius pictus* from the USA, *Pimus pitus* from the USA and a *Retiro* sp. from Peru. We also included an ecribellate representative, *Macrobunus* cf. *multidentatus*, from Chile. Recently Raven and Stumkat (2003) transferred *Poaka* from the

Psechridae into the Amaurobiidae. We discuss *Poaka* under the Psechridae (below) and note that our analysis suggests that placement of that genus in either the Amaurobiidae or Psechridae is problematic.

We have observed *Callobius* and *Pimus* in California, both in the field and in captivity, and have observed *Amaurobius* in California and Denmark. These spiders make irregular webs of cribellate silk that radiate out from a retreat, usually in a cavity (Figs. 206D, G). The cribellate silk carding leg is braced with a mobile leg IV. The spider moves on the web. We never saw amaurobiids wrap their prey. We have not observed living *Retiro*. *Macrobunus* cf. *multidentatus* was found in loose silken cells under logs. Our amaurobiid exemplars have two nearly straight rows of eyes (Fig. 206B) with canoe-shaped tapeta. Tarsal organs are capsulate (Figs. 151D, 153I–K) and there is a single row of tarsal trichobothria that increase in length distally. Trichobothrial bases are transversely ridged in *Amaurobius*, *Callobius* and *Pimus* (Figs. 147B, 156D), but smooth to longitudinally striate in *Macrobunus* and *Retiro* (Fig. 151C, 156E). There are three tarsal claws without tenent or accessory claw setae (Fig. 136G, 138E). The chilum is median (but absent in *Macrobunus*), and the chelicerae have teeth, thickened setae near the base of the fang furrow, and a large boss. In our cribellate representatives the cribellum is divided into two fields of strobilate spigots (Figs 88A, 96A–B) and the spinneret cuticle is ridged but typical cribellate macrobunines have an entire cribellum. Male pedipalpal tibiae have multiple processes, with at least a retrolateral (RTA), dorsal (DTA) and prolateral (PTA) tibial apophysis. The palpal bulb has a tegular apophysis (TA) in addition to the hyaline C and flexibly attached MA, which we code as a sclerotized tegular process (STP), which in most species is broad and blunt. Female genitalia are entelegyne. Details of individual genera, where they differ from this general outline, are discussed below.

Amaurobius fenestralis has apical preening combs of several setae on metatarsi III and IV of both sexes. The respiratory system comprises four simple tracheal tubes (Lamy 1902; Wang 2000). We have examined the spinnerets of a female in detail (Fig. 88A). The ALS (Fig. 88B) has a wide, bare margin with two MAP clustered mesally and a piriform field of more than 30 spigots with rounded base margins and interspersed with tartipores. The PMS has only two AC spigots, a median mAP, one posteromedian CY and two anterior strobilate PC spigots (Fig. 88C). The PLS has an apical MS flanked by two PC. One PC shares a common base with the MS (Fig. 88D). There are ten AC spigots interspersed by tartipores and two CY, one subapical and one subbasal. Wang's (2000) observations agree with ours except that his female specimen had only a single AC spigot on the PMS. Males have epiandrous spigots in two bunches. The cribellate silk of a Californian species of *Amaurobius* has axial fibers and reserve warp (Fig. 122C). The male pedipalpal tibia has four processes: RTA, DTA PTA and VTA. A broad TA extends retrolaterad obscuring the base of the concave MA. The margin of the tegulum has a lobe but there is no corresponding lobe on the subtegulum. The epigynum has small teeth posteriad of the copulatory openings near the epigastriac furrow.

Callobius (Fig. 206B), like *Amaurobius*, has apical preening combs of several setae on metatarsi III and IV of both sexes and a respiratory system of four simple tubes. We have examined the spinnerets of a female in detail (Fig. 89A). The ALS has a wide, bare margin with two mesally clustered MAP, a large tartipore mesad of these and a piriform field of more than 30 spigots with rounded base margins and interspersed with tartipores (Fig. 89B). The PMS (Fig. 89C) has several median to posterior AC spigots, a median mAP, and a retrolateral and a posterior CY. There are three anterior PC spigots with strobilate shafts. The PC spigots arise from single bases, but one *Callobius* individual examined had a pair of shafts arising from a common PC base (Fig. 96C). Abnormal, duplicate shafts are occasionally found in spiders (e.g., Figs. 107C, 111A), hence we have coded *Callobius* PMS PC as arising from a single base. The PLS has an apical MS flanked

by two separate PC. There are more than 20 AC spigots interspersed by tartipores and two CY, one subapical and one subbasal (Fig. 89D). Wang's (2000) observations are similar to ours. Males have epiandrous spigots in two bunches. Cribellate silk has axial fibers and reserve warp (Figs 123A–B). The male pedipalpal tibia has four processes: RTA, DTA, PTA and VTA. The VTA and PTA are short and conical (Figs. 182A, 193A), the RTA is a backward curving hook, and the DTA is bifid with a long, slender process and a short, conical one (Fig. 181C). The MA is convex and hatchet-shaped and the TA is hemispherical (Figs. 182A–B). Unlike *Amaurobius* the epigynum lacks teeth.

Pimus has a prolateral series of thorn-like setae on the male palpal femur (Fig. 147C). Preening combs are lacking. The respiratory system comprises four simple tracheal tubes. We examined the spinnerets of a male and female (Figs. 90A, 91A). The ALS has a narrow, bare margin (Fig. 90B). The female ALS has two mesally clustered MAP and a nearby tartipore (Figs. 90B, 96F). The male (Fig. 91B) has one functional MAP plus nearby nubbin and tartipore. The piriform gland spigots have rounded bases and are interspersed with tartipores. The female PMS has two mAP accompanied by a TP, a single anterior PC, several median AC spigots, and a single posterior CY (Figs. 90C, 96G). The male PMS has a nubbin in place of the PC, and lacks the CY (Fig. 91C). Wang (2000) recorded only one mAP in *Pimus*, but his specimen was somewhat damaged and difficult to interpret. The female PLS has an apical MS flanked by two separate PC (Figs. 90D, 96D, H). There are about 15 AC spigots interspersed by tartipores and two retrolateral CY (Figs. 90D, 96H). The male retains only the AC spigots. The CY are absent and the MS and PC are replaced by apical nubbins (Fig. 91D). Males have epiandrous spigots dispersed along the epigastric furrow (Fig. 161E). The cribellate silk has axial fibers and reserve warp. Reserve warp fibers are visible in Figures 123C–D; the axial fibers are hidden, but present. The male pedipalpal tibia has long, slender and pointed DTA and RTA, and a short conical PTA (Fig. 181D). The embolus is a slender, curved spine, the C hyaline, and the TA is flattened and arched, covering the base of the MA (Fig. 182C). The epigynum lacks teeth.

Retiro differs in many features from the other amaurobiid exemplars, especially in the tracheal system, epiandrous region, and trichobothrial bases. The tracheal system comprises two thick median trunks that give rise to bunches of fine lateral tracheoles in the abdomen, and penetrate the cephalothorax where they give rise to two lateral and a terminal bunch of fine tracheoles. The lateral tracheae comprise a fine, simple tube on each side, which is confined to the abdomen. Male epiandrous spigots are absent. The trichobothrial bases are smooth to longitudinally striate (Fig. 156E), the cheliceral boss is small, and preening combs are lacking. We have examined the spinnerets of a female (Fig. 92A) and male (Fig. 93A). The female ALS (Fig. 92B) has a narrow field margin and a single MAP and posterior nubbin at the edge of the spinning field. A second apparent nubbin mesad of these appears to be a PI spigot with a broken shaft. The piriform spigots have rounded base margins. The male ALS is the same (Fig. 93B). The female PMS has five AC spigots, an anterior mAP and two lateral CY (Fig. 92C). Unlike other amaurobiids, PMS PC are absent. The male PMS has the mAP and five AC but lacks the CY spigots (Fig. 93C). The female PLS (Fig. 92D) has several AC spigots, two median CY and an apical MS but no PC (Fig. 96E). The male PLS lacks the CY and the MS is replaced by an apical nubbin (Fig. 93D). The male pedipalpus has a forward-curving RTA and an elongate, transverse VTA (Figs. 182D–E), a short, stout PTA and a short, curved, bifid DTA (Fig. 181B). The bulb has a broad, trifid TA that obscures the C base and a slender, apically hooked MA (Figs. 181A, 182D–E). The epigynum lacks teeth posteriad of the copulatory openings but has small pockets.

Macrobunus has simple lateral tracheae, and slightly branched median tracheae, limited to the abdomen. Male epiandrous spigots are absent (Fig. 158H). The chelicerae have a very long fang, three promarginal teeth, and a long retromarginal series of 8 teeth plus 6–10 tightly packed denti-

cles. The tarsal organ has an oval orifice (Fig. 151D), the proximal hood of the trichobothrial base is longitudinally striate (Fig. 151C), and the cuticle is smooth with some ridged areas. The male femur II has a ventral, basal, conical process. We present scans of male and female spinning organs (Figs. 94–95). The colulus is broad and covered by setae (Figs. 94A–B, 95A). The ALS has about 27 PI spigots with rounded bases and thin shafts; the female has two MAP spigots with a tartipore (Fig. 94C), while the male has the posterior MAP replaced by a nubbin (Fig. 95B). The PMS has one mAP spigot without traces of nubbin or tartipore, and many AC spigots with long, thin shafts (Figs. 94D, 95C); in addition to these, the female has two larger CY spigots on the mesal and posterior margins. The PLS has several AC and no traces of MS or nubbins, and the female has one CY spigot on the anterior external margin (Figs. 94E, 95D). The male pedipalpus has a complex RTA with several processes and ridges (Figs. 183A, 193B–C), a simple DTA, and a small, rounded VTA. The DTA has a membranous area on its base. One of the processes of the RTA is flat, translucent, closely appressed to a concave area of the cymbium (Fig. 183A); on closer inspection this concave area has regularly disposed ridges, apparently a stridulatory apparatus (Fig. 183B). Similar stridulatory fields were found in other macrobunine genera as well (*Anisacate*, Ramírez pers. obs.; *Rubrius* and *Emmenomma*, Fig. 183C–D). The bulb (Fig. 193B–C) has an apical hyaline C, a large, articulate sclerite that we identify as a MA, and a small sclerotized plate surrounded by a membranous area that we identify as a TA. The embolus is fused with the tegulum and has a complex basal process; the embolar base is projected in a lobe, which has no corresponding lobe in the subtegulum. The epigynum lacks teeth.

Amphinectidae Forster and Wilton, 1973

Amphinectidae comprise 34 genera and 181 described species from Australia, New Zealand and South America (Platnick 2004). At least *Metaltella simoni* is introduced to the USA. There are cribellate and ecribellate amphinectids, and there are several cases in which cribellates and ecribellates are closely related, e.g., *Maniho* and *Amphinecta* (Forster and Wilton 1973). Cribellate amphinectids build small space webs for prey capture, whereas ecribellate amphinectids are wandering hunters.

Our amphinectid exemplars are *Maniho ngaitahu* from New Zealand and *Metaltella simoni* (Fig. 206A) from California (this species also occurs in the southern USA and in South America). We have also examined *Metaltella rorulenta* from Chile. We have observed *Maniho* species in the wild in New Zealand and *Metaltella simoni* in captivity. *Maniho* occurred beneath logs and stones. *Metaltella simoni* built irregular space webs in captivity and spent most of the time hanging upside down in these webs. The cribellate silk carding leg is braced with a mobile leg IV. We never observed prey wrapping. *Metaltella* cribellate silk has reserve warp and axial fibers (Figs. 124A–C).

Our amphinectid exemplars have two nearly straight rows of eyes with canoe-shaped tapeta. The chelicerae have teeth, thickened setae near the base of the fang furrow, and a large boss. Tarsal organs are capsulate (Figs. 147D, 153E) and there is a single row of tarsal trichobothria with smooth bases (Figs. 155I, 156A). There are three claws and preening combs occur at the apices of metatarsi III and IV, but serrate accessory setae and scopulae are lacking. Male epiandrous spigots are absent (Fig. 160D). The cribellum is divided into two fields of strobilate spigots and the spinneret cuticle is ridged. Female genitalia are entelegyne, the epigynum has lateral teeth (Fig. 180D) and the vulva is complex with convoluted ducts (Fig. 164F). Male pedipalpal tibiae have a simple, apical RTA and a proximal DTA (Fig. 180C, 189C). The cymbium lacks chemosensory scopulae but has trichobothria. The palpal bulb has a sclerotized C, an MA and an additional TA that arises near

the embolic base, but details differ dramatically between *Maniho* (Figs. 180A–B, 189C) and *Metaltella* (Fig. 179D). Amphinectids are heterogeneous in several other features. *Maniho* has deeply notched trochanters, whereas those of *Metaltella* are unnotched. Tarsal trichobothria form a single row and are irregular in length in *Maniho* but increase in length distally in *Metaltella*. *Maniho* has feathery scales (Fig. 147D) but *Metaltella* lacks them. The chilum is median in *Metaltella* but bilateral in *Maniho*.

We examined the spinning organs of both sexes of *Maniho* (Figs. 75A, 76A). The ALS has a wide bare margin. The female ALS has two MAP clustered at the mesal margin and a piriform field of more than 30 spigots with rounded base margins and interspersed with tartipores (Fig. 75B). The male ALS is similar except that the posterior MAP is replaced by a nubbin (Fig. 76B). The female PMS (Fig. 75C) has several AC spigots, one anterior mAP, and a median and lateral CY. There is a median row of 10–11 PC with strobilate shafts. Most PC have multiple shafts emerging from a common base (Fig. 82D). The male PMS lacks the CY, and the PC are replaced by a median row of nubbins (Fig. 76C). The female PLS (Fig. 75D) has two basal CY, more than 20 AC, and an apical MS flanked by two PC (Fig. 82E). The male PLS lacks the CY and has the MS and PC replaced by nubbins (Fig. 76D). The male pedipalpus (Figs. 180A–C, 189C) has a trapezoidal tegulum, a transverse, curved MA, and a ribbon-like embolus that spirals to encircle the tegulum. The large C opposes the embolus tip. Near the embolic base is a short, semicircular TA (Figs. 180B, 189C).

Metaltella spinnerets resemble those of *Maniho* (Figs. 77A, 78A). The ALS has a wide bare margin. The female ALS has two MAP clustered at the mesal margin and a piriform field of more than 30 spigots with rounded base margins and interspersed with tartipores (Fig. 77B); the male posterior MAP is replaced by a nubbin (Fig. 78B). The female PMS (Fig. 77C) has one large anterior mAP, two posterior CY and several AC. There is a median group of 10–11 PC with strobilate shafts. Most PC have single shafts but a few have multiple shafts emerging from a common base. The PC are replaced by a median group of nubbins in the male (Fig. 78C). The female PLS (Fig. 77D) has a basal CY, more than 20 AC, and an apical MS flanked by two PC (Fig. 82C). The MS and PC are replaced by nubbins in the male (Fig. 78D). The male palpal bulb appears relatively simple (Fig. 179D), but has an astonishing internal complexity (Figs. 191, 192). The MA is elongate, with a concavity facing retrolaterally (identified as primary conductor by Davies 1998). The broad shaft of the C (identified as secondary conductor by Davies 1998) arises retrolaterally on the tegulum and is inrolled to form a near cylinder that contains the threadlike embolus; the hypertrophied C base forms most of the visible part of the tegulum. We have distinguished the approximate limit between tegulum and conductor by the origin of the embolus, and by a furrow that seems to mark the suture line between them (Fig. 192B–C, tegulum grayed). The origin of the embolus is totally concealed by the C (E* in Fig. 192A); after digestion of tissues, the long embolus can be seen describing several internal loops before emerging from a slit in the C shaft; a dissection of the tegulum shows that the embolus runs through convoluted cuticular foldings of the C (C* in Fig. 192A). The embolar base has a sclerotized process that arises apically from the tegulum (E** in Fig. 192A); there is no subtegular lobe opposing this embolar lobe. The female vulva has long, convoluted copulatory ducts (*cf.* Fig. 164F), an indication of a correspondingly long intromittent embolus. This suggests that a significant part of the embolus comes out through the conductor slit during mating. A high hydrostatic pressure in the bulb may produce the membranous internal foldings of the conductor to push the embolus out of the copulatory bulb. This unique conductor form is characteristic of metaltellines (Davies 1998); a similar disposition of the embolus origin internal to the conductor is reported here also for *Desis*, although not as dramatically developed as in metaltellines.

Araneoidea Simon, 1895

This worldwide superfamily comprises the ecribellate orb weavers and their kin, including the families Anapidae, Araneidae, Cyatholipidae, Linyphiidae, Mysmenidae, Nesticidae, Pimoidae, Symphytognathidae, Synsphyridae, Synotaxidae, Tetragnathidae, Theridiidae, and Theridiosomatidae, and includes at least 11022 described species (Platnick 2004). This is a large and important taxon comprising 29% of described spider species and including the second (Linyphiidae) and third (Araneidae) largest families. Griswold, Coddington, Hormiga and Scharff (1998, Fig. 211) proposed a comprehensive phylogeny for the superfamily. Recent work by Karin Schütt (Schütt 2000, 2002, Fig. 210, 2003) suggests that the minute Micropholcommatidae, previously included in Palpimanoidea, may belong in Symphytognathoidea, a relatively derived group within Araneoidea. *Araneus* (Araneidae), our selected exemplar taxon, is, for the characters treated herein, a good representative of the groundplan of Araneoidea, as optimized at the base of the superfamily. We also illustrate some characters as seen in other araneoid taxa.

In *Araneus* the eyes have a canoe-shaped tapetum and the chelicerae have a small boss and teeth on the fang furrow but lack thickened setae near the fang base. The chilum is bilateral. The legs lack tarsal trichobothria and have only one subapical metatarsal trichobothrium, trichobothrial bases are smooth and the capsulate tarsal organ has a round orifice (Fig. 149A), and there are three claws with conspicuous serrate accessory setae (sometimes called “false claws”) associated (Fig. 137C, arrow). Hairs are serrate (Figs. 148F, 149A). Preening combs, scopulae and claw tufts are absent. The posterior respiratory system comprises four simple tracheal tubes. Araneoids are ecribellate, and lack characters associated with the cribellum, calamistrum and cribellate silk and silk spinning. The ALS has a narrow, bare margin surrounding the spinning field. The female ALS has a single MAP accompanied by a nubbin and a tartipore, all at the edge of the spinning field, separated by a deep furrow from the PI field (Figs. 20E–F). The piriform spigots have rounded bases and their field is interspersed with tartipores. Some derived Araneoidea have lost their PI spigot bases (Fig. 20F) but round bases optimize as the groundplan state. The male’s ALS is identical to the female. The female PMS has a single posterior mAP and associated nubbin and tartipore, several AC spigots and 1–2 CY. The female PLS has a peripheral triplet of a flagelliform gland (FL) and two aggregate gland (AG) spigots (Figs. 38C, E) responsible for the gluey silk capture line (Fig. 119C–E). There are also numerous AC spigots and two CY on the PLS. Appendage cuticle is squamate (Fig. 149A). Males have epiandrous spigots evenly distributed along the epigastric furrow. The male pedipalpal tibia has simple, rounded ventral processes and the cymbium has a paracymbium (Fig. 171F) but lacks trichobothria or chemosensory scopulae. The male palpal tarsus is rotated so that the cymbium is prolateral and the bulb retrolateral. The bulb has a sclerotized C of the “uloborid” type (see character 118 state 3 below) and a flexibly attached, convex MA (Fig. 171E). The entelegyne female genitalia comprise an epigynum that lacks teeth and has a simple vulva. Araneoids are orb builders and all behaviors that build the orb web apply, i.e., construction of a frame, radius, hub, temporary spiral and sticky spiral. Araneoids hang beneath the web and wrap their prey before biting.

Archaeidae C.L. Koch and Berendt, 1854

Archaeidae comprise three genera and 25 species from Africa, Madagascar, and Australia (Platnick 2004). Our exemplar is *Archaea workmani* from Madagascar. *Archaea* make no webs for prey capture but use silk for drag lines and to wrap their eggs. They prey upon other spiders (Fig. 195D).

The eight eyes are in two nearly straight rows and have a canoe-shaped tapetum. All but the

AME are very small. The pars cephalica is extremely prolonged into a “neck” and sclerotized completely around the base of the elongate chelicerae (Figs. 127A, 195D). The chelicerae lack a boss or stout setae near the fang base but have peg teeth and a few true teeth (Fig. 127B) and a patch of stridulatory striae on the outer margin (Fig. 127D). The cheliceral gland opens on a mound (Fig. 127C). The labrum has lateral extensions (Fig. 127E). Two faint sclerotizations above the cheliceral base suggest a bilateral chilum. The elongate legs are spineless, all hairs are plumose and the cuticle is squamate (Figs. 134D, 149C). Tarsal trichobothria are absent and there is only a single subapical trichobothrium on the metatarsus. The trichobothrial base hood is transversely ridged (Fig. 149H) and the capsulate tarsal organ has round orifice (Fig. 149C). There are three claws but claw tufts, preening combs and scopulae are absent. The setae below the claws resemble serrate accessory setae (Fig. 134E–F). Forster and Platnick (1984) and Platnick et al. (1991) did not record serrate accessory setae in *Archaea*, but we code them as present. The median claw is elongated, remarkably similar to that of symphytognathoid araneoids (Griswold et al. 1998: character 63). A pair of posterior spiracles (Fig. 127F) each leads to a single tracheal tube (Forster and Platnick 1984, fig. 305); lateral tracheae are absent. The male lacks epiandrous spigots. The spinnerets of *Archaea* were described by Platnick et al. (1991, figs. 228–233). We examined male, female and immature *Archaea workmani* from Madagascar (Figs. 20A–D, 21–22). *Archaea* are ecribellate. The ALS of both sexes have a wide spinning field margin, one MAP spigot plus a tartipore and a reduced MAP, all on the mesal margin, and a field of more than 25 PI spigots with short, sharp bases and interspersed with tartipores (Figs. 21B, 22B). The immature has two normally developed MAP, suggesting that the posterior reduced MAP in adults is homologous with the nubbin found in other spiders (Fig. 20B). The MAP field is separated from the PI field by a deep furrow (Figs. 20B, 22B). The female PMS has an anteromedian mAP, a median AC, and a lateral and posterior CY (Fig. 21C). The male retains only the AC and mAP (Fig. 22C), but the immature seems to have two mAP and two AC (Fig. 20C). The female PLS has a median row of five AC spigots and three large CY spigots in the anterior, mesal and posterior positions (Fig. 21D). The male retains only the five AC (Fig. 22D), while the immature has only two AC (Fig. 20D). The male palpus lacks tibial processes, and the cymbium lacks trichobothria or chemosensory scopulae (Figs. 168A–C). The apex of the *Archaea* tegulum has two sclerotized ridges that spiral around a central pit that contains the E and MA (Fig. 168D). We code these ridges as an apical C. The haplogyne female genitalia lack an epigynum (Fig. 165); there is a large, membranous median seminal receptacle with patches of gland ductules on its dorsal side. Internally, the epigastric fold bears two strong apodemes for muscle insertion (Fig. 165 A–B).

Austrochilidae Zapfe, 1955

Austrochilidae comprise three genera: the monotypic *Hickmania* from Tasmania, and *Austrochilus* and *Thaida* with eight described species between them from Argentina and Chile (Platnick 2004). The family was established by Gertsch and Zapfe (in Zapfe 1955) and considered a senior synonym of Thaididae and Hickmaniidae by Forster et al. (1987:25), contra Lehtinen (1967:299) and Marples (1968:30).

Our exemplars are *Thaida peculiaris* from Chile and *Hickmania troglodytes* from Tasmania. Austrochilids make and hang beneath extensive sheet webs (Figs. 198A–F) (*Thaida*: Forster et al. 1987: fig. 118; *Hickmania*: Morrison and Morrison 1990:148). Lopardo, Ramírez, Grismado and Compagnucci (2004) report that in *Thaida peculiaris* and *Austrochilus forsteri* the cribellate silk carding leg is braced with a mobile leg IV (an “advanced” entelegyne behavior) (Fig. 198B) and that they occasionally wrap prey after biting (Fig. 198F). We examined the cribellate silk of *Hickmania* and *Thaida*. In both cases the cribellate mass is puffed, and the fibrils have the regular-

ly spaced nodules reported by Eberhard and Pereira (1993) for entelegyne spiders (Figs. 118A–D, 119F). Carlson (*in lit.*) also examined the fine structure of *Hickmania* cribellate silk, which has axial fibers but lacks reserve warp (Figs. 120A–C). Although there are wavy fibers in the cribellate mass (Fig. 120C), these lack the characteristic spiral of reserve warp and are probably axial fibers. She also noted nodules on the cribellar fibers.

Austrochilids have primitive tapeta and chelicerae without a boss but with teeth and thickened setae along the fang furrow. The chilum is absent at least in *Thaïda*. The clypeal hood makes examination of the chilum difficult. Tarsal trichobothria are lacking and there is only a single, subapical trichobothrium on the metatarsus: the base is smooth and has a distal notch. The tarsal organ is exposed (Figs. 148D, 150A, 152A). There are three claws and serrate accessory setae (Figs. 133A–D); scopulae and claw tufts are lacking. The palpal femora of *Thaïda* have probasal thickened setae modified as thorns; such thorns are lacking in *Hickmania*. *Thaïda* has some feathery scales (Fig. 148D) whereas those of *Hickmania* are only plumose. Males have numerous epiandrous spigots in two bunches (Fig. 158A). The respiratory systems of austrochilids vary. *Hickmania* has four booklungs. *Thaïda* has a wide posterior spiracle that leads to modified organs that resemble vestigial booklungs in the hatching immatures, which become elongate and similar to tracheae through successive stages (Forster and Platnick 1984; Ramírez 2000). We reflect this ambiguity as a polymorphic scoring. *Hickmania* and *Thaïda* have similarly projecting female genital regions that we code as an epigynum, but *Thaïda* has in addition a sclerotized area posterior to the genital opening. The haplogyne female genitalia of *Thaïda* and *Hickmania* have a genital opening anterior to the epigastric fold, which leads to a median sperm receptacle (in *Thaïda*) or to four slender spermathecae (in *Hickmania*) and also to the uterus externus (Figs. 163A–B). In *Thaïda* the genital opening is also exposed in the male (Fig. 158A), whereas that of *Hickmania* is hidden by the epigastric fold. The epigastric fold leads to a blind invagination that serves as a muscle attachment.

Forster, Platnick and Gray (1987) and Platnick et al. (1991) described the spinning organs of *Austrochilus melon*, *Thaïda peculiaris* and *Hickmania troglodytes*, but some of our interpretations here differ from those previously published. We scanned the spinning organs of both sexes of *Thaïda peculiaris* from Argentina and Chile. Like hypochilids they have entire cribella (Fig. 13A), but in other aspects they resemble entelegynes. The male and female ALS of *Thaïda* have two large MAP at the median edge of the spinning field, flanked by a huge tartipore (Figs. 11B, 12B, 14A). The margin of the spinning field is narrow. There are more than 50 piriform spigots with rounded bases. The piriform spinning field is interspersed with tartipores and is separated from the MAP and large tartipore by a wide, semicircular bare area (Fig. 11B). The female PMS has about 6 AC spigots, a large median mAP accompanied by a tartipore, and 11 large posterior spigots (Fig. 11C) that we code as CY. A row of 10 PC spigots encircles the anterior side of the spinneret. Each PC base gives rise to a single shaft. The PC shafts have numerous closely-spaced annulations (Figs. 11C, 13D). The female PLS is flattened (Fig. 11D), has numerous AC spigots, an anterior-external line plus a basal group of large spigots, and an apical MS spigot flanked by one PC and one very small nubbin (Figs. 13E–F). Close to this group, there is a spigot with a shaft of intermediate morphology between AC and PC (Fig. 13E, asterisk), which we code as a second PLS PC. The male PMS retains two PC spigots, but the other PC are replaced by long nubbins, and the large posterior spigots are absent (Fig. 12C). The male PLS has only AC spigots, plus the apical nubbins of the MS, its tiny accompanying nubbin, and the nubbin of the PC spigot (Fig. 12D). Because the numerous large spigots on the female PMS and PLS are absent in the male, while all the other spigots (or their corresponding nubbins) occur in the same relative position, we identified the large spigots as cylindricals (Figs. 11C–D, 13D–F). These spigots fulfill our ontogenetic and morphological crite-

ria for CY. This conclusion is novel: previous morphological (Forster et al. 1987) and phylogenetic (Platnick et al. 1991, Griswold et al. 1999) studies coded CY spigots as absent in austrochilids.

We scanned the spinning organs of both sexes of *Hickmania troglodytes* from Tasmania. The male and female ALS has two large MAP at the median edge of the spinning field, flanked by a huge tartipore (Figs. 7B, 8B, 10D). The ALS PI spigots gradually increase their size towards the external border (Figs. 7B, 8B, 10C). The PMS PC encircle the spinneret anteriorly (Fig. 7C), and, like *Thaïda*, the shafts have closely-spaced annulations (Fig. 10F). In the male PMS, several PC spigots are replaced by nubbins, but about 15 still retain their shafts (Fig. 8C). There is one median mAP spigot, with a short conical base, flanked by a tartipore (Figs. 7C, 8C, 10E). A second, similar but more posterior spigot is probably a mAP as well. There are about 20 small AC spigots. A group of large CY spigots with thicker shafts encircle the PMS posteriorly and at the sides. The PLS are very flat, have numerous small AC spigots and an apical MS spigot, but PC are lacking (Figs. 7D, 8D, 9A–D). The female PLS has an anterior line of CY spigots. As in *Thaïda*, we identified these as CY spigots because they are absent in the male. A further class of spigots occurs on the PMS and PLS of both males and females (Figs. 7C, 9A–D). They have large bases, and the shafts are intermediate in size between those of AC and CY. We tentatively identified them as a second class of AC spigots (marked with ‘?’ on the plates). These large spigots occur on a median and a posterior line on the PLS.

The male pedipalpi of austrochilids lack tibial processes and cymbial chemosensory scopulae and trichobothria, but the bulbs are diverse. The bulb of *Hickmania* is simple, lacking C and MA (Forster et al. 1987, figs. 343–346). Nevertheless, the tegulum and subtegulum are distinguishable, and the bulb is not spindle-shaped, so we do not code it as piriform. *Thaïda* has a complex bulb with several processes (Figs. 166C, 187A). The embolus is a broad, twisted flange that contains the membranous sperm duct. The MA is a slender spine that arises from soft cuticle and the C is sclerotized and has a serrate trip. The embolus and C, the latter with a serrate apex, are both elongate cones that are in close association in the unexpanded bulb (Fig. 166C) but arise far from each other in the expanded bulb (Fig. 187A). The subtegulum has a sclerotized hook, noted with an arrow in Figure 166C. Our interpretation of bulb processes differs from the interpretation of Forster et al. (1987), who considered the slender MA spine to be the embolus and the broad embolic flange to be a C.

Ctenidae Keyserling, 1877

Ctenidae comprise a large, worldwide family of 39 genera and 450 described species (Platnick 2004). Most are ecribellate, but *Acanthoctenus* and three other genera retain the cribellum. Ctenids, or “tropical wolf spiders,” are fast moving, running hunters that make little use of silk. Traditional synapomorphies for this family are the 2-4-2 eye pattern and claw tufts. Although the monophyly of Ctenidae including *Acanthoctenus* is dubious (e.g, Griswold 1993, Fig. 213; Silva Dávila 2003, Fig. 214), we accept the current broad limits of the family and choose a few species of *Acanthoctenus* (Fig. 208C) as our exemplar.

The eyes have a grate-shaped tapetum and the chelicerae have a large boss, teeth on the fang furrow and thickened setae near the fang base. The chilum is bipartite. The legs are very spinose (more than 7 pairs of ventral spines on the first tibia), hence *Acanthoctenus*. The capsulate tarsal organ has an oval orifice (Fig. 153M) and the trichobothrial bases have transverse ridges (Figs. 148C, 156H). Two to three dorsal rows of trichobothria occur on the tarsi. The short, basal calamistrum is oval (Figs. 145I–J). The ITC is absent and there are well-developed claw tufts (Fig. 139E), and at least the posterior tarsi of females have scopulae. The respiratory system consists of 4 simple tracheal tubes.

We describe the spinning organs of male and female *Acanthoctenus* specimens from Panama and Peru. The narrow, deep cribellum is divided into two fields of strobilate spigots that are clumped in short, longitudinal linear rows (Figs. 97A, G). The ALS has a narrow, bare margin, a pair of large MAP and numerous PI spigots interspersed with tartipores (Figs. 115B, 116B, 117A). There is a large tartipore close to the MAP (Figs. 115B, 117A). The PMS (Figs. 115D, 117B–C) lacks a paracribellum, and has two mAP spigots with short, stout bases and cylindrical shafts, with a large tartipore in between (Figs. 115D, 116C). Posteriad of these are more than 20 small AC spigots with cylindrical bases and slender shafts. The female has in addition three large CY spigots with conical bases and long, conical shafts, interspersed posteriorly among the AC (Figs. 115C–D, 117C). The conical apical segment of the PLS has numerous AC and an apical anterior MS (Figs. 115E, 117D) which is replaced by a nubbin in the male (Fig. 116D). The female has in addition three large CY spigots similar to those on PMS. Males lack epiandrous spigots. The structure of *Acanthoctenus* cribellate silk is unknown.

The male pedipalpus has a simple, triangular, apical RTA and the cymbium has a dorsal chemosensory scopula. The bulb has retrolateral locking lobes on the tegulum and subtegulum and two processes in addition to the embolus: an apical, hyaline C that opposes the tip of the embolus and a flexibly attached, concave MA. The epigynum lacks teeth and vulva is simple.

Deinopidae C.L. Koch, 1851

Deinopidae comprise four genera and 57 species, and occur worldwide except in New Zealand (Platnick 2004). All are cribellate. Our deinopid exemplars are *Deinopis spinosus* from Costa Rica (Figs. 200D–E) and Florida in the USA and *Menneus camelus* from Kenya and South Africa (Fig. 200C). We have not examined a male of *Menneus*, so our data come from the only published description (Tullgren 1910), which is not complete.

We have observed *Deinopis* in many parts of the world, especially Florida and Costa Rica, and have observed *Menneus* in South Africa. The fine structure of the cribellate silk of *Menneus* was studied by Akerman (1926) and that of *Deinopis* by Kullman (1975) and Peters (1992a) and summarized by Eberhard and Pereira (1993). The puffed cribellate band has both reserve warp and axial fibers, and the cylindrical cribellar fibrils have nodules. Deinopids build a characteristic, highly modified orb web (Figs. 200C–D) (Coddington 1986b) that we term “deinopid web architecture.” In addition to the suite of orb web building behaviors, deinopids locate sticky silk with leg IV (SS localization with L4). Like other Orbiculariae, deinopids brace the silk carding leg with a mobile leg IV and wrap their prey after biting it.

Deinopid eyes lack a tapetum and the posterior eye row is strongly recurved. At least in *Deinopis* the PME are greatly enlarged, hence the common name, “ogre-faced” spiders (Fig. 200E). The tarsi lack trichobothria and there is but a single trichobothrium near the apex of the metatarsus. The trichobothrial bases are smooth to weakly ridged (Figs. 135B, 154E) and the capsulate tarsal organ has a round (Figs. 148A, 152H) orifice. The legs have numerous feathery scales (Figs. 135A, 148A) as well as plumose hairs with short barbs (Fig. 147F, 148A). These latter have been called “pseudoserrate” (Green 1970; Coddington 1986a; Griswold et al. 1998) but differ only slightly from typical plumose hairs. *Deinopis* have a characteristic line of stout setae on the hind tarsi, the “deinopoid tarsal comb” (Figs. 141B–C). Only a few such setae are found in *Menneus* (Fig. 140B). There are three claws and serrate accessory setae (Figs. 135C–E) but the legs lack scopulae, preening combs or claw tufts. The large chelicerae have teeth on the fang furrow but lack a thickened seta near the fang base or a boss. We have been unable to find and score the chilum. Lamy (1902) recorded a respiratory system comprising four simple tracheal tubes in *Deinopis*.

Males have epiandrous spigots arranged in several groups sunk into pits along the epigastric furrow (Figs. 159C–D).

The spinning organs of *Deinopis* have been discussed previously (Coddington 1989; Peters 1992a). We here illustrate the spinnerets of *Menneus* as well as some details of *Deinopis*. In most details *Menneus* and *Deinopis* are alike. The spigots have ridged cuticle (Figs. 44D–E) and the cribellum is entire with strobilate spigots (Fig. 43A). The female ALS has five MAP clustered at the inner edge of the spinning field (Fig. 43B), two large tartipores proximad of these (Fig. 44C) and a large, bare semicircular region separating these from the rest of the spinning field. Similar ALS bare regions are found in uloborids (Fig. 45B) and *Thaida* (Fig. 11B). The piriform spinning field is interspersed with tartipores and comprises more than 50 piriform spigots with flat base margins. The female PMS (Fig. 43C) has numerous anterior to median AC spigots, an anterior mAP, and several posterior and posterobasal CY. Peters (1992a) found two PMS mAP spigots in a *Deinopis*, but we have found only one in our *Deinopis* and *Menneus* specimens. However, one of the mAP found by Peters is much smaller, and our images of *Deinopis* do not permit certain identification. We scored two mAP in *Deinopis*, following Peters, but one in *Menneus*. There are numerous PC bunched along the anterior margin of the PMS, each base supporting a single shaft. The shafts have numerous, closely-spaced annulations, hence the term “deinopoid” PC spigots (e.g., in *Deinopis*, Fig. 45D) used in previous phylogenetic studies (e.g., Griswold et al. 1999). The conical PLS apical segment (Fig. 43D) has several basal CY, several median to apical AC, and an apical MS segregated from the spinning field (Fig. 44D). Both AC and CY spigots have columnar bases with flat margins, but the AC shafts are short cones whereas the CY shafts are long cylinders (Fig. 44E).

The male pedipalpus of *Deinopis* lacks tibial processes, and the cymbium lacks trichobothria or chemosensory scopulae. The bulb has a central lobate C with the embolus spiralling around it, and there is no MA (Fig. 171D). The published figure of the male palpus of *Menneus* (Tullgren 1910: fig. 2) shows a similar organ. The entelegyne female genitalia comprise an epigynum that lacks teeth posteriad of the copulatory openings.

Desidae Pocock, 1895

Desidae comprise 38 genera and 180 described species (Platnick 2004), mostly occurring in Australia, New Zealand, New Caledonia and southeast Asia. *Porteria* occurs in Chile, and the intertidal genera *Desis* and *Paratheuma* occur on Indopacific coastlines. At least *Phryganoporus candidus* may be subsocial. *Badumna longinqua* is a synanthropic invader in California, New Zealand and Uruguay. Desidae are a heterogeneous family with cribellate and ecribellate genera, the former occurring primarily in Australia and New Zealand.

Our desid exemplars are the cribellate *Phryganoporus candidus* from Australia, *Badumna longinqua* (Figs. 205B–C) from California, New Zealand and Uruguay (this species is probably native to Australia), *Matachia australis* and *M. marplei* from New Zealand (Figs. 205D–G), and the ecribellate *Desis formidabilis* (Fig. 205A) from South Africa. Our desid exemplars are alike in having eight eyes with canoe-shaped tapeta in two nearly straight rows, plumose setae, capsulate tarsal organs (Figs. 151H, 153G–H), and three tarsal claws but no claw tufts, serrate accessory hairs or scopulae (Forster 1970 reported scopulae in *Desis*, but they have only a dense cover of plumose setae). The chelicerae have teeth and a large basal boss, epiandrous spigots are lacking, and the spinnerets have ridged or smooth cuticle, tartipores, and when present, strobilate PC spigot shafts. The respiratory systems have highly branched median and lateral tracheae (Forster 1970: *Matachia* and *Badumna longinqua*; Gray 1983: *Phryganoporus* [as *Badumna candida*]). The male palpus has a MA and a typical C that arises laterally on the bulb near the embolic base and cradles the embo-

lus in a groove that extends to the embolic apex and embraces half to all of the embolus (Figs. 178A, 189D), totally hiding the embolus in *Desis* (Fig. 190). The female genitalia are entelegyne and the epigynum has teeth.

The fine structure of the cribellate silk has been studied by Eberhard and Pereira (1993) for *Paramatachia* and *Phryganoporus* (as *Badumna candida*) and by Carlson (*in lit.*) for *Badumna longinqua*. We use Eberhard and Pereira's data from *Paramatachia* to code *Matachia* in our matrix. The *Paramatachia* cribellate band is puffed and the fine structure lacks both axial lines and reserve warp whereas the band of *Badumna* lacks puffs but has both reserve warp and axial fibers (Fig. 122D). We have observed *Badumna longinqua* in the field and lab. This species builds webs (Fig. 205C) with sheets of cribellate silk radiating out from a central, funnel-like retreat. The spider walks on these sheets, braces the cribellate silk carding leg with a mobile leg IV (Fig. Fig. 205B), and has not been observed to wrap prey. *Matachia* builds and walks on a similar web (Figs. 205D–G), but other details of its behavior are unknown. *Desis* is an intertidal spider (Fig. 205A) that actively hunts its prey (Robson 1878; Lamoral 1968).

Badumna and *Phryganoporus* are alike in numerous details, but differ in numerous details from *Matachia* and *Desis*. *Badumna*, *Phryganoporus* and *Matachia* have one row of tarsal trichobothria, while *Desis* has two; in *Badumna* and *Phryganoporus* the tarsal trichobothria are of irregular lengths whereas in *Matachia* and *Desis* they increase in length distally; *Badumna*, *Phryganoporus* and *Matachia* have smooth trichobothrial bases (Figs. 156B–C), but those of *Desis* have transverse ridges (Fig. 151G); *Desis* has reduced leg spination, elongated trochanters, and characteristically pointed maxillae (Forster 1970: fig. 35); *Matachia* and *Desis* have smooth tarsal cuticle, whereas that of *Badumna* and *Phryganoporus* is ridged (the tibial cuticle in *Desis* is squamate); *Badumna*, *Phryganoporus* and *Desis* have unnotched trochanters whereas those of *Matachia* are notched; *Badumna* and *Phryganoporus* have a bilateral chilum whereas those of *Matachia* and *Desis* are median; *Badumna*, *Phryganoporus* and *Desis* lack preening combs on the hind metatarsi but these occur in *Matachia*; *Badumna* and *Phryganoporus* cribella are divided but that of *Matachia* is entire; *Badumna* and *Phryganoporus* PMS PC are median and have several shafts arising from a common base whereas those of *Matachia* are anterior and single; and *Badumna* and *Phryganoporus* have simple vulvae whereas *Matachia* and *Desis* vulvae have convoluted ducts.

The spinning organs of *Phryganoporus candidus* comprise a divided cribellum in the female (Fig. 84A) which is still visible as two bare plates in the male (Fig. 85A) and ALS with a wide, bare margin. The female ALS has two MAP clustered at the mesal edge of the spinning field plus a large tartipore, and a field of more than 25 piriform spigots with flat base margins (Fig. 84B). Males have the posterior MAP replaced by a nubbin (Fig. 85B). The female PMS has only two identifiable AC spigots at the anterior margin of the spinneret, an anteromedian mAP and three posterior CY. The PC arise in the middle of the spinning field: 7 to 15 shafts arise from each of two large PC spigot bases (Fig. 84C). The male PMS lacks the CY, and three posteromedian nubbins replace the PC (Fig. 85C). The female PLS (Fig. 84D) has at least one basal CY, several AC, and the apex has an MS and two PC, one of which shares a common base with the MS (Fig. 87B). The apex of the male PLS has a large and a small nubbin, the former probably representing the fused MS and PC of the female (Fig. 85D).

Badumna longinqua spinnerets (Figs. 86A–D, 87C–D, F) are like those of *Phryganoporus candidus* in most details except that the female ALS piriform spigots have their bases more rounded (Fig. 86B), the PMS has at least six AC and seven CY spigots and the numerous PC spigot shafts arise from five thick common bases (Fig. 86C). There is a huge anteromedian mAP, visible in Figure 87C but hidden in Figure 86C. The PLS has at least four CY spigots (Fig. 86D).

We have studied only the female spinnerets of *Matachia*. Unlike *Badumna* and *Phryganoporus* the cribellum is entire (Figs. 83A, 87E), but like these genera the ALS has a wide, bare margin and two MAP clustered at the mesal edge of the spinning field but the piriform spigots have rounded base margins (Fig. 83B). The PMS has a median mAP and more than 20 posterior spigots with long, cylindrical bases and short conical shafts (Fig. 83C). As these are all similar to one another we cannot distinguish AC from CY and so code these all as AC spigots. Numerous PC spigots, each with a shaft arising from a single base, are bunched at the anterior margin of the spinneret (Fig. 83C). As on the PMS, the PLS has numerous spigots with long, cylindrical bases and slender conical shafts (Fig. 83D); again, these are all coded as AC. The PLS apex has an MS and an single PC (Fig. 87A).

We present scans of male and female spinning organs of *Desis formidabilis* (Figs. 79–81). The colulus is broad and covered by setae (Figs. 79A, 80A). The ALS is densely covered by setae, which must be removed to expose the spigots. On the prolateral external side of the terminal article there is a field of short, curved setae with bare smooth tips (Fig. 79B). There is one MAP spigot with one tartipore and no nubbin; the placement of the MAP is unusual, on the anterior margin (Figs. 79B, 80B). There are many PI spigots with long, smooth shafts (Fig. 79B). At the side of the MAP there is a subtle mound that could be a vestige of a nubbin of a posterior MAP (Figs. 81C–D). The PMS are very large, and together with the PLS, have a dense cover of small AC spigots, as occur in other intertidal spiders that build dense, waterproof silken retreats (for example, the cybaeid *Argyroneta aquatica* and the anyphaenid *Amaurobioides*; Ramírez 2003:53). There is one mAP spigot with a short base, without traces of nubbin or tartipore (Figs. 79C, 80C, 81E), and the female also has three posterior CY spigots. The PLS (Figs. 79D, 81F) has one median spigot similar to the mAP, that we identify as a MS, and the female also has two CY spigots on its prolateral mesal margin (Figs. 79D, 81F).

The male pedipalpal tibiae vary among desids. *Matachia* and *Desis* have a bifid RTA, formed by a wide more ventral blade and a dorsal spine (Fig. 177E; Forster 1970: fig. 52), *Phryganoporus* has a simple process (Fig. 189D), and *Badumna* has several processes (Figs. 178B–C). *Phryganoporus* also has a basal DTA (Fig. 189D). Our desid representatives have the characteristic “desid-amphinectid” C and a MA. The latter is concave in *Badumna* and *Phryganoporus* (Figs. 178A, 189D) and *Desis* (Fig. 177B–D) but hooked in *Matachia* (Forster 1970: figs. 52–54).

The copulatory bulb of *Desis* is very particular. The origin of the embolus is completely hidden among the complex foldings of the C, even in the expanded bulb (Fig. 190), suggesting that the basal part of the C became integrated with the tegulum, embracing the embolus from its origin, as occurs with the metaltellines (Amphinectidae). There is a fleshy membranous tegular sclerite (MTP) in addition to the MA and C (Figs. 177B, 190B). Davies (1998:212, fig. 7) illustrated the expanded bulb, but missed the long loop of the sperm reservoir before the entrance to the embolus.

Dictynidae O.P.-Cambridge, 1871

Dictynidae is a large, worldwide family of 48 genera and 555 described species (Platnick 2004). It is relatively poor in species in Australia and South America. The family is heterogeneous, containing cribellate and ecribellate forms, and the placement in this family of most of the ecribellates is uncertain. We include exemplars from each of the subfamilies that include cribellate species: Cicuriniinae (*Lathys*), Dictyninae (*Dictyna* and *Nigma*, and some silk data from *Mallos*), and Tricholathysinae (*Tricholathys*), which we refer to as “typical dictynids.” We also include the enigmatic genus *Aebutina*, currently placed in Dictynidae. *Aebutina* differs from typical dictynids in so many ways that we discuss it separately at the end of the family treatment.

Typical dictynids make webs with a central, funnel-like retreat and multiple cribellate sheets in different planes on which they walk (Fig. 200B). In *Dictyna* the cribellate silk carding leg is braced with a mobile leg IV, and we have never observed them to wrap captured prey. The fine structure of the cribellate silk of *Dictyna* was studied by Eberhard and Pereira (1993) and that of *Mallos* by Carlson (*in lit.*). We add the *Mallos* observations to our matrix to code *Nigma*. The cylindrical cribellar fibrils have nodules. The cribellate band is puffed (Fig. 120E) and axial fibers are absent (Fig. 120F) but the reserve warp may be absent (*Dictyna*) or present (*Mallos*: Fig. 120F).

Common characteristics of our typical dictynid exemplars are the distinctive respiratory system and male palpal bulb. The dictynid tracheal system comprises thick median tracheal trunks that extend into the cephalothorax and have many fine lateral branches; lateral tracheae are absent (Lamy 1902; Forster 1970; Griswold and Ramírez, pers. obs.). The male palpal bulb lacks a median apophysis and has a characteristic sclerotized conductor that arises laterally on the bulb near the embolic base and cradles the embolus in a groove. The conductor extends distad but the apex turns back proximad, in most species extending past the base of the bulb (Figs. 175A–B, D) to the tibia. The conductor apex of *Tricholathys* forms a spiral (Figs. 175C–D) and that of *Lathys* fits through a notch behind the RTA (Fig. 176C). Our dictynid exemplars are also alike in having canoe-shaped tapeta, capsulate tarsal organs (Figs. 152K, 153A–B), smooth trichobothrial bases (Figs. 155B–E), no palpal trichobothria or cymbial chemosensory scopulae (Fig. 175C), few spines on the legs, a linear calamistrum (Figs. 145D–E), only plumose hairs, and three claws but no serrate accessory setae, claw tufts, preening combs or scopulae (Fig. 136F). The chelicerae have teeth (Figs. 131C, E), thickened setae near the fang base and a basal boss (Figs. 129C–D). The chilum is absent or impossible to discern in the specimens that we examined. Male epiandrous spigots are absent (Fig. 160C), the cribellum is entire (though at least some *Mallos* have divided cribella) with strobilate cribellar spigots (Figs. 59A, 66D–E) and ridged spigot cuticle (Figs. 63C, 65C). The female ALS has only one MAP spigot accompanied by a large tartipore and nubbin (Fig. 59B), which is very small in *Lathys* (Fig. 63B). All spinning fields are interspersed with tartipores. Female genitalia are entelegyne and the epigyna lack teeth.

Below we describe individually the peculiarities of our “typical dictynid” exemplars *Dictyna*, *Nigma*, *Lathys* and *Tricholathys*, including spinning organs and male genitalia.

Dictyna has two nearly straight rows of eyes (Fig. 200A), strongly bowed male chelicerae (Fig. 129D) and legs lacking tarsal trichobothria and having only a single distal metatarsal. We scanned both female (Fig. 59A) and male (Fig. 60A) spinnerets. The female ALS has a single MAP at the mesal edge of the spinning field flanked posteriorly by a nubbin and mesally by a tartipore (Fig. 59B) and a field of eighteen piriform spigots with flat base margins. The male ALS is similar, with several large tartipores in the piriform field (Fig. 60B), more conspicuous in the male. The female PMS has only three or four AC spigots, an anteromedian mAP and a posterior CY. The CY shape is unusual: the base is short and concave and the shaft long and nearly cylindrical. The PC encircle the spinnerets anteriorly and laterally, and the PC spigot bases may give rise to one to many shafts (Fig. 59C). The male PMS lacks the CY, has the median mAP and several AC, and the PC spigots are replaced by an encircling series of nubbins (Fig. 60C). The female PLS (Fig. 59D) has two median CY, again with short, concave bases, several AC, and an MS and PC at the apex (Fig. 66C). The male PLS has only AC spigots, several tartipores, and apical nubbins representing the MS and PC of the female (Fig. 60D).

Like *Dictyna*, *Nigma* has two nearly straight rows of eyes and strongly bowed male chelicerae and the legs lack tarsal trichobothria and have only a single distal metatarsal. We scanned both female (Fig. 61A) and male (Fig. 62A) spinnerets. Like *Dictyna* the female ALS has a single MAP at the mesal edge of the spinning field flanked posteriorly by a nubbin and a tartipore (Figs. 61B).

There are only nine piriform spigots with flat base margins. The male ALS is similar (Fig. 62B). The female PMS (Fig. 61C) has three AC spigots, but the mAP is posterior. Posteromesad of the mAP is a spigot slightly larger than the AC. There is no spigot in the corresponding position in the male, therefore we code the female spigot as a CY. The PC encircle the spinnerets anteriorly and laterally, and the PC spigot bases may give rise to one to many shafts (Fig. 66B). The male PMS has the posterior mAP and three AC, and the PC spigots are replaced by an encircling series of nubbins (Fig. 62C). The female PLS (Fig. 61D) has a single basomedian CY, several AC, and the apex has an MS and PC (Fig. 61D). The CY morphology is normal for entelegynes and contrasts with that of *Dictyna*: the CY base is long and tapers slightly, as does the shaft. The male PLS has only AC spigots and apical nubbins representing the MS and PC of the female (Fig. 62D).

Lathys humilis has two nearly straight rows of eyes, whereas *L. delicatula* has only six eyes (the AME are absent). *Lathys* has normal male chelicerae (Fig. 129C) and rows of several trichobothria on the tarsus (Fig. 147E) and one or two on the metatarsus. We scanned both female (Fig. 63A) and male (Fig. 64A) spinnerets. Like other dictynids the female ALS has a single MAP at the mesal edge of the spinning field and a tartipore, but the posterior MAP nubbin is very small (Fig. 63B). The eight piriform spigots have rounded base margins. The male ALS is similar (Fig. 64B). The female PMS (Fig. 63C) has three AC spigots, a posteromedian mAP, and two posterior CY. The four PC encircle the spinnerets anteriorly, and the PC spigot bases give rise to only one shaft each (Fig. 63C). The male PMS retains the posterior mAP and has three AC, and the PC spigots are replaced by an encircling series of four nubbins (Fig. 64C). The female PLS (Fig. 63D) has a mesal CY, five AC, and the apex has an MS but lacks a PC. The CY base and shaft are long and tapering. The male PLS has only four AC spigots and an apical nubbin representing the MS of the female (Fig. 64D).

Like *Lathys* but unlike *Dictyna* and *Nigma*, *Tricholathys* has normal male chelicerae and rows of trichobothria on the tarsus and metatarsus. There are two nearly straight rows of eyes. The tarsal trichobothria increase in length distally. We present a complete description of the female spinnerets (Fig. 65A). Like other dictynids the ALS has a single MAP at the mesal edge of the spinning field, a large MAP nubbin posteriad of this and a mesal tartipore (Fig. 65B). The eight piriform spigots have rounded base margins. The PMS (Figs. 65C, 66F) has six or seven AC spigots, a median mAP, and three posterior CY. A single, large central PC base gives rise to several strobilate shafts (Fig. 66A), and is replaced by a large nubbin in the male (Fig. 66G). The PLS (Fig. 65D) has only AC and a lateral CY: we are unable to discern MS or PC.

Typical dictynid male palps exhibit a characteristic C and lack a MA (Figs. 175A–D), but the tibia is variable. All except *Nigma* have an RTA, i.e., *Tricholathys* (Fig. 175C), *Lathys* (Fig. 176C), and *Dictyna* (Figs. 176D–E). *Nigma* has a blade-shaped, apical DTA and a patellar process as well (Fig. 176A), whereas *Dictyna* has a basal DTA surmounted by two short spines (Figs. 176B, D–E).

Aebutina, a monotypic genus known from Ecuador and Brazil, is currently placed in the Dictynidae (Platnick 2004). The placement of *Aebutina* has long been uncertain. Simon (1892) considered its external morphology intermediate between *Uloborus* and *Dictyna*, with the balance of affinity with the former. Petrunkevitch (1928) placed it in the Dictynidae, where it has remained ever since. Millot (1933a) examined the internal anatomy of *Aebutina* and found well developed, endocephalic venom glands, refuting placement in Uloboridae and supporting Dictynidae. Avilés (1993) has recently described social behavior in *A. binotata* from Ecuador. This species maintains communal nests and cooperatively captures and feeds on prey. Cribellate silk fine structure, silk carding behavior and prey wrapping are unknown. The spiders spend much of the time beneath leaves, so we code their web posture as inverted.

Our exemplars of *A. binotata* are from Ecuador. *Aebutina* has eight eyes with canoe-shaped

tapeta in two nearly straight rows. The faint chilum is median. The chelicerae have a large basal boss and teeth on the fang furrow, but lack the characteristic stout seta at the retromargin of the fang (Fig. 130E). Spines are absent from the legs, all leg setae are plumose, the calamistrum is linear and extends for nearly the whole length of the fourth metatarsus (Fig. 142E), and the leg metatarsi and tarsi have short rows of two trichobothria each. The trichobothrial base hood has transverse ridges (Fig. 150C), and the capsulate tarsal organ has a round opening. There are three claws but preening combs, serrate accessory setae, claw tufts and scopulae are absent (Fig. 142F). Male epiandrous spigots are absent (Fig. 157C). Millot (1933a) found no tracheae, but our preparations revealed four simple tracheae. The median tracheae are flat, wide, until a point where they are abruptly truncated, then extending into a thin tube. The truncate border has the ragged texture typical of muscle attachments.

We report on *Aebutina* spinning organs for the first time. We scanned both female (Figs. 56A–C, 57A) and male (Fig. 58A) spinnerets. The cribellum is divided and covered with evenly spaced strobilate spigots (Fig. 157A) and the spinneret cuticle texture is ridged. The female ALS has a narrow spinning field margin, a pair of MAP at the mesal edge of the spinning field, a large tartipore mesad of these, and a field of twenty-four piriform spigots with flat base margins and interspersed with tartipores (Fig. 57B). The male ALS is similar, but the posterior MAP is replaced by a flat-topped nubbin (Fig. 58B). The female PMS lacks PC spigots, and has a large anteromedian spigot with a short cylindrical base and long, tapering shaft, and two posterior spigots with tapering bases and cylindrical shafts (Fig. 57C). Comparison with the male PMS reveals that the large posterior spigots are missing, but the larger anteromedian one remains (Fig. 58C). We suggest that the former are CY and the latter is a mAP. The female PMS also has eight small spigots, seven with relatively long bases and short shafts and another, close to the mAP, that has a relatively long shaft. Comparison to the male reveals that the seven small spigots are present but that the one near the mAP is replaced by a flat-topped nubbin similar to that of the posterior MAP on the ALS. We suggest that this spigot is a second mAP, and that the others are AC. The domed apical segment of the female PLS has more than 15 apical AC spigots, two lateral CY, and an apical spigot with a long, cylindrical shaft that we code as an MS (Fig. 57D). Two additional spigots occur anterobasolaterally on the female PLS (arrows in Figs. 56B, 57D) well separated from the main spinning field. These spigots differ from AC, and from each other, but at least the basal one resembles the apical MS (Fig. 56C). The CY and MS are absent in the male, the latter replaced by an apical nubbin, and two other nubbins replace the basolateral spigots (Fig. 58D). Because these spigots are replaced by nubbins in the male we suggest that these are the two flanking spigots of the triad that are displaced to a basal position (see character 96).

The male pedipalpus is unique among dictynids and lacks the characteristic dictynid C (Fig. 169D). The tibia has a pointed apical RTA (Fig. 169C). The cymbium lacks trichobothria, chemosensory scopulae or processes. The bulb has a slender embolus that arises laterally, and a retroventral, bifid process. This process is flexibly attached, and because of the position, far from the embolus, and type of attachment, we code this as an MA. This in turn suggests that the C is absent. The entelegyne female genitalia have a simple vulva and an epigynum with median and lateral lobes but lacking teeth.

Eresidae C.L. Koch, 1851

Eresidae comprise 10 genera and 102 species (Platnick 2004). Their center of richness is in Africa but eresids occur across Eurasia. They are absent from the Americas except for two species of *Stegodyphus* from Brazil, and they are absent from Australia and New Zealand. All are cribel-

late except *Wajane*. Our exemplars are *Eresus cinnaberinus* and *E. sandaliatus* from Eurasia and *Stegodyphus mimosarum* from Africa.

Eresids are both solitary and social (three species of *Stegodyphus*). The solitary species make webs with a central, funnel-like retreat and an irregular cribellate mass appressed to the substrate or multiple cribellate sheets in different planes on which they walk. The social species make a large nest of silk, plant debris and chitinous remains of their insect prey, and large sheets of cribellate silk may extend out in several directions (Figs. 199A, C–D). The spiders walk upon or hang beneath these sheets: we code them as walking on the silk like the solitary species. The cribellate silk carding leg is braced with a mobile leg IV, and the margins of the cribellate band are entire. We have never observed them to wrap captured prey. The fine structure of the cribellate silk of *Stegodyphus* was studied by Kullman (1975) who recorded both axial fibers and reserve warp and noted that the cribellar fibrils are cylindrical in cross section.

Eresids have eight eyes lacking tapeta, with the posterior row strongly recurved. The anterior margin of the carapace is truncated, giving it a “square” look when viewed from above (Fig. 199B). The chelicerae may have a small boss (Fig. 129A) and small teeth near the fang furrow, but the elongate thickened seta behind the fang is absent (Figs. 131A–B, D). The paturon is extended slightly toward the fang tip, but we do not score this as homologous to the chela of filistatids and other haplogynes. We could not detect a chilum beneath the characteristic clypeal hood (Fig. 129A). The legs are stout and spines are few. Tarsal trichobothria are lacking and there is only a single, subapical trichobothrium on the metatarsus: the base has transverse ridges (Fig. 154D). There are only plumose hairs and the tarsal organ is capsulate (Fig. 152C). Eresids have a linear calamistrum and a dorsal patch of smaller calamistral setae (i.e., with lines of teeth, Figs. 144D–F). In some specimens of *Eresus* the line of larger setae is not clearly distinguishable from the dorsal patch. There are three claws but serrate accessory setae, scopulae, claw tufts and preening combs are lacking (Fig. 136B). A series of partially serrated hairs occur at the sides of the superior claws (Fig. 136A) but these differ in position from typical serrate accessory setae. Males have numerous scattered epianthous spigots (Fig. 159A). The posterior respiratory system comprises four simple tracheal tubes (Lamy 1902, Griswold, pers. obs. *Stegodyphus*). Males lack apophyses on the palpal tibia, and the cymbium lacks processes, trichobothria, or chemosensory scopulae. The male palpal bulb has only an apical, sclerotized conductor that embraces the embolus (Fig. 170D). The enigmatic ecribellate eresid *Wajane* is reported to have a tibial apophysis and MA (Lehtinen 1967). Female genitalia are entelegyne and the epigynum has median and lateral lobes but lacks teeth.

The silk glands and spinnerets have been discussed previously but their interpretation remains controversial. Kovoor and Lopez (1979) studied the silk glands of the eresids *Eresus cinnaberinus* (as *E. niger*) and *Stegodyphus dufouri*. Peters (1992b) studied the spigots of two species of *Stegodyphus* and traced the origin of the fibers that composed the cribellate strands. Eresid spinnerets have been studied with scanning electron microscopy and coded in matrices by Coddington (1990b), Platnick et al. (1991), Griswold et al. (1999) and Schütt (2002). In this paper we make several changes from codings in previous phylogenetic studies. Kovoor and Lopez (1979) identified pseudoflagelliform glands of the sort that we assume to serve the PLS MS. These spigots were overlooked in eresids by Griswold et al. (1999), but in this new study we recognize MS spigots in eresids. Kovoor and Lopez (1979) further asserted that eresids have numerous ampullate and cylindrical glands but lack aciniform glands. Previous phylogenetic studies (Griswold et al. 1999) relied upon these gland data to code eresids as having numerous MAP, mAP, and CY and lacking AC, but here we rely upon our ontogenetic data and recognize AC spigots as present. Schütt (2002) also coded eresids as having a brush of AC spigots.

We here illustrate the spinnerets of an *Eresus cinnaberinus* male from Greece (Figs. 32A–D,

33E–F) and provide data for females from Morocco (Figs. 31A–D, 33A–D), and Switzerland (Figs. 34B, E). We also illustrate the female spinnerets of *Eresus sandaliatus* from Denmark (Figs. 34A, C). We also discuss the male and female spinnerets of *Stegodyphus mimosarum* from Malawi (Figs. 34D, F, 35A–D, 36A–D) and of a female *S. mimosarum* from South Africa (Figs. 33G–J, 37A–D). In most details *Eresus* and *Stegodyphus* are alike. The spigot cuticle lacks the characteristic “fingerprint” ridges of most entelegynes. Eresids are unique in that their ampullate shafts have small papillae or imbricate protrusions (Figs. 33C, E, 34B, D, 37C). The cribellum is divided (Fig. 34A) into two parts (*Dresserus* has the cribellum transversely divided into four parts) with strobilate spigots (Fig. 34C) and paracribellar spigots are absent from both the PMS and PLS.

The female ALS of *Stegodyphus* has at least five or more MAP scattered throughout the spinning field of more than thirty PI spigots with rounded bases (Figs. 35B, 37B). A large nubbin may be present near the MAP that are clustered at the inner edge of the spinning field (Fig. 35B), and other nubbins and tartipores occur amongst the PI spigots. The MAP are conspicuously larger than the PI, and their bases are squat and larger in relation to their shafts than those of the PI. The ALS of the male is similar, though with fewer spigots of both types (Fig. 36B). The spigots on the PMS and PLS are difficult to interpret and females from Malawi and South Africa differ in details. The Malawian female (Fig. 35C) and male (Fig. 36C) each have at least one large spigot with a squat base and nearly cylindrical shaft: these resemble the MAP of the ALS, and we code these as mAP. The South African female has two mAP (Fig. 37C). The female PMS has a large tartipore and smaller spigots of two types. There are 15–25 small spigots with narrow bases and cylindrical shafts and at least two spigots of intermediate size with conical bases and shafts (Figs. 35C, 37C). The former also occur in males but the intermediate size spigots are absent (Fig. 36C). The females have more than twenty additional spigots of various sizes, whereas the male has fewer than twelve. The female PLS also has more spigots than the male. Ontogenetically this resembles a pattern in which the female has both AC and CY spigots, but the male retains only the AC. Although Kooroor and Lopez (1979) state that eresids lack the glands that serve AC spigots, but have multiple ampullate and tubuliform (cylindrical) glands, in this case we accept the ontogenetic evidence and suggest that female *Stegodyphus* have AC, mAP and CY spigots, with the latter absent in males. It is difficult to differentiate these types: the largest spigots with squat bases are probably mAP (Figs. 35C, 36C), the intermediate size with cylindrical bases may be CY, and the smallest spigots may be AC (Figs. 35C, 37C). On the anterior, basal margin of the apical segment of the male and female PLS, well separated from the rest of the spinning field, there is a triad of slender spigots, one of them larger (Figs. 37D, 33J, inset in 36A, D); of this triad, we coded the larger one as a MS, in agreement with Peters' (1992b) interpretation, who also found that these spigots produce the axial fibers in the cribellate strands. In the female from South Africa the PLS are also unusual in having some nubbins interspersed among the AC spinning field (Fig. 33I). *Eresus* female spigots (Figs. 31A–D) are like those of *Stegodyphus* except that there are eight to eleven recognizable ampullate gland spigots (Fig. 31B). The ALS appears to have more MAP with squat bases (Fig. 34B), including six to eight concentrated near the median margin and two to four more scattered through the PI spinning field (Fig. 31B). Males have fewer MAP and PI (Fig. 32B). The PMS of both females and males have at least four large mAP along the anterior and median margins (Figs. 31C, 32C, 34E). The female PMS has more than 30 small spigots of varying sizes, probably representing both CY and AC (Fig. 31C), whereas the male has only five or six small AC spigots (Fig. 32C). The AC and CY spigots of *Eresus* are not so clearly differentiated as in *Stegodyphus*. The difference in spigot number between female and male suggests that there may be several CY in the female but we have not attempted to label these. The female PLS has a field of more than 40 small spigots and a basal triad of spigots with large, squat bases (Fig. 31D); as in *Stegodyphus*, we coded the larger one as a

MS. In the male, this basal group has the two (Fig. 32D) or three (Fig. 33F) accompanying spigots vestigial or reduced to nubbins.

Filistatidae Ausserer, 1867

Filistatidae are a nearly cosmopolitan family of 16 genera and 108 species, absent only from New Zealand (Platnick 2004). All are cribellate.

Our exemplars are *Filistata insidiatrix* from Spain and Italy (Fig. 196A) and *Kukulcania* spp. from Argentina (Figs. 197A–C) and from Florida and California in the USA. Filistatids make webs of cribellate silk radiating out from a retreat and appressed to the substrate (Figs. 196A–B). The spider walks on top of the web. Filistatids have the primitive cribellate silk carding behavior using a mobile leg III to support the combing leg IV (Fig. 196E). We have observed *Kukulcania* to bite prey and then wrap it using slow alternating movements of legs IV. Cribellate silk of *Filistata* was studied by Lehmensick and Kullman (1956) and that of *Kukulcania* by Eberhard and Pereira (1993) using a transmission electron microscope (TEM). The cribellate band is highly folded (Figs. 118E, 196C). Filistatid cribellate silk is peculiar: axial fibers and reserve warp are present but the cribellar fibrils lack nodules. Eberhard and Pereira (1993) observed that the cribellar fibrils are flattened but our SEM preparations of *Kukulcania* silk do not show flattened fibrils (Fig. 118F).

Filistatids are peculiar in many ways, combining primitive and derived character states. There are eight eyes on a mound (Figs. 196D, F, 197B); the tapetum is “primitive” (Homann 1971), and sigilla are found on the sternum. Lucrecia Nieto (*in lit.*) found that the intestine of *Kukulcania hibernalis* is M-shaped, as in other primitive Araneomorphae (Marples 1968). The chelicerae (Figs. 126A–C) are fused together at the base and lack a basal boss, teeth or a stout seta at the fang base, but the paturon is prolonged to meet and form a chela with the fang tip (Fig. 126B). We could not detect a chilum. Tarsal trichobothria are lacking but there is a row of several trichobothria on the metatarsus: the base is smooth (Figs. 154A–B). There are only plumose hairs, autospasy is at the patella-tibia joint, and the tarsal organ is capsulate (Fig. 152B). There are three claws but serrate accessory setae, scopulae, claw tufts and preening combs are lacking (Fig. 136C). Filistatids have the calamistral setae in three staggered rows (Fig. 143B). The calamistral setae have multiple rows of large teeth. Males have numerous scattered epiandrous spigots. The posterior respiratory system comprises a wide spiracle leading to two stiff median tubes, and two lateral flat extensions (Lamy 1902; Ramírez and Grismado 1997; Griswold, pers. obs.); Ramírez found that the hatching instars of *Filistata* and *Kukulcania* have about three booklung lamella in place of the flat extensions. We scored both genera as having reduced posterior booklungs. Males lack apophyses on the palpal tibia, and the cymbium lacks processes, trichobothria, or chemosensory scopulae. The male palpal bulb is piriform: spindle-shaped with the subtegulum and tegulum fused (Figs. 166D, 167D), and it retains the claw flexor and claw extensor muscles M29 and M30 (Fig. 167D). The female is haplogyne and lacks an epigynum (Fig. 164E).

The spinning organs of filistatids were described in detail by Platnick et al. (1991) and we supplement those observations with new scans of *Filistata*. Filistatid cribella are divided (Figs. 3A, 5A, 14D), tartipores are absent, and the cribellate sigots are “claviform”: nearly smooth and thicker apically (Figs. 5B–C, 14E). The female ALS of *Filistata* has numerous PI spigots with rounded bases and three MAP spigots: two near the outer margin and one within the PI spinning field (Figs. 3B, 5F). The ALS has three segments and a posterior fan of large setae with teeth (Figs. 5D–E). The male ALS is similar, though there are fewer PI spigots (Fig. 4B). The PMS has a median MAP spigot with a squat base and slender shaft, at least three slender spigots with cylindrical bases and shafts that we code as AC, and three peculiar posterior spigots with cylindrical bases and flattened, transversely-ridged, “floppy” shafts, which we code as PC (Figs. 3C, E, 4C). These presumed PC

are like the PC of other neocribellate spiders in that they occur on both the PMS and PLS, and the morphology resembles the cribellar spigots of the same species: shafts of these spigots may be pointed or claviform (Fig. 14C) These differ from typical PC in being posterior on the PMS (Figs. 3C, 4C). Like some other “lower” araneomorphs (e.g., *Thaida*, *Hickmania*), some PC may occur in the male as well as the female. The female PLS has more than fifty AC spigots and two floppy PC spigots at the apex (Figs. 3D, F); the male is similar (Fig. 4D). *Kukulcania* females resemble *Filistata* in having three ALS MAP, two on the field margin and one within the PI spinning field (Fig. 6B), three AC on the PMS and many AC on the PLS, and floppy PC posteriorly on the PMS (Figs. 6A, C) and apex of the PLS (Fig. 6D).

Gradungulidae Forster, 1955

Gradungulidae comprise seven genera and 16 species (Platnick 2004). They occur only in Australia and New Zealand. All are ecribellate except *Macrogradungula moonya* from Queensland and two species of *Progradungula* from New South Wales and Victoria, Australia. At least the cribellate *Progradungula carraiensis* wraps prey after ensnaring it (Forster et al. 1987:59). The cribellate species are very rare and we cannot add to the data presented by Forster et al. (1987) and the analysis of Platnick et al. (1991). We included as exemplar the ecribellate *Gradungula sorenseni* from New Zealand.

The colulus is represented by a pilose area. All spigots are interspersed with tartipores and small orifices (asterisks in Figs. 17A, D–E). The ALS has three segments (Figs. 15B, 16B). The mesal sector of the ALS spinning field has 12–14 MAP spigots and several tartipores (Fig. 17B). Two slightly larger MAP are set apart with a nearby tartipore (Fig. 17C). The PI closer to the margins have longer bases and shafts. The PMS (Figs. 15C, 16C) has a central area with small AC spigots, more numerous in the female, and encircled by larger spigots with thicker shafts (Figs. 17D–E). Because these larger spigots are present in both sexes, we tentatively identified them as a second class of AC (marked with ‘?’ in Figs. 15C–D, 16C–D). We cannot recognize CY spigots. The PLS has a conical terminal segment, with spigots as in the PMS, and lacks an MS (Figs. 15D, 16D, 17F).

Gradungulids have characteristically modified tarsi I and II, with the raptorial proclaw much larger than the retroclaw (Forster et al. 1987: figs. 185–189). The male palp of *Gradungula* lacks an apophysis on the tibia and the bulb has a complex, divided embolus and a second small, flexibly-attached process on the bulb that Forster et al. (1987) classify as a MA. We code the MA present for *Gradungula* and code the C as absent. The female genitalia of *Gradungula* were described by Forster et al. (1987). As in the austrochilids, the epigastric fold leads to a blind fold, which has the attachment of abdominal muscles. The female genital area is protruding, with some sclerotizations, and the genital opening is exposed on the posterior face, well out of the epigastric fold. The genital opening leads to the spermathecae, and to the uterus externus. The male has numerous epiandrous spigots dispersed in a transverse line, and the genital opening is exposed, in the same way as in the female.

Huttoniidae Simon, 1893

This monotypic family is endemic to New Zealand (Platnick 2004). In addition to *Huttonia palpimanoides* O.P.-Cambridge, there appear to be several undescribed species. Long considered a member of the Stenochilidae, Huttoniidae was elevated to family status by Forster and Platnick (1984). Our exemplar is *Huttonia palpimanoides* from near Dunedin, New Zealand. We choose the Huttoniidae for this phylogenetic study because of all the families representing the “classic”

Palpimanoidea (Huttoniidae, Palpimanidae and Stenochilidae) only huttoniids retain all six spinnerets.

The eight eyes are in two nearly straight rows and have a canoe-shaped tapetum. The chelicerae lack a boss, stout setae near the fang base or true teeth, but have peg teeth. The chilum is absent. The legs are spineless, the first tarsus, metatarsus, and tibial apex have a prolateral scopula (like palpimanids and stenochilids), all hairs are plumose and the cuticle is ridged (Figs. 134A–C). Tarsal trichobothria are absent and there is only a single subapical trichobothrium on the metatarsus. The trichobothrial base hood is transversely ridged (Fig. 149I) and the capsulate tarsal organ has a round orifice (Fig. 149D). There are three claws but serrate accessory setae and claw tufts are absent. Metatarsi III have apicoventral preening combs. Forster and Platnick (1984: fig. 304) recorded a single thick median trunk and two simple, lateral tracheal tubes. Epiandrous spigots are absent from the male. The spinnerets of *Huttonia palpimanoidea* O.P.-Cambridge were described by Platnick et al. (1991: figs. 246–248, 305–310). We scanned the spinning organs of both sexes of a probably undescribed *Huttonia* species from Orongorongo, New Zealand. *Huttonia* are cribellate (Figs. 23A, 24A) and lack a colulus. The female ALS has a narrow field margin, a single MAP spigot on the mesal margin, a small adjacent nubbin and tartipore, and a field of about 10 PI spigots with short, rounded bases and interspersed with tartipores (Fig. 23B). The male ALS is similar (Fig. 24A). The posterior spinnerets have numerous long hairs that make the identification of spigots difficult. The female PMS is fused basally and has 13–15 AC spigots with long, filiform shafts, and two posterior CY spigots with long, thicker shafts (Fig. 23C). Platnick et al. (1991) identified a larger anterior spigot in the female PMS of *Huttonia palpimanoidea* as an mAP, but it is absent in both sexes of our specimens. Because they did not find a similar spigot in the male, it might be a CY spigot instead. We scored the mAP absent. The male retains only 10–12 AC (Fig. 24C). The female PLS has numerous AC spigots, and four basal CY spigots (Fig. 23D). The male retains only the AC (Fig. 24D). Both sexes have a central papillate mark on the PLS. The male palpus lacks tibial processes, and the cymbium lacks trichobothria or chemosensory scopulae. *Huttonia* has an almost piriform bulb. The embolus is a short apical spine accompanied by a small pointed process that we code as the C (Forster and Platnick 1984: figs. 350–352). The haplogyne female genitalia lack an epigynum.

Hypochilidae Marx, 1888

Hypochilidae comprise two genera: the Chinese *Ectatosticta* (one species) and the North American *Hypochilus* (ten species) (Platnick 2004).

Hypochilus makes a peculiar, “lampshade” web (Figs. 195A–B). The spider hangs beneath a central retreat surrounded by a circular curtain of cribellate silk. Shear (1969), Eberhard (1988) and Catley (1994) have studied the behavior of *Hypochilus*. Cribellate silk carding behavior is primitive: a mobile leg III supports the combing leg IV. They have never been observed to wrap prey. Cribellate silk of *Hypochilus* was studied by Eberhard and Pereira (1993) who found that axial fibers and reserve warp are present but that the cribellar fibrils lack nodules.

Hypochilids are peculiar in many ways, retaining primitive and exhibiting derived character states. There are eight eyes with “primitive” tapeta (Homann 1971); the posterior eye row is recurved (Fig. 195C). Sigilla are found on the labium and sternum, and the serrula consists of a plate bearing several rows of teeth. Internally, the venom glands are confined to the chelicerae, the coxal glands have highly convoluted ducts, diverticula of the proximal portion of the midgut (the thoracenteron) extend anteriorly into the base of the chelicerae, the pharyngeal dilators originate on an apodeme of the rostrum, the posterior midgut is M-shaped, and they retain four heart ostia, two

pairs of booklungs and the fifth abdominal endosternite, which is lost in the remaining araneomorphs. The large chelicerae (Fig. 130A) have teeth but lack a basal boss or a stout seta at the fang base. Hypochilids have distinct concavities on the inner subbasal face of the paturon into which the fang tips fit when closed (Fig. 130B). We could not detect a chilum. Tarsal trichobothria are lacking and there is only a single subdistal trichobothrium on the metatarsus: the base has a smooth proximal hood with a marginal ridge and is embedded distally (Fig. 150B). There are only plumose hairs, and the tarsal organ is exposed. There are three claws (Fig. 132A) but serrate accessory setae, scopulae, claw tufts and preening combs are lacking. Hypochilids have the calamistral setae forming two rows (Fig. 143A). Males have numerous scattered epiandrous spigots. Males lack apophyses on the palpal tibia, and the cymbium lacks trichobothria or chemosensory scopulae but has a lateral lobe that we code as a paracymbium (Fig. 166A). The male palpal bulb retains a clear separation between the subtegulum and tegulum, an apical C embraces and spirals with the embolus, and there is a lobe on the tegulum which, in keeping with Catley's (1994: fig. 4) interpretation, we code as an MA (Fig. 166B). The female is haplogyne and lacks an epigynum (Figs. 164A–B).

The spinning organs of *Hypochilus pococki* were described in detail by Platnick et al. (1991), and we supplement those findings here with our own scans of a female *H. pococki* from North Carolina. The cribellum is entire with strobilate spigots (Figs. 1A, 2A–B), tartipores and paracribellar spigots are lacking and the spigot cuticle is annulate (Figs. 1C, 2C). The ALS field margin is narrow and at least ten MAP spigots with tapering shafts are clustered at the mesal margin of the spinning field (Fig. 1B). The two anterior MAP are larger (Fig. 2C). The PMS has only AC spigots (Fig. 1C). The PLS has numerous AC spigots and at the apex are two or three (one shaft is broken in all our scans) large spigots with slender shafts (Fig. 1D). The wide-shafted spigots depicted in Platnick et al. (1991: figs. 11, 12) were broken. Though they resemble the MAP spigots on the ALS, we code these as PLS modified spigots (MS), homologous to the similar spigots in neocribellates and the pseudoflagelliform and flagelliform gland spigots of Orbiculariae. It is noteworthy that the Chinese *Ectatosticta* seems to have two MS on the PLS, but those are smaller than the AC (Fig. 2E). There are no CY spigots.

Mimetidae Simon, 1881

This worldwide family comprises twelve genera and 154 species (Platnick 2004). They are not known to build webs. So far as is known, all invade the webs of other spiders and prey on them. Our exemplar is *Mimetus hesperus* from North America.

The eight eyes are in two nearly straight rows and have a canoe-shaped tapetum (Figs. 128B–C). The chelicerae are fused at the base (Fig. 128C), lack a boss (Fig. 128A) or stout setae near the fang base but have peg teeth and a few true teeth (Figs. 128D, 130D). The cheliceral gland opens through a very low mound. The chilum is absent. There is an evident diastema (Fig. 128A, Schütt 2002), i.e., a wide space between chelicerae and endites. The legs have spines, and legs I and II have characteristic series of raptorial spines along the anterior prolateral surfaces of tibiae and metatarsi (Fig. 142C). All hairs are serrate and the cuticle squamate (Fig. 149B). Tarsal trichobothria are absent and there is only a single subapical trichobothrium on the metatarsus. The trichobothrial base hood is smooth (Fig. 149G) and the capsulate tarsal organ has a round orifice (Fig. 149B). There are three claws and serrate accessory setae but claw tufts and scopulae are absent (Fig. 142B). Forster and Platnick (1984: fig. 306) recorded four simple tracheal tubes. Male epiandrous spigots are scattered anterior of the epigastric furrow (Fig. 157E). We describe the spinnerets of a female (Fig. 25A) and male (Fig. 26A). Mimetids are ecribellate and have a triangular colulus surmounted by a few setae (Fig. 26A). The female ALS (Fig. 25B) has a broad spinning

field margin with a single MAP accompanied by a posterior nubbin at the inner mesal margin, and a tartipore mesad of these. The MAP field is separated from the PI field by a deep furrow. There are more than 40 PI spigots with very short bases and interspersed with tartipores. The male is similar (Fig. 26B). The PMS has a median row of four AC spigots, a posterior mAP with squat base and tapering shaft accompanied by a nubbin and a tartipore, and a remarkable anterior spigot with very broad base and hemispherical, grooved shaft (Fig. 25C). Comparison with the male, which lacks this spigot, suggests that this is a CY spigot. The male PMS also lacks the posterior tartipore (Fig. 26C). The female PLS has 14 AC spigots and a large anterior CY spigot of similar morphology to that on the PMS (Fig. 25D). The male retains only the AC spigots (Fig. 26D). The male palpal tibia has simple, rounded ventral processes and the cymbium lacks trichobothria or chemosensory scopulae. There is a retrolateral paracymbium and dorsal and lateral slender spinous processes as well (Figs. 169A–B). Like araneids, the palpal tarsus is rotated so that the cymbium is prolateral and the bulb retrolateral. The tegulum of *Mimetus* has several sclerotized processes including an anterior ridge with groove for the embolus, a subapical hook, two small median teeth, and two broad retrolateral flanges. We code the C, MA and TA's as present although we cannot easily specify which is which. The entelegyne female genitalia have an epigynum.

Neolanidae Forster and Wilton, 1973

This monogeneric family comprises three cribellate species of *Neolana* from New Zealand (Platnick 2004). We have chosen *Neolana dalmasi* (Figs. 204C, G) as our exemplar. *Neolana dalmasi* were observed in the Waipoua Forest of North Island, where they make characteristic webs on the trunks of huge Kauri (*Agathis australis*) and other large trees (Figs. 204A–B). These webs comprise a vertical curtain of cribellate silk placed on the outside of a concavity in the bark (Fig. 204B; Forster and Wilton 1973: fig. 951). The spiders hang head down on the inside of this curtain. We have not observed their silk carding or prey capture behavior, and the fine structure of their cribellate silk is unknown.

The eight eyes are in two nearly straight rows (Figs. 204C, G) and have a canoe-shaped tapeum. There are two rows of metatarsal and one of tarsal trichobothria (including the palpal tarsus), which have smooth to longitudinally ridged trichobothrial bases (Fig. 155G). Tarsi have three claws but no claw tufts, serrate accessory hairs or scopulae (Fig. 132B). The capsulate tarsal organ has a teardrop-shaped orifice (Fig. 153D). The chelicerae have a large boss, teeth on the fang furrow and thickened setae near the fang base. The chilum is bilateral. Forster and Wilton (1973) recorded four simple tracheal tubes. We could not discern epiandrous spigots in the male.

We describe *Neolana* spinning organs for the first time. We had only females suitable for scanning (Fig. 67A). The wide, short cribellum is divided into two fields of strobilate spigots. The ALS has a wide, bare margin surrounding the spinning field, two mesal MAP plus a tartipore, and a PI field of more than 40 spigots interspersed with tartipores (Fig. 67B). The anterior margin of the PMS (Fig. 67C) has two thick shafts each giving rise to bundles of 10–12 strobilate PC spigots. There are five AC spigots, a large mesal mAP posterad of these, and a posterior CY. The mAP spigot has a shorter, stouter base than does the CY. The conical apical segment of the PLS has an apical MS flanked by two PC spigots (Fig. 68A). There are 7–10 AC spigots interspersed by tartipores and one or two large CY spigots along the mesal margin (Fig. 67D).

The male pedipalpus has a simple apical RTA and a proximal DTA (Fig. 178E). The RTA and DTA are connected by a ridge. The bulb has a central, sclerotized knob that we score as the C and a small, probasal protuberance that we score as a MA (Fig. 178D). The epigynum has a simple median lobe and lateral lobes without teeth, and the vulva is simple.

Nicodamidae Simon, 1898

Nicodamidae comprise nine genera and 29 species from Australia, New Guinea and New Zealand (Platnick 2004). Only the two monotypic genera from New Zealand, *Forstertyna* and *Megadictyna*, are cribellate. *Megadictyna* was long classified as a dictynid, while the ecribellate Australian *Nicodamus* made up the Nicodamidae. Forster (1970) was the first to place *Megadictyna* in Nicodamidae. Harvey (1995) revised the family and provided a phylogeny. We chose *Megadictyna thilenii* from New Zealand (Figs. 203A–B) and *Nicodamus mainae* from Australia as exemplars. Our *Megadictyna thilenii* specimens were from the Nelson and Marlborough regions of northern South Island, New Zealand, and behavioral observations were made in the field and on captive individuals. These spun sheets of cribellate silk beneath concavities, and hung beneath the webs (Figs. 203C–D). The cribellate silk carding leg is braced with a mobile leg IV and prey was wrapped with legs IV after being bitten. Carlson (*in lit.*) provides data on the cribellate capture line (Figs. 122A–B). The cribellate band contains a pair of reserve warp fibers and a pair of slightly thinner axial lines. The cribellate mass is not puffed, and its fibers are cylindrical, with nodules.

Nicodamids (Figs. 203A–B) have eight eyes with a canoe-shaped tapetum arranged in two nearly straight rows. The large chelicerae lack a boss or thickened setae near the fang base but have teeth on the fang furrow. We did not observe a chilum. Leg cuticle is smooth in *Megadictyna* (Fig. 154F) but squamate in *Nicodamus* (Fig. 149J). Tarsal trichobothria are lacking and there is only a single, subapical trichobothrium on the metatarsus; trichobothrial bases have a nearly smooth hood but may be smooth (*Nicodamus*, Fig. 149J) or longitudinally ridged distally (*Megadictyna*, Fig. 154F), and the capsulate tarsal organ has a round orifice (Figs. 149E, 152G). The legs have three pectinate claws (Figs. 137A, 139A). *Megadictyna* has thick accessory claw setae with weaker serrations than in Austrochilidae and Orbiculariae, but we code them as homologous. In *Nicodamus* (Fig. 139A) the accessory setae are similar to those of *Archaea* (Figs. 134E–F) but weaker, and we code them as uncertain. Tarsus IV has a series of stout ventral setae (Figs. 140D, 141A), but claw tufts, preening combs and scopulae are lacking. Forster (1970) recorded a respiratory system comprising a pair of highly branched median tracheae and a pair of simple lateral tracheae in *Megadictyna*; the lateral tracheae are absent in *Nicodamus*. Male *Megadictyna* have numerous epianidrous spigots scattered in bunches along the epigastric furrow (Figs. 161A, C).

We describe the spinning organs of *Megadictyna* (Figs. 39, 40) and *Nicodamus* (Figs. 41, 42) in detail. In *Megadictyna* the cribellum is entire, wide and short, and set with numerous strobilate spigots (Fig. 38D). The ALS has a narrow, bare margin (Figs. 39B, 40B) and spigot cuticle is ridged (Fig. 38B). Both males and females have a pair of large MAP at the mesal margin and 90–100 PI spigots interspersed with tartipores. The anterior margin of the female PMS is encircled by more than a dozen single-shaft PC spigots (Fig. 38B); males have a series of nubbins in this position (Fig. 40C). The mAP spigot is posterior, as in Araneoidea (Fig. 39C). The female PLS has a conical apical segment with a MS and single PC spigot at the tip (Fig. 38A): males have a large and small nubbin in this position (Fig. 40D). The PMS and PLS of males and females have numerous identical spigots with long cylindrical shafts and short tips that we presume to be AC spigots. We are not able to distinguish any potential CY spigots, although the greater number of these uniform spigots in females relative to males (PMS - 90:65; PLS - 110:70) suggests that AC and CY spigots may be externally indistinguishable. We have coded the CY spigot characters as unknown in *Megadictyna*. *Nicodamus mainae* is ecribellate with a well defined, triangular colulus (Figs. 41A, 42A). The ALS has two segments, and there is a pair of mesal MAP spigots and a large tartipore, with slender shafts in the male (Figs. 41B, 42B). The PI spigots have a short base with sharp edge. The PMS has a very atypical complement of spigots, which we can only homologize tentatively

(Figs. 41C, 42C). One median spigot with a thick, cylindrical base, present in both male and female, we identified as mAP. The nubbin posterior to the male mAP in Figure 42C is not present on the opposite PMS. A lateral spigot with a long base and thick shaft, on the female PMS, we identified as CY. There is a central group of spigots with large, blunt shafts, and numerous spigots with thin shafts, encircling the PMS except in the median line. We tentatively identified those spigots as two different classes of AC. They occur in females and males. The female PLS (Fig. 41D) has a group of four CY spigots (the most anterior has two shafts on the same base) and lacks an MS. The male is similar but lacks the CY spigots (Fig. 42D); the apical nubbin is absent on the other PLS.

The male pedipalpus of both *Megadictyna* and *Nicodamus* has a characteristic large, curved, proximal DTA (Figs. 171A, C, 172A–C). The bulb of *Megadictyna* is simple with only one process in addition to the embolus. We code this as a sclerotized, central C (Figs. 171A–B). There is no MA. *Nicodamus* has a similar spiral embolus but differs in having a large, distad-projecting C and similar MA that originate near the center of the bulb (Figs. 172B, D). *Nicodamus* has the retromargins of the tegulum and subtegulum with interlocking lobes (Figs. 172A, D); such lobes are absent in *Megadictyna*. Nicodamids are entelegyne with simple vulvae and epigyna with scape-like projections.

Oecobiidae Blackwall, 1862

Oecobiidae comprises six genera and 101 species (Platnick 2004) occurring worldwide, although the wide distribution is due in part to cosmopolitan synanthropic species of *Oecobius*. Oecobiids are both cribellate and ecribellate. The ecribellate genera are restricted to Africa and Eurasia. Our exemplars are *Oecobius navus* from the USA and undetermined species of *Uroctea* from India, Namibia (Figs. 199E–F) and South Africa.

Oecobiids make silken retreats with upper and lower sheets and trip lines radiating out in all directions. Prey may be wrapped during “whirligig” behavior, i.e., with the spider running rapidly around the prey swathing it with silk from the elongate PLS, and Eberhard (1967) recorded *Oecobius* wrapping prey with alternate movements of legs IV. The fine structure of *Oecobius* cribellate silk was reported by Zimmerman (1975), who found cylindrical cribellar fibrils with nodules and a cribellate band with reserve warp (summary in Eberhard and Pereira 1993).

The cribellate *Oecobius* and ecribellate *Uroctea* share some striking features. The carapace is heart-shaped to round in dorsal view and the eight eyes are arranged in a tight group (Figs. 199E–F). The chelicerae are small, not extending vertically past the endites (Fig. 129B), and lack a basal boss, teeth on the fang furrow, and thickened setae near the fang base (Fig. 130C). The anal tubercle is enlarged, nearly as long as the elongate PLS, and set with a marginal ring of setae (Figs. 27A, 30A). The male palpal bulb has several peculiar processes that are difficult to homologize with those of other spiders (Figs. 170A, C, 187B). Oecobiid legs have only plumose hairs, trichobothria are lacking from the tarsi and there is only a single subdistal trichobothrium on the metatarsi, and the capsulate tarsal organ has a round orifice (Fig. 152D). The legs have three claws but lack claw tufts, scopulae, serrate accessory claw setae or preening combs (Figs. 136E, 140C). Apart from differences in spinning organs (see below), *Oecobius* and *Uroctea* differ in several other features. *Oecobius* has a primitive tapetum, whereas the tapetum of *Uroctea* combines features of the primitive and canoe-shaped type (Homann 1971); the trichobothrial bases of *Uroctea* are smooth (Fig. 154C), whereas those of *Oecobius* have transverse ridges on the hood; *Uroctea* males have epiandrous spigots (Fig. 159B) whereas *Oecobius* males lack them. *Uroctea* has three ALS segments, whereas *Oecobius* has two.

Kovoor (1980) made an extensive study of the silk glands of *Uroctea* and *Oecobius*, but close examination of the spinnerets and spigot morphology has not been presented before. We scanned

Oecobius females from California and Georgia and a male from Washington D.C. in the USA, and female and male *Uroctea* from Garies, South Africa.

Oecobius is cribellate and has a divided cribellum (Fig. 27A). The female ALS has a single large MAP spigot at the inner margin and a field of eight PI spigots with round bases and interspersed by tartipores (Fig. 27B); the male ALS is similar (Fig. 28B). Interestingly, Millot (1938) described two ampullates for the ALS of *Oecobius*. Kooor also refers to two pairs of ampullates, but it is not clear if she was referring to both major and minor ampullates. We find only one spigot on the ALS that has the larger size and peripheral position characteristic of MAP. The female PMS has a central series of thirteen small spigots with slender, barrel-shaped bases and narrow shafts, and single larger spigots anteriorly and posteriorly (Fig. 27C). Comparison with the male (Fig. 28C) shows that the median series and anterior large spigot remain but the large posterior spigot is absent, suggesting that the anterior spigot is a mAP and the medians AC. Although Kooor (1980) states that “tubuliform” glands seem absent in *Oecobius*, the size and ontogeny of the posterior spigot suggest that it is a CY. The female PLS has an elongate apical segment with numerous small spigots resembling the AC of the PMS and three larger spigots along the outer margins of the AC row (Fig. 27D). These larger spigots are absent from the male (Fig. 28D), and, again, we suggest that these may be CY spigots.

Uroctea differs, of course, in lacking the cribellum, but in many other characteristics as well. The female ALS has several large and small spigots (Fig. 29A), and the male ALS has a similar array of spigots, only fewer (Fig. 30B). Kooor (1980) recorded 9–18 pairs of ampullate glands and 20 pairs of piriform glands in *Uroctea*: we consider the large ALS spigots to serve MAP glands and the small to serve PI. Kooor recorded only CY and AC glands serving the PMS of *Uroctea*. Our scans of the female PMS reveal numerous small spigots with slender, conical shafts, and a few larger spigots with cylindrical shafts (Fig. 29B). The male PMS has only the smaller type of spigot (Fig. 30C), which we code as AC. The larger spigots are probably CY. The female PLS has the same spigot types as on the PMS (Figs. 29C–D). Numerous small AC spigots form a broad longitudinal band, and eight larger CY spigots occur along the outer margin of this band. Males lack the CY (Fig. 30D).

The male palpus of oecobiids lacks tibial processes and has no cymbial processes, trichobothria, or chemosensory scopulae. The palpal bulbs have a readily recognizable embolus and three additional processes that are difficult to homologize. Shear (1970) recognized a conductor, stipes and radix on the oecobiid tegulum, whereas Coddington (1990a) referred to an oecobiid embolic apophysis (OEA), probably Shear’s conductor, an oecobiid tegular apophysis (OTA) and two lobes (OTL II and II). Because there are three processes in addition to the embolus, by default we code a C, MA, and TA, but cannot determine which process is homologous to those processes in other spiders. All are listed as TA (Figs. 170A, C, 187B). The female genitalia of oecobiids are also remarkable (Baum 1972). The copulatory duct leads to an anterior large, membranous sac, from where another long, sclerotized duct runs to the posterior margin, where the fertilization ducts discharge. *Oecobius* has in addition a membranous sac at the base of the fertilization duct.

Pararchaeidae Forster and Platnick, 1984

This family comprises one genus and seven species from Australia and New Zealand (Platnick 2004). Our exemplar is a *Pararchaea* species from Fiordland on South Island, New Zealand with additional data from Forster and Platnick (1984), Platnick et al. (1991), and Schütt (2000).

There are eight eyes and the tapetum is canoe-shaped. The pars cephalica is prolonged into a short “neck” and sclerotized completely around the base of the chelicerae. The chelicerae lack a

boss, have no stout setae near the fang base nor true teeth but have peg teeth. There is an evident diastema between the chelicera and endite. The chilum could not be observed. The legs are spineless, all hairs are serrate and the cuticle is squamate. Tarsal trichobothria are absent and there is only a single subapical trichobothrium on the metatarsus. The trichobothrial base hood is smooth and the capsulate tarsal organ has a round orifice. There are three claws and serrate accessory setae but claw tufts, preening combs and scopulae are absent. Forster and Platnick (1984: fig. 307) recorded four simple tracheal tubes and two bunches of epiandrous spigots along the male epigastic furrow. Data on the spinning organs of *Pararchaea* have been gleaned from Platnick et al. (1991) and Schütt (2000). In neither paper were the spinnerets fully illustrated, so some characters, especially for the ALS, cannot be scored. *Pararchaea* are ecribellate. The spinneret cuticle is squamate and there are tartipores. The PMS has two AC spigots and a CY spigot with a long, tapering shaft (Schütt 2000, fig. 10C). The occurrence of ampullate gland spigots on the ALS and PMS and PI spigot morphology remain unknown. The male palpus lacks tibial processes, and the cymbium lacks trichobothria or chemosensory scopulae but has a paracymbium. The apex of the *Pararchaea* tegulum has a “complex distal plate” (Forster and Platnick 1984: fig. 237) with two flanges, a hook, and a broad scaly surface, which we code as a C. The entelegyne female genitalia have an epigynum.

Phyxelididae Lehtinen, 1967

Phyxelididae comprise 12 genera and 54 described species (Platnick 2004) that occur in Africa and Madagascar, the southeastern Mediterranean, and south east Asia (*Vytfutia*).

Lehtinen (1967) treated Phyxelidinae as a subfamily of the Amaurobiidae. Griswold (1990) revised this subfamily, adding *Vytfutia* from the Agelenidae. Griswold Coddington, Platnick and Forster (1999) raised Phyxelididae to family rank and suggested sister group relationship with the Titanoecidae (Fig. 212, “Titaneocoids”).

We have observed the behavior of several genera of phyxelidids, including *Xevioso* in the field and *Phyxelida* in the field and lab. All build cribellate webs. *Xevioso* (Figs. 202B, E–F) builds an appressed web radiating out from a retreat, as does *Vidole* (Fig. 202A; Griswold 1990: fig. 1a): it walks erect on the web. There may sheet-like cribellate components (Fig. 202F). *Phyxelida* builds webs with more three-dimensional structure, typically with small sheet-like components beneath which the spider hangs inverted (Figs. 202D). In phyxelidids the cribellate silk carding leg is braced with a mobile leg IV and at least *Phyxelida* and *Ambohima* wrap prey with slow alternating movements of legs IV after first biting it. Carlson (*in lit.*) has studied the fine structure of *Phyxelida tanganensis* cribellate silk. The cribellate band is entire, cribellar fibrils are cylindrical with nodules, and axial fibers and reserve warp are present (Figs. 121A–C).

Phyxelidids have eight eyes in two nearly straight rows (Figs. 202A–C), canoe-shaped tapeta, chelicerae with a large boss and teeth and thickened setae along the fang furrow (Fig. 131F). The cheliceral gland does not open on a mound (Griswold 1990: fig. 14c, d). The chilum may be entire (*Vytfutia*) or divided (*Phyxelida* and *Xevioso*). Tarsal trichobothria are lacking and there is only a single, subapical trichobothrium on the metatarsus: the base has transverse ridges (Figs. 147A, 155A). The capsulate tarsal organ has a round orifice (Fig. 152J). Most have only plumose setae (Fig. 147A), but at least *Malaika* has feathery scales as well. The palpal femora of both sexes have probasal thickened setae modified as thorns (Figs. 173D–E). Males of most species have metatarsus I modified with a posterolateral projection that may be surmounted by a spine and a distal concavity (Figs. 173F, 202C). At least in *Phyxelida tanganensis* the male grasps the female by her second trochanter with this clasping organ while they hang face to face during copulation. There are three claws but serrate accessory setae, claw tufts and scopulae are absent (Figs. 132C–D).

Preening combs on metatarsi III and IV may be present (*Xevioso*: Fig. 141G) or absent. The phyxelidid calamistrum is linear and located in the middle of metatarsus IV (Fig. 143D). Deeleman-Reinhold (1986) reports that *Vytfutia* has four simple tracheae; *Xevioso* and *Phyxelida* each have simple lateral tracheae and median tracheae with few to many branches. Males of at least *Xevioso* and *Phyxelida* have epiandrous spigots grouped into two lateral bunches (Figs. 160A–B); epiandrous spigots are absent in *Vytfutia* (Fig. 161G).

All phyxelidids have divided cribella (Fig. 47A) with fields of uniformly distributed strobilate cribellate spigots. Numerous (13–29) PC spigots encircle the anterior margin of the female PMS (Figs. 47C, 49C). The bases are elongate and pressed together and flattened, and each is surmounted by a single strobilate shaft (Figs. 46C, 47C). Spigot cuticle is ridged. Phyxelidini and Vidoliini have a characteristic, stout, curved seta laterally on the PLS (Fig. 49D), but we couldn't find this seta in *Vytfutia*. It may have broken off in our specimens. Otherwise phyxelidid spinning organs vary. Griswold (1990) briefly described phyxelidid spigots based on *Namaquarachne tropata* and *Xevioso amica*: here we elaborate on this discussion, redescribing *Xevioso* and describing *Phyxelida* and *Vytfutia* for the first time. The female ALS of *Phyxelida tangansensis* has a narrow, bare margin (Fig. 49A). There are two MAP at the inner edge and a field of more than 30 PI spigots with round base margins and interspersed with tartipores (Fig. 49B). The male ALS is similar except that the posterior MAP is replaced by a nubbin (Fig. 50B). The female PMS anterior margin is encircled by at least 16 PC, there is a large mAP and a nubbin and tartipore posteriad of these, and posteriorly 8–10 AC spigots (Fig. 49C). We identify only one posterior CY. The male PMS has the PC replaced by an encircling row of nubbins, a large median tartipore and a nubbin that replaces the mAP (Fig. 50C). The female PLS has a domed apical segment and a stout lateral seta. There is an apical MS, a field of about 15 AC and two mesal CY spigots (Fig. 49D). Males lack the CY and have the MS replaced by a large nubbin (Fig. 50D) that resembles a tartipore in being apically dimpled. *Xevioso amica* females (we have not scanned the male) resemble *P. tangansensis* in most details except that the PMS has a single large nubbin and at least four CY spigots and the PLS has a single PC spigot and a slender nubbin ("cuticular finger") next to the MS spigot (Griswold 1990: figs. 30a–f). Most of the PLS spinning field of our specimen is infolded and obscured: only one CY spigot is visible, but there may be others. The PLS is similar to *Namaquarachne*, which has an apical MS, slender nubbin, and two CY (Fig. 46B). *Vytfutia pallens* differs from these in several details. Both females (Fig. 47B) and males (Fig. 48B) have only a single anterior MAP and posterior nubbin on the ALS. The PMS of both sexes have a large median mAP but lack nubbins: the female has four CY spigots, three of which are visible in Figure 47C. The PLS appears to lack the stout lateral setae characteristic of other phyxelidids (they may be broken off in our specimens), and the female has an apical MS, one PC, and at least two CY (Fig. 47D). There is a spigot adjacent to the MS that differs from all others. Unlike the AC it has a slender, cylindrical shaft without longitudinal striations. Although it lacks the encircling ridges characteristic of PC, we code it as a PC (Fig. 47D: PC). It, as well as the MS spigot, is replaced by nubbins on the male PLS (Fig. 48D): this is typical of MS and PC ontogeny.

The male palpal tibia of all phyxelidids has a dorsoapical process that may be simple and sclerotized (e.g., *Namaquarachne*, *Vytfutia*), partly sclerotized and partly hyaline (*Xevioso* and *Vidole*) or bifid with the larger part rolled (*Ambohima*, *Phyxelida*) (Figs. 173A–B). *Vytfutia* has an additional RTA. The cymbium lacks trichobothria or chemosensory scopulae (Fig. 173A). Male palpal bulbs are diverse (Figs. 170B, 173C, 188C–D). All have at least two processes: C and MA. Conductors are fleshy to sclerotized and may oppose (*Vytfutia*, *Xevioso*) or embrace (*Phyxelida*) the embolus. *Xevioso* C may be hyaline at the outer edge (Fig. 170B). Both *Phyxelida* (Figs. 173C, 188C–D) and *Vytfutia* have flexibly attached, cylindrical MA whereas *Xevioso* (Fig. 170B) has

three to five conical processes including an MA and extra tegular processes (e.g. TA1, TA2, TA3, TA3a and TA4: Griswold 1990). We label these all as TA, but assume that one is the MA homologue. Epigyna are simple with median and lateral lobes without teeth (Fig. 170E).

Psechridae Simon, 1890

Psechridae comprise two genera and 24 species (Platnick 2004). *Psechrus* and *Fecenia* occur from southeast Asia to northern Australia. The New Zealand endemics *Haurokoa* and *Poaka*, although lacking the psechrid peculiarities of three claws plus claw tufts, grate-shaped tapeta and an elongate, “rectangular” calamistrum, were placed in this family by Forster and Wilton (1973). Recently Raven and Stumkat (2003) moved *Poaka* to the Amaurobiidae and *Haurokoa* to the Tengellidae. We discuss *Poaka* morphology under the Psechridae below and note that its placement in the Amaurobiidae, Psechridae, or elsewhere is still problematic. Our exemplars are *Psechrus* species from China (Fig. 208A–B, D–E), India, Nepal, Papua New Guinea and Thailand, and *Poaka graminicola* from New Zealand. All are cribellate. Because of their numerous differences we discuss these genera separately.

We have observed *Psechrus* in the field in Yunnan, China. There they build huge (0.5 to 1m across) webs comprising a cribellate sheet (Fig. 208E). At one edge is a circular retreat that leads to a cave, rock crevice, or other cavity (Fig. 208A). The spider hangs beneath the web (Fig. 208B) and the cribellate silk carding leg is braced with a mobile leg IV (Fig. 208D). We never saw them wrap pray. The fine structure of *Psechrus* cribellate silk has not been studied.

The eight eyes are in two nearly straight rows (Fig. 208B) and have a grate-shaped tapetum, the chelicerae have a large boss, teeth on the fang furrow and thickened setae near the fang base, and the chilum is bilateral. The legs have three claws, and remarkably, claw tufts (Figs. 132E–F, 139C), but no serrate accessory setae or preening combs and no scopulae on the posterior legs of females. The legs have only plumose hairs and there are two rows of metatarsal and one of tarsal trichobothria on the legs, but none on the palpal tarsus. The trichobothrial bases have transverse ridges on the hood and the capsulate tarsal organ has a round orifice (Fig. 149L; Griswold 1993: fig. 65). The calamistrum comprises several irregular rows of calamistral setae and is a modified form of the “oval calamistrum” typical of the Lycosoidea and their kin (Figs. 143H, 145F). The posterior respiratory system comprises four simple tracheal tubes (Lamy 1902:168). The male lacks epiandrous spigots.

We scanned female (Fig. 109A) and male (Fig. 110A) spinnerets. The cribellum is divided and evenly covered with strobilate cribellar spigots (Figs. 97B, E). Paracribellar spigots are absent from both the PMS and PLS. The female ALS has numerous piriform spigots with round bases; at the mesal margin are two large MAP spigots and a tartipore (Fig. 109B). The male ALS is similar except that the posterior MAP is replaced by a nubbin (Fig. 110B). The female PMS (Figs. 109C, 111A) has an anterior large spigot with a squat base, which we interpret as an mAP, and a smaller spigot with a nearby tartipore, which we tentatively identify as a mAP as well because this spigot is replaced by a nubbin in the male (Figs. 110C, 112A–B). Posterior to this group is a field of more than twenty small spigots with slender bases and shafts and at least six larger spigots each with a long, cylindrical base and conical shaft (Figs. 109C, 111A–B, 112A). Both types of spigots also occur on the female PLS, but only the small type occurs on the male PMS and PLS (Figs. 110C–D). We interpret the smaller spigots as AC, and the larger as CY. The female PLS has a broad band of more than twenty AC and about 11 CY spigots in a band along the outer margin of the AC spigot field (Fig. 109D). At the PLS apex the female has a presumed MS spigot (Fig. 111D), flanked by two small nubbins in males (Fig. 112C): the MS occurs in a male from Papua New Guinea (Figs.

110D, 112D) but is replaced by a nubbin in a male from Thailand (Fig. 56D).

The male genitalia of *Psechrus* are in many ways both typical and atypical for Lycosoidea. There is no apophysis on the palpal tibia, but the cymbium has a well developed dorsal chemosensory scopula (Fig. 167A). The tegulum and subtegulum have interlocking lobes, but the C is fleshy rather than hyaline and there is no MA (Figs. 167B–C). Psechrids are typical lycosoids, though: the related genus *Fecenia* has an RTA, hyaline C and a MA (Levi 1982). The entelegyne female genitalia have an epigynum that lacks lateral teeth (Figs. 164C–D).

Poaka graminicola was placed “with considerable doubt” (Forster and Wilton 1973:297) in the Psechridae. Raven and Stumkat (2003:106) moved *Poaka* to the Amaurobiidae because of its similarities to *Manjala*, an Australian spider described in the Amaurobiidae by Davies (1990). As our analysis suggests, the definition of Amaurobiidae is still unsettled, and the ultimate placement of *Poaka* remains an open question. This monotypic genus is endemic to New Zealand, where the spider is common in grasslands and lives by hunting without constructing a snare.

Poaka has eight eyes in two straight rows, and, unlike typical psechrids, the tapeta are canoe-shaped. We were unable to discern a chilum. The chelicerae have a large basal boss, teeth on the fang furrow, and the characteristic stout seta at the retromargin of the fang. The legs are spinose and sexually dimorphic: female tibiae and metatarsi I and II have several pairs of ventral spines, though there are few spines on these segments in males. All leg setae are plumose and the calamistrum is linear and extends for the basal half of the fourth metatarsus (Fig. 142D). The leg metatarsi have two irregular rows of trichobothria and the tarsi have a single row of three to five trichobothria that increase in length distally. The trichobothrial base has a smooth hood (Fig. 150D), and the capsulate tarsal organ has a round (Fig. 150D) to keyhole-shaped (Fig. 150E) opening. There are three claws but unlike typical psechrids claw tufts are absent (Fig. 142A). Preening combs, serrate accessory setae, and scopulae are also absent. The male lacks epiandrous spigots (Fig. 157F). The tracheal system comprises four simple tubes.

We report on *Poaka* spinning organs for the first time. We scanned both female and male spinnerets (Figs. 107A–D, 108A–D). The cribellum is divided (Fig. 157B) and covered with evenly spaced strobilate spigots and the spinneret cuticle texture is ridged (Fig. 157D). The female ALS has a narrow spinning field margin and a single MAP flanked by a posterior nubbin at the median edge (Fig. 107B). There are about fifteen PI gland spigots with rounded base margins. The male ALS is similar, with the PI field interspersed with tartipores (Fig. 108B). The female PMS has a large anterior spigot with squat base and tapering shaft that we code as mAP (Fig. 107C). The central part of the PMS spinning field has several AC spigots and several PC spigots with a single strobilate shaft emerging from each base. The PC extend from the anterior margin to the middle of the spinning field. We code as CY two large spigots at the posterior margin of the spinneret with shafts much stouter than the mAP. The male PMS retains only the anterior mAP and four AC spigots (Fig. 108C). Surprisingly, there are no nubbins representing vestiges of the PC of the female. The domed apical segment of the PLS of our female is slightly collapsed making spigot interpretation difficult (Fig. 107D). There are several AC spigots but we cannot confirm the presence or absence of CY or PC spigots. One apical spigot has a shaft much stouter than the others: we provisionally code this as an MS. The male retains only several AC and has several nubbins (Fig. 108D).

The male palpal tibia has four retrolateral processes: an apical blade, two posteromedian teeth and a median stout cone (Fig. 184F). We code this as a “complex RTA.” The cymbium lacks processes or chemosensory scopulae but has at least one trichobothrium. The complex palpal bulb has a tegulum with a prolateral straight, slender embolus. The base of the embolus extends forward in a sclerotized projection that parallels the embolus and embraces its apex (arrows in Figs. 184 C–E). There are two flexibly-attached tegular apophyses, one arising near the embolic base that we

code as the C, and the other near the retroapex of the bulb that we code as a MA (Figs. 184A–C, E). The entelegyne female genitalia have a simple vulva and an epigynum with median and lateral lobes that lack teeth.

Segestriidae Simon, 1893

Segestriidae comprise three genera and 106 species (Platnick 2004). The genera *Ariadna* and *Segestria* are cosmopolitan, and *Gippsicola*, known from only one species, is known only from Australia. Segestriids occupy tubular cavities, which they line with silk. The web comprises silken “trip lines” that radiate out from the retreat (Fig. 202G). They are members of Dysderoidea, a homogeneous group of haplogyne families including dysderids, oonopids, and orsolobids (Forster and Platnick 1985). Dysderoids have a peculiar tracheal system (described, among others, by Lamy 1902, Purcell 1910, and Forster and Platnick 1985). The lateral tracheae are advanced just behind the epigastric furrow, bearing two separate spiracles similar to the booklung spiracles (Fig. 162A). Each spiracle leads to a broad, anteriorly directed tracheal trunk that splits in many thin tracheoles, serving both the abdomen and the carapace (Fig. 162B–F). The internal female genitalia of dysderoids are also distinctive (described, among others, by De la Serna de Esteban 1976, Uhl 2000, and Burger et al. 2003). The posterior wall of the atrial cavity connects to a large posterior receptacle (Fig. 162B), while the anterior part leads to an anterior, often bilobate receptacle.

Our representatives are *Ariadna boesenbergi* from Argentina and *Ariadna maxima* from Chile. There are six eyes with primitive tapeta, the anterior medians having been lost. The carapace is elongate, and the thoracic fovea is absent. There are no sternal or labial sigillae. The chelicera has three teeth on its anterior margin, and a small apical retromarginal tooth (Fig. 130F). The cheliceral lamella found in other haplogyenes is absent. A cheliceral boss is absent, but in its place there is a transversely elevated ridge.

The third leg is characteristically oriented forwards, an apparent adaptation to the tubular silk retreat (Fig. 202G). The tarsal organ is exposed (Fig. 151B; Forster and Platnick 1985: fig. 862). Tarsal trichobothria are lacking (Fig. 138B) and there is only a single subdistal trichobothrium on the metatarsus. The trichobothrial bases have a transverse ridge (Fig. 151A). The tarsal cuticle is smooth. There are three tarsal claws (Fig. 138A) and no accessory claws, claw tufts, or scopulae. The setae are of the plumose type and there are no scales of any kind, including feathery scales. There is a preening comb on the retrolateral apical margin of metatarsus IV. The male metatarsus I is cylindrical, although other *Ariadna* species bear clasping processes. Male epiandrous spigots are absent.

We have scanned the spinnerets of male and female *Ariadna boesenbergi* (Figs. 18, 19). Our observations concur with those compiled in Platnick et al. (1991) for *Ariadna* and the other two segestriid genera. The spinnerets are not sexually dimorphic. The colulus is well defined and pilose. The ALS has three segments, with the basal segment crossed by a diagonal membranous area, giving the impression of a four-segmented spinneret (Figs. 18A, 19B). There is only one MAP spigot without accompanying nubbins or tartipores, and about 11–12 PI (Figs. 18C, 19B). The PMS have one mAP and one AC (Figs. 18E, 19C), and the PLS have 4 AC (Figs. 18F, 19D). The ALS PI and the PLS AC have elongated, curved shafts and flattened bases. We have not found tartipores, except for a scar corresponding to one of the male PLS AC; because this scar occurred on only one side, we scored tartipores absent, which concurs with previous findings (Platnick et al. 1991).

The male palp has a simple, cylindrical tibia without processes, and a very short tarsus, where the piriform copulatory bulb arises. There is no hematodocha other than the articulation of the bulb with the tarsus, and no bulb sclerites or processes other than the simple embolus.

Stiphidiidae Dalmas, 1917

Stiphidiidae comprise 13 genera and 94 species occurring primarily in Australia and New Zealand (Platnick 2004). Records of *Ischalea* from Madagascar and Mauritius are dubious until modern material is available for study. Stiphidiids are both cribellate and ecribellate.

As exemplars we chose *Stiphidion facetum*, which we observed in New Zealand and Australia, and *Pillara griswoldi* (recently described by Gray & Smith 2004), observed in the Barrington Tops area of New South Wales, Australia. *Pillara* was identified as “*Baiami*” in Griswold et al (1999). *Stiphidion* makes a characteristic web, dubbed the “sombbrero web,” which has a central conical retreat encircled by a loosely-hanging curtain of cribellate silk (Figs. 204D–F). The spider hangs beneath the web. *Pillara* makes a flat sheet of cribellate silk beneath which the spider hangs: there is a retreat at one corner of the web. Cribellate silk carding has not been observed in either genus, and we never observed *Stiphidion* to wrap prey that it had caught. The fine structure of *Stiphidion* cribellate silk was studied by Eberhard and Pereira (1993), who found the cribellate mass entire, cribellar fibrils cylindrical with nodules, and axial fibers and reserve warp in the cribellate silk.

Our stiphidiid exemplars have two rows of eyes with grate-shaped tapeta. Homann (1971) depicts a weakly undulate grate-shaped tapetum in *Stiphidion*; *Pillara* has the tapetum making a few broad loops (Griswold, pers. obs). We code the tapeta of each genus as grate-shaped. The PER of *Pillara* is straight, but that of *Stiphidion* is recurved. The chelicerae have teeth, thickened setae near the base of the fang furrow, and a large boss, and the chilum is median. *Pillara* has deeply notched trochanters, whereas those of *Stiphidion* are entire. Feathery scales are present on the legs in both genera (Fig. 147I). There are three claws but serrate accessory setae, preening combs, claw tufts and scopulae are lacking. Tarsal organs are capsulate (Figs. 153C) and there is a single row of tarsal trichobothria with smooth bases (Figs. 147I, 155F); the tarsal trichobothria increase in length distally. The calamistrum is linear. Male epiandrous spigots are absent. The posterior respiratory system consists of four simple tubes (Griswold pers obs., *Pillara*; Forster and Wilton 1973, *Stiphidion*).

We examined the spinning organs of both sexes of *Pillara* and *Stiphidion*. The cribellum (Figs. 69A, 71A) is divided into two fields of strobilate spigots (Fig. 72A), spinneret cuticle is ridged (Fig. 71C) and the ALS has a wide bare margin surrounding the spinning field (Figs. 69B, 71B). The female ALS of *Stiphidion* has two MAP clustered at the mesal margin: the anterior is much larger than the posterior. The PI field comprises nearly 40 spigots with rounded base margins interspersed with tartipores (Fig. 69B). The male ALS is similar except that the posterior MAP is replaced by a nubbin (Fig. 70B). There is a conspicuous tartipore near the MAP nubbin. The female PMS (Fig. 69C) has nearly thirty AC spigots, one anterior mAP, and a posterior and lateral CY. The PC comprise two huge bases on the anterior margin of the spinning field with six to eight strobilate shafts emerging from each base (Fig. 68B). The male PMS lacks the CY, and the PC are replaced by two or three large anterior nubbins (Fig. 70C). The conical apical segment of the female PLS (Fig. 69D) has two basomedian CY (only one is visible in Fig. 69D), more than 40 AC, and an apical MS flanked by three PC (Fig. 68D). The male PLS lacks the CY and the apex has the MS and PC replaced by four nubbins (Fig. 70D). *Pillara* spinnerets resemble those of *Stiphidion* (Figs. 71A–D, 72B–D). The female ALS has two MAP clustered at the mesal margin and a PI field of about 30 spigots with rounded base margins interspersed with tartipores (Fig. 71B); the male retains only the anterior MAP with the posterior replaced by a nubbin (Fig. 72B). The female PMS (Fig. 71C) has one large anterior mAP, one posterior CY and only five AC spigots. Two huge PC bases on the anterior margin of the spinneret give rise to 15 and 7 strobilate spigot shafts. The lateral PC base has a single PC base and shaft emerging from its side. The male retains the mAP and

seven AC and the PC are replaced by two anterior nubbins (Fig. 72C). The female PLS (Fig. 71D) has a basal and a median CY, about 15 AC, and an apical MS flanked by three PC (Fig. 68C). The MS and PC are replaced by nubbins in the male (Fig. 72D).

Male pedipalpal tibiae (Figs. 179F, 189A) have a VTA and an RTA that may be simple (*Stiphidion*) or complex (*Pillara*). The cymbium lacks chemosensory scopula but has trichobothria. The palpal bulb lacks a MA: in our analysis this optimizes as a synapomorphy for Stiphidiidae, but this may be artifactual, as at least some ecribellate stiphidiid genera (e.g., *Cambridgea*, *Ischalea*) may have MA (Forster and Wilton 1973). The C is sclerotized and embraces the embolus. We score this as a "desid" type C, but these are heterogeneous in stiphidiids. The C of *Stiphidion* is broadly T-shaped, with two points extending retrolaterad and embracing the embolus and the other simple one pointing prolaterad (Fig. 179E). *Pillara* has a C that embraces only the embolus tip. Female genitalia are entelegyne, the epigynum lacks lateral teeth and the vulva is simple.

Tengellidae Dahl, 1908

Tengellidae comprise eight genera and 32 described species (Platnick 2004). Most occur in the Americas. *Tengella* is the type genus. Our exemplars are *Tengella radiata* from Costa Rica (Fig. 206C, E–F) and an unidentified *Tengella* species from Mexico.

We have observed *Tengella radiata* in the field in Costa Rica and in the lab. They make a large sheet of cribellate silk with a funnel-shaped retreat at one side, and run on top of the sheet (Figs. 206C, E). The cribellate silk carding leg is braced with a mobile leg IV. We never saw them wrap prey. The fine structure of *Tengella* cribellate silk was studied by Eberhard and Pereira (1993) who found that the uniform cribellate silk band has both axial fibers and reserve warp, and that the cylindrical cribellar fibrils have nodules.

Tengella has eight eyes in two rows (Fig. 206F), a canoe-shaped tapetum, chelicerae with a large boss and teeth and thickened setae near the fang furrow. The chilum is bilateral. There are multiple rows of trichobothria on the tarsi; trichobothrial bases have transverse ridges (Fig. 149K). The tarsal organ is capsulate with a round orifice (Fig. 149F; Griswold 1993: fig. 64). There are three claws and scopulae but claw tufts are lacking (Fig. 139B). The calamistrum is oval and females have dense scopulae beneath the posterior tarsi. There are four simple tracheae.

We report on the spinning organs of a male and two female *Tengella radiata* from Costa Rica (Figs. 98A, 99A). The cribellum has a divided spinning field with strobilate spigots uniformly distributed. The ALS has a narrow, bare margin. The female has two MAP (Figs. 100C) at the mesal margin with a nearby tartipore, and a field of numerous PI spigots interspersed with tartipores (Figs. 98B). The male is similar except that the posterior MAP is replaced by a nubbin (Fig. 99B). The female PMS lacks PC spigots, has two mAP with squat bases and long, conical shafts, the external one accompanied by a tartipore, and two posterior CY spigots interspersed with about 40 AC spigots (Fig. 98C). The male is similar, retaining the two mAP spigots but lacking the CY (Fig. 99C). The female PLS has more than 30 AC spigots and two basal and one median CY spigots (Figs. 98D, 100A–B). There is an apical MS on the anterior margin, flanked by two presumably AC spigots (Fig. 98D inset). The group is replaced by nubbins in the male (Figs. 99D, F). Both PMS and PLS have some marginal spigots slightly larger than the AC, which we tentatively identify as a different class of AC (marked with arrows on plates). The males lack epiandrous spigots.

The male palpal tibia has a simple retrolateral process. The cymbium lacks a chemosensory scopula. *Tengella* palpal bulbs are typical of primitive Lycosoidea and their kin (Griswold 1993; Wolff 1977: fig. 3). They have interlocking lobes on the tegulum and subtegulum, and two processes in addition to the embolus on the tegulum: an apical hyaline C and a median, convex, flexibly

attached MA. The epigynum has an enlarged median lobe; the lateral lobes lack teeth (Wolff 1977: fig. 5).

Titanoecidae Lehtinen, 1967

Titanoecidae comprise five genera and 46 described species (Platnick 2004). Most occur in Eurasia and the Americas though a few species occur in Africa, Madagascar, and New Guinea. All are cribellate. Our exemplars are *Goeldia* species from South America (Figs. 203F–H) and *Titanoeca* species (Fig. 203E) from the USA.

Titanoecids make cribellate webs that radiate from a retreat (Figs. 203F, G). These webs may be appressed to the substrate and may include sheet-like components. Szlep (1966) has described the web and spinning behavior of *Titanoeca albomaculata* from Israel. She states that the spider emerges from the retreat at night and “sits on the catching web.” We have observed the behavior of *Titanoeca nigrella* in captivity. They moved on top of the web and were never observed to wrap prey after biting it. Carlson (*in lit.*) has studied the fine structure of cribellate silk of *Titanoeca nigrella*. The cribellate silk has both axial fibers and reserve warp (Fig. 121D).

Titanoecids have eight eyes in two nearly straight rows (Fig. 203H), canoe-shaped tapeta, chelicerae with a large boss and teeth and thickened setae along the fang furrow. The chilum is entire. Tarsal trichobothria are lacking and there is only a single, subapical trichobothrium on the metatarsus: the base has transverse ridges (Figs. 154H, I). The capsulate tarsal organ has a round to oval orifice (Figs. 152I, L). There are three claws, but claw tufts, serrate accessory setae, preening combs and scopulae are lacking. The linear calamistrum begins near the base and extends for nearly the entire length of metatarsus IV (Fig. 143E). The posterior respiratory system comprises four simple tracheae. Males of *Titanoeca americana* have numerous epiandrous spigots scattered anteriorly of the epigastric furrow (Figs. 161B, D). We were unable to observe this region in our *Goeldia* male specimens and code their epiandrous spigots as unknown.

We illustrate titanoecid spinning organs for the first time. All titanoecids have divided cribella (Fig. 51A) with fields of uniformly distributed strobilate cribellate spigots. Paracribellar spigots are absent from the PMS but present on the PLS. The female ALS of a *Goeldia* from Chile has the bare margin narrow surrounding the spinning field at least anteriorly (Fig. 53B). There are two MAP with a nearby tartipore and a field of about 30 PI spigots with rounded bases and interspersed with tartipores. The MAP and tartipore are removed from the mesal margin of the spinneret and are partially surrounded by the PI spinning field. The male ALS is similar except that the posterior MAP is replaced by a nubbin (Fig. 54A). The female PMS (Fig. 53C) has a large anterior mAP with a squat base and a single AC mesad and two AC laterad of the mAP. Posteriorly there are two conical CY with stout, conical shafts. The male PMS has the mAP replaced by a huge dimpled nubbin, and retains only the three AC spigots (Figs. 54C–D). The female PLS has a domed apical segment with a terminal field of about nine AC and a single PC (Fig. 53D). There is a lateral CY and near the base are at least two PC spigots (Fig. 55E). There is no sign of an MS near the apical PC (Fig. 55F). Males have only the AC spigots and a large nubbin (Fig. 54B), presumably of the PC. The spinnerets of *Titanoeca* are similar but differ in several features. Like *Goeldia* the MAP are removed from the mesal margin of the spinneret and partially surrounded by the PI field (Figs. 51B, 52B, 55A) and the female PMS has a large mAP and two posterior CY (Fig. 51C) with the mAP replaced by a huge nubbin in the male (Fig. 52C). The PMS has more AC spigots than *Goeldia*: five (Fig. 52C) or six (Fig. 51C). The *Titanoeca americana* female PLS is also like that of *Goeldia* in lacking an MS and having an apical and three basal PC spigots (Fig. 51D). A peculiar, elongate nubbin appears to replace the apical PC on the male PLS (Fig. 52D) and other nubbins replace the proximal PC. *Titanoeca nigrella* is identical to *T. americana* (Figs. 52A, 55A, C). The nubbins that

replace the mAP and PC are peculiar in titanoeuids, resembling tartipores in having folds or dimples (Figs. 52C, 54C). Coddington (1990b: 70) scored *Titanoeca silvicola* as having a MS on the female PLS, but we are unable to find such a spigot in the other titanoeuid species. Because Coddington's *T. silvicola* female was damaged, we consider the presence of a MS ambiguous, and code *Titanoeca* as lacking this spigot.

The male palpal tibia of all titanoeuids has a complexly folded dorsoapical process (Figs. 174A, C, E, 188A–B). Male palpal bulbs have at least two processes in addition to the embolus. A convex process is flexibly attached to the center of the tegulum: we code this as an MA because of its similarity in form and position to the unambiguous MA of other families (Figs. 174B, 188A–B). There is a triangular process near the embolic base, which we code as a conical extra tegular process (Figs. 174D, 188B). There is no obvious C, but the embolus inserts in a unique groove along the outer margin of the tegulum (Fig. 174D, 188B). The female genitalia are entelegyne and the epigyna are simple with median and lateral lobes without teeth.

Uloboridae Thorell, 1869

Uloboridae is a worldwide family comprising 18 genera and 248 species (Platnick 2004, Grismado 2004). All are cribellate. Our exemplars are *Octonoba octonaria* from the USA, several species of *Uloborus*, and *Hyptiotes* from California.

Uloborids are the only spiders that build typical orb webs with cribellate capture lines (Figs. 201A–C, 206C), although some genera make webs reduced to a single sticky line (*Miagrammopes*, Lubin 1986). They exhibit the whole suite of behaviors that go into constructing the orb web. Uniquely, tertiary radii are doubled during orb construction (Eberhard 1982, Coddington 1986a). They hang beneath the orb, card cribellate silk with the carding leg braced by the other, mobile leg IV, and wrap their prey before biting. The fine structure of uloborid cribellate silk has been studied extensively (Friedrich and Langer 1969; Opell 1989a, b, 1995, 2001; Peters 1983, 1984, 1987). The cylindrical cribellar fibrils have nodules. The cribellate band is puffed (Figs. 119A–B) and axial fibers are present but the reserve warp is absent (R. Carlson, *in lit.*). The cribellate threads of *Hyptiotes* are typical (Fig. 120D).

Uloborids are small to medium-sized spiders. There are eight eyes that lack tapeta. The large chelicerae have teeth on the fang furrow but lack stout setae near the fang base. A basal boss may be small (*Octonoba*) or absent (*Uloborus*). The chilum is not visible. Uloborids, together with the Mesothele (Haupt 2003), are unique among spiders in lacking venom glands. The legs have feathery scales (Figs. 147H, 148B), the tarsi lack trichobothria and there is but a single subapical trichobothrium on the metatarsi, but a row of trichobothria occurs on femur IV. Trichobothrial bases are smooth (Figs. 147H, 154G) and the minute tarsal organ is capsulate (Figs. 152E–F). There are three claws with associated serrate accessory claw setae (Figs. 137D, 140A) and the hind tarsus has a series of stout setae that we code as the “deinopoid tarsal comb” (Fig. 140A). Claw tufts, scopulae and preening combs are absent. The linear calamistrum begins basally and extends for most of metatarsus IV length (Figs. 145A–C). The posterior respiratory system comprises two thick median trunks with lateral branches (Lamy 1902, Opell 1979, 1987) and simple lateral tracheae. Male epandrous spigots are scattered along the epigastric furrow.

The spinning organs of Uloboridae have been extensively studied (*Octonoba octonarius*: Coddington 1989: figs. 6–9; *Uloborus*: Kooor 1978, Peters 1983, 1984, Peters and Kooor 1980, 1989). We present some details of *Octonoba* (Figs. 44A–B) and *Uloborus* (Figs. 45A–C). The cribellum is entire (Fig. 44A) and the spigots have ridged texture. Unlike deinopids but like araneoids, the ALS of *Uloborus* has a single MAP spigot accompanied by a nubbin (Fig. 45B). Like

Deinopidae (Fig. 43B) and Austrochilidae (Fig. 11B) there is a wide, bare region between the MAP and the PI field (Fig. 45B). The PI spigots of the ALS have sharp apical margins. The PMS has an apical mAP with a squat base and short shaft, several median AC and several posterior CY (Fig. 45C). There appears to be a tartipore next to the mAP in our *Uloborus* individual illustrated (Fig. 45C) but there is a nubbin in that place in *Octonoba* (Coddington 1989), *Waitkera* (Platnick et al. 1991), and *Conifaber* (Grismado 2004). The AC and CY are similar in structure, with long cylindrical bases, sharp base margins, and short conical shafts. In another *Uloborus* that we examined both a nubbin and tartipore accompany the mAP. The CY are recognizable by their larger size and their absence in males. Bunched along the anterior margin of the PMS are more than 20 PC spigots that have closely-spaced annulations on the shafts (Fig. 45C). These have previously been classified as being of the “deinopoid” type (Griswold *et al.* 1999: character 82, state 0). The PLS of *Octonoba* has CY and AC spigots with the same morphology as in *Uloborus* and an apical MS set well apart from the spinning field (Fig. 44B).

The male palpal tibia of uloborids lacks processes, and the cymbium lacks chemosensory scopulae, trichobothria or a paracymbium. The bulb has a C and MA. The C is large, sclerotized, and flexibly attached. We code this as the “uloborid” type, similar only to that of araneids. The entelegyne female genitalia have an epigynum. Teeth are lacking, although some *Uloborus* have paired projections anterior of the epigynal median sector.

Zorocratidae Dahl, 1913

Zorocratidae comprise five genera and 21 described species from Mesoamerica, Africa, Madagascar, and Sri Lanka (Platnick 2004). Most are cribellate but at least *Campostichomma manicatum* and some *Uduba* are ecribellate. The family name was first used by Dahl (1913). The genera *Campostichomma*, *Raecius*, *Uduba*, *Zorocrates* and *Zorodictyna* were associated as a clade by Griswold (1993) in a study of lycosoid spiders and their relatives (Fig. 213), and Dahl’s family name was applied to this clade by Griswold et al. (1999, Fig. 212, “Zorocratidae”). In their analysis the zorocratid exemplars *Raecius* and *Uduba* were joined by the male tibial crack (Fig. 141F), clumped cribellar spigots (Figs. 97C–D, F), and a male palpal tibial ventroapical process (Figs. 185B, 194C). Zorocratidae are nevertheless heterogeneous (e.g., all known *Zorocrates* lack the male tibial crack and clumped cribellar spigots). Subsequent work by Silva (2003) associated *Zorocrates* and *Tengella*, apart from other zorocratids (Fig. 214). Raven and Stumkat (2005) placed zorocratids as a subfamily of Zoropsidae (Fig. 215, “Zorocratinae”).

Our exemplars are *Zorocrates* from North America (Fig. 207B), *Raecius* from Africa (Figs. 207G, H), and *Uduba* from Madagascar (Figs. 207A, C–F). We have observed *Raecius* in the field in Cameroon and Tanzania, *Uduba* in the field in Madagascar, *Zorocrates* in the field in Arizona and Mexico, and all three genera in captivity. Zorocratids may be running hunters or fossorial predators. There may be a collar (Figs. 207F, G) or funnel (Fig. 207E) of cribellate silk extending out from the retreat. Leg autospasy readily occurs at the tibial crack of *Uduba*, in contrast to *Zoropsis* (see below). *Zorocrates* lacks a tibial crack. Webs comprise irregular cribellate lines or sheets that radiate out from a burrow or retreat, although some *Uduba* make no webs and wander in search of prey. The cribellate silk carding leg is braced with a mobile leg IV; we never observed prey wrapping after the initial bite. Carlson (*in lit.*) has studied the fine structure of the cribellate silk from a juvenile *Raecius scharffi* from Tanzania. The cribellate silk has both axial fibers and reserve warp (Figs. 124D, 125C).

Zorocratids have eight eyes in two nearly straight rows (Figs. 207A–B, D, H) and canoe-shaped tapeta (Homann 1971: fig. 27B), chelicerae with a large boss and teeth and thickened setae

near the fang furrow (Fig. 130I). The chilum is bilateral. There are multiple rows of trichobothria on the tarsi (Fig. 141D); trichobothrial bases have transverse ridges (Figs. 151E, 156G). The tarsal organ is capsulate with a round (Figs. 151F, 153L) to multilobed orifice: in *Campostichomma* and some *Uduba* the orifice may make an asterisk-like or stellate pattern (Fig. 153O). There are three claws and dense scopulae that may obscure the ITC, but claw tufts are absent (Fig. 146A–C). At least *Raecius* has feathery scales (Fig. 147J), but *Zorocrates* has only cylindrical scales (Fig. 146D). The calamistrum is oval (Fig. 143C, 146E–G) and females have dense scopulae beneath the posterior tarsi (Fig. 141D); males of most species (but not in *Zorocrates*) have a tibial crack (Fig. 141F). There are four simple tracheae.

We report on the spinning organs of a female *Raecius asper* from Cameroon, a male and female of *Raecius jocquei* from Côte d'Ivoire (Figs. 105A–D, 106A–D), both sexes of two species of *Uduba* from Madagascar (Figs. 104A–D) and of two *Zorocrates* species from North America (Figs. 101A–D, 102 A–F, 103A–G). The spinning organs of *Raecius* have recently been discussed (Griswold 2002), but some of our interpretations here differ from those previously published. In all species the cribellum has linear groups of strobilate spigots (Fig. 97D); PC spigots are lacking from the PMS and PLS; three or more CY spigots occur on the PMS and PLS, and male epiandrous spigots are absent (Fig. 161H). Female *Raecius* have an entire, wide and short cribellum (Fig. 97D). The ALS has a narrow, bare margin surrounding the spinning field, two mesal MAP, a large tartipore mesad of these, and a field of more than 30 PI spigots with rounded bases and interspersed with tartipores (Fig. 105B). The male ALS is similar except that the posterior MAP is replaced by a nubbin (Fig. 106B). The PMS of *R. jocquei* has a large anterior mAP with a broad, squat base and slender shaft, several AC spigots (one anterior to the mAP and several behind) and there appears to be a second, slender mAP next to a large tartipore (Fig. 105C). There are three CY spigots. Males lack the CY spigots but retain the anterior mAP, AC and tartipore, and have a large nubbin next to the tartipore (Fig. 106C). We interpret this as a mAP nubbin, and conclude that at least *R. jocquei* has two PMS mAP (this differs from the conclusions in Griswold [2002], which considered the second mAP as a possible CY). The female PLS has a domed apical segment with more than 20 AC spigots and three large, conical CY spigots (Fig. 105D). We identify an MS spigot at the apex, and the male has an apical nubbin that may be an MS vestige (Fig. 106D). The female of *Raecius asper* resembles *R. jocquei* except that there are four CY on the PMS and five on the PLS (Griswold, 2002). The two exemplar species of *Uduba* are alike in having a divided cribellum (Figs. 97C, 104A). The ALS has two mesal MAP and large tartipore mesad of these in females, an MAP and nubbin in males, and a field of more than fifty PI with rounded bases and interspersed with tartipores (Fig. 104B). The female PMS has two large anterior mAP, a possible second small mAP near it, 8–12 AC, and 5–10 CY spigots on the posterior surface (Fig. 104C). Males retain only the mAP and a few AC spigots, and have a large nubbin that is probably the vestige of the second mAP. The female PLS has a domed apical segment with more than 20 AC spigots with long, slender shafts, and six large, conical CY spigots (Fig. 104D). A spigot with a stouter shaft closely flanked by two smaller spigots is identified as a MS spigot. Males have only the AC spigots. We present scans of the spinning organs of a female of *Zorocrates* cf. *mistus* and a male of *Zorocrates* sp. (Figs. 101–103). The cribellum is wide, bipartite, and the cribellar spigots are strobilate, uniformly distributed (Figs. 101A–B). The male has only a few vestigial cribellar spigots (Fig. 103G). The female ALS has two MAP and a tartipore (Fig. 102B), while in the male ALS the posterior MAP is replaced by a nubbin (Fig. 103B). The female PMS has two mAP spigots and a tartipore, several small AC spigots, and 4 or 5 large CY spigots on its posterior side (Fig. 102C–D). The male has only one mAP and a tartipore and the AC spigots (Fig. 103C–D). The female PLS has two large basal CY spigots, many AC spigots with interspersed setae, and one external MS spigot (Fig.

102E). There is some asymmetry in the PLS of this female: in the right PLS the MS is flanked by one vestigial shaft sharing the base with the MS, and one nubbin (Figs. 101C, 102E), while in the left side the MS has the fused shafts and accompanying spigots well developed. The male PLS has only AC and the three nubbins of the MS and its accompanying spigots (Fig. 103E–F).

The zorocratid male palpal tibia has only a retrolateral process in *Zorocrates* (Fig. 186D–E), and this plus a ventral process in *Uduba* and *Raecius* (Figs. 185B, 194B–C). In most species there is a cymbial scopula of chemosensory setae, though some species of *Raecius* and *Zorocrates* lack this. *Raecius* palpal bulbs are typical of primitive Lycosoidea and their kin (Griswold 1993). They have interlocking lobes on the T and ST (Figs. 186F, 194C), and three processes in addition to the embolus on the tegulum: an apical hyaline C, a median, flexibly attached MA, and a large sclerotized process (a TA that we code as “sclerotized tegular process” or STP) (Figs. 185A, 194C). In *Zorocrates* the embolus is articulated, and the tegular locking lobe corresponds with the embolar base (Fig. 186A, 194A); there is no subtegular locking lobe. The palpal bulb of *Uduba* is highly modified (Figs. 185C, 194B). There is no obvious vestige of interlocking lobes on the tegulum and subtegulum. The elongate embolus is flexibly attached and passes behind the bifid, deeply concave tegulum. There is a flexibly attached MA and a hyaline ridge on the retrolateral lobe of the tegulum that is probably the hyaline C. Another lobe of the tegulum is a TA. The epigynum has a median and lateral lobes. Teeth are lacking in *Uduba* and *Zorocrates* but may be present or absent in *Raecius*: the female exemplar of *Raecius congoensis* that was coded for the previous study (Griswold et al. 1999) lacked them.

Zoropsidae Bertkau, 1882

Platnick (2004) records five genera and 22 species in the Zoropsidae. Traditionally containing only *Zoropsis*, the family was enlarged by Lehtinen (1967), who proposed *Takeoa* for the East Asian *Z. nishimurai*, and by Bosselaers (2002) who proposed *Akamasia* for *Z. cyprogenia*, from Cyprus. Raven and Stumkat (2003, 2005) have recently studied zoropsid relationships in depth and greatly enlarged the family. They added the the Australasian genera *Uliodon* and *Huntia*, described four new Australasian genera (*Birrana*, *Kilyana*, *Krukt* and *Megateg*) and moved the subfamilies Zorocratinae (formerly Zorocratidae) and Griswoldiinae (formerly Miturgidae, comprising *Devendra*, *Griswoldia* and *Phanotea*) into the Zoropsidae (Fig. 215). Zorocratine exemplars are discussed above under Zorocratidae. Our zoropsid exemplar summarizes the data from two species of *Zoropsis*. *Zoropsis* is widespread in Eurasia, especially the circum-Mediterranean region. *Zoropsis spinimana* has recently been introduced into North America (Griswold and Ubick 2001). All are cribellate.

We observed captive *Zoropsis spinimana* from California and France. *Zoropsis* are running hunters that make no apparent use of silk for prey capture but spin a curtain of cribellate silk to surround a retreat where they make their eggsac (Fig. 208F). The cribellate silk carding leg is braced with a mobile leg IV. Carlson (*in lit.*) has examined the fine structure of *Zoropsis* cribellate silk. The cribellate mass is irregular and contains both axial fibers and reserve warp (Fig. 125A–B). We never observed prey wrapping. Male *Zoropsis* have a crack near the base of leg tibiae. In contrast to *Uduba* (see above), leg autospasy at the tibial crack did not occur in teathered individuals.

There are eight eyes with the posterior row strongly recurved (Fig. 208G) and the tapetum grate-shaped. The chelicerae have a large boss, teeth on the fang furrow and thickened setae near the fang base, and the chilum is bipartite. The legs are very spinose (more than 7 pairs of ventral spines on the first tibia), the capsulate tarsal organ has an oval orifice (Fig. 153N) and the trichobothrial bases have transverse ridges (Fig. 156I). Two to three dorsal rows of trichobothria

occur on the tarsi. The short, basal calamistrum is oval (Figs. 143G, 145G, H). The ITC is reduced and there are well developed claw tufts (Figs. 139D, 141E), and at least the posterior tarsi of females have scopulae. The respiratory system consists of 4 simple tracheal tubes. Males lack epiandrous spigots.

We describe the spinning organs of a female of *Zoropsis spinimana* (Fig. 113A) and a male of *Zoropsis rufipes* (Fig. 114A). The cribellum is broad and short, with strobilate spigots distributed in transversal bands across a divided spinning field (Figs. 113C–E; Silva Dávila 2003: figs. 32A–B). The ALS has a narrow, bare margin, a mesal pair of large MAP and a tartipore, and numerous (>60) PI spigots interspersed with tartipores (Fig. 113B, 114B). The bases of the PI spigots have a flat margin around the origin of the shaft. The PMS (Fig. 113F) lacks a paracribellum and has two large anterior spigots with short stout bases and tapering shafts: we identify them as mAP. The male has the shaft broken, but one of them remains and the mAP can be identified by their bases (Fig. 114C). A large tartipore occurs anterior of the mAP (Fig. 100E). Posterior of these are two or three small AC spigots with cylindrical bases and slender shafts, interspersed posteriorly with at least 10 large CY spigots with conical bases and long, conical shafts (Fig. 100F). The domed apical segment of the PLS has five to six AC and a small distal spigot that we presume to be the MS (Figs. 100D, G). Laterally and basally on the PLS are 10 large CY spigots with conical bases and long, conical shafts (Figs. 100D, 113G). The male lacks the CY, and has the MS and the two accompanying spigots reduced to nubbins (Fig. 114D).

The male pedipalpus has a simple, triangular apical RTA (Fig. 185D) and the cymbium has a dorsal chemosensory scopula (Fig. 185F). The bulb (Fig. 185E) has retrolateral locking lobes on the tegulum and subtegulum and three processes in addition to the embolus: an apical, hyaline C that opposes the tip of the embolus, a flexibly attached, concave MA, and a fleshy to membranous TA arising near the embolic base, which we code as an extra tegular process (“MTP” = membranous tegular process of Griswold 1993). The epigynum has lateral lobes without teeth and a scape-like median lobe, and the vulva is simple.

CHARACTERS

All character scorings are listed in Appendix 2. Comments for specific cells are listed in Appendix 3.

LEGS.— These characters were scored by our observations of voucher specimens. Trichobothria were scored present if observed with light microscopy but are recorded as absent from tibiae, metatarsi and tarsi only if absence was confirmed by scanning electron microscopy.

1. Femoral trichobothria: **(0)** absent; **(1)** present.

In our dataset femoral trichobothria are unique to uloborids. Although we didn’t scan the femora of all exemplars, the femoral trichobothria are typically long and conspicuous, and their presence and absence are adequately observed with light microscopy.

2. Tarsal organ: **(0)** exposed; **(1)** capsulate.

Exposed tarsal organs (state 0) have the nerve endings visible on the cuticle (Figs. 150A, 152A). The capsulate form (state 1) has the nerve endings invaginated into a pocket and accessible to the outside through a hole. This hole may be simple and round to oval (Figs. 152B–L, 153A–N) or have elaborately scalloped, stellate edges (Fig. 153O)

3. Tarsal trichobothria: **(0)** absent; **(1)** present.

Tarsal trichobothria are absent in hypochilids, austrochilids, filistatids, eresids, oecobiids, Orbiculariae, nicodamids, palpimanoids, phyxelidids and titanocoids, and are present (Fig. 147E) in most dictynids (but absent in *Dictyna* and *Nigma*), neolanids, stiphidiids, agelenids, amphinecids, desids, amaurobiids and the Lycosoidea and their kin.

4. Tarsal trichobothrial rows: **(0)** one; **(1)** two or more.

We code a single line of trichobothria as one row (Fig. 147E). An arrangement of trichobothria that is staggered or forming two or more rows (Fig. 141D) we code as two or more.

5. Metatarsal trichobothria: **(0)** one or two; **(1)** three or more.

A single, subapical to apical metatarsal trichobothrium occurs in hypochilids, austrochilids, eresids, oecobiids, Orbiculariae, palpimanoids, nicodamids, phyxelidids and titanocoids. A row of three or more occurs in filistatids, neolanids, stiphidiids, agelenids, amphinectids, desids, amaurobiids and the Lycosoidea and their kin. Most dictynids have only one or two but *Tricholathys* has a row of several trichobothria.

6. Tarsal trichobothria: **(0)** normal; **(1)** longer distally.

A row of tarsal trichobothria that increase in length distally is a classic key character (e.g.; Kaston 1972: couplet 38a, fig. 107). We code as “normal” a line or lines of trichobothria of equal or of irregular, differing lengths.

7. Palpal tarsal trichobothria: **(0)** absent; **(1)** present.

We have examined male cymbia for palpal tarsal trichobothria.

8. Trichobothrial base hood texture: **(0)** smooth; **(1)** with transverse ridges.

We code as smooth all trichobothrial hoods that are all smooth (Figs. 154A–C). We also code as smooth those with fine wrinkles or striations that don’t differ from the surrounding cuticle and that may be transverse (Figs. 135B) or longitudinal (Figs. 154G, 155F, G). We code as having transverse ridges those hoods with deep, broad transverse grooves that are larger than surrounding cuticular ridges (Figs. 147B, 149H, 154D, H, I)

9. Trichobothrial base: **(0)** simple; **(1)** notched.

A trichobothrial base is simple if it has an evenly curved, entire, distal margin (Fig. 156E). Forster et al. (1987: figs. 103–105) observed a small notch on the distal margin of the base in austrochilids.

10. Leg cuticle texture: **(0)** fingerprint; **(1)** squamate; **(2)** smooth.

We scored most of our terminals from scans of the tarsal cuticle. Most representatives have cuticular sculpturing forming a fingerprint pattern (Figs. 148A, F). *Araneus* (Fig. 149A), *Mimetus* (Fig. 149B), *Nicodamus* (Fig. 149E), and to a lesser degree *Archaea* (Fig. 149H), *Huttonia* (Fig. 149I), and *Desis* (on tibiae, Fig. 151J, but not on tarsi, Fig. 151I) all have squamate cuticle. Smooth cuticles are less common, e.g., in *Megadictyna* (Fig. 154F) and *Matachia* (Fig. 156B). A few representatives are scored polymorphic (0, 2) because they only have faint fingerprint marks (*Nigma*, *Retiro*) or differ among tarsal and tibial cuticle (*Desis*). This classification of cuticle texture was proposed by Lehtinen (1996).

11. Deep trochanteral notch: **(0)** absent; **(1)** present.

We code as notched only those trochanters that have a deep, semicircular notch (e.g., Griswold 1993: fig. 2).

12. Tarsal claws: **(0)** three; **(1)** two.

Three claws occur in most of our exemplar taxa (Figs. 132B–C, F, 133A, 137C). Loss of the ITC leaving only two claws occurs only in ctenids (Fig. 139E) and zoropsids (Fig. 141E).

13. Claw tufts: **(0)** absent; **(1)** present.

Tufts are dense groups of setae in the pretarsal region, set on a separate plate beside the claws, and obscuring the pretarsus and ITC (if present). These are absent in most of our exemplar taxa (Figs. 132B–C, 133A, 137C). Claw tufts are present in spiders with three (Figs. 132E–F, 139C) or two (Figs. 139E, 141E) claws. Extended scopulae that obscure the ITC may be confused with claw tufts, e.g., as in tengellids (Fig. 139B) and zorocratids (Fig. 141D) that have dense scopula but lack tufts.

14. Serrate accessory claw setae: (0) absent; (1) present.

Many three clawed spiders that hang beneath webs have modified setae beneath the STC and near the ITC. These setae are serrate along the lower margin, and may be flattened. They may function to grasp and release the silken line, and for this reason are sometimes called “false claws.” Such modified setae occur in austrochilids (Figs 133A–D), Orbiculariae (Figs. 135C–E, 137C–D), in the nicodamids (Figs. 137A–B, 139A) and in the “palpimanoids” *Mimetus* (Fig. 142B), *Pararchaea*, and *Archaea* (Figs. 134E–F). Serrate accessory claw setae are absent from other spiders in our dataset, including some that hang beneath webs, e.g. *Hypochilus* (Fig. 132A), *Neolana* (Fig. 132B) and *Phyxelida* (Figs. 132C–D).

15. Male palpal femoral thorns: (0) absent; (1) present.

Setae that are conspicuously thickened, or which at least have thickened bases, we refer to as “thorns.” These occur on the inner surface of the male palpal femur of some austrochiloids, some amaurobiids (e.g., *Pimus*: Fig. 147C) and all phyxelidids (Figs. 173D–E). Most of our exemplar taxa lack thorns.

16. Female palpal femoral thorns: (0) absent; (1) present.

Palpal femoral thorns similar to those in males occur in females of all phyxelidids, in *Thaida*, *Huttonia*, and at least *Retiro* in the Amaurobiidae.

17. Hair type. (0) plumose; (1) serrate.

Plumose hairs (sensu Lehtinen 1975) have many fine, short to long barbs arranged in spiral whorls around the shaft (Figs. 147B, 154B). Serrate hairs, typical of the Araneoidea, have flattened, overlapping scales along the shaft (Fig. 147G). These also occur in *Mimetus* and *Pararchaea*. Pseudoserrate plumose hairs (Fig. 147F) were reported to be present in deinopids and uloborids (Green 1970:8; Coddington 1986a: 327), but after a wider taxon sampling was examined, the distinction between plumose and pseudoserrate became unclear (compare Figs. 148A–D).

18. Feathery scales: (0) absent, (1) present.

Hill (1979) studied the diversity of shapes in scales, a specific type of seta. Scales are thinner than hairs, are bent in an angle just above the socket (Fig. 146D), and lack innervation. Scales may have lateral prolongations, named *setules* by Hill. Flattened scales with long setules are traditionally named “feathery hairs” (Figs. 135A, 147D, H–J, 148A–B). State 0 (absent) applies to those terminals lacking scales of the feathery type, or lacking scales at all.

19. Metatarsal preening combs: (0) absent; (1) present.

We define preening combs as setae that form an even series at the apex of a leg segment, and that differ conspicuously from surrounding setae (Fig. 141G). We don’t know if these combs are actually used in preening. Such combs occur in the phyxelidid *Xevioso*, the agelenid *Neoramia*, the desid *Matachia* (but not other desids), in amphinectids, in the amaurobiids *Amaurobius* and *Callobius*, and in *Huttonia*.

20. Tibial ventral spine number: (0) fewer than seven pairs; (1) seven or more pairs.

The anterior tibia of *Zoropsis* and *Acanthoctenus* is very spinose, with more than seven pairs of ventral spines. Females, but not males, of *Poaka* also have very spinose first tibiae and metatarsi. No other exemplar taxon has more than five pairs of ventral spines on the anterior tibiae.

21. Reduced leg spination: (0) no; (1) yes.

Most of our exemplar taxa have extensive leg spination: e.g., dorsal spines on the leg femora, pairs of ventral spines on tibiae and metatarsi I and II, and spines on most surfaces of tibiae and metatarsi III and IV. Those taxa in which spines are absent or reduced to a few scattered examples, i.e., *Hypochilus*, *Archaea*, *Huttonia*, and *Pararchaea*, eresids, and dictynids (including *Aebutina*), are coded as “reduced”.

22. Male metatarsus I: (0) unmodified; (1) modified.

Among the Phyxelididae the male first metatarsus (and second as well in *Ambohima*) is modified with a deep median concavity and, in most species, a clasping spine (Figs. 173F, 202C). At least in *Phyxelida tanganensis* the male grasps the female by her second trochanter with this clasping organ while they hang face to face during copulation.

23. Male tibial crack: (0) absent; (1) present.

The male tibial crack is a conspicuous suture line visible through the cuticle at the base of the leg tibiae of most male Zorocratidae and in *Zoropsis* just distal to the basal pair of ventral spines; it is visible on the surface as a shallow, depressed ring, and autospasy may occur at this point (Fig. 141F; Griswold 1993: figs. 3–4). Autospasy through the base of the tibia apparently does not occur easily in *Zoropsis* but occurs readily in *Uduba* (Griswold, pers. obs.). The tibial crack differs from patella-tibia autospasy, which is found in *Thaيدا*, where it occurs through the base of the tibia, and in Filistatidae, where it occurs at the patella-tibia joint.

24. Female posterior leg scopula: (0) absent; (1) present.

Females of tengellids, zorocratids, and lycosoids (except *Psechrus*) have dense scopulae of tenent setae beneath the hind tarsi and metatarsi (Fig. 141D). Other spiders may have scopulae, at least in males, but extensive development in females is unique to the exemplars listed above.

25. Deinopoid tarsal comb: (0) absent; (1) present.

The thick and blunt tarsus IV macrosetae (Figs. 140A, 141B–C) that form a clear line in deinopids and uloborids have previously been suggested as a synapomorphy for the Deinopoidea (Coddington 1986a, 1990a, 1990b; Griswold et al. 1998). This result is corroborated by our analysis (although these setae are absent in the deinopid *Menneus*, Fig. 140B). Austrochiloids and basal Entelegynae typically have tarsal macrosetae. *Megadictyna* has thick setae uniformly distributed (Fig. 141A), and *Menneus*, *Oecobius*, and *Nicodamus* (compare Fig. 140A with B–D), as well as *Araneus* and *Mimetus*, all have tarsal macrosetae, but not forming a clear line. We code the deinopid tarsal comb present only if the macrosetae form a clear line, a coding more restrictive than in previous studies (e.g., Griswold et al. 1999). The sustentaculum, a tarsal macroseta found in araneids, may be a vestige of this comb.

26. Calamistral rows: (0) two; (1) one; (2) three.

Most of our cribellate exemplar taxa have the calamistral setae in a single row (state 1; Figs. 143D–F). In *Hypochilus* the calamistral setae occur in two parallel rows (state 0; Fig. 143A). *Kukulcania* and *Filistata* have the calamistral setae in three staggered rows (state 2, Fig. 143B), but the more basal calamistral setae still show the triseriate arrangement found in the basal filistatine *Sahastata* and the Prithinae. We do not score this character for those taxa with an oval patch of calamistral setae (see character 14 below) except for Eresidae, which have a single linear row as well as an oval patch of calamistral setae (Fig. 144D).

27. Calamistrum: (0) linear, with a straight row or rows of calamistral setae; (1) oval to rectangular.

Most of our cribellate exemplar taxa have linear calamistra, with a single (Figs. 143D–F) or double (i.e., *Hypochilus*: Fig. 143A) row of calamistral setae (state 0). We code the filistatids, which have staggered rows, as state 0 also. An oval to rectangular patch, with the bases of calamistral setae not forming a line, occurs in the Lycosoidea and their kin (state 1; Figs. 143C, G, H, 145F–J). Eresids have a linear calamistrum and a dorsal patch of smaller calamistral setae (i.e., with lines of teeth, Fig. 144D–F). In some specimens of *Eresus* the line of larger setae is not clearly distinguishable from the dorsal patch. We did not score the eresids differently (e.g., as a polymorphism with both states) because other terminals (e.g., *Dictyna*, Fig. 145D–E) have a similar patch, but there the calamistral setae lack the lines of teeth, thus are not easily distinguishable from the normal setae.

28. Calamistrum origin: (0) basal to subbasal; (1) median.

Calamistrum origins were classified based on the following formula: length from the metatarsus base to calamistrum origin divided by the metatarsus length. A ratio of less than 0.30 was considered basal to subbasal (Figs. 143E, 145A). A ratio of greater than 0.30 was considered median origin (Figs. 143D, 144A).

CARAPACE.— Most characters were scored by examination of exemplars. Character data taken from the literature include the suite of classical characters from spider internal anatomy (characters 51–56; Platnick 1977, ex Millot 1931a, b, 1933a–c, 1936, Marples 1968, 1983, Homann 1971). Some past studies have assumed the states for many unexamined taxa (e.g., Platnick et al. 1991; Griswold et al. 1998; Griswold et al. 1999), but here we have coded only those for which there are observations. We have been conservative in the scoring of these characters, only using data from congeneric representatives, thus many of the cells are empty. Whenever possible tapetum form was scored from exemplars, but classical data from Homann (1971) and from Levi's translation of Homann (*in lit.*) were also included. The “primitive” tapetum fills the eyecup with shiny reflective surface. If a tapetum was oval and bisected by a straight dark line it was considered canoe-shaped (Homann 1971: figs. 10A, 27B, 32A). The grate-shaped tapetum is a complex structure in which the rhabdoms are bilaterally arranged in a folded row that penetrates the tapetum (Homann 1971), giving the shiny tapetum an appearance like that of a fireplace grate or barbecue grill. It is this complexly folded structure that causes the “sparkling” eyeshine of lycosids, pisaurids, and other Lycosoidea. We have not examined the morphology of the retina: if the tapetum had the appearance of a folded grate, resembling that figured by Homann (1971: figs. 28a–d, 32d, e), it was scored as grate-shaped.

29. Carapace shape: (0) oval; (1) square; (2) round.

In dorsal view the carapaces of most taxa studied are oval to pear-shaped, with the cephalic region narrower than the thoracic (state 0; Figs. 196F, 202B, 203H, 208G). Eresids have the carapace anteriorly truncate, giving it a square or rectangular shape (state 1, Fig. 199B). Oecobiids have the carapace heart-shaped to nearly round in outline (state 2, Figs. 199E–F).

30. Clypeal hood: (0) absent; (1) present.

A clypeal hood is a median extension of the clypeal margin over the base of the chelicerae (Fig. 129A). It is typical of austrochiloids and eresids. Absent refers to a clypeal margin that is straight or evenly curved in the center (Figs. 128C, 129B–C).

31. Pars cephalica shape: (0) not elevated; (1) elevated.

Uniquely among our exemplars, in *Archaea* and *Pararchaea* the entire pars cephalica is elevated from the fovea to the clypeus (Figs. 127A, 195D).

32. Carapace anterior shape: (0) normal; (1) prolonged around chelicerae.

In *Archaea* and *Pararchaea* the elevated pars cephalica is prolonged around the chelicerae and the bases of the elongated chelicerae are completely surrounded by sclerotized cuticle. In all other exemplars soft cuticle surrounds the chelicerae ventrally.

33. Cheliceral diastema: (0) absent; (1) present.

In most representatives the bases of the chelicerae are close to the endites. *Mimetus*, *Huttonia*, *Archaea* and *Pararchaea* have an evident diastema (Fig. 128A), i. e., a wide space between the chelicerae and endites. Schütt (2002) first noted the importance of this character.

34. Thickened setae at fang base: (0) absent; (1) present.

There may be a series of thick, plumose setae present along the margins of the fang furrow. One posterior seta may be longer than the others and curves gracefully along the posterior side of the fang (Fig. 130I, 131F). We code this character as present if this one long, curved seta arising

on the retromargin near the fang base is present. Taxa lacking this characteristic seta are scored as absent (state 0) (Figs. 126C–D, 130A–C, 131B, D).

35. Male chelicerae: (0) normal; (1) bowed.

The median margins of the chelicerae of most male spiders in our exemplar set are straight or slightly diverging distally (Fig. 129C). In *Dictyna* and *Nigma* the chelicerae are deeply excavate medially and bowed out laterally (Fig. 129D).

36. Chelicerae: (0) normal; (1) small.

The chelicerae of most of our exemplar spiders are fairly robust (state 0 “normal”) (Fig. 129C). The small chelicerae of oecobiids are weak, short and thin (state 1 “small”) (Fig. 129B).

37. Medial cheliceral concavity: (0) present; (1) absent.

Hypochilids have distinct concavities on the inner subbasal face of the paturon into which the fang tips fit when closed (Fig. 130B); a similar depression occurs in *Desis* (Fig. 130H). Such concavities are lacking in all other taxa in our exemplar set (Figs. 126C, 130C).

38. Chelicerae: (0) free; (1) fused at base.

The chelicerae of most of our exemplar spiders are separate all the way to the clypeal margin (state 0, “free”: Figs. 129B–C), and the articulation between them is membranous and flexible. Filistatid chelicerae have a stiff, sclerotized articulation near the cheliceral margin, and the paturon bases are separated anteriorly and posteriorly by strips of pale, fleshy tissue (state 1: Fig. 126C). *Mimetus* also has the chelicerae with a slightly fused, stiff basal articulation (Fig. 128C).

39. Cheliceral teeth: (0) present; (1) absent.

Teeth, which are non-articulate cuticular projections, are present near the fang furrow in most of our exemplar taxa (state 0). These teeth may be large (Figs. 130A–B, 131C, E–F) or small and difficult to detect, as in the eresids (Figs. 131A–B, D). Filistatids (Fig. 126C), oecobiids (Fig. 130C), *Huttonia* and *Pararchaea* lack cheliceral teeth.

40. Cheliceral chela: (0) absent; (1) present.

In filistatids the apex of the paturon is extended to meet the tip of the fang when flexed, forming a chela (Figs. 126B–C). Our other exemplar taxa lack this modification (Figs. 126D, 130A–B). Eresidae have the apex of the paturon extended toward the tip of the fang but this is not so pronounced as the chela in filistatids (see Figs. 131B, D).

41. Cheliceral peg teeth: (0) absent; (1) present.

The palpimanoids, *Archaea*, *Huttonia*, *Mimetus* and *Pararchaea*, have the chelicerae armed with a series of stout, socketed setae that Forster and Platnick (1984) referred to as “peg teeth” (Figs. 127B, 128D). True teeth, i.e., conical projections of the cheliceral cuticle, may or may not be present in palpimanoids. No other taxa in our exemplar set have peg teeth.

42. Cheliceral gland mound: (0) absent; (1) present.

The cheliceral gland opens through a set of pores on the paturon near the tip of the fang when at rest. The glands of the palpimanoids *Archaea*, *Huttonia*, and *Pararchaea* open on an area of raised cuticle or mound (Fig. 127C). Although mimetids have previously been coded as having a gland mound (Platnick et al. 1991), Schütt (2002) suggests that mimetids lack clearly developed gland mounds. Forster and Platnick (1984: figs. 379, 381) refer to a mimetid mound, but this is a barely raised group of pores. We code mimetids as lacking gland mounds. All others in our exemplar set have the cheliceral gland pores opening through flat cuticle.

43. Cheliceral boss: (0) absent; (1) present.

The boss is a retrobasal swelling on the paturon that varies in size and shape (Figs. 129A, C–D) from a low mound to a prominent, teardrop-shaped protuberance. The boss is absent in many lower araneomorphs (Figs. 126A, 128A), even those with large chelicerae such as hypochilids, austrochilids, and deinopids.

44. Cheliceral boss: (0) small; (1) large.

We differentiate between the low mound found in some eresids and araneoids (state 0, “small”: Fig. 129A), and the prominent, teardrop-shaped protuberance typical of higher entelegynes (state 1 “large”: Figs. 129C–D).

45. Cheliceral stridulatory striae: (0) absent; (1) present.

Some spiders may have transverse ridges on the outer margin of the paturon that presumably function as stridulatory striae. These are prominent in *Archaea* (Fig. 127D). Our *Huttonia* species have a small area with stridulatory ridges, similar to that in *Archaea*. Presence or absence of striae is variable in *Pararchaea* (Forster and Platnick 1984), so we code this genus as polymorphic. Austrochiloids also have striae. *Thaيدا* males have striae, but females have only aligned nodules.

46. Chilum: (0) absent; (1) median; (2) bilateral.

The chilum is a sclerite located in the fleshy tissue at the base of the chelicerae beneath the clypeal margin. Due to the retraction of the cheliceral bases beneath the clypeus in some specimens it was not possible to score this character for all taxa. Nor was scoring possible in most cases for those taxa with clypeal hoods, i.e., austrochilids and eresids. For those taxa in which the precheliceral region was visible we noted that there was no sclerite (state 0: “chilum absent”), a single sclerite in the middle (state 1: “chilum median”) or two sclerites separated in the center by soft cuticle (state 2: “chilum bilateral”).

47. Tapetum: (0) primitive; (1) canoe-shaped; (2) grate-shaped; (3) absent.

A tapetum, when present, occurs only in the indirect eyes: the laterals and posterior medians. Homann (1971) referred to a primitive tapetum (“primitivem Typus”) in which the eye has a complete, even layer of light-reflecting crystals (state 0: primitive). This tapetum type is readily seen in hypochilids, austrochilids and filistatids. We have also scored the tapeta of oecobiids as primitive. Homann referred to *Oecobius* as having the primitive type but noted that the tapetum of *Uroctea* combined primitive and canoe-shaped features. Homann’s canoe-shaped tapetum (“kahnförmigem Tapetum”) has two shiny oval parts bisected by a longitudinal dark line (state 1; Homann 1971: figs. 10A, 27B, 32A). It is typical of most entelegyne spiders. The grate-shaped tapetum (state 2) has each half weakly (e.g., *Stiphidion*: Homann 1971: fig. 32D) to strongly (e.g., Homann 1971: figs. 12C, 32E) folded so that it resembles a fireplace grate or barbecue grill (Homann’s “rostförmigem Tapetum”). This occurs in psechrids (Homann 1971:224, 261; Levi 1982: figs. 73, 74, 88), ctenids (Homann 1971:224, 261; pers. obs.), zoropsids (Homann 1971:261; pers. obs.), and stiphidiids (Homann 1971: fig. 32D; pers. obs.). Tapeta are absent in eresids, deinopids and uloborids (Homann 1971:242–243).

48. Posterior eye row: (0) straight; (1) recurved.

When viewed from above the posterior eye rows of *Hypochilus* (Fig. 195C), eresids (Fig. 199B), deinopids, uloborids, *Stiphidion*, *Zoropsis* (Figs. 208F, G) and *Acanthoctenus* (Fig. 208C) are recurved. All other taxa in our exemplar set have straight posterior eye rows (e.g., Figs. 203A, H, 205A, 207A).

49. Serrula tooth rows: (0) multiple; (1) single.

The serrula is a group of toothlike structures situated at the ventral tip of the anterior surface of the pedipalpal coxal endites. Marples (1968) noted that there are two kinds. In hypochilids the serrula consists of a plate bearing several rows of teeth (state 0; Platnick 1977: figs. 14, 15). In all other taxa the serrula is a single row of closely spaced teeth (state 1; Platnick 1977: figs. 11, 12). We have scored this for all taxa by observation.

50. Sternal sigilla: (0) present; (1) absent.

Sigilla are depressions or dimples in the cuticle of the sternum or labium that correspond to the attachments of ventral extensions of the endosternite. Marples (1968:20) reported labial and

sternal sigilla similar to those of mygalomorphs and mesotheles in the hypochilid *Ectatosticta*, but only a pair of labials in *Hypochilus*. Lehtinen (1967:300) has reported sternal sigilla in filistatids which, in *Filistata* and *Kukulcania*, are depressed, whitish areas in front of coxae III and IV. All other taxa in our exemplar set lack sigilla.

51. Venom gland: **(0)** present; **(1)** absent.

Uloborids are the only spiders among our exemplars that lack venom glands (Millot 1931a). Additional scorings were taken from Millot (1931b, 1933a–c), who made carapace sections to study the midgut diverticula of spiders, and from Forster (1955) and Forster and Platnick (1984).

52. Venom gland: **(0)** endochelicerai; **(1)** extends into carapace.

Petrunkevitch (1933) discovered that the venom glands of *Hypochilus* are confined to the chelicerae and Millot (1933b) found the same configuration in *Ectatosticta*. All examined non-hypochilid araneomorphs with venom glands, including the austrochilids *Hickmania* (Marples 1968) and *Thaida* (Zapfe 1955), have these glands extending into the carapace. The sources of our data are the same as for the previous character.

53. Coxal gland duct: **(0)** convoluted; **(1)** simple.

The coxal glands of hypochilids have highly convoluted ducts (Marples 1968) similar to those of mygalomorphs (Buxton 1913). Other araneomorphs, including austrochiloids, have simple, inverted, U-shaped ducts. Only a few of our exemplar families have been studied, i.e., hypochilids and austrochiloids (Marples 1968), and filistatids, araneids, dictynids, agelenids, and ctenids (Buxton 1913). We scored *Araneus* and *Dictyna* after an unspecified dictynid, both from Buxton (1913), but the ctenids and agelenids that he studied may not be closely related to the terminals in this analysis and we therefore did not code our ctenid and agelenid exemplars.

54. Midgut diverticula in chelicerae: **(0)** present; **(1)** absent.

Hypochilids have diverticula of the proximal portion of the midgut (the thoracenteron) that extend anteriorly into the base of the chelicerae (Millot, in Bristowe 1933; Marples 1968). Austrochiloids (Marples 1968) and the other araneomorphs studied by Millot (1931a) lack these anterior extensions. Platnick (1977) argued that the extension of the thoracenteron into the chelicerae was a synapomorphy for the hypochilids with acquisition of a parallel condition in liphistiids (Millot, in Bristowe 1933).

55. Pharynx dorsal M1 muscle origin: **(0)** carapace; **(1)** rostrum.

The dorsal dilator muscle M1 of the pharynx of most spiders originates dorsally on the carapace (state 0) (Marples 1968, 1983). In hypochilids the pharyngeal dilators originate on an apodeme of the rostrum (state 1), similar to Mesothelae. Our scorings are from Marples (1968, 1983). *Deinopsis* and *Filistata* are scored inapplicable because the M1 muscle is absent (the anterior muscle M2 seems to act as dilator).

ABDOMEN.— Most characters were scored by examination of exemplars. Character data taken from the literature include the suite of classical characters from abdominal internal anatomy (characters 57–58: Platnick 1977, ex Millot 1931a, 1933a–d, 1936; Marples 1968). As with the carapace characters, we only used data from congeneric representatives, thus many data are missing. Respiratory system data came from dissections by Lamy (1902), Forster (1970), Forster and Wilton (1973), Ramírez (2000) or Griswold and Ramírez (pers. obs.). Male epiandrous spigots were examined with SEM and the condition checked in additional specimens with light microscopy.

56. Fifth median abdominal endosternite: **(0)** present; **(1)** absent.

The internal anatomy of the abdomen of spiders was studied by Millot (1933a–d, 1936) and Marples (1968), who indicated that the abdomen of most araneomorphs has four ventral median endosternites (non-cuticular, internal tendonous pieces where muscles insert). *Liphistius* has nine

median abdominal endosternites, including the four from the anterior abdominal segments and five additional representing the primitive abdominal segmentation. Hypochilids retain the first of these additional five (state 0), the fifth abdominal endosternite (Marples 1968), where the muscle dilator of the anus inserts. The fifth endosternite is lost in the remaining araneomorphs (state 1).

57. Intestine: (0) M-shaped; (1) straight or only curved.

Millot (1933b: figs. 1, 2) discovered that the opisthosomal portion of the midgut is M-shaped in *Ectatosticta*, *Liphistius* and mygalomorphs (state 0), as opposed to straight in other araneomorphs (state 1). He did not specify the other taxa studied. He also noted (Millot 1931a:740) that the study of the abdominal intestine is extremely difficult. Millot reported (1933b:228) that the Haplogynae with globose abdomens (*Scytodes*, *Physocyclus*) have very curved, but not M-shaped intestines. Marples (1968) reported that *Ectatosticta* (and to a lesser degree *Hypochilus*) and the austrochiloids also have M-shaped midguts. Lucrecia Nieto (*in lit.*) reported an M-shaped intestine in the filistatid *Kukulcania*. This is a new coding for filistatids, differing from that in previous studies (e.g., Platnick et al. 1991; Griswold et al. 1999).

58. Heart ostia number: (0) four; (1) three or two.

Hypochilids (Petrunkevitch 1933) and austrochiloids (Zapfe 1955; Forster 1955; Marples 1968) have four pairs of heart ostia (state 0), whereas other araneomorphs (the Araneoclada of Platnick 1977) have three or two pairs (state 1). Petrunkevitch (1933) reported the number of heart ostia for filistatids, eresids, oecobiids, deinopids, uloborids, araneids, dictynids, agelenids, desids, amaurobiids, psechrids, zoropsids and ctenids. We scored our exemplars following Petrunkevitch (1933) and Millot (1936) when they studied congeneric representatives. Lucrecia Nieto (*in lit.*) confirmed the presence of three pairs of ostia in *Kukulcania*.

59. Third dorsoventral abdominal muscles: (0) present; (1) absent.

These muscles run from sigillae on the dorsal surface of the abdomen to the ventral median endosternites corresponding to the tracheal (or posterior booklung) segment (IX segment in Millot 1933b, 1936). Many spiders have two pairs of large sclerotized sigillae on the abdominal dorsum, marking the insertions of the dorsoventral muscles corresponding to the genital and tracheal segments. Scorings for this dataset were primarily taken from Millot (1933b, 1936), Crome (1955), Marples (1968), Ramírez and Grismado (1997) and Ramírez (2000). The presence of muscles was in some cases indirectly inferred from the corresponding dorsal abdominal sigillae.

60. Posterior spiracles: (0) two widely separated; (1) one narrow median.

Four lunged spiders such as *Hypochilus*, *Gradungula*, and *Hickmania* have a pair of posterior spiracles united by a furrow (state 0), whereas those with posterior tracheae have but a single spiracle (state 1). *Thaïda*, *Kukulcania* and *Filistata* have similar posterior respiratory systems connecting to a wide furrow (and filistatines have posterior booklungs in the hatching stage, Ramírez pers. obs.) We also code these as state (0). *Archaea* has two separate, round openings (Fig. 127F) that we code as state (0). The general condition in Entelegynae is a narrow spiracle connecting to the tracheae.

61. Posterior booklungs and modifications: (0) booklungs; (1) reduced booklungs; (2) lateral tracheae.

Hypochilus, *Gradungula*, and *Hickmania* retain typical posterior booklungs. The peculiar morphology in *Thaïda* (Forster et al. 1987; Ramírez 2000) is ambiguous, with intermediate morphology between reduced booklungs and lateral tracheae, and is scored here as polymorphic (1, 2). Filistatines have reduced booklungs, with a few leaves in the hatching stage, of which only one is retained later in development (state 1), while other spiders develop the tracheae without passing through cuticular booklung leaves (Ramírez 1995, Anyphaenidae, and pers. obs., *Loxosceles*). In nearly all of our other exemplar taxa the posterior respiratory system comprises median tracheae

derived from the elongated entapophyses of the third abdominal segment and lateral tracheae derived from modification of the posterior booklungs (state 2) (Purcell 1909). We code this character as unknown for those taxa that have lost their lateral tracheae, i.e., *Archaea*, *Nicodamus* and the dictynids *Dictyna*, *Nigma*, *Lathys* and *Tricholathys*.

62. Lateral tracheae: (0) simple; (1) branched; (2) absent (lost).

Most taxa, even those with branched median tracheae, have the lateral tracheae forming a simple, unbranched tube. Desids (*Matachia*, *Desis*, *Phryganoporus* and *Badumna*) are alike in having the lateral tracheae highly branched. The dictynids *Dictyna*, *Lathys* and *Tricholathys* have a thick median tracheal trunk with many fine lateral branches, but lateral tracheae are lacking. Lateral tracheae are also lacking in *Nicodamus* and in *Archaea*. Taxa with posterior booklungs are scored inapplicable.

63. Median tracheae or 3rd entapophyses: (0) muscle apodemes; (1) median tracheae.

The 3rd abdominal entapophyses are cuticular muscle apodemes that occur between the posterior booklungs in primitive spiders with four booklungs, and between the lateral tracheae in some haplogyne spiders (Ramírez 2000). Purcell (1909) demonstrated that these apodemes develop in elongate structures with thin walls, to give the median tracheae, which in some cases still retain their connection with the abdominal muscles (Lamy 1902). Ramírez (2000) found that the median tracheae are a synapomorphy of Entelegynae (convergently with Austrochilinae). *Hypochilus*, *Gradungula*, *Hickmania* and the filistatids have normal muscle apodemes, and *Ariadna* has short muscle apodemes. All other terminals have median tracheae.

64. Median tracheae: (0) simple; (1) branched.

Simple tracheae comprise unbranched tubes. We code as branched those median tracheae that have few to many branches, and both those that branch from a basal rosette and those with thick trunks giving rise to lateral branches. *Huttonia* has a median, unbranched tube (Forster and Platnick 1984). *Aebutina* has median tracheae that are flat and wide, until a point where they are abruptly truncated and then extend into a thin tube. The truncate border has the ragged texture typical of muscle attachments. We code them as simple.

65. Anal tubercle: (0) small; (1) large.

The anal tubercle of most araneomorphs is little longer than the PMS (state 0: Figs. 47A, 59A). Oecobiids have a large anal tubercle, nearly as long as the elongate PLS and much larger than the PMS (Figs. 27A, 30A). Deinopids have an anal tubercle that extends beyond the PMS (Fig. 44A), but is not nearly as large as in oecobiids.

66. Epiandrous spigots: (0) present; (1) absent.

Epiandrous spigots, which presumably serve in making the sperm web, occur in a variety of taxa (Figs. 160A–B, 161A–E). Males of many taxa lack them (Figs. 160C–D, 161F–H); how or if they construct sperm webs is unknown.

67. Epiandrous spigot distribution: (0) dispersed; (1) in two bunches.

Most phxelidid males have the epiandrous spigots grouped into two separate bunches (Figs. 160A–B), as do *Thaida* (Fig. 158A) and *Hickmania*, *Callobius* and *Amaurobius*, and *Pararchaea*. In other males with epiandrous spigots these are scattered along the margin of the epigastric furrow (Figs. 161A–C, E).

SPINNERET MORPHOLOGY.— Spigots were classified according to the criteria in Coddington (1989). Spigots are named for the glands that they presumably serve. Glands and spigots have been associated in several key taxa. Although the glands of most of our exemplar taxa have not been studied, we think that reasonable inferences about their gland types can be made from the structure, number, distribution and ontogeny of spigots. Piriform gland spigots (PI) occur as multiples

on the ALS of both males and females. Ampullate gland spigots (MAP and mAP) are typically present as singles or as a few on the ALS and PMS in both males and females, and if one is missing in a male it is replaced by a nubbin. Paracribellar spigots (PC) may occur on the PMS, PLS, or both, and have a characteristic annulate shaft similar to that of cribellar spigots. These may be present in both sexes of “lower” araneomorphs, but are in most cases replaced by nubbins in the males of higher araneomorphs. The PLS modified spigot (MS) (e.g., “pseudoflagelliform” gland spigot of Kovoor [1977b]) may occur on the PLS of both sexes, or if absent in the male, is replaced by a nubbin. Aciniform gland spigots (AC) occur as multiples on the PMS and PLS of both sexes. Cylindrical gland spigots (CY) occur only in adult females, where they may be found on the PMS and PLS, and are not represented by nubbins in males. We also suggest that shaft morphology is a more reliable indication of spigot type than base morphology. We follow Tillinghast and Townley (1994) and Townley and Tillinghast (2003) in defining nubbins and tartipores. All specimens were critical point dried before scanning electron microscope (SEM) examination of spinning organs.

68. Ampullate spigot shaft texture: (0) smooth or longitudinally striated; (1) with papillae; (2) concentrically striated.

Most of our representatives have smooth or longitudinally striated MAP and mAP shafts (Figs. 65B–C, 71C). Eresids are unique in that their ampullate shafts have small papillae or imbricate protrusions (state 1, Figs. 33C, E, 37C). Filistatids are also unique in having all spigot shafts with faint concentric ridges (state 2, Figs. 3E–F, 5F).

69. Spigot base texture: (0) all squamate; (1) only PMS and PLS squamate; (2) all smooth or with “fingerprint” pattern.

Most of our representatives have smooth or finely striated spigot base cuticle (state 2, Figs. 65B–C, 71C). *Hypochilus* has scale-like annuli encircling all the spigot bases (state 0, Figs. 1A–D, 2C–D). Deinopids and *Nicodamus* have some spigot bases with similar squamate-annulate texture, but only on the posterior spinnerets (state 1, Figs. 41C–D, 43C–D, 44E).

70. Tartipores: (0) absent; (1) present.

Tartipores were first described by Kovoor (1986). We follow the terminology of Townley and Tillinghast (2003) for nubbins and tartipores. They define a tartipore as “a cuticular scar, morphologically singular or multiple, that results, after ecdysis, from a collared opening forming in the exoskeleton during proecdysis; the opening accommodates a silk gland duct, allowing it to remain attached to a spigot on the old exoskeleton during proecdysis.” This mechanism allows spiders to use silk during the proecdysis, through gland ducts that pierce the forming cuticle to remain attached to the shedding spigots (Townley et al. 1993, Tillinghast and Townley 1994). A direct prediction is that hypochilids and filistatids (as well as most haplogynes), which lack tartipores (Figs. 1B, 5F), are unable to produce silk in the days before moulting. Similarly, spiders should be able to use, during proecdysis, only the basic spigot types with tartipores (namely MAP, mAP, PI and AC, but not MS, PC, or cribellum). Tartipores typically have a dimple, scar, or crease (Figs. 9D, 10D). Tartipores of the MAP and mAP are larger than PI or AC tartipores. The ALS of higher entelegynes have a basic complement of two MAP (which may be replaced by a nubbin in the adult), accompanied by one MAP tartipore (Figs. 13C, 86B). The same pattern generally occurs with the mAP in the PMS, but we found more variation there.

71. Cribellum: (0) present; (1) absent.

Most of our exemplars are cribellate (Figs. 2A, 47A) but Palpimanoidea are ecribellate (Fig. 24A). We include a few other ecribellate taxa, i.e., *Gradungula*, *Araneus*, *Nicodamus*, and *Uroctea* (Fig. 30A) that may exemplify character combinations more representative of their higher taxa, and which offer clearer evidence for taxonomic placement. The cribellar spigots are lost in males when they reach maturity.

72. Cribellum: (0) entire; (1) divided.

Hypochilus, austrochilids, Orbiculariae, most dictynids and several other taxa have the cribellate spinning field entire with the spigots spread evenly across (Figs. 2A, 10A, 38D, 43A). Divided cribella have a bare line down the center, dividing the spinning field into two lateral parts (Figs. 5A, 97B–C).

73. Cribellate spigots: (0) uniform; (1) clumped.

In most taxa, whether the cribellum is entire or divided, the cribellar spigots are uniformly spread across the spinning field (Figs. 34C, 97E). In *Acanthoctenus* and some zoroecratids these spigots are clumped into tightly packed groups surrounded by bare cuticle (e.g., *Acanthoctenus*: Figs. 97A, G; *Uduba*: Figs. 97C, F), which may form short, longitudinal segments (*Acanthoctenus*, *Raecius*). *Zoropsis* has two transversal bands of spigots isolated by bare cuticle (Figs. 113C–F), in similar disposition as the aligned clumps of *Acanthoctenus*; we code *Zoropsis* ambiguous for this character.

74. Cribellate spigots: (0) strobilate; (1) claviform.

Strobilate cribellar spigots are cylindrical to tapering at the tip and ringed by evenly spaced, raised annular ridges (Figs. 34C, 96B, 97E). Claviform cribellar spigots, typical of the Filistatidae, are club-shaped, blunt at the tip, and have fine transverse ridging (Figs. 5B–C, 14E).

75. ALS segment number: (0) three; (1) two.

Primitive Araneomorphae retain the intermediate ALS segment as an incomplete lateral ring (Figs. 2A, 32A). Other Araneomorphae have lost this segment (Fig. 76A).

76. ALS MAP: (0) clustered; (1) dispersed.

One or a few ampullate glands serve the ALS and PMS. The large spigots served by these glands are called “major ampullate” (MAP) on the ALS and “minor ampullate” (mAP) on the PMS. They can be distinguished from other spigots on these spinnerets by their large size, usually squat base, and small number. If present in females but absent in males they are typically replaced by a nubbin. In most taxa the MAP are clustered along the inner margin of the spinning field (“clustered”: Figs. 1B, 43A, 113B), but in filistatids, eresids and oecobiids some MAP spigots are interspersed among the piriform spigots (“dispersed”: Figs. 6B, 29A, 35B). We score this for taxa with a single MAP if it is accompanied by a nubbin, but code it “?” for those have only one unaccompanied MAP, i. e., *Oecobius* and *Pararchaea*.

77. ALS MAP field separated by deep furrow: (0) absent; (1) present.

In most Araneomorphae the mesal MAP field is separated from the PI field by more or less flat or weakly folded cuticle (Figs. 67B, 104B). In Araneoidea, *Mimetus* and *Archaea*, the MAP field is separated by a deep furrow (Figs. 20E–F, 21A, 25B). *Huttonia* has only an indentation between both fields (Fig. 24B).

78. ALS MAP number in female: (0) more than three; (1) three; (2) two, or one plus a nubbin.

Hypochilus, *Gradungula*, eresids and deinopids have four or more MAP (state 0, Fig. 43B); filistatids have three (state 1, Fig. 6B); most of our exemplars have a consistent pattern (state 2) of two marginal MAP (Figs. 7B, 49B, 53B) or only one, in that case accompanied by a posterior nubbin (e.g., *Uloborus*, Fig. 45B; dictynids, Figs. 59B, 61B, 63B, 65B; *Retiro*, Fig. 92B). Except in deinopids and *Uroctea*, the other taxa with more than one MAP have two mesal, anterior MAP larger than the rest (Fig. 2C). These are presumably homologues of the two MAP that remain in higher entelegynes. *Ariadna*, *Oecobius*, *Desis* and (presumably) *Pararchaea* are the only representatives with only one MAP and no nubbin (Fig. 27B), so we code them as nonapplicable for this character.

79. ALS female posterior MAP: (0) functional; (1) reduced to nonfunctional nubbin.

There has been extended confusion between nubbins and tartipores, but Townley and Tillingast

(2003) recently presented a coherent terminology. Nubbins are nonfunctional, vestigial spigots, usually in the form of protuberances, in the place where a spigot occurred in the previous instar. They lack the characteristic cuticular scar found in tartipores. Nubbins of MAP only occur in higher entelegynes that have only two MAP. We can identify that it is the posterior MAP that is consistently reduced in the adults. The posterior MAP is the secondary one, that is, the one that remains functional during proecdysis, and produces the tartipore (Townley et al. 1993). The posterior MAP in adult *Archaea* is smaller than the anterior one (although still has a shaft, Figs. 21B, 22B), but both MAP are well developed in the immature (Fig. 20B), thus we interpreted the vestigial adult posterior MAP as a nubbin. We scored this character as inapplicable in *Oecobius* and *Pararchaea*, which seem to have only one MAP.

80. ALS piriform margin: (0) rounded; (1) flat to sharp.

Piriform glands serve multiple spigots on the ALS. These spigots extrude the glue that attaches silken lines. The junction of the base and shaft may be gradual and rounded (Fig. 83B) or the junction may be abrupt, with the edges of the base at the junction forming a shelf or ledge (“flat to sharp”: Figs. 58B, 84B). We score this as nonapplicable in *Mimetus* and *Pararchaea*, which have short, reduced bases (Fig. 25B).

81. PMS mAP: (0) absent; (1) present.

Like the MAP on the ALS, minor ampullate spigots (mAP) occur as one, two, or a few on the PMS (Figs. 40C, 92C). They tend to have squat bases and slender, tapering shafts (e.g., Fig. 111A). Unlike cylindrical gland spigots (CY), these large spigots occur in both females and males or, if absent in males, are replaced by nubbins. Among our exemplars only *Hypochilus* (Fig. 1C), *Gradungula*, *Huttonia* and *Uroctea* (Fig. 29B) lack mAP.

82. PMS mAP number in female: (0) more than two; (1) two; (2) one plus nubbin; (3) one.

The definition of nubbins and tartipores is the same as for the MAP. Many of our exemplar taxa have a single mAP on the PMS (Figs. 40C, 92C). The lycosoids and their kin have two (Figs. 98C, 104B), as do the austrochilids, *Deinopis*, *Pimus*, and the enigmatic *Aebutina*. Araneoids, uloborids, *Mimetus* (Fig. 25C) and some phyxelidids (Fig. 49C) have one mAP plus a nubbin. According to Kooor and Lopez (1979) eresids have numerous ampullate gland spigots opening on the PMS (Fig. 34E).

83. PMS mAP position: (0) median to anterior; (1) posterior.

The mAP is located in the median to anterior part of the PMS spinning field in most of our exemplars (Figs. 59C, 92C). A posterior mAP is found in the Araneoidea, and in *Mimetus*, *Megadictyna* (Fig. 40C) and some dictynids (Fig. 61C).

84. PMS aciniform number: (0) more than three; (1) one to three.

Most of our exemplar taxa have numerous AC spigots on the PMS (Figs. 49C, 60C) but in a few species these are reduced in number to three or fewer (Figs. 64C, 74C, 85C, 113F). Despite the suggestions of Kooor and Lopez (1979), ontogeny compels us to code aciniform gland spigots present in eresids.

85. PMS-PLS AC shaft size: (0) uniform; (1) two size classes.

This character accounts for the finding in *Gradungula*, *Hickmania*, *Uroctea*, *Nicodamus*, and *Tengella* of an uncertain type of spigot on male and female PMS and PLS, which we tentatively describe as a second class of AC (Figs. 17E–F, 30C). These larger spigots generally occur on the margins of the spinning fields, but in *Hickmania* there is also a median line of large spigots on the PLS (Figs. 9A–D). In *Nicodamus* the larger spigots form a central group in the PMS (Figs. 41C, 42C).

86. PMS cylindrical gland spigots: (0) absent; (1) present.

Cylindrical glands serve the PMS and PLS and produce silk used in forming the eggsac.

Therefore, they occur in adult females but are absent from juveniles and males, even as nubbins. In the absence of gland data we rely on ontogeny to identify CY spigots. If a class of spigots occurs on the PMS and PLS of females but not males, we assume these to be CY. Cylindrical gland spigots tend to have slender, tapering bases and shafts, and resemble aciniform gland spigots except in being larger and less numerous (Figs. 49C, 63C, 113F). Cylindrical gland spigots were considered as characteristic of the Entelegynae (Platnick et al. 1991), but we report them from the austrochiloids *Thaida* and *Hickmania*. They are absent in hypochilids (Figs. 1C–D) and Haplogynae including filistatids (Fig. 6C), but putative homologs of CY occur in telemids and leptonetids as well (Platnick et al. 1991). Some entelegyne taxa also lack apparent CY spigots, e.g., *Matachia* (Figs. 83C–D). We are unable to determine if CY spigots occur in *Megadictyna*, and therefore code this and other CY characters as unknown.

87. PMS cylindrical gland spigot number: **(0)** one or two; **(1)** many.

Most of our exemplar taxa with CY spigots have one or two on the PMS (Figs. 53C, 61C, 88C). We code three or more as “many”. The phyxelidids *Vytfutia* and *Xevioso* have three (Fig. 47C). According to Kovoor and Lopez (1979), eresids have numerous CY glands serving the PMS. *Thaida* (Fig. 11C) and *Hickmania* (Fig. 7C) have several PMS CY and deinopoids have several large CY posteriorly on the PMS (Fig. 43C). Zorocratids and Lycosoidea have numerous large CY spigots posteriorly on the PMS: three or four occur in *Raecius* (Fig. 105C), four in *Acanthoctenus* (Fig. 115C), and eight or more occur in *Psechrus* (Fig. 109C), *Uduba* (Fig. 104C) and *Zoropsis* (Fig. 113C).

88. PMS paracribellars: **(0)** absent; **(1)** present.

Spigots with shafts that resemble cribellar spigots may occur on the PMS and/or PLS (Peters and Kovoor 1980). Their function may be to produce fine fibrils that accompany the axial fibrils in the capture threads (Peters 1984; Peters 1987: fig. 65a “ls”). Paracribellars on the PMS occur widely in the Neocribellatae (Figs. 11C, 45C–D, 71C) and are absent in the hypochilids (Fig. 1C) and sporadically absent among the neocribellates (Figs. 27C, 51C, 92C, 113F). They are present in females but in most taxa are replaced by nubbins in males (Figs. 48C, 76C). We code ecribellates as nonapplicable for this character.

89. PMS paracribellar spigots in male: **(0)** present; **(1)** absent.

The adult males of basal Araneomorphae, i.e. filistatids and austrochilids, retain the PC spigots (e. g., *Filistata*, Fig. 4C, *Hickmania*, Fig. 8C, *Thaida*, Fig. 12C), while in our representative entelegynes the PC are reduced to nubbins in the males (Figs. 40C, 50C, 74C). There are many missing entries for this character both because PC are absent in both sexes (i.e., nonapplicable) and because the males of some exemplars have not been scanned (i.e., unknown). The PC shaft found in the male of *Neoramia* (Fig. 82B) is here regarded as abnormal. Even isolated cribellar shafts are occasionally found in males (Fig. 158C).

90. PMS paracribellar form: **(0)** strobilate; **(1)** floppy.

In the majority of taxa with paracribellar spigots their shafts resemble those of the cribellar spigots. Most of our exemplars have strobilate PC shafts, with widely spaced, annular ridges (Fig. 82D) (state 0). Previously we recognized a class of paracribellar spigots that have long shafts with many, closely spaced annuli and that are typical of the Deinopoidea (Figs. 45C–D) (Griswold et al. 1999: character 82, “deinopoid”). Similar PC shafts occur in austrochilids, e.g., *Thaida* (Figs. 11C, 12C) and *Hickmania* (Fig. 10E, Platnick et al. 1991: fig. 45). We no longer recognize separate strobilate and deinopoid states, as some taxa (e.g., *Megadictyna*, Fig. 38B) have an intermediate morphology. The apparent differences in annuli number and position may relate only to the length of the shafts. Filistatid PC morphology is as unique as that of their cribellars (Figs. 3C, F). On the PMS and PLS of filistatids there are peculiar spigots with cylindrical bases and flattened, trans-

versely ridged, “floppy” shafts. The shafts of these spigots may be pointed or claviform (Fig. 4C) (state 1).

91. PMS paracribellar distribution: **(0)** at anterior margin of spinning field; **(1)** mid-field; **(2)** at posterior margin of spinning field.

Among most taxa with PMS paracribellars these occur along the anterior margin of the PMS spinning field (Figs. 49C, 63C, 83C). In the agelenid *Neoramia* (Fig. 73C), among the amphinectids (Fig. 77C) and in some desids (Fig. 87C) and dictynids the PC spigots occur at mid-field, surrounded by AC spigots. Uniquely, the PMS paracribellars of filistatids arise at the posterior margin of the spinning field (Figs. 3C, 4C).

92. PMS paracribellars: **(0)** bunched; **(1)** encircling spinneret anteriorly.

Austrochiloids, phyxelidids, and some other taxa have paracribellar spigots that may be regularly spaced in a row that encircles the PMS anteriorly (Figs. 7C, 11C, 40C, 49C, 60C). In other taxa the anterior PC are irregularly arranged or bunched together (Figs. 43C, 83C).

93. PMS paracribellar shafts: **(0)** arising from single bases; **(1)** grouped.

The paracribellar shafts of most taxa arise from single bases (Figs. 45D, 47C). In stiphidiids, neolanids, amphinectids, and some desids and dictynids several PC shafts may arise from a single, greatly enlarged base (Figs. 66A, 68B, 73C, 87C). We code this striking morphology as “grouped” or “fused.” This character defined in part the “fused paracribellar clade” of Griswold et al. (1999, Fig. 212). In some taxa both single and grouped PC shafts may be found in the same individual, e.g., *Dictyna* (Fig. 59C). We also code these as grouped. Abnormal, duplicate shafts are occasionally found in spiders (Fig. 111A), hence we have coded *Callobius* PMS PC (Fig. 96C) as arising from a single base.

94. PMS paracribellar bases: **(0)** cylindrical; **(1)** long, narrow, flattened.

The encircling PC of phyxelidids are so tightly packed that the bases are laterally flattened to fit together (Figs. 46C, 47C). Other taxa with single PC bases, whether bunched or encircling, have the bases well separated and round in cross section (Fig. 63C). This character is nonapplicable in those taxa for which all PC shafts arise from one or a few common bases.

95. PLS aggregate gland (AG) spigot: **(0)** absent; **(1)** present.

In Araneoidea the paired aggregate gland spigots (Figs. 38C, E) flank the flagelliform gland (FL) spigot and coat the FL fiber with sticky glue as it is spun (Figs. 119C–E). Aggregate glands have been observed in all araneoid families for which gland histology has been studied (Kovoor 1977a), but are absent from other spiders (Figs. 43D, 44B).

96. PLS modified spigot: **(0)** absent; **(1)** present.

At the apex of the PLS in many spiders are one or more enlarged spigots that differ from the AC, CY and PC. Typically they are larger than the nearby AC spigots and have a thick, cylindrical or even clavate shaft (Figs. 68A, D). They are present in females but often replaced by a nubbin in males (compare Figs. 75D and 76D). Glands serving these spigots were first identified in uloborids by Kovoor (1977b), who called them “pseudoflagelliform,” and were subsequently found in amaurobiids, eresids, psechrids and zoropsids, but not in filistatids and dictynids. These glands presumably produce the axial fibers in the cribellate band (Peters 1984). Nevertheless, classifying the spigot type by presumed gland morphology may present a dilemma. For example, pseudoflagelliform glands have not been found in dictynids, and it is therefore not surprising that their cribellate silk does not have axial fibers. But some female dictynids do have an enlarged spigot at the apex of their PLS (Fig. 59D) that is replaced by a nubbin in males (Fig. 60D). We divorce classification of this spigot from data on gland types and refer to these simply as “modified spigots” (MS). We suggest a broad homology between the pseudoflagelliform gland spigot of Deinopoidea, flagelliform gland spigot of Araneoidea, and this peculiar spigot type in other spiders. Typical MS occur wide-

ly (Figs. Fig. 43D, 46B, 82E, 88D, 113G). *Hypochilus* has a set of three or four large spigots with cylindrical shafts at the apex of its PLS (Fig. 1D). We code these as MS although the morphology is unique. The MS is often flanked by one to three spigots, forming a compact group; in many taxa this group is a triad, made of the MS and two smaller spigots, one at each side. This triad is an additional guide to identify the MS in those terminals. In the taxa that possess PC, the flanking spigots in the triad are PC (Figs. 82C, E); in others, they are similar to AC spigots, but differ in being replaced by nubbins in the male (compare Figs. 33D and 33F; 98D and 99F; 100G and 114D). These accompanying spigots similar to AC seem to belong to a further class of spigots for which glands have not yet been identified, because AC do not degenerate into nubbins. We have not attempted to name these spigots. Interestingly, the AG spigots of araneoids also flank the MS forming a triad, suggesting that there may be a broad homology of the otherwise different spigot types accompanying the MS. If that is the case, our character codings involving the PLS-MS triad (PC and MS presence, disposition, and number) only reflect imperfectly these relations. In eresids the MS is anterobasal and separated from the rest of the PLS spinning field (Figs. 31D, 33D, J, 37D) but the spigot is otherwise ontogenetically like typical MS. *Aebutina* has a typical apical MS but also two anterobasal spigots that are replaced by nubbins in the male (Figs. 57D, 58D), which we interpreted as the two flanking spigots of the triad that are displaced to a basal position. Another possible interpretation, which we considered in previous versions of this manuscript, is that all the isolated, basal spigots of eresids and *Aebutina* are also MS. The MS is absent from filistatids (Figs. 3D, 6D), palpimanoids, oecobiids (Fig. 27D), and some dictynids and titanocids. Although Coddington (1990a) codes the MS present for *Titanoeca*, and the male of *Titanoeca* has what could be a MS nubbin (Fig. 52D), we can't identify an MS on the PLS of any *Titanoeca* or *Goeldia* that we have examined.

97. PLS modified spigot position: **(0)** at margin of spigot field; **(1)** segregated.

The modified spigots (MS) of most taxa are located at the margin of the PLS spinning field (Figs. 46B, 105D). Among the Orbiculariae the MS is laterally separated from the spinning field (Figs. 38E, 43D, 44B), as is the case in *Thaida* (Fig. 11D). The eresid MS is distant from the rest of the spinning field. Although *Aebutina* has one MS in the spinning field, the two flanking spigots of the triad seem to be segregated, therefore we code *Aebutina* as uncertain (see below).

98. PLS MS position: **(0)** at field margin or only slightly segregated; **(1)** basal anterior.

In eresids the MS is well separated from the rest of the PLS spinning field (Figs. 31D, 37D). At least the *Eresus* MS is ontogenetically like that of other spiders in occurring in females but being reduced in males (Fig. 32D). In *Stegodyphus* the MS produces the same cribellar axial threads as in *Deinopis* (Peters 1992a), and is accompanied by two small spigots (Fig. 33D, F) that are reduced to nubbins in males (Fig. 33F). *Aebutina* has the MS in the spinning field, but the pair of accompanying spigots is apparently segregated (Figs. 56B, 57D).

99. PLS paracribellar: **(0)** absent; **(1)** present.

Spigots with shafts that resemble cribellar spigots may occur on the PLS. They may function like the PC on the PMS to produce fine fibrils that accompany the axial fibers in the capture threads. Hypochilids (Fig. 1D) lack PLS paracribellars and in the Neocribellatae PLS PC are sporadically present (Fig. 87D) or absent (Fig. 98D). Surprisingly, occurrence of PLS PC does not parallel that of PMS PC. Some taxa with PMS PC lack these on the PLS (Fig. 44B), and, remarkably, titanocids lack PMS PC but have them on the PLS (Fig. 53D). They are present in females but are typically replaced by nubbins in males (Fig. 76D).

100. PLS paracribellar number: **(0)** one; **(1)** two or three.

Megadictyna, *Xevioso* and dictynids (Fig. 59D) have a single PLS PC, whereas two or more occur in filistatids, titanocids (Fig. 51D), some amaurobiids (Fig. 96D), *Neolana*, stiphidiids,

amphinectids and some desids (Figs. 82E, 87B). *Thaida* has one unambiguous PLS PC and a second spigot of intermediate morphology (Fig. 13E). The male has two apparent PC nubbins on the PLS (Fig. 12D), so we code *Thaida* as having two PLS PC.

101. PLS PC distribution: **(0)** apical only; **(1)** with an additional basal external group.

In most representatives the PLS PC spigots are apical and are situated close to the MS (if this spigot is present), often one at each side (Figs. 68D, 88D, 96D). In titanocoids, besides an apical PC, there is a basal external group of three PC, separated from the rest of the PLS spinning field (Fig. 55D).

102. PLS paracribellar and modified spigot: **(0)** separate; **(1)** united.

In most taxa that have both a modified spigot (MS) and PC on the PLS the PC flank the MS (Figs. 59D, 96D). In *Badumna* (Fig. 87D), *Phryganoporus* (Fig. 87B) and *Amaurobius* (Fig. 88D) one PC spigot shares a common base with the MS.

103. PLS apical segment: **(0)** domed to conical; **(1)** elongate.

Most of our exemplars have PLS apical segments that are domed (Fig. 4D), conical (Figs. 40D, 44A, 69D, 72D) or flattened (Figs. 7A, D, 11A). The PLS apical segments of oecobiids are elongate (Figs. 27A, D, 30A). This was character 92 in Griswold et al. (1999) except that domed and conical are no longer distinguished. Upon including more taxa we found that we could no longer code domed and conical segments as distinct states.

104. PLS apical enlarged seta: **(0)** absent; **(1)** present.

Among the phyxelidids the Phyxelidini and Vidoliini have a characteristic, stout seta laterally on the PLS (Fig. 49D). We did not find this seta in *Vytfutia*, though it may have been broken off in our specimen. Such setae are lacking in our other exemplars (Figs. 64A, 69D).

MALE GENITALIA.—Some past phylogenetic studies of spiders, e.g., Coddington (1990b), considered any apophysis on the male palpal tibia to be homologous to the RTA (retrolateral tibial apophysis). Our coding recognizes that a single tibia may have apophyses on as many as four surfaces (prolateral, dorsal, retrolateral and ventral) and that these may occur in a great variety of combinations. We therefore divide the male tibial apophyses into four homology hypotheses (pro-, dorsal, retro- and ventral) and further subdivide some of these in terms of the morphology of the apophysis (e.g., simple or complex) or its origin (e.g., proximal or distal). With regard to apophyses on the tegulum of the male palp, we have arbitrarily chosen to allocate homoplasy in our dataset to the median apophysis rather than to both it and the conductor (Coddington 1990a, Griswold et al. 1998). The embolus is readily identifiable. We code three basic homologies on the bulb in addition to the embolus. If a second apophysis is present, we code it as the conductor (C) (see *Gradungula*, titanocoids and *Aebutina* for exceptions), if a third, the median apophysis (MA), and if a fourth, we code this as an “extra tegular apophysis” (TA) (see characters 126 and 127). We further subdivide each of these homologies in terms of shape, texture, and/or position of origin.

105. Retrolateral tibial process (RTA): **(0)** absent; **(1)** present.

The retrolateral surface of the male palpal tibia may be unarmed (Figs. 166A, 187A) or there may be a spur or projection (RTA: Figs. 175C, 178B, 189B). Although the psechrud *Fecenia* has an RTA, *Psechrus* lacks this (Figs. 167A–B) and we code the RTA as absent.

106. Retrolateral tibial process form: **(0)** simple; **(1)** complex; **(2)** desine incised blade.

The retrolateral surface of the male palpal tibia may have a simple conical spur or blade (state 0; Figs. 175C, 183D, 189A), or two or more (up to four) spurs may arise from the same region (state 1; Figs. 178B, 189B). Desines have a particular configuration of a relatively simple blade, with a deep incision delimiting a narrow more dorsal process (state 2; Fig. 177E; Forster 1970: fig. 52).

107. Ventral tibial process (VTA): **(0)** absent; **(1)** present.

The ventrolateral surface of the male palpal tibia may be unarmed (Figs. 166A, 178C) or there may be a spur or projection (VTA: Figs. 179F, 182A, D, 192A–C). We also consider the large, rounded bumps in *Araneus* and *Mimetus* as potential homologues.

108. Dorsal tibial process (DTA): **(0)** absent; **(1)** apical; **(2)** proximal.

The dorsolateral surface of the male palpal tibia may be unarmed (Figs. 166A, 177A) or there may be a spur or projection (DTA). That process may be near the apex of the segment (“apical”: e.g., *Phyxelida*, Figs. 173A–B, *Titanoeca*, 174C) or arise near the base (“proximal,” e.g., *Megadictyna*, Figs. 171A–C, *Nicodamus*, Figs. 172A–C, *Dictyna*, Figs. 176D–E, *Maniho*, Fig. 180C). The proximal process may be simple (Fig. 178E) or surmounted by stout setae (Fig. 176B).

109. Dorsal tibial process form: **(0)** simple; **(1)** complex, folded.

The dorsal process may be simple (Fig. 178E) or inrolled (Fig. 173B) (state 0: “simple”) or be complexly folded (state 1: Figs. 174C, E) as in the Titanoecidae.

110. “Nicodamid” DTA **(0)** absent; **(1)** present.

The nicodamids *Megadictyna* (Figs. 171A, C) and *Nicodamus* (Figs. 172A–C) have a unique type of DTA that arises basally and forms a broad, sweeping curve.

111. Prolateral tibial process (PTA): **(0)** absent; **(1)** present.

The prolateral surface of the male palpal tibia may be unarmed (Figs. 166A, 172B) or there may be a spur or projection (PTA: Figs. 181B, 182A, 193A).

112. Paracymbium: **(0)** absent; **(1)** present.

The paracymbium is a process arising from the cymbial margin. Absent from most entelegyne families (Figs. 171B, 175C, 182E), the paracymbium is characteristic of the Araneoidea (Figs. 171E–F). *Mimetus* (Fig. 169A) and *Pararchaea* also have paracymbia. We also code a projection from the cymbial margin of *Hypochilus* as a paracymbium (Fig. 166A).

113. Cymbial dorsal scopula: **(0)** absent; **(1)** present.

The dorsum of the cymbium may be clothed with ordinary setae with some interspersed chemosensory setae, similar to leg segments (Figs. 173A, 174C), or may have a dense patch of chemosensory setae (Figs. 167A, 185F).

114. Piriform bulb: **(0)** absent; **(1)** present.

We code as piriform a palpal bulb that has the tegulum and subtegulum fused, lacks processes other than the embolus, and is spindle-shaped (Figs. 166D, 167D). This type is characteristic of the Filistatidae. Other bulbs have additional processes. *Hickmania*, although lacking the conductor and median apophysis, does not have a spindle-shaped bulb and retains clear demarcation between tegulum and subtegulum: we do not code it as piriform.

115. Subtegular locking lobe: **(0)** absent; **(1)** present.

In some taxa the subtegulum has a promarginal lobe on its dorsolateral surface which interlocks with a corresponding lobe on the tegulum (Figs. 186F, 194C) in the unexpanded bulb. At least some taxa with a tegular lobe have no corresponding subtegular lobe (e.g., *Amaurobius*).

116. Tegular locking lobes: **(0)** absent; **(1)** on embolus base; **(2)** on tegulum, far from embolus base.

In some taxa the embolar base has a promarginal lobe on its dorsolateral surface, which interlocks with the subtegulum (Fig. 186F) in the unexpanded bulb (state 1). This lobe may interact with a corresponding lobe on the subtegulum (e.g., in *Tengella*, *Raecius*, *Zoropsis*), but there is no corresponding subtegular lobe in *Amaurobius*, *Macrobnus* and *Zorocrates*. In tengellids, zorocratids, zoropsids and ctenids with embolus fused to the tegulum, this lobe is near the embolic base. In *Zorocrates* (Fig. 186A), which has the embolus articulated by a hematodocha, the locking lobe is a process at the base of embolus; a similar disposition occurs in *Uliodon* (Zoropsidae),

Liocranoides (Tengellidae), and *Xenoctenus* (Zoridae), among others (Ramírez, pers. obs.). A similar lobe, though far from the embolic base (state 2), occurs in *Nicodamus* (Figs. 172A, D).

117. Tegular groove acting as conductor: **(0)** absent; **(1)** present.

In titanoeoids the embolus rests in a complex groove in the tegulum (Figs. 174D, 188A–B).

118. Conductor (C): **(0)** present; **(1)** absent.

If a palpal bulb has one apophysis in addition to the embolus we consider it the conductor. If the bulb has two or three apophysis in addition to the embolus we consider the one that is most closely associated with the embolus to be the conductor. A conductor is present in almost all of the taxa treated here (Figs. 166A, 175A, 182B, 189D). *Hickmania* and filistatids (Figs. 166D, 167D) clearly lack a conductor. We make coding exceptions for the titanoeoids, *Gradungula*, and *Aebutina*. In titanoeoids the embolus rests in a groove in the tegulum (see character 117). Whereas this is not clearly a “process” we code this tegular groove as the conductor for this family. Additional titanoeoid palpal bulb processes are coded as a median apophysis and additional tegular process (see below). Forster et al. (1987) code the small process on the *Gradungula* bulb as a median apophysis, not as a conductor, and we follow this interpretation. The tegulum of *Aebutina* has only a flexibly attached process that arises far from the embolus and resembles the median apophyses of other exemplars (Figs. 169C–D). In this case we code the conductor of *Aebutina* as absent.

119. Conductor position: **(0)** subterminal; **(1)** terminal; **(2)** central.

Hypochilus (Fig. 166A), *Archaea* (Fig. 168A, D), *Huttonia*, *Pararchaea*, and the eresids (Fig. 170D) have the tegular sclerites, which we code as conductors, at the apex of the bulb (state 1). In most other exemplars that have conductors, these originate laterally, or basally on the bulb (state 0). A few terminals have a simple, median lobe in the center of the bulb, which is coded as “central” (state 2: Figs. 171B, D, 178D).

120. Conductor and embolus: **(0)** separate; **(1)** conductor embraces embolus.

Many conductors wrap, cradle or embrace the embolus for part or all of its length (Figs. 166B, 170D, 172A, 175A, 179D–E, 189D).

121. Conductor types: **(0)** sclerotized, relatively simple; **(1)** dictynid posteriorly directed; **(2)** desid-amphinectid type, hiding most embolus; **(3)** complex, large, with many processes; **(4)** hyaline.

We have distinguished a few morphological types of conductors, among the wide variety of known shapes, dispositions and textures of conductors. Sclerotized conductors that are little different in texture and color from the cuticle of the bulb from which they arise, and are relatively simple, are all lumped in state 0 (e.g., Figs. 166B–C, 170B, 171D–E, 179B, 180A, 187A–B). We have indentified the conductor in *Archaea* as the sclerotized ridge that spirals around a central pit that contains the embolus and median apophysis (Fig. 168D). *Huttonia* has an almost piriform bulb. The embolus is a short apical spine accompanied by a small pointed process that we code as a simple conductor (Forster and Platnick 1984: figs. 350–352). The “dictynid” type (state 1) has a long groove that embraces most of the embolus, and the apex is characteristic in turning back proximad, in most species extending proximad of the base of the bulb (Figs. 175A–B, D); the conductor apex may be straight, curved, or form a spiral. We call the “desid-amphinectid” type of conductor (state 2) one that is hypertrophied and accompanies the embolus from its origin, is highly convoluted, and with a membranous furrow that hides the embolus for much of its trajectory (Figs. 178A, C); extreme developments of this kind of conductor occur in *Desis* and *Metaltella* (see character 122). The conductors of araneids (Fig. 171E), mimetids, *Pararchaea*, uloborids, and oecobiids are large, complex articulate structures with many processes (state 3). Oecobiid palpal bulbs have 3–4 processes in addition to the embolus; by default one of these is coded as conductor (one of the TA’s

in *Uroctea*, Figs. 170A or 187B, or in *Oecobius*, Fig. 170C). The tegulum of *Mimetus* has several sclerotized processes including an anterior ridge with groove for the embolus, a subapical hook, two small median teeth, and two broad retrolateral flanges (Figs. 169A–B); one of these TA is the conductor. The apex of the *Pararchaea* tegulum has a “complex distal plate” (Forster and Platnick 1984: fig. 237) with two flanges, a hook, and a broad scaly surface. The hyaline conductor (state 4) presents a characteristic, stereotyped morphology. It is membranous in texture, transparent or translucent, strongly contrasts to the texture of the nearby tegular cuticle (Fig. 193A), is fan-shaped, arises from the retroapex of the bulb, and opposes the embolic tip (Fig. 185E). *Psechrus* has a sclerotized conductor but *Fecenia*, another psechrid, has a hyaline conductor like that of other Lycosoidea.

122. Embolus origin: (0) exposed; (1) internal to complex conductor.

In Metaltellinae and in *Desis* the conductor is greatly developed, forming much of the exposed structure of the copulatory bulb. The origin of the long embolus is entirely hidden in intricate membranous loops of the conductor, and it is only visible by transparency, or by breaking through the conductor (Figs. 190A–B, 191A–B).

123. Median apophysis (MA): (0) present; (1) absent.

If a palpal bulb has two apophyses in addition to the embolus (i.e., three apophyses) and one fits the criteria listed above for conductor (e.g., embracing embolus, hyaline fan opposing embolic apex, etc.), we code the other as a median apophysis. This is typically the farthest apophysis from the embolus origin. Many taxa have a median apophysis (Figs. 166B, 171E, 178A) but this process is typically absent in filistatids (Fig. 166D), eresids (Fig. 170D), deinopids (Fig. 171D), *Megadictyna* (Fig. 171B), dictynids (Fig. 175A), and our stiphidiid exemplars (Fig. 179E). Although the psechrid *Fecenia* has a median apophysis, this is lacking in *Psechrus* (Fig. 167C). Forster et al. (1987) code the small process on the *Gradungula* bulb as a median apophysis. Among the several fixed, sclerotized processes on the tegulum of *Mimetus* we code one as median apophysis. *Archaea* has a hooked MA within the crescent-shaped conductor (Fig. 168D).

124. Median apophysis shape: (0) convex; (1) concave.

Median apophyses exhibit a great variety of origins and shapes including being swollen or resembling cones or blades (state 0 “convex”: Figs. 171E, 188B). We code as a separate state those that have one surface concave or excavate (state 1 “concave”; Griswold 1993: figs. 8,26).

125. Median apophysis attachment: (0) fixed; (1) flexibly attached.

The median apophysis may be fixed to the tegulum (state 0: Figs. 166B, 170B, 178D) or have a characteristic, flexible attachment (state 1: Figs. 171E, 187A, 188C, 193A–C). The median apophysis may be moved at this articulation.

126. ‘Extra’ tegular processes (i.e., in addition to conductor and median apophysis): (0) absent; (1) present.

Many taxa have only the standard conductor and median apophysis (Figs. 166B, 173C, 178A, D). If a palpal bulb has a third apophysis in addition to the embolus (i.e., at least four apophyses) we code that bulb as having a conductor, median apophysis and “extra tegular apophysis” (TA: Figs. 180B, 193A, 194B–C). Deciding which apophysis is which may be problematic. In most cases the conductor is associated with the embolus. Median apophysis assignment may be based on similarity in form and position to the median apophyses in taxa without extra apophyses. The remaining apophysis, without special similarity to conductor or median apophysis, is by default the “extra tegular apophysis”. There may be more than one extra tegular apophysis. In some taxa, e.g. *Xevioso* (Fig. 170B) or *Mimetus* (Fig. 169B) no special similarities enable us to distinguish one of the four tegular apophyses as the median apophysis, yet we code it as present by default. Others, e.g., oecobiids, are even more problematic. These bulbs have several apophyses in addition to the

embolus (Figs. 170A, C, 187B), but none can be chosen over others as median apophysis or conductor, and these, as well as extra tegular apophyses, are coded by default.

127. ‘Extra’ tegular process form: **(0)** conical; **(1)** sclerotized tegular process (STP); **(2)** membranous (MTP).

We distinguish extra tegular apophyses based on their shape and texture. A variety of apophyses are conical (Figs. 170B–C, 180B), and, although they differ among themselves, we cannot subdivide this state (state 0). The STP (sclerotized tegular process, state 1) typical of amaurobiids and zorocratids is a sclerotized plate or blade that arises near the embolic base (Figs. 181A, 182B–C, 185A). Finally, in *Zoropsis* there is a translucent process (state 2, “membranous”) that resembles the STP in origin but differs in texture (Fig. 185E).

128. Palpal tarsus M29 muscle: **(0)** present; **(1)** absent.

Huber (1994, *in lit.*) studied the distribution of muscles that attach to the male palpal bulb. The claw flexor, termed “M29” by Ruhland and Rathmeyer (1978), originates at the palpal tibia and attaches to the basal part of the genital bulb (Fig. 167D). Huber noted the presence of the M29 muscle in *Liphistius*, Mygalomorphae, Haplogynae (except *Oonops*) and *Palpimanus*, and its absence in all entelegynes. Huber (*in lit.*) examined many of our exemplar families including filistatids, oecobiids, eresids, deinopids, uloborids, araneids, dictynids, neolanids, stiphidiids, amphinctids, and amaurobiids and we code our exemplars according to his observations, even if he examined genera different than ours. After Huber’s examination of *Palpimanus*, we code the M29 present in *Huttonia*. We observed cuticular apodemes in the palp of *Kukulcania hibernalis* that seem to correspond to these muscles (Fig. 167D); however Huber (*in lit.*) made sections of the palp of *K. hibernalis* and concluded that the M29 is absent.

129. Palpal tarsus M30 muscle: **(0)** present; **(1)** absent.

Huber (1994, *in lit.*) studied the distribution the claw extensor, termed “M30” by Ruhland and Rathmeyer (1978), which originates at the cymbium and attaches to the basal part of the genital bulb (Fig. 167D). He noted that the M30 is present in lower araneomorphs and absent from entelegynes except *Uroecobius* (Oecobiidae), *Tama* and *Hersilia* (Hersiliidae), *Palpimanus*, *Mecysmauchenius* and *Argyroneta*. Because *Palpimanus* is presumably closely related to *Huttonia*, we code the M30 present in the latter. Although the M30 is present in *Uroecobius*, Huber (1994) notes its absence in both *Oecobius* and *Uroctea*.

FEMALE GENITALIA.— All characters were scored by observation of exemplars.

130. Female genitalia: **(0)** haplogyne; **(1)** entelegyne.

Hypochilids, austrochiloids, filistatids, huttoniids and archaeids lack a separate fertilization duct connecting the spermathecae with the oviduct (state 0, haplogyne) (Figs. 164B, E); all other exemplar taxa have a fertilization duct (state 1, entelegyne) (Figs. 164D, F).

131. Epigynum: **(0)** absent; **(1)** present.

We code as an epigynum any sclerotized modification of the cuticle around the female genital region. Epigyna are typical of entelegyne spiders, but we also code the female genital sclerotization of *Thaïda* as an epigynum. The genital areas in *Hickmania* and *Gradungula* are almost identical to *Thaïda* except for the sclerotization, so we also code these as an epigynum. The palpi-manoids *Archaea* and *Huttonia* lack epigyna but *Mimetus* and *Pararchaea* have epigyna.

132. Epigynum teeth: **(0)** absent; **(1)** present.

Among taxa with epigyna several have paired conical structures arising from the lateral lobes. These may be short or long (Fig. 180D). We code *Raecius* as having teeth although this varies within the genus: *Raecius asper* and *R. jocquei* have teeth but *R. congoensis* lacks them. Many other entelegynes lack teeth (Figs. 164C, 170E).

133. Oecobiid spermathecae: **(0)** absent; **(1)** present.

The entelegyne female genitalia of oecobiids are unique in comprising a copulatory duct that leads to an anterior large, membranous sac, from where another long, sclerotized duct runs to the posterior margin, where the fertilization ducts discharge. In addition *Oecobius* has a membranous sac at the base of the fertilization duct (Baum 1972). This character is inapplicable to haplogynes.

134. Convolute vulval ducts of amphinectid type: **(0)** absent; **(1)** present.

Amphinectid spiders such as *Maniho* and *Metaltella* have characteristic, complex vulvae in which the copulatory ducts make at least three anterior-posterior switchbacks (e.g., Fig. 164F; Forster and Wilton 1973: figs. 531, 534). Most entelegyne taxa treated here have simple lobate vulvae, vulvae with spirals, or with fewer switchbacks (state 0). *Matachia* also has a complex vulva (Forster 1970: figs. 61–65), which we code like the amphinectid vulva (state 1).

135. Gonopore separated from the epigastric fold: **(0)** absent; **(1)** present.

In the austrochiloids *Gradungula*, *Hickmania* and *Thaida*, the gonopore is externally visible in the projecting genital area (Fig. 163A), while in other spiders the opening is hidden in the epigastric fold. In austrochiloids the epigastric fold leads to a blind pocket (the postepigastric fold, Figs. 163A–D), where the strong longitudinal muscles VIII and IX attach (see Millot 1936). Forster et al. (1987) described this posterior structure as a receptacle, but besides having some powerful muscles attached, it lacks any feature commonly associated with sperm receptacles (e.g., a constriction followed by a large lumen, or glandular pores). This invagination is quite general for spiders, but similarly developed posterior extensions were found in palpimanid spiders (Platnick et al. 1991) and by Ramírez (pers. obs.) in several other spiders, including liphistiids, gradungulids, mimetids, and corinnids. This has formerly been coded as a “posterior receptaculum” in Platnick et al. 1991.

SILK.— Silk ultrastructure data are taken from the discoveries and summary in Eberhard and Pereira (1993), from unpublished observations by Carlson (*in lit.*), and from our own observations. Terminology follows Peters (1987) with modifications by Eberhard and Pereira (1993).

136. Cribellate silk axial lines: **(0)** present; **(1)** absent.

Axial lines are the straight thicker fibers associated with the cribellum fibrils (Figs. 120A–C, 121C–D, 122A, 123A, 124A). They are present in most of our exemplars for which data are available, being absent only in *Matachia* and dictynids (Figs. 120E–F).

137. Cribellate silk reserve warp: **(0)** present; **(1)** absent.

Reserve warp lines are the highly-curved or undulating thicker fibers associated with the cribellum fibrils (Figs. 120E–F, 121C–D, 122A, 123A, C, 124A). Reserve warp is present in most of our exemplars for which data are available, being absent only in *Hickmania* (Figs. 120A–C), uloborids (Fig. 120D), *Matachia* and some dictynids.

138. Cribellate silk nodules: **(0)** absent; **(1)** present.

Cribellar fibrils of most Neocribellatae have nodules along their length (Figs. 118B, D). Among taxa studied nodules are lacking only in *Hypochilus* and filistatids (Fig. 118F).

139. Cribellate silk: **(0)** uniform; **(1)** puffed.

The cribellate band is made of up foundation lines (e.g., reserve warp, axial lines) and a mass of numerous, fine cribellar fibrils. In most cribellates the lateral margins of this band are uniform or entire (Figs. 120A, 121C, 123A, 125A). Austrochilids (Figs. 118A, C), uloborids (Figs. 119A–B), deinopoids (Fig. 120D), *Matachia* and dictynids (Fig. 120E) have the edges of the cribellate band with regular puffs. This character is inapplicable for the cribellate bands of filistatids, which are very differently constructed and heavily folded (Fig. 118E, Eberhard and Pereira 1993).

BEHAVIOR.— Behavioral observations were made on living animals in the field or lab. Except where references are cited, these are our personal observations.

140. Web posture: **(0)** inverted; **(1)** erect.

We code this based upon the movement of the spider on the web. We have observed the scored taxa in the field and/or in captivity. Most spiders with space webs or sheet webs hang beneath them (state 0: “inverted”), although some sheet web builders walk on the web, e.g. *Tengella. Tengella*, as well as spiders that have their webs appressed to the substrate and walk on the web, are coded as “erect” (state 1).

141. Combing leg support: **(0)** fixed leg III; **(1)** mobile, braced leg IV.

Eberhard (1988) identified two ways in which spiders spin cribellate silk. In hypochilids and filistatids the combing leg was supported by the contralateral leg III, which was held immobile or nearly so (state 0: “fixed leg III” or “stereotyped combing type 1”); this combing behavior was recently observed for *Filistata insidiatrix* by one of us (M. Ramírez) in specimens from Siena, Italy (Figs. 196D–E). Other cribellates support the combing leg with the other leg IV and move both legs synchronously (state 1: “mobile, braced leg IV” or “stereotyped combing type 2”) (Figs. 205B, 208D). The combing behavior of *Thaidia* has recently been observed by Lopardo et al. (2004): its combing leg is braced by a mobile leg IV.

142. Orb web architecture: **(0)** absent; **(1)** present.

The orb web is characteristic of Orbiculariae (Figs 201A–C).

143. Deinopid web architecture: **(0)** absent; **(1)** present.

Deinopids make a highly modified orb web with sticky cribellate capture silk held by the first two pair of legs (Figs. 200C–D).

144. Frame construction: **(0)** absent; **(1)** present.

Frame construction is one of the components of the behavior sequence in spinning orb webs and is characteristic of Orbiculariae.

145. Radius construction: **(0)** absent; **(1)** present.

Orb weavers make radii according to stereotyped behaviors, which are absent in non orb weavers.

146. Radius construction behavior: **(0)** cut and reeled; **(1)** doubled.

Eberhard (1982) described several ways in which orb weavers lay and connect radii; these behaviors are phylogenetically informative (Coddington 1990a, Hormiga et al. 1995). Most orbicularians cut and reel radii as they are being laid. The spider moves along a pre-existing radius to a vacant spot on the frame, laying out a new line behind. The spider attaches this radius to the frame, and returns to the hub spinning a new radial line. As the spider returns to the hub on the radial line just laid, this radial line is cut, reeled up, and eaten so that the dragline behind forms the only radial line. The result is only one radius for a pass from hub to frame and back (state 1: “cut and reeled”; Eberhard 1982: character F1). Uloborids cut and reel to make frames, but omit cutting and reeling when spinning radii. However, like orbicularians other than nephiline tetragnathids, they attach radii only once to the frame. The result is that uloborid radii are double, with one line laid on the way out and one on the return (state 2: “doubled”; Eberhard 1982: character F4).

147. Hub construction: **(0)** absent; **(1)** present.

Hub construction is one of the components of the behavior sequence in spinning orb webs and is characteristic of Orbiculariae.

148. Temporary spiral construction: **(0)** absent; **(1)** present.

Temporary (non sticky) spiral construction is one of the components of the behavior sequence in spinning orb webs and is characteristic of Orbiculariae.

149. Sticky spiral construction: **(0)** absent; **(1)** present.

Sticky spiral construction, in which threads of flagelliform gland silk are coated with glue from aggregate glands (Figs. 119C–E), is one of the characteristic components of the behavior sequence

in spinning orb webs and is characteristic of Orbiculariae.

150. Sticky silk localization: **(0)** absent; **(1)** present.

Orb weavers use their legs to locate themselves during sticky spiral construction. This behavior has not been observed in spiders that do not make orb webs.

151. Sticky silk localization, type: **(0)** outside leg I; **(1)** inside leg IV.

Eberhard (1982) first pointed out the phylogenetic significance of the different legs used by orb weavers to locate themselves during sticky spiral construction, and systematists have emphasized it ever since (e.g. Coddington 1986a, 1990a, Hormiga et al. 1995). Araneids and uloborids use the outside first leg (away from the hub) to touch the previous sticky spiral before attaching the current segment (state 0). *Deinopis* use the inside fourth leg (towards the hub) (state 1).

152. L4 shift switch during sticky silk construction: **(0)** absent; **(1)** present.

See Coddington (1986a), character 82 in Coddington (1990a) and character 58 in Coddington (1990b).

153. Non-sticky line grip: **(0)** otherwise; **(1)** with leg IV.

See Coddington (1986a), character 81 in Coddington (1990a) and character 57 in Coddington (1990b).

154. Prey wrapping with legs IV: **(0)** absent; **(1)** present.

Many spiders wrap their prey (Fig. 198F) with alternate movements of legs IV, including *Thaida*, filistatids, Orbiculariae, *Oecobius* (Eberhard 1967), *Megadictyna* and phyxelidids. Other spiders have not been observed to wrap. We code this behavior only for those taxa that we have observed in the field or in captivity catching prey and feeding upon it, or for which the behavior is detailed in the literature. Eberhard (1982) referred to this behavior as “attack wrap without rotation in the web” (his character I3).

DISCUSSION

Many of the representatives and characters in this study were used in previous analyses (Coddington 1990a, 1990b; Platnick et al. 1991 [Fig. 209]; Griswold 1993 [Fig. 215]; Griswold et al. 1998 [Fig. 211]; Griswold et al. 1999 [Fig. 212]; Schütt 2000, 2002 [Fig. 210]; Silva Dávila 2003 [Fig. 214]; Raven and Stumkat 2005 [Fig. 215]). Whereas common themes emerge, the phylogenetic hypotheses obtained in those studies are also significantly different from one another, suggesting that we are not yet reaching robust solutions, and that future studies will differ as well (*cf.* Miller 2003). We choose to emphasize the documentation of observations, fundamentally with images, and the conceptualization of homology hypotheses through a wide range of taxa, rather than in trying to produce highly elaborate but ephemeral phylogenetic hypotheses. Our experience in doing this study is that a collection of high-resolution digital images permits a level of analysis and possibilities for discussions that were impossible without this technology. We make available full-resolution versions of the images contained in this study at http://www.calacademy.org/research/entomology/Entomology_Resources/Arachnida/Atlas_of_Entelegynae.htm.

In Figures 218 and 219 we present several indices related with the support of groups. All of them measure different properties of the dataset, and are generally correlated, although imperfectly. For example, although Eresoidea is found through the whole space of the analysis parameters explored, its Bremer support and resampling frequencies are very low. More importantly, our results indicate that all groups highly dependent upon specific conditions of the analysis are also weakly supported for the other estimators, thus downplaying the importance of the selection of a specific method of analysis.

Character Systems and Homoplasy Levels

The homoplasy levels are homogeneously widespread across all character systems (Fig. 220D), except for behavior and the internal anatomy characters from non-cuticular structures, two character systems difficult to record. Their high congruence indices are seemingly related to the elevated proportion of missing or inapplicable entries (Fig. 220A). We diverged from previous analyses (Platnick et al. 1991; Griswold et al. 1999) in not assuming character distributions for the classic characters of internal anatomy. The high proportion of missing entries illustrates a real situation of a much-neglected field of study. When these characters are more adequately sampled, they may show that they have similar levels of homoplasy as any other character system.

Many of our behavioral characters are specific to orb weavers, represented in this dataset by only five representatives in three families. Most of the problematic taxa that interfere with the resolution of orbweavers in this analysis (fundamentally, Palpimanoidea and the nicodamids) do not spin webs, or their spinning behavior has never been observed in detail. The weak support for orb weavers is not due to the missing data, because the results are insensitive to the replacing of missing entries by zeroes in the characters for orb web details (characters 144–153). However, replacing the inapplicable scorings by zeroes in characters 144–153 results in an equal weights tree with Palpimanoidea sister to orbweavers, and Nicodamidae sister to all of them (Fig. 218C), thus approximating the strategy and results of Platnick et al. (1991). We no longer endorse such an approach here.

Groups

NEOCRIBELLATAE.—The monophyly and synapomorphies of Neocribellatae (all Araneomorphae except *Hypochilus*, Fig. 212) are not tested here. Compared to Mesothelae, Mygalomorphae and *Hypochilus* (Haupt and Kovoov 1993; Goloboff 1995), the Neocribellatae evolved a greater diversity of gland spigots on the posterior spinnerets, including paracribellar and minor ampullate gland spigots.

ARANEOCLADA.—The Araneoclada were defined by Platnick (1977:8) for a large group of spiders believed to have 3 pairs of heart ostia and a straight midgut, comprising most of the Araneomorphae (Fig. 212). Equal weights (Fig. 216) and implied weights (Fig. 217) both refute the Araneoclada. The haplogyne spiders are placed as the basal Neocribellate group. Lopardo et al. (2004) already discussed challenging evidence favoring a more basal placement of Filistatidae, outside of Araneoclada (e.g., an M-shaped intestine and traces of posterior booklungs in Filistatidae, Type 2 combing behavior in Austrochilinae). We continued finding evidence in conflict with a monophyletic Araneoclada in this study (e.g., the presence of cylindrical gland spigots in Austrochilidae). Our results are novel in the placement of the representatives of Haplogynae (Segestriidae and Filistatidae) in a more basal position relative to Austrochiloidea. Although we should expect some artificial results from a shallow sampling of such a large and diverse group as Haplogynae, this result clearly indicates that the basal clades of Araneomorphae are far from satisfactorily resolved.

AUSTROCHILOIDEA.—This taxon was proposed by Forster et al. (1987) and corroborated by the quantitative analyses of Platnick et al. (1991 [Fig. 209]) and Griswold et al. (1999 [Fig. 212]). Both equal weights and implied weights support Austrochiloidea, comprising Austrochilidae and Gradungulidae. Our reinterpretation of the female genitalia of austrochiloids renders additional support to the group (the well exposed female gonopore). However, this reinterpretation undermined the support for Austrochilidae, because we identified their “posterior receptacle” as a simple cuticular fold generally found in other Araneomorphae. Also novel is the finding of sexually

dimorphic spigots on the posterior spinnerets of austrochilids. We identify these as cylindricals, previously thought to be restricted to entelegynes. The spinning organs of adult cribellate gradungulids were never examined with SEM. The micrographs of immature *Macrogradungula* in Platnick et al. (1991, figs. 297–304) show a pattern of spigots similar to that found in *Gradungula* (the ALS), and *Hickmania* and *Austrochilus* (PMS and PLS), thus it is unlikely that the examination of the adult spinnerets of cribellate gradungulids will produce any radical change in the resolution of Araneoclada or Austrochiloidea. In our analysis Austrochilidae is not monophyletic, implying an unlikely convergence in the acquisition of booklungs in *Gradungula* and *Hickmania*.

ENTELEGYNÆ.— This group is well established (Figs. 209, 212) and is corroborated by our analysis (Figs. 216–217). The entelegyne condition has seemingly reversed to secondary haplogyny in several taxa (e.g., some Tetragnathidae and Anapidae, all ‘palpimanoids’ except *Holarchaea*, *Pararchaea* and *Mimetus*). We know of only one well-documented convergence to the entelegyne condition, in pholcids of the genus *Metagonia* (Huber 1997). Our analysis under equal weights is consistent with this hypothesis, but under implied weights the palpimanoids *Huttonia* and *Archaea* are placed more basally (thus implying primary haplogyny), while *Pararchaea* and *Mimetus* remain with araneoids. A broader sampling of palpimanoids should shed more light on this problem.

ERESOIDEA.— Eresidae and Oecobiidae were first associated by Platnick et al. (1991 [Fig. 209]) and this grouping was corroborated by Griswold et al. (1999 [Fig. 212]). Equal, successive and implied weights all support this clade in our new analysis (Figs. 216–219). A distinctive characteristic of Eresoidea is the several major ampullate spigots dispersed among the piriform field. *Oecobius*, with only one MAP spigot is an exception, probably associated with its very small size.

CANOE TAPETUM CLADE.— This group was first suggested in the analysis of Platnick et al. (1991) and named by Griswold et al. (1999 [Fig. 212]). The clade is not recovered in our analysis, due to ambiguous placement of the Eresoidea and Orbiculariae.

ORBICULARIAE AND PALPIMANOIDEA.— Two issues about orb weaving phylogeny have been heatedly debated: the origin of orb webs, and the placement of certain non orb weavers within Araneoidea. The first issue had lost its original momentum. After the detailed works of Eberhard (1982) and Coddington (1986a–b), who closely examined the sequences and stereotyped movements that orb weavers use to make their webs, there has been little questioning of the common origin of orb webs. It surely influenced this debate that the hypotheses of repeated convergence in complex ‘adaptive’ traits are not as central to evolutionary debates as was the case years ago. It is nowadays accepted that the cribellate Deinopoidea (Deinopidae and Uloboridae) are the sister group of the ecribellate Araneoidea. As for the second issue (the non orb weaving araneoids), the detailed morphology of the silk spinning organs provided rich support to the affiliation of some non orb weaving families in Araneoidea (Coddington 1989; Griswold et al. 1998 [Fig. 211]), and it seems clear that the orb web was modified or lost several times in the evolution of Orbiculariae (e.g., in Deinopidae, Theridiidae, Linyphiidae, Nesticidae, cyatholipoids and several symphytognathoids). Our analysis does not solve the placement of Palpimanoidea, but none of the trees obtained under the several explored weighting schemes implies a convergence in the orb web.

Schütt (2000, 2002, 2003) recently argued that micropholcommatids and textricellids, previously considered palpimanoids, have the spigot characters typical of symphytognathoids. However, the placement of Mimetidae and other “palpimanoids” (e.g., Archaeidae, Pararchaeidae, Malkaridae) has remained controversial. Schütt (2000, 2002) suggested that Mimetidae, Pararchaeidae and Malkaridae belong with the Araneoidea (Fig. 210). Our analyses concur, also suggesting that at least some “palpimanoids” nest within the Orbiculariae. Implied weights places entelegyne palpimanoids with paracymbia (i.e., Mimetidae and Pararchaeidae) sister to Araneoidea

(Fig. 217). Equal weights and successive weights place all palpimanoids, including the haplogyne Archaeidae and Huttoniidae, closely related to Araneoidea (Fig. 218, when nicodamids are removed, Fig. 219B). The more basal position of *Archaea* plus *Huttonia* suggested by implied weights (Fig. 217) is interesting, because it implies primitive, instead of secondary haplogyny. It is worth noting that Forster (in Forster and Platnick 1984) argued that archaeids are primitively haplogyne and that their peculiar posterior respiratory system evolved directly from booklungs, a scenario plausible given the placement of archeids under implied weights. On the other hand, this placement may be simply an artifact due to shallow taxon sampling.

The Palpimanoidea traditionally included only the families Huttoniidae, Palpimanidae and Stenochilidae, all haplogyne families having characteristic brushes of setae on the tarsi and metatarsi of legs I and II. Foster and Platnick (1984) enlarged and radically redefined the Palpimanoidea, adding to the three traditional families the Mimetidae, Micropholcommatidae, Tetricellidae, Archaeidae, Mecysmaucheniidae, Pararchaeidae, Holarcheidae, and later (Platnick and Forster 1987) the Malkaridae. Palpimanoidea has remained one of the most controversial hypotheses in spider classification. This concept of an enlarged, monophyletic Palpimanoidea survived the quantitative test of Platnick et al. (1991), but not those of Schütt (2002, 2003), and our results are ambiguous.

It seems clear that an adequate test of the limits of Araneoidea and Palpimanoidea should include not only numerous representatives of both superfamilies (comprising 32 families in total), but also sufficient outgroup representatives to leave room for the contentious taxa to be placed elsewhere. The affiliation of palpimanids and archaeids with eresids, and of *Nicodamus* with mimetids in Schütt (2002) seems indicative of undersampling of outgroup taxa. Conversely, the alternative placements of Huttoniidae and Archaeidae in our implied and equal weights analyses suggest the effect of undersampling of araneoids and palpimanoids.

OUTGROUPS TO ORBICULARIAE.— Identifying the phylogenetic intermediates between orb webs and ‘sheet’ or ‘irregular’ webs is the holy grail in understanding the evolution of spider webs, hence the interest in knowing the closer relatives of orb weavers. Some preliminary results (Griswold et al. 1999) suggested that nicodamids are good candidates because of the serrate accessory claw setae and entire cribellum found in *Megadictyna*, resembling those of orb weavers and deinopoids, respectively. In a reexamination of our representatives we found that serrate accessory claw setae are more widely distributed than previously thought, even in spiders with plumose setae (e.g., Austrochilidae, *Megadictyna*), or in spiders that do not use webs to capture prey (Hersiliidae, not shown). *Nicodamus*, an ecribellate Nicodamidae, only has slightly serrate accessory claw setae, which we coded as uncertain (scoring them absent produces the collapsing of Deinopoidea in the equal weights analysis). Our equal weights analysis concurs with that of Griswold et al. (1999 [Fig. 212]) in placing Orbiculariae (including Palpimanoidea) as sister group of all entelegynes other than Eresoidea (Fig. 218, nicodamids removed), but under implied weights (Fig. 219), eresoids and orb weavers are sister groups feebly supported by having the PLS modified spigots at least slightly segregated from the spinning field.

NICODAMIDAE.— Cribellate and ecribellate nicodamids are quite heterogeneous in general morphology. In our dataset they appeared monophyletic only under successive and implied weights (with low support), united by the branched median tracheae and a proximal, curved dorsal process on the male palpal tibia. Harvey (1995) proposed the absence of trichobothria on metatarsus IV as a further synapomorphy of the family, but we have not explored trichobothrial patterns in much detail. Under equal weights, both nicodamid representatives swap around orb weaver groups and their two contiguous branches (Fig. 218).

DIVIDED CRIBELLUM CLADE.— This clade, first recognized by Griswold et al. (1999 [Fig.

212]) includes the derived entelegynes beyond Nicodamidae, and is found here under equal and implied weights (Figs. 216–217), but with low support. The cribellum seems to have transformed from entire to divided at least three times (also in Eresoidea and Filistatidae), and secondarily to entire in some members of the RTA clade.

TITANOECOIDS.— Griswold et al. (1999 [Fig. 212]) proposed this clade for the Titanoecidae plus Phyxelididae. Implied and successive weights produces this grouping (Fig. 219), but with very low support and only under two concavities of the weighting function. Under equal weights (Fig. 218) Phyxelididae and Titanoecidae are successive outgroups to the numerous families comprising the RTA clade.

RTA CLADE.— Coddington and Levi (1991) proposed this group for those spiders having an apophysis in any position on the male palpal tibia. We have scored separately the ventral, dorsal, prolateral and retrolateral processes. This more restrictive RTA clade, comprising taxa with a retrolateral tibial apophysis, was found in the analysis of Griswold et al. (1999 [Fig. 212]). The RTA clade is supported under equal and implied weights (Figs. 218–219), by the RTA itself, and by the increased number of trichobothria on appendages.

AMAUROBIIDAE.— We no longer recover a clade of Amaurobioids (all RTA clade except Dictynidae, Fig. 212). Amaurobiidae itself is problematic under equal weights (because of the macrobunines *Macrobunus* and *Retiro*), though at least a core Amaurobiidae comprising the type genus *Amaurobius* plus *Callobius* and *Pimus* is found (Fig. 216). Under implied and successive weights (Fig. 217) Amaurobiidae is supported by having multiple male palpal tibial processes and an additional tegular sclerite other than conductor and median apophysis. Besides *Macrobunus*, the representatives *Pimus* and *Retiro* are also listed in Macrobininae (Lehtinen 1967). However, we expect changes in the composition of Macrobininae. According to ongoing research by Ramírez and Griswold, the closer cribellate relatives of *Macrobunus* all have entire cribella (*Anisacate*, some *Macrobunus* species, plus some undescribed genera). They are grouped with other cribellate macrobunines close to *Macrobunus* by having a stridulatory area on the male palpal cymbium (Figs. 183A–D). Compagnucci and Ramírez (2000) joined the macrobunines *Anisacate*, *Emmenomma* and *Naevius* by the presence of a gland in the male palpal tibia discharging through a dorsal apophysis. It seems likely that Macrobininae will end up diagnosed by having an entire cribellum (when present) and a stridulatory area on the male palpal cymbium; it will include a group of genera with a male palpal tibial gland.

FUSED PARACRIBELLAR CLADE.— This group (FPC) was proposed by Griswold et al. (1999 [Fig. 212]) for some taxa having the PMS paracribellar spigots with two to several shafts arising from a large, common base, i.e., Stiphidiidae, Neolanidae, Agelenidae, Amphinectidae and Desidae (but not Dictynidae). Successive weights and one of the concavities of implied weights (Fig. 219) excludes the Stiphidiidae but newly groups the Dictynidae, which also have fused paracribellar bases, within FPC, sister to some Desidae (*Desis* and *Matachia*). This striking morphology is at least corroborated as a synapomorphy, although for a different collection of taxa.

STIPHIDIIDS.— Griswold et al. (1999) retrieved a clade uniting Neolanidae with Stiphidiidae (Fig. 212), only supported by a reversion to an inverted posture on the web. Our analyses do not support this clade.

AGELENOIDS.— A clade uniting the cribellate agelenid *Neoramia* with desids and amphinectids (Fig. 212) is not recovered in our analysis.

DESIDAE, AMPHINECTIDAE AND DICTYNIDAE.— Both Desidae and Amphinectidae are paraphyletic in our analysis. Under all concavities other than 6 the amphinectid *Metaltella* and the desid *Desis* are sister groups, joined by the internal origin of the embolus. Dictynidae is supported under equal, successive and implied weights, but we do not reproduce the basal position of Dictynidae in

the RTA clade, as found in Griswold et al. (1999 [Fig. 212]). Instead, in our current results Dictynidae is sister to some Desidae (Figs. 216–217).

OVAL CALAMISTRUM CLADE.— Griswold (1993 [Fig. 213]) proposed a clade for those spiders with an oval to rectangular calamistrum, grouping the lycosoids together with zorocratids and tengellids. This clade passed the quantitative test of Griswold et al. (1999 [Fig. 212]). We obtained an oval calamistrum (OC) clade under equal and implied weights (Figs. 216–217). Under implied weights the group is supported additionally by the tegular and subtegular locking lobes.

LYCOSOIDEA.— The Lycosoidea were defined by having a grate-shaped tapetum in the indirect eyes (Homann 1971). This idea was corroborated by the quantitative test of Griswold (1993 [Fig. 213]) and partially corroborated by Griswold et al. (1999 [Fig. 212]), who grouped the Psecridae, Zoropsidae and Ctenidae but excluded the Stiphidiidae. We no longer obtain a monophyletic Lycosoidea (represented by the cribellate Psecridae, Zoropsidae and Ctenidae), although *Zoropsis* and *Acanthoctenus* appear as sister groups (Figs. 216–217).

Our results differ from those of Griswold et al. (1999) and Griswold (1993), and should be considered in the light of the recent analyses made by Silva Dávila (2003) and Raven and Stumkat (2005). Silva Dávila's (2003) dataset included a dense sampling of Lycosoids and their kin and a fairly broad selection of outgroups, including dionychans and amaurobiids, and rooted the analysis with *Megadictyna*. The dataset comprised the seven OC clade representatives included here, most of the representatives considered in Griswold (1993), a denser sampling within Tengellidae and Ctenidae, and many representatives of ecribellate families allegedly linked to lycosoids (Cycloctenidae, Zoridae, dionychans). She also reviewed and used most of the characters of the previous cladistic analyses, including Griswold et al. (1999). Silva Dávila recovered a clade of spiders with grate-shaped tapetum (GST clade), including lycosoids, but also miturgids, zorids, and the OC clade nested within (Fig. 214). She did not recover Tengellidae and Zorocratidae as monophyletic groups. It is interesting that her analysis suggested that *Tengella* and *Zorocrates* are sister groups (Fig. 214), a result mirrored in our analysis for all but equal weights (Fig. 219). Her dataset implies tiny support values for the relations among the higher groups, and the results differ significantly between equal and implied weights; this, together with the differences obtained from a wider taxon sampling, is indicative of high instability in the relations of lycosoids and their kin. It is notable that the grate-shaped tapetum appears to have little phylogenetic value. Our cladograms (Figs. 216–217) and those of Silva Dávila (Fig. 214) and Raven and Stumkat (Fig. 215) all imply considerable homoplasy in this feature.

ZOROCRATIDAE.— Our implied and successive weights analyses concur with Silva Dávila's (2003 [Fig. 214]) in joining *Zorocrates* with *Tengella*, although the support is weak (Figs. 218–219). Raven and Stumkat (2005) used the densest sampling of lycosoids and their kin of any study to date, though their dataset was not as broad as Silva Dávila's or ours. They enlarged the Zoropsidae to include taxa formerly included in the Zorocratidae, which they considered as a subfamily of Zoropsidae (Fig. 215). Their analysis was rooted with *Tengella*, so does not test the possible relationship between *Tengella* and *Zorocrates*. Our analysis did not recover a clade of Zorocratidae, and in the light of the current evidence, it is unlikely that the family is monophyletic. None of the characters proposed to define Zorocratidae by Griswold et al. (1999), i.e., clumped cribellar spigots, male tibial crack, or tibial ventroapical process, occur in *Zorocrates*.

AEBUTINA AND POAKA.— The placement of the mysterious *Aebutina* at the base of lycosoids and allies is very unconvincing. Excluding *Aebutina* from the equal weights analysis is of no consequence, but under implied weights causes *Macrobunus* to join at the base of the OC clade, as occurs in the equal weight analysis. The relationships of *Poaka* remain an open question, only resolved in the implied weights tree, but involving groupings of very low support.

CONCLUSIONS

We are making progress. Whereas some results conflict with previous studies and even within this study, at least some results are robust. The Austrochiloidea, Entelegynae, Eresoidea, and Divided Cribellum, RTA and Oval Calamistrum clades all survived the tests, and may represent true evolutionary groups. The unique origin of the orb web seems assured, though the composition of the Orbiculariae remains controversial. On the other hand, the weak support for other groups, poor phylogenetic performance of many classic characters, sensitivity of results to taxon sampling and generally ephemeral nature of many phylogenetic hypotheses suggest that we still have a long way to go to understand the big picture of spider evolution.

What do we need to make more progress? We probably have adequate methods of analysis. Our results suggest that some groups are robust and some not, regardless of estimator, which downplays the importance of the selection of a specific method of analysis. This in turn suggests that, given adequate taxon sampling and careful character definition and coding, the currently available analytical methods will give robust and meaningful results. Comparative genomics will undoubtedly contribute a huge amount to understanding spider evolution. Indeed, current support from the U.S. National Science Foundation to the “Assembling the Tree of Life: Phylogeny of Spiders” project promises to make DNA data crucial in reconstructing spider phylogeny. But, this should not obscure the continuing importance of “traditional” disciplines. Examination by SEM of cuticular structures has provided hundreds of new and meaningful comparisons. Comparative anatomy of internal soft structures, a field largely neglected since the pioneering work of Millot, Petrunkevitch and Marples in the 1930s through 1960s, deserves rejuvenation. For example, the recent discovery of the primitive M-shaped intestinal configuration in *Kukulcania hibernalis*, which makes sense given that spider’s primitive silk spinning behavior, proves that there are yet valuable insights to be gained by dissecting, sectioning and staining. Conversely, the disappointing behavior of the tapetum (as currently coded) as a phylogenetic character, suggests that reinvestigation of this system is imperative. Field studies of behavior also have much to offer. The discovery of evolutionarily advanced spinning behavior in austrochilines foretold their movement up the spider cladogram. Moreover, behavior is intensely interesting to biologists of all stripes. As we firm up the phylogenetic tree of spiders, the need for behavioral data to map on this tree will grow. Finally, it is clear that denser taxon sampling is necessary. Much of the disconnect between the various phylogenetic studies considered herein may be due to sparse, and different, taxon sampling. This in turn argues that further collecting, especially in inaccessible, undersampled regions, and the continued conservation and study of existing collections, is essential.

Forty years ago Pekka Lehtinen and Ray Forster started a revolution in spider taxonomy. They brought a worldwide perspective to the subject and focused on the tropics and especially the austral regions. This revolution continues, and the importance of taxa and data from the southern hemisphere suggests that a continued focus on the austral regions will be crucial to understanding spider evolution.

LITERATURE CITED

- AKERMAN, C. 1926. On the spider, *Menneus camelus* Pocock, which constructs a moth-catching, expanding snare. *Annals of the Natal Museum* 5:411–422.
- AVILÉS, L. 1993. Newly-discovered sociality in the Neotropical spider *Aebutina binotata* Simon (Dictynidae?). *The Journal of Arachnology* 21:184–193.
- BAUM, S. 1972. Zum “Cribellaten-Problem”: Die Genitalstrukturen der Oecobiinae und Urocteinae (Arach.: Aran: Oecobiidae). *Abhandlugen und Verhandlungen des Naturwissenschaftlichen Vereins in Hamburg*

- (N.F.) 16:101-153.
- BOSSELAERS, J. 2002. A cladistic analysis of Zoropsidae (Araneae), with description of a new genus. *Belgian Journal of Zoology* 132(2):141–154.
- BRISTOWE, W. 1933. The liphistiid spiders. With an appendix on their internal anatomy by J. Millot. *Proceedings of the Zoological Society of London, 1932*:1015–1057.
- BURGER, M., W. NENTWIG, AND C. KROPP. 2003. Complex genital structures indicate cryptic female choice in a haplogyne spider (Arachnida, Araneae, Oonopidae, Gamasomorphinae). *Journal of Morphology* 255:80–93.
- BUXTON, B.H. 1913. Coxal glands of the arachnids. *Zoologische Jahrbücher, II Abteilung für Systematik* 14:231–282.
- CATLEY, K.M. 1994. Descriptions of new *Hypochilus* species from New Mexico and California with a cladistic analysis of the Hypochilidae (Araneae). *American Museum Novitates* 3088:1–27.
- CHAMBERLIN, R.V., AND W. IVIE. 1941. North American Agelenidae of the genera *Agelenopsis*, *Calilena*, *Ritalena* and *Tortolena*. *Annals of the Entomological Society of America* 34:585–628.
- CODDINGTON, J.A. 1983. A temporary slide-mount allowing precise manipulation of small structures. *Verhandlungen des Naturwissenschaftlichen Vereins in Hamburg* 26:291–292.
- CODDINGTON, J.A. 1986a. The monophyletic origin of the orb web. Pages 319–363 in W. A. Shear, editor, *Spiders: Webs, Behavior, and Evolution*. Stanford University Press, Stanford, California, USA.
- CODDINGTON, J.A. 1986b. Orb webs in ‘non-orb weaving’ ocre faced spiders (Araneae: Deinopidae): a question of genealogy. *Cladistics* 2(1): 53–67.
- CODDINGTON, J.A. 1989. Spinneret silk spigot morphology: Evidence for the monophyly of orb-weaving spiders, Cyrtophorinae (Araneidae), and the group Theridiidae plus Nesticidae. *The Journal of Arachnology* 17:71–95.
- CODDINGTON, J.A. 1990a. Ontogeny and homology in the male palpus of orb-weaving spiders and their relatives, with comments on phylogeny (Araneoclađa: Araneoidea, Deinopoidea). *Smithsonian Contributions to Zoology* 496:1–52.
- CODDINGTON, J.A. 1990b. Cladistics and spider classification: araneomorph phylogeny and the monophyly of orbweavers (Araneae: Araneomorphae; Orbiculariae). *Acta Zoologica Fennica* 190:75–87.
- CODDINGTON, J.A., AND H.W. LEVI. 1991. Systematics and evolution of spiders (Araneae). *Annual Review of Ecology and Systematics* 22:565–592.
- CODDINGTON, J.A., AND N. SCHARFF. 1994. Problems with zero-length branches. *Cladistics* 10:415–423.
- COMPAGNUCCI, L.A., AND M.J. RAMÍREZ. 2000. A new species of the spider genus *Naevius* Roth from Argentina (Araneae, Amaurobiidae, Macrobnuninae). *Studies on Neotropical Fauna and Environment* 35:203–207.
- CROME, W. 1955. Die Beziehungen zwischen dem dorsalen Zeichnungsmuster und der Metamerie des Spinnenabdomens, II. *Zoologische Jahrbücher, Systematik* 83:541–638.
- DAHL, F. 1913. Vergleichende Physiologie und Morphologie der Spinnentiere unter besonderer Berücksichtigung der Lebensweise. 1. *Die Beziehungen des Körperbaues und der Farben zur Umgebung, Jena*, pp. 1–112.
- DAVIES, V.T. 1998. A revision of the Australian metaltellines (Araneae: Amaurobioidea: Amphinectidae: Meteltellinae). *Invertebrate Taxonomy* 12:211–243.
- DAVIES, V.T. 1990. Two new spider genera (Araneae: Amaurobiidae) from rainforests of Australia. *Acta Zoologica Fennica* 190:95–102.
- DEELEMEN-REINHOLD, C. 1986. A new cribellate amaurobioid spider from Sumatra (Araneae: Agelenidae). *Bulletin of the British Arachnological Society* 7:34–36.
- DE LA SERNA DE ESTEBAN, C.J. 1976. Algunas observaciones anatómo-histológicas sobre el aparato reproductor de la hembra de *Ariadna mollis* (Holmberg, 1876) (Araneae, Labidognatha, Haplogynae). *Phycis C* 35:139–146.
- EBERHARD, W.G. 1967. Attack behavior of diguetid spiders and the origin of prey wrapping in spiders. *Psyche* 74:173–181.
- EBERHARD, W.G. 1982. Behavioral characters for the higher classification of orb-weaving spiders. *Evolution* 36:1067–1095.

- EBERHARD, W.G. 1988. Combing and sticky silk attachment behavior by cribellate spiders and its taxonomic implications. *Bulletin of the British Arachnological Society* 7:247–251.
- EBERHARD, W.G., AND F. PEREIRA. 1993. Ultrastructure of cribellate silk of nine species in eight families and possible taxonomic implications (Araneae: Amaurobiidae, Deinopidae, Desidae, Dictynidae, Filistatidae, Hypochilidae, Stiphidiidae, Tengellidae). *The Journal of Arachnology* 21:161–174.
- FARRIS, J.S. 1969. A successive approximation approach to character weighting. *Systematic Zoology* 18:374–385.
- FORSTER, R.R. 1955. Spiders of the family Archaeidae from Australia and New Zealand. *Transactions of the Royal Society of New Zealand* 83:391–403.
- FORSTER, R.R. 1970. The Spiders of New Zealand, III. *Otago Museum Bulletin* 3:1–184.
- FORSTER, R.R., AND N.I. PLATNICK. 1984. A review of the archaeid spiders and their relatives, with notes on the limits of the superfamily Palpimanoidea (Arachnida, Araneae). *Bulletin of the American Museum of Natural History* 178:1–106.
- FORSTER, R.R., AND N.I. PLATNICK. 1985. A review of the austral spider family Orsolobidae (Arachnida, Araneae), with notes on the superfamily Dysderoidea. *Bulletin of the American Museum of Natural History* 181:1–230.
- FORSTER, R.R., N.I. PLATNICK, AND M.R. GRAY. 1987. A review of the spider superfamilies Hypochiloidea and Austrochiloidea (Araneae, Araneomorphae). *Bulletin of the American Museum of Natural History* 185(1): 1–116.
- FORSTER, R. R., AND C.L. WILTON. 1973. The Spiders of New Zealand, Part IV. *Otago Museum Bulletin* 4:1–309.
- FRIEDRICH, V., AND R. LANGER. 1969. Fine structure of cribellate spider silk. *American Zoologist* 9:97–101.
- GIRIBET, G. 2003. Stability in phylogenetic formulations and its relationship to nodal support. *Systematic Biology* 52:554–564.
- GOLOBOFF, P.A. 1993a. Estimating character weights during tree search. *Cladistics* 9:83–91.
- GOLOBOFF, P.A. 1993b. *Nona 2.0*. Computer program available at <<http://www.cladistics.com>>.
- GOLOBOFF, P.A. 1995. A revision of the South American spiders of the family Nemesiidae (Araneae, Mygalomorphae). Part 1: Species from Peru, Chile, Argentina, and Uruguay. *Bulletin of the American Museum of Natural History* 224:1–189.
- GOLOBOFF, P.A., J.S. FARRIS, M. KÄLLERSJÖ, B. OXELMAN, M.J. RAMÍREZ, AND C.A. SZUMIK. 2003. Improvements to resampling measures of group support. *Cladistics* 19:324–332.
- GOLOBOFF, P.A., J.S. FARRIS, AND K. NIXON. 2003–2004. *TNT: Tree analysis using new technology*. Version 1.0. Program and documentation, available from the authors, and at <<http://www.zmuk.dk/public/phylogeny>>.
- GRAY, M.R. 1983. The taxonomy of the semi-communal spiders commonly referred to the species *Ixeuticus candidus* (L. Koch) with notes on the genera *Phryganoporus*, *Ixeuticus* and *Badumna* (Araneae, Amaurobioidea). *Proceedings of the Linnean Society of New South Wales* 106:247–261.
- GRAY, M.R., AND H.M. SMITH. 2004. The “striped” group of stiphidiid spiders. Two new genera from north-eastern New South Wales, Australia (Araneae: Amaurobioidea: Stiphidiidae). *Records of the Australian Museum* 56:123–138.
- GREEN, L.A. 1970. *Setal structure and spider phylogeny*. M.S. thesis. Southern Illinois University, Carbondale, Illinois, USA.
- GRISMADO, C.J. 2004. Two new species of the spider genus *Conifaber* Opell 1982 from Argentina and Paraguay, with notes on their relationships (Araneae, Uloboridae). *Revista Ibérica Aracnología* 9:291–306.
- GRISWOLD, C.E. 1990. A revision and phylogenetic analysis of the spider subfamily Phyxelidinae (Araneae, Amaurobiidae). *Bulletin of the American Museum of Natural History* 196:1–206.
- GRISWOLD, C.E. 1993. Investigations into the phylogeny of the lycosoid spiders and their kin (Arachnida, Araneae, Lycosoidea). *Smithsonian Contributions to Zoology* 539:1–39.
- GRISWOLD, C.E. 2002. A revision of the African spider genus *Raecius* Simon, 1892 (Araneae, Zorocratidae). *Proceedings of the California Academy of Sciences* 53 (10):117–149.
- GRISWOLD, C.E., J.A. CODDINGTON, G. HORMIGA, AND N. SCHARFF. 1998. Phylogeny of the orb-web building spiders (Araneae, Orbicularia: Deinopoidea, Araneoidea). *Zoological Journal of the Linnean Society*

- 123:1–99.
- GRISWOLD, C.E., J.A. CODDINGTON, N.I. PLATNICK, AND R.R. FORSTER. 1999. Towards a phylogeny of entelegyne spiders (Araneae, Araneomorphae, Entelegynae). *The Journal of Arachnology* 27:53–63.
- GRISWOLD, C.E., AND D. UBICK. 2001. Zoropsidae: a spider family newly introduced to the USA (Araneae, Entelegynae, Lycosoidea). *The Journal of Arachnology* 29:111–113.
- GRISWOLD, C.E., AND X.P. WANG. 2001. *Character Data to accompany “Towards a phylogeny of entelegyne spiders (Araneae, Entelegynae)” by Griswold, C., J. Coddington, N. Platnick, and R. Forster. 1999. J. Arachnol. 27:53–63.* <<http://www.calacademy.org/research/entomology/griswold/n/.html>>
- HARVEY, M.S. 1995. The Systematics of the Spider Family Nicodamidae (Araneae: Amaurobioidea). *Invertebrate Taxonomy* 9:279–386.
- HAUPT, J. 2003. The Mesothele — a monograph of an exceptional group of spiders (Araneae: Mesothele). *Originalabhandlungen aus dem Gesamtgebiet der Zoologie, Stuttgart* 154:1–102.
- HAUPT, J., AND J. KOVOOR. 1993. Silk-gland system and silk production in Mesothelae (Araneae). *Annales des Sciences Naturelles, Zoologie, Paris* 14:35–48.
- HILL, D.E. 1979. The scales of salticid spiders. *Zoological Journal of the Linnean Society (London)* 65:193–218.
- HOMANN, H. 1971. Die Augen der Araneae: Anatomie, Ontogenese und Bedeutung für die Systematik (Chelicerata, Arachnida). *Zeitschrift für Morphologie der Tiere* 69:201–272.
- HORMIGA, G., W.G. EBERHARD, AND J.A. CODDINGTON. 1995. Web-construction behaviour in Australian *Phonognatha* and the phylogeny of nephiline and tetragnathid spiders (Araneae: Tetragnathidae). *Australian Journal of Zoology* 43:313–364.
- HUBER, B.A. 1994. Genital bulb muscles in entelegyne spiders. *The Journal of Arachnology* 22:75–76.
- HUBER, B.A. 1997. On American ‘*Micromerys*’ and *Metagonia* (Araneae, Pholcidae), with notes on natural history and genital mechanics. *Zoologica Scripta* 25:341–363.
- KASTON, B.J. 1972. *How to know the spiders*. 2nd Ed. William C. Brown Co., Dubuque, 289 pp.
- KOVOOR, J. 1977a. La soie et les glandes séricigènes des Arachnides. *L’année biologique* 16:97–141.
- KOVOOR, J. 1977b. L’appareil séricigène dans le genre *Uloborus* Latr. (Araneae: Uloboridae). I. Anatomie. *Revue Arachnologique* 1:89–102.
- KOVOOR, J. 1978. L’appareil séricigène dans le genre *Uloborus* (Araneae, Uloboridae). II. Données histo-chimiques. *Annales des Sciences Naturelles Zoologie et Biologie Animale* 20:3–25.
- KOVOOR, J. 1980. Les glandes séricigènes d’*Uroctea durandi* (Latreille) (Araneae: Oecobiidae). Revision, histo-chimie, affinités. *Annales des Sciences Naturelles, Zoologie, Paris* 1(3): 187–203.
- KOVOOR, J. 1986. L’appareil séricigène dans les genres *Nephila* Leach et *Nephilengys* Koch: anatomie microscopique, histo-chimie, affinités, avec d’autres Araneidae. *Revue Arachnologique* 7(1):15–34.
- KOVOOR, J., AND A. LOPEZ. 1979. Présence de glandes à soie mélanisées chez des Eresidae solitaires (Araneae). *Revue Arachnologique* 2 (3):89–102.
- KULLMAN, E. 1975. Die Produktion und Funktion von Spinnenfäden und Spinnengewebe. Pages 318–378 in *Netze in Natur und Technik* (Inst. Leichte Flächentragwerke ed.). Stuttgart-Vaihingen.
- LAMORAL, B.H. 1968. On the ecology and habitat adaptations of two intertidal spiders, *Desis formidabilis* (O.P. Cambridge) and *Amaurobioidea africanus* Hewitt, at the Island (Kommetjie, Cape Peninsula) with notes on the occurrence of two other spiders. *Annals of the Natal Museum* 20(1):151–193.
- LAMY, E. 1902. Recherches anatomiques sur les trachées des araignées. *Annales des Sciences Naturelles, Paris* {Zoologie 8} vol. 15:149–280.
- LEHMENSICK, R., AND E. KULLMAN. 1956. Über den Feinbau der faden einiger Spinnen (Vergleich des Aufbaues der Fangfaden cribellater und ecribellater Spinnen). *Zoologischer Anzeiger, Supplement*: 123–129.
- LEHTINEN, P.T. 1967. Classification of the cribellate spiders and some allied families. *Annales Zoologici Fennici* 4:199–468.
- LEHTINEN, P.T. 1975. Notes on the phylogenetic classification of Araneae. *Proceedings of the 6th International Congress of Arachnology, Amsterdam* 1974:26–29.
- LEHTINEN, P.T. 1996. The ultrastructure of leg skin in the phylogeny of spiders. *Revue Suisse de Zoologie, Genève hors. Série* 1975:399–421.

- LEVI, H. W. 1982. The spider genera *Psechrus* and *Fecenia* (Araneae: Psechridae). *Pacific Insects* 24:114–138.
- LOPARDO, L., M.J. RAMÍREZ, C.J. GRISMADO, AND L.A. COMPAGNUCCI. 2004. Web building behavior and the phylogeny of austrochiline spiders. *The Journal of Arachnology* 32:42–54.
- LUBIN, Y.D. 1986. Web building and prey capture in the Uloboridae. Pages 132–171 in W.A. Shear, ed., *Spiders: Webs, Behavior, and Evolution*. Stanford University Press, Stanford, California, USA.
- MARPLES, B.J. 1968. The hypochilomorph spiders. *Proceedings of the Linnean Society London* 179:11–31.
- MARPLES, B.J. 1983. Observations on the structure of the fore-gut of spiders. *Bulletin of the British Arachnological Society* 6:46–52.
- MCKEOWN, K.C. 1936. *Spider Wonders of Australia*. Angus & Robertson, Sydney, Australia. xii+252 pp.
- MILLER, J.A. 2003. Assessing progress in systematics with continuous jackknife function analysis. *Systematic Biology* 52:55–65.
- MILLOT, J. 1931a. Les diverticules intestinaux du cephalothorax chez les Araignées vrais. *Zeitschrift Morphologie und Ökologie der Tiere* 21:740–764.
- MILLOT, J. 1931b. Les glandes venimeuses des Aranéides. *Annales des sciences naturelles, Zoologie, Paris* 14:113–147.
- MILLOT, J. 1931c. Anatomie comparee de l'intestin moyen céphalo-thoracique chez les Araignées vraies. *Compte rendu des l'Académie des sciences, Paris* 192:375–377.
- MILLOT, J. 1933a. Le genre *Aebutina* (Aranéides). *Bulletin de la Société Entomologique de France, Paris* 58:92–95.
- MILLOT, J. 1933b. Notes complémentaires sur l'anatomie des Liphistiides et des Hypochilides, a propos d'un travail recent de A. Petrunkevitch. *Bulletin de la Société Entomologique de France, Paris* 58:217–235.
- MILLOT, J. 1933c. L'anatomie interne des Dinopides. *Bulletin de la Société Entomologique de France, Paris* 57:537–542.
- MILLOT, J. 1933d. L'anatomie interne des Liphistiides. In Bristowe, W.S. The Liphistiid Spiders. *Proceedings of the Zoological Society, London*. 1933:1045–1055.
- MILLOT, J. 1936. Metamerisation et musculature abdominale chez les Araneomorphes. *Bulletin de la Société Entomologique de France, Paris* 61:181–204.
- MILLOT, J. 1938. L'Appareil séricigène d'*Oecobius cellariorum* Dugès, suivi de quelques considérations générales sur les glandes sécrétrices de soie des Aranéides. *Travaux de la Station zoologique de Wimereux* 13:479–487.
- MILLOT, J. 1949. Classe des Arachnides (Arachnida). I. Morphologie générale et anatomie interne. In P. Grasse. *Traité de Zoologie*. Paris 6:263–319.
- MORRISON, R., AND M. MORRISON. 1990. *Australia: the Four Billion Year Journey of a Continent*. Facts on File, New York, New York, USA. 334 pp.
- NIXON, K. 1999. The parsimony ratchet, a new method for rapid parsimony analysis. *Cladistics* 15:407–414.
- OPELL, B. 1979. Revision of the genera and tropical American species of the spider family Uloboridae. *Bulletin of the Museum of Comparative Zoology* 148:443–549.
- OPELL, B. 1987. The influence of web monitoring tactics on the tracheal systems of spiders in the family Uloboridae (Arachnida, Araneida). *Zoomorphology* 107:255–259.
- OPELL, B. 1989a. Functional associations between the cribellum spinning plate and capture threads of *Miagrammopes animotus* (Araneida, Uloboridae). *Zoomorphology* 108:263–267.
- OPELL, B. 1989b. Measuring the stickiness of spider prey capture threads. *The Journal of Arachnology* 17:112–114.
- OPELL, B. 1995. Ontogenetic changes in cribellum spigot number and cribellar prey capture thread stickiness in the spider family Uloboridae. *Journal of Morphology* 224:47–56.
- OPELL, B. 2001. Cribellum and calamistrum ontogeny in the spider family uloboridae: linking functionally related but separate silk spinning features. *The Journal of Arachnology* 29:220–226.
- PETERS, H.M. 1983. Struktur und Herstellung der Fangfäden cribellater Spinnen (Arachnida: Araneae). *Verhandlungen des Naturwissenschaftlichen Vereins in Hamburg* 26:241–253.
- PETERS, H.M. 1984. The spinning apparatus of Uloboridae in relation to the structure and construction of capture threads (Arachnida, Araneida). *Zoomorphology* 104:96–104.

- PETERS, H.M. 1987. Fine structure and function of capture threads, In W. Nentwig ed., *Ecophysiology of Spiders*, Pp. 187–202, Springer, New York.
- PETERS, H.M. 1992a. On the spinning apparatus and the structure of the capture threads of *Deinopis subrufus* (Araneae, Deinopidae). *Zoomorphology* 112:27–37.
- PETERS, H.M. 1992b. Über Struktur und Herstellung von Fangfäden cribellater Spinnen der Familie Eresidae (Arachnida, Araneae). *Verhandlungen des Naturwissenschaftlichen Vereins in Hamburg* 33:213–227.
- PETERS, H.M., AND J. KOVOOR. 1980. Un complément à l'appareil séricigène des Uloboridae (Araneae): le paracribellum et ses glandes. *Zoomorphology* 96:91–102.
- PETERS, H.M., AND J. KOVOOR. 1989. Die Herstellung der Eierkokons bei der Spinne *Polonecia producta* (Simon, 1873) in Beziehung zu den Leistungen des Spinnapparates. *Zoologische Jahrbücher, Abteilung Allgemeine Zoologie und Physiologie der Tiere* 93:125–144.
- PETRUNKEVITCH, A. 1928. Systema Araneorum. *Transactions of the Connecticut Academy of Arts and Sciences* 28:1–270.
- PETRUNKEVITCH, A. 1933. An inquiry into the natural classification of spiders, based on the study of their internal anatomy. *Transactions of the Connecticut Academy of Arts and Sciences* 31:299–389.
- PETRUNKEVITCH, A. 1939. The Status of the Family Archaeidae and the Genus *Landana*. *Annals of the Entomological Society of America* 32:479–501.
- PLATNICK, N.I. 1977. The hypochiloid spiders: A cladistic analysis, with notes on the Atypoidea (Arachnida, Araneae). *American Museum Novitates* 2627:1–23.
- PLATNICK, N.I. 2004. *The world spider catalog, version 5.0*. American Museum of Natural History, online at <http://research.amnh.org/entomology/spiders/catalog/INTRO1.html>.
- PLATNICK, N.I., J.A. CODDINGTON, R.F. FORSTER, AND C.E. GRISWOLD. 1991. Spinneret evidence and the higher classification of the haplogyne spiders (Araneae, Araneomorphae). *American Museum Novitates* 3016:1–73.
- PLATNICK, N.I., AND R.R. FORSTER. 1987. On the first American spiders of the subfamily Sternodinae (Araneae, Malkaridae). *American Museum Novitates* 2894:1–12.
- PLATNICK, N.I., AND W.J. GERTSCH. 1976. The suborders of spiders: a cladistic analysis. *American Museum Novitates* 2607:1–15.
- PURCELL, W.F. 1909. Development and origin of respiratory organs in Araneae. *Quarterly Journal of the Microscopical Society (N.S.)* 54:1–25.
- PURCELL, W.F. 1910. The phylogeny of the Tracheae in Araneae. *Quarterly Journal of the Microscopical Society (N.S.)* 54:519–564.
- RAMÍREZ, M.J. 1995. A phylogenetic analysis of the subfamilies of Anyphaenidae (Arachnida, Araneae). *Entomologica Scandinavica* 26:361–384.
- RAMÍREZ, M.J. 2000. Respiratory system morphology and the phylogeny of haplogyne spiders (Araneae, Araneomorphae). *The Journal of Arachnology* 28:149–157.
- RAMÍREZ, M.J. 2003. A cladistic generic revision of the spider subfamily Amaurobioidinae (Araneae, Anyphaenidae). *Bulletin of the American Museum of Natural History* 277:1–262.
- RAMÍREZ, M.J., AND C.J. GRISMADO. 1997. A review of the spider family Filistatidae in Argentina (Arachnida, Ataneae), with a cladistic reanalysis of filistatid genera. *Entomologica Scandinavica* 28:319–349.
- RAMÍREZ, M.J., C. GRISMADO, AND T. BLICK. 2004. Notes on the family Agelenidae in Southern South America (Arachnida: Araneae). *Revista Ibérica Aracnología* 9:179–182.
- RAVEN, R.J., AND K. STUMKAT. 2003. Problem solving in the spider families Miturgidae, Ctenidae and Psecridae (Araneae) in Australia and New Zealand. *The Journal of Arachnology* 31(1):105–121.
- RAVEN, R.J., AND K. STUMKAT. 2005. Revisions of Australian ground-hunting spiders: II: Zoropsidae (Lycosoidea: Araneae). *Memoirs of the Queensland Museum* 50(2):347–423.
- ROBSON, C.H. 1878. Notes on a marine spider found at Cape Campbell. *Transactions of the New Zealand Institute* 10:299–300.
- RUHLAND, M., AND W. RATHMEYER. 1978. Die Beinmuskulatur und ihre Innervation bei der Vogelspinnen *Dugesiella hentzi* (Ch.) (Araneida, Avaiculariidae). *Zoomorphologie* 89:33–46.
- SCHÜTT, K. 2000. The limits of the Araneoidea (Arachnida: Araneae). *Australian Journal of Zoology* 48:135–153.

- SCHÜTT, K. 2002. *The limits and phylogeny of the Araneoidea (Arachnida, Araneae)*. Thesis submitted to Mathematisch-Naturwissenschaftlichen Fakultät I der Humboldt-Universität zu Berlin. 153 pp.
- SCHÜTT, K. 2003. Phylogeny of Symphytognathidae *s.l.* (Araneae, Araneoidea). *Zoologica Scripta* 32:129–151.
- SHEAR, W.A. 1969. Observations on the predatory behavior of the spider *Hypochilus gertschi* Hoffman (Hypochilidae). *Psyche* 76:407–417.
- SHEAR, W.A. 1970. The spider family Oecobiidae in North America, Mexico, and the West Indies. *Bulletin of the Museum of Comparative Zoology* 140:129–164.
- SIERWALD, P. 1990. Morphology and ontogeny of female copulatory organs in American Pisauridae, with special reference to homologous features (Arachnida: Araneae). *Smithsonian Contributions to Zoology* (484):1–24.
- SILVA DÁVILA, D. 2003. Higher-level relationships of the spider family Ctenidae (Araneae: Ctenoidea). *Bulletin of the American Museum of Natural History* 274:1–86.
- SIMON, E. 1892. *Histoire naturelle des Araignées*, vol. 1, pt. 1. Encyclopédie Robet, Paris, France. 256 pp.
- SZLEP, R. 1966. Evolution of the web spinning activities: the web spinning in *Titanoeca albomaculata* Luc. (Araneae, Amaurobidae). *Israel Journal of Zoology* 15:83–88.
- TILLINGHAST, E.K., AND M.A. TOWNLEY. 1994. Silk glands of araneid spiders: Selected morphological and physiological aspects. Pages 29–44 in D. Kaplan, W.W. Adams, B. Farmer, and C. Viney, eds., *Silk Polymers: Materials Science and Biotechnology*. American Chemical Society Symposium, Series 544. American Chemical Society, Washington, D.C., USA.
- TOWNLEY, M.A., E.K. TILLINGHAST, AND N.A. CHERIM. 1993. Moulting-related changes in ampullate silk gland morphology and usage in the araneid spider *Araneus cavaticus*. *Philosophical Transactions of the Royal Society of London, B* 340:25–38.
- TOWNLEY, M.A., AND E.K. TILLINGHAST. 2003. On the use of ampullate gland silks by wolf spiders (Araneae, Lycosidae) for attaching the egg sac to the spinnerets and a proposal for defining nubbins and tartipores. *The Journal of Arachnology* 31(2): 209–245.
- TULLGREN, A. 1910. *Araneae*. In *Wissenschaftliche Ergebnisse der Schwedischen Zoologischen Expedition nach dem Kilimandjaro, dem Meru und den umgebenden Massaiesteppen Deutsch-Ostafrikas 1905-1906 unter Leitung von Prof. Dr Yngve Sjöstedt*, Stockholm, 20(6):85–172.
- UHL, G. 2000. Two distinctly different sperm storage organs in female *Dysdera erythrina* (Araneae: Dysderidae). *Arthropod Structure and Development* 29:163–169.
- WANG, X.P. 2000. A revision of the genus *Tamagrina* (Araneae: Amaurobiidae), with notes on amaurobiid spinnerets, tracheae and trichobothria. *Invertebrate Taxonomy* 14:449–464.
- WOLFF, R.J. 1977. The cribellate genus *Tengella* (Araneae: Tengellidae?). *The Journal of Arachnology* 5(2): 139–144.
- ZAPFE, H. 1955. Filogenia y función en *Austrochilus manni* Gertsch y Zapfe (Araneae-Hypochilidae). *Trabajos del Laboratorio de Zoología Facultad de Filosofía Y Educación Universidad de Chile* 2:1–53.
- ZIMMERMAN, W. 1975. *Biologische und rasterelektronenmikroskopische Feststellungen an Oecobiinae, Uroecobiinae und Urocteinae (Araneae: Oecobiidae) als Beitrag zum "Cribellaten-Ecribellaten Problem."* Thesis. Universität Bonn, Bonn, Germany.

APPENDICES

Appendix 1. Taxa Examined to Provide Exemplar Data

Exemplar specimens have labels reading “Entelegyne phylogeny atlas exemplar”

Taxa marked with an asterisk * are not coded in our data matrix,
but reference SEM preparations, photographs, or other observations.

AGELENIDAE

Neoramia sana Forster: ♂ ♀ from Saddle Hill, Dunedin, New Zealand, 29 October 1992, R. Forster, CAS; ♀ from Saddle Hill, 5 km W Dunedin, elev. 280–380 m, ca. 45°56'S; 170°20'E, native bush, 14 April 1995, C. Griswold and T. Meikle, CAS (Meikle photo voucher).

AMAUROBIIDAE

Amaurobius fenestralis (Stroem): ♂ ♀ from Tisvilde, Denmark, 19 May 1991, C. Griswold, CAS and USNM.

Amaurobius sp.: ♀ from Page Mill Boulevard, 0.3 mi. from Skyline Drive, 1600 ft. elev., Santa Clara Co., California, USA, 5 July 1996, R. Carlson and C. Griswold, CAS (R. Carlson silk study voucher).

Callobius sp.: ♀ from redwood forest, 0.7 mi NE Fort Ross, Sonoma Co., California, USA, 21 June 1996, C. E. Griswold, R. Carlson, CAS (R. Carlson silk study voucher).

Callobius bennetti (Blackwall): ♂ ♀ from Piscataquis Co., Maine, USA, June 1978, D. Jennings, CAS; ♂ from Soubunge Mountain, Maine, USA, 8 June 1978, D. Jennings, CAS; ♀ from Hampshire Co., West Virginia, USA, 9 June 1985, USNM.

Callobius gauchama Leech: ♂ ♀ from Seven Oaks, elev. 5600ft., San Bernardino Mts., San Bernardino Co., California, USA, 17–19 May 1996, R. Vetter, CAS (R. Carlson silk study voucher).

Callobius nevadensis (Simon): ♀ from Norden, California, USA, T. Davies, CAS (Davies photo voucher).

Callobius pictus (Simon): ♀ from Olympia, Washington, USA, 16 March 1931, H. Exline, CAS; ♀ from Elum, Washington, USA, 20 May 1934, H. Exline, CAS.

Macrobunus cf. *multidentatus* (Tullgren): 2 ♂ 1 ♀ from Arroyo Cole Cole, 25 km N Cucao, Chiloé, Chile, 8–11 February 1991, M. Ramírez, MACN, (MACN-Ar, SEM preparations MJR 958–962, temporary mount MJR 973).

Pimus pitus Chamberlin: ♀ from Kyburz, California, USA, 15 September 1959, W. Gertsch and V. Roth, AMNH; ♂ from Yosemite, California, USA, 14 September 1959, W. Gertsch and V. Roth, AMNH.

Pimus napa Leech: 4 ♀ paratypes from Napa Co., 3 mi W Oakville, California, USA, 15 February 1954, Roth and Schuster, AMNH (SEM preparation MJR 761–763); ♂ paratype from 2 mi W Oakville, Napa Co., California, USA, 31 December 1953, AMNH (SEM preparation MJR 764).

Pimus spp.: ♂ ♀ from Mendocino Co., California, USA, 15 September 1990, D. Ubick, CAS; ♀ from Eel River, Mendocino Co., California, USA, 20 September 1990, D. Ubick, CAS; ♀ from Page Mill Road, 0.3 mi. from Skyline Boulevard, Santa Clara Co., California, USA, 1600 ft. elev., 5 July 1996, R. Carlson and C. Griswold, CAS (R. Carlson silk study voucher).

Retiro sp.: ♂ ♀ from Lima, Peru, H. Exline, CAS.

AMPHINECTIDAE

Maniho ngaitahu Forster and Wilton: ♂ ♀ from Kaituna valley, South Island, New Zealand, 13 April 1964, R. Forster, CAS.

Maniho pumilio Forster and Wilton: ♂ ♀ from Butterfly Creek, Eastbourne, New Zealand, *Nothofagus*/tree fern forest, 18 April 1996, L.J. Boutin, CAS (R. Carlson silk study voucher).

Maniho tigris Marples: ♀ from Butterfly Creek, Eastbourne, New Zealand, *Nothofagus*/tree fern forest, 18 April 1996, L.J. Boutin, CAS (R. Carlson silk study voucher).

**Metaltella rorulenta* (Nicolet): ♀ from Malalcahuello, Chile, 25 January 1985, N. Platnick, CAS; ♂ from Nahuelbuta, Chile, M. Irwin and E. Schlinger, CAS.

Metaltella simoni (Keyserling): ♂ ♀ from Riverside, California, USA, 7 July 1996, R. Vetter, CAS (R. Carlson silk study voucher); 3 ♂ 11 ♀ from St. Tammany Co., Pearl River, Louisiana, USA, AMNH; 2 ♂ 2 ♀ from same locality, 1965, L. Roddy, AMNH; ♂ from Villa Madero, Buenos Aires, Argentina, August 1998, C. Scioscia, MACN (MACN-Ar, preparation MJR 975); ♂ from El Palmar, Entre Ríos, Argentina, November

1988, M. E. Galiano, MACN (MACN-Ar, preparation MJR 976); ♂ from Puerto Obligado, Buenos Aires, Argentina, March 1983, E. Maury and P. Goloboff, MACN (MACN-Ar, preparation MJR 977); juv. from Whittier, California, USA, March 2005, L. Vincent, CAS (Vincent photo voucher).

**Metaltellinae* sp.: 2 ♀ from Llanquihue, Concordia, Fundo Pedernales, Chile, 4 February 1986, T. Cekalovic, AMNH.

ANAPIDAE

**Crassanapis chilensis* Platnick and Forster: 2♂ 4♀ from Parque Nacional Puyehue, Aguas Calientes, Osorno, Chile, Moczarski-Tullgren extractor, 13–17 December 1998, M. Ramírez, L. Compagnucci, C. Grismado and L. Lopardo, MACN (MACN-Ar, 1♂ and 1♀ mounted for SEM, preparation MJR 677).

ARANEIDAE

Araneus diadematus Clerck: ♂ from Seattle, Washington, USA, 3 September 1933, H. Exline-Frizzell, CAS; 1♂4♀ from Swansea, W of High Park, Ontario, Canada, 43°41'N, 79°28'W, 1 September 1945, W. Ivie and T. Kurata, AMNH (SEM preparations MJR 819–822).

**Argiope argentata* (Fabricius): 1♀ from 1 mi. S. Millers Landing, Baja California, Mexico, in coastal sand dunes, 6 July 1973, S. Williams and K. Blair, CAS.

**Metepeira atascadero* Piel: ♂ ♀ from Guanajuato, Mexico, September 1976, C. Griswold and R. Jackson, CAS.

ARCHAEIDAE

Archaea workmani (O. P.-Cambridge): ♂ ♀ from Vohiparara, Parc National de Ranomafana, ca. 21°14'S, 47°24'E, elev. 1100 m., Fianarantsoa Prov., Madagascar, April 1998, C. Griswold, D. Kavanaugh, M.J. Raherilalao and D. Ubick, CAS; 3♂ 3♀ and immatures from Parc Nationale Ranomafana, Talatakely, 21°14.9'S, 47°25.6'E, Fianarantsoa Prov., Madagascar, 5–18 April 1998, C. Griswold, D. Kavanaugh, N. Penny, M. Raherilalao, J. Ranorianarisoa, J. Schweikert, D. Ubick, CAS (SEM preparations MJR 791–797). (Coville photo voucher)

AUSTROCHILIDAE

**Austrochilus forsteri* Grismado, Lopardo & Platnick: ♀ from Contulmo, Chile. February 1992, M. Ramírez, MACN (Ramírez photo voucher).

**Austrochilus melon* Platnick: juvenile from Cuesta Pucalan, Chile, 19 September 1966, E.I. Schlinger, USNM.

Hickmania troglodytes (Higgins and Petterd): ♂ ♀ from cave at Mole Creek, Tasmania, Australia, 3 June 1996, J. Boutin, CAS; silk from Newdegate Cave, Tasmania, Australia, 11 October 1998, J. Boutin, CAS (R. Carlson silk study voucher); silk samples from Tasmania, L. Trimmer Cave, 15 July 2000, N. Dioran, MACN (MACN-Ar, SEM preparations MJR 74, 77); 1♂ 1♀ from W of Deloraine, Mole Creek Cave, in small Cavern, Tasmania, Australia, 3 June 1996, L.J. Boutin, CAS (SEM preparations MJR 787, 788).

Thaïda peculiaris Karsch: ♂ ♀ from Los Lagos, Valdivia, Neltumo, Chile, 23 November 1988, V. and B. Roth, CAS; ♂ ♀ from Region Pucón by Lago Villarica, Chile, 14 December 1988, V. and B. Roth, CAS; immature from Osorno, Chile, 12 February 1985, USNM; silk samples from Puerto Blest, Neuquén, Argentina, 7–20 January 2000, L. Lopardo and A. Quaglino, MACN (SEM preparations MJR 72, 78); 1♀ from Puerto Blest, Parque Nacional Nahuel Huapi, Argentina, 7–20 January 2000, L. Lopardo and A. Quaglino, MACN (MACN9976, SEM preparations MJR 675, 676, 839); 1♂ from Bellavista, N shore Lago Villarrica, elev. 310 m, site 655, window trap, valdivian rainforest, Cautín, Chile, 15–30 December 1982, A. Newton and M. Thayer, AMNH (SEM preparation MJR 765); ♀ from Puyehue, Chile, 15 December 1998, M. Ramírez, MACN (Ramírez photo voucher).

CTENIDAE

Acanthoctenus spiniger Keyserling: ♂ from Ecuador, collected on bananas in New York, USNM; ♀ from Changuinola, Panama, 1965, J. Harrison, CAS; ♀ from Tegucigalpa, Honduras, 1953, Gilbert, USNM.

Acanthoctenus cf. *spinipes* Keyserling: 2♂ 1♀ from Río Samiria, Loreto, Peru, fogging, May 1990, T. Erwin et al., MUSM.

Acanthoctenus sp.: ♀ from Río Samiria, Peru, 15 May 1990, D. Silva, MUSM.

Acanthoctenus sp.: ♀ from 25km N Formosa, 25°59'S, 58°12'W, Estancia Guaycolec, Argentina, elev. 185m, 26 February to 10 March 1999, S. Heydon and J. Ledford, CAS (Griswold photo voucher).

DEINOPIDAE

Deinopis spinosus Marx: ♂ ♀ from Gainesville, Florida, USA, 1 July 1994, C. Griswold, CAS; ♀ from Alachua Co., Florida, USA, J. Coddington, 3 August 1985, USNM; ♀ from Finca La Selva, Heredia Province, Costa Rica. October 1981, C. Griswold and R. Coville, CAS (Coville photo voucher); ♀ from same locality, 13 August 1985, J. Coddington, USNM (Coddington photo voucher).

Menneus camelus Pocock: ♀ from Twin Streams near Mtunzini, Natal, Zululand, South Africa, 19–20 January 1984, T. Meikle and C. Griswold, NMSA (Meikle photo voucher); ♀ from Mpumalanga Prov., Songimvelo Nature Reserve, Kromdraai, 26°2'33"S, 31°0'5"E, 800m elev., South Africa, 16–23 March 2001, D. and S. Ubick, CAS; ♀ from Kaibos, Kenya, 23 May 1980, B. Lamoral, USNM.

Menneus sp.: 1 ♀ from Tembe Elephant Park, elev. 115 m, 27°2'32.8"S, 32°25'24.4"E, KwaZulu-Natal, South Africa, 9–12 April 2001, M. Ramírez, MACN (SEM preparations MJR 623).

DESIDAE

Badumna longinqua (L. Koch): ♂ ♀ from Montevideo, Uruguay, 5 November 1961, R. Capocasale, CAS; ♂ ♀ from San Francisco, California, USA, July 1996, R. Carlson, CAS (R. Carlson silk study voucher); 1 ♀ from Maui, Hawaii, USA, Lennox, MM85-19, USNM; 1 ♂ 1 immature from Ship Cr., Haast, New Zealand, 8 December 1977, E. I. Schlinger, CAS; 2 ♀ 1 ♀ subadults from Pacifica, San Mateo Co., California, USA, 13 May 1995, K. Ribardo, CAS.

**Badumna* sp.: ♀ from from Waitomo, near caves, ca. 38°14'S, 175°08'E, North Island, New Zealand, 3 April 1995, C. Griswold and T. Meikle, CAS (Meikle photo voucher).

Desis formidabilis (O. P.-Cambridge): 1 ♂ 3 ♀ from "The Island", Kommetje, Cape Peninsula, Western Cape, South Africa, May 1966, B. Lamoral, CAS (identified by B. Lamoral, SEM preparation MJR 274, temporary preparation MJR 974); ♂ ♀ from same locality, 34°9'S, 18°20'E, 30 air km S Cape Town, intertidal zone, under rocks, 13 March 2001, K. Muller, S. Prinsloo, L. Prendini, D. and S. Ubick, CAS (SEM preparations MJR 275–280); ♂ ♀ from Lüderitz, Namibia, among intertidal rocks, October 1985, C. Griswold and T. Meikle, NMSA (Meikle photo voucher).

Matachia australis Forster: ♀ from Saddle Hill, Dunedin, New Zealand, 29 October 1992, R. Forster, CAS.

Matachia marplei Forster: ♂ from Helena Bay, North Island, New Zealand, 3 February 1994, E. Schlinger, CAS.

Matachia spp.: ♀ from Parakaunui Falls, Catlins Coastal Rainforest Park, 10.8km 201°S Owaka, S46.51592°, E169.55887°, elev. 20m, *Nothofagus/podocarp* forest, Otago Prov., New Zealand, 16 February 2005, C. Griswold, D. Silva and H. Wood, OMD (Wood photo voucher); ♀ from Banks Peninsula, Hay Scenic Reserve nr. Pigeon Bay, elev. 50 m, ca. 43°42'S, 172°54'E, native forest, 10 April 1995, C. Griswold and T. Meikle, CAS (Meikle photo voucher).

Phryganoporus candidus (L. Koch): ♂ ♂ ♀ ♀ from Black Mountain, Canberra, Australia, 7 August 1990, C. Griswold and T. Meikle, CAS and USNM.

DICTYNIDAE

Aebutina binotata Simon: ♂ ♀ from Rio Cuyabeno, near via Atipishea, Sucumbos, Ecuador, August 1995, G. Cañas, CAS; ♂ from Aguas Negras, near Tarapuy, Napo, Ecuador, 1984, L. Avilés, CAS; 1 ♂ and several ♀, from Divisoria, 1700 m, Huanuco, Peru, 23 September–3 October 1946, F. Woytkowski, AMNH.

Dictyna arundinacea (Linnaeus): ♂ ♀ from Tuva, Russia, 9 June 1995, Y. Marusik, CAS; ♂ ♀ from Lyngby, Denmark, 26 May 1991, C. Griswold and N. Scharff, USNM; 9 ♀ from Skibo Castle, Dornoch, Sutherland, Scotland, August 1935, R. Miller, AMNH; 2 ♂ 1 ♀ from Helsingfors, Haga, Finland, 3 June 1951, W. Hackman, AMNH (SEM preparation MJR 818).

Dictyna bostoniensis Emerton: ♂ ♀ from Minnesota, USA, 27 June 1936, H. Exline-Frizzell, CAS.

Dictyna sp.: ♀ from Whittier, California, USA, March 2005, L. Vincent, CAS (Vincent photo voucher).

Lathys delicatula (Gertsch and Mulaik): ♀ from Southwestern Research Station, Portal, Arizona, USA, 19 September 1972, D. Ubick, CAS.

- Lathys humilis* (Blackwall): ♂ ♀ from Eastling, Kent, United Kingdom, 16 May 1993, A. Russell-Smith, CAS.
Lathys immaculata (Chamberlin and Ivie): ♂ from Bradley, Arkansas, USA, 2 February 1964, CAS.
 **Mallos* sp.: ♂ ♀ from Chiricahua Mountains, Arizona, USA, 26 May 1975, D. Ubick, CAS.
 **Mallos* sp.: ♀ from Mt. Lemon, Arizona, USA, D. Ubick, CAS (R. Carlson silk study voucher).
Nigma linsdalei (Chamberlin and Gertsch): ♂ ♀ from San Francisco, California, USA, June 1994, D. Ubick, CAS.
Tricholathys spiralis Chamberlin and Ivie: ♂ ♀ from Lenore Lake, Washington, USA, 8 May 1938, Hatch, CAS.
Tricholathys sp.: ♀ from San Francisco, California, USA, 15 April 1992, K. Dabney, CAS.

ERESIDAE

- **Dresserus subarmatus* Tullgren: ♂ ♀ from Nairobi, Kenya, AMNH.
 **Dresserus* sp.: ♂ ♀ from Mazumbai, Muheza District, Tanzania, elev. 1600–1800 m, 4°49'S, 38°30'E, 11–20 November 1995, C. Griswold, D. Ubick, and N. Scharff, CAS.
 **Dresserus* sp.: immature from Tembe Elephant Park, elev. 115m, 27°2'32.8"S, 32°25'24.4"E, KwaZulu-Natal, South Africa, 9–12 April 2001, M. Ramírez, MACN.
Eresus cinnaberinus (Olivier): ♂ ♀ from Fiesch Wallis, Switzerland, Schenkel, AMNH.
Eresus cf. *cinnaberinus* (Olivier): 1 ♂ from Peloponesus, Mistras, Greece, 19 June 1982, B. and H. Malkin, AMNH (SEM preparations MJR 809, 810); 1 ♀ from Igrherm, Anti Atlas, elev. 1600–1700 m, Morocco, 23–29 May 1974, B. Malkin, AMNH (SEM preparations MJR 811, 831).
Eresus sandaliatus (Martini & Goeze): ♂ ♀ from road between Rye to Gl. Salten, 9°35'E, 56°05'N, SE of Silkeborg, Denmark, 25 November 1994, P. d. place Bjørn, CAS.
Stegodyphus dumicola Pocock: ♂ ♀ from Spieonkop Dam, south shore, 30 km SW Ladysmith, elev. 900m, 28°41'S, 29°28'E, mixed grassland and dry bushveld, KwaZulu-Natal, South Africa, December 1985, T. Meikle and C. Griswold, CAS; ♂ ♀, same data, 9 January 1986, CAS.
Stegodyphus mimosarum Pavesi: ♂ ♀ from Spieonkop Dam, south shore, 30 km SW Ladysmith, elev. 900m, 28°41'S, 29°28'E, mixed grassland and dry bushveld, KwaZulu-Natal, South Africa, December 1985, T. Meikle and C. Griswold, CAS NMSA (Meikle photo voucher); ♂ ♀ from 31 mi. SE Ft. Hill, elev. 1600m, Malawi, 20 February 1958, E. Ross, CAS; 1 juv. from Parc National de Ranomafana, Vohiparara, ca. 21°14'S, 47°24'E, elev. 1100 m., Fianarantsoa Prov., Madagascar, 5–7 November 1993, C. Griswold, CAS; 1 ♀ from Phinda Resource Reserve, elev. 38 m. S 27°50'43", E 32°18'49.1", KwaZulu-Natal, South Africa, 13–15 April 2001, M. Ramírez, MACN (SEM preparations MJR 767, 768).
Stegodyphus sp.: ♀ from ShweSettaw Wildlife Reservation, Magway Division, Myanmar, N20°47.4", E94°35'2.8", elev. 137m, deciduous forest, at night, 29 September 2003, C. Griswold, P. Sierwald, D. Ubick, Aye Aye Cho and Tin Mya Soe, CAS (Dong Lin photo voucher).

FILISTATIDAE

- Filistata insidiatrix* (Forskål): ♂ ♀ from rock wall in park, Barcelona, Spain, 13 October 1986, J. Coddington, USNM; several females and eggsacs with spiderlings from Siena, 4 km S San Giminiano, Fattoria Voltrona, Reg. Toscana, Italy, 12 July 2001, M. Ramírez, MACN (SEM preparations MJR 798–803, 835).
 **Filistatinella* sp.: ♀ from Arroyo Seco, Monterey Co., California, USA, 7 May 1995, D. Ubick, CAS.
Kukulcania hibernalis (Hentz): ♂ ♀ from Archbold Biological Station, 8 mi. S. Lake Placid, Highlands Co., Florida, USA, 26 June 1978, C. Griswold, CAS; ♂ ♀ from Clearwater, Pinella Co., Florida, USA, December 1962 – February 1963, O. Paulus, CAS; 1 ♀ from Alachua Co., Florida, USA, 8 August 1985, USNM; ♀ and spiderlings from eggsac reared in lab, from Las Gamas, 20km W Vera, Santa Fe, Argentina, 27–30 October 1994, M. Ramírez and J. Faivovich, MACN (SEM preparations MJR 33–37); silk samples from Buenos Aires, Argentina, 11 January 2001, L. Lopardo, MACN (SEM preparation MJR 73); ♂ ♀ from Buenos Aires, Argentina, 1 January 2005, M. Ramírez, MACN (Ramírez photo voucher); 1 ♂ from Savanna, Georgia, USA, 18 August 2001, T. Sullivan, AMNH (SEM preparation MJR 838).
Kukulcania sp.: ♂ from Kings Co., 25th Ave. near Parejo Hill, 35°37'14"N, 119°54'52"W, California, USA, 18 May 1997, D. Ubick and W. Savary, CAS (penultimate observed carding cribellate silk); silk samples, ♀ from North Carolina, USA, unspecified locality, alive in AMNH.

**Misionella mendensis* (Mello-Leitão): ♀ from Misiones, Argentina, M. Ramírez, MACN (Ramírez photo voucher).

**Priiha nana* (Simon): ♀ from Bolzano, Italy, M. Ramírez, MACN (Ramírez photo voucher).

GRADUNGULIDAE

Gradungula sorenseni Forster: ♂ ♀ from Saltwater Forest, west coast, South Island, New Zealand, 2 December 1991, P. Walsh, CAS; 7 ♂ 3 ♀ from South Island, west coast, Saltwater Forest, pit trap in rimu forest, New Zealand, 1 December 1991, P. Walsh, CAS (SEM preparations MJR 789, 790).

HUTTONIIDAE

Huttonia palpimanoides O. P.-Cambridge: ♂ ♀ from dead fern fronds in Leith Saddle forest, Dunedin, South Island, New Zealand, 3 January 1975, R. Forster, CAS.

Huttonia sp.: 1 ♀ from Orongorongo Res. Project, Wellington, New Zealand, 1 June 1992, OMD (SEM preparations MJR 827–829); 1 ♂ with same data, OMD; 1 ♀ from Kapiti Island, off SW Coast of North Island, New Zealand, 40°52'S, 174°55'E, ex pitfall trap, 1996, J. Mclartney, CAS (SEM preparation MJR 830); 1 immature from Otago, Trotters Gorge, New Zealand, from ferns, 6 February 1979, R. R. Forster, USNM (tracheae examined).

HYPOCHILIDAE

Hypochilus sheari Platnick: ♂ from Yancey Co., Crabtree Meadows, 25 mi. N Marion, North Carolina, USA, 4 September 1976, C. Griswold and R. Jackson, CAS.

Hypochilus pococki Platnick: ♂ ♀ from Ramsey Cascade, Great Smokey Mts. N.P. elev. 2080 ft., Sevier Co., Tennessee, USA, 10 August 1995, F. Coyle, CAS; ♀ from Haywood Co., North Carolina, USA, 3 October 1960, USNM; many ♂ and ♀ from above Crabtree to Betsey's Gap, 3956 ft. elev., Haywood Co., North Carolina, USA, 3 October 1960, W. Gertsch, W. Ivie, AMNH (SEM preparations MJR 735, 836, 837, 863).

Hypochilus kastoni Platnick: ♀ from Mount Shasta, California, USA, J. Ledford, CAS (Ledford photo voucher).

**Ectatosticta* sp.: 1 ♀ from Taibai Shan S flanks, above Houshenzi, mixed coniferous/*Rhododendron* forest, elev. 3050 m, Shaanxi Prov., China, 12–13 June 1997, P. Jäger and B. Martens, JGU (SEM preparation MJR 755).

MIMETIDAE

Mimetes hesperus Chamberlin: ♂ from Baboquivari Canyon, Baboquivari Mts., Pima Co. Arizona, USA, 21 July 1952, H. B. Leech and J. W. Green, CAS; ♀ from Tampico, Tamulipas, Mexico, summer 1966, CAS; 2 ♀ from Kingston Camp, 30 mi S Austin, Toiabe Range, elev. 3700 ft, Lander Co., Nevada, USA, 12 August 1966, F.P. and M. Rindge, AMNH (SEM preparations MJR 823, 824); 1 ♀ from Valles, San Luis Potosí, Mexico, 19 July 1956, W. Gertsch, V. Roth, AMNH; 1 ♂ from Brown Canyon, Baboquivari Mts., Arizona, USA, 9 July 1952, M. Cazier and W. Gertsch, AMNH (SEM preparation MJR 825).

NEOLANIDAE

Neolana dalmasi (Marples): ♂ ♀ from Lake Okataina, New Zealand, 20 October 1984, D. Court, OMD; ♂ ♀ from Trounsen's Kauri Park, Waipoua Forest, North Island, New Zealand, 6 April 1995, C. Griswold, CAS (Meikle photo voucher).

NICODAMIDAE

Megadictyna thilenii Dahl: ♂ ♀ from Queen Charlotte Sound, South Island, New Zealand, January 1996, J. Boutin, CAS; ♀ from Hicks Bay, North Island, New Zealand, 15 February 1995, J. Boutin, CAS; ♂ from Orongorongo, New Zealand, 1 March 1992, M. Fitzgerald, CAS; ♀ from W Taupo District, New Zealand, 26 January 1956, R.K. Dell, USNM; ♂ ♀ juvs. from Town Belt, Wellington, New Zealand, January-April 1996, L.J. Boutin, CAS (R. Carlson silk study vouchers); 1 ♂ from Moerangi, North Island, New Zealand, elev. 625 m, mixed podocarp forest, berlese forest litter, 4–9 June 1980, A. Newton and M. Thayer, AMNH; 1 ♀ from Tuna Saddle, N of Taumararui, New Zealand, 10 January 1967, R.R. Forster, AMNH;

♀ from Onamalutu Scenic Reserve, Mt. Richmond Forest Park, 20.6km 263° W Blenheim, S41.45844°, E173.70388°, elev. 90m, South Island, New Zealand, 24 February 2005, C. Griswold, D. Silva and H. Wood, OMD (Wood photo voucher).

Nicodamus mainae Harvey: 1 ♀ from Coalseam Park, Miners picnic site, by head-torch at night, under rock, Irwin River Bank, 29°01'S, 115°29'E, Western Australia, Australia, 11 November 1999, J.W. Waldock, AMNH; 1 ♂ from Bush Bay, 25°06'49"S, 113°43'52"E, Western Australia, Australia, 28 September, 1998, M.S. Harvey et al., AMNH; ♂ ♀ from 30 mi. E. Southern Cross, elev. 350m., Western Australia, Australia, 16 September 1962, E. Ross and D.Cavagnaro, CAS.

OECOBIIDAE

Oecobius navus Blackwall: ♀ from Golden Gate Park, in California Academy of Sciences building, San Francisco, California, USA, 11 June 1973, J. Hjelle, CAS; ♂ ♀ juvs. from S. slope Burdell Mountain, N of Novato, grassland on serpentine soil under stones, Marin Co., California, USA, 28 November 1992, C. Griswold, CAS; ♀ ♂ from Richmond, Contra Costa Co., California, USA, 28 March 1961, P. Craig, CAS; ♀ ♂ from Smithsonian Natural History building, Washington DC, USA, USNM; 4 ♂ 4 ♀ from 1 mi N Sylvania, Georgia, USA, 10 April 1943, W. Ivie, AMNH (SEM preparation MJR 826).

Uroctea spp.: ♂ ♀ from Garies, Namaqualand, South Africa, 14 November 1949, B. Malkin, CAS; juvenile from Julwania, M. P., India, elev. 800m, 14 January 1962, E. Ross and D. Cavagnaro, CAS; ♂ ♀ from Noordoeuer, at Orange River, Namibia, October 1985, C. Griswold and T. Meikle, NMSA (Meikle photo voucher).

PARARCHAEIDAE

Pararchaea sp.: ♂ ♀ from moss in *Nothofagus* forest, Kelper Track, S end of Lake Te Anau, 45°25'S, 167°40'E, Fiordland, South Island, New Zealand, 21 April 1995, C. Griswold and T. Meikle, CAS.

PHYXELIDIDAE

**Ambohima sublima* Griswold: ♂ ♀ from Ambohimanga, Antananarivo Prov., Madagascar, 2 December 1993, C. Griswold, CAS.

**Namaquarachne tropata* Griswold: ♂ ♀ from Grootvadersbosch, Western Cape Province, South Africa, 8–10 November 1985, C. Griswold and T. Meikle, CAS.

Phyxelida bifoveata (Strand): ♂ ♀ from Mazumbai, Muheza District, Tanzania, elev. 1600–1800 m, 4°49'S, 38°30'E, 11–20 November 1995, C. Griswold, D. Ubick, and N. Scharff, CAS.

Phyxelida tanganyensis (Simon and Fage): ♂ ♀ from Amani, East Usambara Mts., Tanzania, 5°5.7'S, 38°38'E, elev. 950 m, 1–10 November 1995, C. Griswold, CAS (R. Carlson silk study voucher).

**Vidole capensis* (Pocock): ♀ from Buffels Bay, Cape of Good Hope, South Africa, 25–29 October 1985, in trees in white milkwood thicket, C. Griswold, T. Meikle and J. Doyen, NMSA (Meikle photo voucher).

Vytfutia pallens Deeleman-Reinhold: ♂ ♀ paratypes from Niah Cave, Sarawak, Malaysia, 10 April 1984, C. Deeleman and C. Hug, RMNH.

Vytfutia bedel Deeleman-Reinhold: holotype ♂ and paratype ♀ from Gunung Leuser, N. Sumatra, Indonesia, 15 November 1983, C. Deeleman-Reinhold, RMNH.

Xeviosio amica Griswold: ♂ ♀ from Lake St Lucia, Zululand, South Africa, 19 November 1985, C. Griswold and T. Meikle, CAS, NMSA.

Xeviosio orthomeles Griswold: ♀ from Sodwana Bay National Park, Mgoboseleni trail, KwaZulu-Natal, South Africa, elev. 50 m, 27°32'34.9"S, 32°39'48.7"E, 6–8 April 2001, G. Hormiga and M. Ramírez, USNM (Hormiga photo voucher).

*Phyxelidid undet. sp.: ♂ from Périnet, Madagascar, 1 August 1992, V. and B. Roth, CAS.

*Phyxelidid undet. sp.: ♂ from Ranomafana, Fianarantsoa Prov., Madagascar, April 1998, C. Griswold, CAS.

PSECHRIDAE

Poaka graminicola Forster and Wilton: ♂ ♀ from Lincoln, South Island, New Zealand, swept from grass, 9 April 1997, A. McLachlan, CAS.

Psechrus sp.: ♂ ♀ from Tham Lot Cave, Thailand, 11 March 1990, V. and B. Roth, CAS.

Psecchus himalayanus Simon: ♂ from Kooloo Valley, India, 1870's, M.M. Carlton, MCZ; ♀ from forest W. of Landrung, Gandaki Zone, Nepal, 21 Oct 1985, J. A. Coddington, USNM.

Psecchus argentatus (Doleschall): 2♂ 2♀ from Camp 1, Menapi, Cape Vogel Peninsula, Papua New Guinea, 21 March–4 May 1953, G. Tate Archbold Expedition, AMNH (SEM preparations MJR 462–467).

Psecchus sp.: ♀ and juveniles from, Bawan, Baoshan Prefecture, Yunnan, China, 24°57'N, 98°50'E, el. 950m, weedy vegetation and road cuts, 8 November 1998, C. Griswold and D. Kavanaugh, CAS and HNU (Griswold photo voucher).

SEGESTRIIDAE

Ariadna boesenbergi Keyserling: ♂ from Sarandí, Buenos Aires, Argentina, January 1998, C. Griswold, MACN (MACN-Ar 10242; SEM preparation MJR 933); 4♀ from Sierras de Olavarría, Buenos Aires, Argentina, 3–6 December 1992, M. Ramírez, MACN (MACN-Ar 10201; SEM preparations MJR 934–936).

Ariadna sp.: ♀ from Phinda Resource Reserve, KwaZulu-Natal, South Africa, elev. 38 m, S 27°50'43", E 32°18'49.1", 13–15 April 2001, M. Ramírez, MACN (Hormiga photo voucher).

STIPHIDIIDAE

Stiphidion facetum Simon: ♂ from Binna Burra, Queensland, Australia, Y. Lubin, QMB; ♂ ♀ from Whalipu, North Island, New Zealand, 25 January 1994, E. Schlinger, CAS; ♀ from Royal National Park, NSW, Australia, 13 August 1990, T. Meikle and C. Griswold, USNM; ♀ from Bundeeena, NSW, Australia, 13 August 1990, T. Meikle and C. Griswold, USNM; ♀ from Piper's Creek, Kosciusko N.P., elev. 5000 ft., NSW, Australia, 26–27 December 1977, E. Schlinger, CAS; ♂ ♀ from Lamington Plateau, Queensland, Australia, V. Davies, QMB; 1♀ from 4 mi S Glencoe, elev. 1280 m, NSW, Australia, 29 November 1962, E. S. Ross and D. Q. Cavagnaro, CAS; 1♂ from Lake St. Caire National Park, Woodland Nature Walk, 42°07'S, 146°10'E, Tasmania, Australia, under rocks, 17 May 1996, L. J. Boutin, CAS; ♀ from Waitomo, North Island, New Zealand, near caves; ca. 36°16'S, 175°33'E, 3 April 1995, C. Griswold and T. Meikle, CAS (Meikle photo voucher); ♀ from Waipoua Forest campground, North Island, New Zealand, on buildings and exotic trees, S35.65233°, E173.55222°, elev. 95m, 43.2 km 299° NNW Dargaville, 9–13 February 2005, C. Griswold, D. Silva and H. Wood, LNZ (Wood photo voucher).

Pillara griswoldi Gray: ♂ ♂ ♀ ♀ from Barrington Tops, NSW, Australia, 14 August 1990, C. Griswold and T. Meikle, CAS and USNM.

TENGELLIDAE

**Liocranoides unicolor* Keyserling: 1♂1♀ from Piper Cave, Smith Co., Tennessee, USA, 5 February 1961, T.C. Barr, AMNH (SEM preparations MJR 524, 525); 3♀ from Fox Cave, Sumner Co., Castalian Springs, Tennessee, USA, 24 March 1949, Jones and Archer, AMNH (SEM preparations MJR 521–523).

Tengella radiata (Kulczynski): ♂ ♀ from Finca La Selva, Costa Rica, October 1981, C. Griswold, CAS; ♂ ♀ from Finca La Selva, Costa Rica, 3 May 1994, G. Hormiga and J. Coddington, USNM (Hormiga photo voucher); ♀ from Finca La Selva, Costa Rica, 1989, J. Coddington, USNM; 1♀ from several km N of Tilaran, 700 m, rotting logs in dense forest and pasture, Guanacaste, Costa Rica, 12 August 1983, F. Coyle and J. Carico, AMNH (SEM preparations MJR 514, 515); 2♂ from Sector Cocori, 30 Km al N. Cariari, Limón, Costa Rica, elev. 100m, Malaise LN 286000 567500 #4525, December 1994, E. Rojas, INBio (SEM preparations MJR 698).

Tengella sp.: ♀ from Palenque, Chiapas, Mexico, 25 August 1977, C. Griswold and T. Meikle, CAS.

TETRAGNATHIDAE

**Nephila* sp.: ♀ from Sodwana Bay National Park, Mgboseleni trail, elev. 50 m, 27°32'34.9"S, 32°39'48.7"E, KwaZulu-Natal, South Africa, 6–8 April 2001, M. Ramírez, USNM (web sample MJR), 6 April 2001 (SEM preparation MJR 267), MACN.

TITANOECIDAE

Goeldia spp.: ♂ ♀ from Colonia Perene, Peru, 3 January 1955, E. Schlinger and E. Ross, CAS; ♂ ♀ from

Zapallar, Chile, 27 November 1950, E. Ross and A. Michelbacher, CAS; ♂ from Colombia, 17 April 1965, P. Craig, CAS; ♀ from Valparaiso, Chile, November 1981, N. Platnick, USNM; ♀ from Parque Nacional Iguazú, 6 km E seccional Yacuy, Misiones, Argentina, 14–16 December 1999, M. Ramírez and L. Lopardo, MACN (Ramírez photo voucher); ♀ from Parque Nacional Pilcomayo, Laguna Blanca, Formosa, Argentina, November 1990, M. Ramírez, MACN (Ramírez photo voucher).

Titanoeca americana Emerton: ♂ ♀ from Portle Springs, Missouri, USA, 2 June 1965, W. Peck, CAS; 4♂ 4♀ from Lambertville, 74°26'W, 40°22'N, New Jersey, USA, June 1952, W. Ivie, AMNH.

Titanoeca nigrella (Chamberlin): ♂ ♀ from Cave Creek, Arizona, USA, 2 July 1996, D. Ubick, CAS (R. Carlson silk study voucher, Coville photo voucher).

ULOBORIDAE

**Conifaber guarani* Grismado: ♂ ♀ from Parque Nacional Iguazú, RN 101, 6km E seccional Yacuy, Misiones, Argentina, 14–16 December 1999, M. Ramírez and L. Lopardo, MACN (MACN-Ar 9878 MJR16.XII.99/7, SEM preparations CJG1, 2); ♂ ♀ with same data, MACN (MACN-Ar 9870 MJR16.XII.99/15, SEM preparation MJR 206).

**Hyptiotes* sp.: juv. from 1.4 mi W. of Cazadero on Ft. Ross Rd, Sonoma Co., California, USA, redwood/douglas fir forest, 21 June 1996, C.E. Griswold and R. Carlson, CAS (R. Carlson silk study voucher).

**Miagrammopes zenzesi* (Mello-Leitão): ♀ from Parque Nacional Iguazú, Misiones, Argentina, February 1995, M. Ramírez, MACN (Ramírez photo voucher); Departamento Cainguás, Parque Provincial Salto Encantado, Misiones, Argentina, 27°07'S, 54°48'E, sendero al Salto La Olla, 10–11 January 2005, C. Grismado, L. Lopardo, L. Piacentini, A. Quaglino and G. Rubio, MACN (Lopardo photo voucher).

**Octonoba octonaria* (Muma): ♀ from Washington Co., Arkansas, USA, 7 September 1965, W.B. Peck, CAS; ♀ from St. Charles Co., Missouri, USA, June 1986, USNM.

**Philoponella* cf. *fasciata* (Mello-Leitão): ♀ from Parque Nacional Iguazú, Misiones, Argentina, July 1992, M. Ramírez, MACN (Ramírez photo voucher).

Uloborus diversus Marx: ♀ from Howell Mt., Napa Co., California, USA, 28 April 1973, H.B. Leech, CAS.

Uloborus glomosus (Walckenaer): 2 ♀ from Mast, 10 mi W Boone on U. S. 421, North Carolina, USA, 18–24 July 1954, E. E. B., AMNH; 1 ♂ from Clemson, South Carolina, USA, 82°50'W, 34°41'N, 6 August 1962, A. Payne, AMNH (SEM preparations MJR 815–817).

Uloborus trilineatus Keyserling: ♀ from Pipeline Rd., Canal Zone, Panama, B. Opell, USNM.

Uloborus spp.: ♂ ♀ from Redding, Shasta Co., California, USA, August 1947, H. Chandler, CAS; ♂ subadult from Sodwana Bay National Park, Mgoboseleni trail, elev. 50 m, 27°32'34.9"S, 32°39'48.7"E, KwaZulu-Natal, South Africa, 6–8 April 2001, M. Ramírez, MACN (web sample MJR 6.IV.01/2, SEM preparation MJR 271).

**Zosis* sp.: ♂ ♀ from Horneman Farm, elev. 220m, Isla Santa Cruz, Galapagos Archipelago, Ecuador, 18 April 1964, D.Q. Cavagnaro, CAS.

ZORIDAE

**Xenoctenus* sp.: 1♂ 1♀ 2 immatures from Embalse Los Sauces, La Rioja, Argentina, 7–8 October 1965, E. Maury, MACN (MACN-Ar, SEM preparations MJR 665, 666); other specimens from Santa Catalina, Santiago del Estero, Argentina, 26 October 1963, M. E. Gali.

ZOROCRATIDAE

Raecius asper (Thorell): ♀ from Mann's Spring, Mount Cameroon, Cameroon, 25 January 1992, C. Griswold, CAS; ♀ from grassland and forest near Mann's Spring, Mt. Cameroon, elev. 2050m, 4°08'N, 9°07'E, 21–25 January 1992, C. Griswold, J. Coddington, G. Hormiga and S. Larcher, USNM (Hormiga photo voucher); ♂ from Moca, Bioko Island, Equatorial Guinea, 1–11 October 1998, D. Ubick and K. Dabney, CAS.

Raecius jocquei Griswold: ♂ ♀ from Appouesso, forêt classée de la Bossematie, Côte d'Ivoire, pitfall traps, 31 October 1994, R. Jocqué and N. Seabé, MRAC.

Raecius congoensis Griswold: holotype ♀ from Lulimbi, embouchure de la riv. Ishasha dans le lac Edward (Sud-Est) baie de Kyangiro, D.R. Congo, "dans le sol prélève," July–August 1976, M. Lejeune, MRAC.

- Raecius scharffi* Griswold: juvenile from 12 km SE Amani, Kihuhwi-Zigi Forest Reserve, 5°6.3'S, 38°40.6'E, 400–450m elev., East Usambara Mountains, Tanzania, 2–4 November 1995, C. Griswold, CAS (R. Carlson silk study voucher).
- Uduba dahlí* Simon: ♂ ♀ from Madagascar, Forsyth Major, BMNH; ♂♂ from 7 km W Ranomafana, Fianarantsoa Prov., Madagascar, 22–31 October 1988, W. Steiner, USNM; ♀ from Andohahela, Toliara Prov., Madagascar, 7–17 November 1995, S. Goodman, FMNH.
- Uduba madagascariensis* (Vinson): ♂ from Ambohimanga, Antananarivo Prov., Madagascar, 18°44'S, 47°34'E, elev. 1400m., 31 October 1993, C. Griswold, S. Larcher, N. Scharff and J. Coddington, CAS (Scharff photo voucher).
- Uduba* spp.: ♂ ♀ from 3 km 41° NE Andranomay, 11.5 km 147° SSE Anjozorobe, Antananarivo Prov., Madagascar, 5–13 December 2000, Fisher-Griswold Arthropod Team, CAS; ♀ from Ranomafana, Fianarantsoa Prov., Madagascar, 10 May 1992, V. and B. Roth, CAS; juvenile from Talataky, Parc Nationale Ranomafana, Fianarantsoa Province, Madagascar, 21°14.9'S, 47°25.6'E, ca. 900m elev., April 1998, C.E. Griswold, CASC (Griswold photo voucher).
- Zorocrates* cf. *mistus* O. P.-Cambridge: 1 ♀ ♀ penultimate from Los Llanos, Chiapas, Mexico, 29 August 1972, Mitchell and Russell, AMNH (SEM preparations MJR 448–452).
- Zorocrates* sp.: ♂ ♀ from Big Bend National Park, The Basin, 6000 ft., Texas, USA, 25 August 1967, W. Gertsch, Hastings, AMNH (SEM preparations MJR 453, 454); 3 ♂ 1 ♀ penultimate from El Tablón, 7 mi SE Zimapan, Hidalgo, Mexico, 20°40'N, 99°20'W, 19 August 1964, J. and W. Ivie, AMNH (voucher D. Silva study, 2000; respiratory system examined from subadult female; temporary mount of expanded male palp MJR 972); ♀ from Chiricahua Mts., Arizona, USA, CAS (Coville photo voucher).
- *Zorocratidae undet. sp.: ♂ ♀ from English Camp, Ankarana, 12°54'34"S, 49°6'36"E, Madagascar, 20–26 August 1992, V. and B. Roth, CAS.

ZOROPSIDAE

- **Uliodon* cf. *frenatus* (L. Koch): ♀ from Wellington town belt, top of Harriet Street, North Island, New Zealand, 24 April 1995, J. Boutin, CAS (SEM preparations MJR 344–347, 389, 512).
- Zoropsis rufipes* (Lucas): ♀ from La Gomera, Canary Islands, J. Wunderlich, CAS; ♂ and ♀ from Tenerife, Canary Islands, November 1975, P. Oromí, AMNH; 1 ♀ from Tenerife, Canary Islands, November 1975, P. Oromí, AMNH; 1 ♂ with same data, AMNH; 1 ♀ from Tenerife, Canary Islands, November 1975, P. Oromí, AMNH (SEM preparations MJR 456–459); 1 ♂ with same data, AMNH (SEM preparations MJR 460, 461).
- Zoropsis spinimana* (Dufour): ♂ from Sunnyvale, California, USA, 12 February 1996, M. Beaugard, CAS; ♂ ♀ Sunnyvale, California, USA, inside house, January–March 1999, V. Romano, CAS (Griswold photo voucher); ♀ from Oakland, SE side of Lake Merritt, in house, Alameda Co., California, USA, 24 September 1997, K. Lundstrom, CAS; ♀ from near Barcelona, Roses, Spain, July 1980, MRAC; ♂ from Vernet-les-Bains, Pyrénées-Orientales, France, 22 August 1989, J.A. Coddington, USNM; ♀ ♀ from Grottes des Canaletes, Pyrénées-Orientales, France, 21 August 1990, J.A. Coddington, USNM; ♀ from Sunnyvale, California, USA, 1996, CAS (R. Carlson silk study voucher).
- Zoropsis media* Simon: ♀ from Pyrénées-Orientales, France, 22 March 1968, H.W. Levi, MCZ.

APPENDIX 2. Data matrix. Terminals scored with more than one state are coded as: a = [01], b = [02], c = [12]

0	<i>Hypochoilus</i>	1234	56789	1111	11111	22222	22222	33333	33333	44444	44444	55555	55555	66666	66666	77777	77777
1	<i>Gradungula</i>	000-	0-001	00000	00000	00000	00000	00000	00000	0000-	00000	10000	10000	00-0-	00000	00000	00000
2	<i>Thaïda</i>	000-	0-001	00001	11010	00000	01010	10001	00100	0000-	10011	01000	00-10	01002	10000	00020	00000
3	<i>Hickmania</i>	000-	0-001	00001	00000	00000	01010	10001	00100	0000-	10011	01000	00-0-	00102	10000	00020	00000
4	<i>Filiistata</i>	010-	1-000	20000	00000	00000	02000	00000	00011	1000-	02011	00101	01-0-	00022	00101	01010	01010
5	<i>Kukulcania</i>	010-	1-000	20000	00000	00000	02000	00000	00111	1000-	00011	00212	00210	01-0-	00022	00101	01010
6	<i>Ariadna</i>	000-	0-010	20000	00001	00000	00000	00000	00100	0000-	00011	101??	00210	0210-	01-02	01-000	00000
7	<i>Stegodyphus</i>	010-	0-010	20000	00000	01000	01001	10000	00100	00010	00301	1????	?????	12010	00012	10100	01000
8	<i>Eresus</i>	010-	0-010	20000	00000	01000	01001	10000	00100	00010	00301	10121	01110	12010	00012	10100	01000
9	<i>Uroctea</i>	010-	0-000	20000	00000	00000	00000	00000	01101	0000-	00011	10121	01110	12010	10002	11-000	01000
10	<i>Oecobius</i>	010-	0-010	00000	00000	01000	01002	00000	01101	0000-	00011	10121	01110	12010	11-02	10100	1-0-0-
11	<i>Deinopis</i>	010-	0-000	00001	00010	00000	11000	00000	00100	0000-	00301	10121	-?210	12010	00001	10000	00000
12	<i>Menneus</i>	010-	0-?00	00001	?0010	00000	01000	00000	00100	0000-	00301	10121	?????	1?210	00001	10000	00000
13	<i>Uloborus</i>	110-	0-000	00001	00010	00000	11000	00000	00100	0000-	00301	11-?1	01110	12011	00002	10000	00021
14	<i>Octonoba</i>	110-	0-?00	00001	00010	00000	11000	00000	00100	00010	00301	11-??	?????	1?210	00002	10000	00021
15	<i>Araneus</i>	010-	0-000	11001	00100	10000	00000	00000	00100	00010	02111	10111	01110	12010	00002	11-000	00121
16	<i>Megadictyna</i>	010-	0-000	20001	00000	00000	01000	00000	00100	0000-	00111	1????	?????	12011	00002	10000	10020
17	<i>Nicodamus</i>	010-	0-000	1000a	00000	00000	00000	00000	00100	0000-	00111	101??	?????	1-211	00001	11-000	10020
18	<i>Dictyna</i>	010-	0-000	00000	00000	01000	01000	00001	10100	00011	02111	10111	00210	1-211	01-02	10000	10021
19	<i>Nigma</i>	010-	0-000	b0000	00000	01000	01000	00001	10100	00011	00111	1????	?????	1?210	01-02	10000	10021
20	<i>Tricholathys</i>	0110	11000	00000	00000	01000	01000	00001	00100	00011	00111	1????	?????	1-211	01-02	10000	10021
21	<i>Lathys</i>	0110	00000	00000	00000	01000	01000	00001	00100	00011	02111	1????	?????	1-211	01-02	10000	10021
22	<i>Titanoeca</i>	010-	0-010	00000	00000	00000	01000	00001	00100	00011	01111	1????	?????	12010	00002	10100	10020
23	<i>Goeldia</i>	010-	0-010	00000	00000	00000	01000	00001	00100	00011	01111	1????	?????	12010	00002	10100	10020
24	<i>Vyffutia</i>	010-	0-010	00000	11000	00100	01010	00001	00100	00011	01111	1????	?????	12010	01-02	10100	00021
25	<i>Xevioso</i>	010-	0-010	00000	11001	00100	01010	00001	00100	00011	02111	1????	?????	12011	01002	10100	00020
26	<i>Phyxelida</i>	010-	0-010	00000	11000	00100	01010	00001	00100	00011	02111	1????	?????	12011	01002	10100	00020
27	<i>Neolana</i>	0110	11000	00000	00000	00000	01000	00001	00100	00011	02111	1????	?????	12010	01-02	10100	00020
28	<i>Stiphidion</i>	0110	11100	00000	00010	00000	01000	00001	00100	00011	01201	1????	?????	12010	01-02	10100	10020
29	<i>Pillara</i>	0110	11100	01000	00010	00000	01000	00001	00100	00011	01211	1????	?????	12010	01-02	10100	10020
30	<i>Neoramia</i>	0110	11000	b0000	00001	00000	01000	00001	00100	00011	02111	1????	?????	12010	01-02	10100	10020
31	<i>Maniho</i>	0110	10100	01000	00011	00000	01000	00001	00100	00011	02111	1????	?????	12010	01-02	10100	10020
32	<i>Metalrella</i>	0110	11100	b0000	00001	00000	01000	00001	00100	00011	01111	1????	?????	12010	01-02	10100	10020
33	<i>Desis</i>	0111	10110	c0000	00000	01000	00000	00000	00000	00011	01111	1????	?????	12111	01-02	11-000	10000
34	<i>Matachia</i>	0110	11100	21000	00001	00000	01000	00001	00100	00011	01111	1????	00210	12111	01-02	10000	10020
35	<i>Phryganoporus</i>	0110	10100	?0000	00000	00000	01000	00001	00100	00011	02111	1????	?????	12111	01-02	10100	10020
36	<i>Bačuma</i>	0110	10100	00000	00000	00000	01000	00001	00100	00011	02111	1????	00210	12111	01-02	10100	10020
37	<i>Macrobnus</i>	0110	11100	b0000	00000	00000	00000	00001	00100	00011	00111	1????	?????	12011	01-02	11-000	10020
38	<i>Retiro</i>	0110	11000	b0000	11000	00000	01000	00001	00100	00011	01111	1????	?????	12011	01-02	10100	10021
39	<i>Pimus</i>	0110	11110	00000	10000	00000	01000	00001	00100	00011	01111	1????	?????	12010	00002	10100	10020
40	<i>Amaurobius</i>	0110	11110	00000	00001	00000	01000	00001	00100	00011	01111	1????	00210	12010	00102	10100	10020
41	<i>Callobius</i>	0110	11110	00000	00001	00000	01000	00001	00100	00011	01111	1????	?????	12010	00102	10100	10020

APPENDIX 2 (continued). Data matrix. Terminals scored with more than one state are coded as: a = [01], b = [02], c = [12]

	1234	56789	1111	11111	22222	22222	33333	33333	44444	44444	55555	55555	66666	66666	77777	77777
42 <i>Tengella</i>	0111	10010	01000	00001	0-100	00001	00100	00100	00111	02111	1????	?????	12010	01-02	10100	10020
43 <i>Zorocrates</i>	0111	10010	01000	00001	0-100	00001	00100	00100	00111	02111	101??	?????	12010	01-02	10100	10020
44 <i>Raecius</i>	0111	10010	00000	00010	0-100	00001	00100	00100	00111	02111	1????	?????	12010	01-02	10010	10020
45 <i>Uguba</i>	0111	10010	00000	00000	00011	0-100	00001	00100	00111	02111	1????	?????	12010	01-02	10110	10020
46 <i>Psechrus</i>	0110	10010	00010	00000	00000	0-100	00001	00100	00011	02211	1????	0?P10	12010	01-02	10100	10020
47 <i>Zoropsis</i>	0111	10010	00110	00000	10011	0-100	00001	00100	00011	02201	101?1	0?P10	12010	01-02	101a0	10020
48 <i>Acanthoctenus</i>	0111	10010	01110	00000	10001	0-100	00001	00100	00011	02201	1????	?????	12010	01-02	10110	10020
49 <i>Aebutina</i>	0110	00100	00000	00000	01000	01000	00000	00100	00011	01111	101??	?????	12010	01-02	10100	10020
50 <i>Poaka</i>	0110	11100	00000	00000	10000	01000	00001	00100	00011	0?111	1????	?????	12010	01-02	10100	10021
51 <i>Huttonia</i>	010-	0-010	10000	01001	10000	0-0-0	00010	00101	0110-	10111	101??	?????	12010	01-02	11- - -	10021
52 <i>Mimetus</i>	010-	0-000	10001	01000	00000	0-0-0	00010	00110	0100-	00111	1????	?????	12010	00002	11- - -	00121
53 <i>Pararchaea</i>	010-	0-000	10001	00100	01000	0-0-0	01110	00101	0110-	a0111	10???	?????	12010	001?2	11- - -	1????
54 <i>Archaea</i>	010-	0-010	10001	00000	01000	0-0-0	01110	00100	0110-	12111	101??	?????	0-210	01-02	11- - -	10121

APPENDIX 2 (continued). Data matrix. Terminals scored with more than one state are coded as: a = [01], b = [02], c = [12]

	88888	88888	99999	99999	11111	11111	11111	11111	11111	11111	11111	11111	11111	11111	11111	11111
0 <i>Hypocheilus</i>	00-0	00-0	01000	01000	00000	00000	01234	56789	01234	56789	01234	56789	01234	56789	01234	56789
1 <i>Gradungula</i>	00-0	10- - -	0- - - -	0- - - -	0- - - -	0- - - -	0- - - -	0- - - -	0- - - -	0- - - -	0- - - -	0- - - -	0- - - -	0- - - -	0- - - -	0- - - -
2 <i>Thaida</i>	01100	01110	00100	01101	10000	0-00	-0000	00000	00000	10-00	010-0	10011	01000	00000	0-001	0-001
3 <i>Hickmania</i>	01100	11110	00100	01000	-00	0-00	-0000	0001-	- - - 1	- - - ??	010-0	10111	0?00?	?????	?????	?????
4 <i>Filiastata</i>	01301	00-10	12000	00-1	10-00	0-00	-0001	0001-	- - - 1	- - - ??	00-0	0000-	1?00?	?????	?????	?????
5 <i>Kukulcania</i>	01301	00-10	12000	00-1	10-00	0-00	-0001	0001-	- - - 1	- - - 10	00-0	0000-	10000	00000	0-001	0-001
6 <i>Ariadna</i>	01301	00- - -	- - - - -	00- - -	- - - 0	0-00	00001	0001-	- - - 1	- 0-??	00- - -	0- - - -	1-00?	???00	0-000	0-000
7 <i>Stegodyphus</i>	01000	0110-	- - - - -	01110	- - - 0	0-00	-0000	00001	1001-	- - - ??	11000	000?0	11000	00000	0-000	0-000
8 <i>Eresus</i>	01000	0110-	- - - - -	01110	- - - 0	0-00	-0000	00001	1001-	- - - 11	11000	0????	1?00?	?????	?????	?????
9 <i>Uroctea</i>	00-0	110- -	- - - - -	00- - -	- - - 0	0-00	-0000	00000	03000	01011	11010	0- - - -	?-00-	- - - - -	- - - - -	- - - - -
10 <i>Oecobius</i>	01300	0100-	- - - - -	00-0	- - - 0	0-00	-0000	00000	03000	01011	11010	0?01?	1100?	?????	?????	?????
11 <i>Deinopis</i>	11100	0111?	00000	01100	- - - 0	0-00	-0000	00002	0001-	- - - 11	11000	00011	01111	11111	11111	11111
12 <i>Menneus</i>	11300	0111?	00000	01100	- - - 0	0-00	-00?0	00002	0001-	- - - ??	11000	000?1	0111?	?????	?????	?????
13 <i>Uloborus</i>	11200	0111?	00000	01100	- - - 0	0-00	-0000	00000	03000	00-11	11000	00111	01101	12111	10111	10111
14 <i>Octonoba</i>	11200	0111?	00000	01100	- - - 0	0-00	-0000	00000	03000	00-??	11000	0?1?1	01101	12111	10111	10111
15 <i>Araeus</i>	01210	010-	- - - - -	1110-	- - - 0	0-10	-1000	00000	03000	10-11	11000	0- - - -	0-101	11111	10111	10111
16 <i>Megadictyna</i>	01310	0?P11	00100	01001	00000	0-020	10000	00002	0001-	- - - ??	11000	00010	0100?	?????	?????	?????
17 <i>Nicodamus</i>	11300	110-	- - - - -	00- - -	- - - 0	0-020	10000	12000	10000	10-??	11000	0- - - -	- - - - -	- - - - -	- - - - -	- - - - ?
18 <i>Dictyna</i>	11300	01011	00110	01001	00000	10020	00000	00000	1101-	- - - 11	11000	01111	11000	00000	0-000	0-000
19 <i>Nigma</i>	11311	01011	00110	01001	00000	0-010	00000	00000	1101-	- - - ??	11000	01011	1?00?	?????	?????	?????
20 <i>Tricholathys</i>	01300	01111	01-1-	01- - 0	- - - 0	1000-	-0000	00000	1101-	- - - ??	11000	0????	?????	?????	?????	?????

APPENDIX 3. Comments on Matrix

Character	Terminal	Comment
2	1	With protruding spine, Forster et al. (1987: figs. 387–391)
8	1	Not photographed, but not described otherwise (see Forster et al. 1987: 61)
9	1	Also crenulate
10	19, 30, 32	Intermediate
10	33	Polymorphic because the tibial cuticle is squamate
10	37	Some ridged areas
10	38	Intermediate
10, 69, 75, 78, 79, 82, 88, 95, 96, 99	53	Schütt (2002)
15	53	Should also be variable, because some species have stridulatory ridges
16	51	Only one, basal
16	53	Should also be variable, because some species have stridulatory ridges
20	15	Many spines, not well paired
20	17	Not paired
22	6	Other <i>Ariadna</i> species bear clasping processes
25	10	Several macrosetae, but not aligned
25	17	Some thick setae, not aligned
45	2	But females with aligned nodules
45	53	Variable through species (Forster and Platnick 1984)
51	0	Marples (1968)
51	1	Forster (1955), Marples (1968)
51	2	After <i>Austrochilus</i> from (Marples 1968)
51	3	Marples (1968)
51, 52	4, 8–10, 15, 18, 47	From Millot (1931a–c), who made sections to study the midgut diverticula
51, 52	11, 12	From Millot (1933c), who made sections to study the midgut diverticula of <i>Menneus</i> and <i>Deinopis</i>
51, 52	49	Millot (1933a)
51	53	Forster et al. (1984)
51	54	Petrunkevitch (1939)
53, 54, 56	1, 3	Marples (1968)
53, 54, 56	2	After <i>Austrochilus</i> from (Marples 1968)
53	5	Buxton (1913)
53	15	After <i>Araneus trifolium</i> from Buxton (1913)
53	18	After unspecified Dictynidae from Buxton (1913)
54	0	Millot (in Bristowe 1933)
54	4, 8–13, 18, 47	Millot (1931a–c)
54	6	Absent in <i>Segestria</i> (Millot 1931a)
54	15	After <i>Araneus</i> and <i>Tetragnatha</i> from Millot (1931a)
55	0, 1	Marples (1968, 1983)
55	2	Marples (1983); also in <i>Austrochilus</i> from Marples (1968)
55	3	Marples (1968, 1983)
55	4	After " <i>Filistata</i> " from Marples (1983), also " <i>Filistatidae</i> " in Marples (1968). The M1 is absent, only the anterior M2 muscle is present, from carapace (1983: fig. 9).
55	6, 9, 10, 13, 15, 18, 34, 36, 40, 46, 47	Marples (1983)

55	11	Marples (1983), also Marples (1968). The M1 is absent, only the anterior M2 muscle is present, from carapace (1983: fig. 9).
56	4	Millot (1936)
56	6	Absent in <i>Segestria</i> (Millot 1936)
56	8, 9, 13	Millot (1936)
56	15	After <i>Tetragnatha</i> from Millot (1936)
57	0	Interpreted as in Marples (1968), after comparison with <i>Ectatosticta</i> (Millot 1933b: fig. 2). <i>Hypochilus</i> has a much more attenuate, almost straight intestine (Marples 1968: fig. 4b).
57	2	After <i>Austrochilus</i> (Marples 1968: fig. 4e)
57	3	Marples (1968: fig. 4c)
57	4	Note also that Marples (1968) remarked that the intestine in <i>Filistata</i> and <i>Segestria</i> was well defined, instead of diffuse
57	5	From L. Nieto (in lit. to MJR). Haplogynae with globose abdomen (<i>Scytodes</i> , <i>Physocyclus</i>) observed by Millot (1933b: 228), not M-shaped, only curved. He generalized the condition "straight" (including curved) to Araneomorphae except Hypochilidae, without specifying representatives.
57	6	Straight in <i>Segestria</i> (Marples 1968)
57	8–10, 13	Tentatively scored from Millot (1936, 1938), because his illustrations were presumably made from sagittal sections, and he (1949) later said that a M-shaped intestine is characteristic of Araneomorphae other than Hypochilidae.
57	15	After <i>Tetragnatha</i> , tentatively from Millot (1936)
58	1	Forster (1955), Marples (1968)
58	3	Marples (1968)
58	5	Petrunkevitch (1933) and L. Nieto (in lit. to Ramírez)
58	6	Two, from Petrunkevitch (1933)
58	8, 9, 15	Petrunkevitch (1933), Millot (1936)
58	10, 11, 13, 18, 41, 46– 48, 52, 54	Petrunkevitch (1933)
59	0	From Petrunkevitch (1933) and Marples (1968). See discussion of differences between <i>Ectatosticta</i> and <i>Hypochilus</i> in Marples (1968: 22)
59	1	From Marples (1968) and Ramírez (2000)
59	2	After <i>Austrochilus</i> from Marples (1968) and Ramirez pers obs.
59	3	Marples (1968)
59	4, 8, 9, 13, 15	Millot (1936)
59	5	Ramírez and Grismado (1997)
59	6	Dorsal sigillae absent; also after <i>Segestria</i> from Millot (1936) and Crome (1955)
59	7, 16– 18, 22, 28, 30, 32, 33, 35–37, 39, 40, 42, 43, 46–48	From the dorsal sigillae
59	11, 40, 46	Crome (1955)
59	18	Dorsal sigillae, also after unspecified dictynid in Millot (1936)
59	51	Probably reduced, dorsal sigillae absent
62	2	Ambiguous interpretation
62	4, 5	Interpreted as reduced booklung
64	6	Absent

64	51	Fused in a median tube
68	6	Irregular, almost smooth
79	6	Inapplicable, only one MAP
79	10	Inapplicable, only one MAP; there are several tartipores, none of them larger
79	14	Coddington (1989)
79	21	A small nubbin attached to the MAP base
79	33	Inapplicable, only one MAP
79	54	The nubbin is not smooth. Immature has two MAP.
80	15	But at high magnification there is a sharp margin, tightly enclosing the shaft
82	51	None
89	11	Peters (1992a)
96	7	Peters (1992b) noted the particular placement of the triad, and traced the function of the MS spigot to the axial fibers in the cribellate band
96	20	Present with a nubbin at side
96	26	It is strange that the male has a tartipore in that position
101	4	MS absent but PC in similar position as in other terminals
101	5	MS absent but PC in similar position as in other terminals
102	43	United, but not PC
108	39	But medial in <i>Pimus napa</i>
111	15, 52	Flat lobe, not scored as a process
117	32, 33	Internal origin, T and C without well defined limits
128, 129	0–54	All scorings after Huber in lit. to Griswold
128	51	Scored present after <i>Palpimanus</i> , from Huber in lit. to Griswold
131	1	Similar as in <i>Thaida</i> , less protruding but more sclerotized
131	3	Similar as in <i>Thaida</i> , less sclerotized
133	8	Seemingly contra Schütt (2002). The morphology is similar to that of oecobiids in that the copulatory opening leads directly into large, globose SP2, with thick, not much sclerotized walls. The oecobiid condition is much more radical, and <i>Eresus</i> is scored absent.
140	33	No web, behavioral data from Lamoral (1968)
154	12	Wrap-bite attack (Ackerman 1926, McKeown 1936, cited by Peters 1992a)

ILLUSTRATIONS

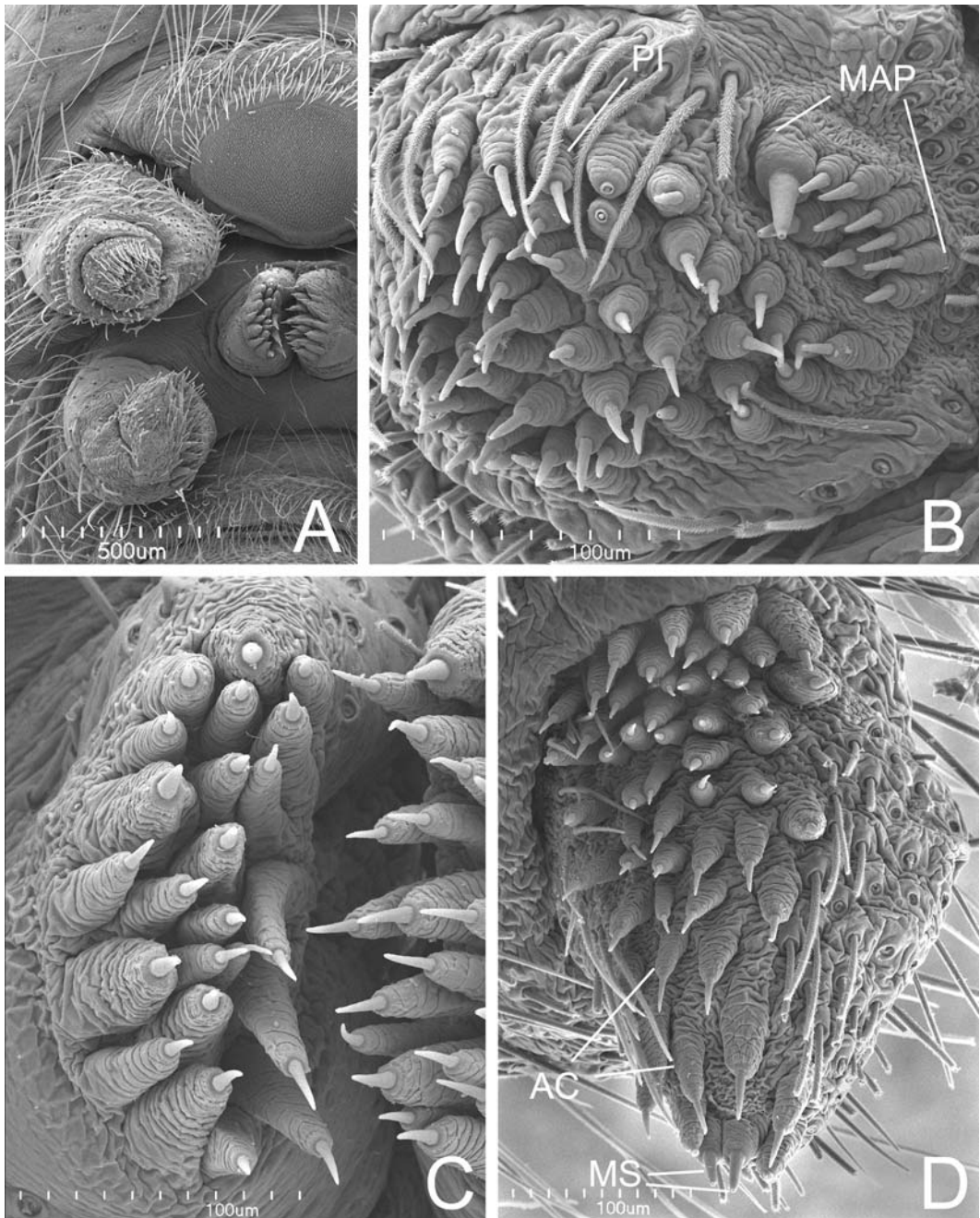


FIGURE 1. Right spinnerets of *Hypochilus pococki* female from Haywood Co., North Carolina, USA. A. Spinnerets and cribellum, overview. B. ALS. C. PMS. D. PLS. AC = aciniform gland spigot(s), MAP = major ampullate gland spigot(s), MS = PLS modified spigot (s), PI = piriform gland spigots. Scale bars: A = 500µm, B–D = 100µm.

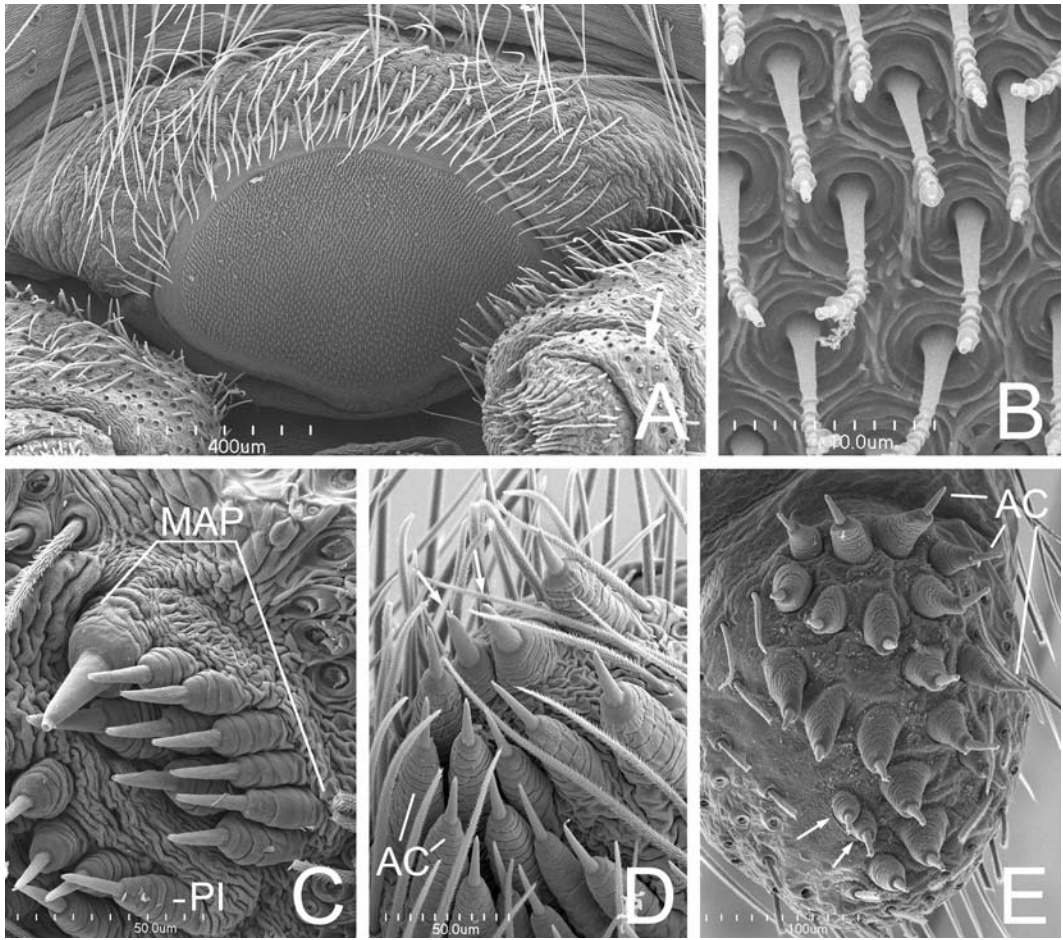


FIGURE 2. Details of female spinnerets. A–D. *Hypochilus pococki* from Haywood Co., North Carolina, USA. A. Cribellum and left ALS. Arrow to intermediate ALS segment. B. Cribellar spigots, close up. C. Right ALS, MAP field: two MAP spigots larger than the rest. D. Right PLS: arrows to two (possibly three, one broken shaft) apical spigots larger than the AC. E. *Ectatosticta* sp. from Shaanxi Province, China, right PLS: arrows to two apical spigots smaller than the AC. AC = aciniform gland spigot(s), MAP = major ampullate gland spigot(s), PI = piriform gland spigots. Scale bars: A = 400µm, B = 10µm, C, D = 50µm, E = 100µm.

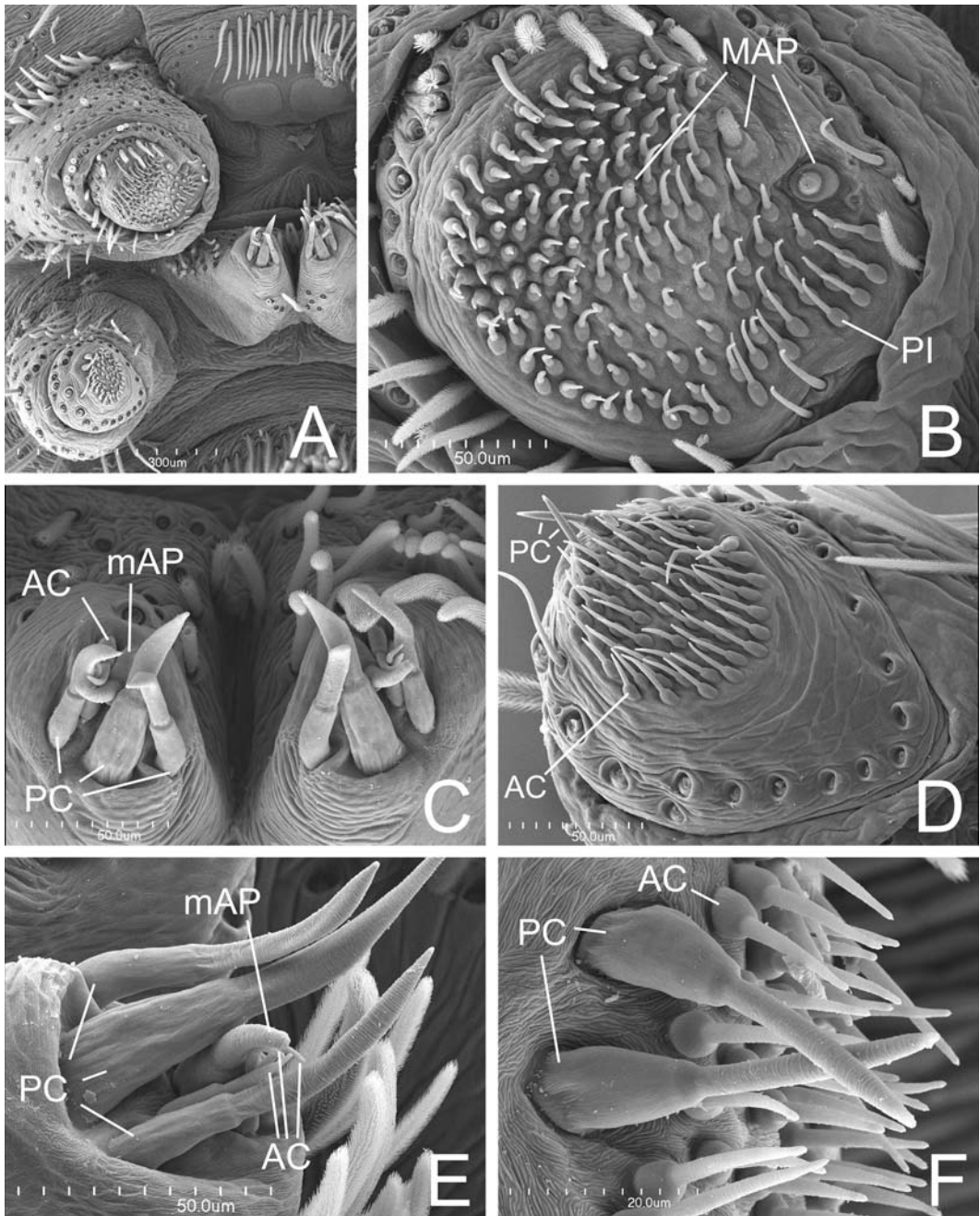


FIGURE 3. Spinnerets of female *Filistata insidiatrix* from Siena, Italy. A. Overview, right. B. Right ALS. C. PMS. D. Right PLS. E. Right PMS. F. Right PLS, detail of PC. AC = aciniform gland spigot(s), MAP = major ampullate gland spigot(s), mAP = minor ampullate gland spigot(s), PC = paracribellar spigot(s). Scale bars: A = 300µm, B–E = 50µm, F = 20µm.

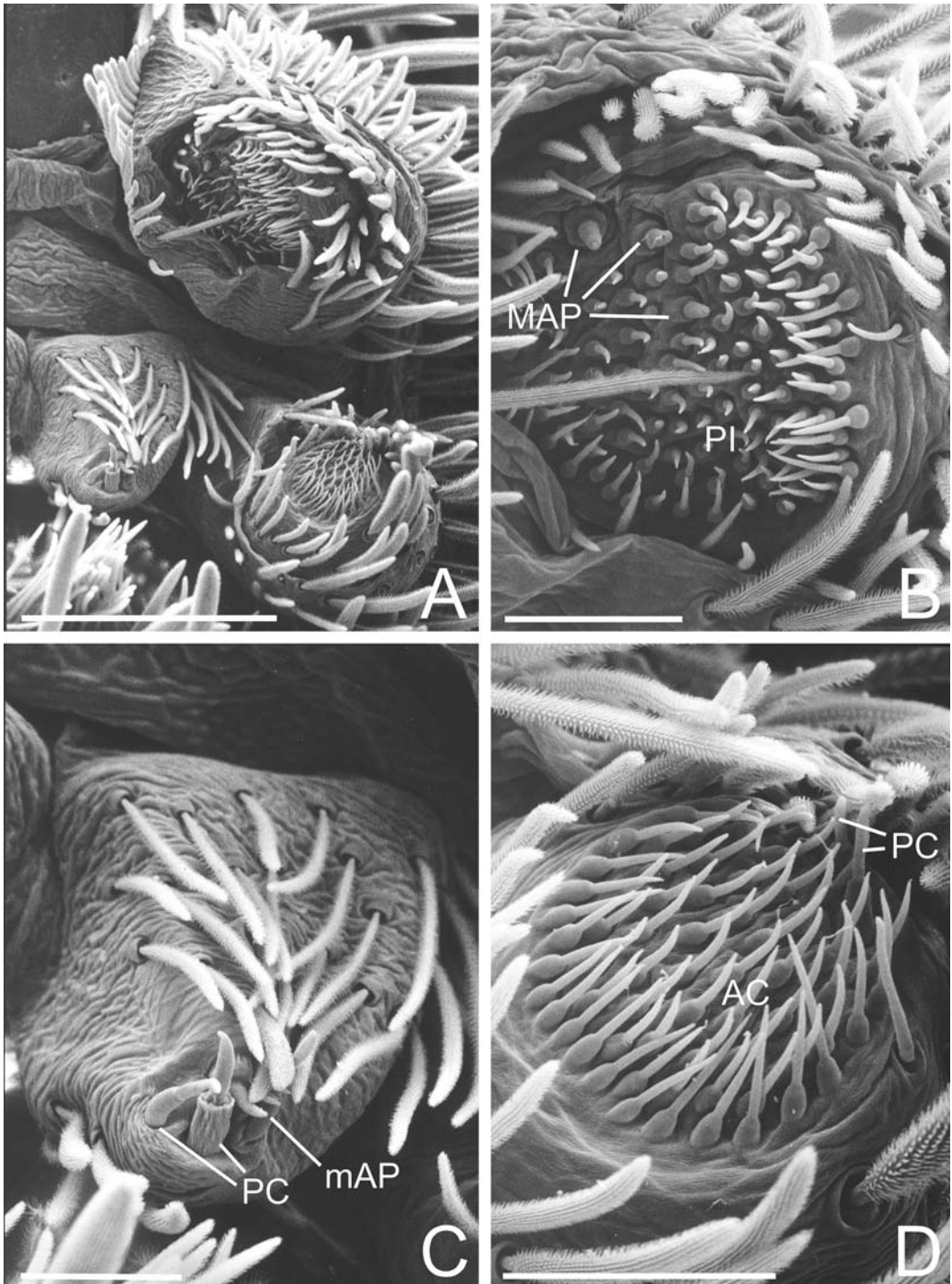


FIGURE 4. Left male spinnerets of *Filistata insidiatrix* from Barcelona, Spain. A. Spinneret overview. B. ALS. C. PMS. D. PLS. AC = aciniform gland spigot(s), MAP = major ampullate gland spigot(s), mAP = minor ampullate gland spigot(s), PC = paracribellar spigot(s), PI = piriform gland spigot(s). Scale bars: A = 200µm, B–D = 50µm.

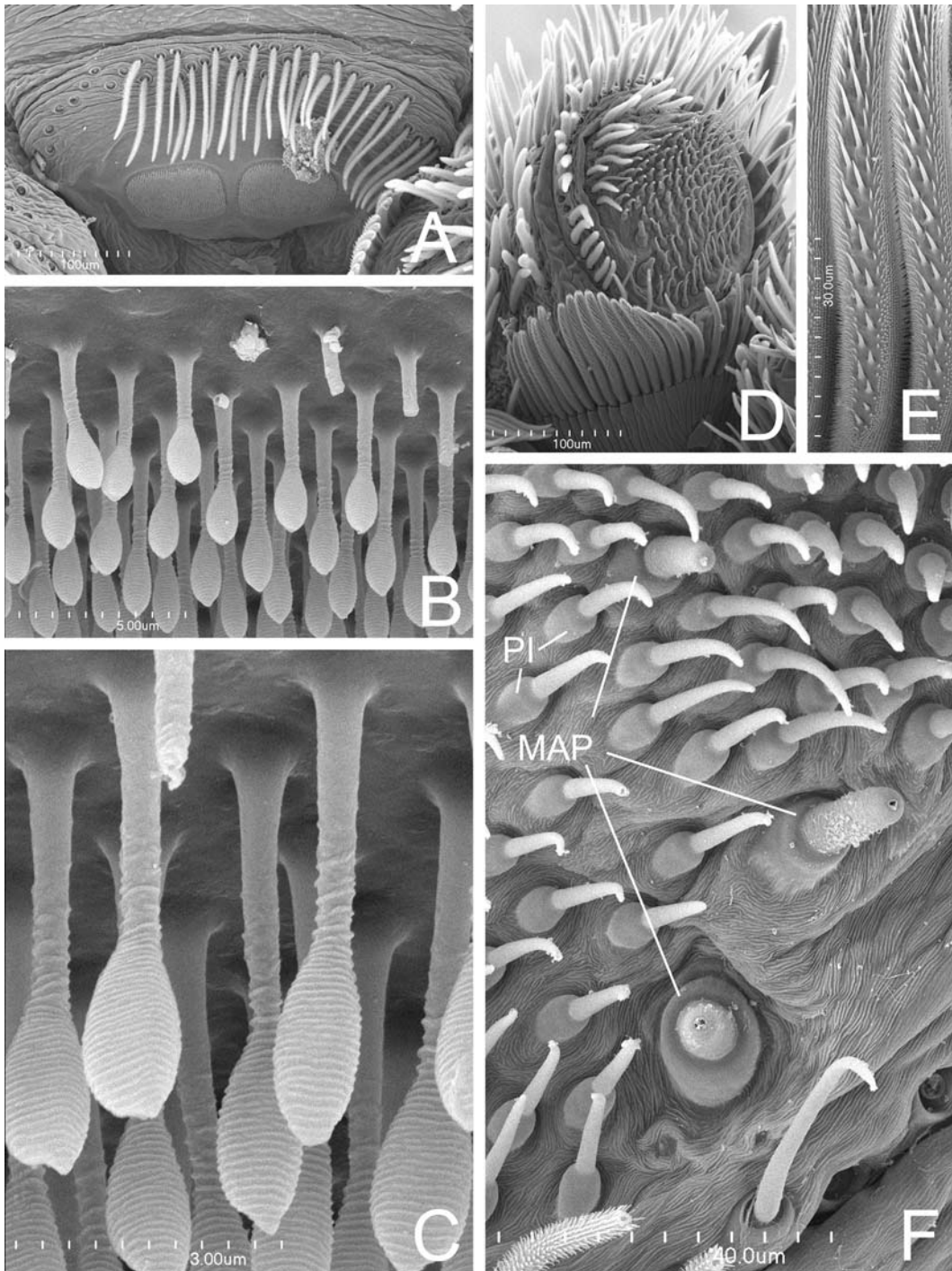


FIGURE 5. Details of spinnerets of *Filistata insidiatrix* female from Siena, Italy. A. Cribellum. B–C. Cribellar spigots. D. Left ALS. Note modified setae posteriorly. E. Left ALS, detail of modified setae. F. Right ALS showing three MAP, one of them among the PI. Note absence of tartipores. MAP = major ampullate gland spigot(s), PI = piriform gland spigot(s). Scale bars: A, D = 100µm, B = 5µm, C = 3µm, E = 30µm, F = 40µm.

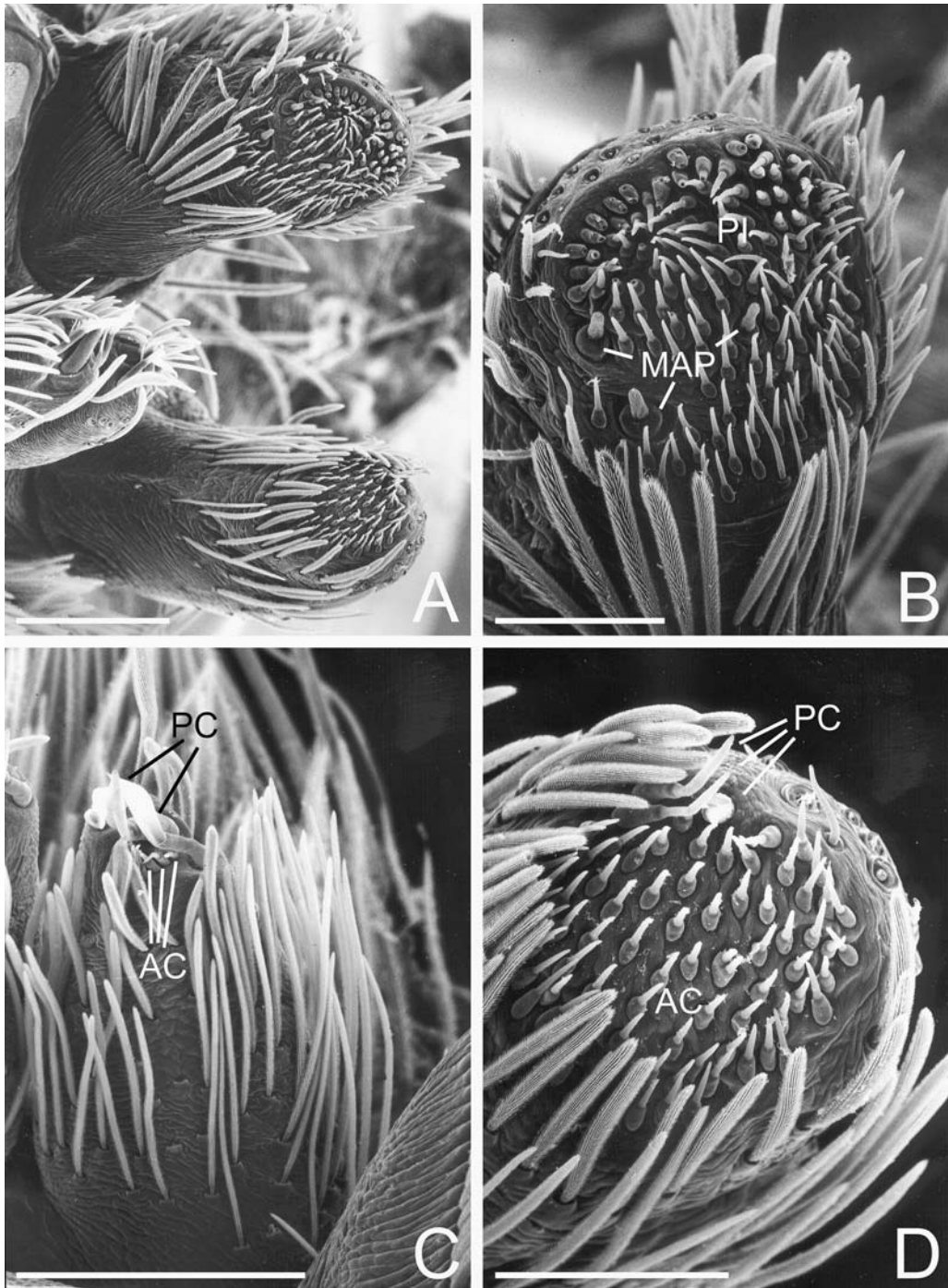


FIGURE 6. Left spinnerets of *Kukulcania hibernalis* female from Alachua Co., Florida, USA. A. Overview. B. ALS. C. PMS, anterior view, with mAP hidden. D. PLS. Note absence of tartipores. AC = aciniform gland spigot(s), MAP = major ampullate gland spigot(s), PC = paracribellar spigot(s), PI = piriform gland spigot(s). Scale bars: A, C = 200 μ m, B, D = 100 μ m.

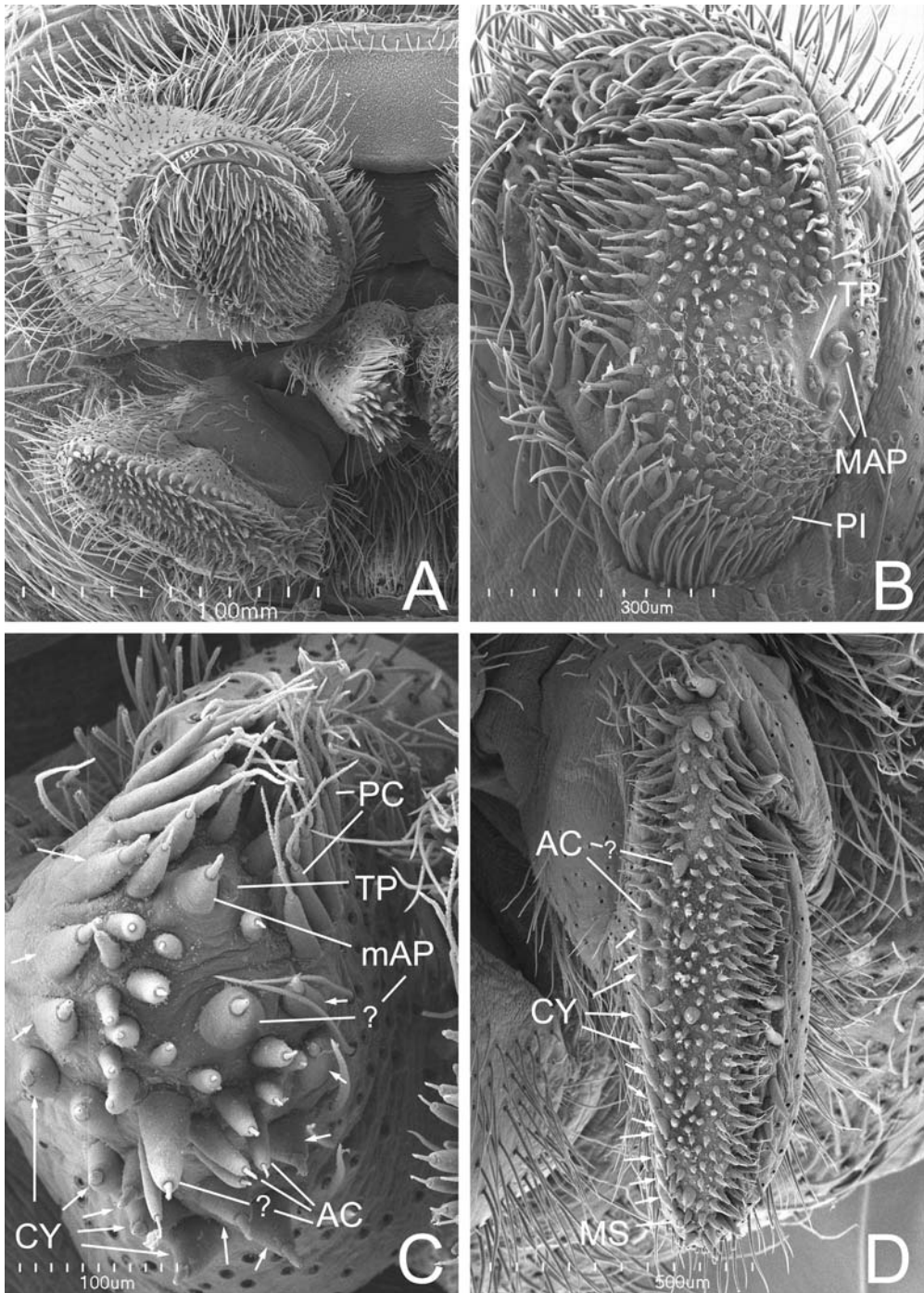


FIGURE 7. Right spinnerets of female *Hickmania troglodytes* from Mole Creek Cave, Tasmania, Australia. A. Spinnerets, overview. B. ALS. C. PMS. D. PLS. Arrows to CY spigots. AC = aciniform gland spigot(s), CY = cylindrical gland spigot(s), MAP = major ampullate gland spigot(s), mAP = minor ampullate gland spigot(s), MS = PLS modified spigot, PC = paracribellar spigot(s), TP = tartipore(s). Scale bars: A = 1.0mm, B = 300µm, C = 100µm, D = 500µm.

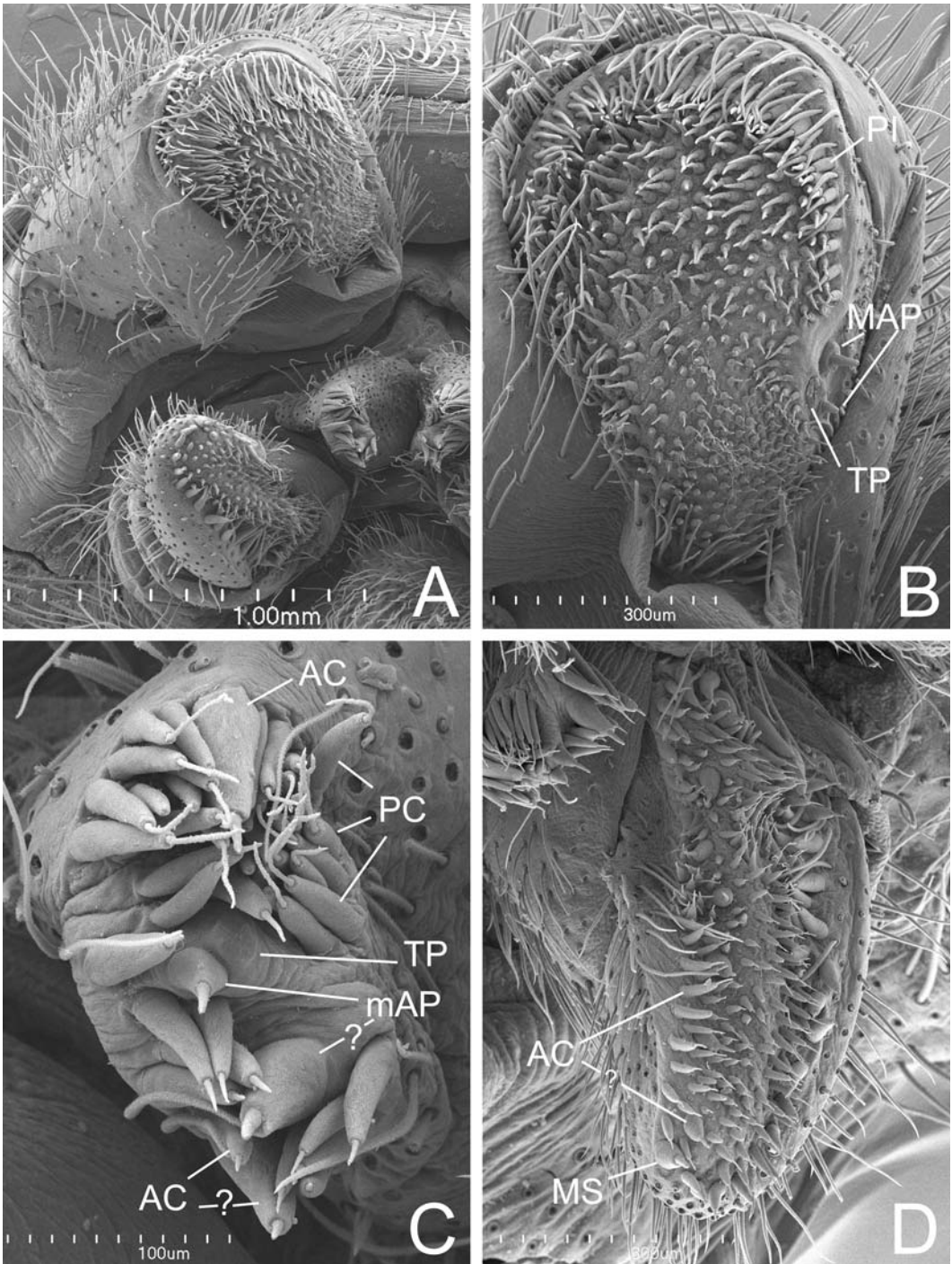


FIGURE 8. Right spinnerets of male *Hickmania troglodytes* from Mole Creek Cave, Tasmania, Australia. A. Spinnerets, overview. B. ALS. C. PMS: Question marks to presumed AC and mAP spigots with larger shafts. D. PLS. AC = aciniform gland spigot(s), MAP = major ampullate gland spigot(s), mAP = minor ampullate gland spigot(s), MS = PLS modified spigot, PC = paracribellar spigot(s), PI = piriform gland spigot(s), TP = tartipore(s). Scale bars: A = 1.0mm, B, D = 300µm, C = 100µm.

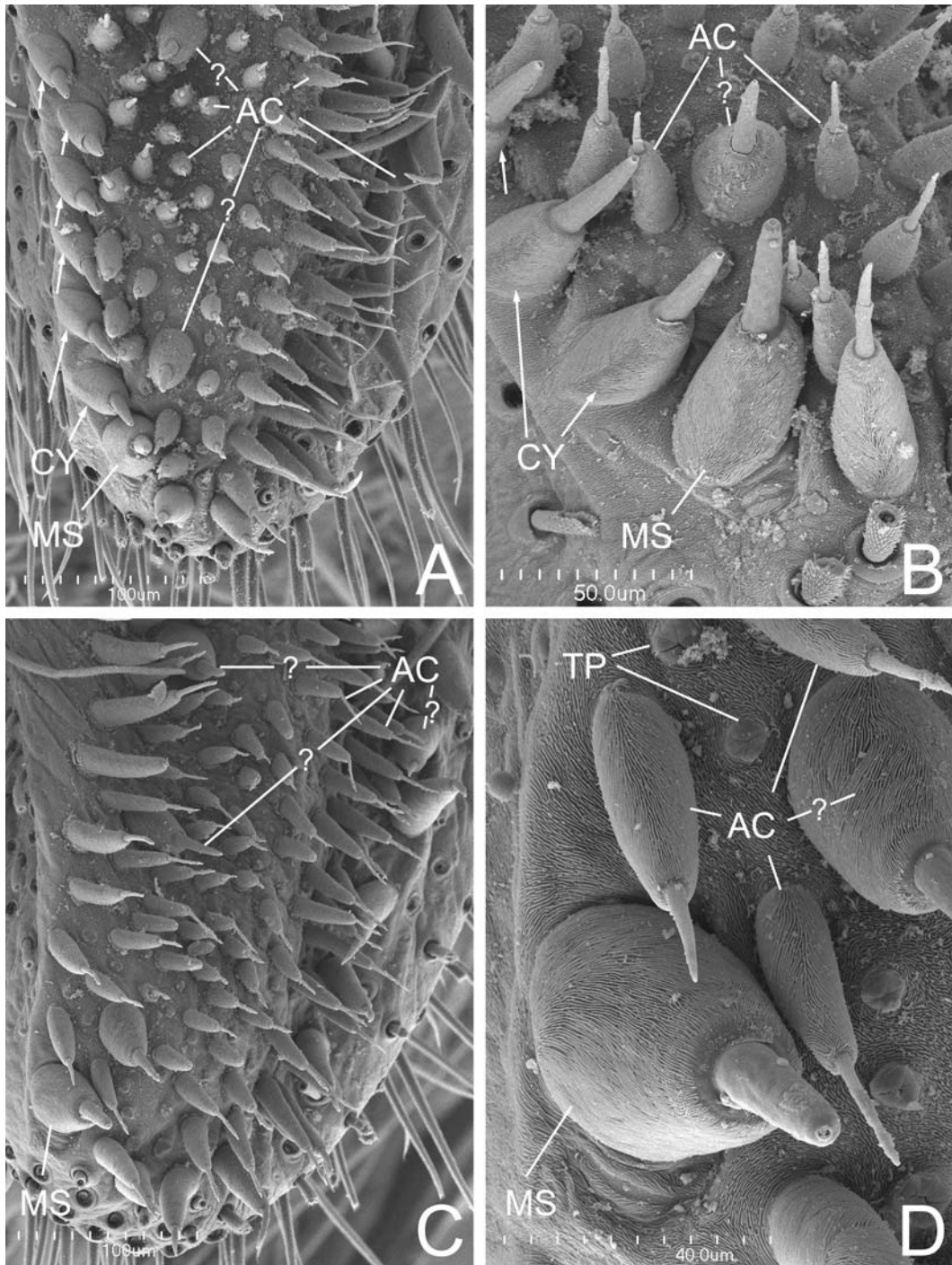


FIGURE 9. Right male and female PLS of *Hickmania troglodytes* from Mole Creek Cave, Tasmania, Australia. A-B. Female PLS showing CY spigots forming an external-anterior row, and two sizes of AC spigots. C-D. Male PLS showing two sizes of AC spigots. AC = aciniform gland spigot(s), CY = cylindrical gland spigot(s), MS = PLS modified spigot, TP = tartipore(s). Scale bars: A, C = 100µm, B = 50µm, D = 40µm.

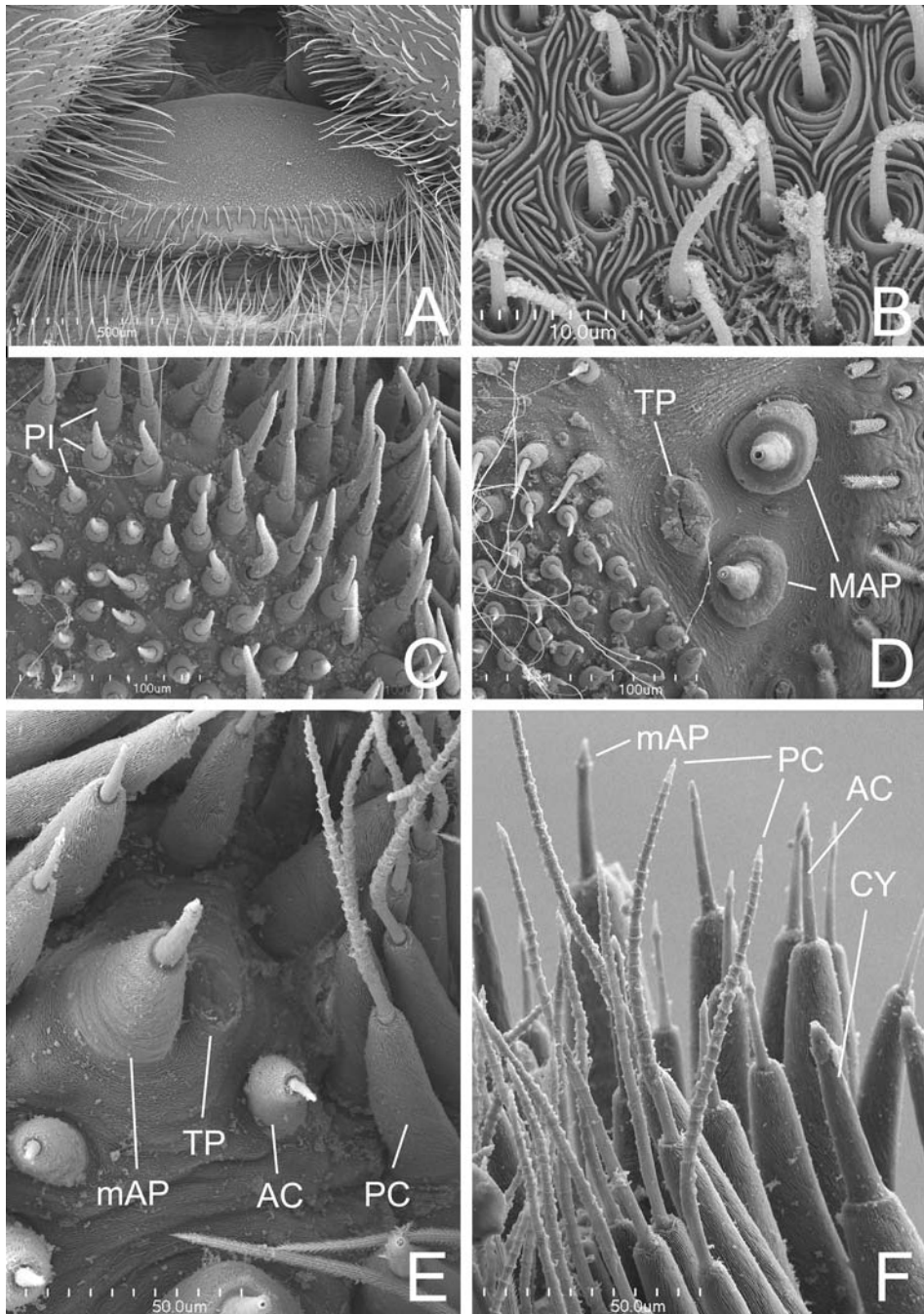


FIGURE 10. Details of spinnerets of female *Hickmania troglodytes* from Mole Creek Cave, Tasmania, Australia. A–B. Cribellum. C–F. Right spinnerets. C. ALS: the marginal PI are larger. D. ALS showing marginal pair of MAP and tarpitopore. E. PMS showing mAP with accompanying tarpitopore. F. PMS showing long paracribellars, and two size classes of AC. AC = acini-form gland spigot(s), CY = cylindrical gland spigot(s), MAP = major ampullate gland spigot(s), mAP = minor ampullate gland spigot(s), PC = paracribellar spigot(s), PI = piriform gland spigot(s), TP = tarpitopore(s). Scale bars: A = 500µm, B = 10µm, C, D = 100µm, E, F = 50µm.

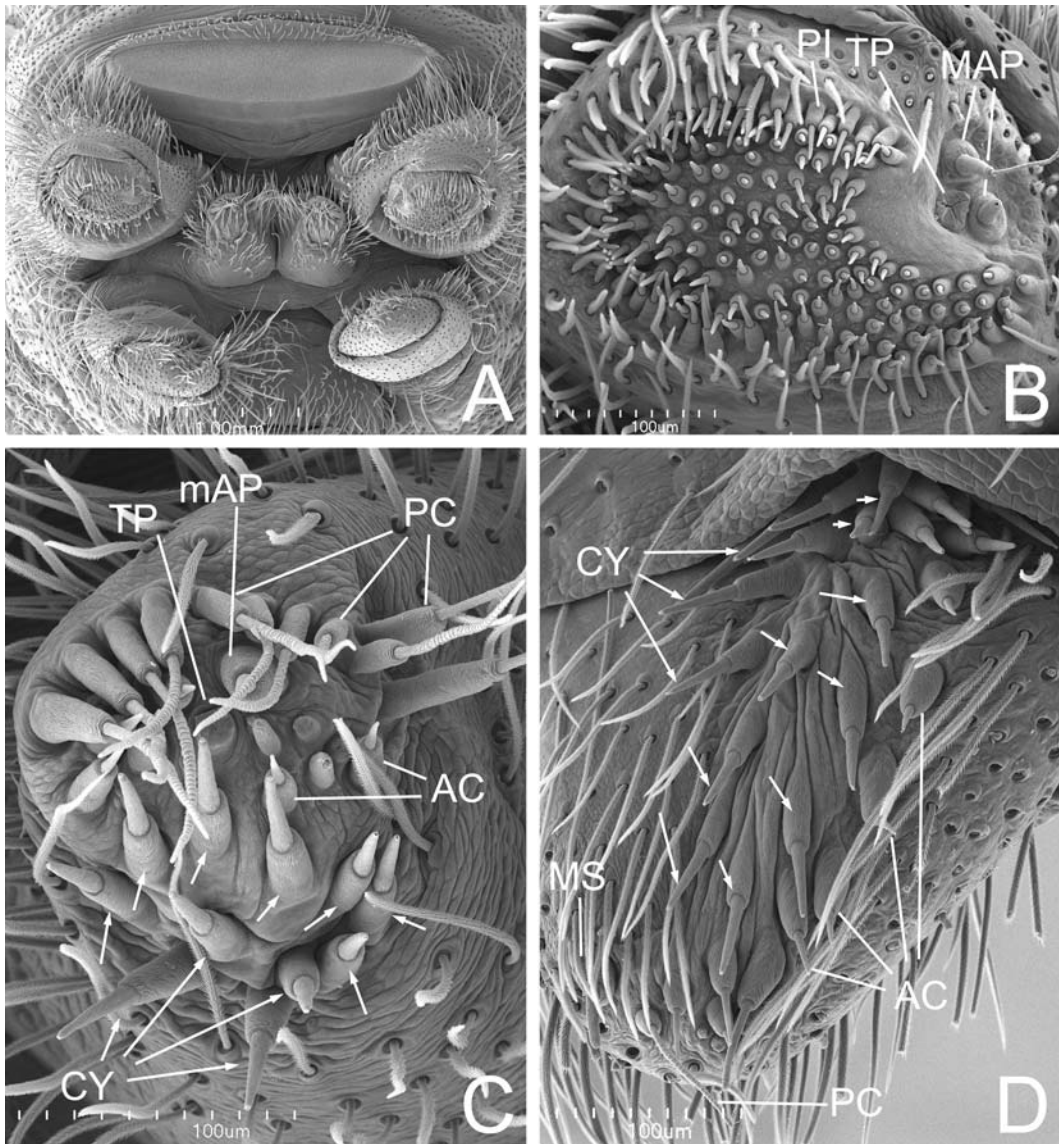


FIGURE 11. Female spinnerets of *Thaidia peculiaris* from Puerto Blest, Argentina. A. Spinnerets and cribellum, overview. B–D. Right spinnerets. B. ALS. C. PMS. D. PLS. AC = aciniform gland spigot(s), CY (and arrows) = cylindrical gland spigot(s), MAP = major ampullate gland spigot(s), mAP = minor ampullate gland spigot(s), PC = paracribellar spigot(s), MS = PLS modified spigot, PI = piriform gland spigot(s), TP = tartipore(s). Scale bars: A = 1.0mm, B–D = 100µm.

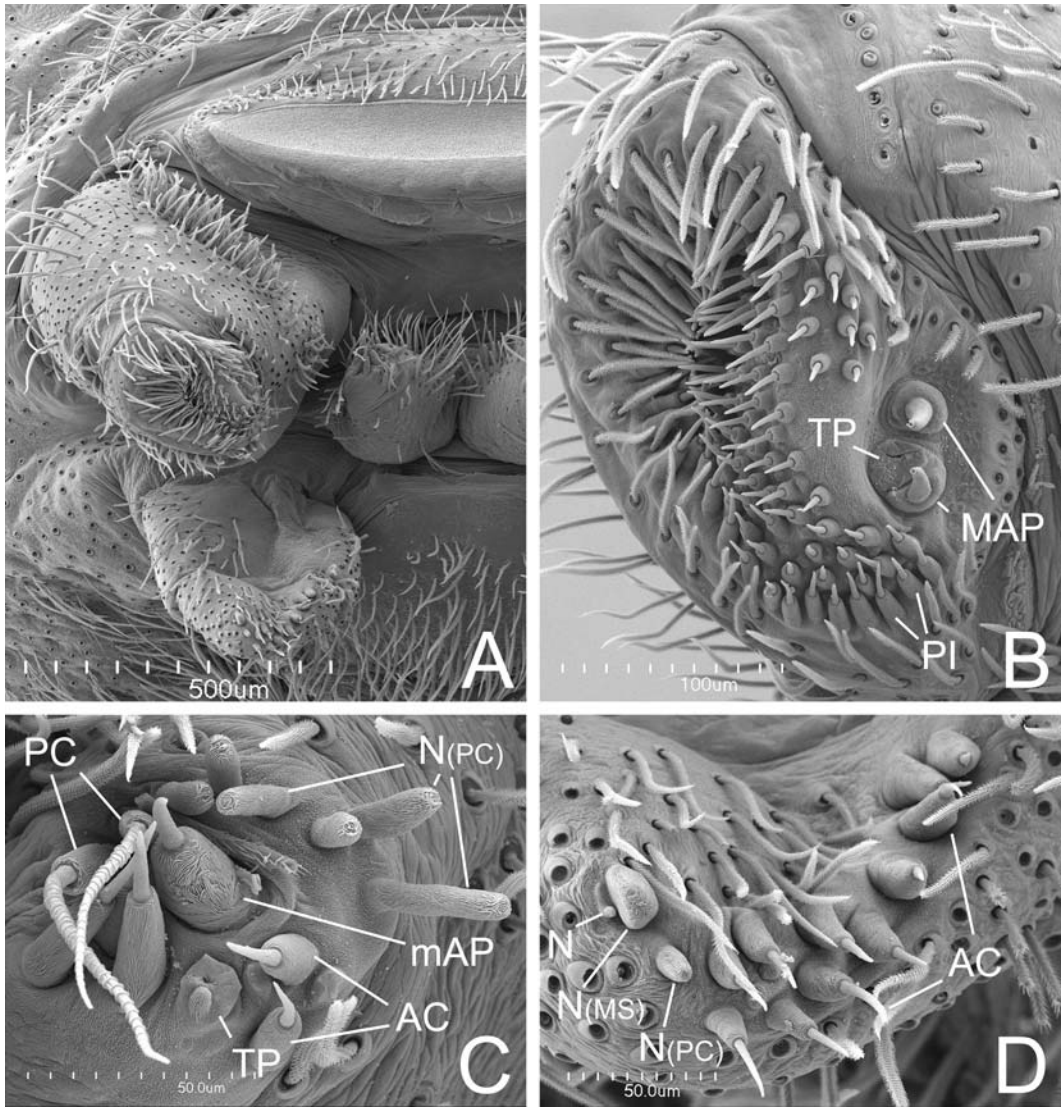
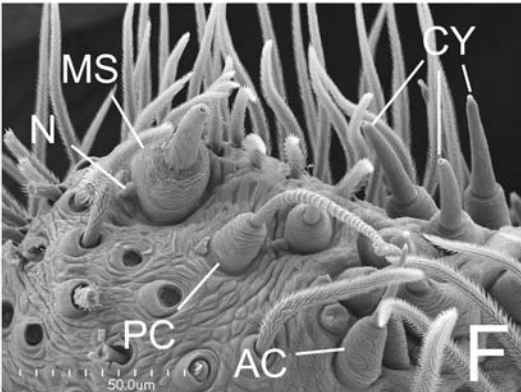
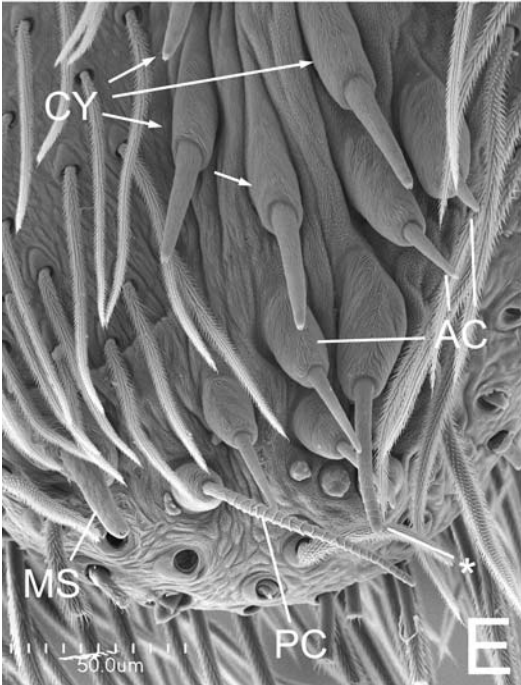
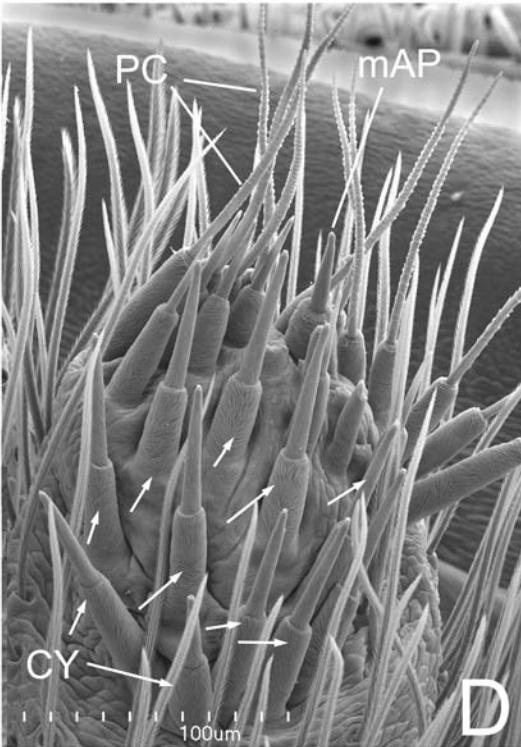
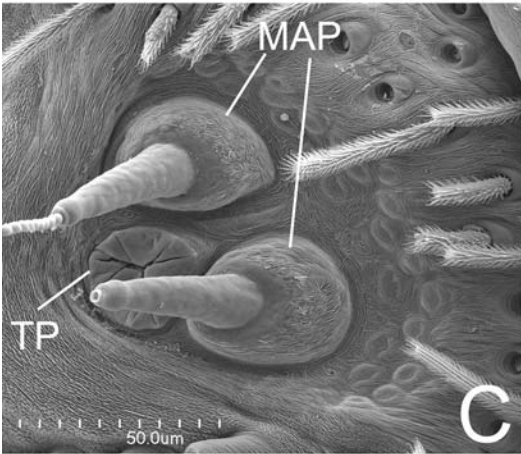
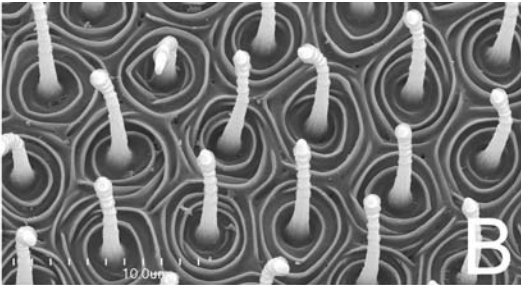
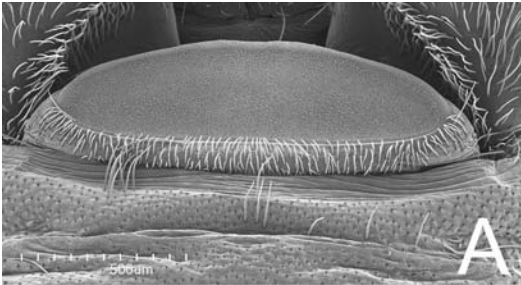


FIGURE 12. Right male spinnerets of *Thaida peculiaris* from Cautin, Chile. A. Spinnerets and cribellum, overview. B. ALS. C. PMS. D. PLS. AC = aciniform gland spigot(s), MAP = major ampullate gland spigot(s), mAP = minor ampullate gland spigot(s), MS = PLS modified spigot nubbin, N = nubbins, PC = paracribellar spigot and nubbins, TP = tartipore(s). Parenthetical notations, i.e., (PC) and (MS) refer to nubbins. Scale bars: A = 500µm, B = 100µm, C, D = 50µm.



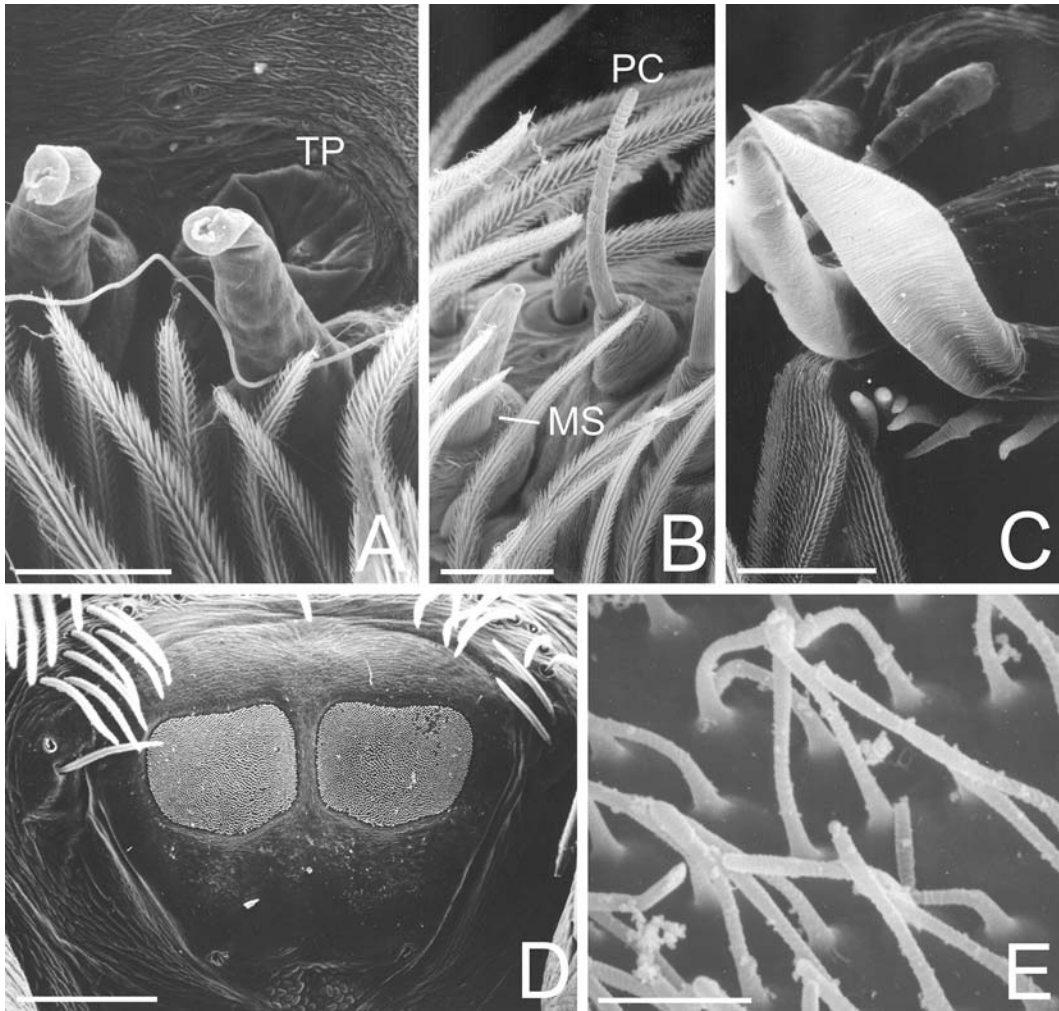


FIGURE 14 (above). Spinning organs of female filistatids and austrochilids. A, B. *Thaidia peculiaris* from Osorno, Chile. A. Left ALS, MAP and tartipore. B. PLS apex. C, D. *Kukulcania hibernalis* from Alachua Co., Florida, USA. C. PMS, showing PC spigots. D. Cribellum. E. *Filistatinella* sp. from Arroyo Seco, California, USA, clavate cribellar spigots. MS = PLS modified spigot, PC = paracribellar spigot(s), TP = tartipores. Scale bars: A–C = 20 μ m, D = 100 μ m, E = 3 μ m.

FIGURE 13 (left). Details of female spinnerets of *Thaidia peculiaris* from Puerto Blest, Argentina. A. Cribellum. B. Cribellar spigots. C. Right ALS, MAP and TP. D. Right PMS, posterior view. E–F. Apex of right PLS: asterisk to intermediate paracribellar shaft with only partial sculpturing. AC = aciniform gland spigot(s), CY and arrows = cylindrical gland spigot(s), MAP = major ampullate gland spigot(s), mAP = minor ampullate gland spigot(s), MS = PLS modified spigot, N = nubbin, PC = paracribellar spigot(s), TP = tartipore(s). Scale bars: A = 500 μ m, B = 10 μ m, C, E, F = 50 μ m, D = 100 μ m.

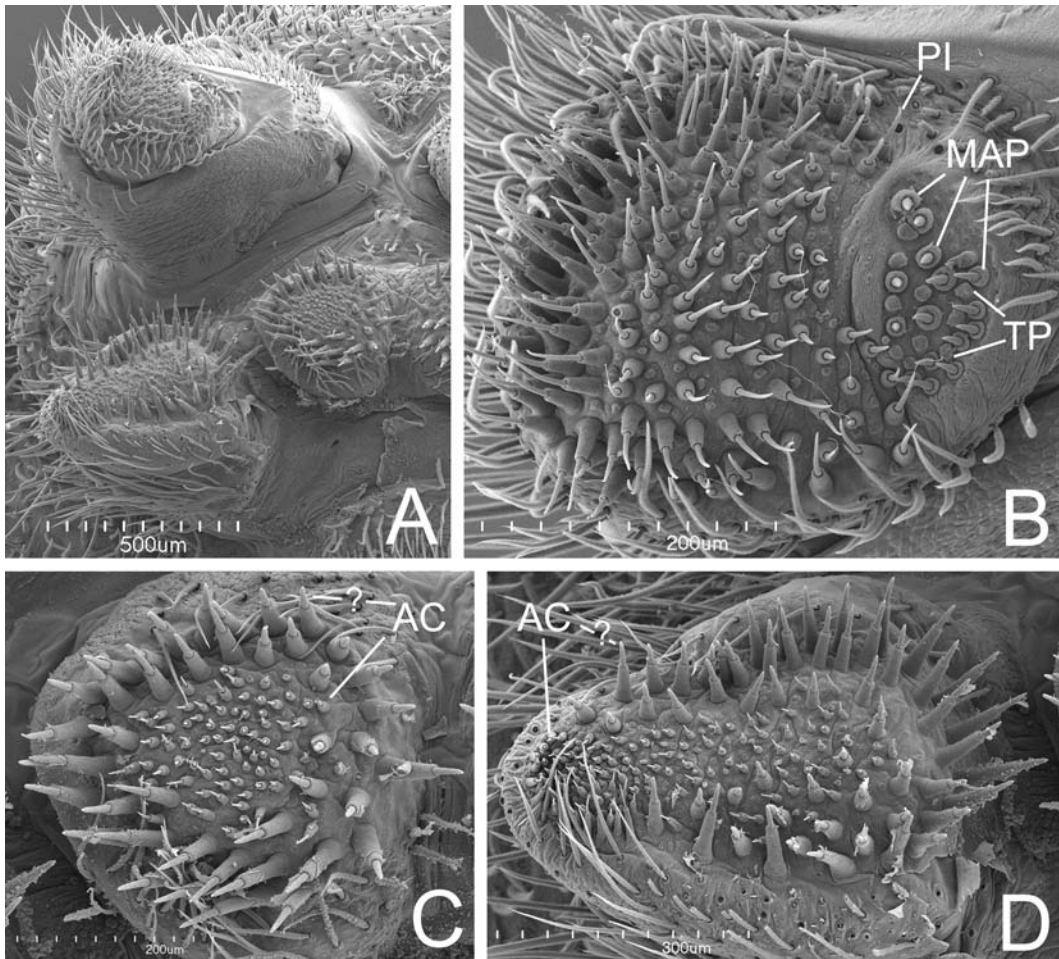


FIGURE 15. Right spinnerets of *Gradungula sorenseni* female from Saltwater Forest, New Zealand. A. Spinnerets, overview. B. ALS. C. PMS. D. PLS. AC = aciniform gland spigot(s), MAP = major ampullate gland spigot(s), PI = piriform gland spigot(s), TP = tartipore(s). Scale bars: A = 500µm, B, C = 200µm, D = 300µm.

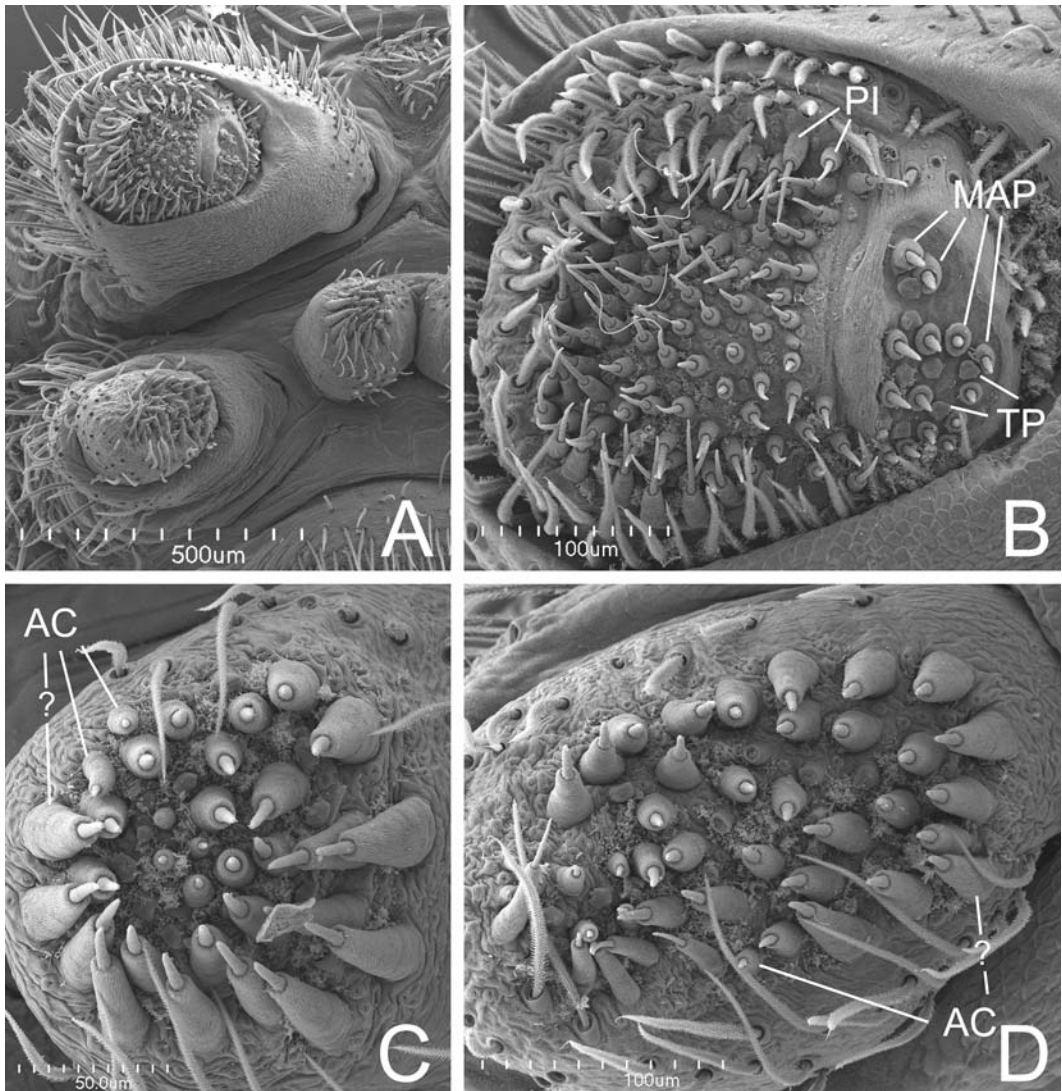


FIGURE 16. Right spinnerets of *Gradungula sorenseni* male from Saltwater Forest, New Zealand. A. Spinnerets, overview. B. ALS. C. PMS. D. PLS. AC = aciniform gland spigot(s), MAP = major ampullate gland spigot(s), PI = piriform gland spigot(s), TP = tarpitopore(s). Scale bars: A = 500µm, B, D = 100µm, C = 50µm.

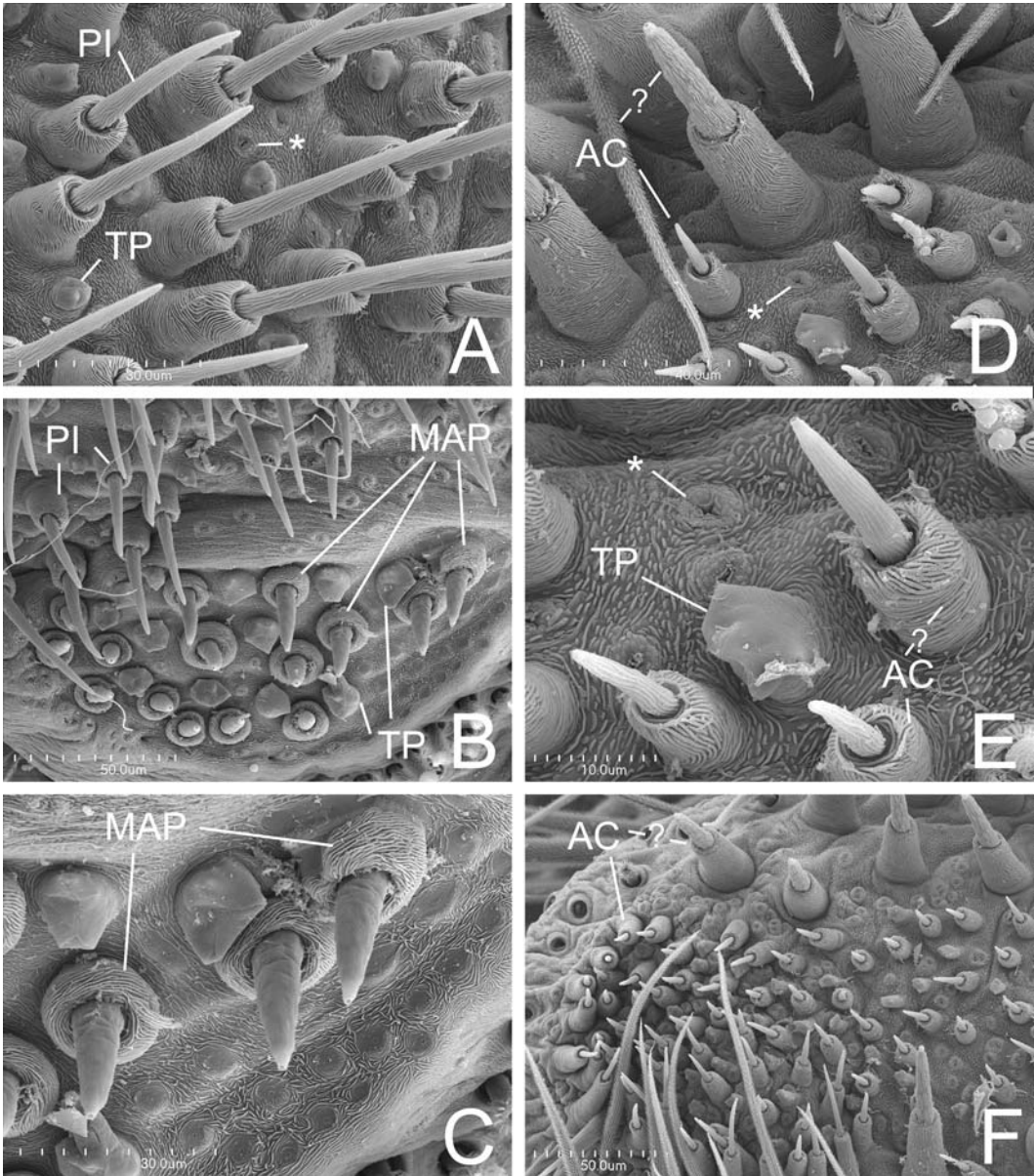
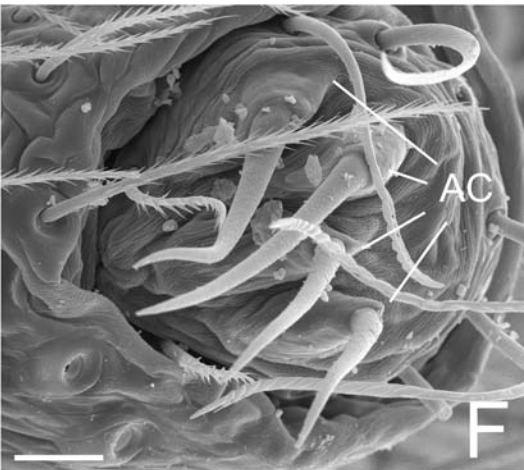
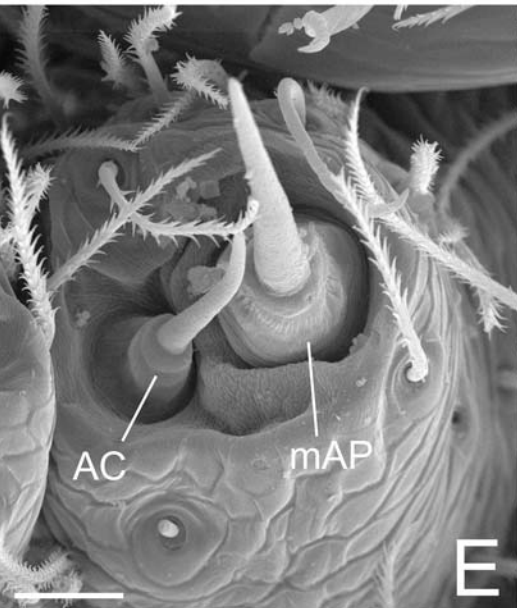
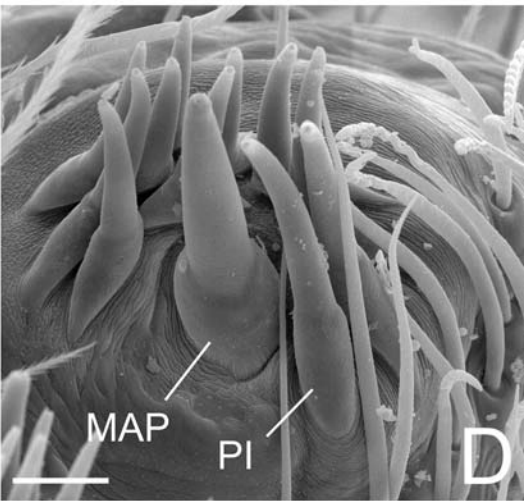
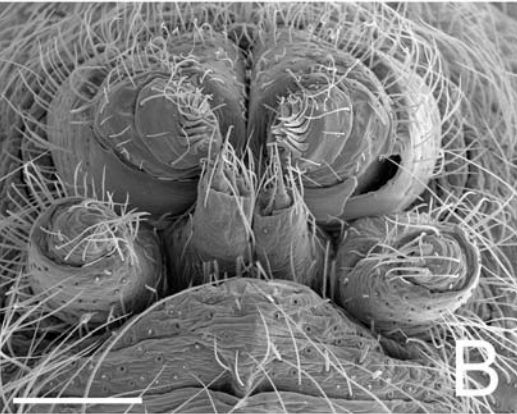
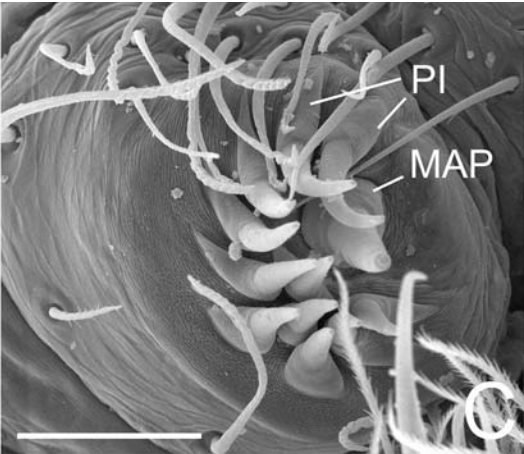
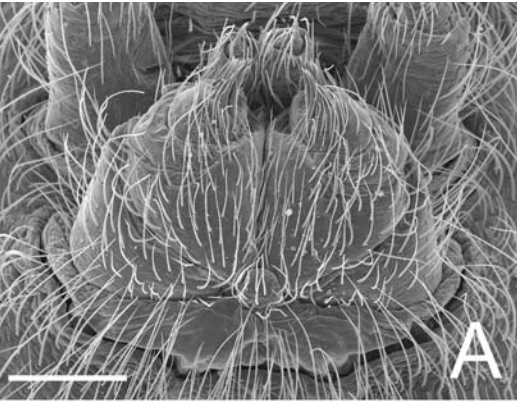


FIGURE 17 (above). Details of right spinnerets of *Gradungula sorenseni* female from Saltwater Forest, New Zealand. A. ALS, PI. B-C. ALS, MAP field. D-E. PMS. F. PLS, large AC at top, small in center. AC = aciniform gland spigot(s), MAP = major ampullate gland spigot(s), PI = piriform gland spigot(s), TP = tartipore(s). * denotes small orifices. Scale bars: A, C = 30µm, B, F = 50µm, D = 40µm, E = 10µm.

FIGURE 18 (right). Female spinnerets of *Ariadna boesenbergi* from Buenos Aires, Argentina. A. Spinnerets, anterior-ventral view. B. Spinnerets, posterior-ventral view. C, D. Right ALS. E. Left PMS. F. Left PLS. AC = aciniform gland spigot(s), MAP = major ampullate gland spigot(s), mAP = minor ampullate gland spigot(s), PI = piriform gland spigot(s). Scale bars: A = 200 µm, B = 50 µm, C, D = 200 µm, E, F = 20 µm.



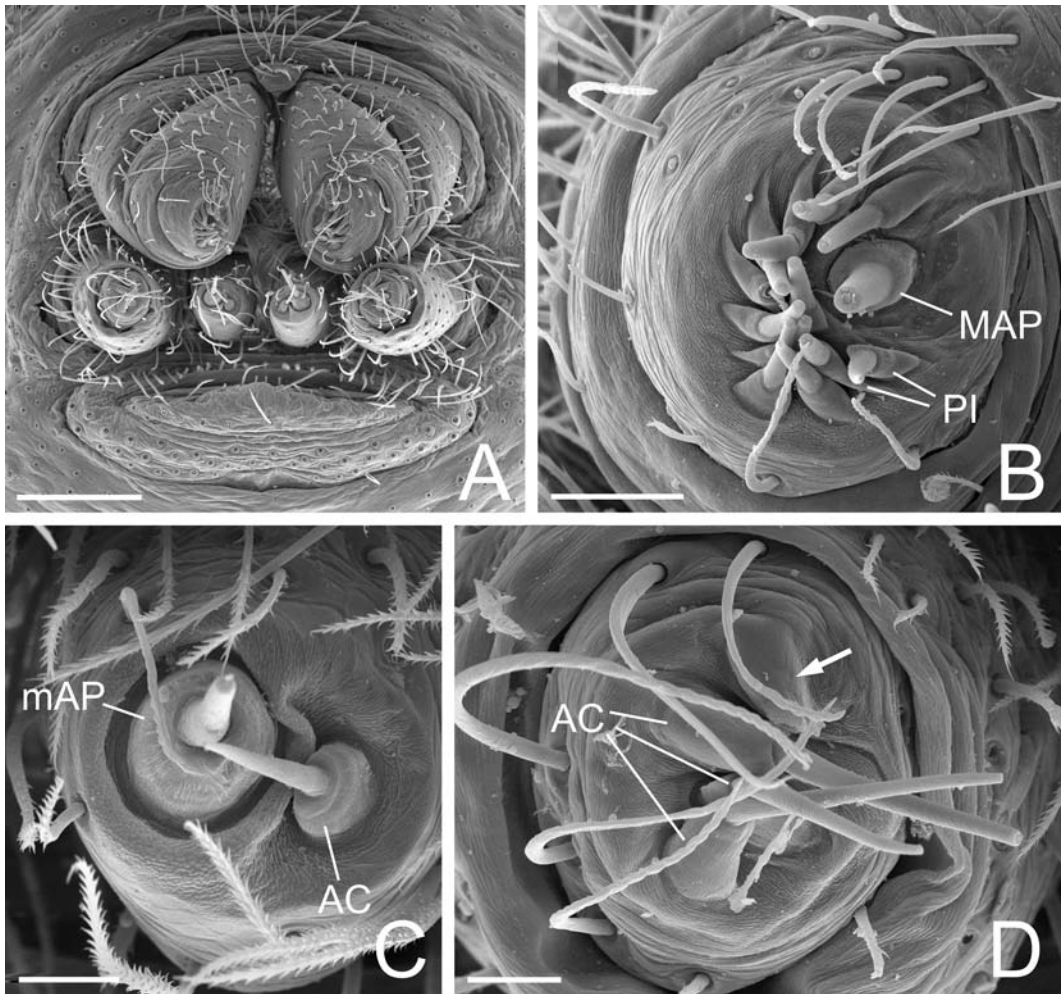


FIGURE 19. Male spinnerets of *Ariadna boesenbergi* from Buenos Aires, Argentina. A. Spinnerets. B. Right ALS. C. Right PMS. D. Right PLS (arrow to reduced AC spigot, present in the left PLS). AC = aciniform gland spigot(s), MAP = major ampullate gland spigot(s), mAP = minor ampullate gland spigot(s), PI = piriform gland spigot(s). Scale bars: A = 200 μ m, B = 40 μ m, C = 20 μ m, D = 20 μ m.

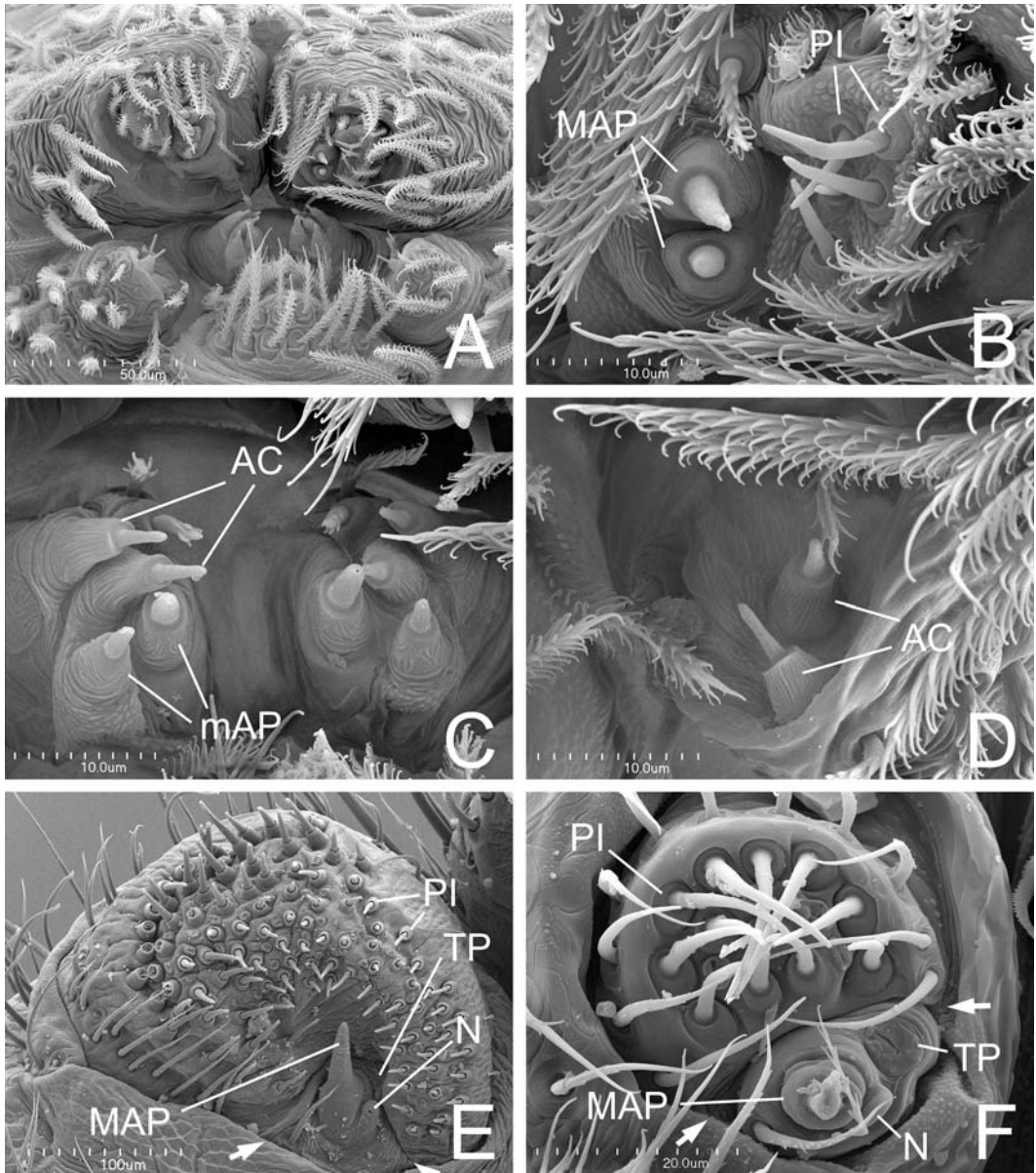


FIGURE 20. Spinnerets of Archaedidae and Araneoidea. A–D. *Archaea workmani* immature from Ranomafana, Madagascar. A. Spinnerets. B. Left ALS: the tartipore is probably hidden in the fold around MAP. C. PMS. D. Left PLS. E. *Araneus diadematus* female from Ontario, Canada, left ALS (arrow to fold separating MAP field). F. *Crassanapis chilensis*, female from Osorno, Chile, right ALS (inverted, arrows to fold separating MAP field). AC = aciniform gland spigot(s), MAP = major ampullate gland spigot(s), mAP = minor ampullate gland spigot(s), N = nubbin, PI = piriform gland spigot(s), TP = tartipore(s). Scale bars: A = 50 μ m, B–D = 10 μ m, E = 100 μ m, F = 20 μ m.

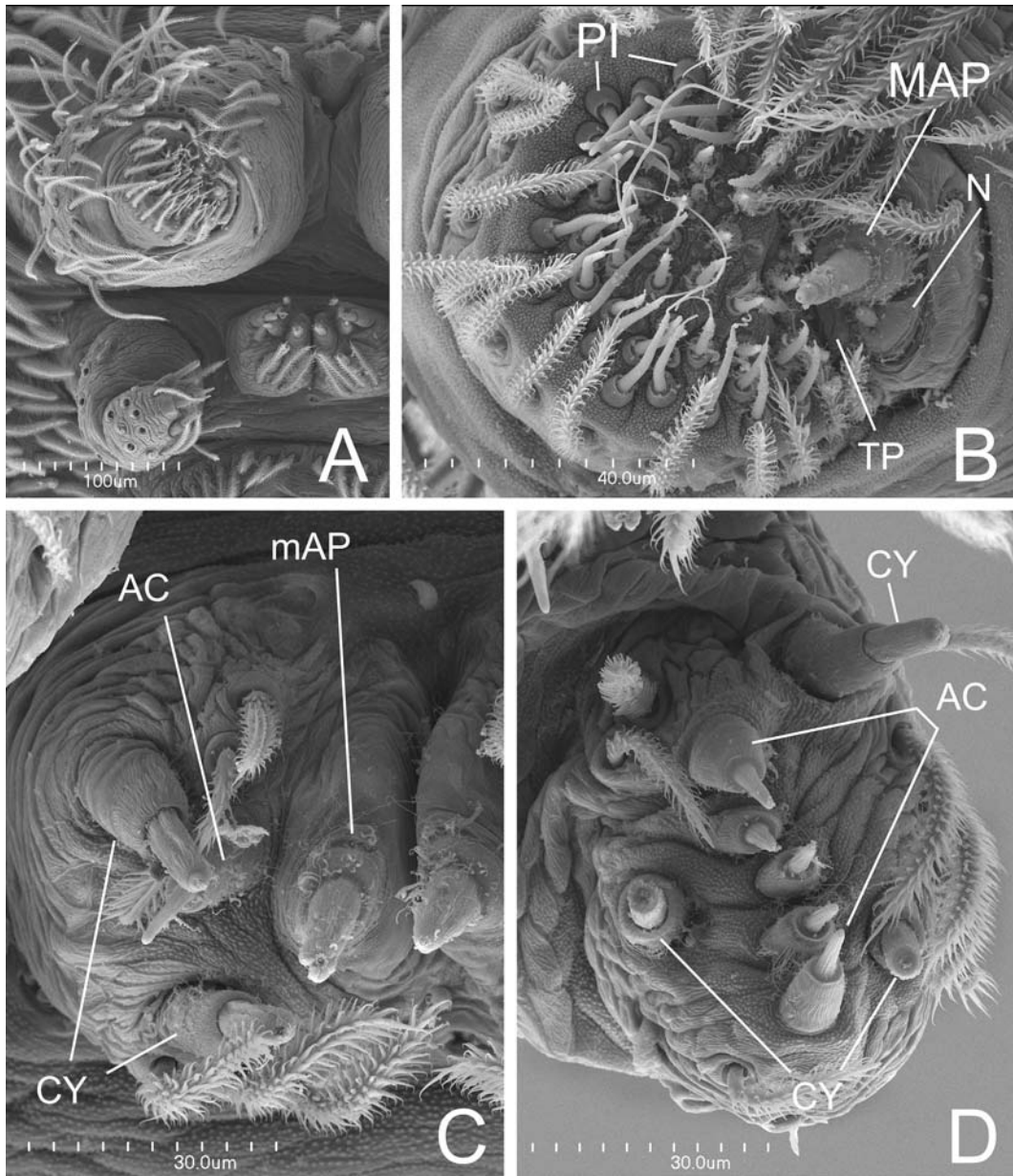


FIGURE 21. Right spinnerets of female *Archaea workmani* from Ranomafana, Madagascar. A. Spinneret overview. B. ALS. C. PMS. D. PLS. AC = aciniform gland spigot(s), CY = cylindrical gland spigot(s), MAP = major ampullate gland spigot(s), mAP = minor ampullate gland spigot(s), N = nubbin, PI = piriform gland spigot(s), TP = tartipore(s). Scale bars: A = 100µm, B = 40µm, C, D = 30µm.

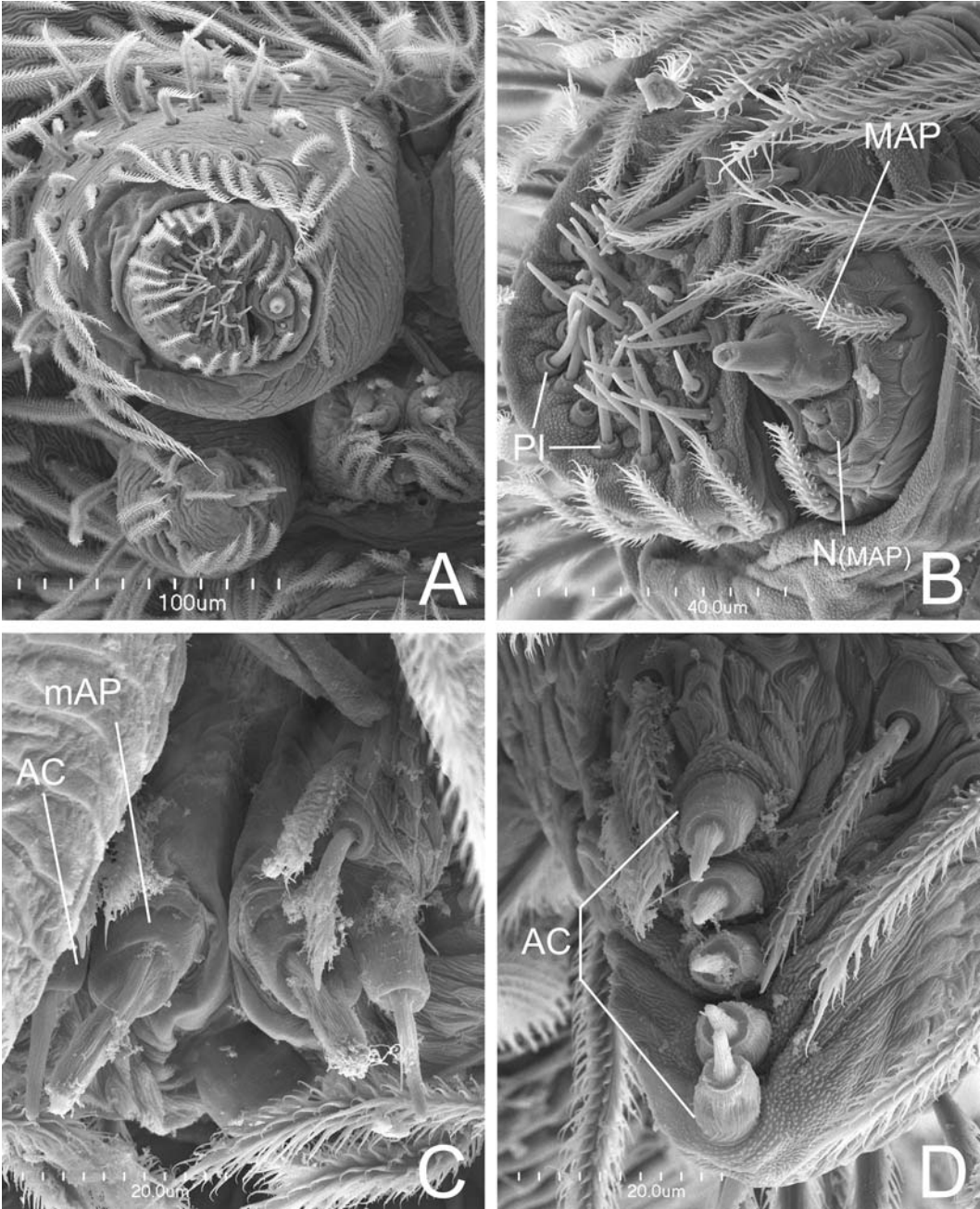


FIGURE 22. Spinnerets of male *Archaea workmani* from Ranomafana, Madagascar, left, inverted. A. Overview. B. ALS. C. PMS. D. PLS. AC = aciniform gland spigot(s), MAP = major ampullate gland spigot(s), mAP = minor ampullate gland spigot(s), N = nubbin of posterior MAP. Scale bars: A = 100µm, B = 40µm, C, D = 20µm.

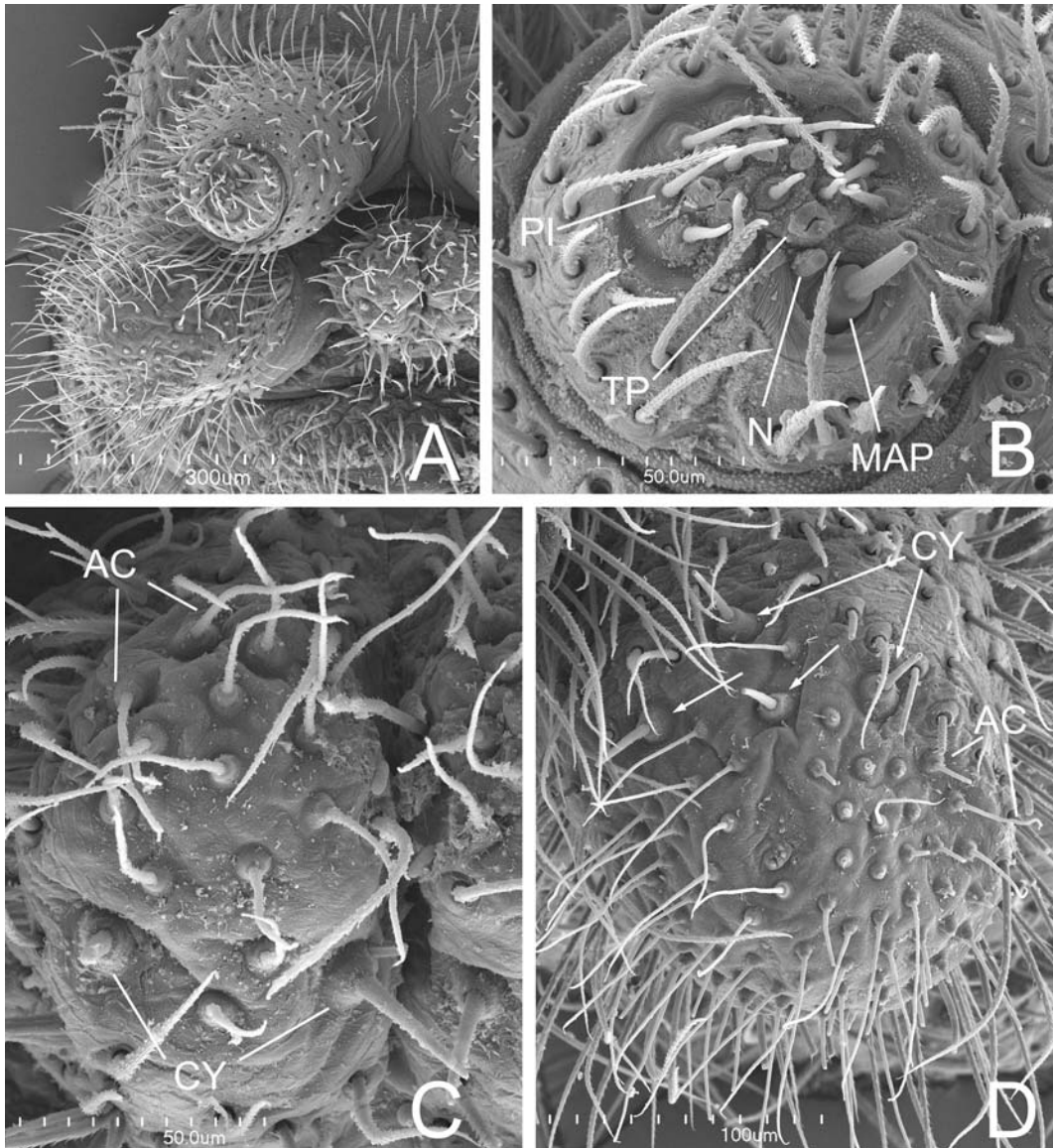


FIGURE 23. Left spinnerets of *Huttonia* sp. female from Orongorongo, New Zealand. A. Overview. B. ALS. C. PMS. D. PLS. AC = aciniform gland spigot(s), CY and arrows = cylindrical gland spigot(s), MAP = major ampullate gland spigot(s), N = nubbin, PI = piriform gland spigot(s), TP = tartipore(s). Scale bars: A = 300µm, B, C = 50µm, D = 100µm.

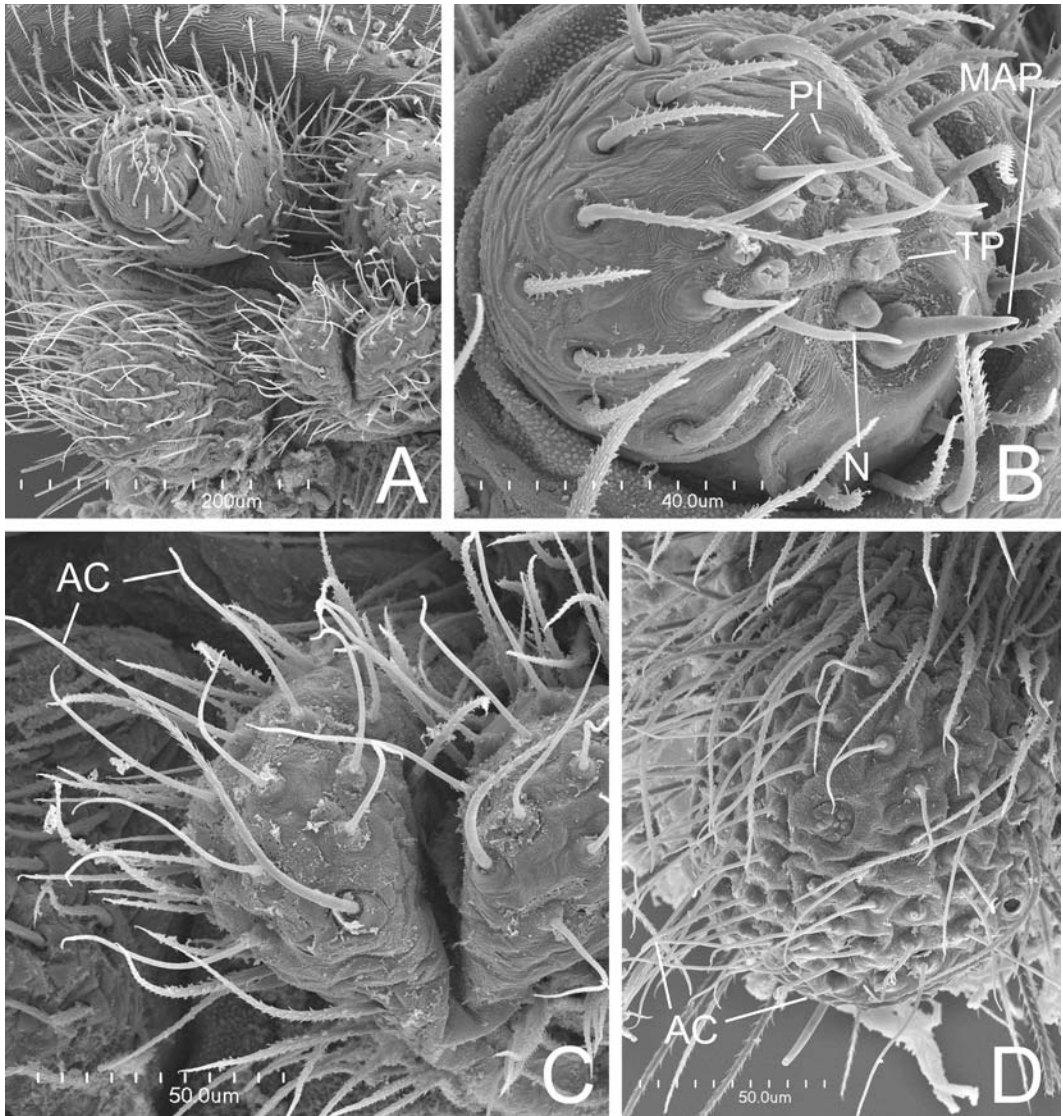


FIGURE 24. Left spinnerets of *Huttonia* sp. male from Orongorongo, New Zealand. A. Overview. B. ALS. C. PMS. D. PLS. AC = aciniform gland spigot(s), MAP = major ampullate gland spigot(s), N = nubbin, PI = piriform gland spigot(s), TP = tartipore(s). Scale bars: A = 200µm, B = 40µm, C, D = 50µm.

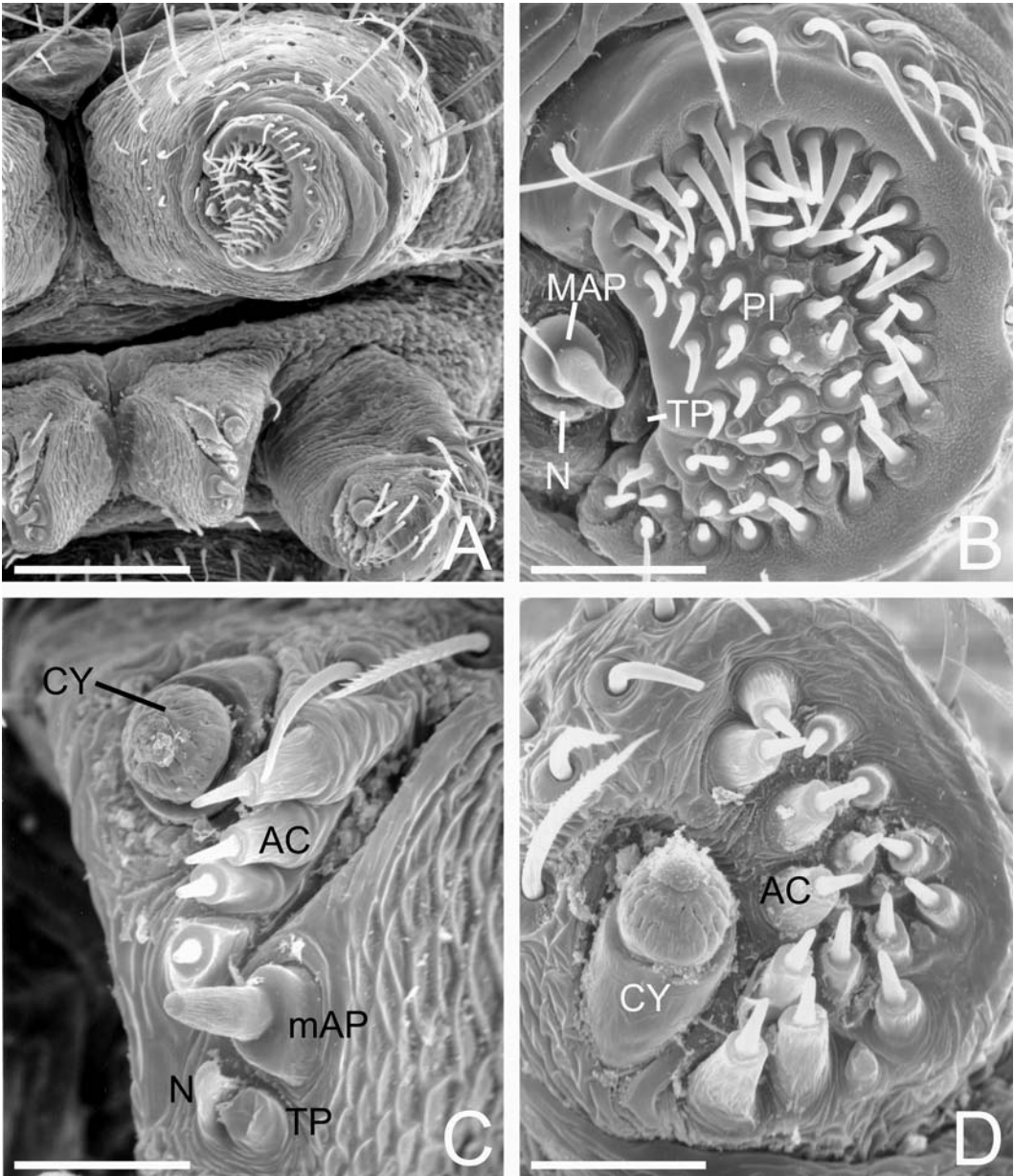


FIGURE 25. Spinnerets of female *Mimetus hesperus* from Tampico, Mexico. A. Left overview. B. Left ALS. Note very short PI bases. C. Right PMS. D. Left PLS. AC = aciniform gland spigot(s), CY = cylindrical gland spigot(s), MAP = major ampullate gland spigot(s), mAP = minor ampullate gland spigot(s), N = nubbin (in white, of posterior ALS MAP, in black, of PMS mAP), PI = piriform gland spigot(s), TP = tartipore (s). Scale bars: A = 115µm, B = 30µm, C, D = 25µm.

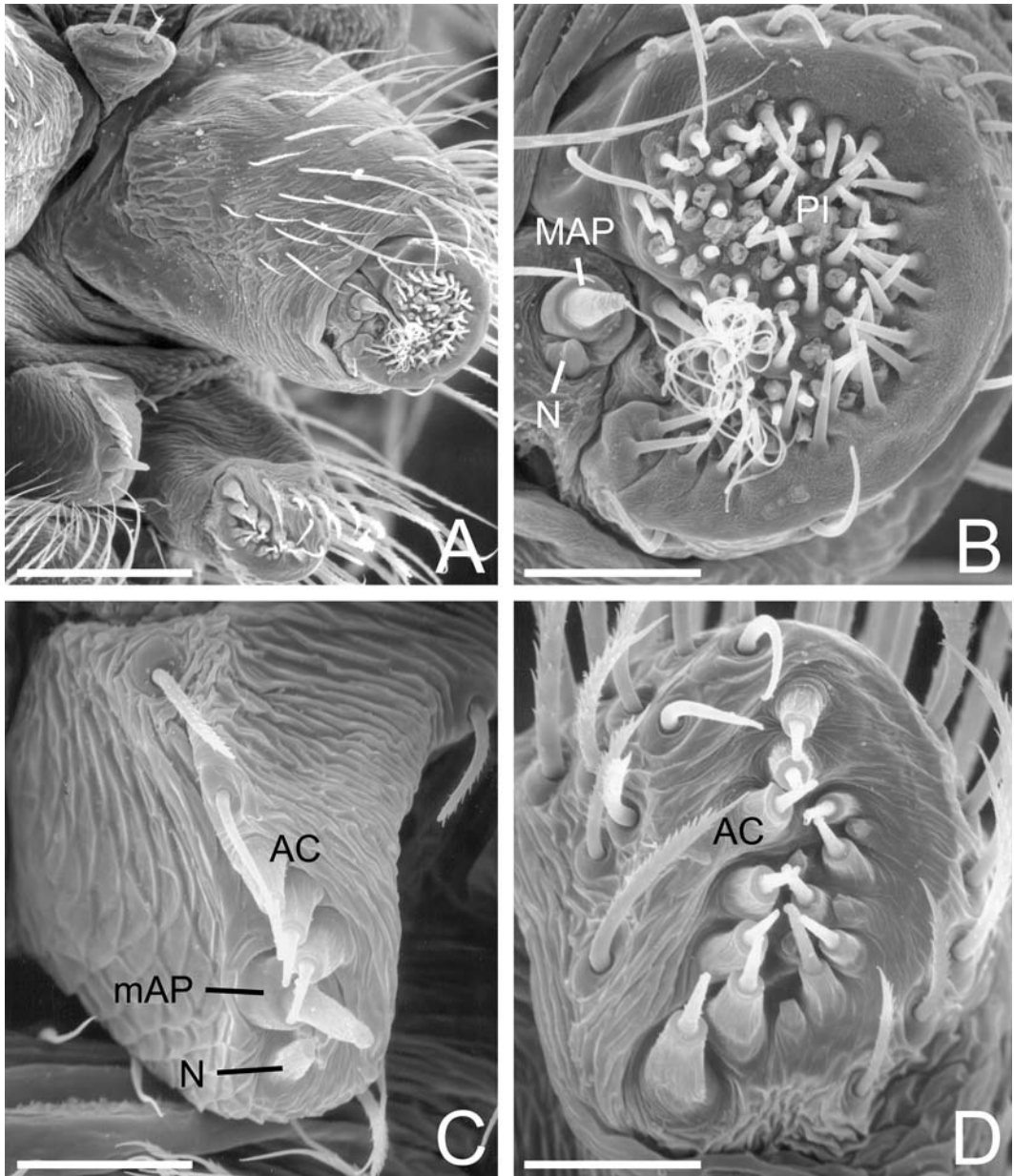


FIGURE 26. Left spinnerets of male *Mimetes hesperus* from Baboquivari Mts., Arizona, USA. A. Overview. B. ALS. C. PMS. D. PLS. AC = aciniform gland spigot(s), MAP = major ampullate gland spigot(s), mAP = minor ampullate gland spigot(s), N = nubbin (in white, of posterior ALS MAP, in black, of PMS mAP), PI = piriform gland spigot(s). Scale bars: A = 100 μ m, B, C = 30 μ m, D = 25 μ m.

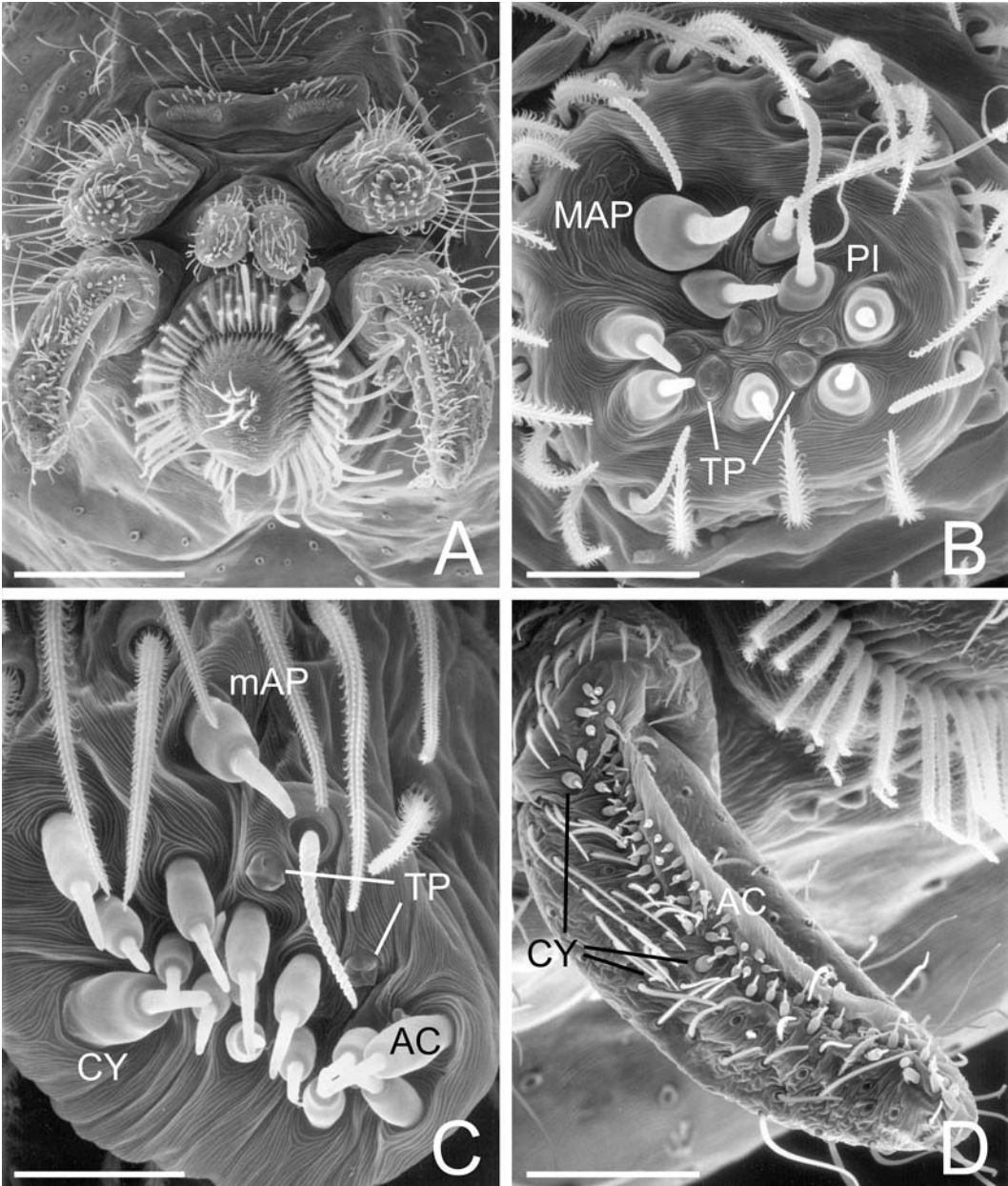
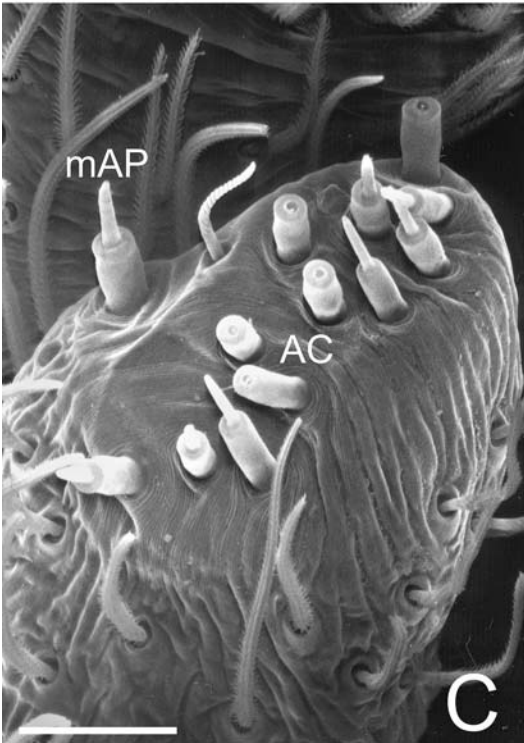
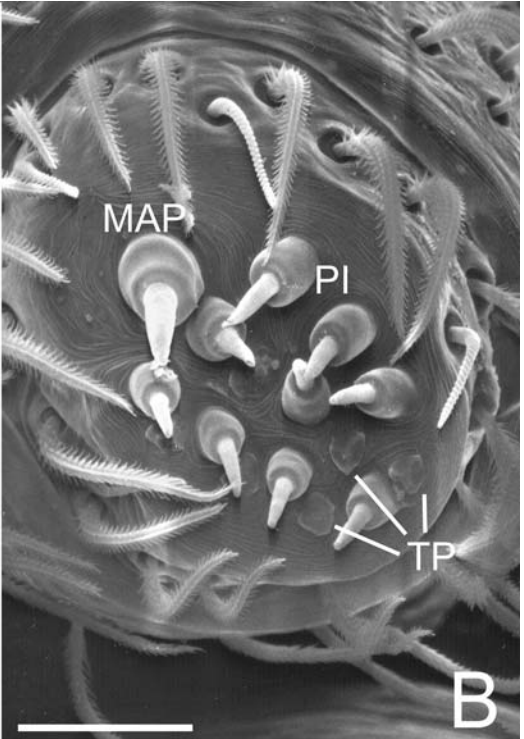


FIGURE 27 (above). Spinnerets of female *Oecobius navus* from Richmond, California, USA. A. Overview. Note divided cribellum, elongate PLS and enlarged anal tubercle. B. Left ALS. C. Left PMS, with median field of AC. D. Left PLS, with numerous AC. AC = aciniform gland spigot(s), CY = cylindrical gland spigot(s), MAP = major ampullate gland spigot(s), mAP = minor ampullate gland spigot(s), PI = piriform gland spigot(s), TP = tartipore(s). Scale bars: A = 200µm, B = 20µm, C = 15µm, D = 75µm.

FIGURE 28 (right). Spinnerets of male *Oecobius navus* from Washington D.C, USA. A. Overview of spinnerets. B. Left ALS. C. Left PMS, anterior to bottom. D. Right PLS, with only AC spigots. AC = aciniform gland spigot(s), MAP = major ampullate gland spigot(s), mAP = minor ampullate gland spigot(s), PI = piriform gland spigot(s), TP = tartipore(s). Scale bars: A = 200µm, B,C = 20µm, D = 100µm.



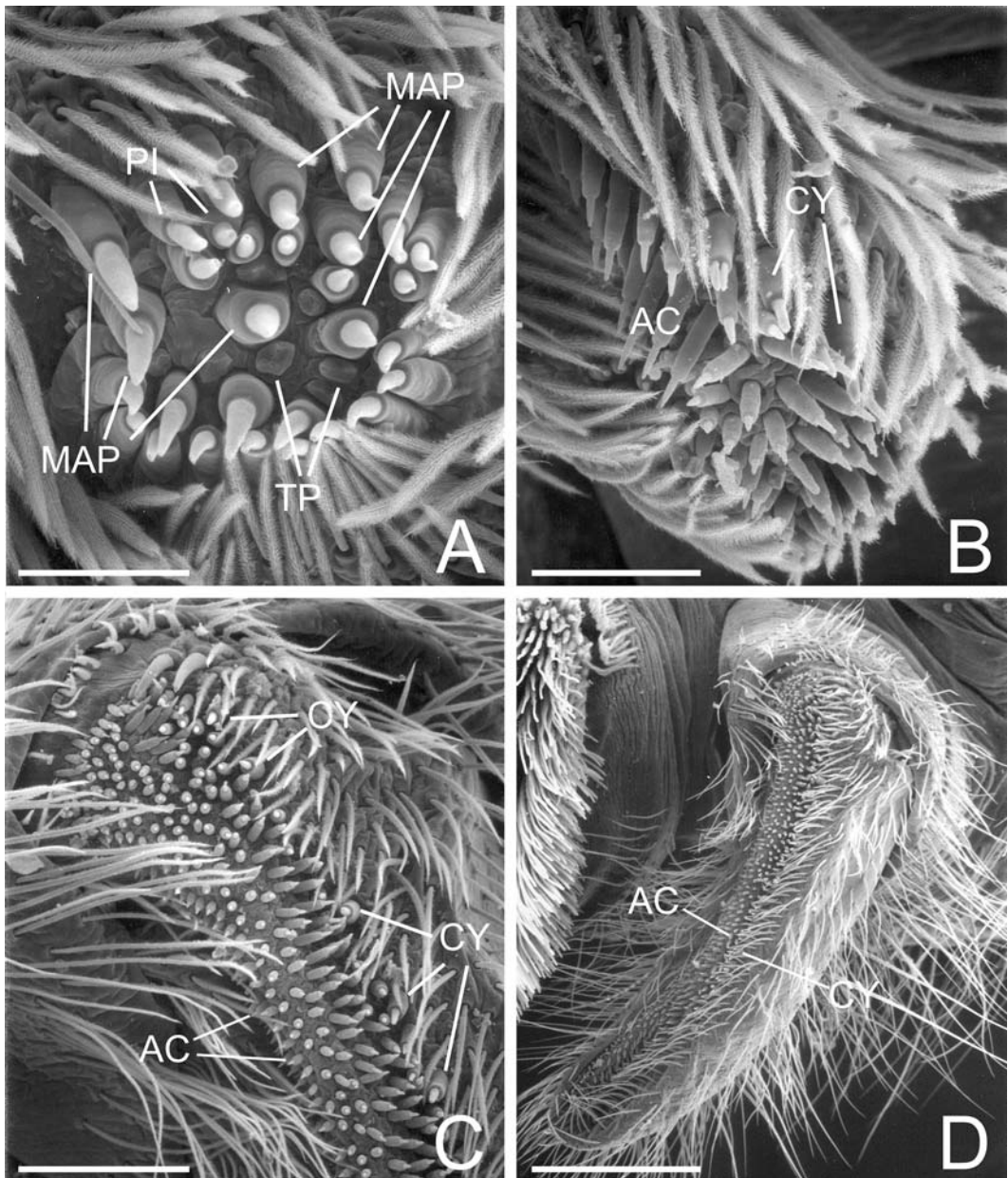


FIGURE 29. Spinnerets of female *Uroctea* sp. from Garies, South Africa. A. Left ALS. B. Left PMS, with no apparent mAP. C. Base of left PLS, with numerous AC. D. Left PLS. AC = aciniform gland spigot(s), CY = cylindrical gland spigot(s), MAP = major ampullate gland spigot(s), PI = piriform gland spigot(s), TP = tartipore(s). Scale bars: A, B = 75 μ m, C = 150 μ m, D = 430 μ m.

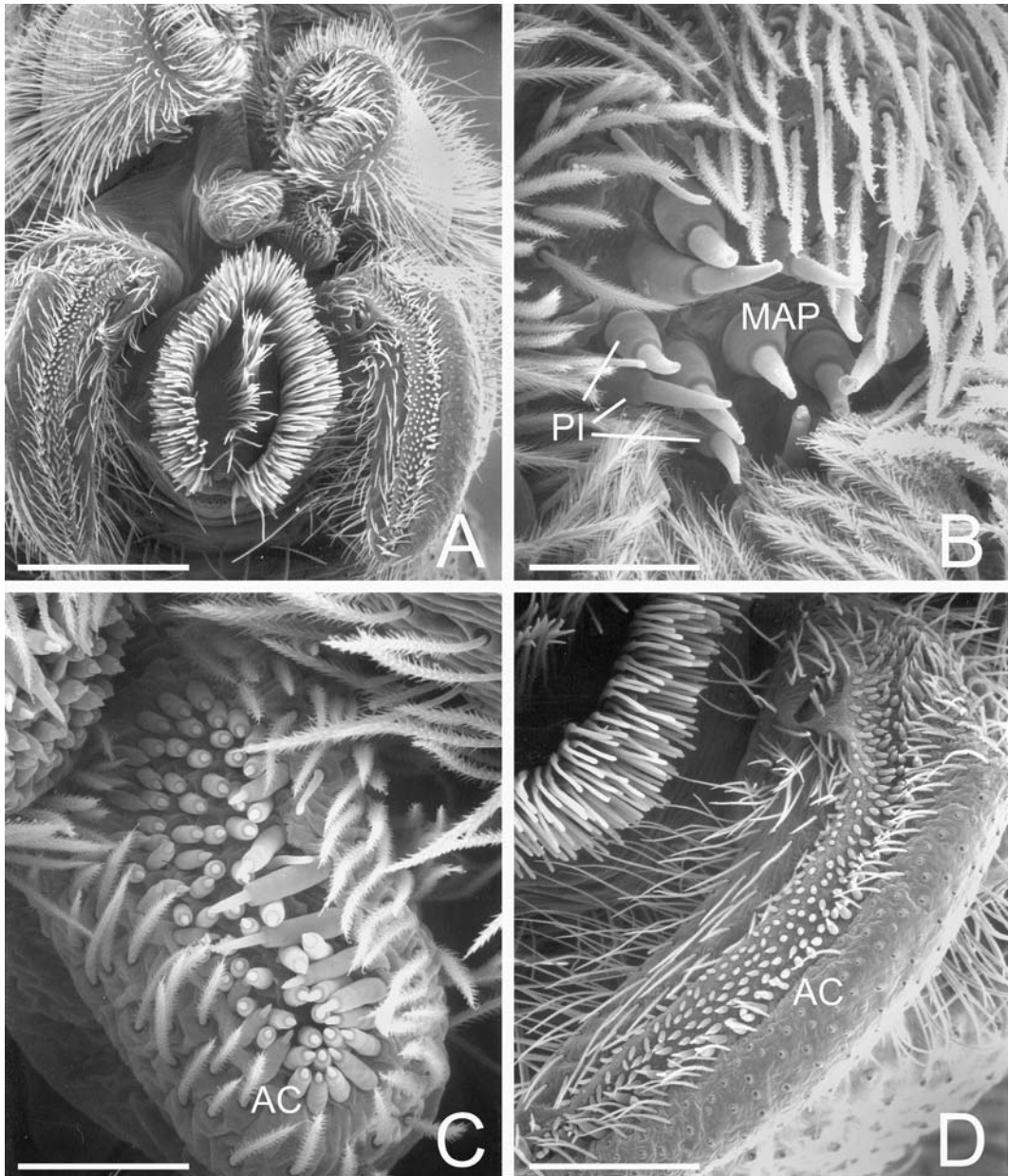


FIGURE 30. Spinnerets of male *Uroctea* sp. from Garies, South Africa. A. Spinneret overview. Note elongate PLS and enlarged anal tubercle. B. Left ALS, showing mostly MAP spigots. C. Left PMS, probably with only AC spigots. D. Left PLS showing only AC spigots. AC = aciniform gland spigot(s), MAP = major ampullate gland spigot(s), PI = piriform gland spigot(s). Scale bars: A = 430 μ m, B, C = 60 μ m, D = 200 μ m.

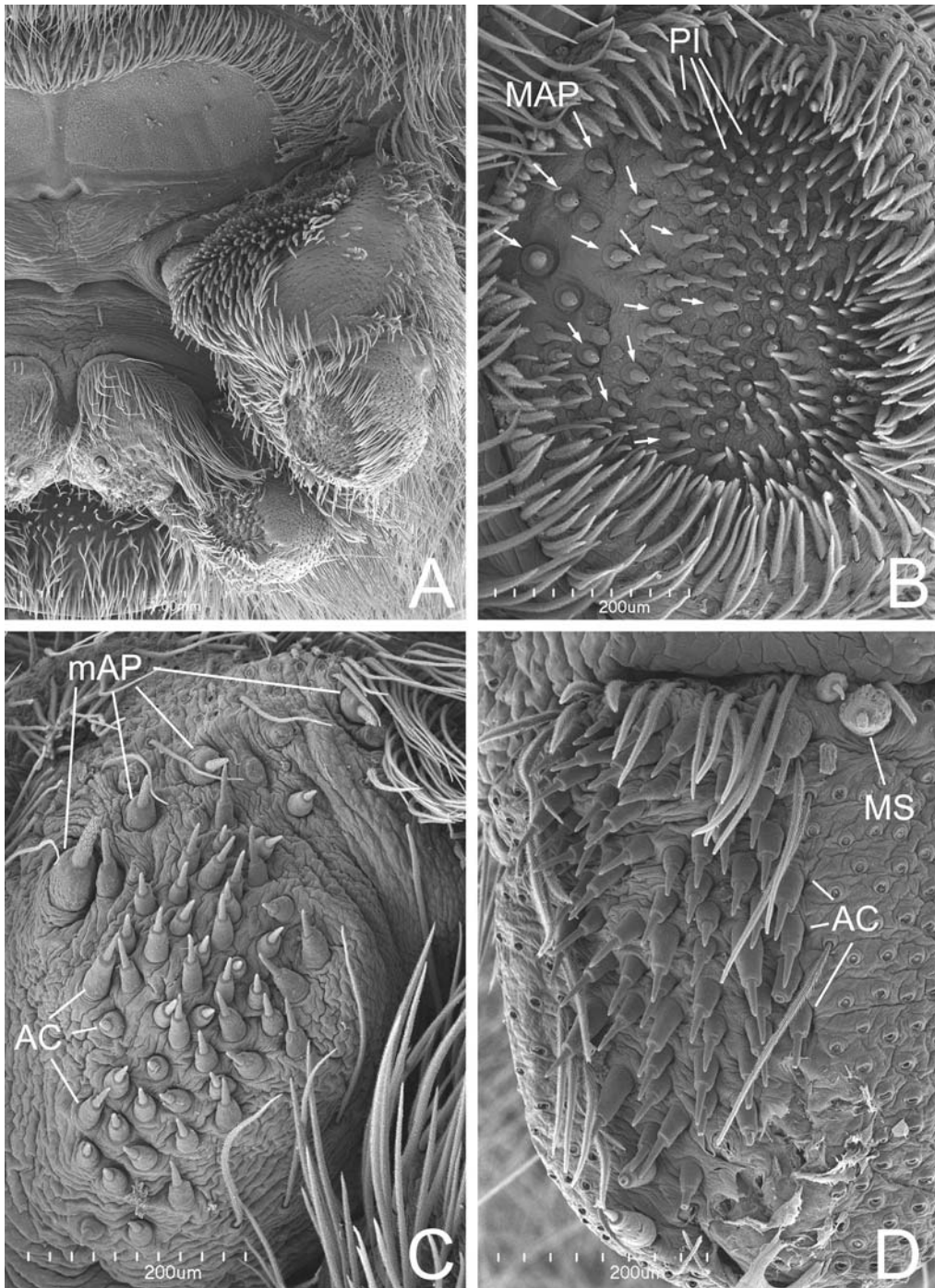


FIGURE 31. Spinnerets of female *Eresus* cf. *cinnaberinus* from Igrherm, Morocco. A. Overview. B. Left ALS: larger spigots (arrows) are presumably MAP, smaller PI. C. Right PMS: larger spigots are presumably mAP and CY, smaller AC. D. Left PLS (inverted). AC = aciniform gland spigot(s), MAP = major ampullate gland spigot(s), mAP = minor ampullate gland spigot(s), MS = PLS modified spigot PI = piriform gland spigot(s). Scale bars: A = 1.0mm, B–D = 200µm.

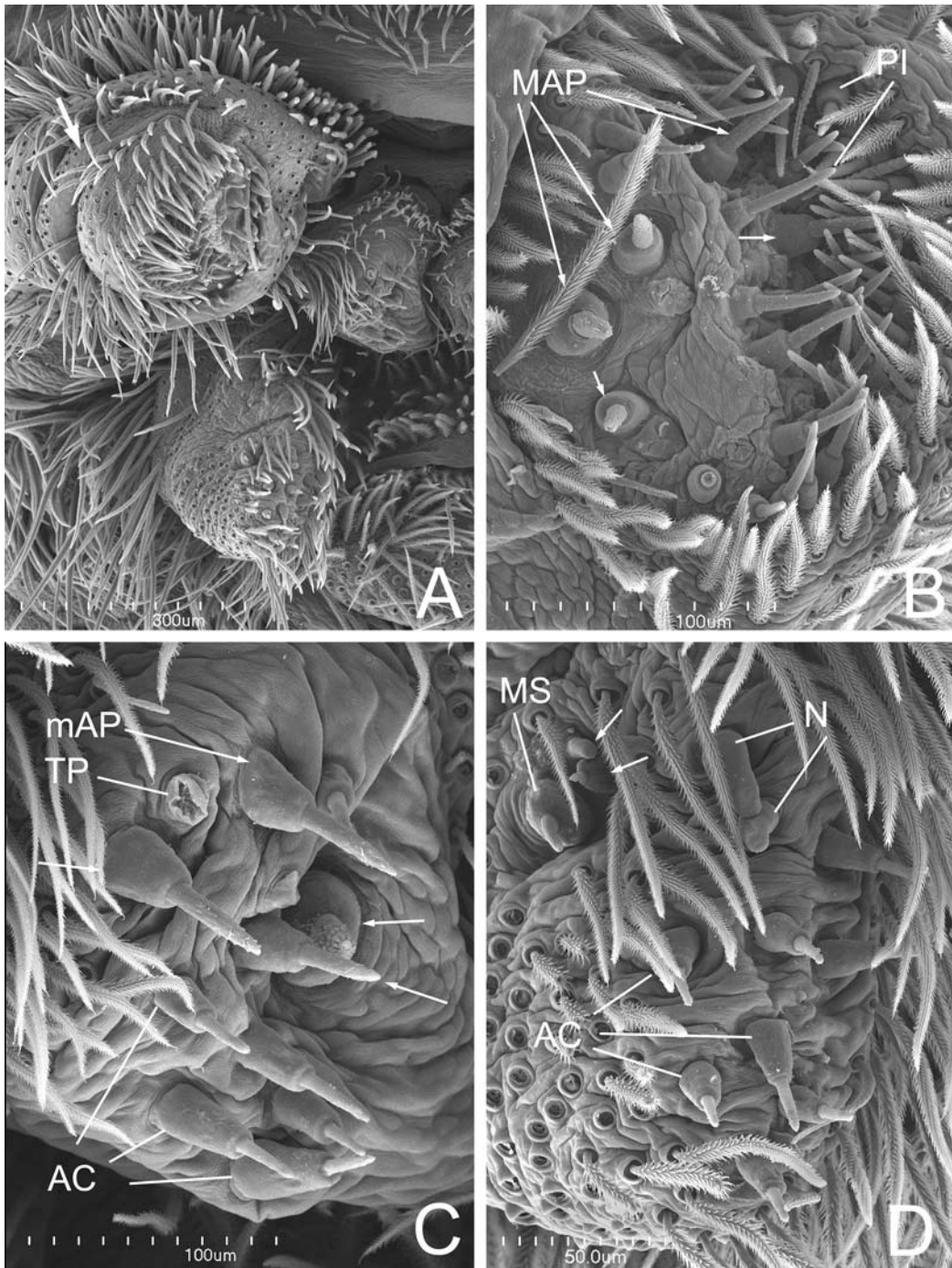


FIGURE 32. Right spinnerets of male *Eresus* cf. *cinnaberinus* from Mistras, Greece. A. Spinneret overview. Arrow to intermediate ALS segment. B. ALS, arrows to MAP. C. PMS, arrows to mAP. D. PLS, arrows to vestigial spigots accompanying the MS. AC = aciniform gland spigot(s), MAP = major ampullate gland spigot(s), mAP = minor ampullate gland spigot(s), MS = PLS modified spigot, N = nubbin(s), PI = piriform gland spigot(s). Scale bars: A = 300µm, B, C = 100µm, D = 50µm.

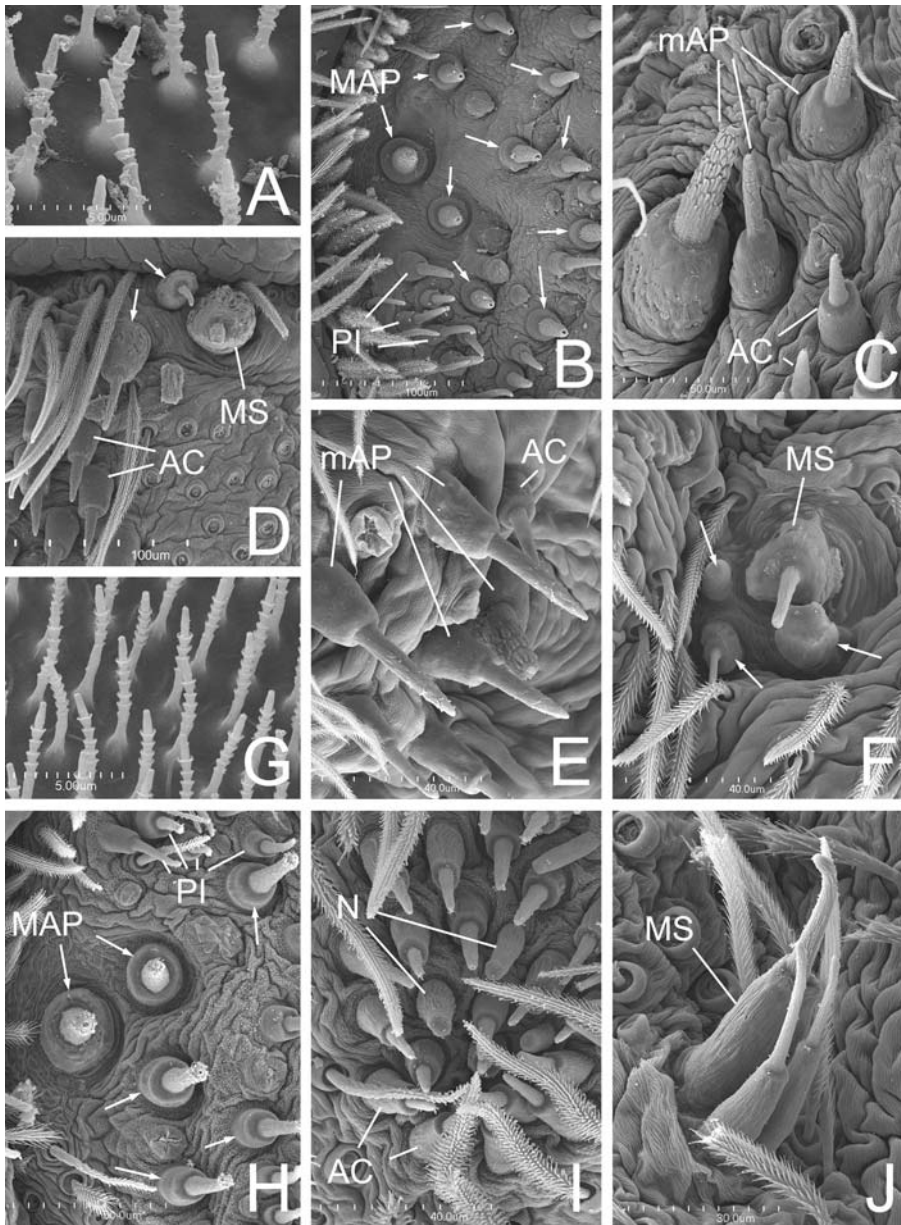


FIGURE 33. Spinnerets of Eresidae. A–F. *Eresus* cf. *cinnaberinus*. A–D. Female from Igrherm, Morocco. E, F. Male from Mistras, Greece. A. Cribellar spigots. B. Detail of right female ALS, showing MAP (arrows) interspersed among PI spigots; the large tartipores correspond to MAP, the small to PI. C. Detail of right female PMS: the ampullate shafts are characteristically sculptured. D. Detail of female base of right PLS (inverted), showing MS and accompanying spigots (arrows). E. Detail of right male PMS: one of the mAP is much larger than the rest. F. Detail of base of right male PLS (inverted), showing MS and vestigial accompanying spigots (arrows). G–J. *Stegodyphus mimosarum* female from Phinda, South Africa. G. Cribellar spigots. H. Detail of right ALS showing MAP (arrows) interspersed among PI spigots; the large tartipores correspond to MAP, the small to PI. I. Apical detail of right PLS: several nubbins among the AC. J. Detail of base of right PLS: showing MS and two accompanying spigots. AC = aciniform gland spigot(s), MAP = major ampullate gland spigot(s), mAP = minor ampullate gland spigot(s), MS = PLS modified spigot, N = nubbin(s), PI = piriform gland spigot(s). Scale bars: A, G = 5 μ m, B, D = 100 μ m, C, H = 50 μ m, E, F, I = 40 μ m, J = 30 μ m.

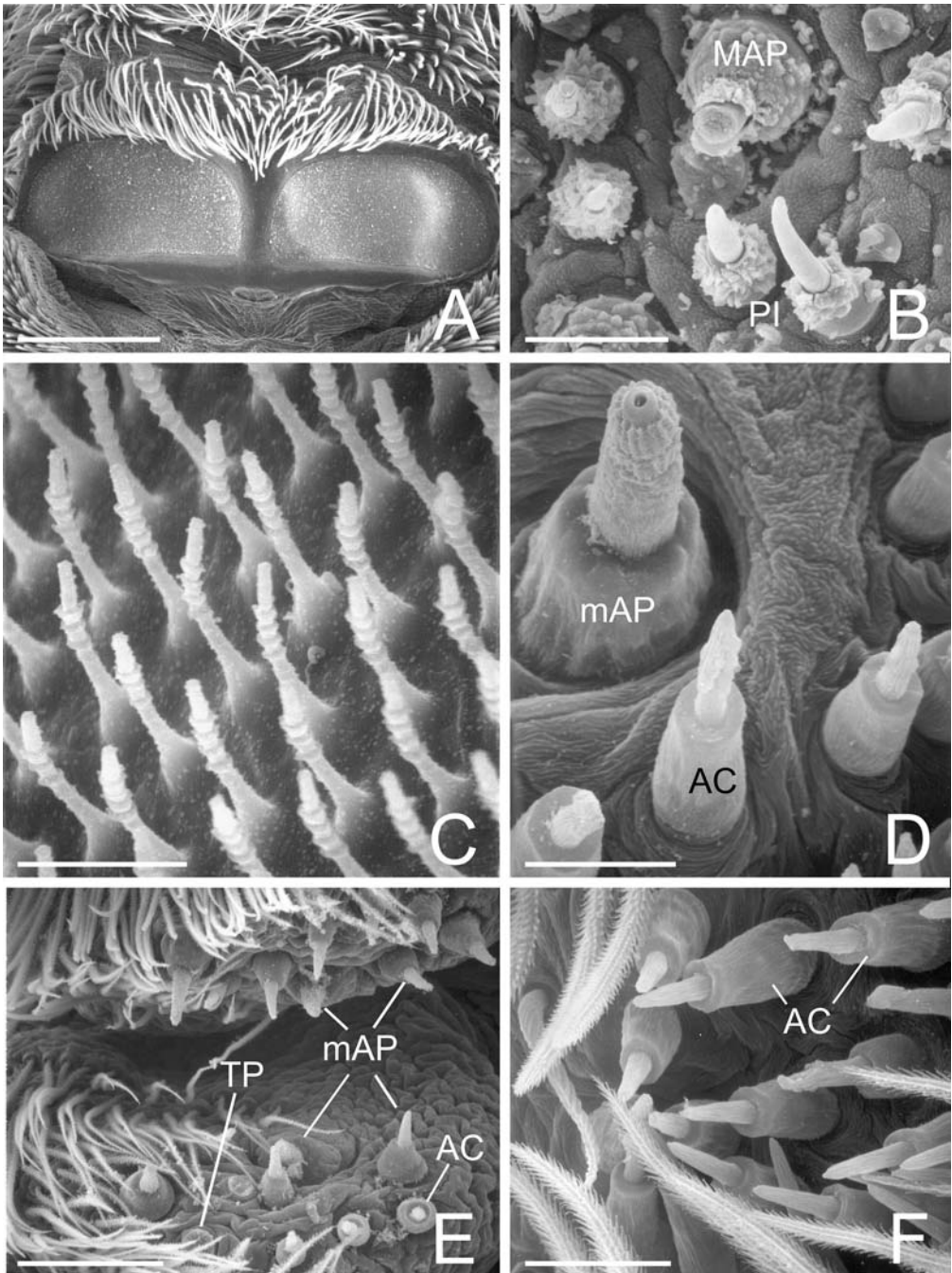


FIGURE 34. Spinnerets of female Eresidae. A, C. *Eresus sandaliatus* from Silkeborg, Denmark. B, E. *Eresus cinnaberinus* from Fiesch Wallis, Switzerland. D, F. *Stegodyphus mimosaurum*, from Fort Hill, Malawi. A. Cribellum. B. Left ALS, detail. C. Strobilate cribellar spigots. D. Left PMS, detail. Note characteristic sculpturing of ampullate shaft. E. PMS. F. Right PLS apex. AC = aciniform gland spigots, MAP = major ampullate gland spigot(s), mAP = minor ampullate gland spigot(s), PI = piriform gland spigot(s), TP = tartipore(s). Scale bars: A = 300 μ m, B = 25 μ m, C = 4.3 μ m, D = 15 μ m, E = 60 μ m, F = 20 μ m.

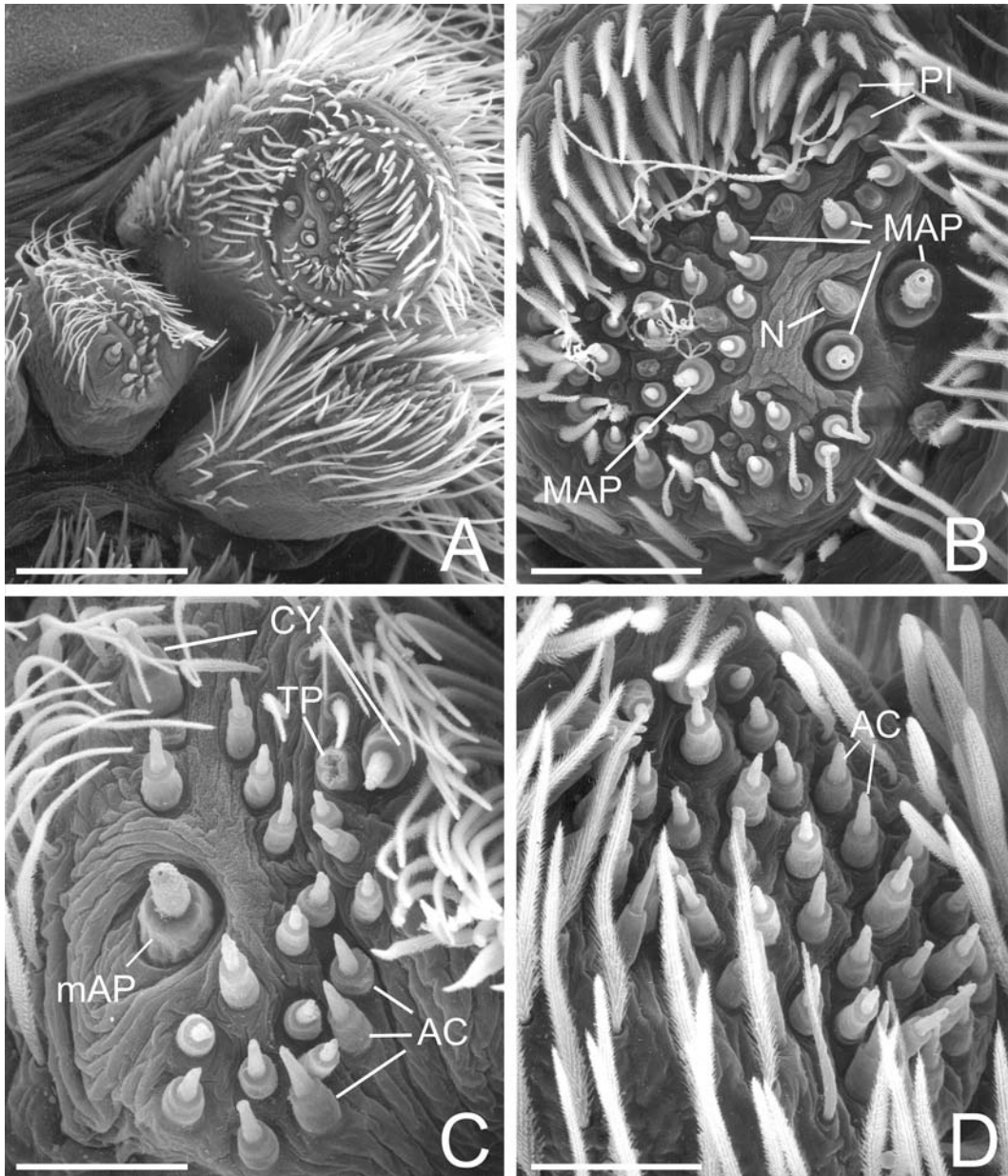


FIGURE 35. Spinnerets of female *Stegodyphus mimosarum* from Fort Hill, Malawi. A. Left spinneret overview. B. Right ALS. Smaller spigots are presumably PI. C. Left PMS. D. Right PLS. AC = aciniform gland spigots, CY = cylindrical gland spigot(s), MAP = major ampullate gland spigot(s), mAP = minor ampullate gland spigot(s), N = nubbin(s), PI = piriform gland spigot(s), TP = tartipore(s). Scale bars: A = 200µm, B = 60µm, C, D = 43µm.

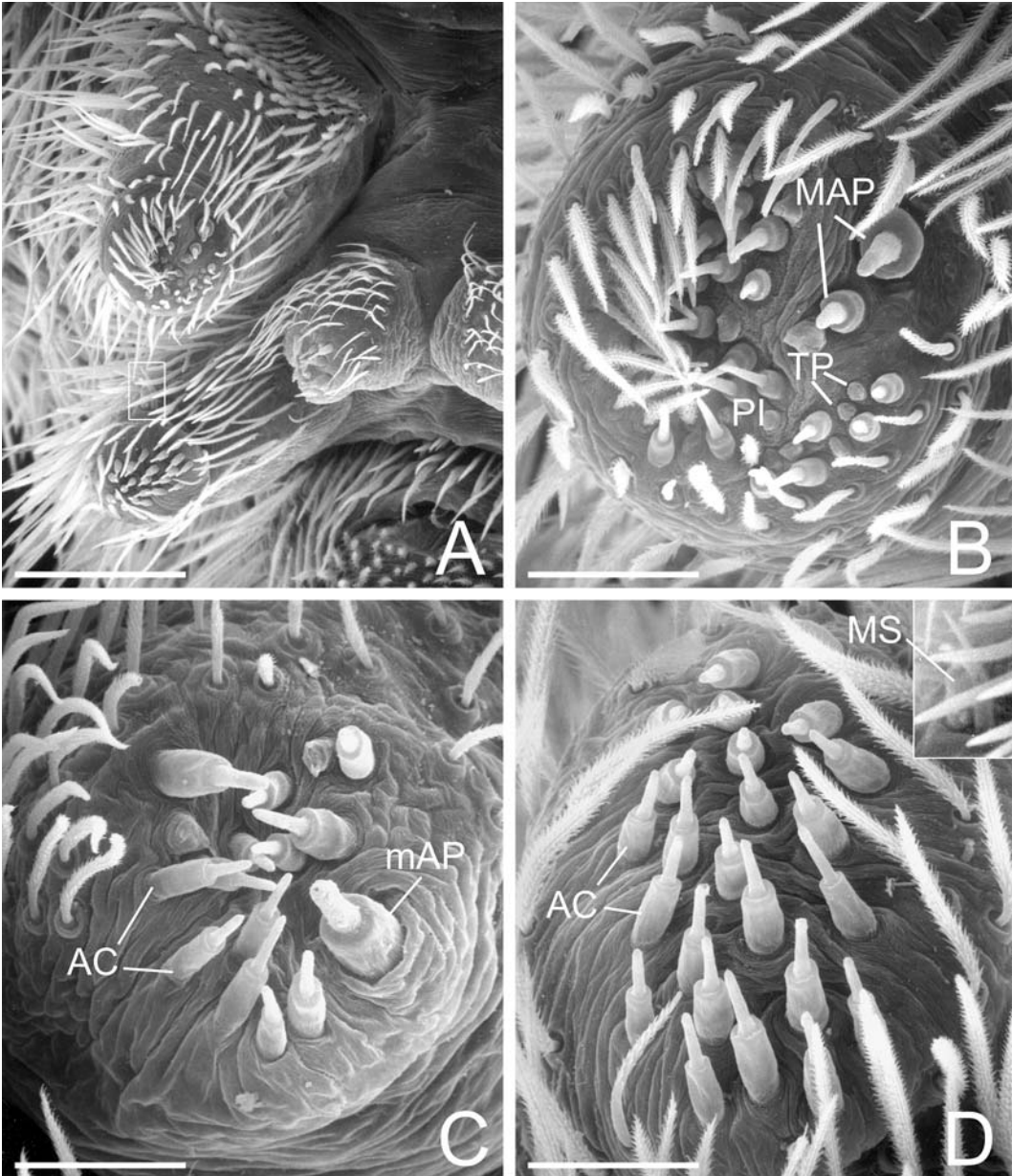


FIGURE 36. Right spinnerets of male *Stegodyphus mimosarum* from Fort Hill, Malawi. A. Overview (inset enlarged in D). B. ALS. C. PMS. D. PLS, inset to MS (area marked in A). AC = aciniform gland spigots, MAP = major ampullate gland spigot(s), MS = PLS modified spigot, PI = piriform gland spigot(s), TP = tartipore(s). Scale bars: A = 150 μ m, B = 43 μ m, C, D = 30 μ m.

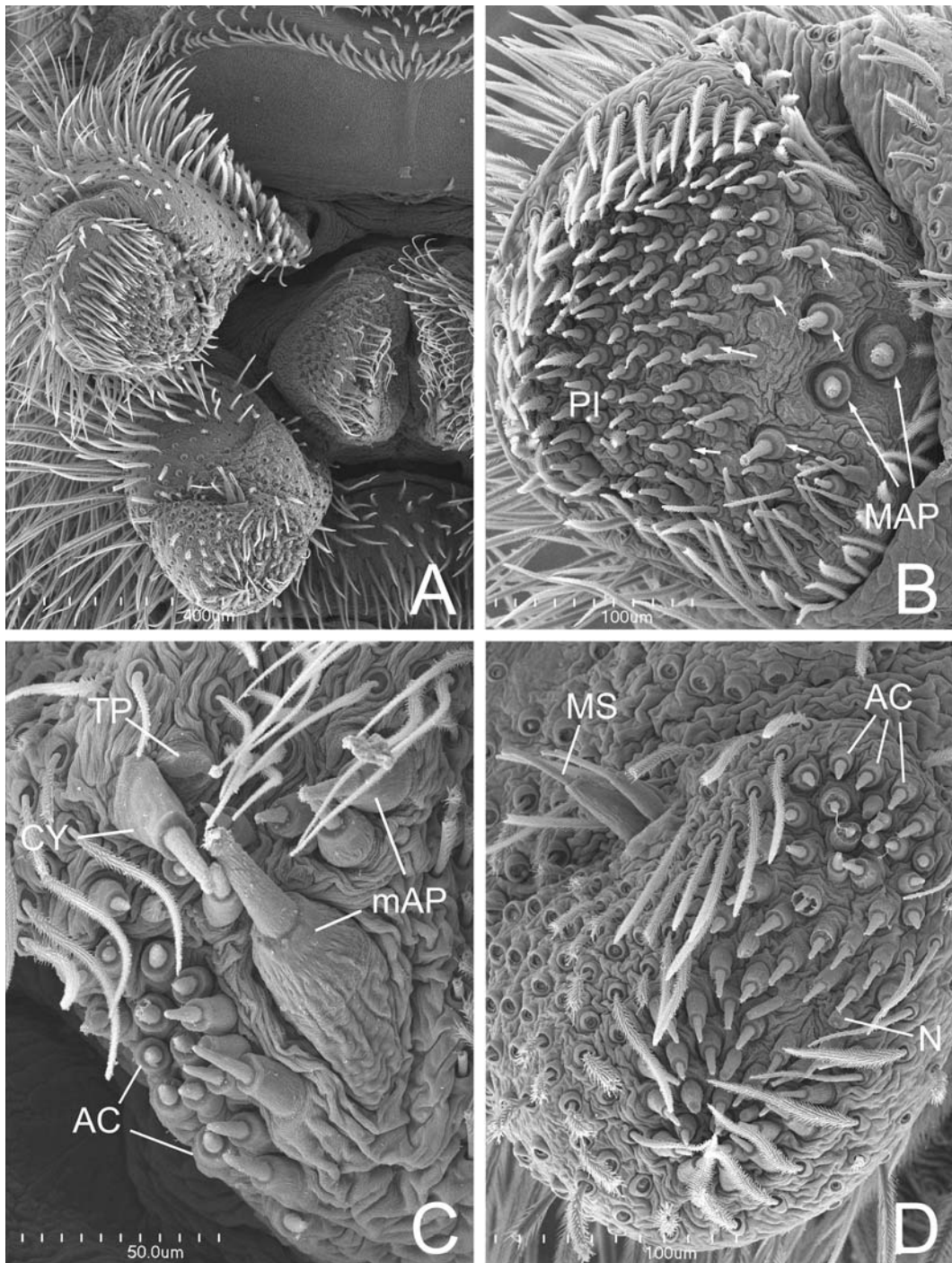


FIGURE 37. Right spinnerets of female *Stegodyphus mimosarum* from Phinda, South Africa. A. Overview of cribellum and spinnerets. B. ALS. Arrows to MAP. C. PMS. D. PLS. CY = cylindrical gland spigot, MAP = major ampullate gland spigot(s), mAP = minor ampullate gland spigot(s), MS = PLS modified spigot, PI = piriform gland spigot(s), TP = tartiportes. Scale bars: A = 400µm, B, D = 100µm, C = 50µm.

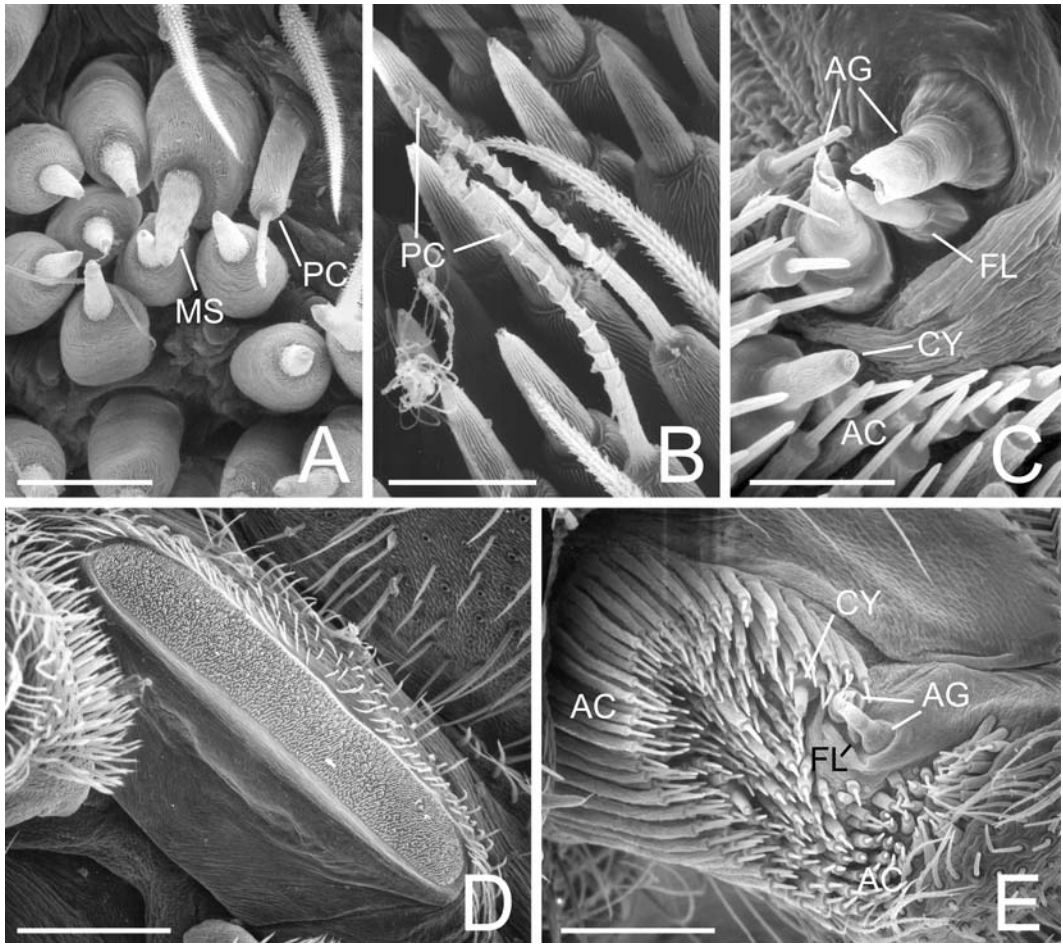


FIGURE 38. Spinnerets of Nicodamidae and Araneidae. A, B, D. *Megadictyna thilenii*. A, D. Female from Hick's Bay, New Zealand. B. Juvenile from Cherry Bay, New Zealand. C, E. Female *Argiope argentata* from Baja California, Mexico. A. Apex of left PLS showing PC, MS and AC spigots. B. PMS, showing PC and AC spigots. C. Triplet of AG and FL spigots at apex of PLS. D. Cribellum. E. Left PLS. AC = aciniform gland spigot(s), AG = aggregate gland spigots, CY = cylindrical gland spigot(s), FL = flagelliform gland spigot, MS = PLS modified spigot, PC = paracribellar spigot(s). Scale bars: A = 30 μ m, B = 15 μ m, C = 43 μ m, D, E = 150 μ m.

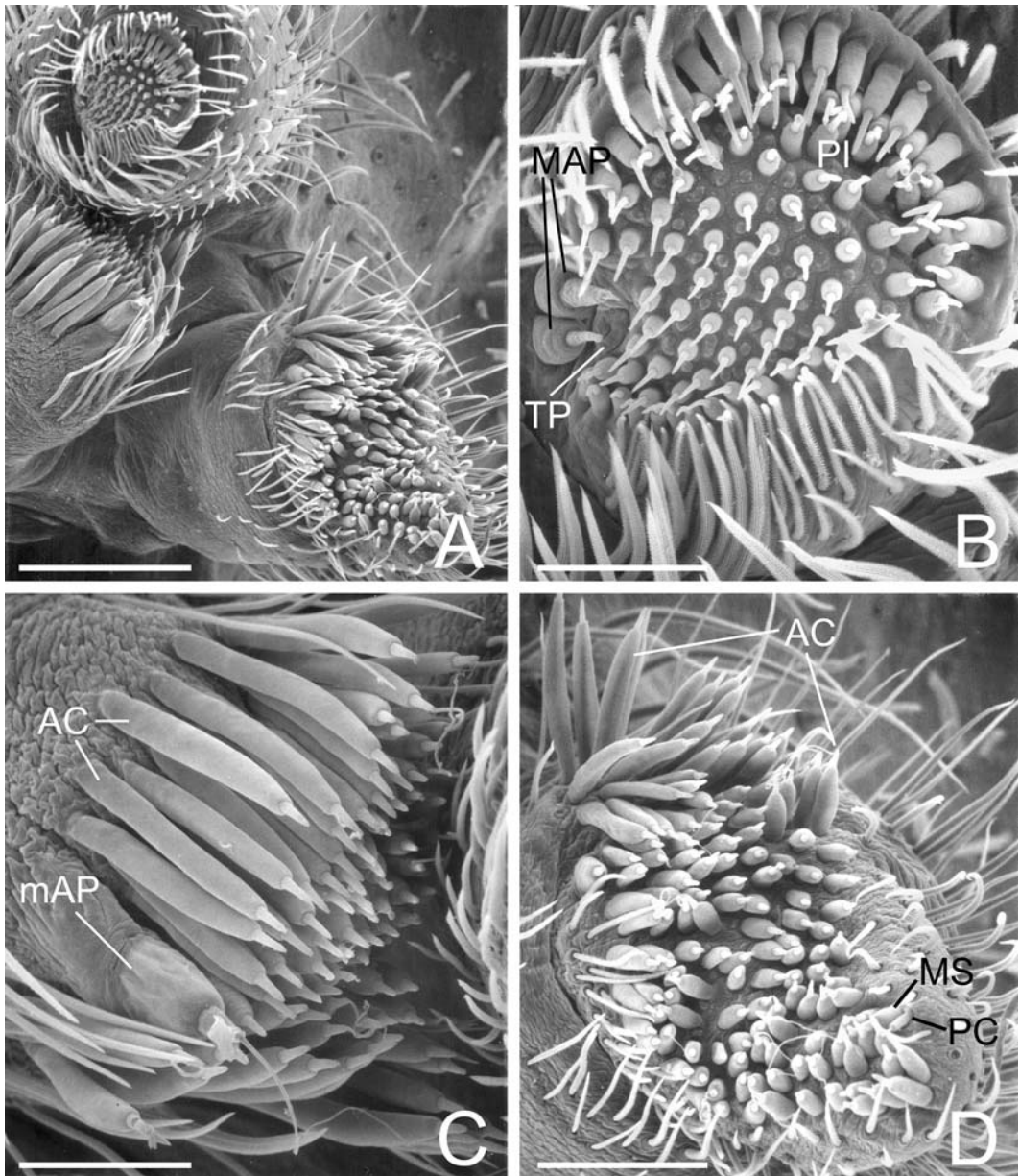


FIGURE 39. Left spinnerets of female *Megadictyna thilenii* from Hicks Bay, New Zealand. A. Overview. B. ALS. C. PMS. Note posterior mAP. PC spigots are hidden. D. PLS. AC = aciniform gland spigots, MAP = major ampullate gland spigot(s), mAP = minor ampullate gland spigot(s), MS = PLS modified spigot, PC = paracribellar spigot(s), PI = piriform gland spigot(s), TP = tartipore(s). Scale bars: A = 300µm, B = 75µm, C = 100µm, D = 150µm.

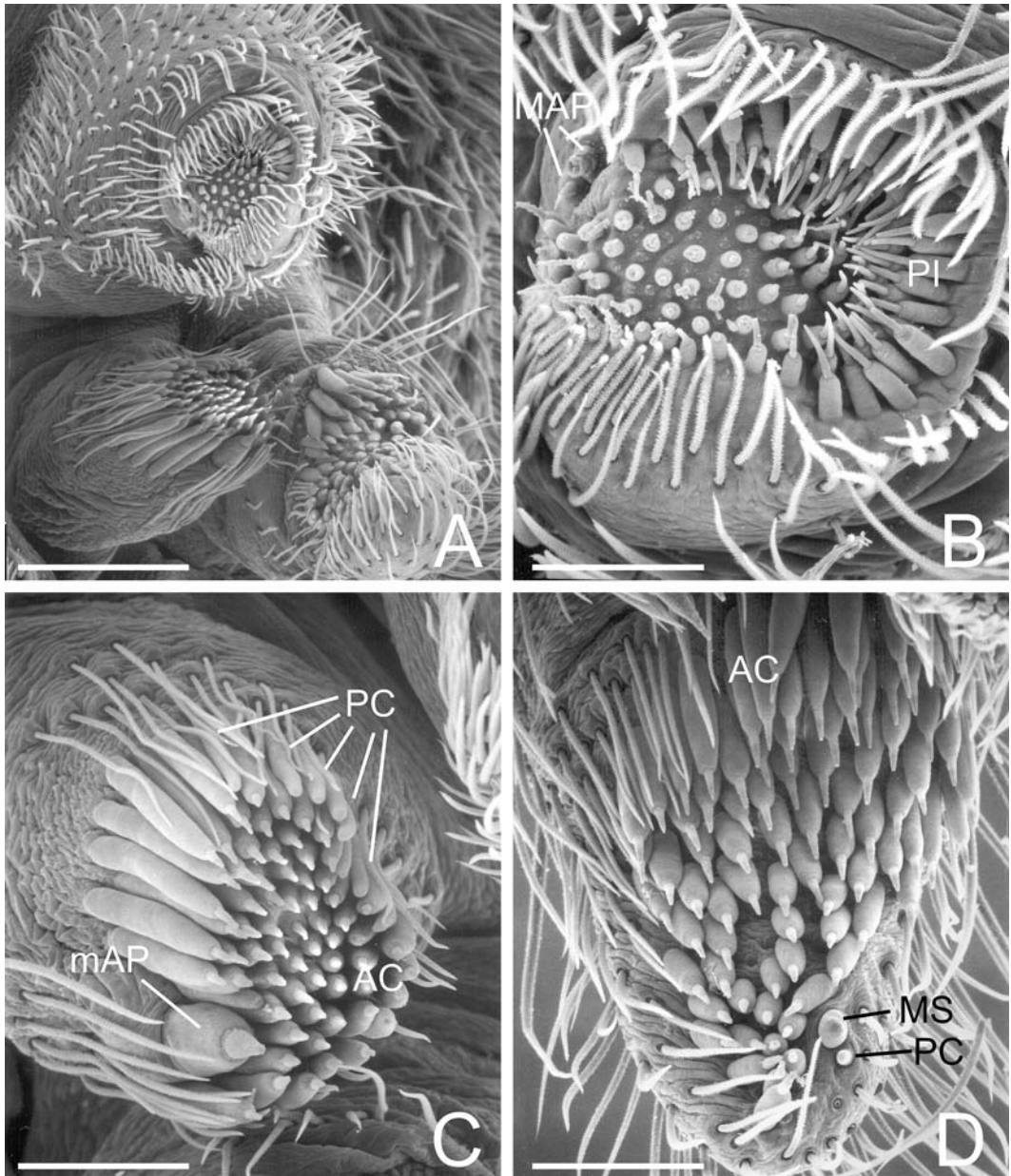


FIGURE 40. Left spinnerets of male *Megadictyna thilenii* from Orongorongo, New Zealand. A. Overview. B. ALS. Note difference in size between anterior and posterior MAP. C. PMS. Note posterior mAP and anterior encircling line of PC spigot nubbins. D. PLS. Note apical nubbins of MS and PC. AC = aciniform gland spigot(s), MAP = major ampullate gland spigot(s), mAP = minor ampullate gland spigot(s), MS = PLS modified spigot nubbin, PC = paracribellar spigot nubbins, PI = piriform gland spigot(s). Scale bars: A = 254 μ m, B = 75 μ m, C, D = 100 μ m.

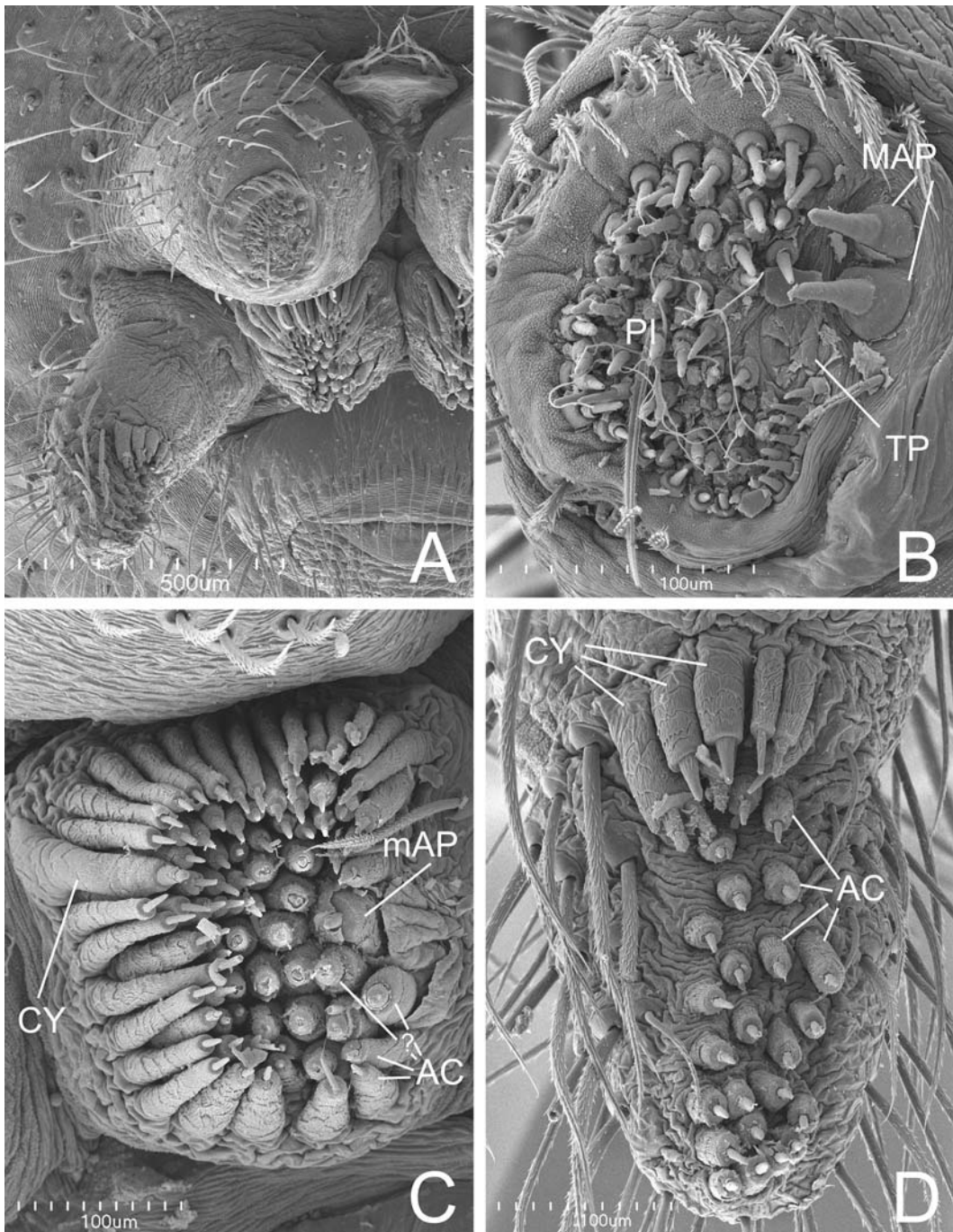


FIGURE 41. Right spinnerets of female *Nicodamus mainae* from Coalseam Park, Western Australia, Australia. A. Spinneret overview. B. ALS. C. PMS. D. PLS. AC = aciniform gland spigot(s), CY = cylindrical gland spigot(s), MAP = major ampullate gland spigot(s), mAP = minor ampullate gland spigot(s), PI = piriform gland spigot(s), TP = tartipore(s). Scale bars: A = 500µm, B–D = 100µm..

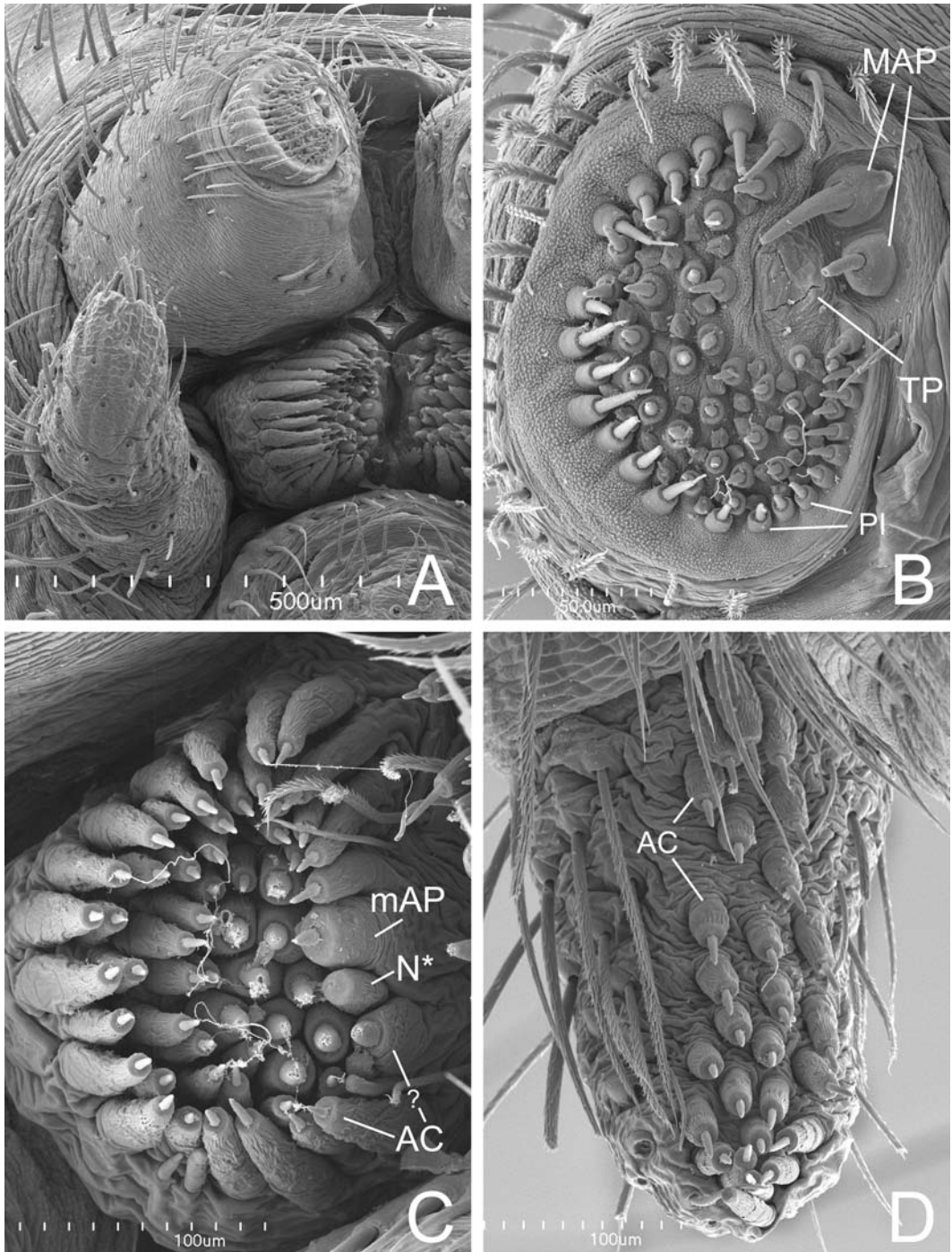


FIGURE 42. Left spinnerets (inverted) of male *Nicodamus mainae* from Bush Bay, Western Australia, Australia. A. Spinneret overview. B. ALS. C. PMS, nubbin posterior to mAP is absent on right spinneret. D. PLS, apical nubbin is absent on right spinneret. AC = aciniform gland spigot(s), MAP = major ampullate gland spigot(s), mAP = minor ampullate gland spigot(s), N = nubbins, PI = piriform gland spigot(s), TP = tartipore(s). Scale bars: A = 500µm, B = 50µm, C, D = 100µm.

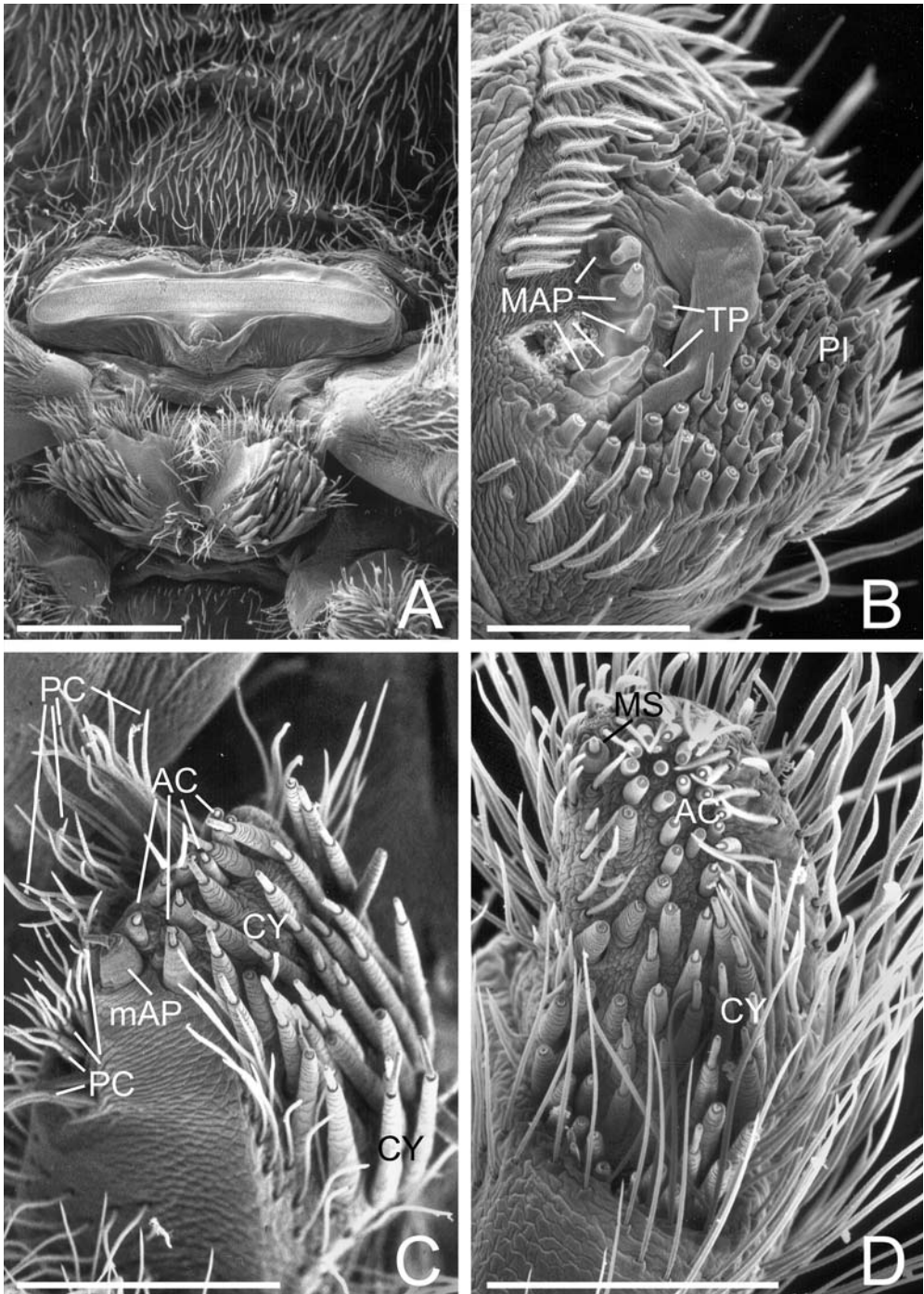


FIGURE 43. Spinnerets of female *Menneus camelus* from Zululand, South Africa. A. Cribellum and PMS. B. Left ALS. C. Left PMS. D. Left PLS. AC = aciniform gland spigot(s), CY = cylindrical gland spigot(s), MAP = major ampullate gland spigot(s), mAP = minor ampullate gland spigot(s), MS = PLS modified spigot, PC = paracribellar spigot(s), PI = piriform gland spigot(s), TP = tartipore(s). Scale bars: A = 500 μ m, B = 100 μ m, C–D = 200 μ m.

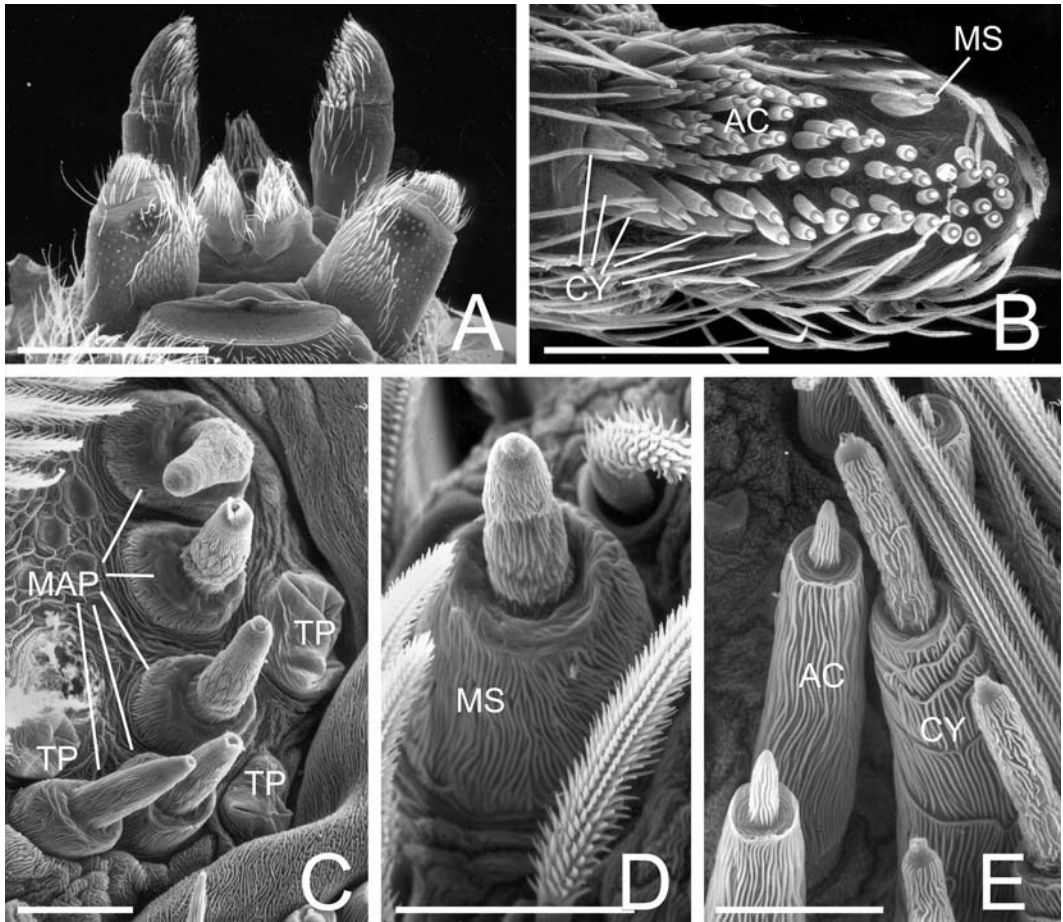
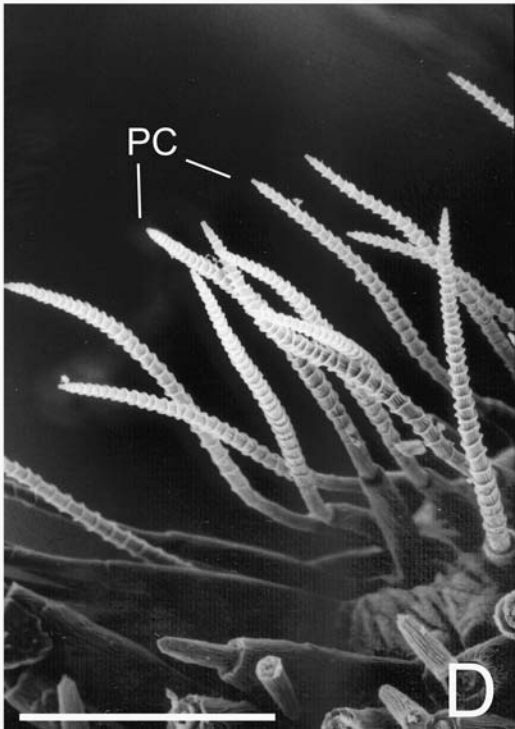
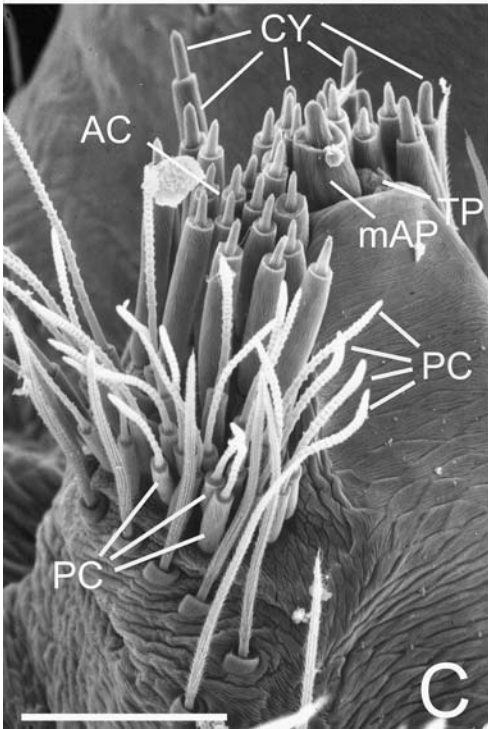
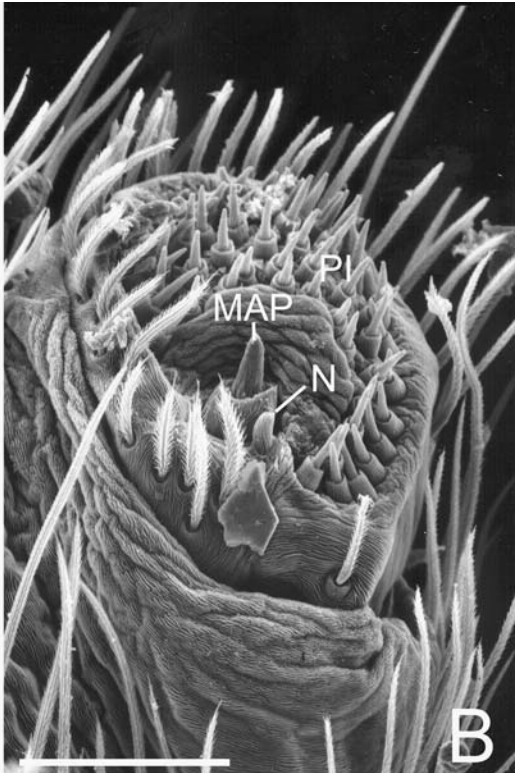
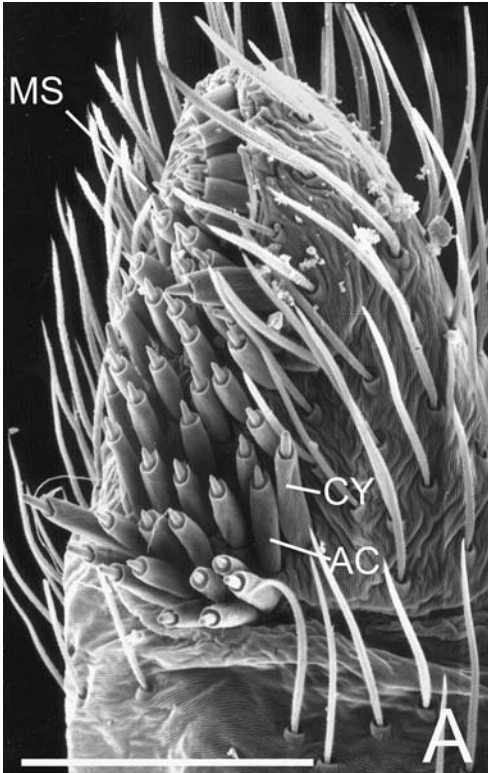


FIGURE 44. Spinneret details of female Deinopoidea. A, B. *Octonoba octonaria* from St. Charles Co., Missouri, USA. A. Spinnerets, anteroventral view. B. PLS. C–E. *Menneus camelus* from Zululand, South Africa. C. ALS MAP. D. PLS apex, showing modified spigot. E. PLS detail. AC = aciniform gland spigot(s), CY = cylindrical gland spigot(s), MAP = major ampullate gland spigot(s), MS = PLS modified spigot, TP = tartipore(s). Scale bars: A = 500µm, B = 50µm, C–E = 20µm.



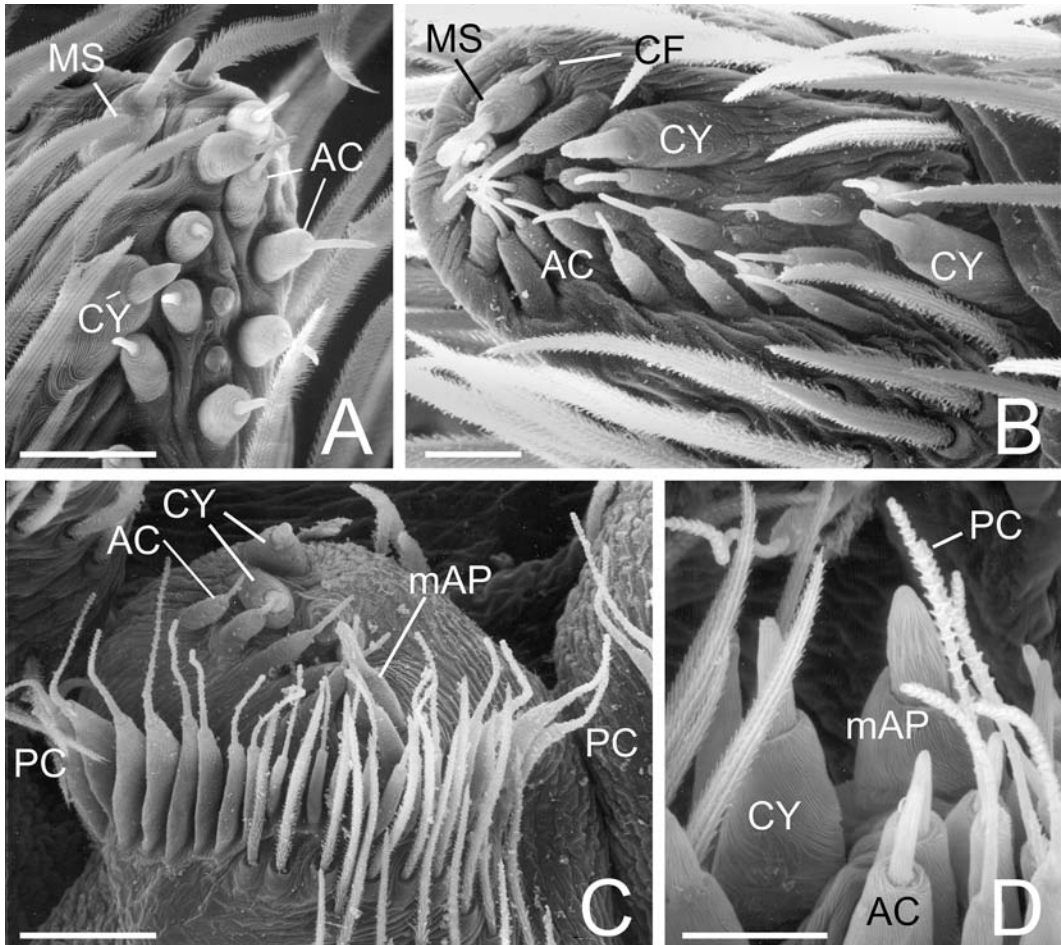


FIGURE 46 (above). Spigots of female Phyxelididae. A. *Phyxelida tanganyensis* from Amani, Tanzania, apex of left PLS showing CY, MS and AC spigots. B. *Namaquarache tropata* from Grootvadersbosch, South Africa. B. PLS apex. C. PMS anterior, with PC labelling ends of encircling row of PC spigots with flattened bases. D. *Vyfytia pallens* from Sarawak, Malaysia, left PMS apex. AC = aciniform gland spigot(s), CF = cuticular finger, CY = cylindrical gland spigot(s), mAP = minor ampullate gland spigot(s), MS = PLS modified spigot, PC = paracribellar spigot(s). Scale bars: A, B = 20µm, C = 40µm, D = 15µm.

FIGURE 45 (left). Spinnerets of female Orbiculariae. A–C. *Uloborus trilineatus* from Pipeline Road., Panama. A. PLS. B. ALS. C. PMS. D. *Deinopis spinosus* from Alachua Co., Florida, USA, PMS paracribellars. AC = aciniform gland spigot(s), CY = cylindrical gland spigot(s), MAP = major ampullate gland spigot(s), mAP = minor ampullate gland spigot(s), MS = PLS modified spigot, N = nubbin(s), PC = paracribellar spigot(s), PI = piriform gland spigot(s), TP = tarapore(s). Scale bars: A = 100µm, B–D = 50µm.

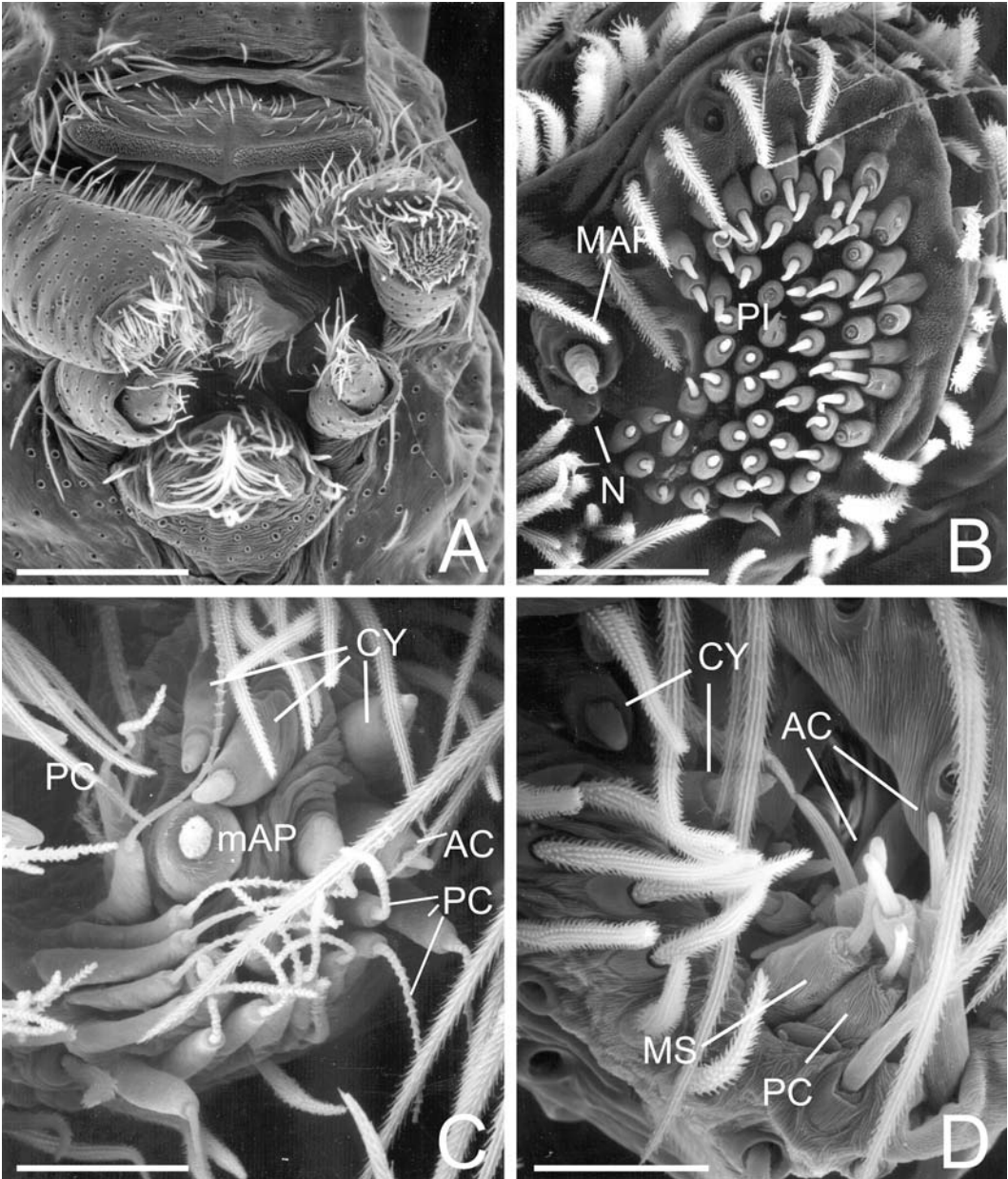


FIGURE 47. Spinnerets of female *Vytfutia pallens* from Sarawak, Malaysia. A. Spinneret overview. B. Left ALS. Note nubbin of MAP spigot and cuticular fold mesad of MAP spigot. C. Right PMS with PC labeling ends of encircling row of PC spigots. Note flattened bases of PC spigots. D. Right PLS. AC = aciniform gland spigot(s), CY = cylindrical gland spigot(s), MAP = major ampullate gland spigot(s), mAP = minor ampullate gland spigot(s), MS = PLS modified spigot, N = nubbin(s), PC = paracribellar spigot(s), PI = piriform gland spigot(s). Scale bars: A = 150 μ m, B = 35 μ m, C = 25 μ m, D = 20 μ m.

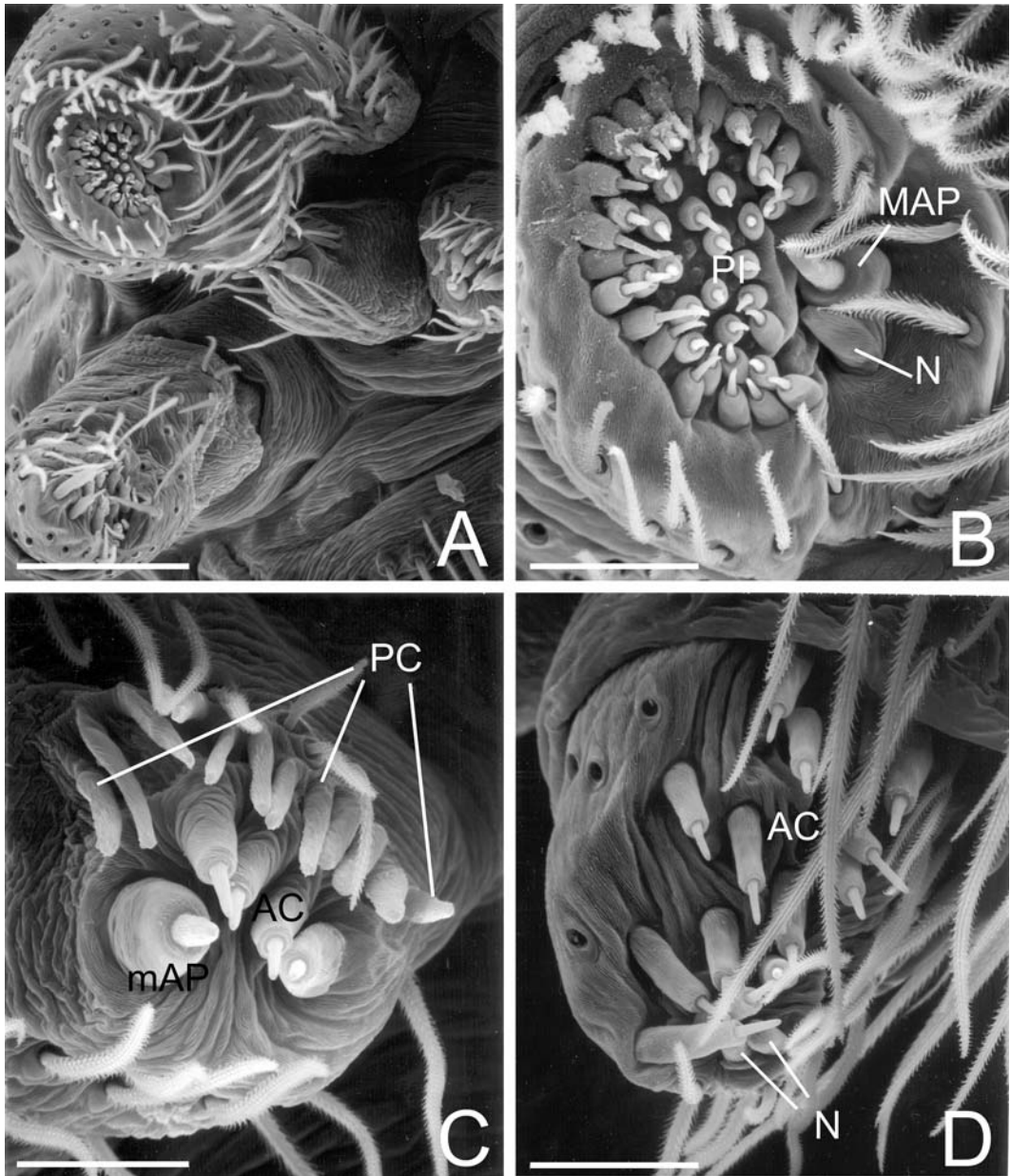


FIGURE 48. Spinnerets of male *Vityftia pallens* from Sarawak, Malaysia. A. Right spinneret overview. B. Right ALS showing nubbin of posterior MAP spigot. C. Left PMS, showing nubbins of PC spigots. D. Left PLS showing nubbins of MS and PC spigots. AC = aciniform gland spigot(s), MAP = major ampullate gland spigot(s), mAP = minor ampullate gland spigot(s), N = nubbins, PC = paracribellar spigot nubbins on PMS, PI = piriform gland spigot(s). Scale bars: A = 100 μ m, B, D = 30 μ m, C = 25 μ m.

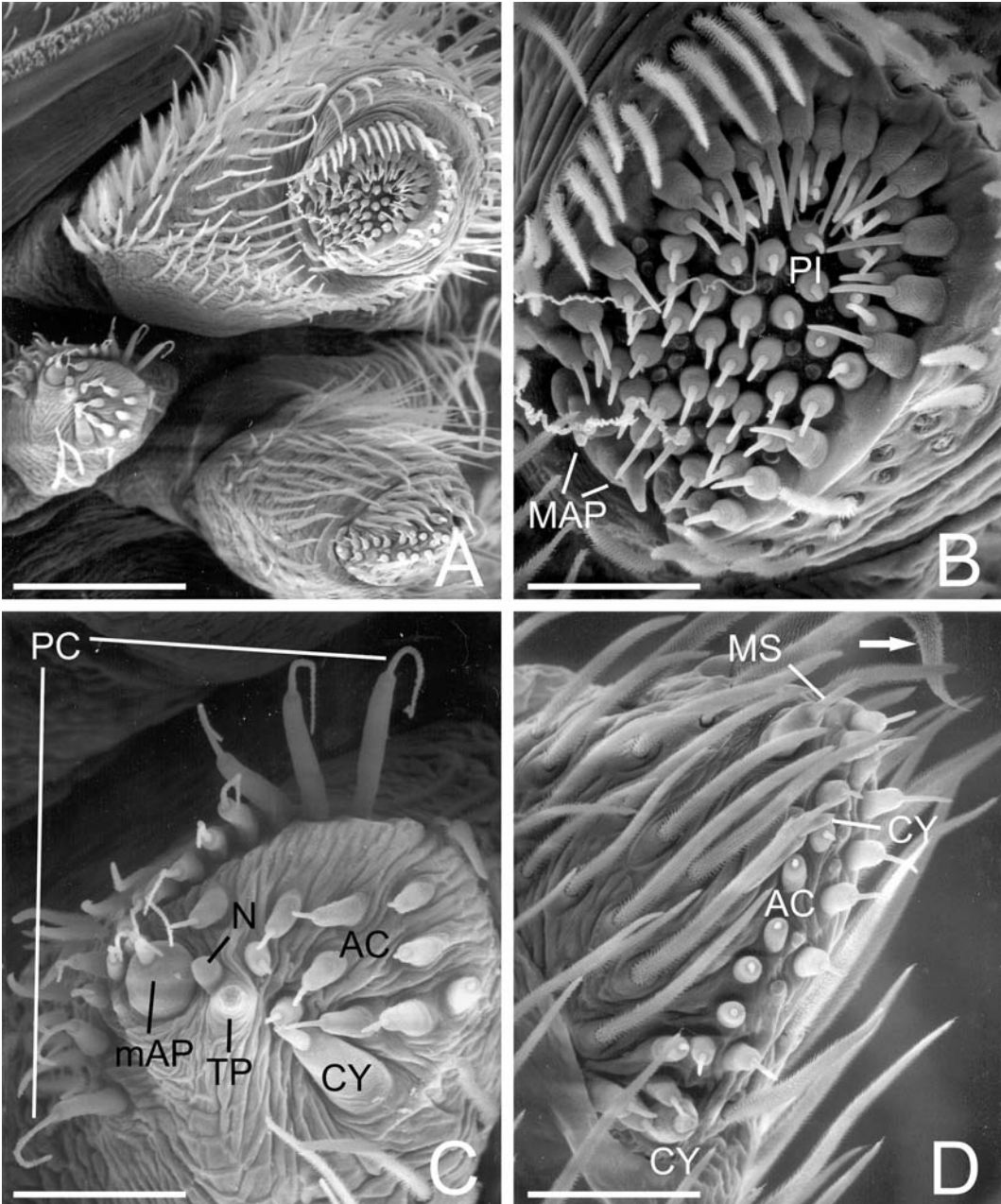


FIGURE 49. Left spinnerets of female *Phyxelida tanganyensis* from Amani, Tanzania. A. Overview. B. ALS. C. PMS. Lines point to ends of encircling row of PC spigots. D. PLS. Arrow to stout seta near PLS apex. AC = aciniform gland spigot(s), CY = cylindrical gland spigot(s), MAP = major ampullate gland spigot(s), mAP = minor ampullate gland spigot(s), MS = PLS modified spigot, N = nubbin, PC = paracribellar spigot(s), PI = piriform gland spigot(s), TP = tartipore. Scale bars: A = 150µm, B, D = 43µm, C = 46µm.

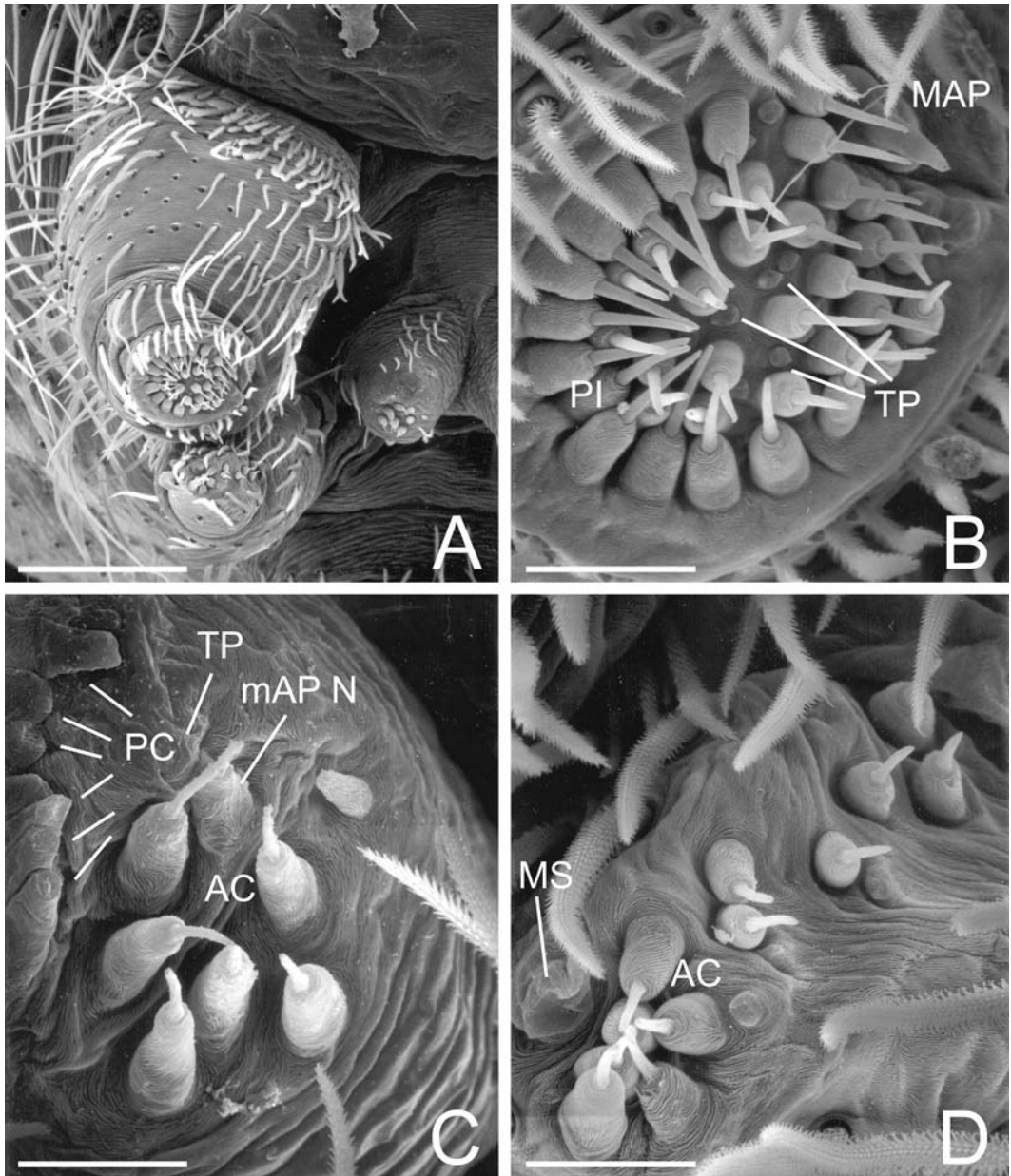


FIGURE 50. Right spinnerets of male *Phyxelida tanganyensis* from Amani, Tanzania. A. Overview. B. ALS. C. PMS. Note large TP. D. PLS, showing nubbin of MS at apex. AC = aciniform gland spigot(s), MAP = major ampullate gland spigot(s), mAP N = minor ampullate gland spigot nubbin, MS = nubbin of PLS modified spigot, PC = nubbins of PC spigots, PI = piriform gland spigot(s), TP = tartipore(s). Scale bars: A = 150µm, B = 30µm, C, D = 20µm.

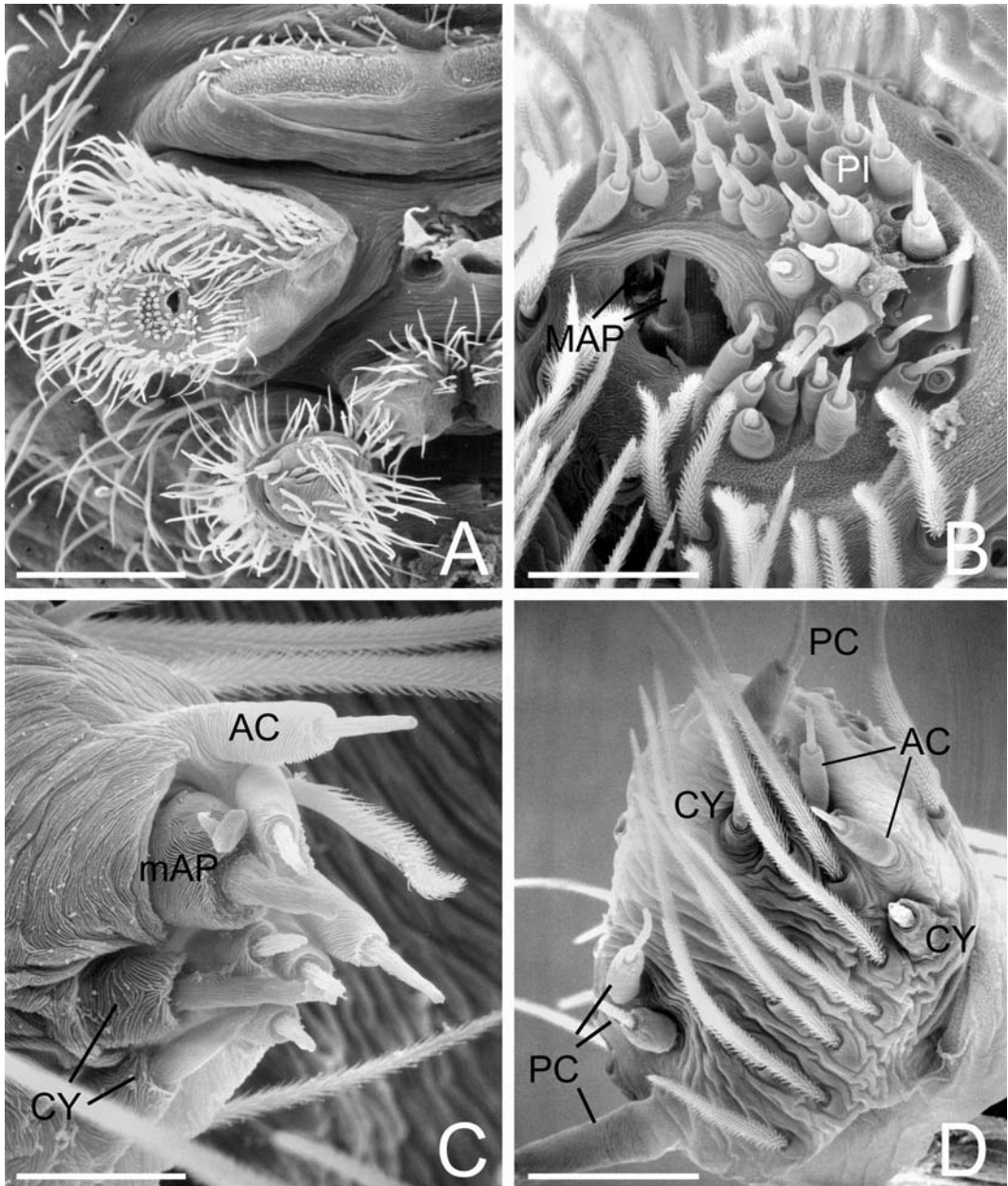


FIGURE 51. Spinnerets of female *Titanoecca americana* from Johnson Co., Missouri, USA. A. Right spinneret overview. B. Left ALS. MAP are sunken into broken cuticle. C. Left PMS. D. Right PLS. AC = aciniform gland spigot(s), CY = cylindrical gland spigot(s), MAP = major ampullate gland spigot(s), mAP = minor ampullate gland spigot(s), PC = paracribellar spigot(s), PI = piriform gland spigot(s). Scale bars: A = 200 μ m, B = 30 μ m, C = 20 μ m, D = 43 μ m.

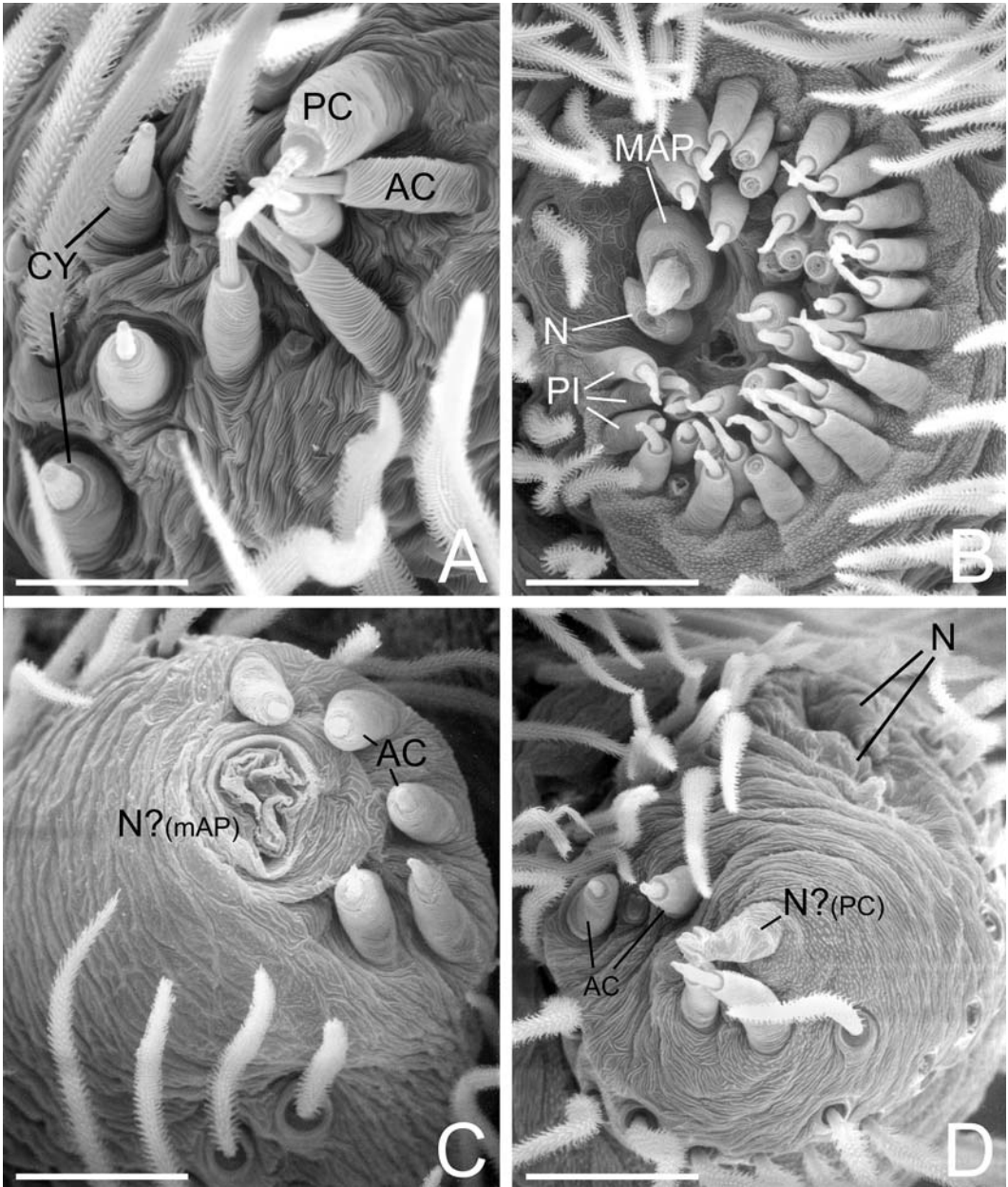


FIGURE 52. *Titanoeoca* spinnerets. A. Female *Titanoeoca nigrella* from Cave Creek, Arizona, USA, PLS apex. B–D. Male *Titanoeoca americana* from Johnson Co., Missouri, USA, left. B. ALS. C. PMS showing AC spigots and large nubbin of mAP. D. PLS, showing AC spigots and nubbins of apical and basal PC. AC = aciniform gland spigot(s), CY = cylindrical gland spigot(s), N = nubbin(s), PC = paracribellar spigot(s), PI = piriform gland spigot(s). Scale bars: A = 43 μ m, B, D = 30 μ m, C = 25 μ m.

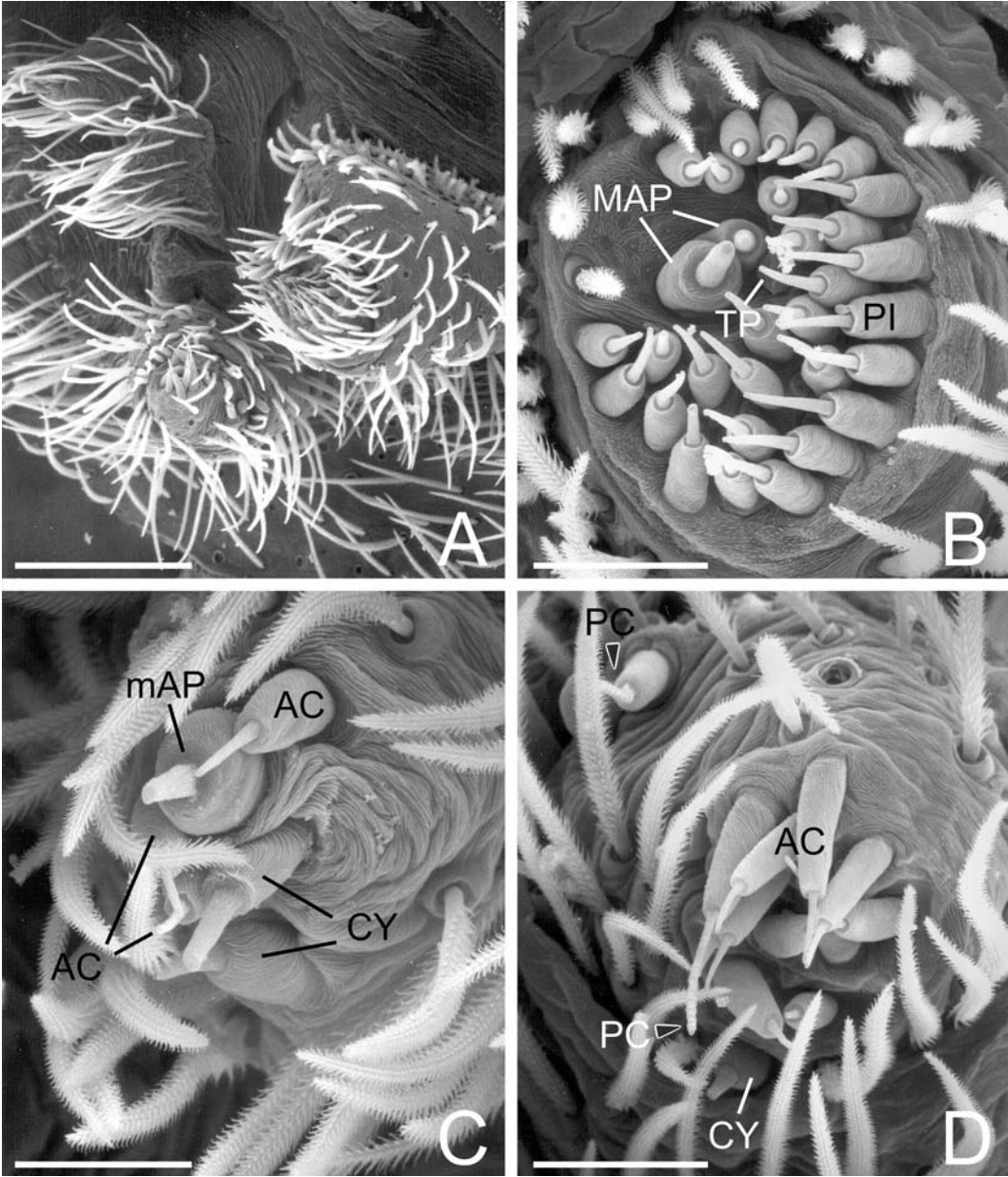


FIGURE 53. Spinnerets of female *Goeldia* sp. from Zapallar, Chile. A. Left overview. B. Right ALS. C. Right PMS. Note absence of PC. D. Left PLS. Basal and apical PC labeled. AC = aciniform gland spigot(s), CY = cylindrical gland spigot(s), MAP = major ampullate gland spigot(s), mAP = minor ampullate gland spigot(s), PC = paracribellar spigot(s), PI = piriform gland spigot(s), TP = tartipore. Scale bars: A = 150µm, B, D = 30µm, C = 20µm.

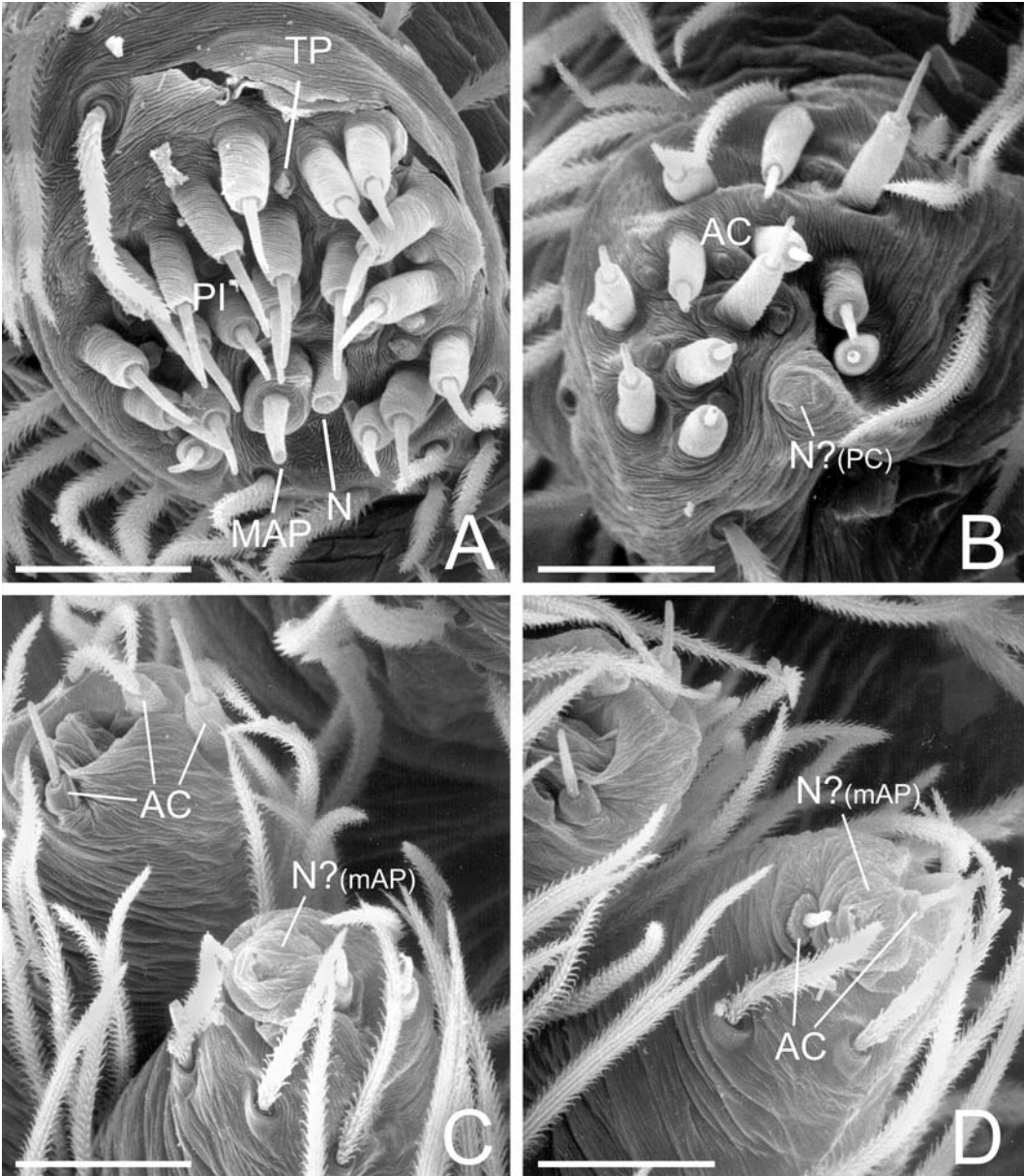


FIGURE 54. Spinnerets of male *Goeldia* sp. from Zapallar, Chile. A. Right ALS. B. Right PLS. Note nubbin of apical PC. C, D. PMS. Nubbin is probably vestige of mAP. C. Lateral. D. Posterior. AC = aciniform gland spigot(s), MAP = major ampullate gland spigot(s), N = nubbin(s), PC = nubbin of paracribellar spigot, PI = piriform gland spigot(s), TP = tartipore(s). Scale bars: A–D = 25µm.

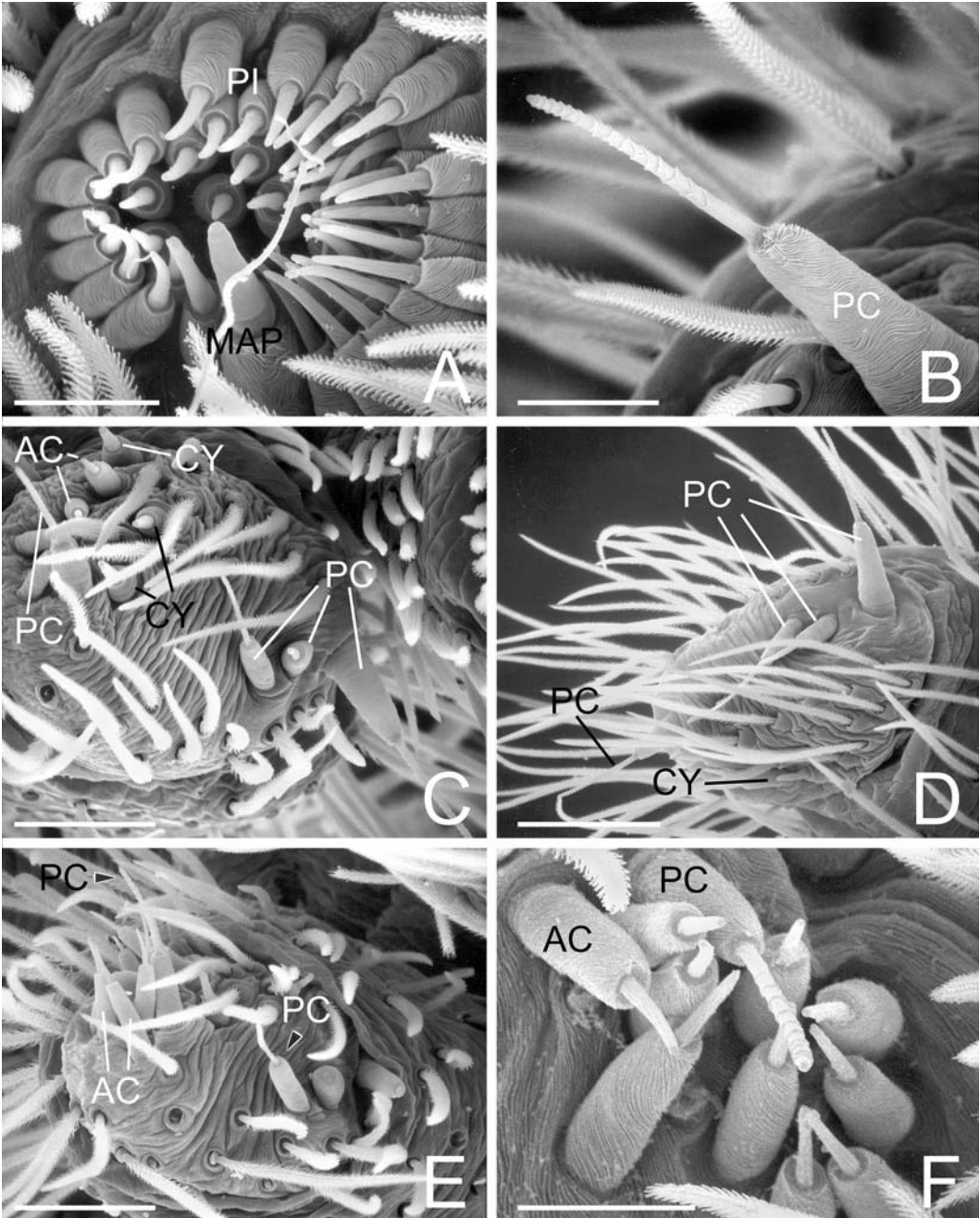


FIGURE 55. Spinnerets of female Titanoeidae. A, C. *Titanoeoca nigrella* from Cave Creek, Arizona, USA. A. Right ALS. C. Left PLS. B, D. *Titanoeoca americana* from Johnson Co., Missouri, USA. B. Right PLS apex, showing PC spigot. D. Right PLS. E, F. *Goeldia* spp. E. Zapallar, Chile, left PLS. F. Valparaiso, Chile, right PLS. AC = aciniform gland spigot(s), CY = cylindrical gland spigot(s), MAP = major ampullate gland spigot(s), PC = paracribellar spigot(s), PI = piriform gland spigot(s). Scale bars: A, B = 20µm, C = 43µm, D = 60µm, E = 43µm, F = 20µm.

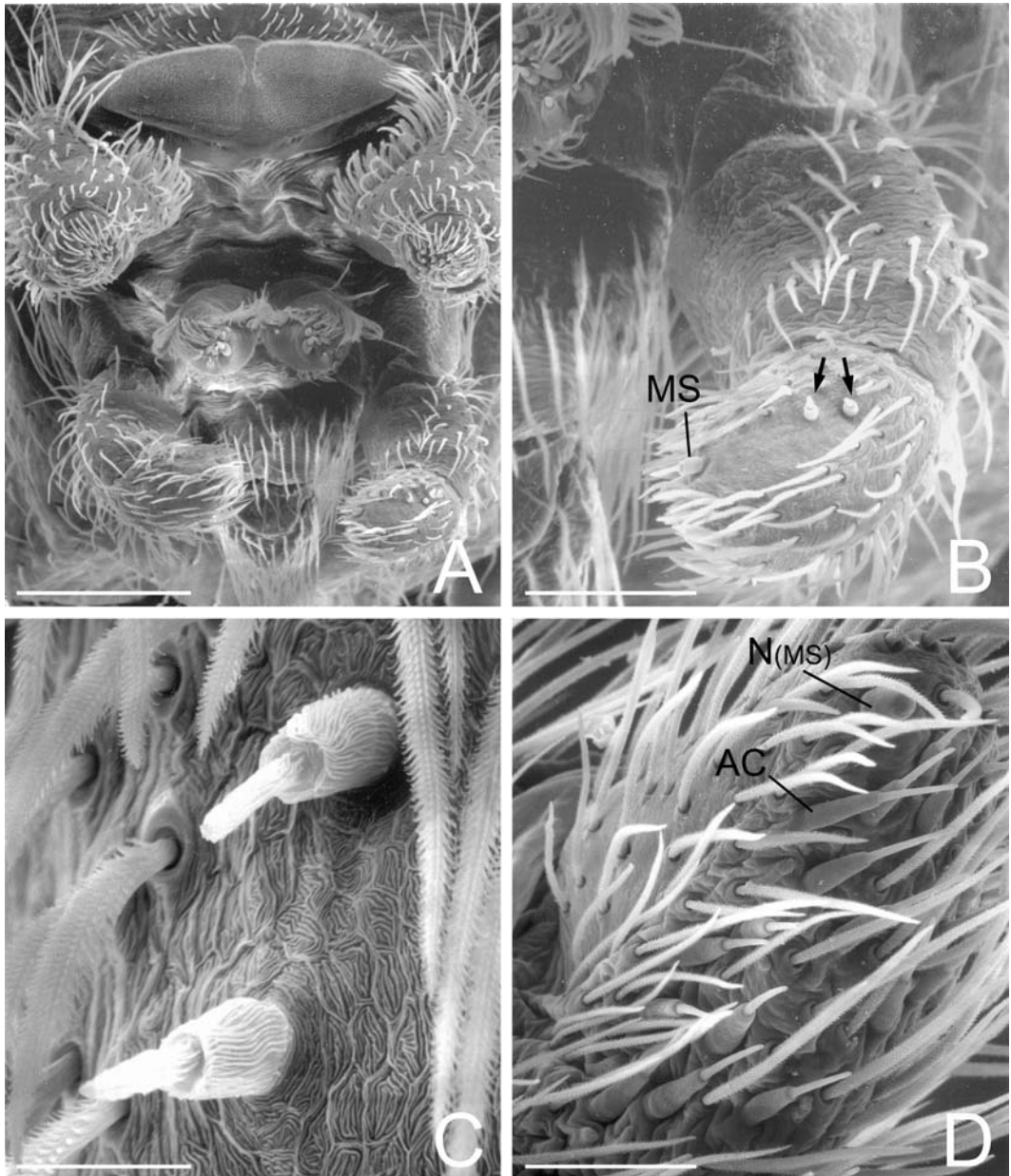


FIGURE 56. Spinneret details. A–C. *Aebutina binotata* female from Tarapuy, Ecuador. Black line to MS spigots and black arrows to flanking spigots of triad. A. Overview. B. Left PLS. C. Left PLS, base of apical segment showing presumed flanking spigots of MS triad. D. *Psechrus* sp. male from Tham Lot Cave, Thailand, left PLS. AC = aciniform gland spigot(s), MS = PLS modified spigot, N = nubbin of MS spigot. Scale bars: A = 250 μ m, B = 100 μ m, C = 15 μ m, D = 60 μ m.

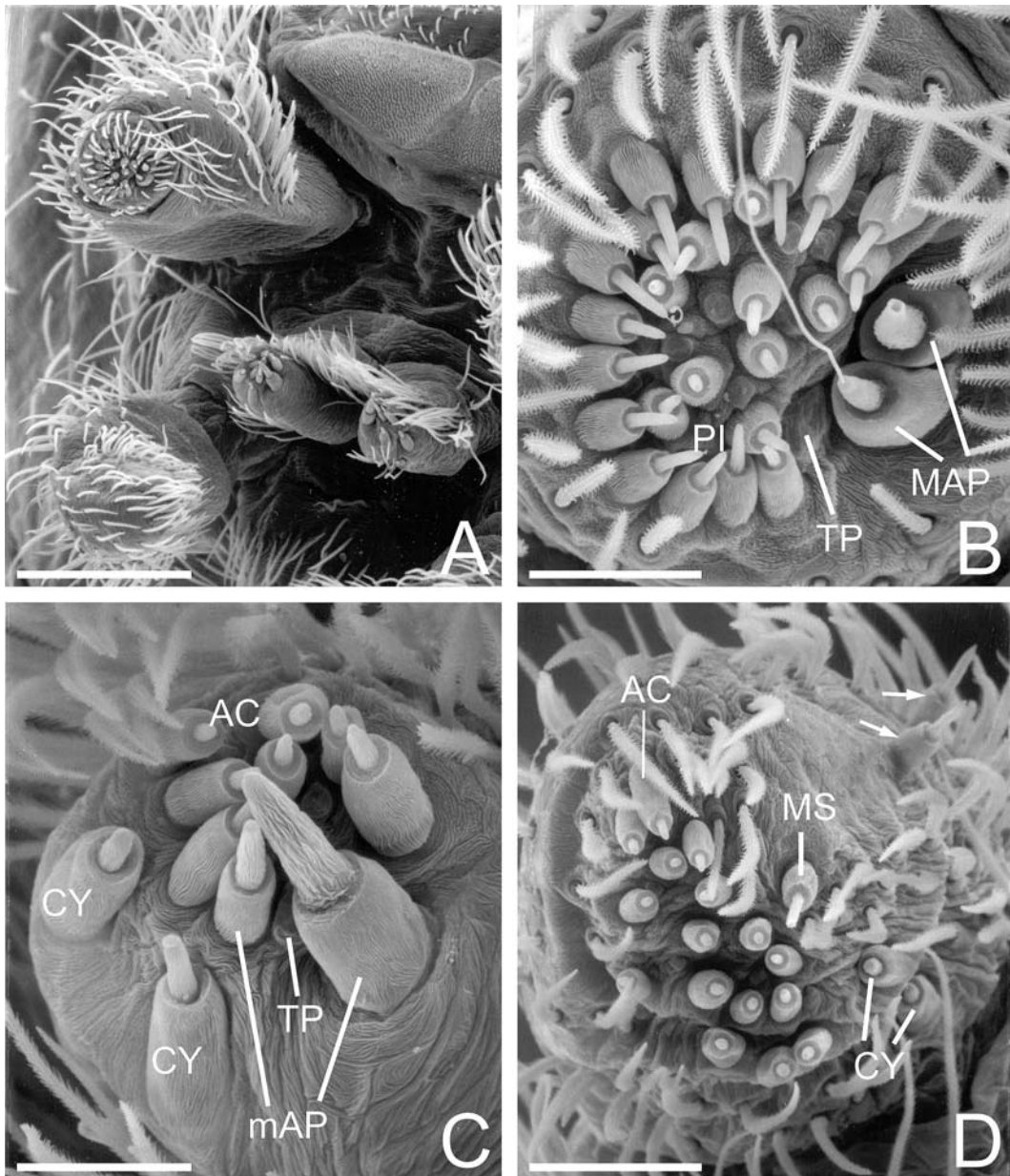


FIGURE 57. Spinnerets of female *Aebutina binotata* from Rio Cuyabeno, Ecuador. A. Overview. B. Right ALS. C. Right PMS. D. Left PLS: note basal MS and flanking spigots of triad (arrows). AC = aciniform gland spigot(s), CY = cylindrical gland spigot(s), MAP = major ampullate gland spigot(s), mAP = minor ampullate gland spigot(s), MS = PLS modified spigot(s), PI = piriform gland spigot(s), TP = tartipores. Scale bars: A = 200µm, B = 30µm, C = 25µm, D = 43µm.

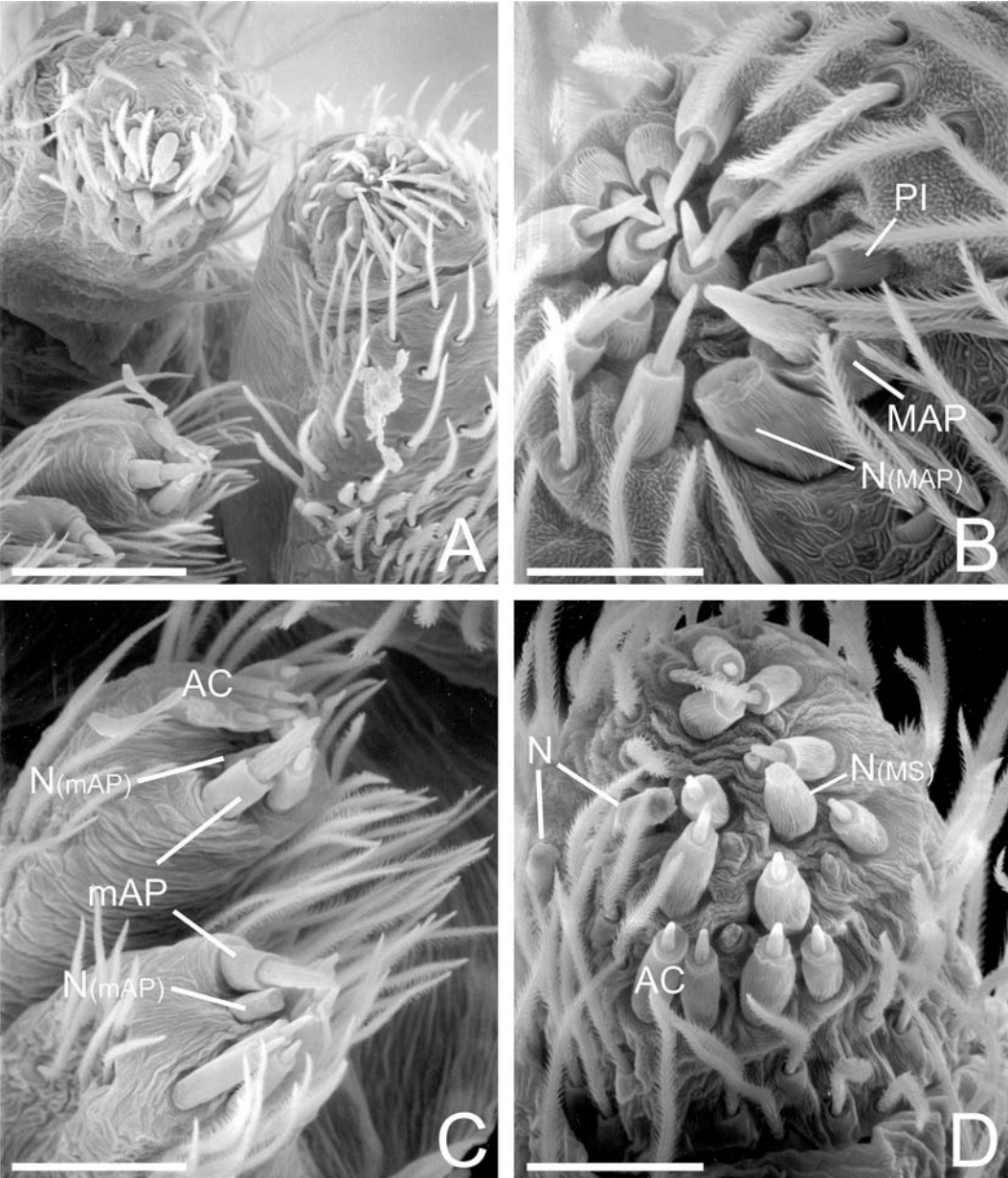


FIGURE 58. Spinnerets of male *Aebutina binotata* from Tarapuy, Ecuador. A. Right overview. B. Right ALS. C. PMS. D. Left PLS. Note anterior basal nubbins of MS and flanking spigots of triad. AC = aciniform gland spigot(s), MAP = major ampullate gland spigot and nubbin, mAP = minor ampullate gland spigot(s), mAP N = minor ampullate gland spigot nubbins, MS = nubbin of PLS modified spigot, N = nubbins of anterobasal PLS spigots. Scale bars: A = 75µm, B = 20µm, C = 43µm, D = 30µm.

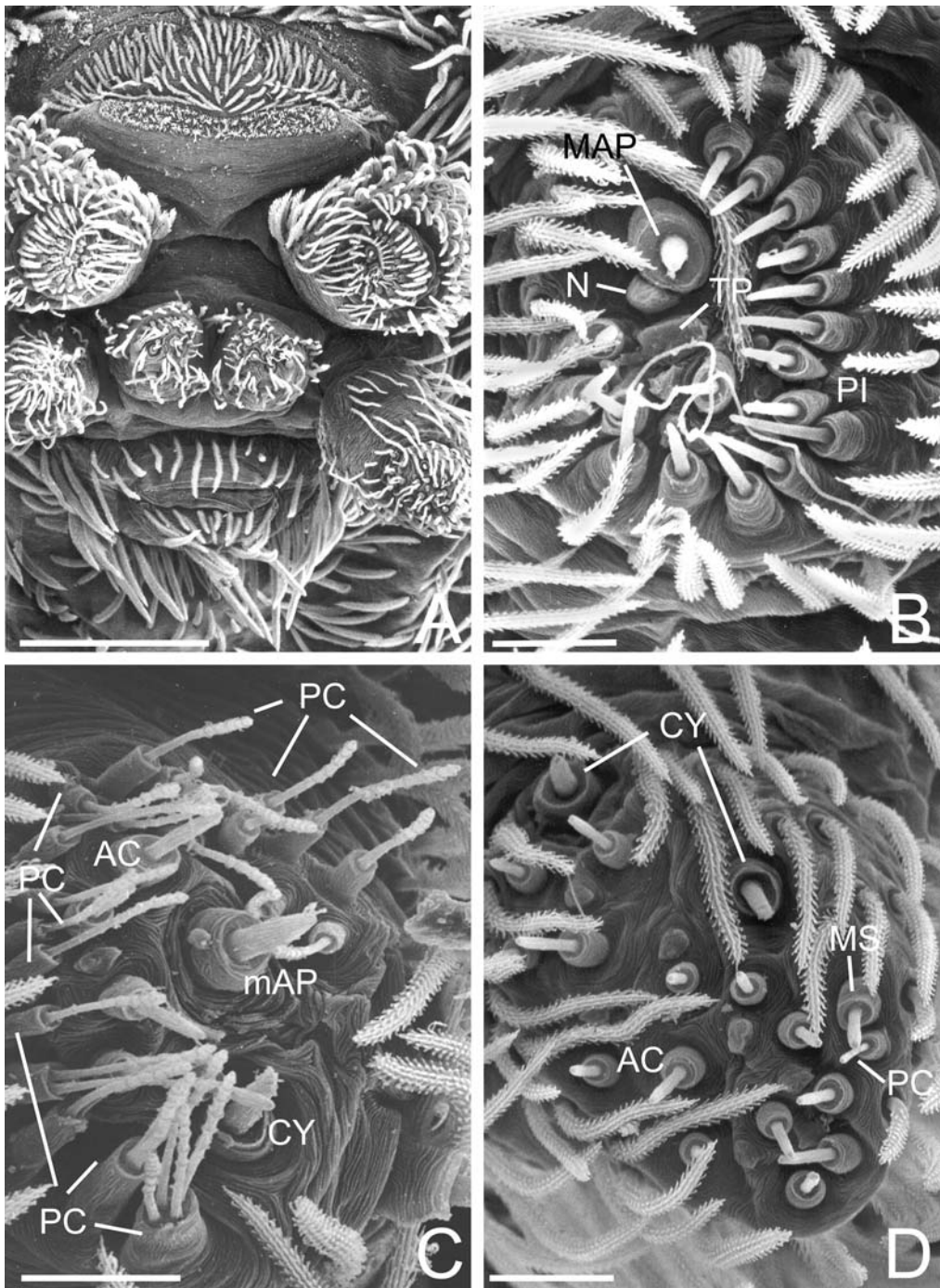


FIGURE 59. Spinnerets of female *Dictyna arundinacea* from Lingby, Denmark. A. Overview. B. Left ALS. C. Left PMS, anterior to left. Note PC spigots encircling top and left side of image, and multiple PC spigots emerging from single large base at bottom. D. Left PLS. AC = aciniform gland spigot(s), CY = cylindrical gland spigot(s), MAP = major ampullate gland spigot(s), mAP = minor ampullate gland spigot(s), MS = PLS modified spigot, N = nubbin(s), PC = paracribellar spigot(s), PI = piriform gland spigot(s), TP = tartipore. Scale bars: A = 200 μ m, B–D = 20 μ m.

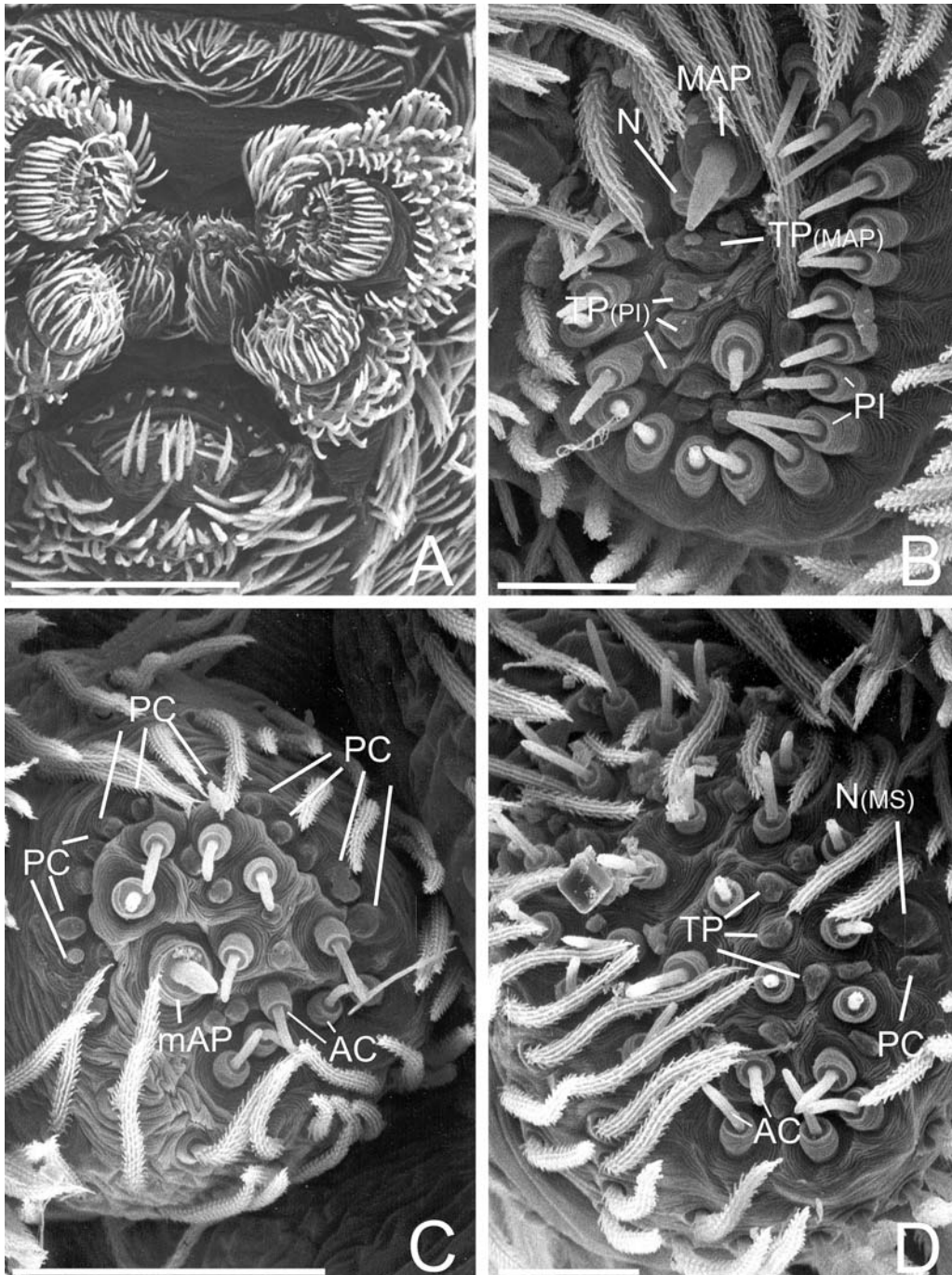


FIGURE 60. Spinnerets of male *Dictyna arundinacea* from Lingby, Denmark. A. Overview. B. Left ALS. C. Left PMS, showing PC nubbins encircling spinneret anterolaterally. D. Left PLS, showing tartipores amid AC spigot field. AC = acini-form gland spigot(s), MAP = major ampullate gland spigot(s), mAP = minor ampullate gland spigot(s), N = nubbin(s), N(MS) = nubbin of PLS modified spigot, PC = paracribellar spigot nubbins, PI = piriform gland spigot(s), TP = tartipore(s), TP (MAP) = tartipore of MAP from previous instar. Scale bars: A = 200µm, B, D = 20µm, C = 50µm.

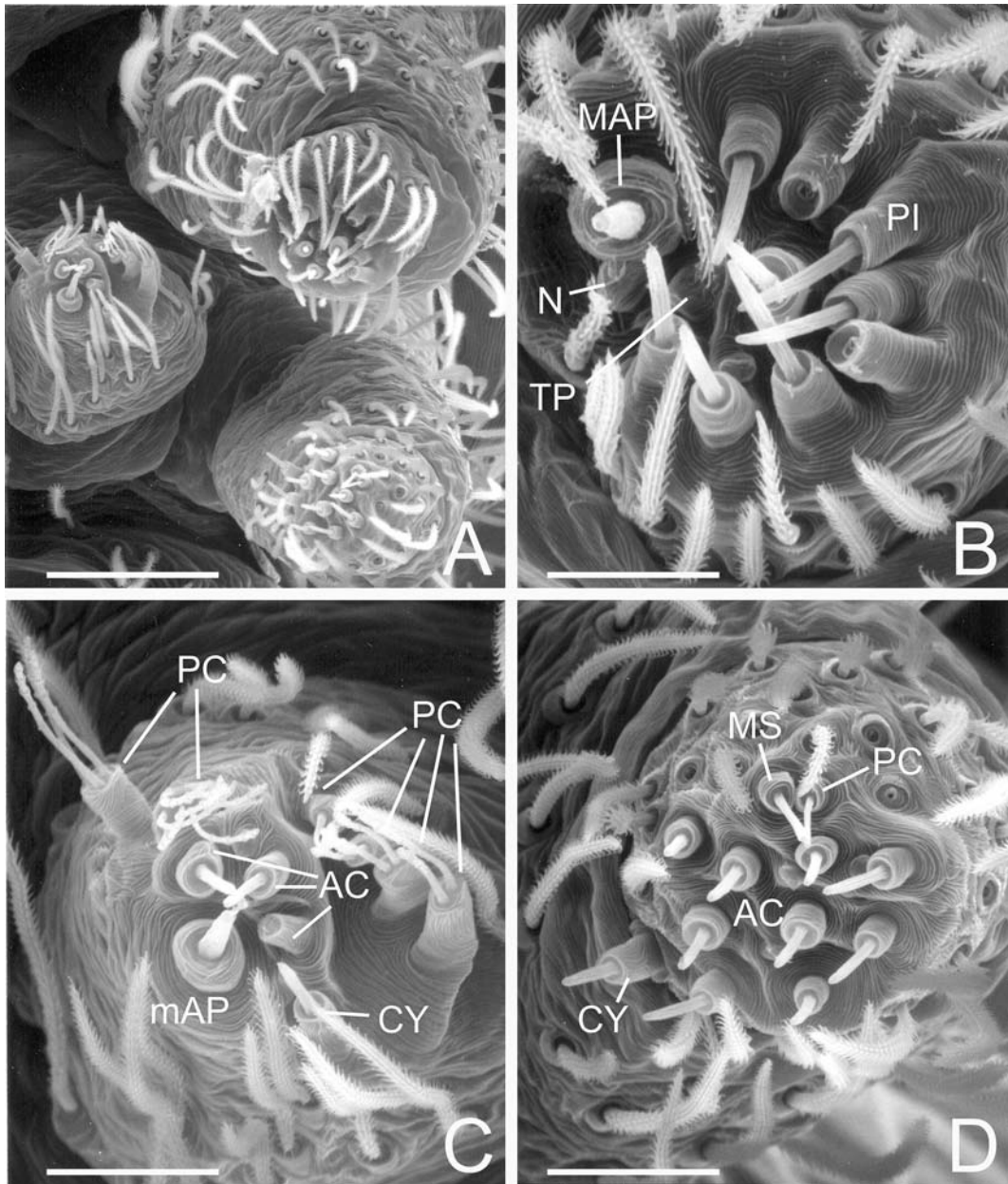


FIGURE 61. Left spinnerets of female *Nigma linsdalei* from San Francisco, California, USA. A. Overview. B. ALS. C. PMS. Note PC spigots encircling spinneret, several that have multiple shafts emerging from a common base. D. PLS. AC = aciniform gland spigot(s), CY = cylindrical gland spigot(s), MAP = major ampullate gland spigot(s), mAP = minor ampullate gland spigot(s), MS = PLS modified spigot, N = nubbin of MAP, PC = paracribellar spigot(s), PI = piriform gland spigot(s), TP = tartipore(s). Scale bars: A = 59 μ m, B = 15 μ m, C, D = 20 μ m.

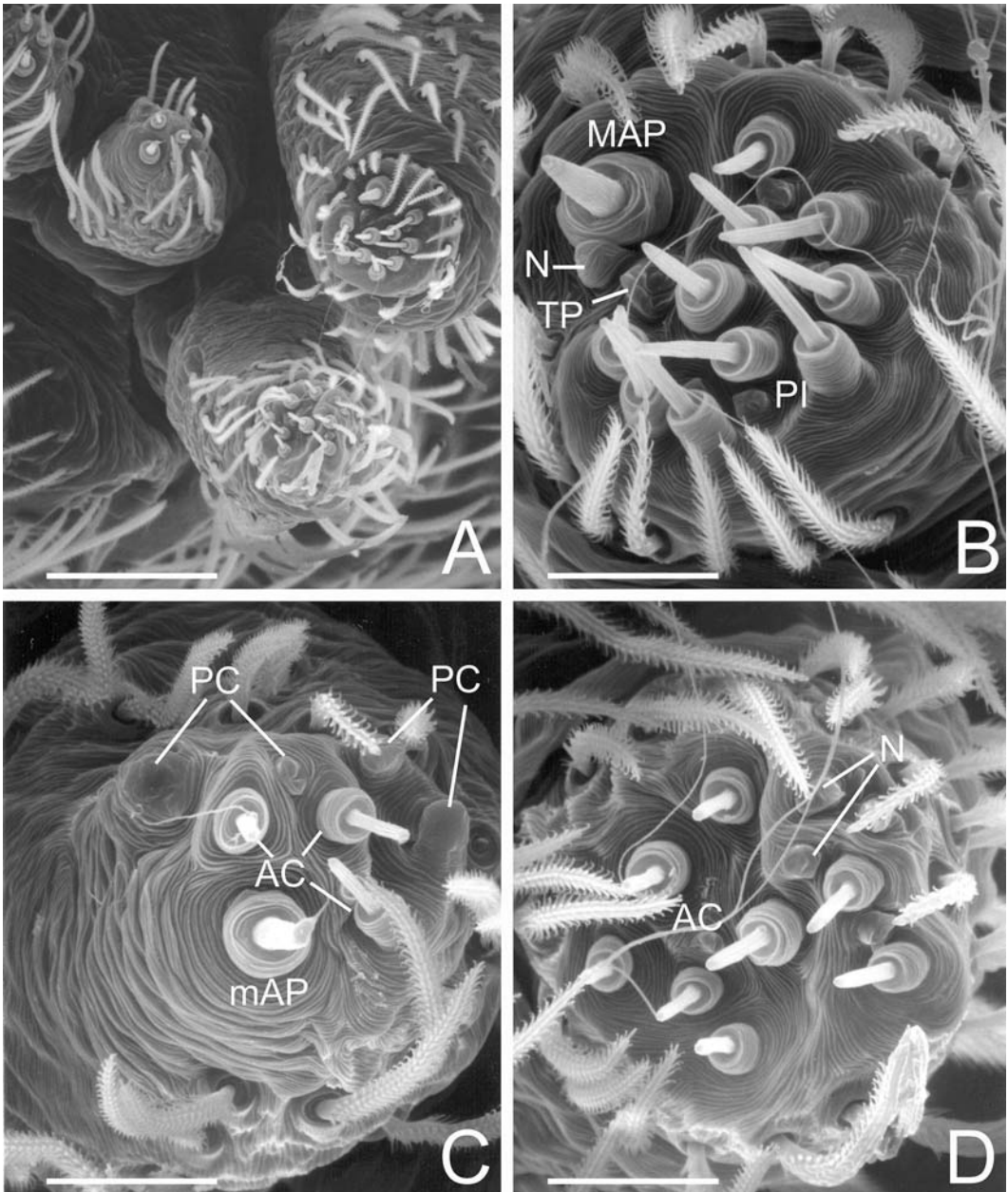


FIGURE 62. Left spinnerets of male *Nigma linsdalei* from San Francisco, California, USA. A. Overview. B. ALS. C. PMS. D. PLS. AC = aciniform gland spigot(s), MAP = major ampullate gland spigot(s), mAP = minor ampullate gland spigot(s), N = nubbins of ALS MAP and PLS PC and MS, PC = nubbins of PMS paracribellar spigots, PI = piriform gland spigot(s), TP = tartipore. Scale bars: A = 60µm, B–D = 15µm.

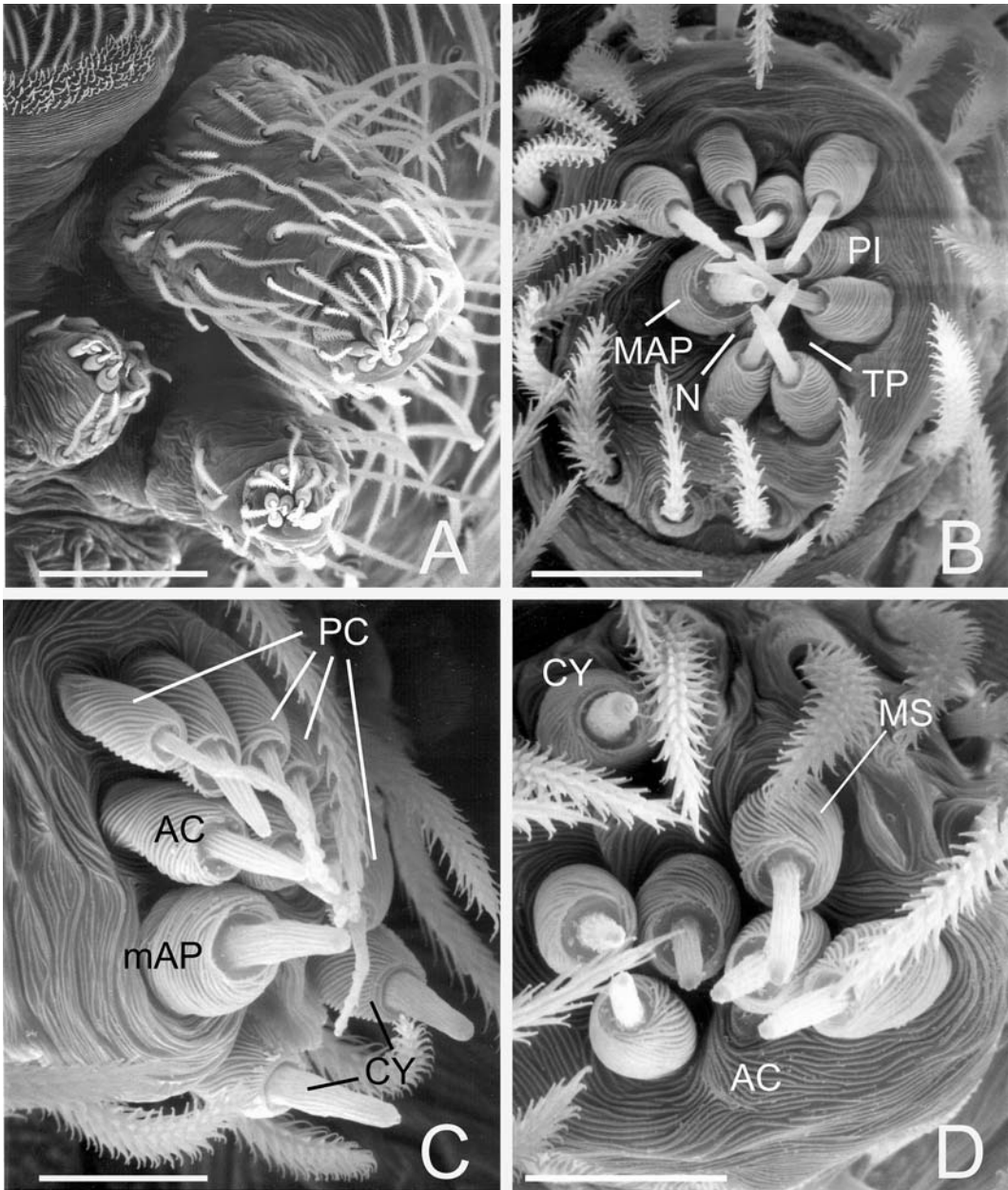


FIGURE 63. Left spinnerets of female *Lathys humilis* from Kent, United Kingdom. A. Overview. B. ALS. C. PMS. D. PLS. AC = aciniform gland spigot(s), CY = cylindrical gland spigot(s), MAP = major ampullate gland spigot(s), mAP = minor ampullate gland spigot(s), MS = PLS modified spigot, N = nubbin, PC = paracribellar spigot(s), PI = piriform gland spigot(s), TP = tartipore. Scale bars: A = 60µm, B = 15µm, C, D = 10µm.

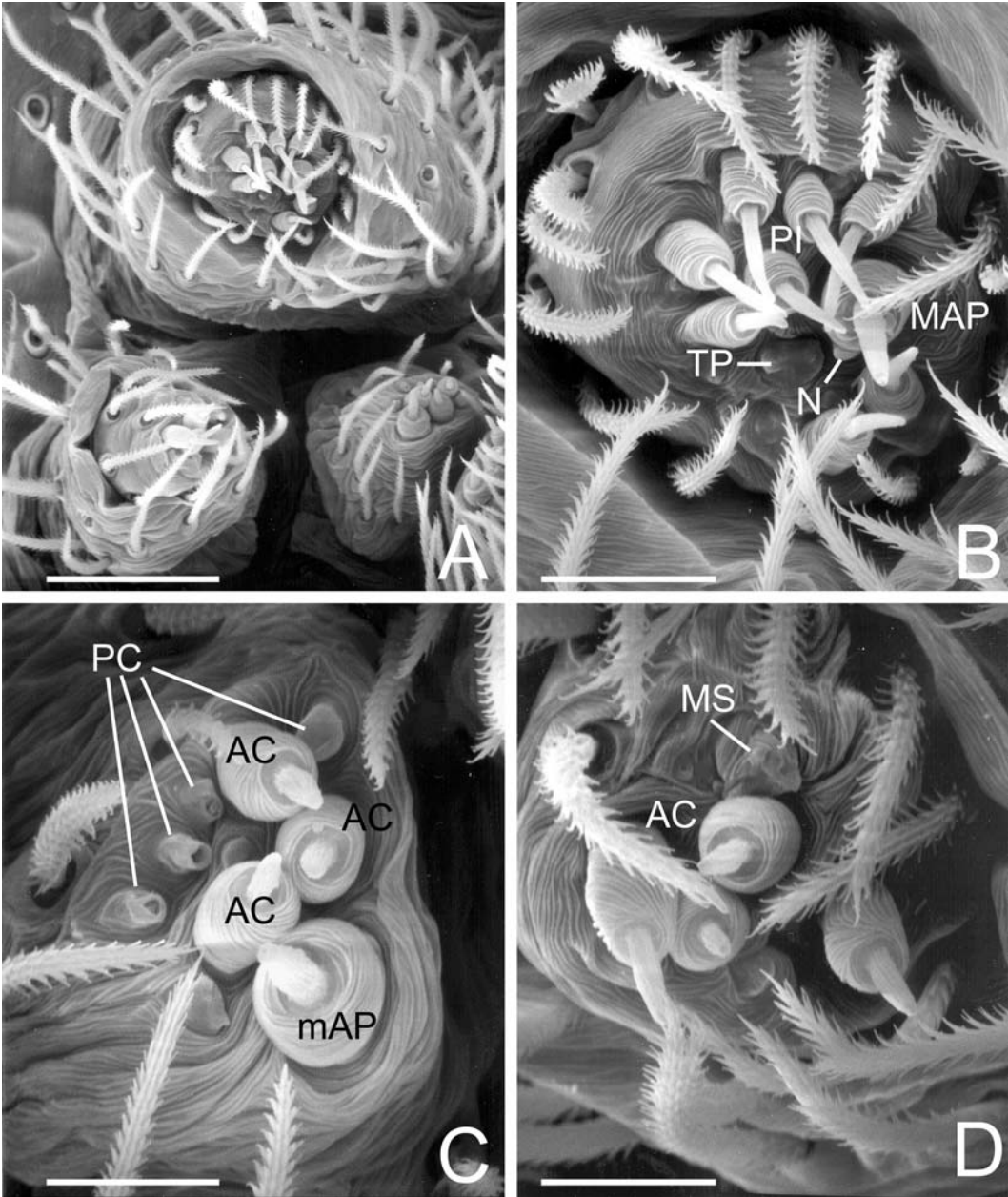


FIGURE 64. Right spinnerets of male *Lathys humilis* from Kent, United Kingdom. A. Overview. B. ALS. C. PMS. D. PLS. AC = aciniform gland spigot(s), MAP = major ampullate gland spigot(s), mAP = minor ampullate gland spigot(s), MS = PLS modified spigot nubbin, N = nubbin of posterior MAP, PC = paracribellar spigot nubbins, PI = piriform gland spigot(s), TP = tartipore. Scale bars: A = 43µm, B = 15µm, C, D = 10µm.

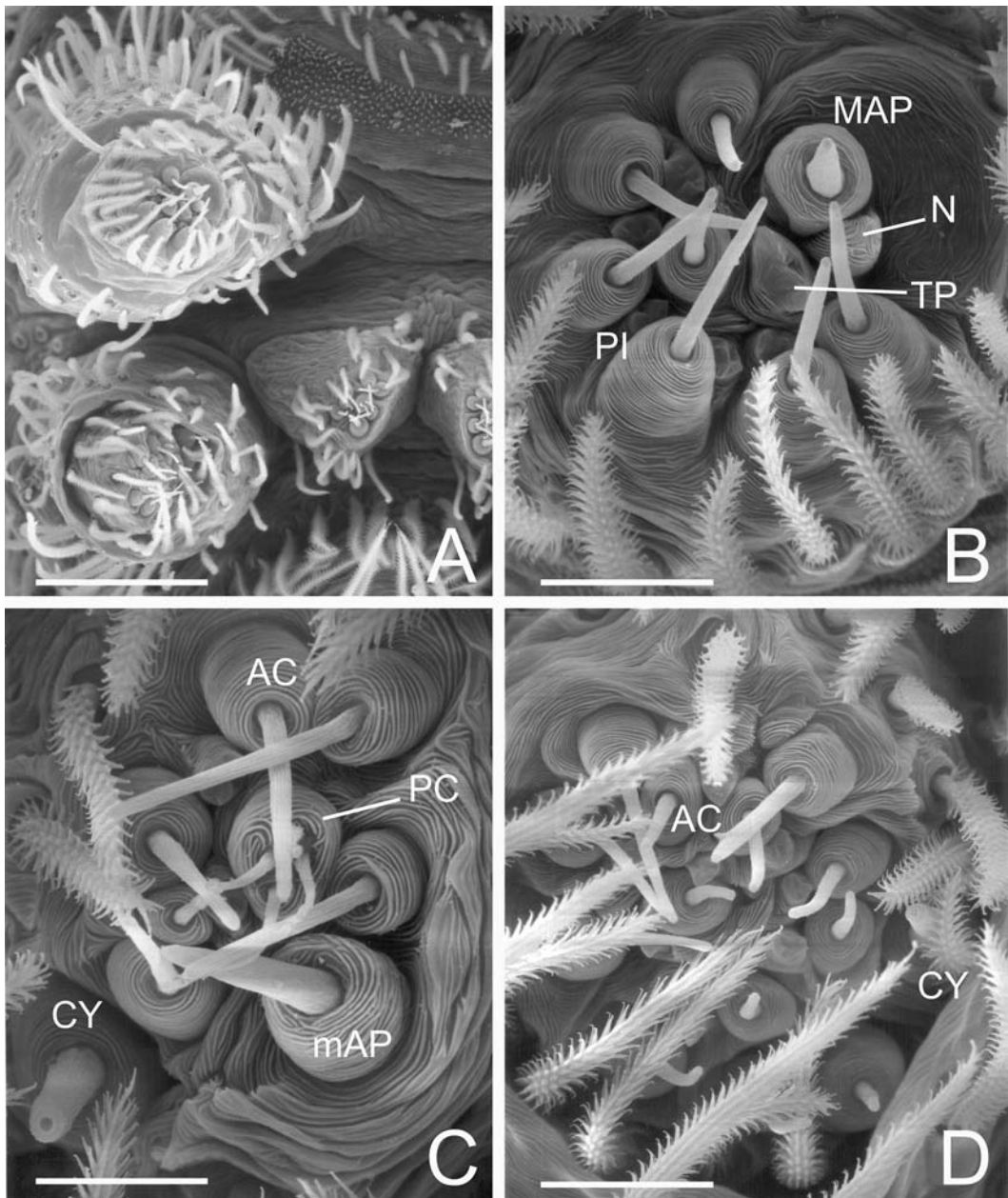


FIGURE 65. Right spinnerets of female *Tricholathys* sp. from San Francisco, California, USA. A. Overview. B. ALS. C. PMS apex. D. PLS. AC = aciniform gland spigot(s), CY = cylindrical gland spigot(s), MAP = major ampullate gland spigot(s), mAP = minor ampullate gland spigot(s), N = nubbin(s), PC = paracribellar spigot(s), PI = piriform gland spigot(s), TP = tartipore(s). Scale bars: A = 75µm, B, D = 15µm, C = 10µm.

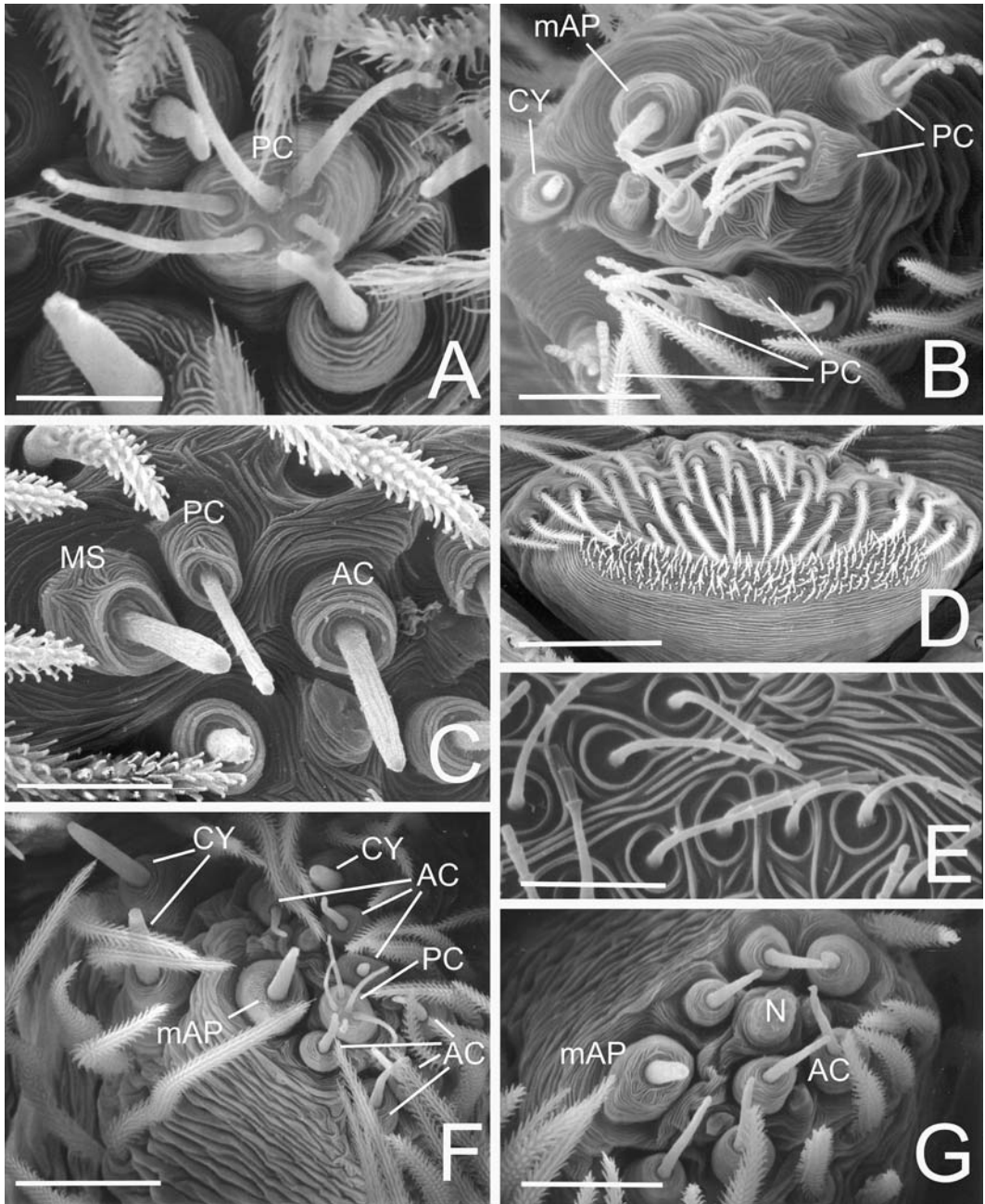


FIGURE 66. Spinning organs of Dictynidae. A, F, G. *Tricholathys spiralis* from Lenore Lake, Washington, USA. A. Left female PMS PC with multiple shafts emerging from wide base. F. Right female PMS. G. Left male PMS. B. *Nigma linsdalei* female from San Francisco, California, USA, left PMS showing PC with multiple shafts per base encircling spinneret. C. *Dictyna arundinacea* female from Lingby, Denmark, PLS apex. D. *Lathys humilis* female from Kent, United Kingdom, cribellum. E. *Nigma linsdalei*, female from San Francisco, California, USA, cribellar spigots. AC = aciniform gland spigot(s), CY = cylindrical gland spigot(s), mAP = minor ampullate gland spigot(s), MS = PLS modified spigot, N = nubbin of paracribellar spigot(s), PC = paracribellar spigot(s). Scale bars: A = 7.5 μ m, B = 15 μ m, C = 10 μ m, D = 43 μ m, E = 6 μ m, F = 25 μ m, G = 20 μ m.

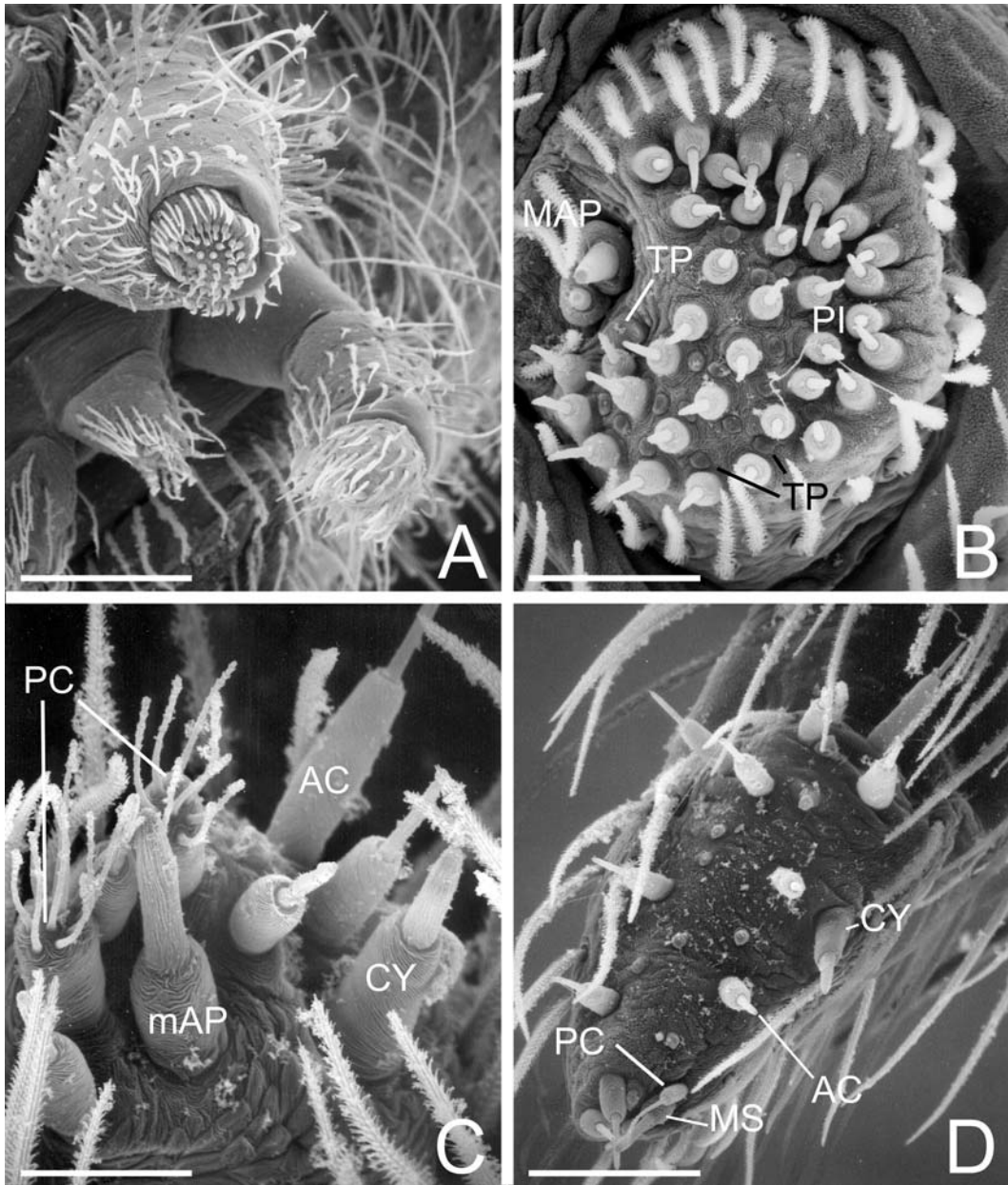


FIGURE 67. Left spinnerets of female *Neolana dalmasi* from Waipoua Forest, New Zealand. A. Overview. B. ALS. C. PMS. D. PLS. AC = aciniform gland spigot(s), CY = cylindrical gland spigot(s), MAP = major ampullate gland spigot(s), mAP = minor ampullate gland spigot(s), MS = PLS modified spigot, PC = paracribellar spigot(s), PI = piriform gland spigot(s), TP = tartipore(s). Scale bars: A = 200µm, B = 43µm, C = 25µm, D = 60µm.

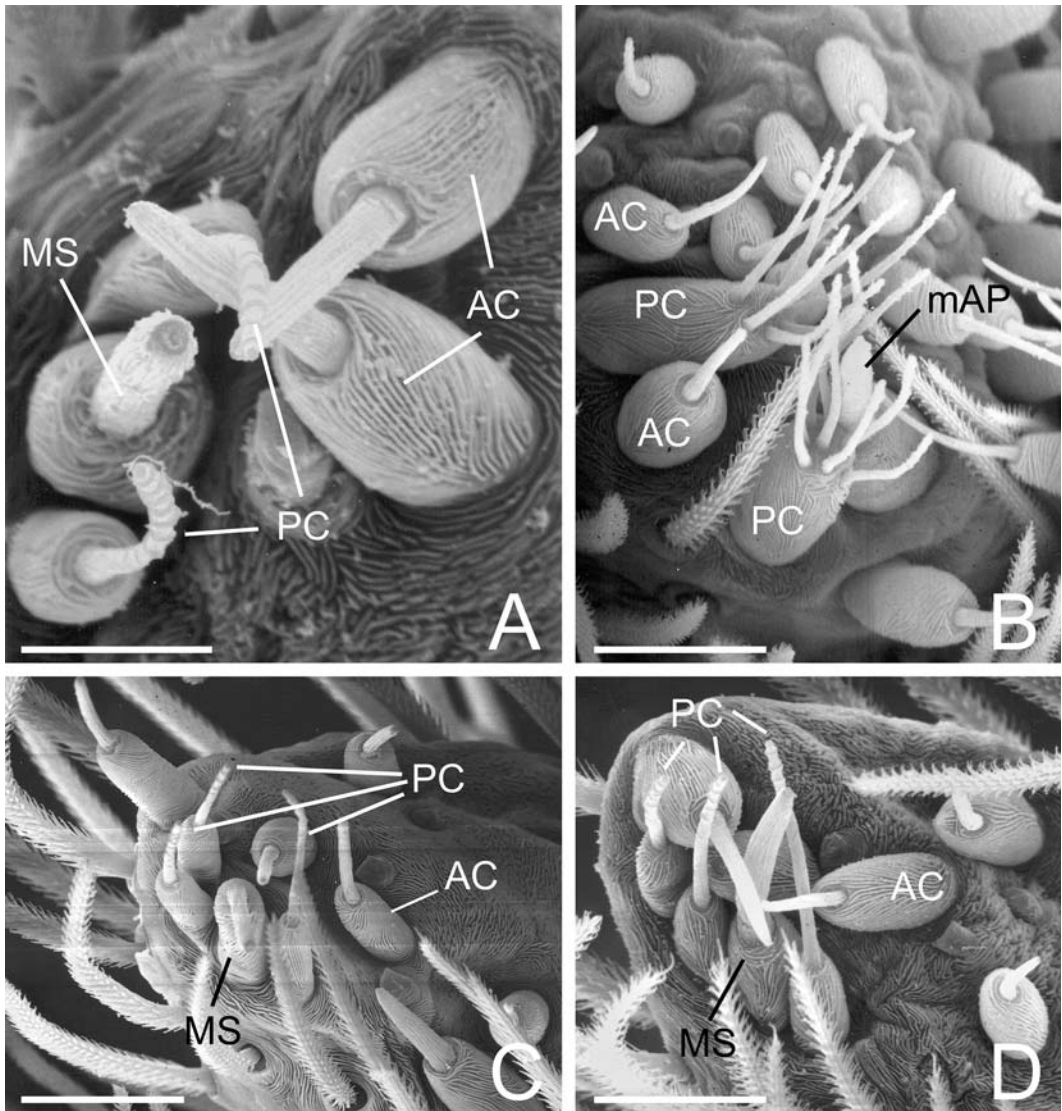


FIGURE 68. Spinneret details of female Neolanidae and Stiphidiidae. A. *Neolana dalmasi* from Waipoua Forest, New Zealand, PLS apex. B, D. *Stiphidion facetum* from Bundeena, New South Wales, Australia. B. PMS. D. PLS apex. C. *Pillara griswoldi* from Barrington Tops, New South Wales, Australia, PLS apex. AC = aciniform gland spigot(s), mAP = minor ampullate gland spigot(s), MS = PLS modified spigot, PC = paracribellar spigot(s). Scale bars: A = 100 μ m, B–D = 20 μ m.

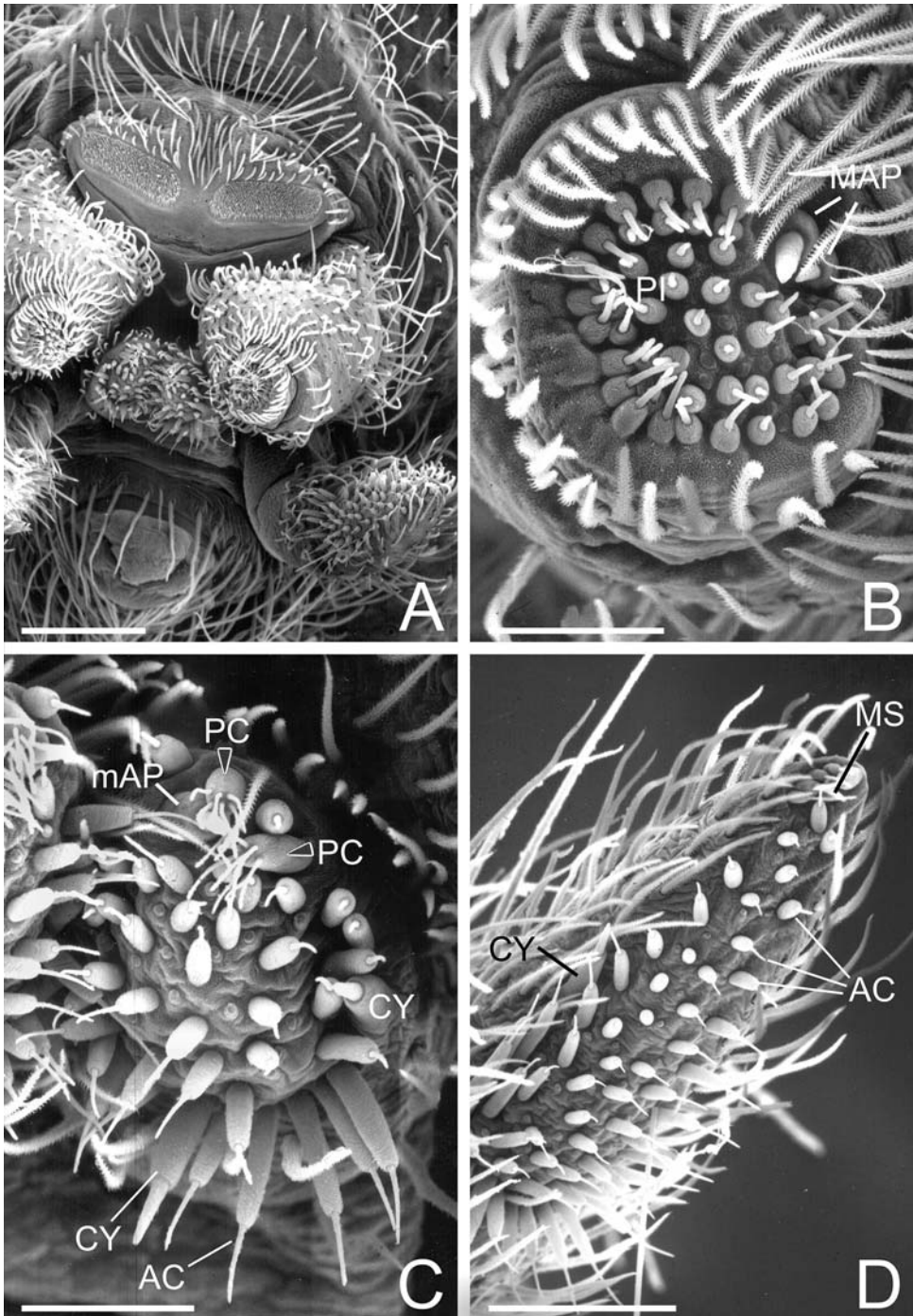


FIGURE 69. Spinnerets of female *Stiphidion facetum* from Bundeena, New South Wales, Australia. A. Overview. B. Left ALS. C. Left PMS. D. Left PLS. CY = cylindrical gland spigot(s), MAP = major ampullate gland spigot(s), mAP = minor ampullate gland spigot(s), MS = PLS modified spigot(s), PC = paracribellar spigot(s), PI = piriform gland spigot(s). Scale bars: A = 200µm, B, C = 50µm, D = 100µm.

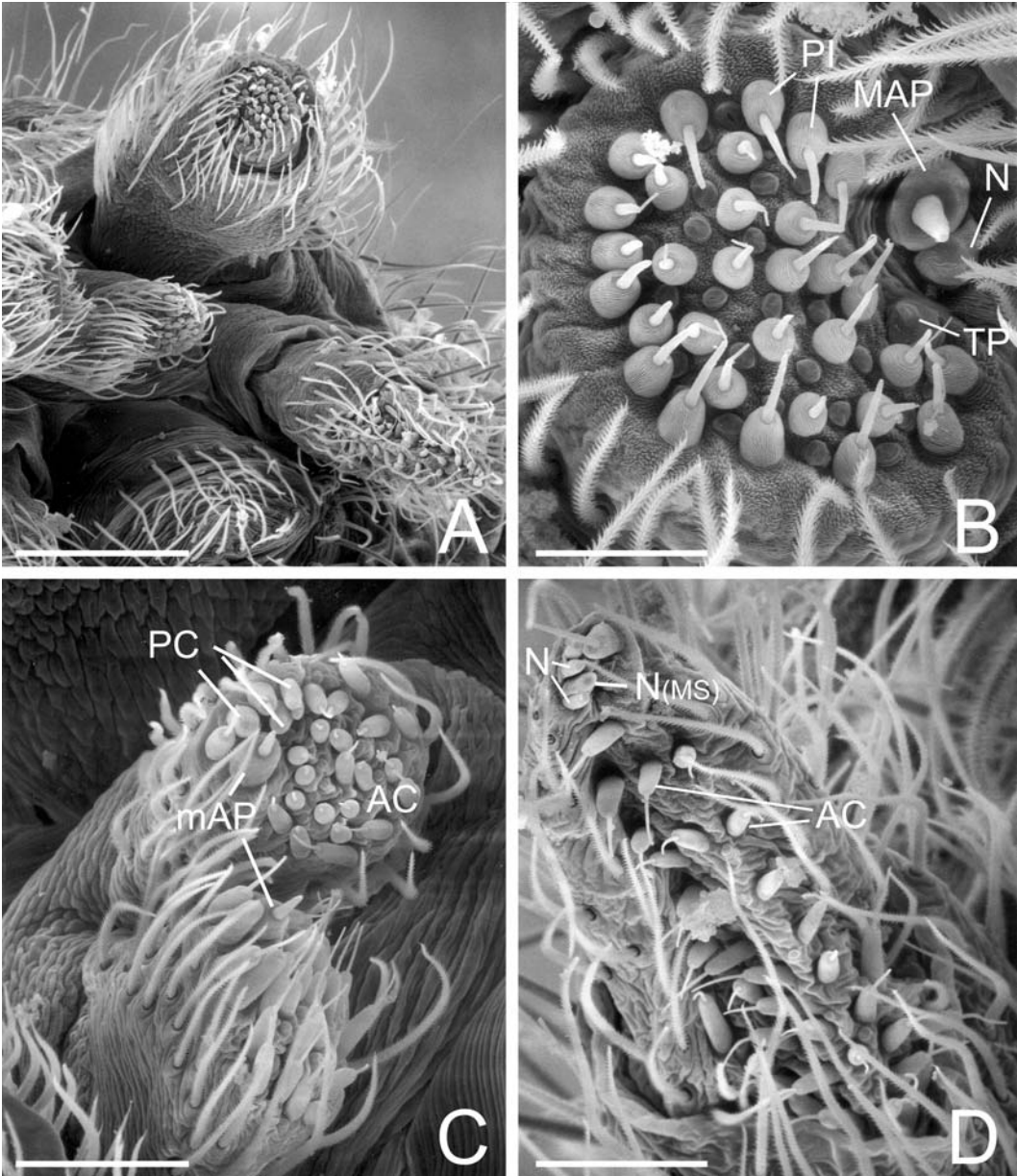


FIGURE 70. Spinnerets of male *Stiphidion facetum* from Whalipu, New Zealand. A. Overview. B. Right ALS. C. PMS. D. Right PLS. AC = aciniiform gland spigot(s), mAP = minor ampullate gland spigot(s), N = nubbins of PC and MS on PLS apex, PC = paracribellar spigot nubbins on PMS, TP = tartipore(s). Scale bars: A = 200µm, B = 30µm, C, D = 60µm.

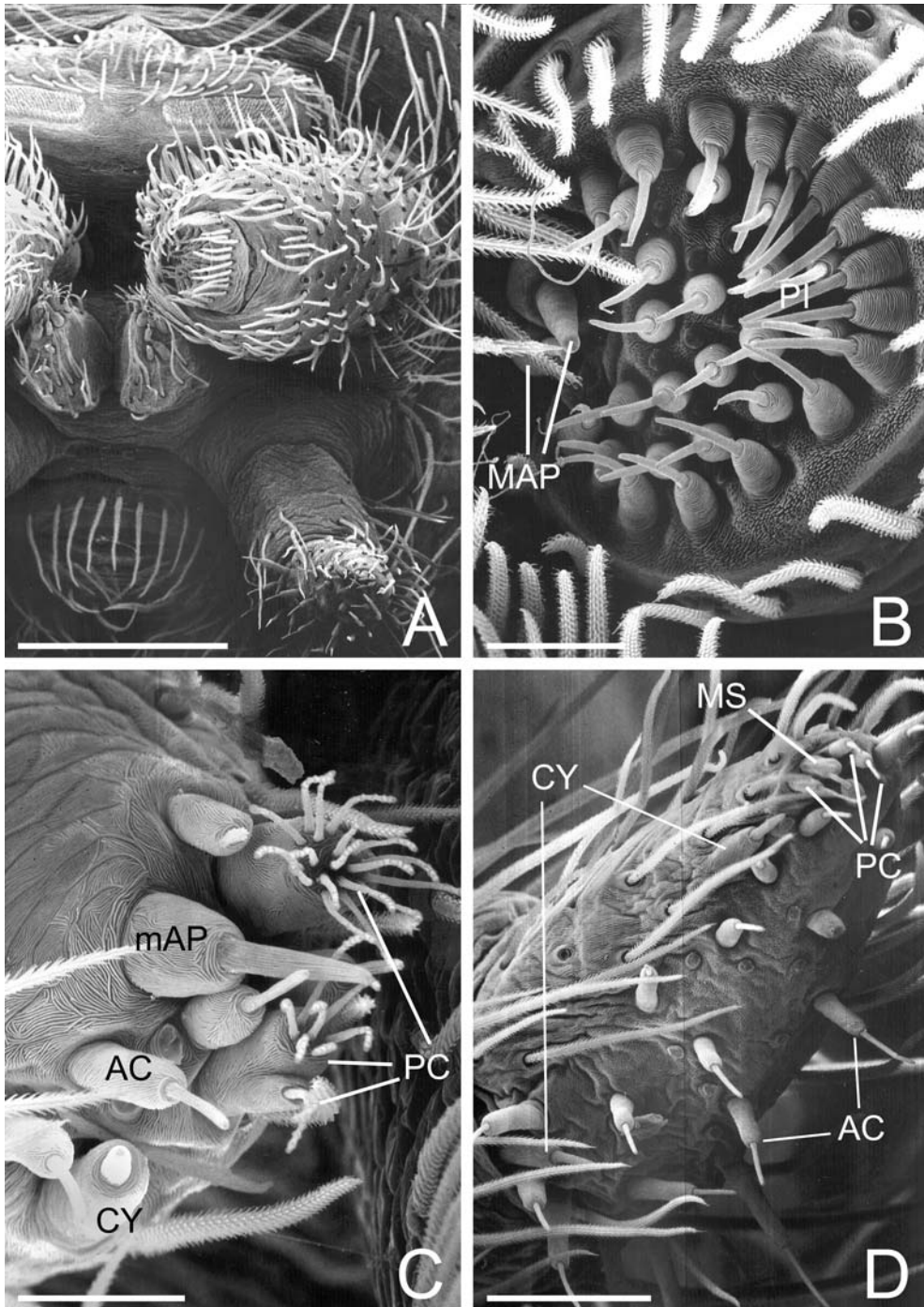


FIGURE 71. Spinnerets of female *Pillara griswoldi* from Barrington Tops, New South Wales, Australia. A. Overview. B. Left ALS. C. Left PMS. D. Left PLS. AC = aciniform gland spigot(s), CY = cylindrical gland spigot(s), MAP = major ampullate gland spigot(s), mAP = minor ampullate gland spigot(s), MS = PLS modified spigot, PC = paracribellar spigot(s), PI = piriform gland spigot(s). Scale bars: A = 200µm, B, C = 20µm, D = 50µm.

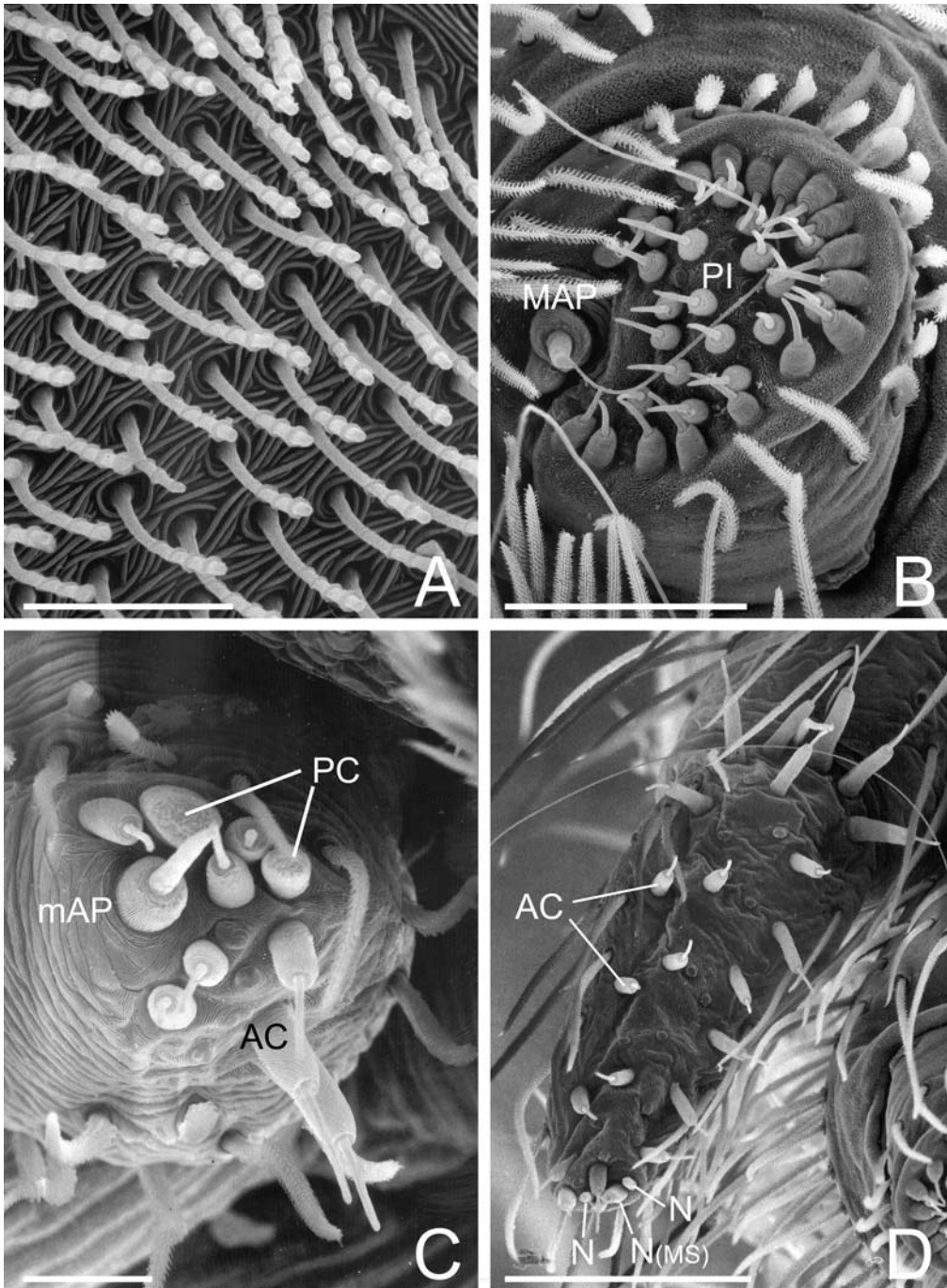


FIGURE 72. Spinnerets of *Pillara griswoldi* from Barrington Tops, New South Wales, Australia. A. Strobilate cribellar spigots of female. B. Male right ALS. C. Male right PMS. D. Male right PLS. AC = aciniform gland spigot(s), MAP = major ampullate gland spigot(s), mAP = minor ampullate gland spigot(s), N = nubbins of PC and MS on PLS apex, PC = paracribellar spigot nubbins on PMS, PI = piriform gland spigot(s). Scale bars: A = 10 μ m, B = 50 μ m, C = 20 μ m, D = 100 μ m.

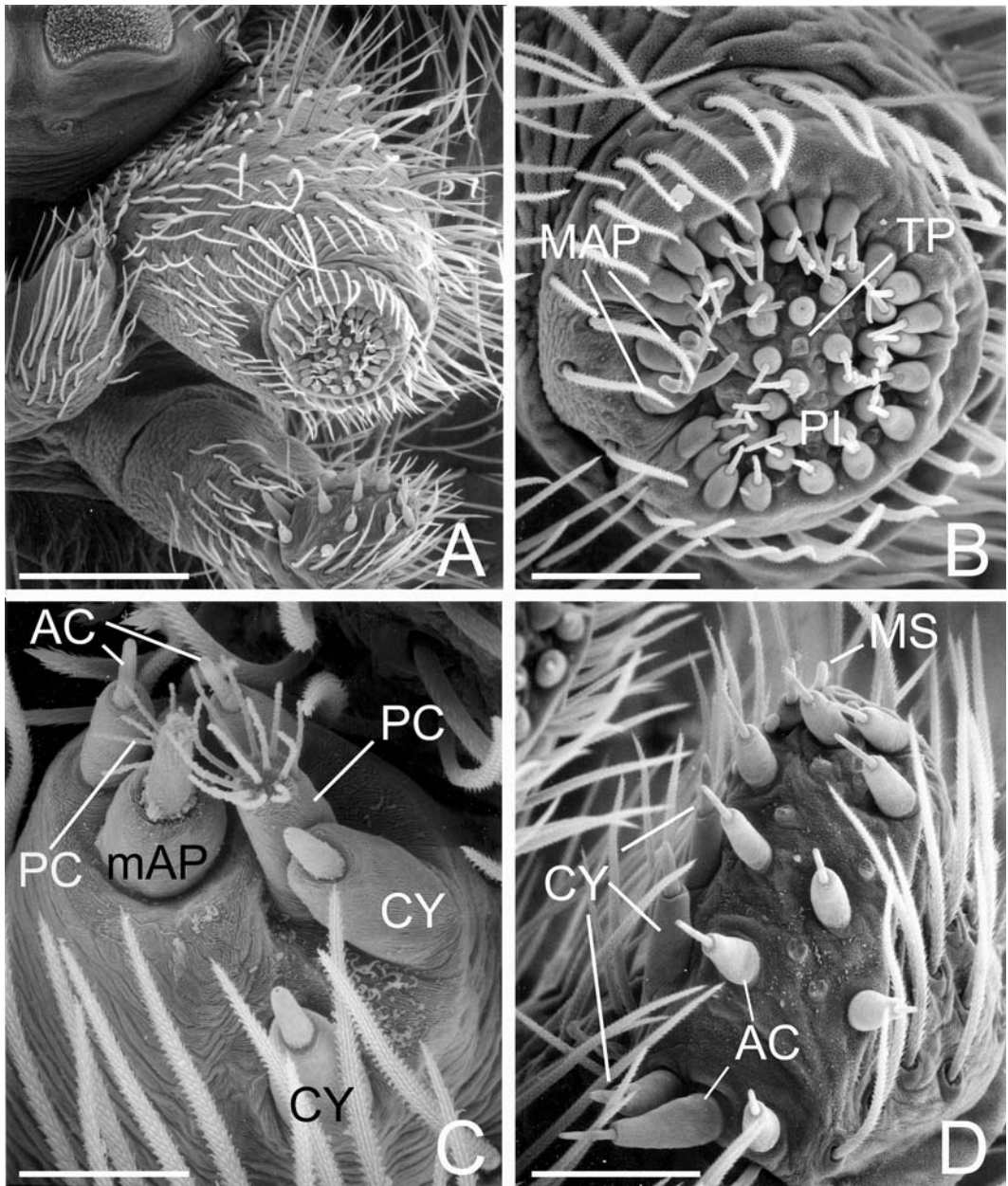


FIGURE 73. Left spinnerets of female *Neoramia sana* from Dunedin, New Zealand. A. Overview. B. ALS. C. PMS. D. PLS. AC = aciniform gland spigot(s), CY = cylindrical gland spigot(s), MAP = major ampullate gland spigot(s), mAP = minor ampullate gland spigot(s), MS = PLS modified spigot, PC = paracribellar spigot(s), PI = piriform gland spigot(s), TP = tartipore(s). Scale bars: A = 200µm, B, D = 60µm, C = 30µm.

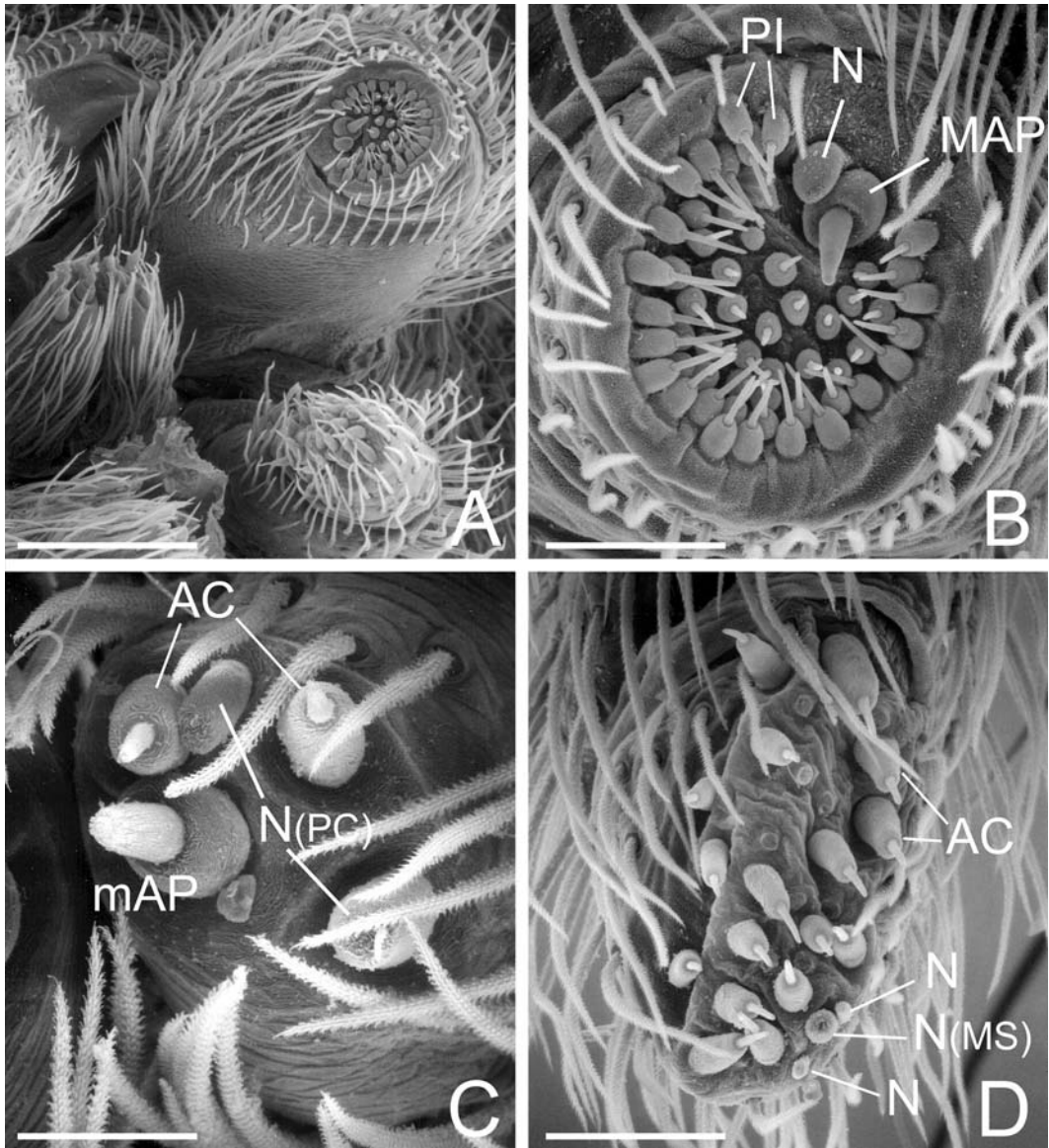


FIGURE 74. Left spinnerets of male *Neoramia sana* from Dunedin, New Zealand. A. Overview. B. ALS. C. PMS. D. PLS. MAP = major ampullate gland spigot(s), mAP = minor ampullate gland spigot(s), N = nubbins, PC = PMS paracribellar spigot nubbins. Scale bars: A = 200µm, B, D = 60µm, C = 30µm.

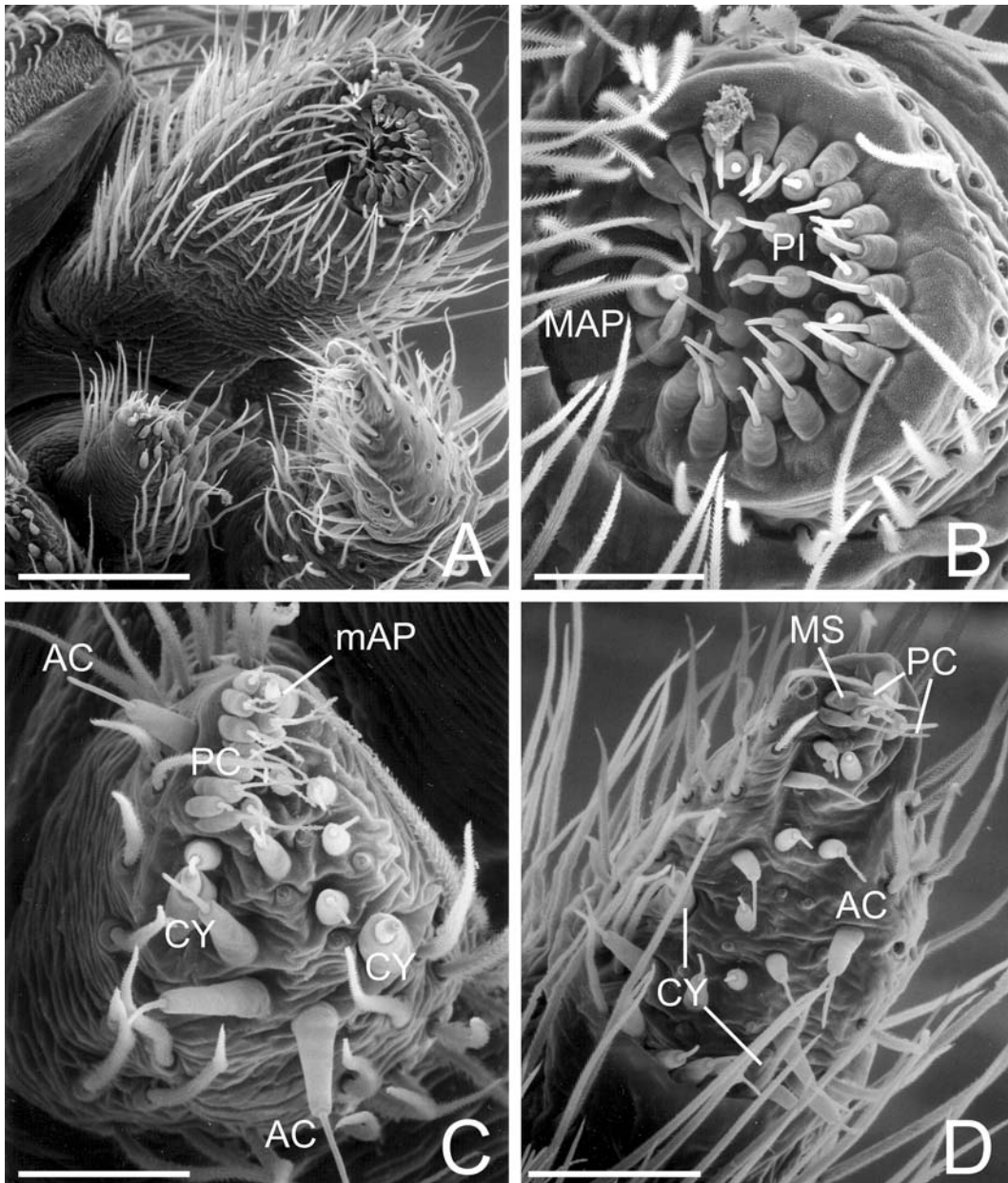


FIGURE 75. Spinnerets of female *Maniho ngaitahu* from Kaituna Valley, New Zealand. A. Left overview. B. Left ALS. C. Right PMS, showing median row of PC spigots. D. Left PLS. AC = aciniform gland spigot(s), CY = cylindrical gland spigot(s), MAP = major ampullate gland spigot(s), mAP = minor ampullate gland spigot(s), MS = PLS modified spigot, PC = paracribellar spigot(s), PI = piriform gland spigot(s). Scale bars: A = 150 μ m, B, C = 43 μ m, D = 60 μ m.

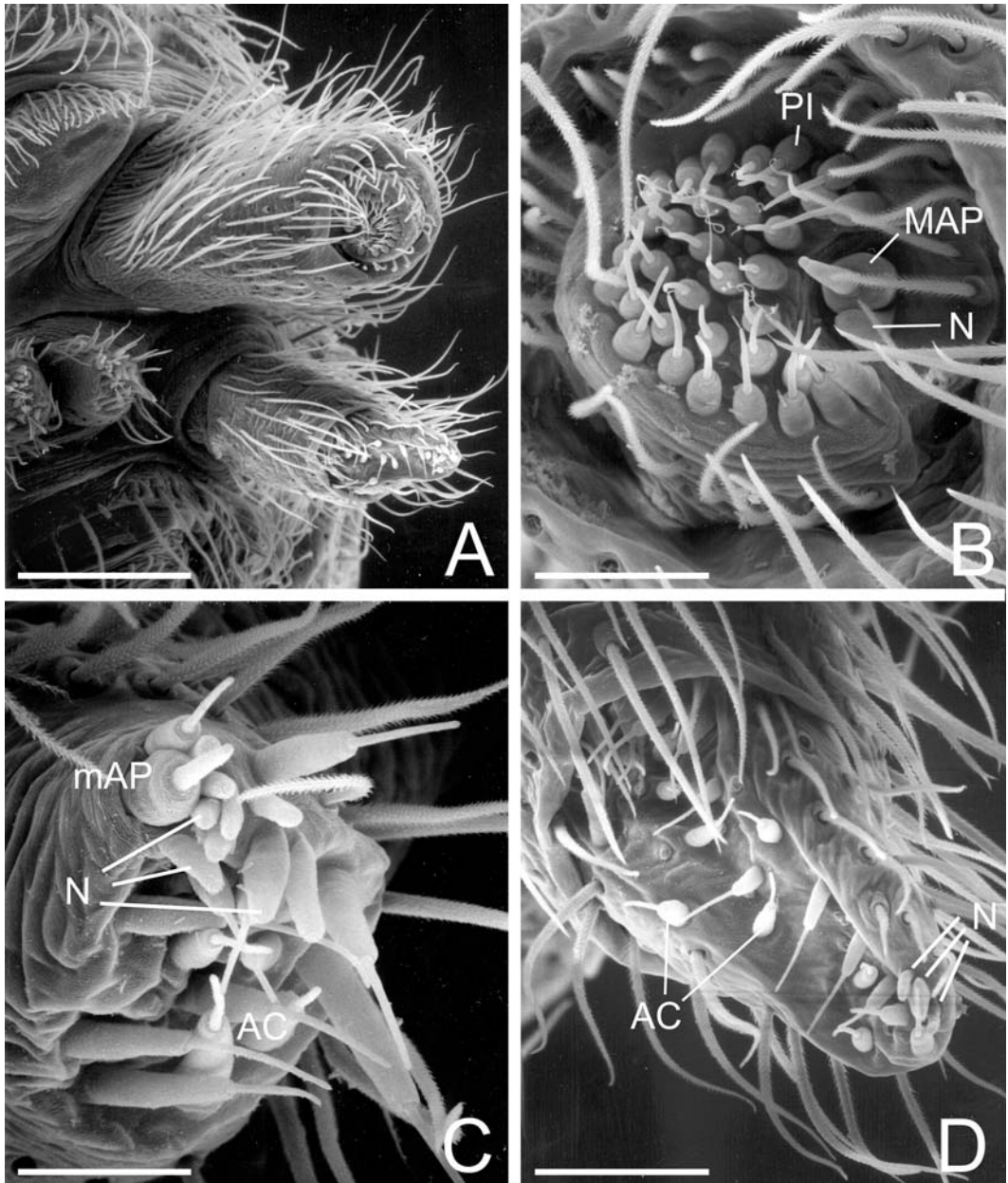


FIGURE 76. Spinnerets of male *Maniho ngaitahu* from Kaituna Valley, New Zealand. A. Left overview. B. Right ALS. C. Left PMS. D. Left PLS. AC = aciniform gland spigot(s), mAP = minor ampullate gland spigot(s), N = nubbins (of PC spigots on PMS, of PC and MS spigots on PLS). Scale bars: A = 150µm, B = 43µm, C = 30µm, D = 60µm.

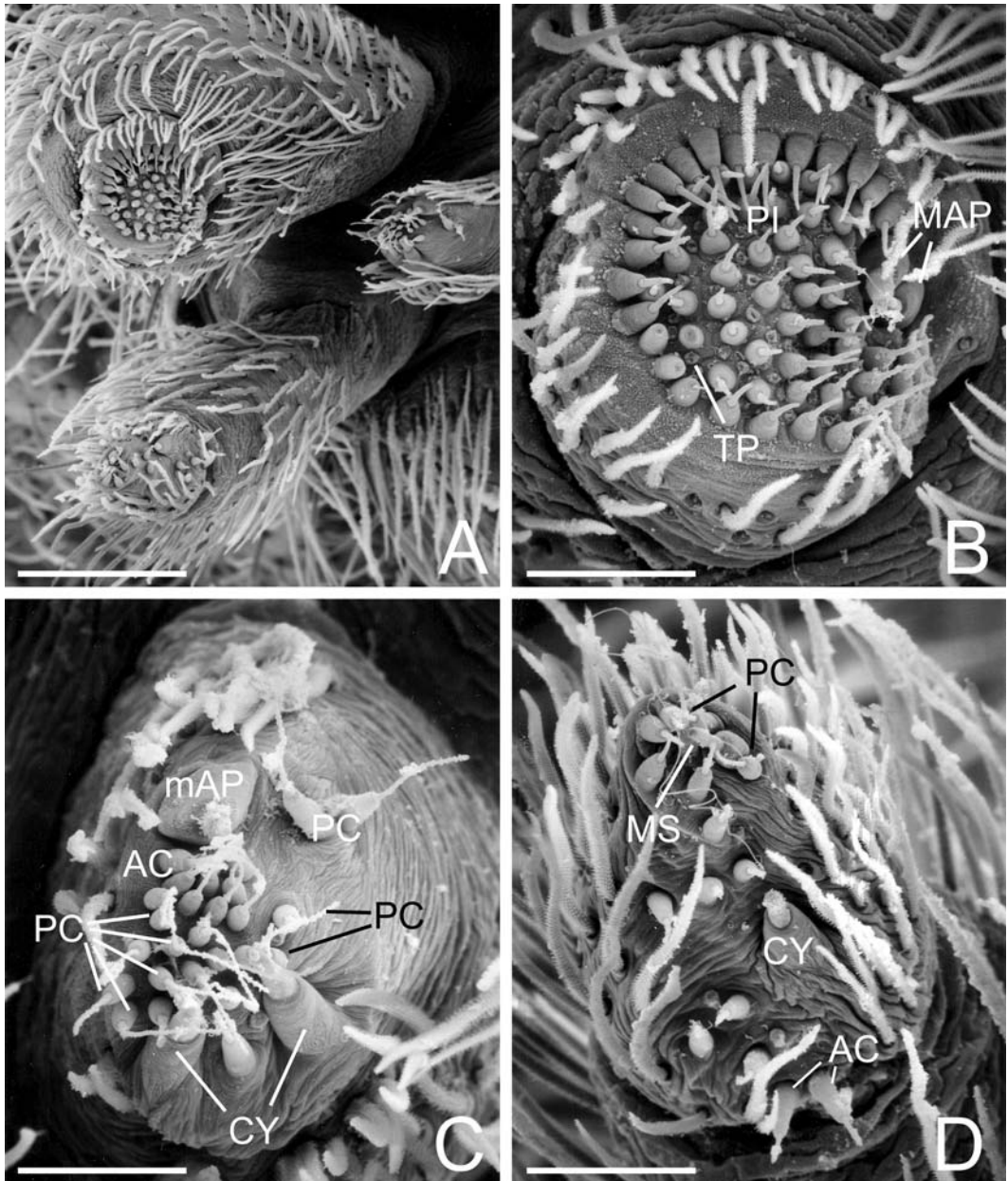


FIGURE 77. Right spinnerets of female *Metaltella simoni* from Riverside, California, USA. A. Overview. B. ALS. C. PMS, showing median field of PC spigots. D. PLS. AC = aciniform gland spigot(s), CY = cylindrical gland spigot(s), MAP = major ampullate gland spigot(s), mAP = minor ampullate gland spigot(s), MS = PLS modified spigot, PC = paracribellar spigot(s), PI = piriform gland spigot(s), TP = tartipore(s). Scale bars: A = 200 μ m, B, D = 60 μ m, C = 43 μ m.

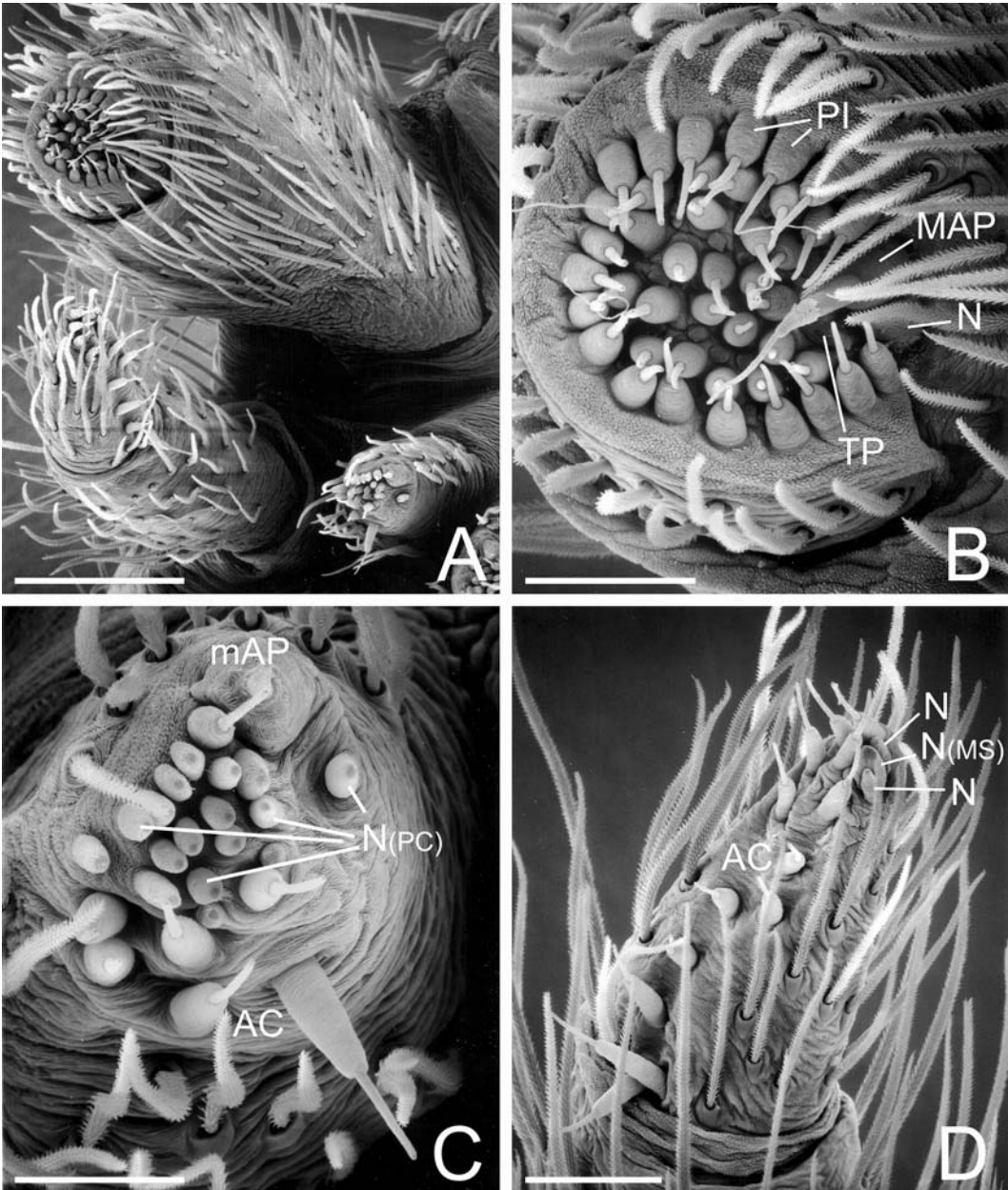


FIGURE 78. Right spinnerets of male *Metaltella simoni* from Riverside, California, USA. A. Overview. B. ALS. C. PMS. Note median field of PC nubbins. D. PLS. AC = aciniform gland spigot(s), MAP = major ampullate gland spigot(s), mAP = minor ampullate gland spigot(s), N = nubbins of MS and PLS PC, PC = nubbins of PMS PC, TP = tartipore(s). Scale bars: A = 150µm, B = 43µm, C = 30µm, D = 60µm.

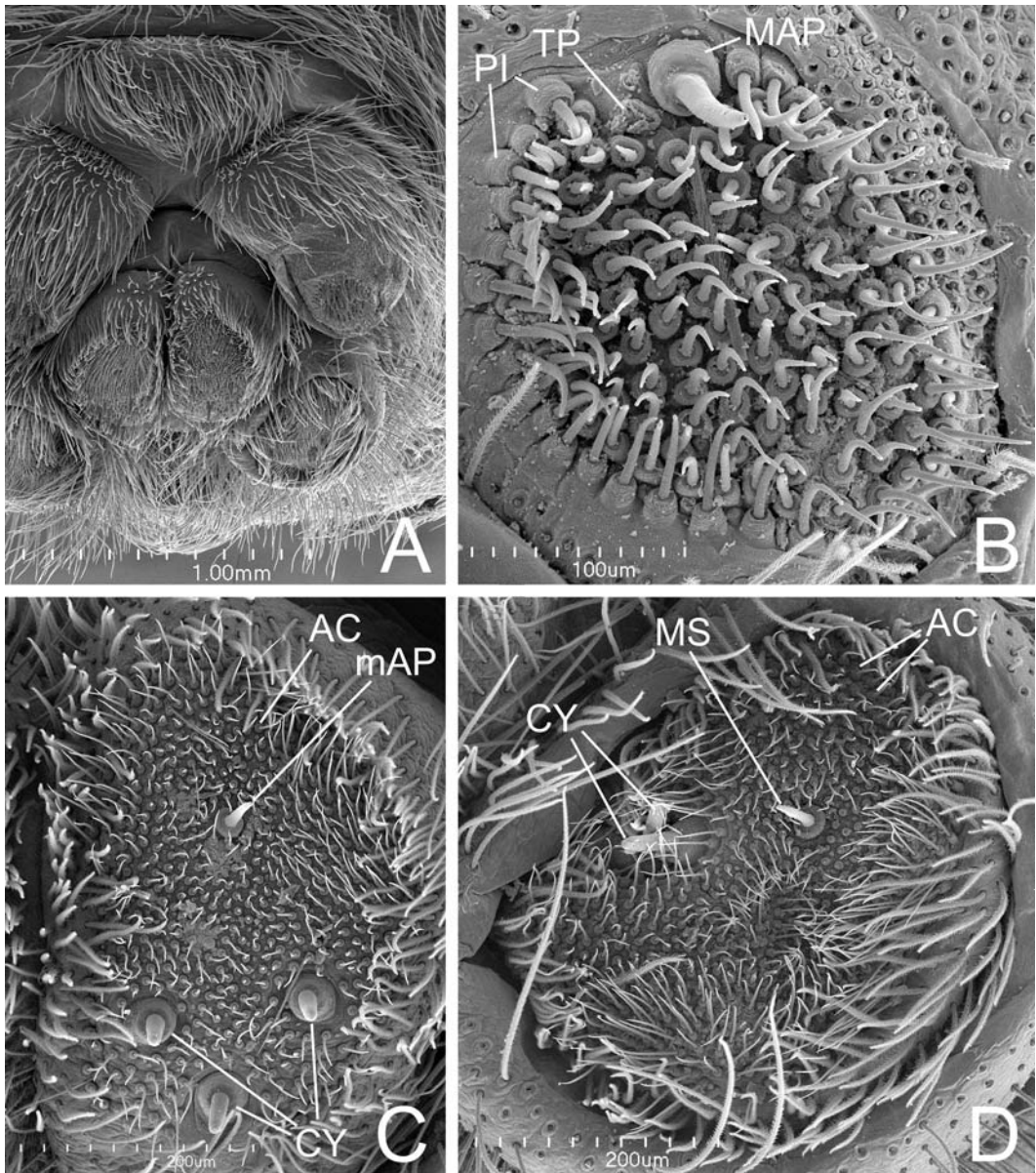


FIGURE 79. Female spinnerets of *Desis formidabilis* from Cape Peninsula, South Africa. A. Spinneret overview. B. Left ALS. C. Left PMS. D. Left PLS. AC = aciniform gland spigot(s), CY = cylindrical gland spigot(s), MAP = major ampullate gland spigot(s), mAP = minor ampullate gland spigot(s), MS = PLS modified spigot, PI = piriform gland spigot(s), TP = tartipore(s). Scale bars: A = 1.0mm, B = 100µm, C, D = 200µm.

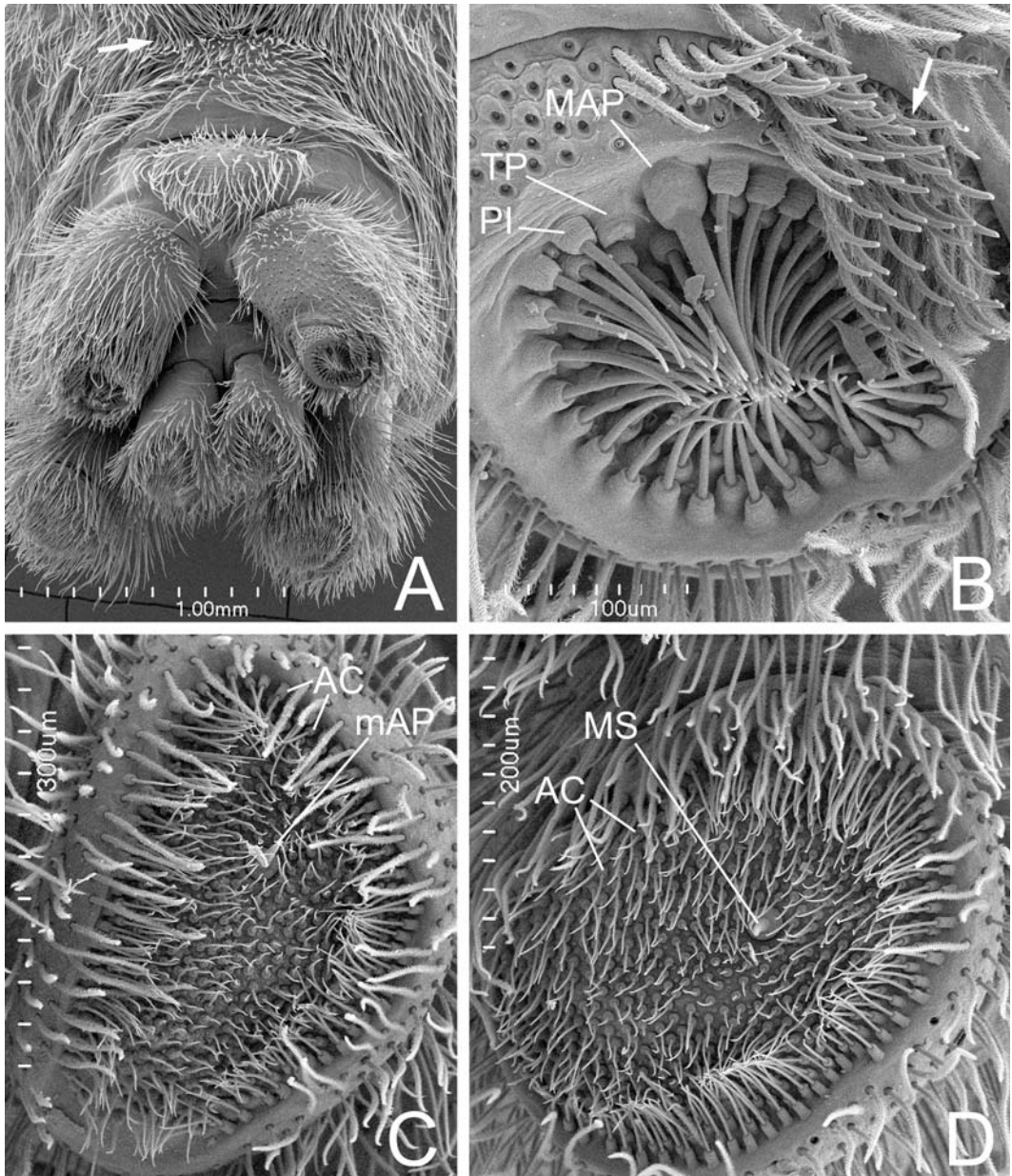


FIGURE 80. Male spinnerets of *Desis formidabilis* from Cape Peninsula, South Africa. A. Spinnerets (arrow to tracheal spiracle). B. Left ALS, arrow to modified setae. C. Left PMS. D. Left PLS. AC = aciniform gland spigot(s), MAP = major ampullate gland spigot(s), mAP = minor ampullate gland spigot(s), MS = PLS modified spigot, PI = piriform gland spigot(s), TP = tartipore(s). Scale bars: A = 1.0mm, B = 100µm, C = 300µm, D = 200µm.

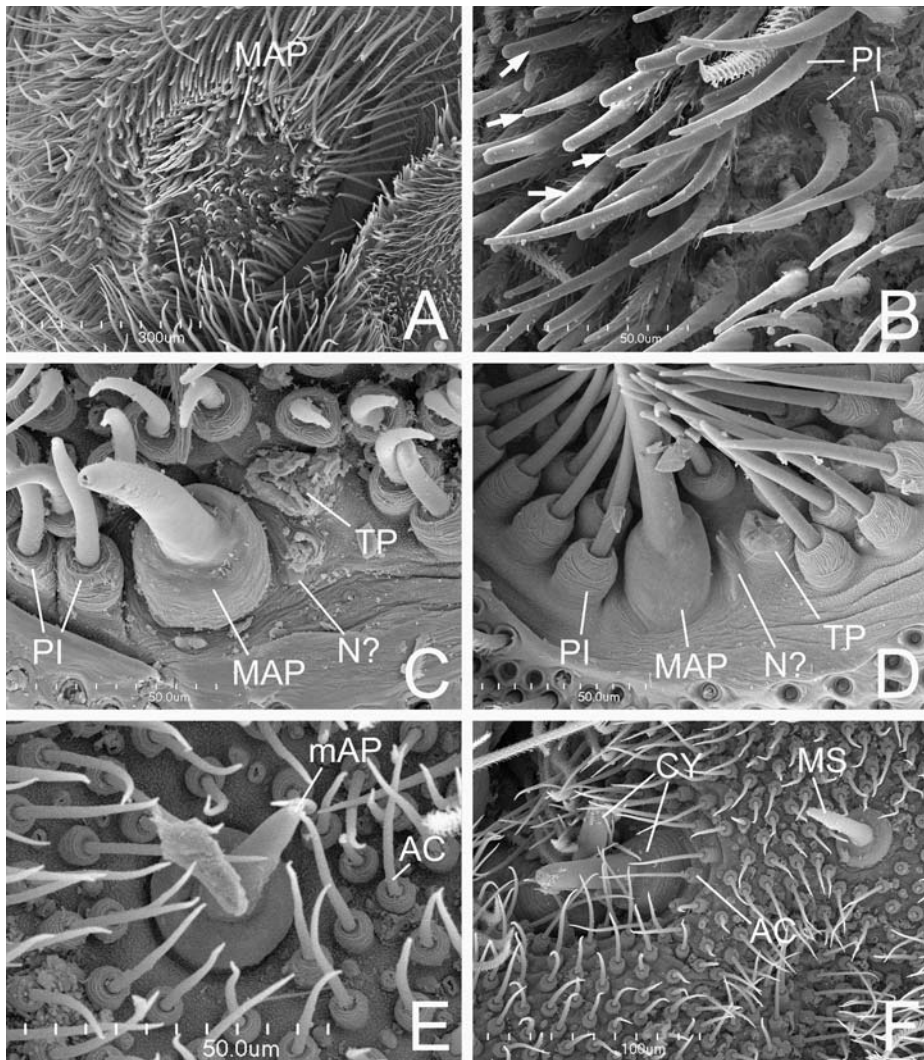


FIGURE 81. Spinnerets and spigots of *Desis formidabilis* from Cape Peninsula, South Africa. A. Female right ALS, note the dense setal cover. B. Detail of female right ALS spinning field, arrows to modified setae. C. Detail of female left ALS, the small mound (N?) between MAP and TP may correspond with the nubbin of a MAP. D. Same, male left ALS. E. Detail of male left PMS. F. Detail of female left PLS. AC = aciniform gland spigot(s), CY = cylindrical gland spigot(s), MAP = major ampullate gland spigot(s), mAP = minor ampullate gland spigot(s), MS = PLS modified spigot, N = nubbin, PI = piriform gland spigot(s), TP = tartipore(s). Scale bars: A = 300µm, B—E = 50µm, F = 100µm.

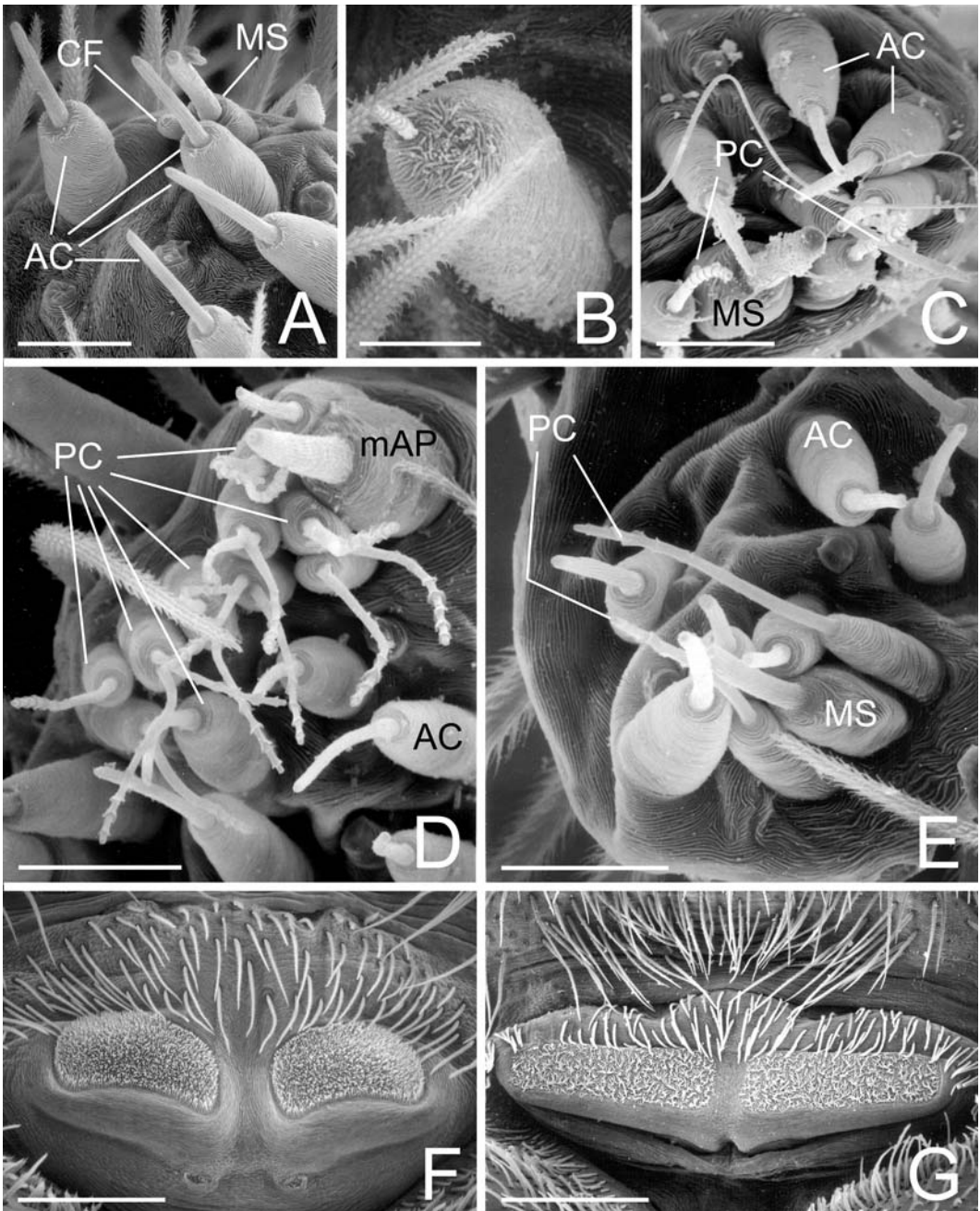


FIGURE 82. Spinnerets. A, B, F. *Neoramia sana* from Dunedin, New Zealand. A. Apex of female PLS. B. Nubbin on male PMS with PC spigot. F. Cribellum. C, G. *Metaltella simoni* female from Riverside, California, USA. C. Apex of PLS. G. Cribellum. D, E. *Maniho ngaitahu* female from Kaituna Valley, New Zealand. D. Right PMS apex. E. Left PLS apex. AC = aciniform gland spigot(s), CF = cuticular finger, mAP = minor ampullate gland spigot(s), MS = PLS modified spigot, PC = paracribellar spigot(s). Scale bars: A = 20 μ m, B = 10 μ m, C = 6 μ m, D, E = 15 μ m, F = 150 μ m, G = 250 μ m.

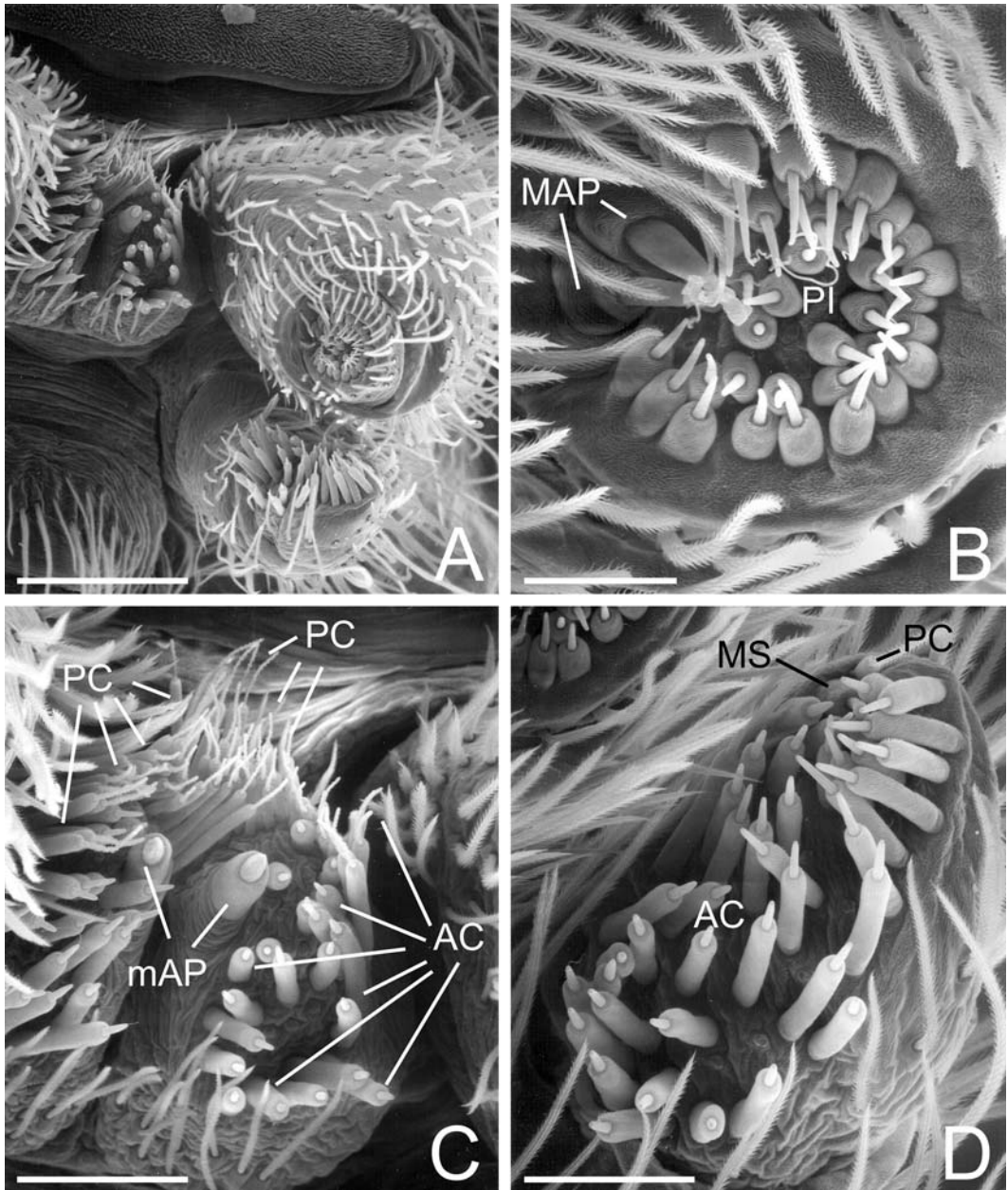


FIGURE 83. Left spinnerets of female *Matachia australis* from Dunedin, New Zealand. A. Overview. B. ALS. C. Left and right PMS. Note numerous PC spigots with one shaft per base. D. PLS. AC = aciniform gland spigot(s), MAP = major ampullate gland spigot(s), mAP = minor ampullate gland spigot(s), MS = PLS modified spigot, PC = paracribellar spigot(s), PI = piriform gland spigot(s). Scale bars: A = 150µm, B = 30µm, C = 60µm, D = 43µm.

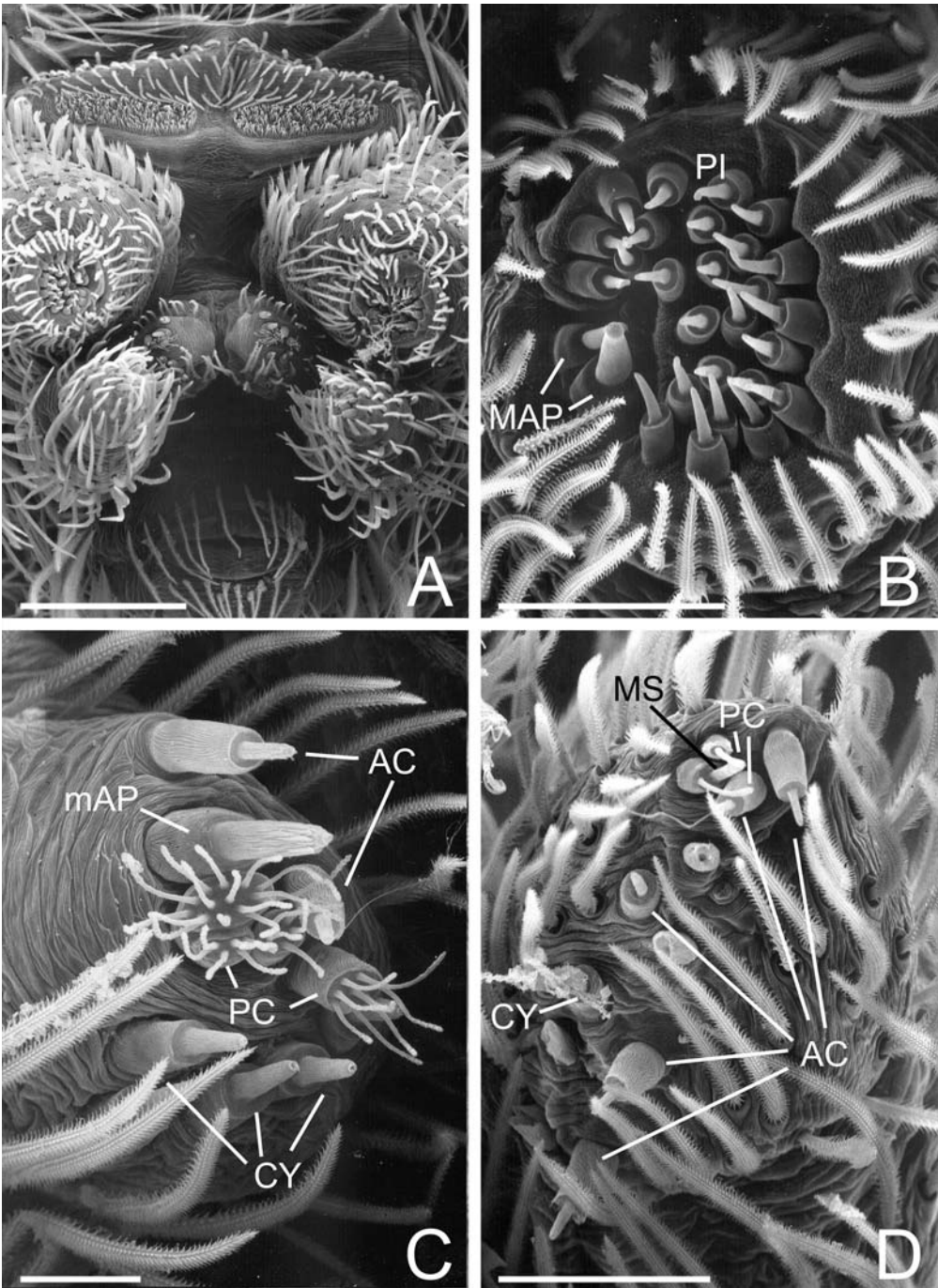


FIGURE 84. Female spinnerets of *Phryganoporus candidus* from Canberra, Australia. A. Spinnerets. B. Left ALS. C. Left PMS. D. Left PLS. AC spigots with shafts labelled, of others only bases remain. Note common base of PC and MS. AC = aciniform gland spigot(s), CY = cylindrical gland spigot(s), MAP = major ampullate gland spigot(s), mAP = minor ampullate gland spigot(s), MS = PLS modified spigot, PC = paracribellar spigot(s), PI = piriform gland spigot(s). Scale bars: A = 200µm, B, D = 50µm, C = 20µm.

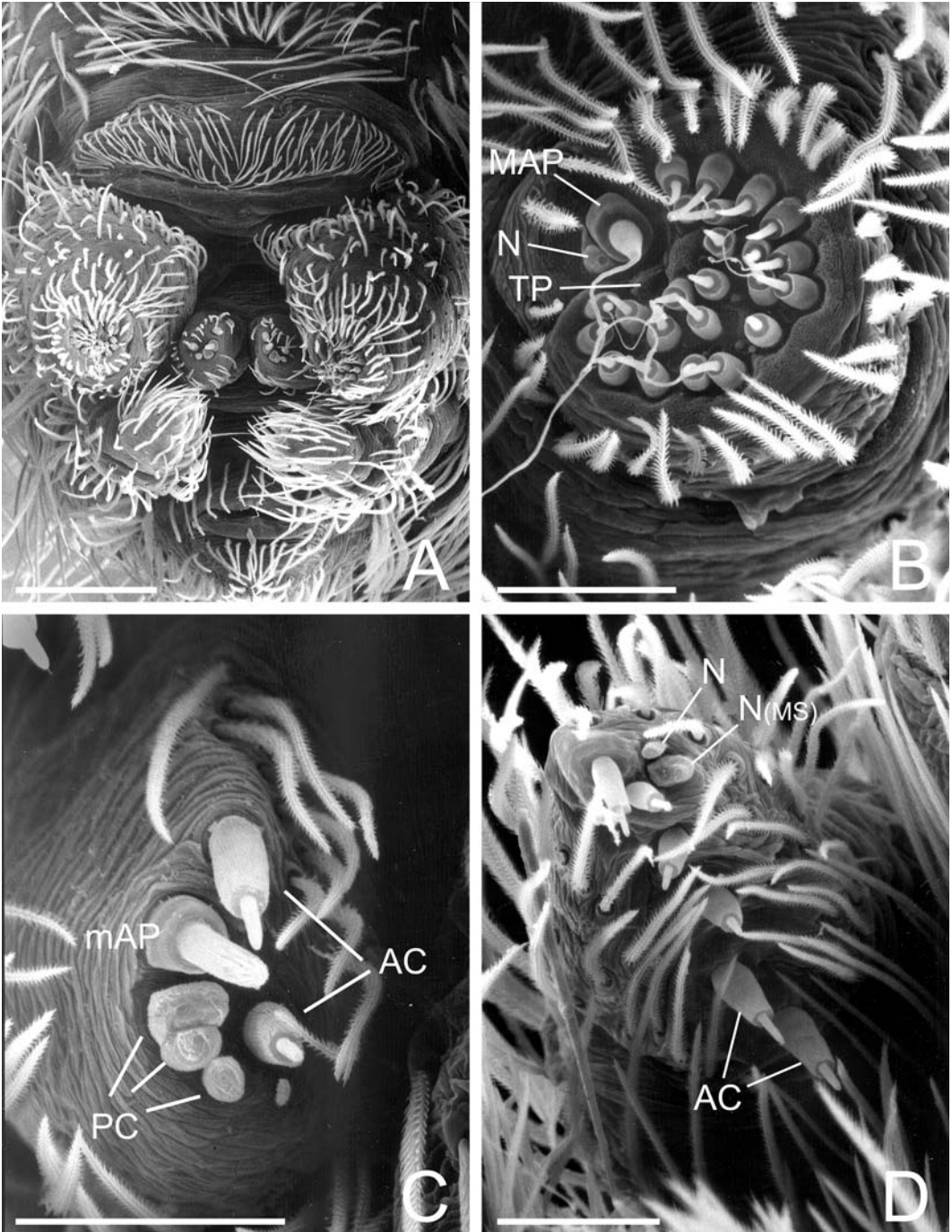


FIGURE 85. Male spinnerets of *Phryganoporus candidus* from Canberra, Australia. A. Spinnerets. B. Right ALS. C. Right PMS. Note PC nubbins. D. Right PLS. Note nubbins of PC and of common base to PC and MS. AC = aciniform gland spigot(s), MAP = major ampullate gland spigot(s), mAP = minor ampullate gland spigot(s), N = nubbins of posterior MAP on ALS, PC and MS on PLS, PC = paracribellar spigot nubbins on PMS, TP = tartipores. Scale bars: A = 200µm, B-D = 50µm

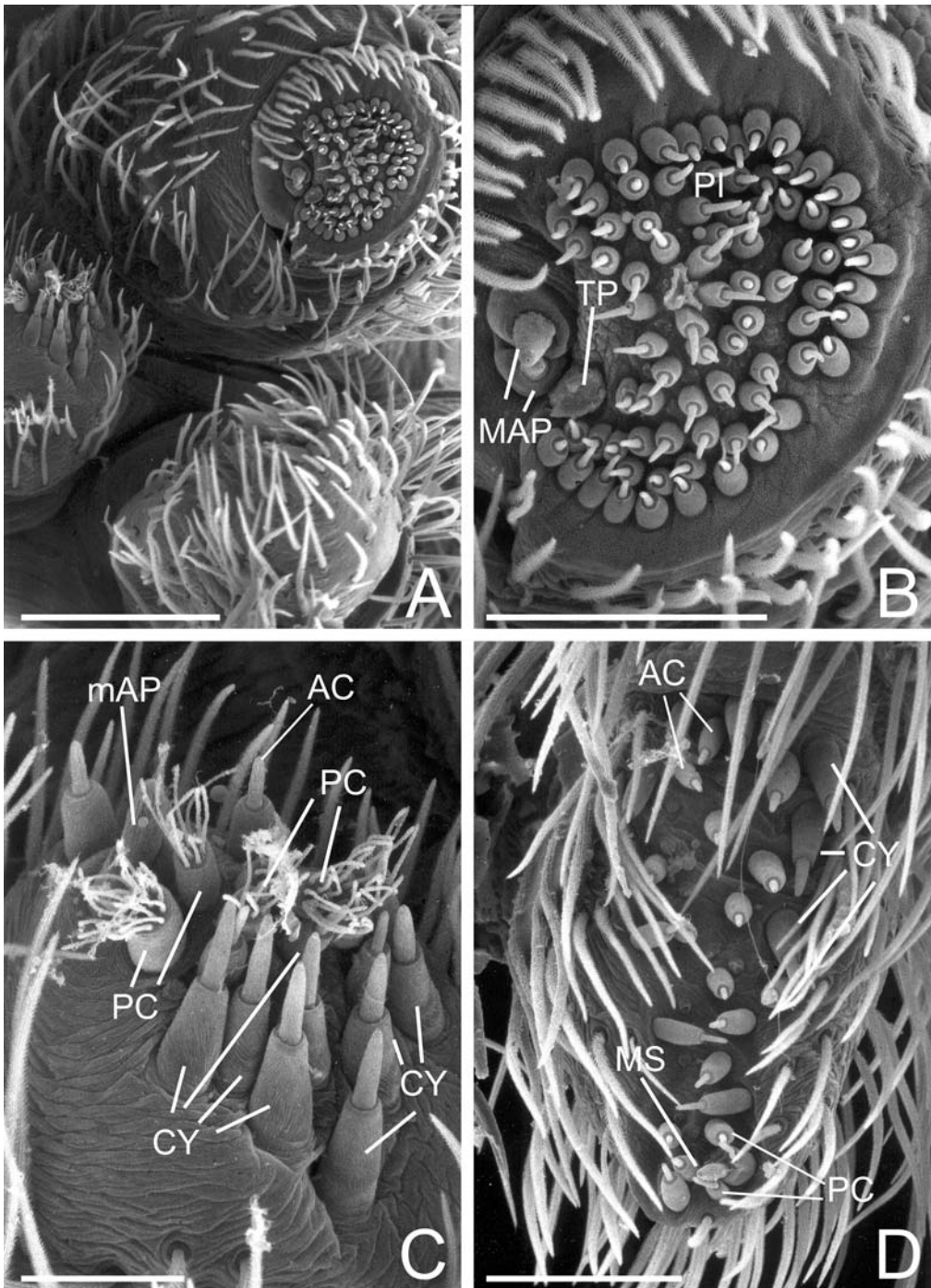


FIGURE 86. Left female spinnerets of *Badumna longinqua* from Maui, Hawaii, USA. A. Overview. B. ALS. C. PMS. D. PLS. AC = aciniform gland spigot(s), CY = cylindrical gland spigot(s), MAP = major ampullate gland spigot(s), mAP = minor ampullate gland spigot(s), MS = PLS modified spigot, PC = paracribellar spigot(s), PI = piriform gland spigot(s), TP = tartipore(s). Scale bars: A = 200µm, B, D = 100µm, C = 50µm.

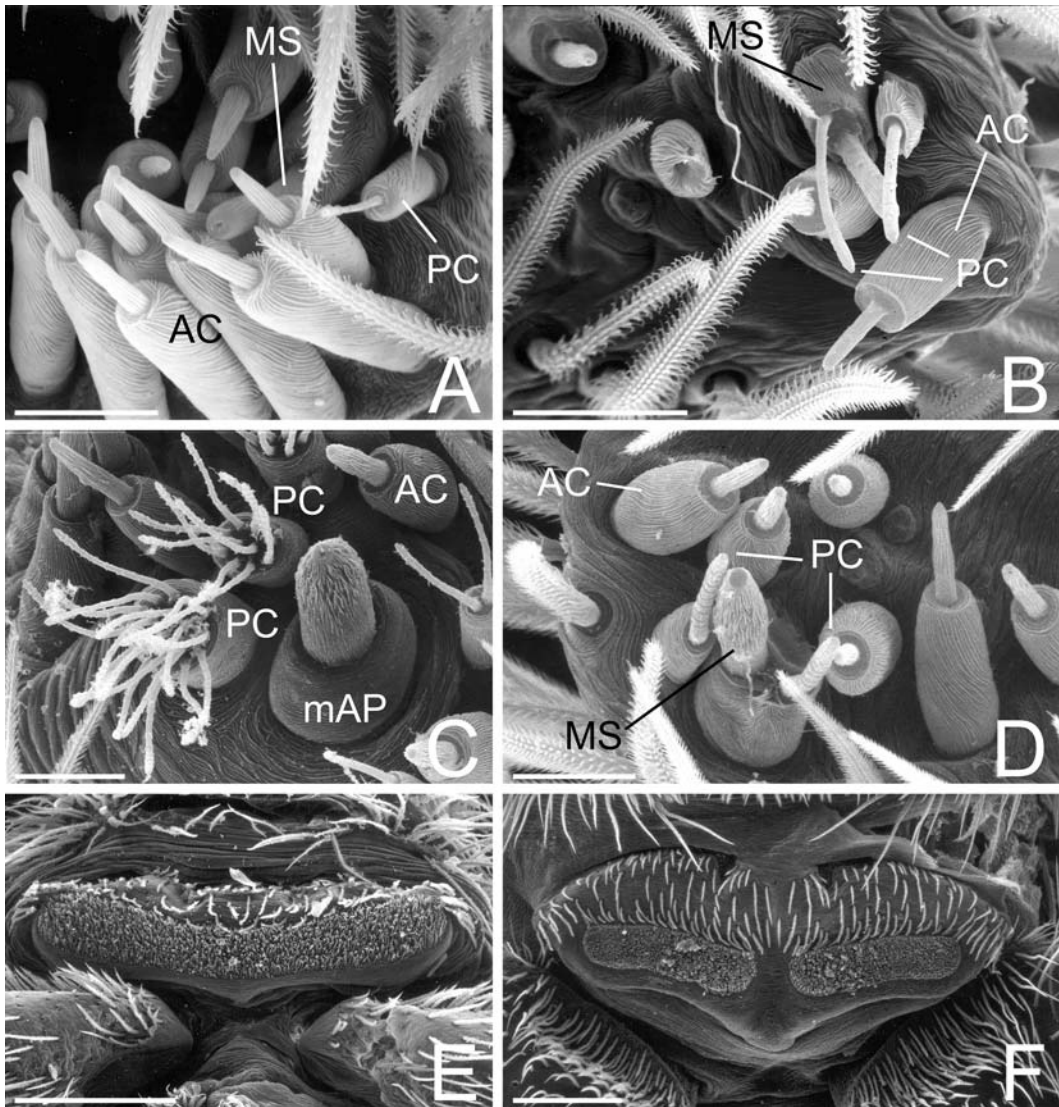


FIGURE 87. Female spinnerets of Desidae. A, E. *Matachia australis* from Dunedin, New Zealand. B. *Phryganoporus candidus* from Canberra, Australia. C, D, F. *Badumna longinqua* from Maui, Hawaii, USA. A. Left PLS apex, showing PC and MS amid AC spigots. B. PLS apex, showing PC and MS with common base, and AC with sharp-edged base. C. PMS showing mid-spinning-field PC with multiple shafts from each base. D. Left PLS apex, showing PC and MS with common base, and AC with sharp-edged base. E, F. Cribella. AC = aciniform gland spigot(s), mAP = minor ampullate gland spigot(s), MS = PLS modified spigot, PC = paracribellar spigot(s). Scale bars: A = 15 μ m, B–D = 20 μ m, E, F = 200 μ m.

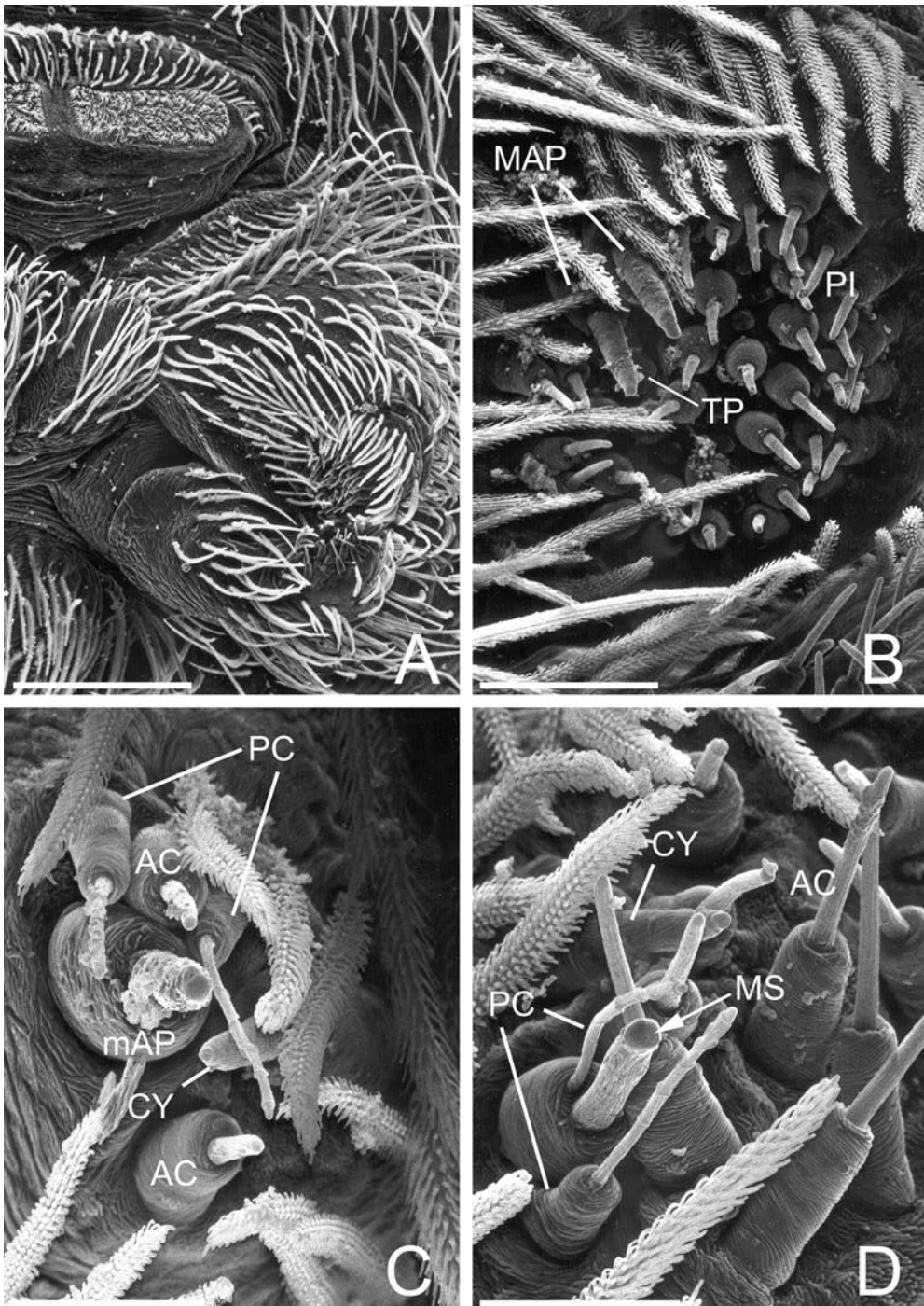


FIGURE 88. Left spinnerets of female *Amaurobius fenestralis* from Tisvilde, Denmark. A. Overview. B. ALS. C. PMS. D. PLS, showing PC and MS arising from common base. AC = aciniform gland spigot(s), CY = cylindrical gland spigot(s), MAP = major ampullate gland spigot(s), mAP = minor ampullate gland spigot(s), MS = PLS modified spigot, PC = paracribellar spigot(s), PI = piriform gland spigot(s), TP = tartipore(s). Scale bars: A = 200µm, B, D = 50µm, C = 20µm.

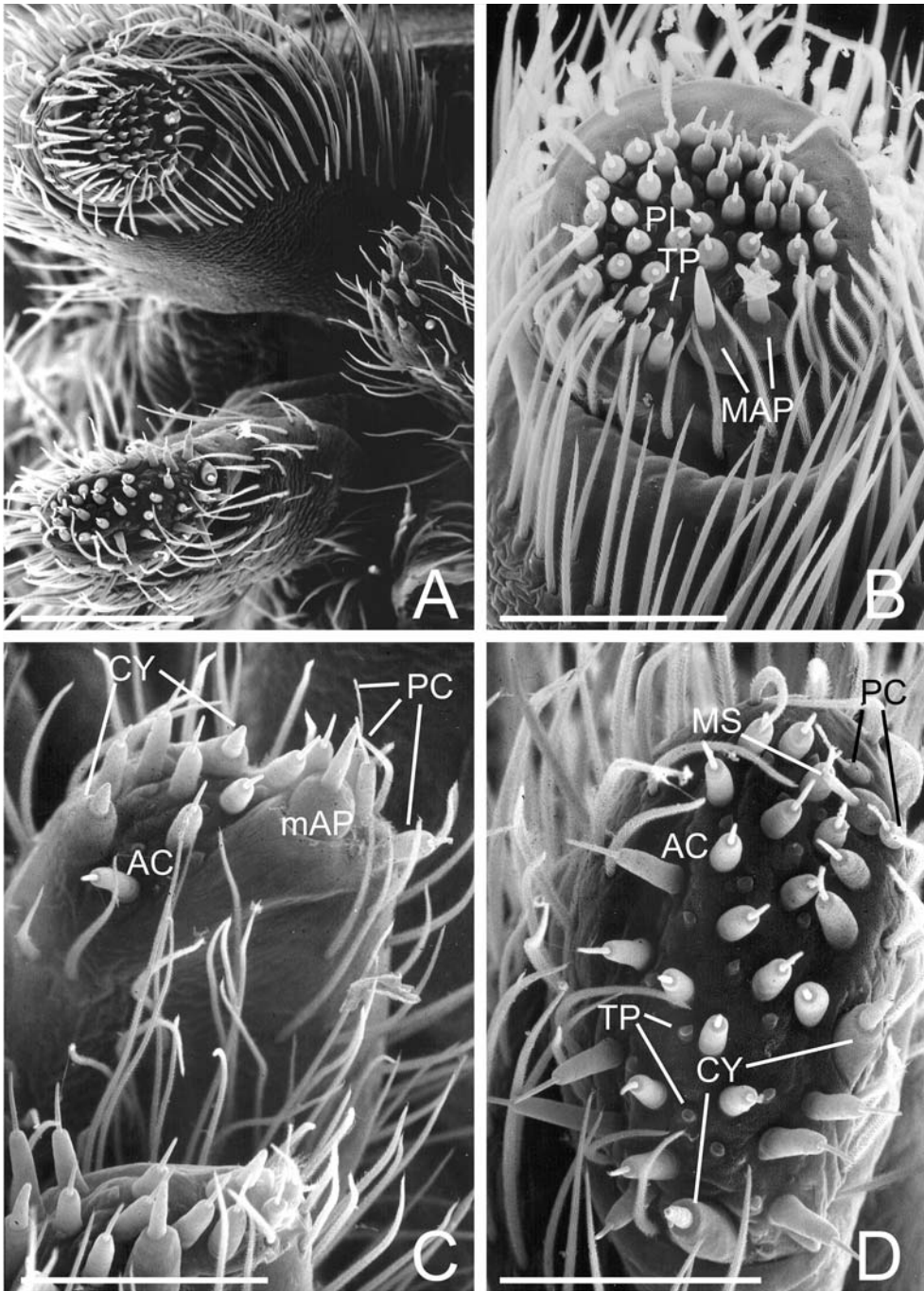


FIGURE 89. Spinnerets of female *Callobius bennetti* from Hampshire Co., West Virginia, USA. A. Right overview. B. Right ALS, showing wide field margin around spinning field. C. PMS. D. Right PLS. AC = aciniform gland spigot(s), CY = cylindrical gland spigot(s), MAP = major ampullate gland spigot(s), mAP = minor ampullate gland spigot(s), MS = PLS modified spigot, PC = paracribellar spigot(s), PI = piriform gland spigot(s), TP = tartipore(s). Scale bars: A = 200 μ m, B–D = 100 μ m.

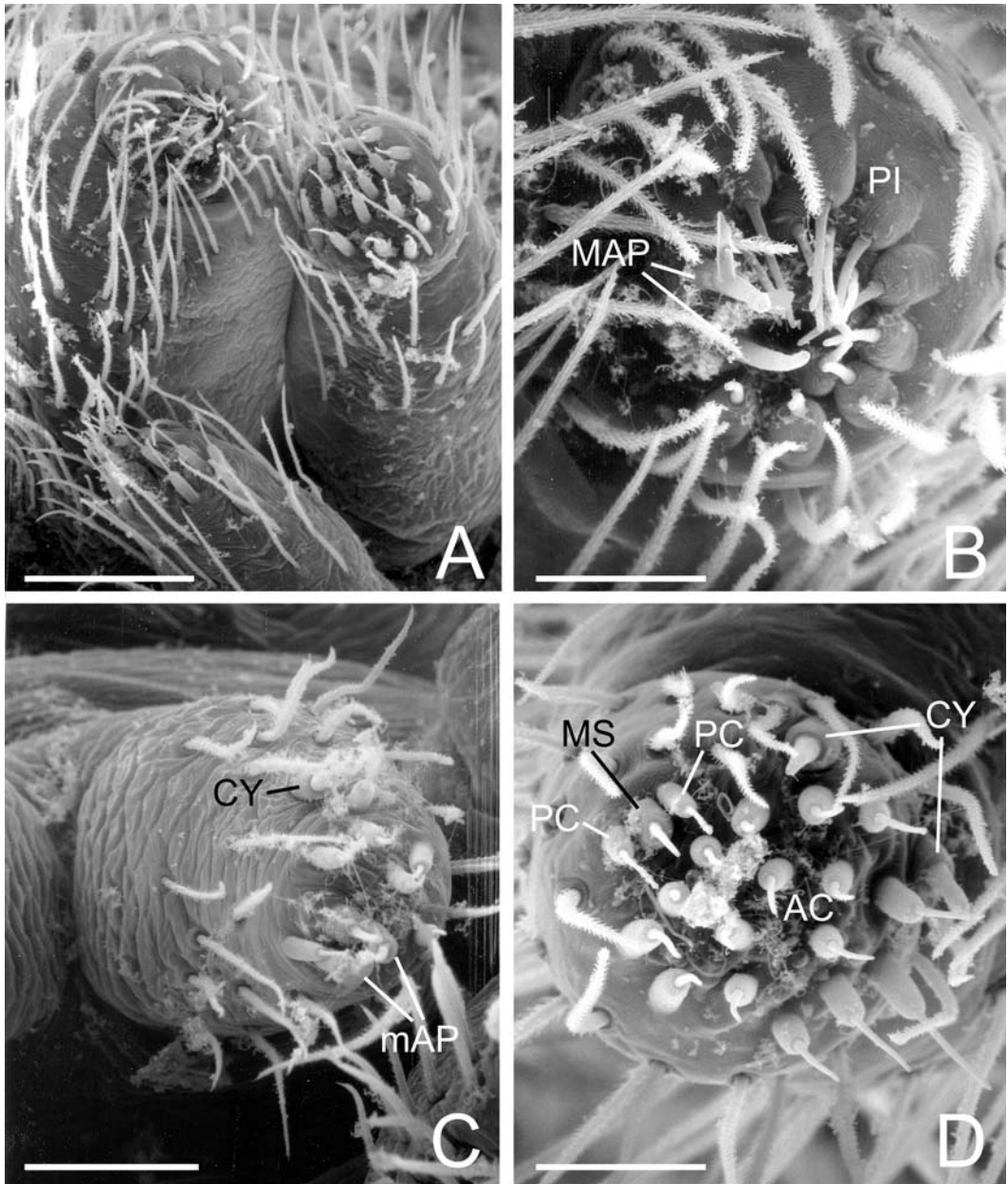


FIGURE 90. Spinnerets of female *Pimus* sp. from Mendocino Co., California, USA. A. Left overview. B. Left ALS. C. Left PMS. Debris obscures the spinning field, but comparison with the male suggests that there are two mAP and one PC. D. Right PLS. AC = aciniform gland spigot(s), CY = cylindrical gland spigot(s), MAP = major ampullate gland spigot(s), mAP = minor ampullate gland spigot(s), MS = PLS modified spigot, PC = paracribellar spigot(s), PI = piriform gland spigot(s). Scale bars: A = 75 μ m, B = 25 μ m, C = 43 μ m, D = 30 μ m.

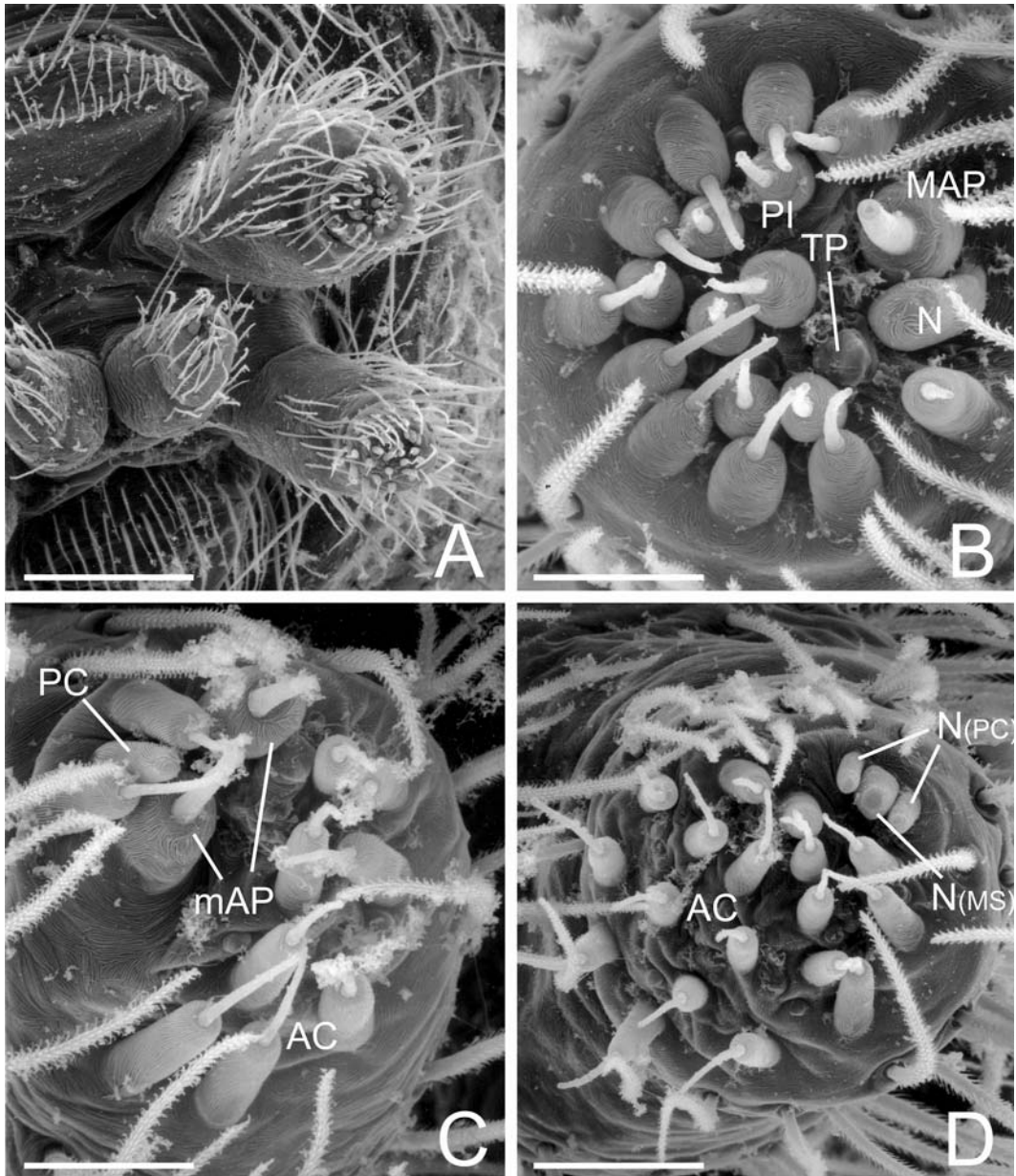


FIGURE 91. Spinnerets of male *Pimus* sp. from Mendocino Co., California, USA. A. Left overview. B. Right ALS, showing MAP, nubbin and tartipore. C. Left PMS. Note two large spigots that may be mAP. D. Left PLS showing nubbins of two PC and one MS spigots. AC = aciniform gland spigot(s), MAP = major ampullate gland spigot(s), mAP = minor ampullate gland spigot(s), MS = nubbin of PLS modified spigot, N = MAP nubbin, PC = paracribellar spigot nubbins, PI = piriform gland spigot(s), TP = tartipore(s). Scale bars: A = 150 μ m, B, C = 20 μ m, D = 30 μ m.

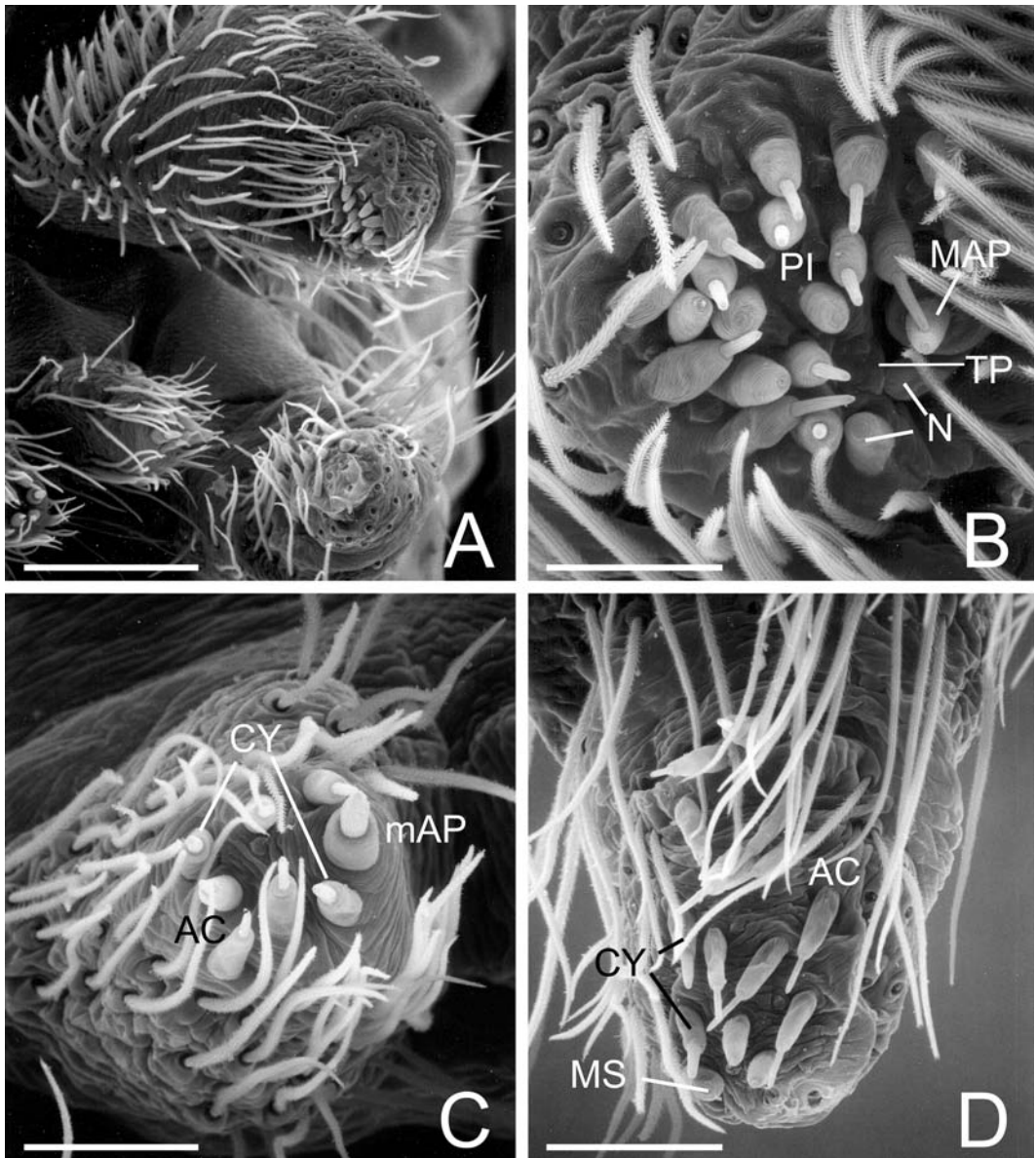


FIGURE 92. Spinnerets of female *Retiro* sp. from Lima, Peru. A. Left overview. B. Right ALS, with only one MAP and nubbin. The second nubbin may be a PI with broken shaft. C. Right PMS. D. Right PLS. Apical MS spigot shaft broken off. AC = aciniform gland spigot(s), CY = cylindrical gland spigot(s), MAP = major ampullate gland spigot(s), mAP = minor ampullate gland spigot(s), MS = PLS modified spigot, N = nubbin(s), PI = piriform gland spigot(s), TP = tartipore(s). Scale bars: A = 150 μ m, B = 30 μ m, C = 43 μ m, D = 60 μ m.

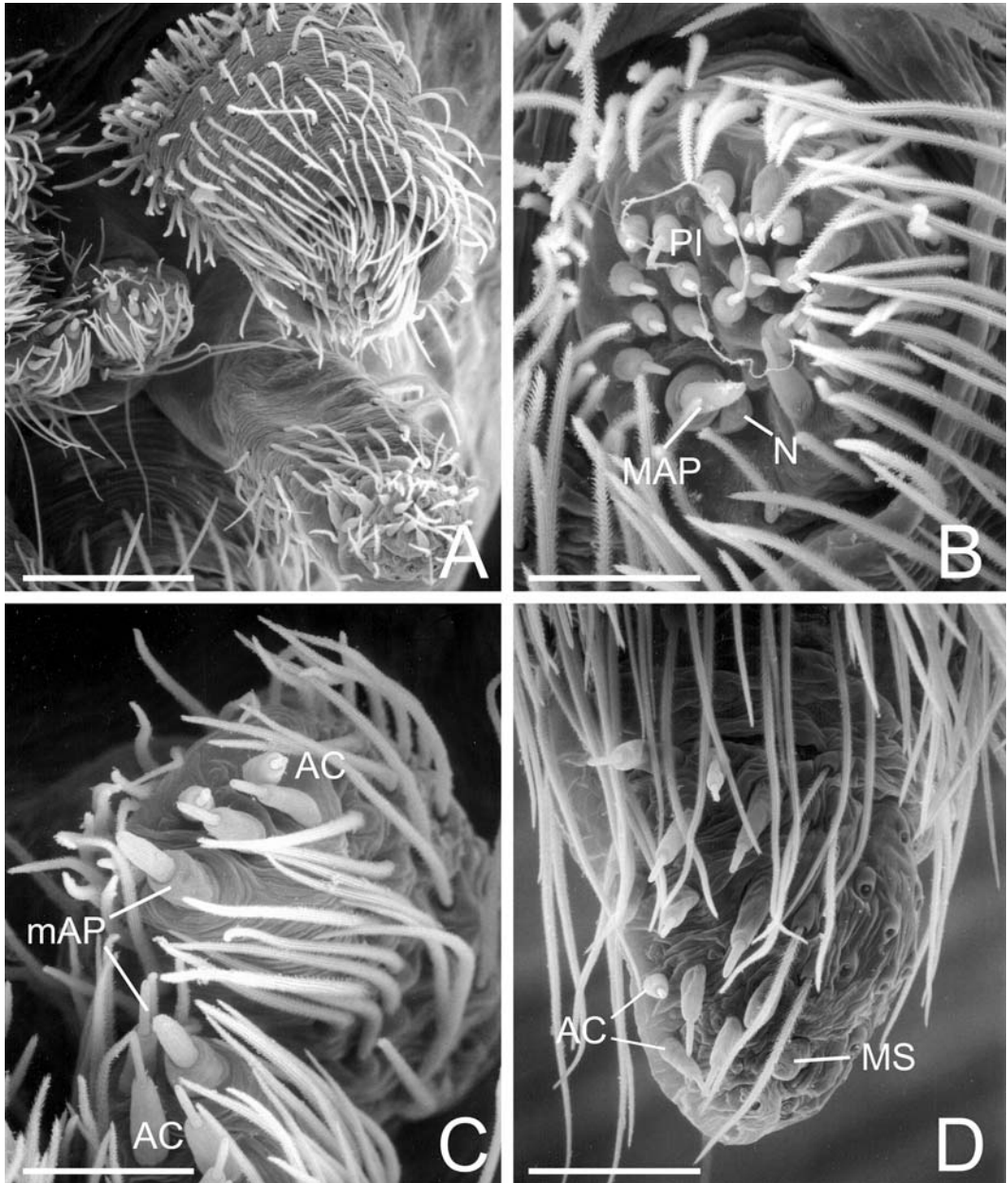


FIGURE 93. Left spinnerets of male *Retiro* sp. from Lima, Peru. A. Overview. B. ALS. C. Left and right PMS. D. PLS, showing AC spigots and MS nubbin. AC = aciniform gland spigot(s), MAP = major ampullate gland spigot(s), mAP = minor ampullate gland spigot(s), MS = PLS modified spigot nubbin, N = nubbin of posterior MAP, PI = piriform gland spigot(s). Scale bars: A = 150 μ m, B, C = 43 μ m, D = 60 μ m.

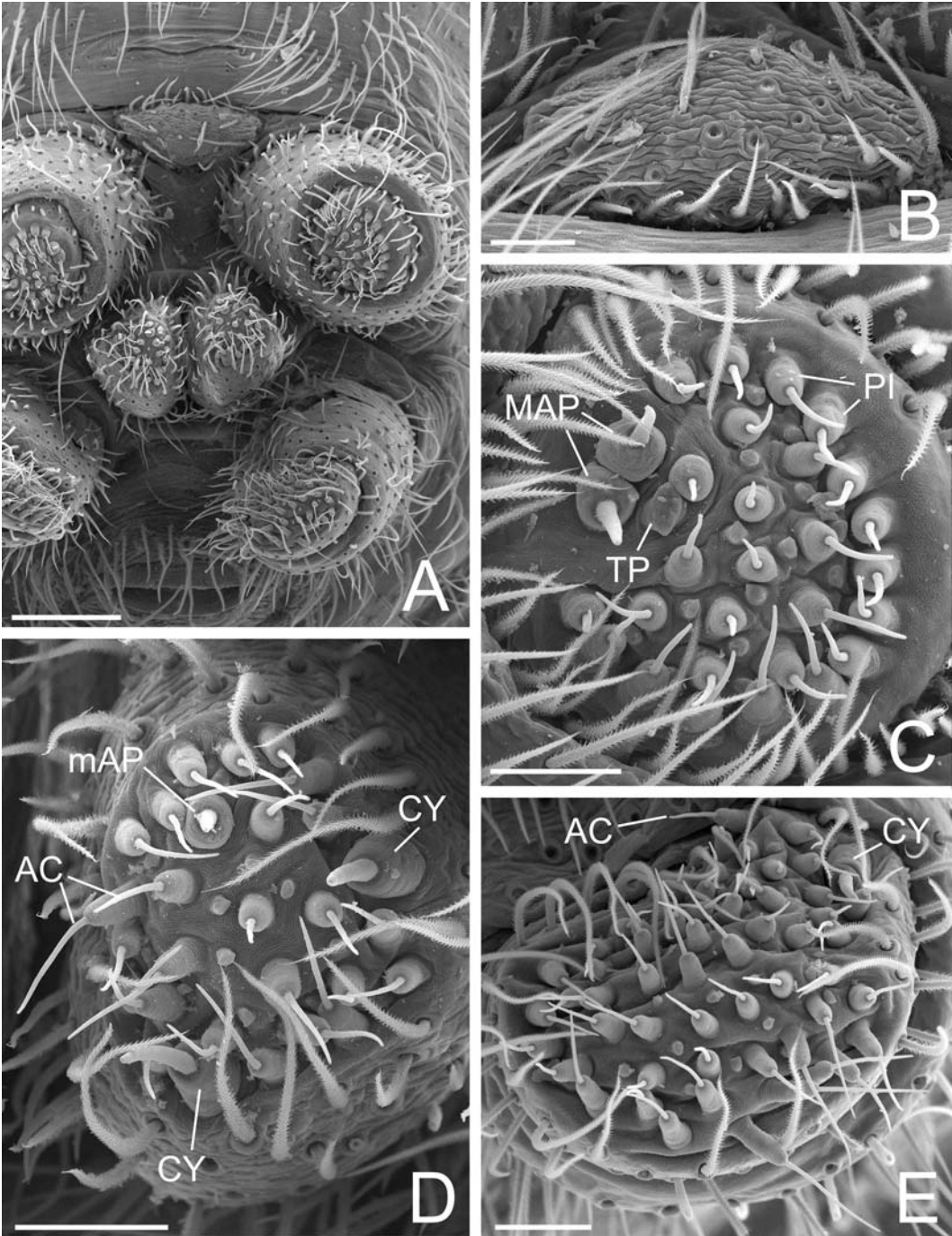


FIGURE 94. Female spinnerets of *Macrobnus multidentatus* from Chiloé, Chile. A. Spinnerets. B. Colulus. C. Left ALS. D. Left PMS. E. Left PLS. AC = aciniform gland spigot(s), CY = cylindrical gland spigot(s), MAP = major ampullate gland spigot(s), mAP = minor ampullate gland spigot(s), PI = piriform gland spigots, TP = tartipore. Scale bars: A = 200 μ m, B-E = 50 μ m.

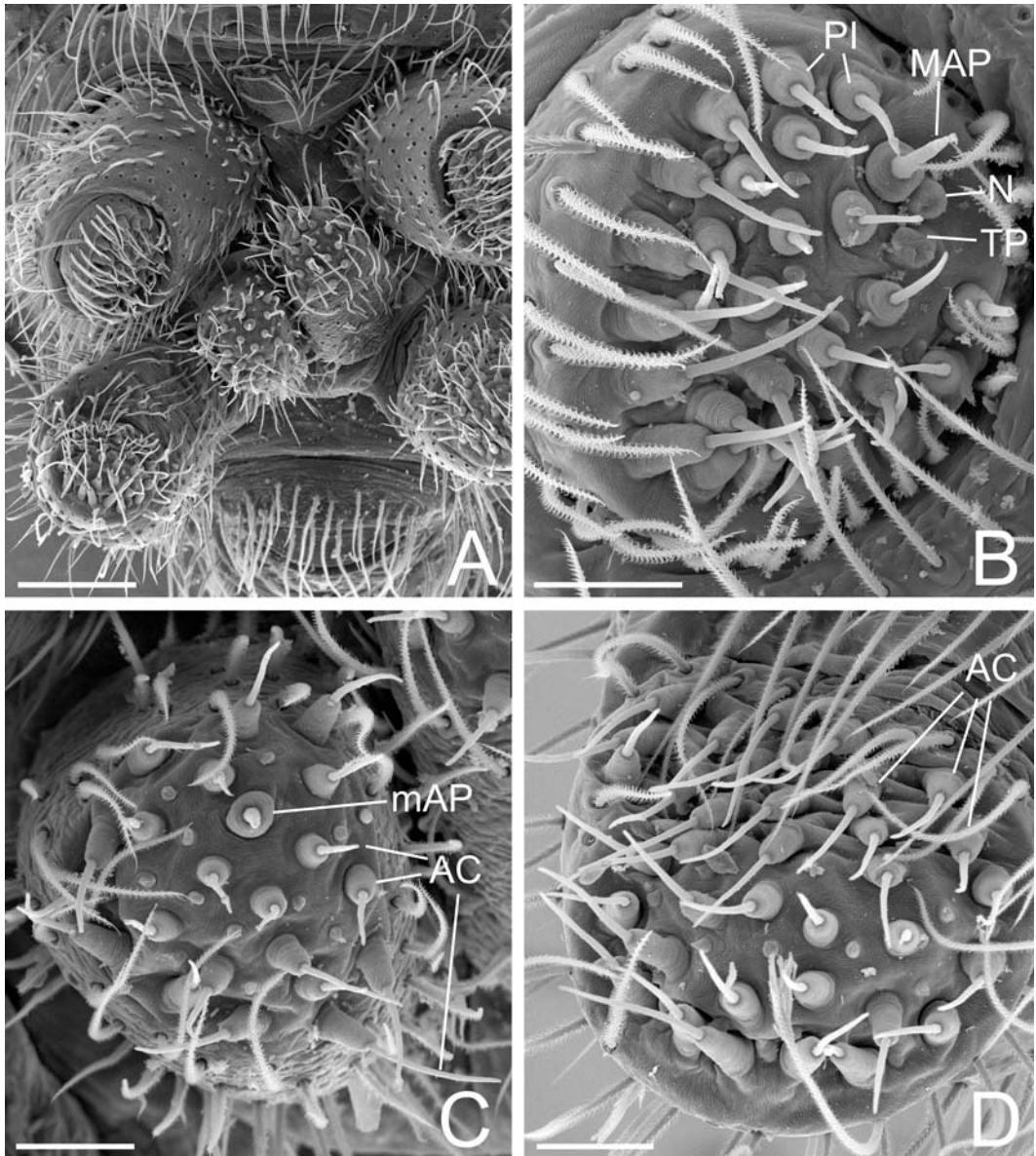


FIGURE 95. Male spinnerets of *Macrobnus multidentatus* from Chiloé, Chile. A. Spinnerets. B. Right ALS. C. Right PMS. D. Right PLS. AC = aciniform gland spigot(s), MAP = major ampullate gland spigot(s), mAP = minor ampullate gland spigot(s), N = nubbin(s), PI = piriform gland spigots, TP = tartipore. Scale bars: A = 200 μ m, B, C, D = 50 μ m.

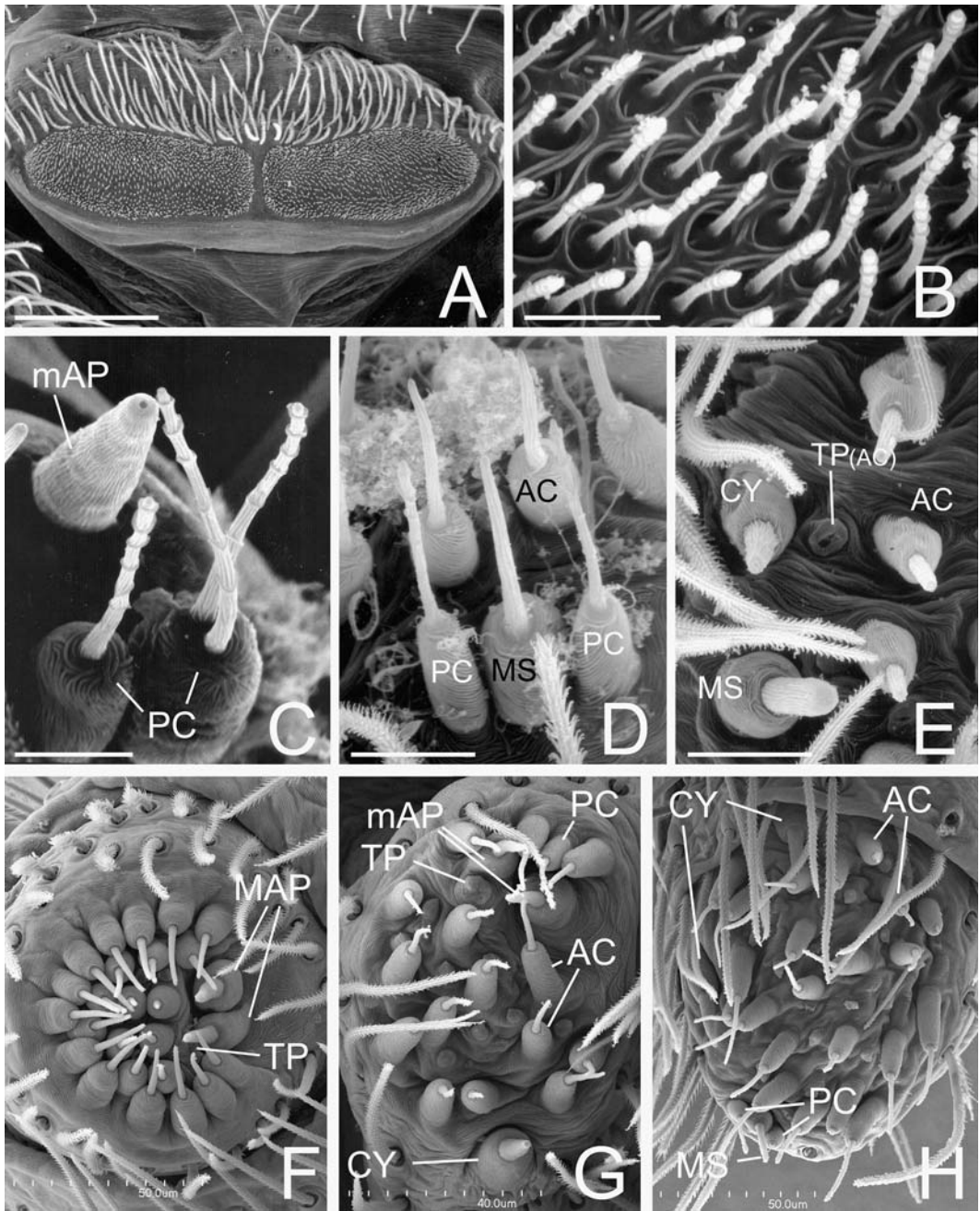


FIGURE 96. Female spinnerets. A, B, E. *Retiro* sp. from Lima, Peru. A. Cribellum. B. Close up of strobilate cribellar spigots. E. Apex of right PLS. C. *Callobius bennetti* from Hampshire Co., West Virginia, USA, PMS apex, showing PC bases with single and multiple shafts. D. *Pimus* sp. from Mendocino Co., California, USA, apex of right PLS. F–H. *Pimus napa* from Napa Co., California, USA, right spinnerets. F. ALS. G. PMS. H. PLS. AC = aciniform gland spigot(s), CY = cylindrical gland spigot(s), MAP = major ampullate gland spigot(s), mAP = minor ampullate gland spigot(s), MS = PLS modified spigot, PC = paracribellar spigot(s), TP = tartipore. Scale bars: A = 150µm, B = 6µm, C, D = 10µm, E = 15µm, F, H = 50µm, G = 40µm.

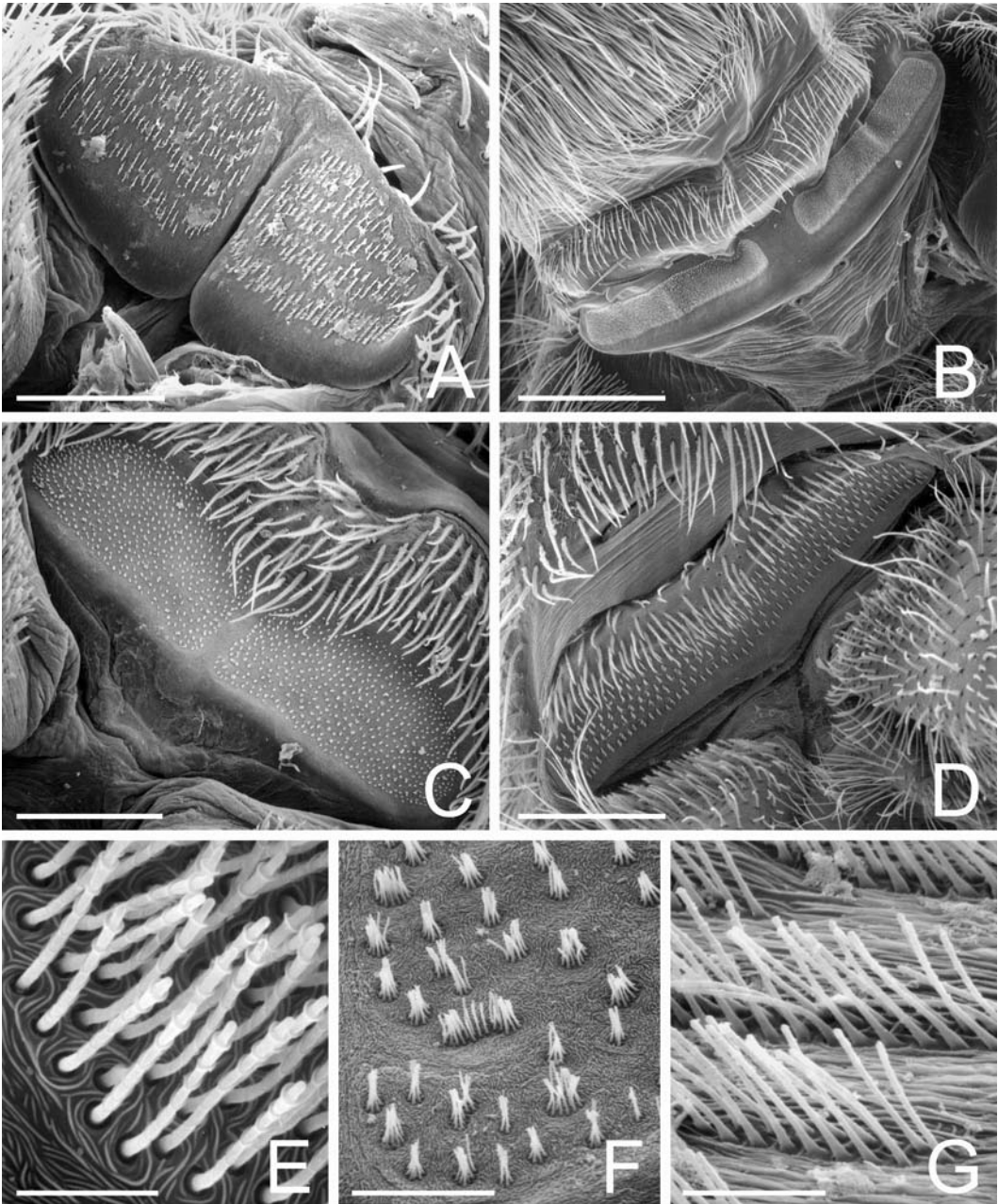


FIGURE 97. Female cribellar spinning organs. A, G. *Acanthoctenus* sp. from Changuinola, Panama. B, E. *Psechrus* sp. from Tham Lot Cave, Thailand. C, F. *Uduba* sp. from Ranomafana, Madagascar. D. *Raecius jocquei* from Appouesso, Côte d'Ivoire. A–D. Cribella. E–G. Details of cribellar spigots. Scale bars: A = 150 μ m, B = 430 μ m, C = 200 μ m, D = 201 μ m, E, G = 7.5 μ m, F = 25 μ m.

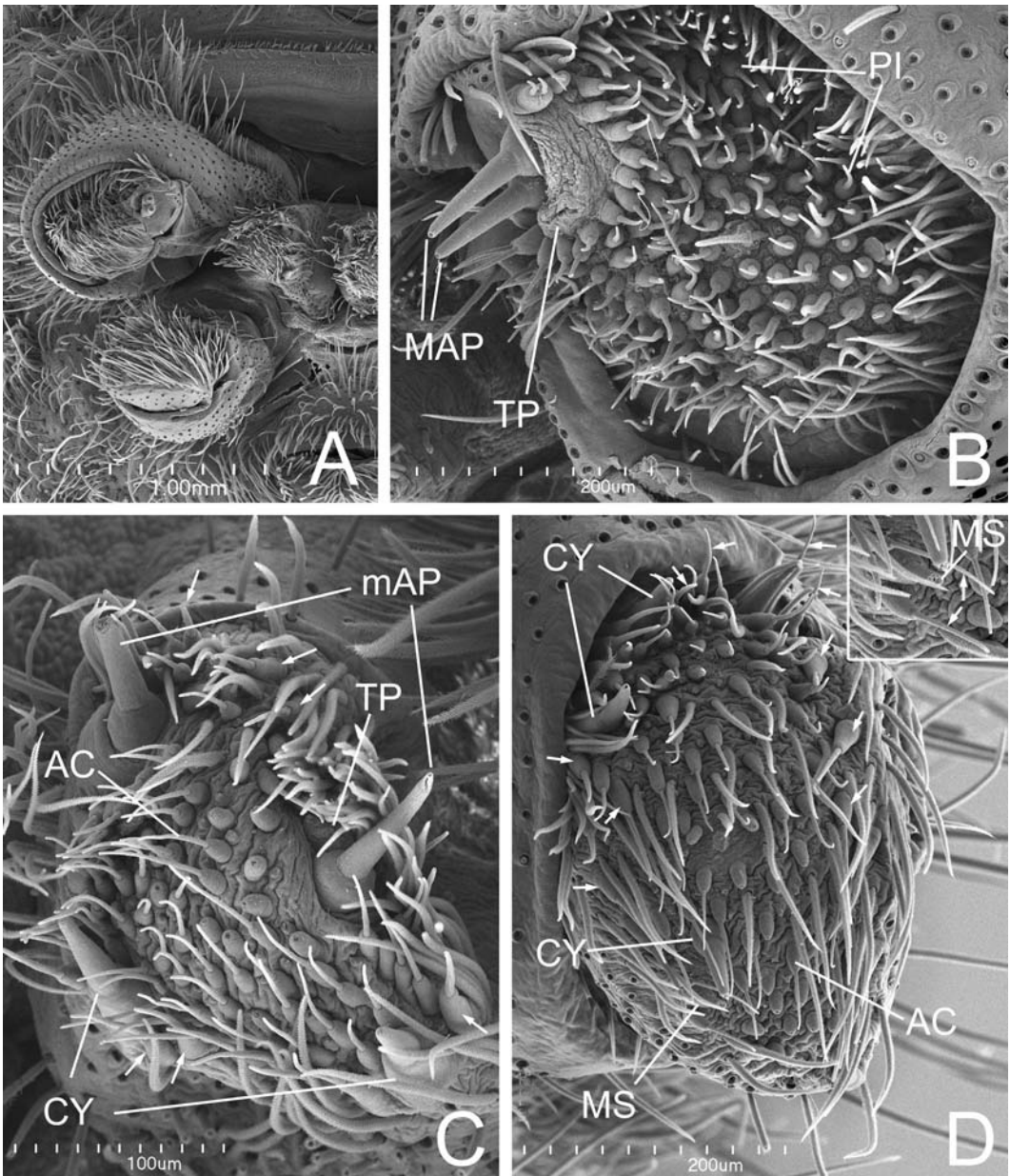


FIGURE 98. Spinnerets of female *Tengella radiata* from Guanacaste, Costa Rica. A. Right spinnerets, overview. B. Left ALS. C. Left PMS: Arrows to larger 'AC'. D. Right PLS. Arrows to larger 'AC'. Inset: MS and two flanking spigots (arrows). AC = aciniform gland spigot(s), CY = cylindrical gland spigot(s), MAP = major ampullate gland spigot(s), mAP = minor ampullate gland spigot(s), MS = PLS modified spigot, PI = piriform gland spigots, TP = tartipore(s). Scale bars: A = 100µm, B, D = 200µm, C = 100µm.

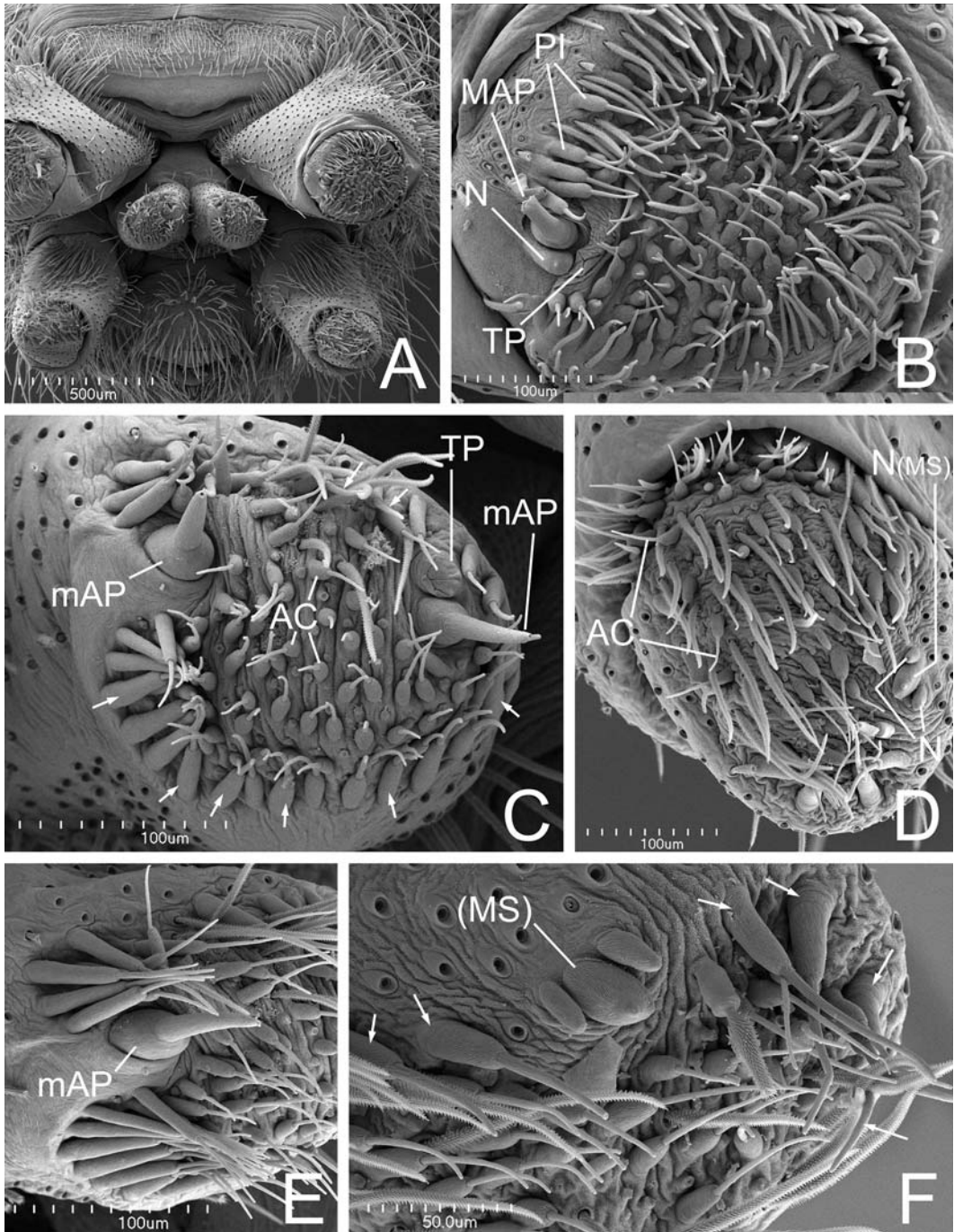


FIGURE 99. Left spinnerets of male *Tengella radiata* from Limón, Costa Rica. A. Spinnerets, overview. B. ALS. C. PMS. D. PLS. E. Detail of PMS, anterior view. F. Detail of PLS: arrows to larger 'AC'. Note the intermediate spigot-seta to the right of the MS nubbin. AC = aciniform gland spigot(s), MAP = major ampullate gland spigot(s), mAP = minor ampullate gland spigot(s), MS = nubbin of PLS modified spigot, N = MAP nubbin, PI = piriform gland spigots, TP = tartipore(s). Scale bars: A = 500µm, B-E = 100µm, F = 50µm.

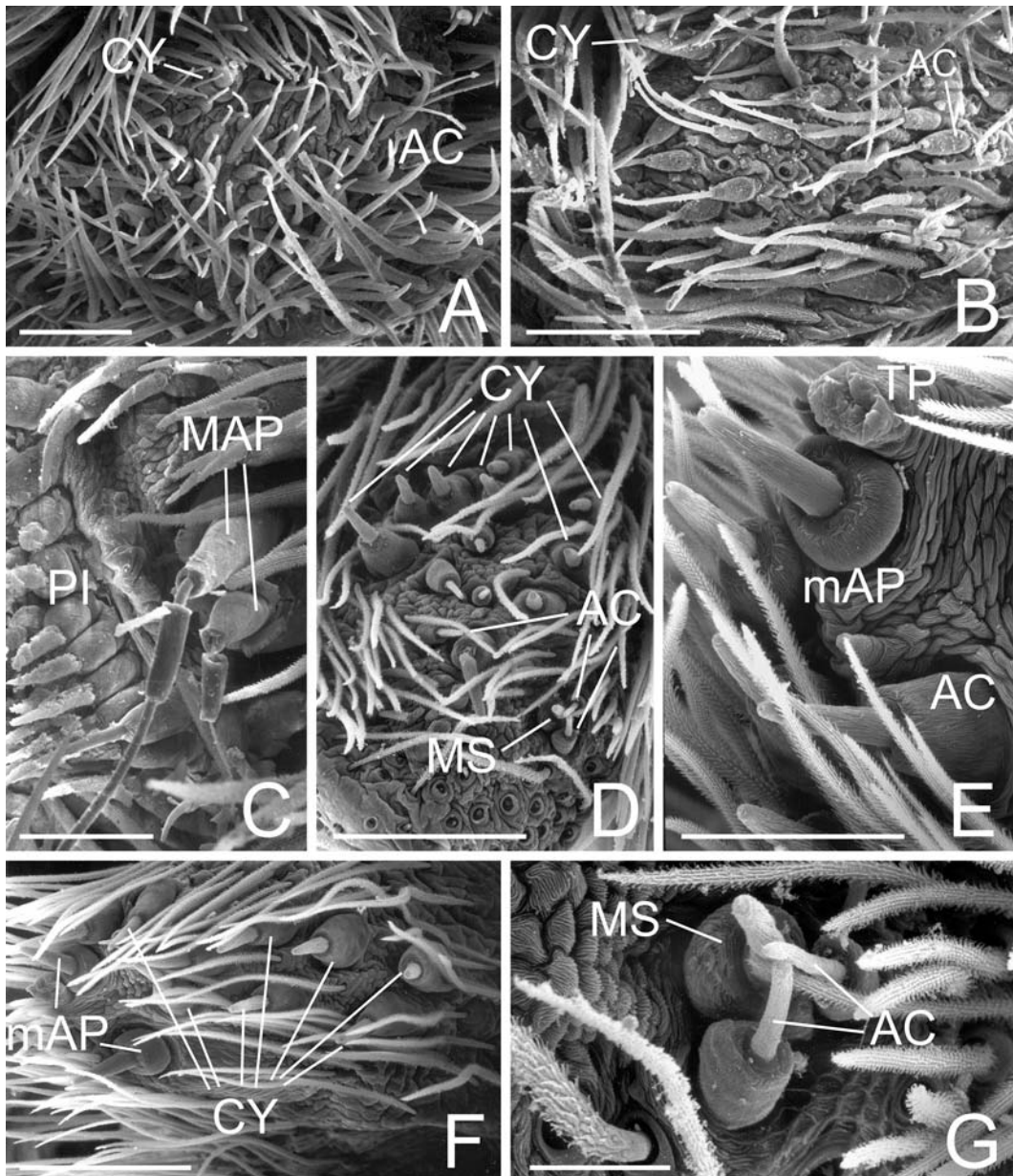


FIGURE 100. Spinnerets of female Tengellidae and Zoropsidae. A–C. *Tengella radiata* from La Selva, Costa Rica. A. Left PLS apex. B. Right PLS apex. C. Right ALS, MAP with broken shafts and PI. D–G. *Zoropsis spinimana* from Barcelona, Spain. D. Left PLS apex. E. PMS apex. F. Left PMS, posterior view. G. Left PLS, ectal. AC = aciniform gland spigot(s), CY = cylindrical gland spigot(s), MAP = major ampullate gland spigot(s), mAP = minor ampullate gland spigot(s), MS = PLS modified spigot, PI = piriform gland spigot(s), TP = tartipore(s). Scale bars: A, B, D, F = 100µm, C, E = 50µm, G = 20µm.

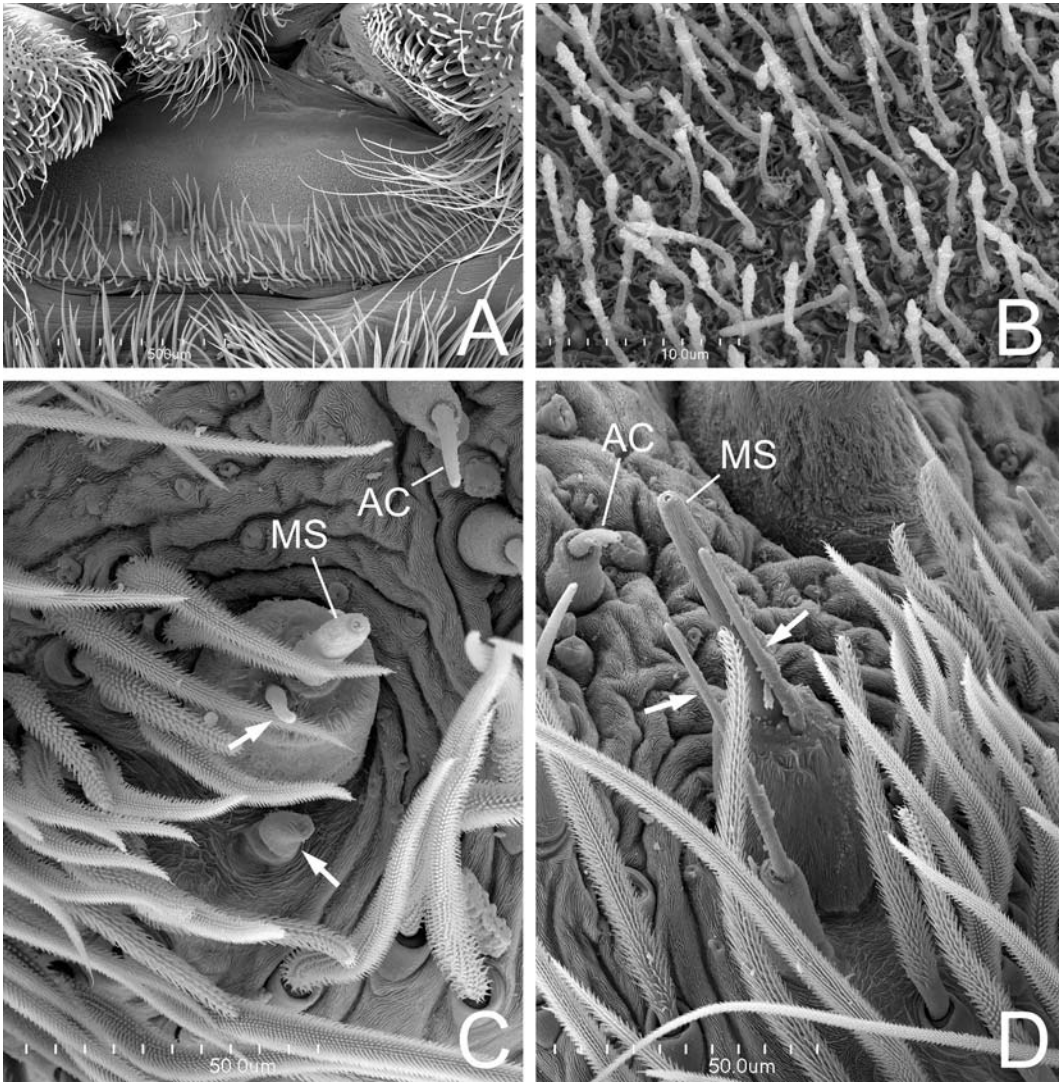


FIGURE 101. Spinnerets of female *Zoroocrates* cf. *mistus* from Los Llanos, Chiapas, Mexico. A. Cribellum. B. Cribellar spigots. C. Detail of left PLS, showing MS and nubbins of the two accompanying spigots (arrows). D. Detail of right PLS, showing MS and the two accompanying spigots (arrows), one of them arising from the MS base. AC = aciniform gland spigot(s), MS = PLS modified spigot. Scale bars: A = 50µm, B = 10µm, C, D = 50µm.

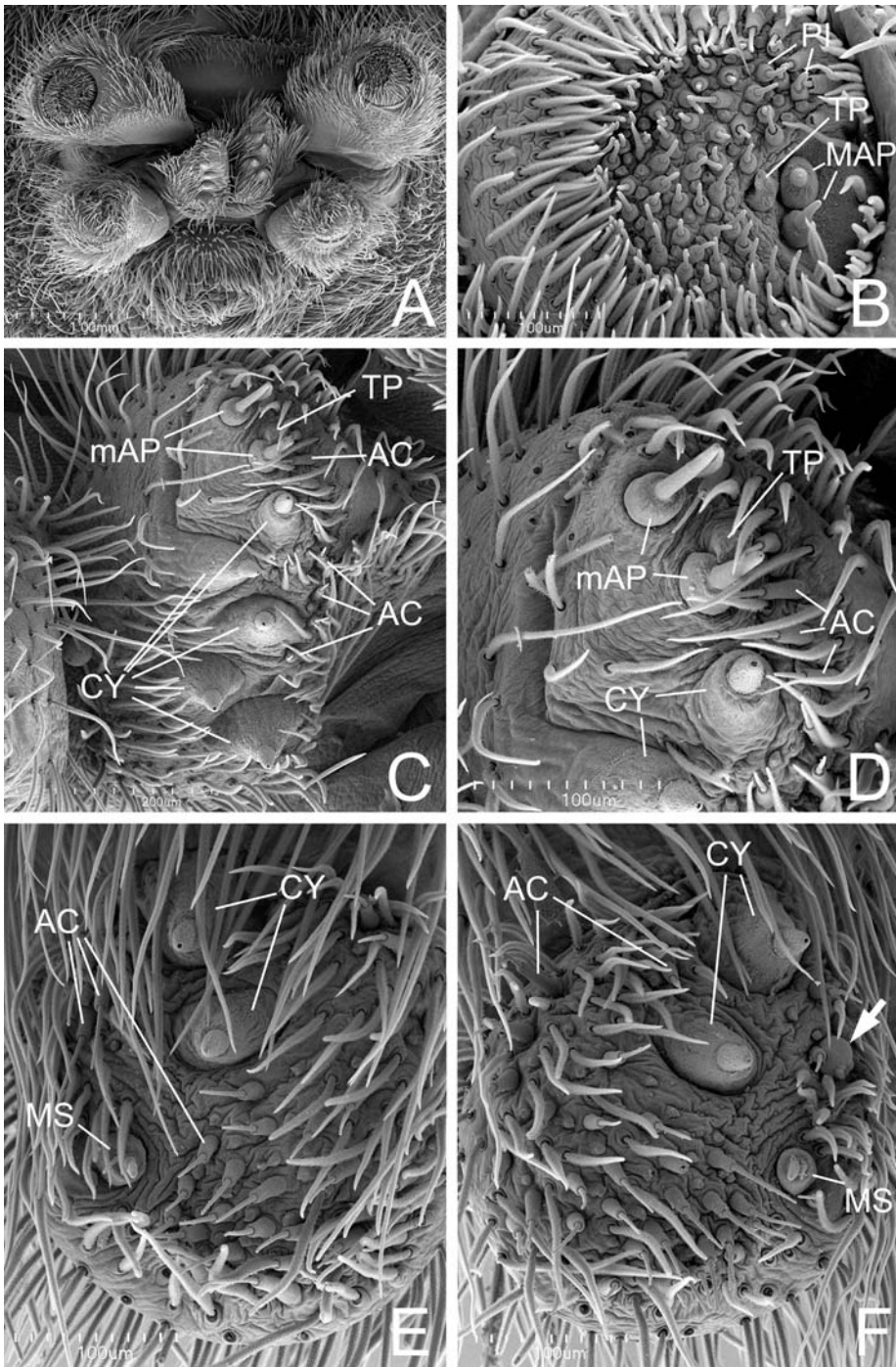


FIGURE 102. Spinnerets of female *Zorocrates* cf. *mistus* from Los Llanos, Chiapas, Mexico. A. Spinnerets. B. Right ALS. C. Left PMS, posterior view. D. Left PMS, detail. E. Right PLS. F. Left PLS (arrow to scar similar to a nubbin). AC = aciniform gland spigot(s), CY = cylindrical gland spigot(s), MAP = major ampullate gland spigot(s), mAP = minor ampullate gland spigot(s), MS = PLS modified spigot, TP = tartipore(s). Scale bars: A = 1.0mm, B, D—F = 100µm, C = 200µm.

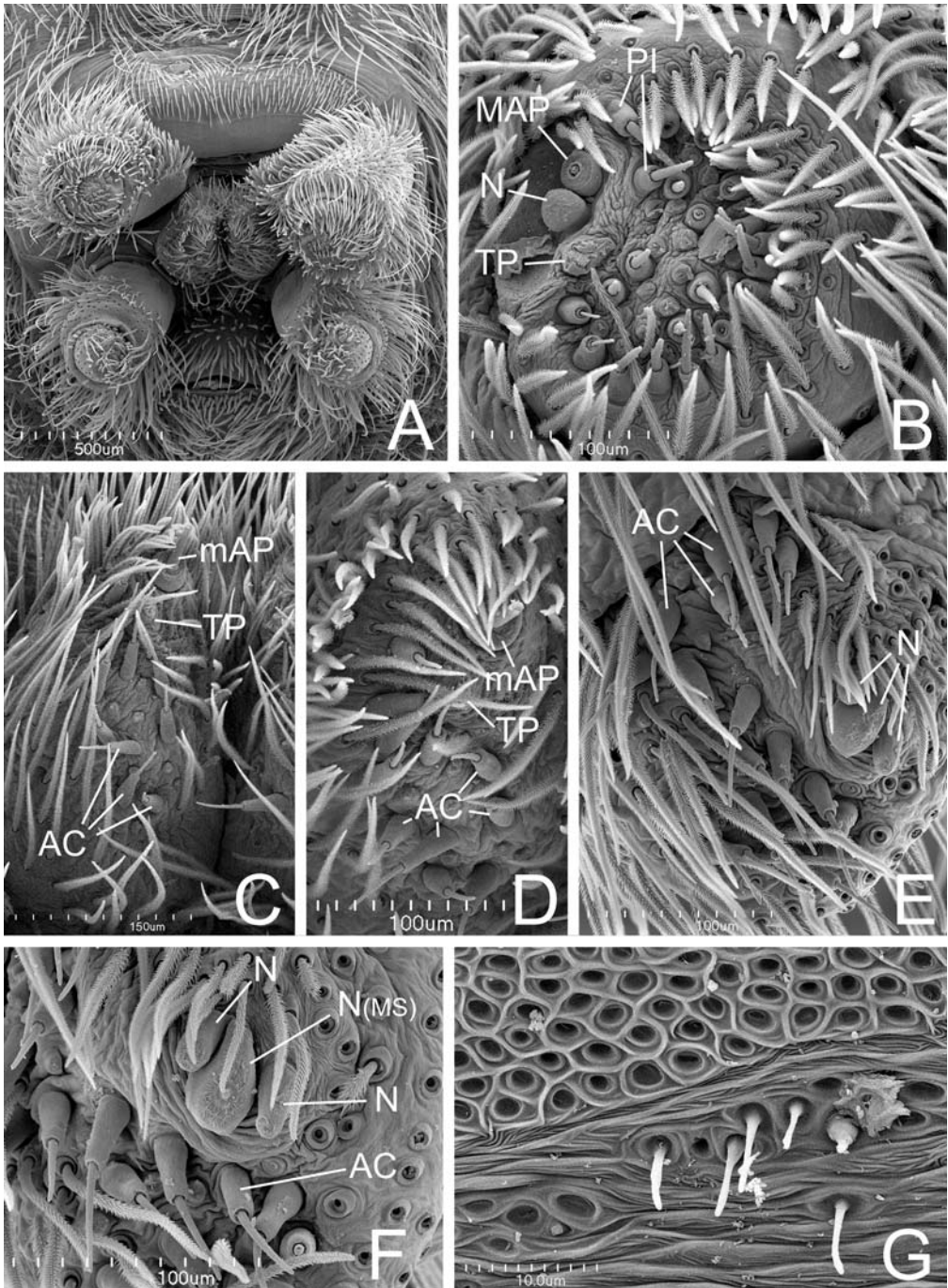


FIGURE 103. Spinnerets of male *Zorocrates* sp. from Big Bend National Park, Texas, USA. A. Spinnerets. B. Left ALS (MAP shaft broken). C. Right PMS, posterior view. D. Right PMS. E. Left PLS. F. Left PLS, detail of nubbin from MS and its accompanying spigots. G. Vestiges of cribellum. AC = aciniform gland spigot(s), MAP = major ampullate gland spigot(s), mAP = minor ampullate gland spigot(s), N = nubbin(s), PI = piriform gland spigots, TP = tartipore(s). Scale bars: A = 500µm, B, D—F = 100µm, C = 150µm, G = 10µm.

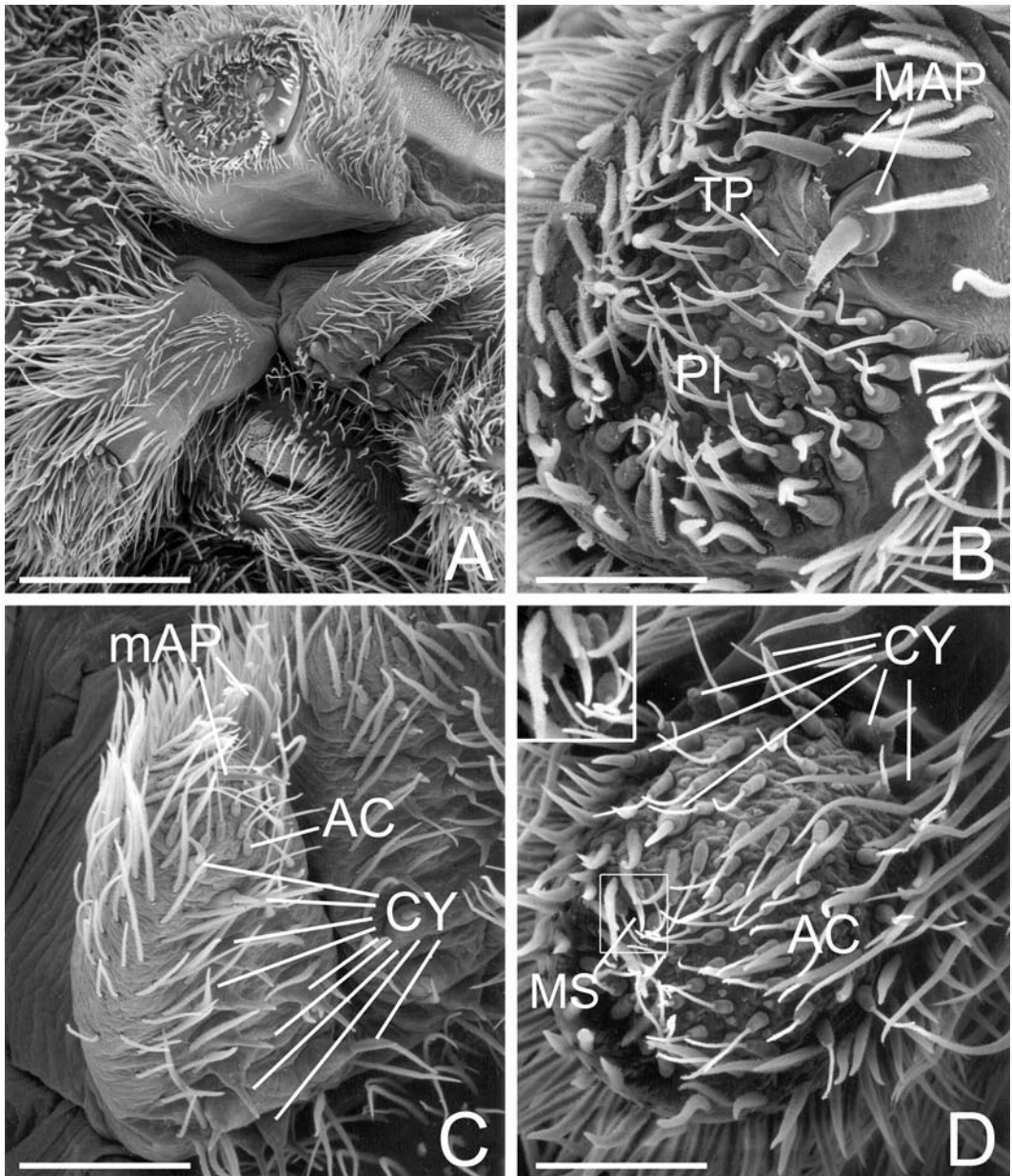


FIGURE 104. Right spinnerets of female *Uduba* sp. from Ranomafana, Madagascar. A. Overview. B. ALS. C. PMS. D. PLS. Inset: MS and two flanking spigots. AC = aciniform gland spigot(s), CY = cylindrical gland spigot(s), MAP = major ampullate gland spigot(s), mAP = minor ampullate gland spigot(s), MS = PLS modified spigot, PI = piriform gland spigot(s), TP = tartipore(s). Scale bars: A = 440 μ m, B, D = 100 μ m, C = 150 μ m.

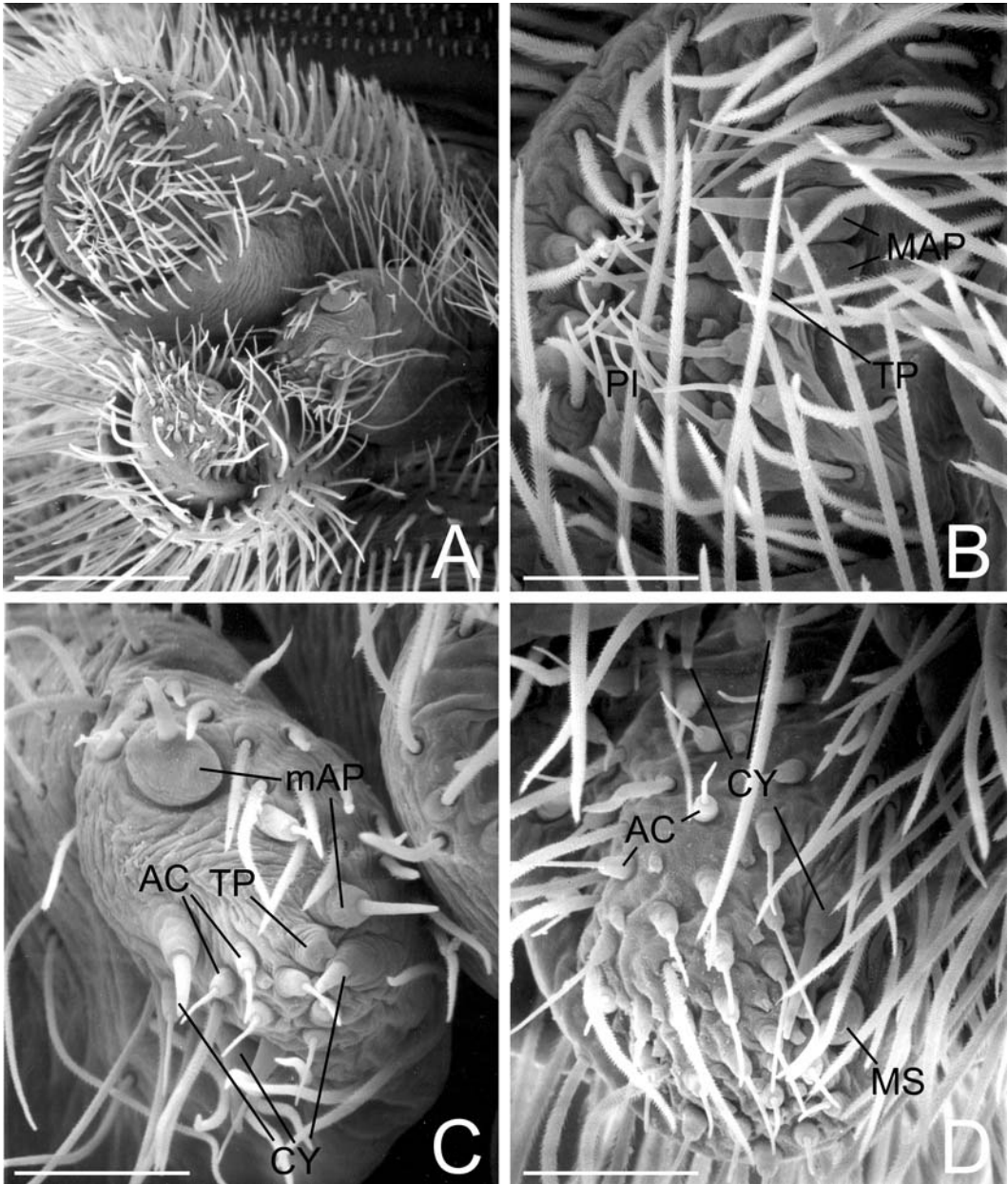


FIGURE 105. Right spinnerets of female *Raecius jocquei* paratype. A. Overview. B. ALS. C. PMS. D. PLS. AC = aciniform gland spigot(s), CY = cylindrical gland spigot(s), MAP = major ampullate gland spigot(s), mAP = minor ampullate gland spigot(s), MS = PLS modified spigot, PI = piriform gland spigot(s), TP = tartipore(s). Scale bars: A = 150 μ m, B–D = 43 μ m.

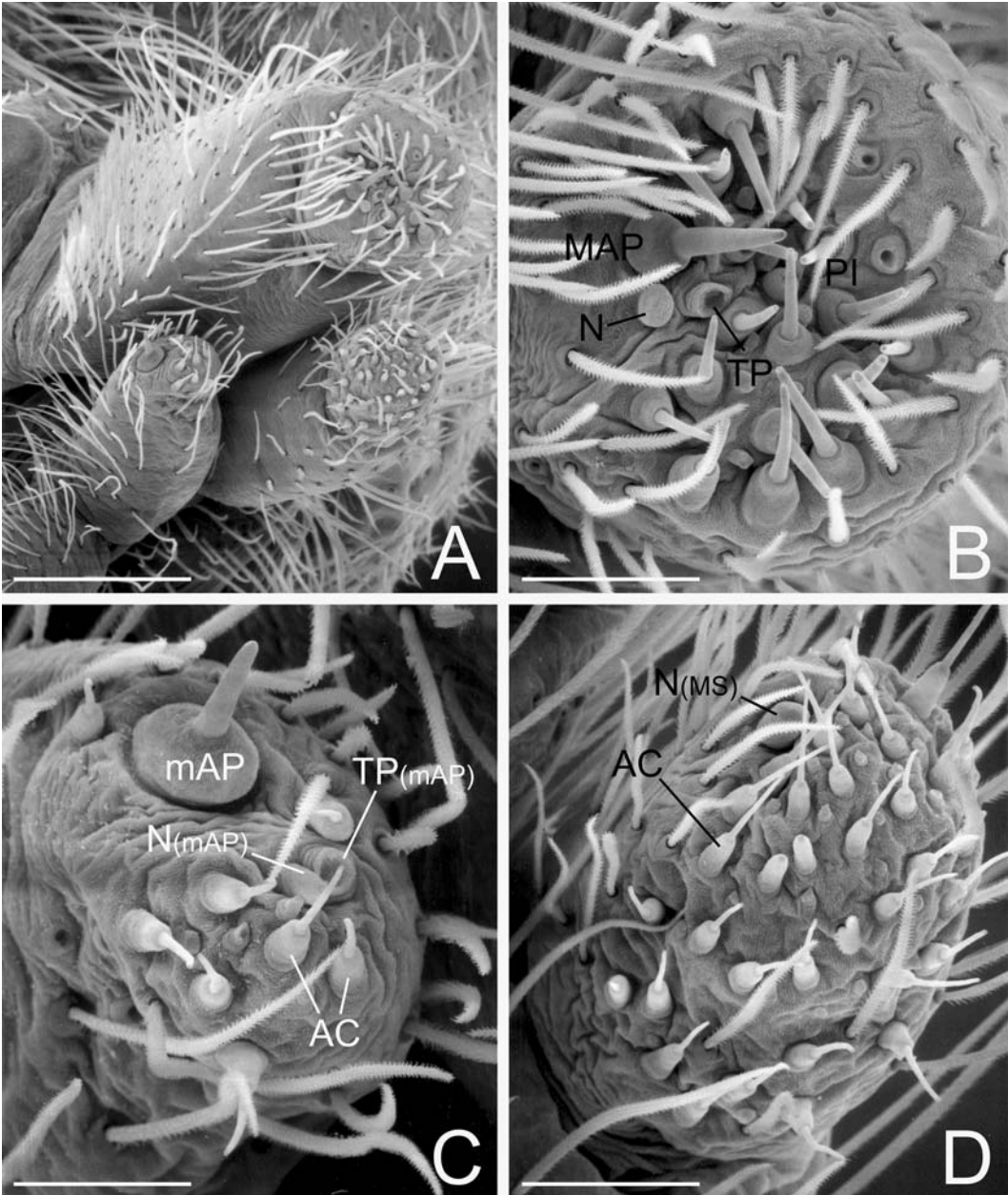


FIGURE 106. Left spinnerets of male *Raecius jocquei* paratype. A. Overview. B. ALS. C. PMS. D. PLS. AC = acini-form gland spigot(s), MAP = major ampullate gland spigot(s), mAP = minor ampullate gland spigot(s), mAP N = minor ampullate gland nubbin, MS N = nubbin of PLS modified spigot, N = MAP nubbin, PI = piriform gland spigot(s), TP = tar-tipore(s). Scale bars: A = 150µm, B–D = 43µm.

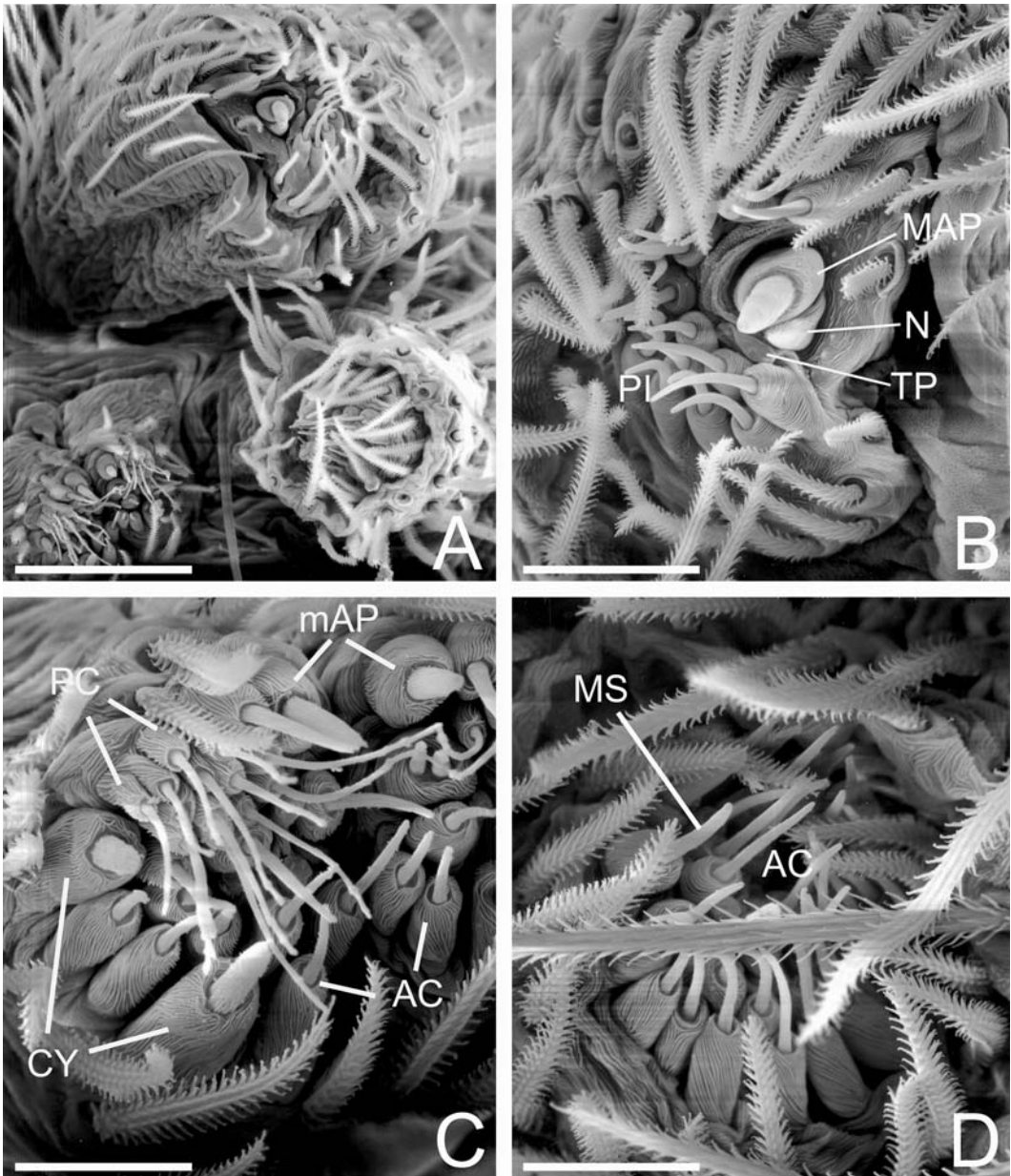


FIGURE 107. Spinnerets of female *Poaka graminicola* from Lincoln, New Zealand. A. Left overview. B. Right ALS. C. PMS. D. Right PLS. AC = aciniform gland spigot(s), CY = cylindrical gland spigot(s), MAP = major ampullate gland spigot(s) and nubbin, mAP = minor ampullate gland spigot(s), MS = PLS modified spigot, PC = paracribellar spigot, PI = piriform gland spigot(s), TP = tartipores. Scale bars: A = 75µm, B = 30µm, C, D = 20µm.

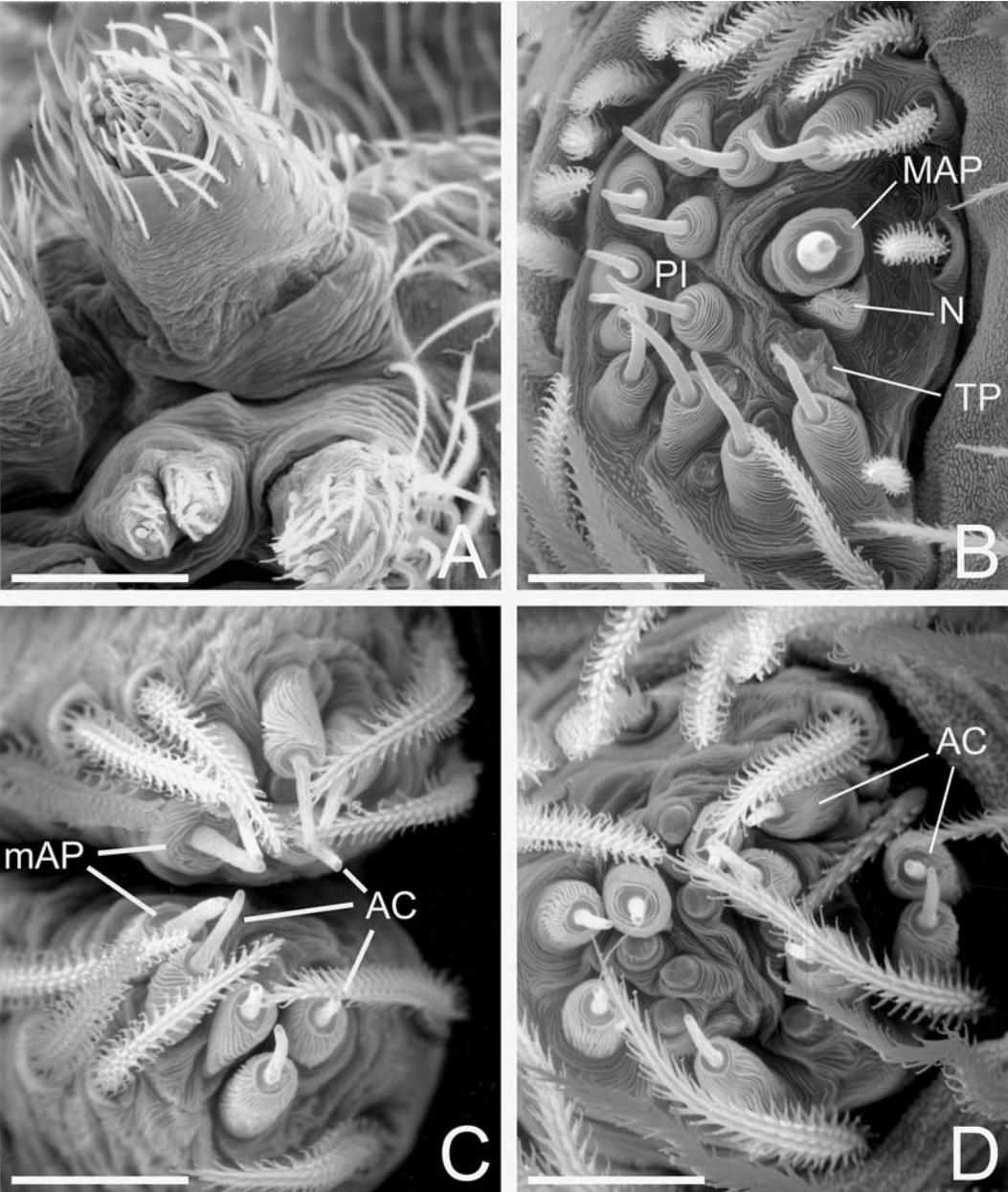


FIGURE 108. Spinnerets of male *Poaka gramnicola* from Lincoln, New Zealand. A. Left overview. B. Right ALS. C. PMS. D. Right PLS. AC = aciniform gland spigot(s), MAP = major ampullate gland spigot and nubbin, mAP = minor ampullate gland spigot(s), PI = piriform gland spigot(s), TP = tartipores. Scale bars: A = 100µm, B = 20µm, C, D = 15µm.

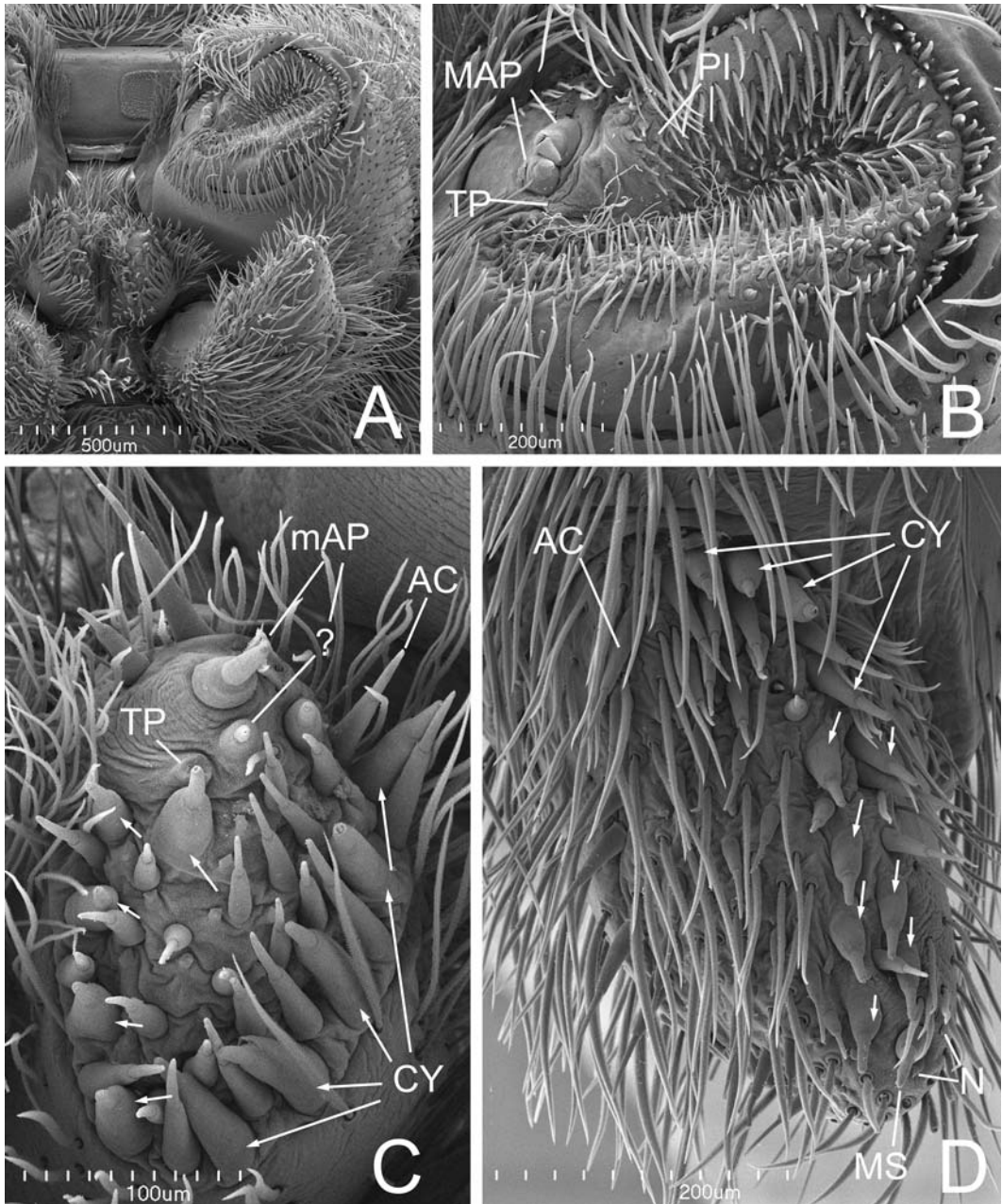


FIGURE 109. Left spinnerets of female *Psechrus argentatus* from Cape Vogel Peninsula, Papua New Guinea. A. Spinneret overview. B. ALS. C. PLS. D. PLS. AC = aciniform gland spigots, CY = cylindrical gland spigot(s), MAP = major ampullate gland spigot(s), mAP = minor ampullate gland spigot(s), MS = PLS modified spigot, PI = piriform gland spigots, TP = tartipore(s). Scale bars: A = 500µm, B, D = 200µm, C = 100µm.

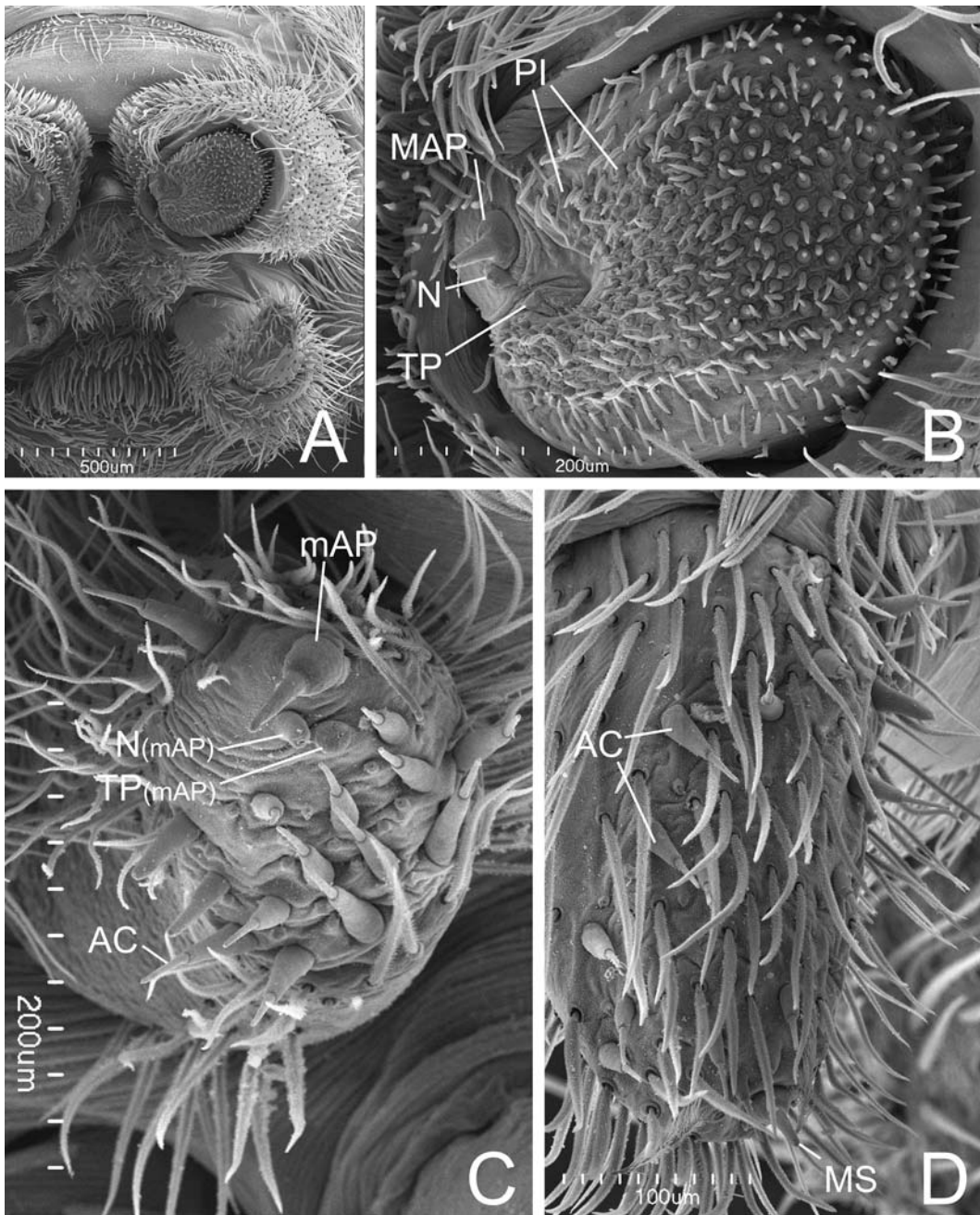


FIGURE 110. Left spinnerets of male *Psecurus argentatus* from Cape Vogel Peninsula, Papua New Guinea. A. Spinneret overview. B. ALS. C. PMS. D. PLS. AC = aciniform gland spigot(s), MAP = major ampullate gland spigot(s), mAP = minor ampullate gland spigot(s), MS = nubbin of PLS modified spigot, N = nubbin, PI = piriform gland spigot(s), TP = tartipore(s). Scale bars: A = 500µm, B, C = 200µm, D = 100µm.

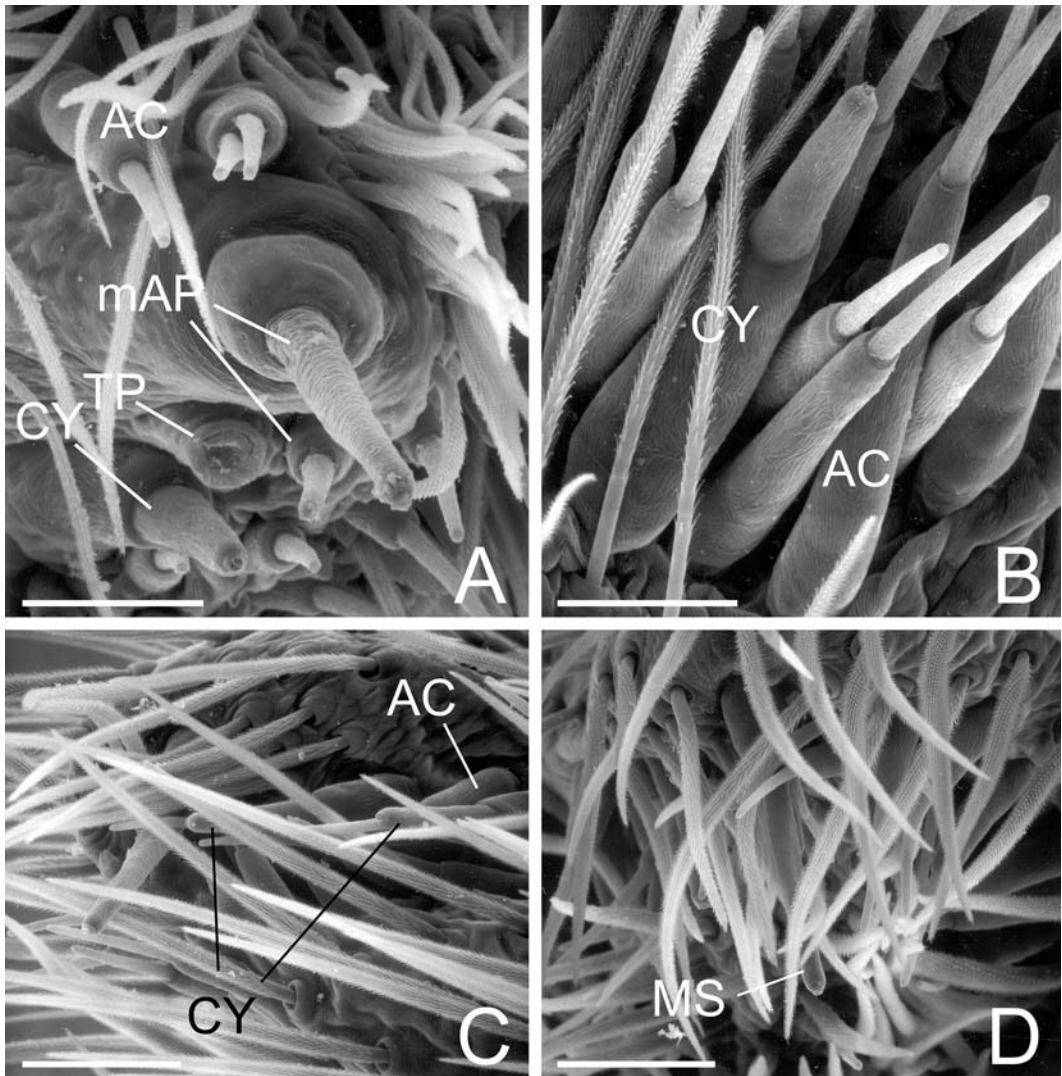


FIGURE 111. Spinnerets of female *Psechrus* sp. from Tham Lot Cave, Thailand. A. Left PMS apex. B. Base of right PMS. C. Left PLS base. D. Left PLS apex. AC = aciniform gland spigot(s), CY = cylindrical gland spigot(s), mAP = minor ampullate gland spigot(s), MS = PLS modified spigot, TP = tartipores. Scale bars: A, B = 30 μ m, C, D = 43 μ m.

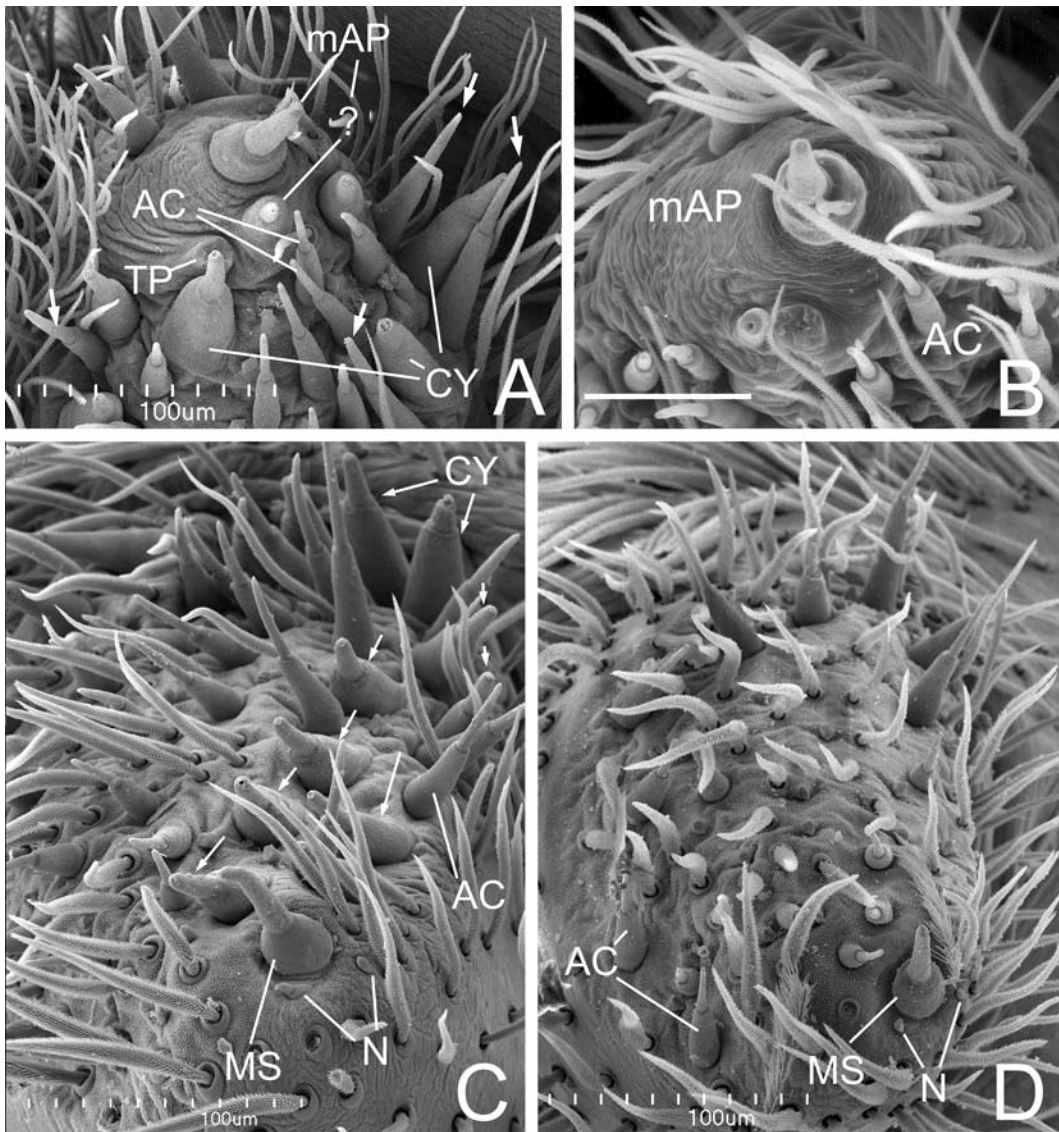
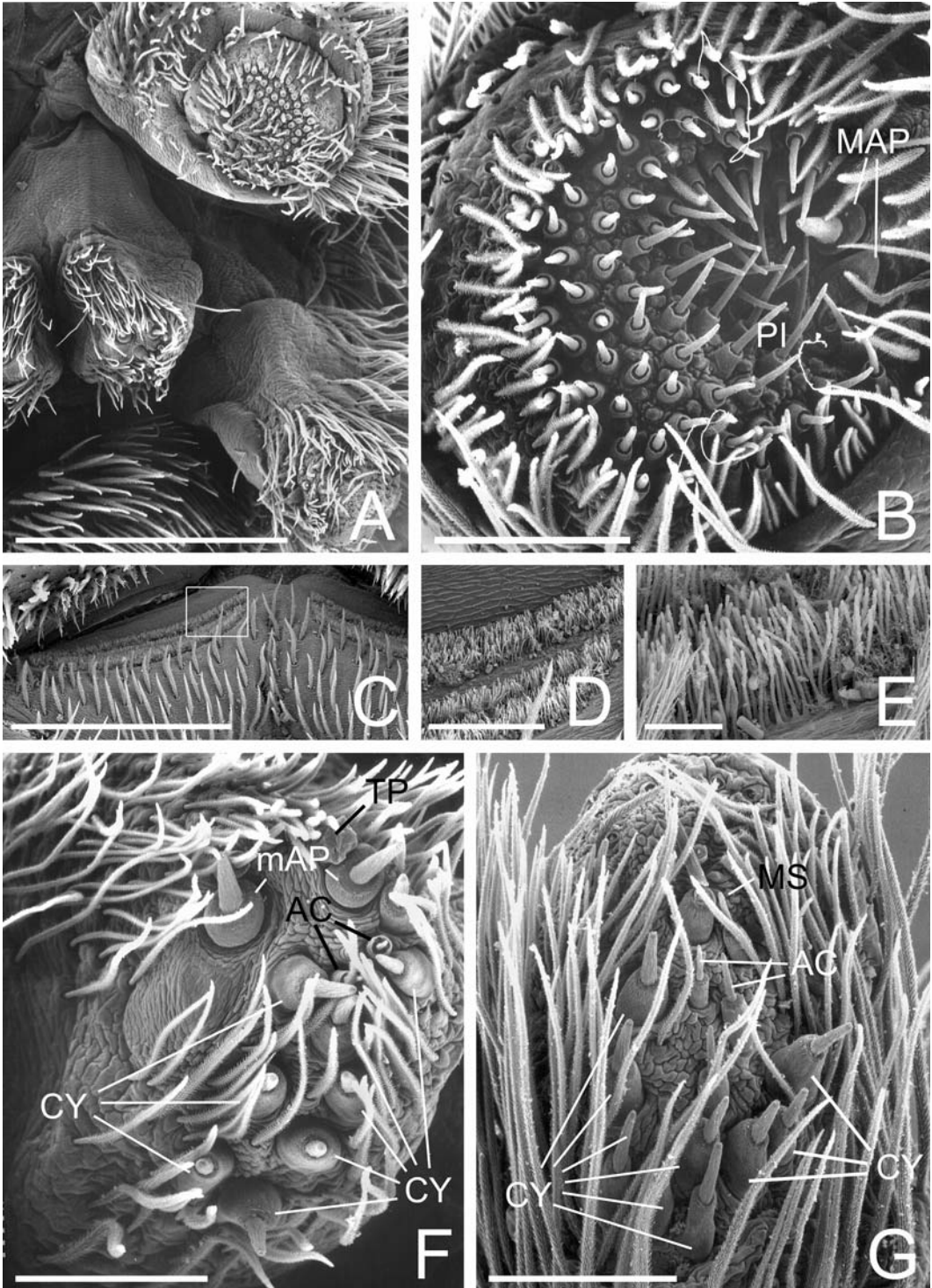


FIGURE 112. Details of left spinnerets of *Psechrus* spp. A, C, D. *Psechrus argentatus* from Cape Vogel Peninsula, Papua New Guinea. B. PMS of male *Psechrus* sp. from Tham Lot Cave, Thailand. A. Female PMS: arrows to larger AC (or smaller CY). C. Female PLS: the nubbins at sides of the MS are small, similar to the tartipores among the AC. D. Male PLS: note the two small nubbins as in the female. AC = aciniform gland spigot(s), CY = cylindrical gland spigot(s), mAP = minor ampullate gland spigot(s), MS = PLS modified spigot, N = nubbin, TP = tartipore(s). Scale bars: A, C, D = 100µm, B = 43µm.



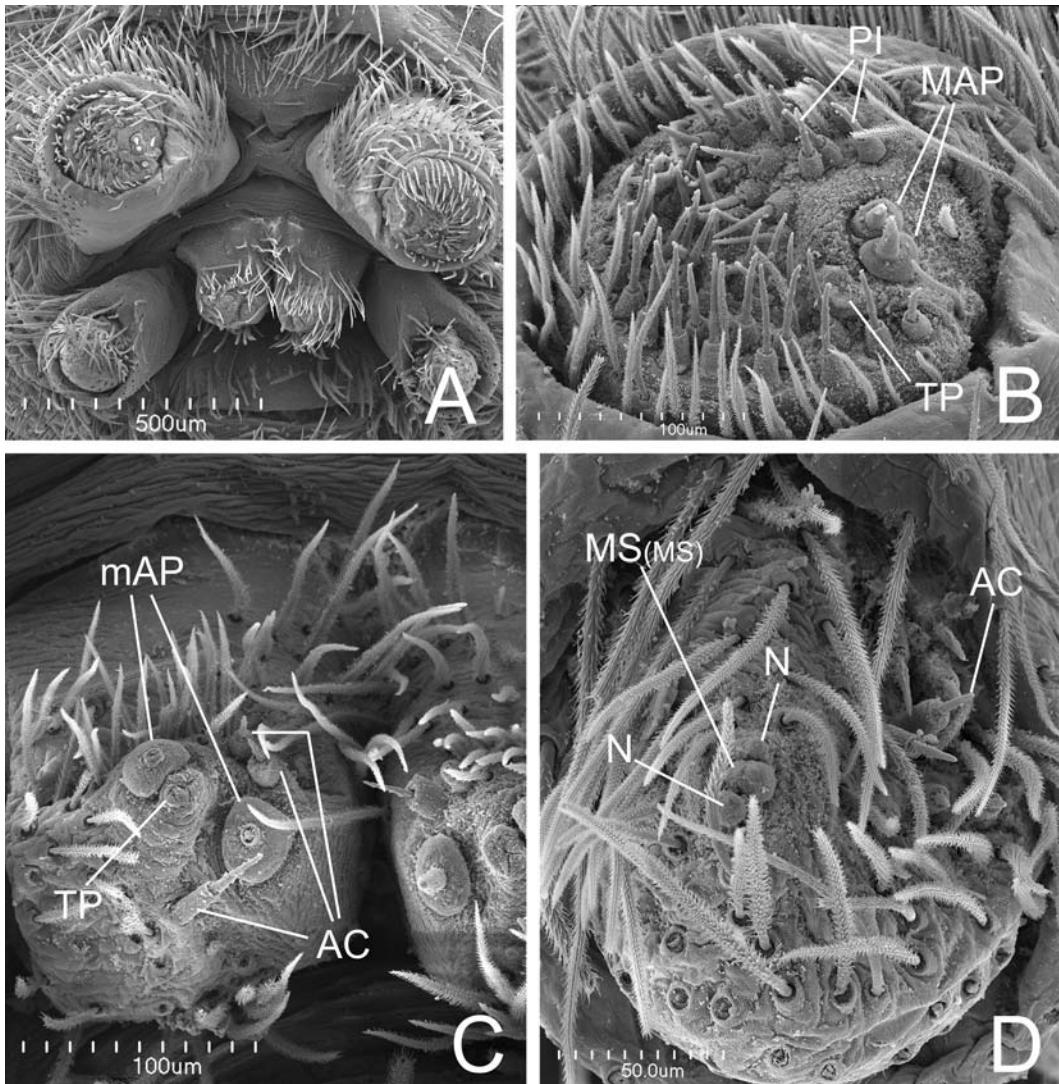


FIGURE 114 (above). Spinnerets of male *Zoropsis rufipes* from Tenerife, Canary Islands. A. Overview. B. Right ALS. C. Right PMS. D. Right PLS. AC = aciniform gland spigot(s), MAP = major ampullate gland spigot(s), mAP = minor ampullate gland spigot(s), MS = PLS modified spigot nubbins, N = nubbins, PI = piriform gland spigots, TP = tartipore(s). Scale bars: A = 500µm, B, C = 100µm, D = 50µm.

FIGURE 113 (left). Spinnerets of female *Zoropsis spinimana* from Barcelona, Spain (A, B, F, G) and Canary Islands (C–E). A. Left overview. B. Right ALS. C. Cribellum. D. Detail of cribellum, showing the transversal bands of spigots. E. Detail of cribellar spigots. F. Left PMS. G. Left PLS. AC = aciniform gland spigot(s), CY = cylindrical gland spigot(s), MAP = major ampullate gland spigot(s), mAP = minor ampullate gland spigot(s), MS = PLS modified spigot, PI = piriform gland spigot(s), TP = tartipore(s). Scale bars: A = 500µm, B, F, G = 100µm, C = 300µm, D = 50µm, E = 10µm.

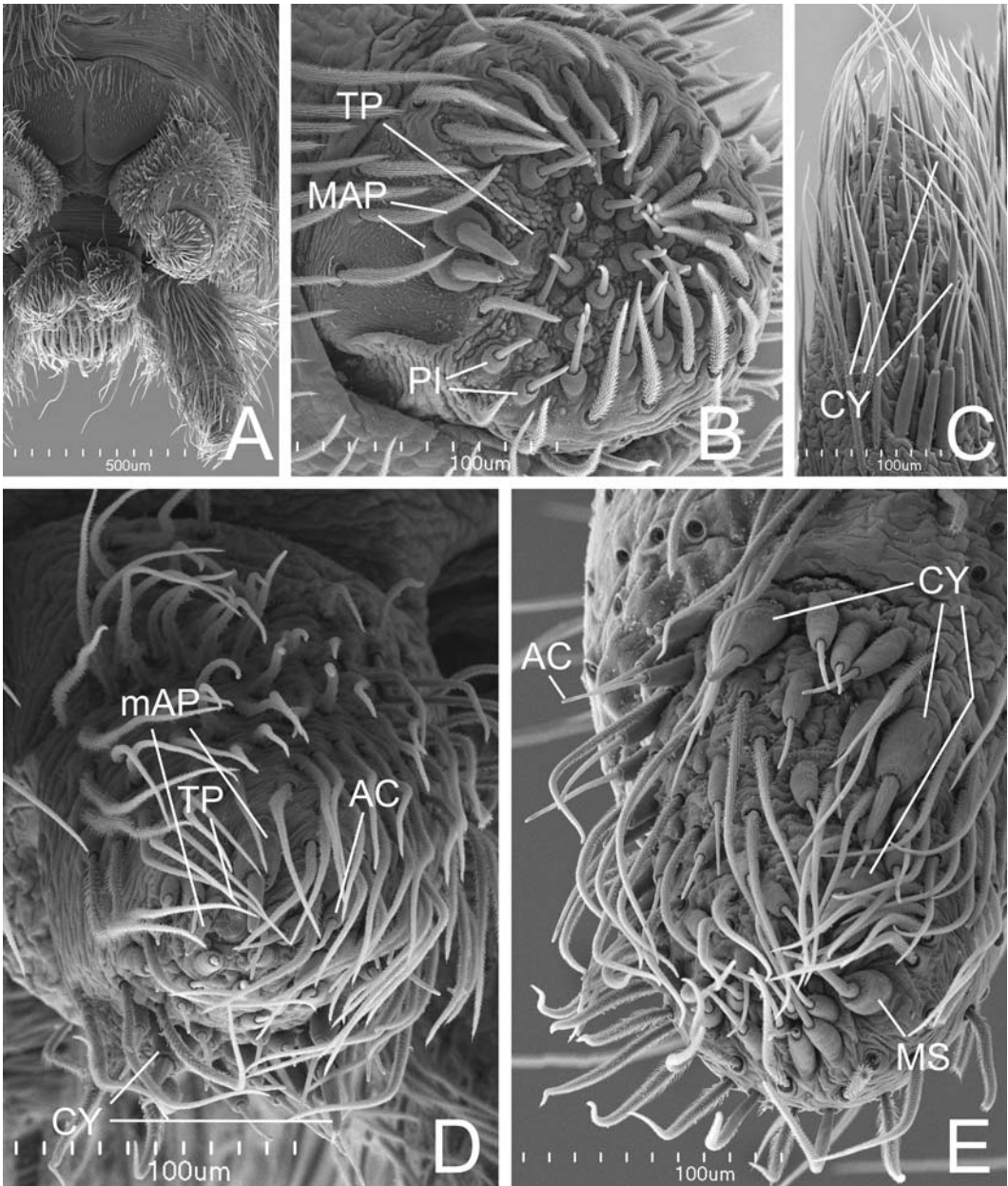


FIGURE 115. Left spinnerets of female *Acanthoctenus* cf. *spinipes* from Loreto, Peru. A. Spinnerets, overview. B. ALS. C. PMS, posterior view. D. PMS. E. PLS. AC = aciniform gland spigots, CY = cylindrical gland spigot(s), MAP = major ampullate gland spigot(s), mAP = minor ampullate gland spigot(s), MS = PLS modified spigot, PI = piriform gland spigots, TP = tartipore(s). Scale bars: A = 500µm, B–E = 100µm.

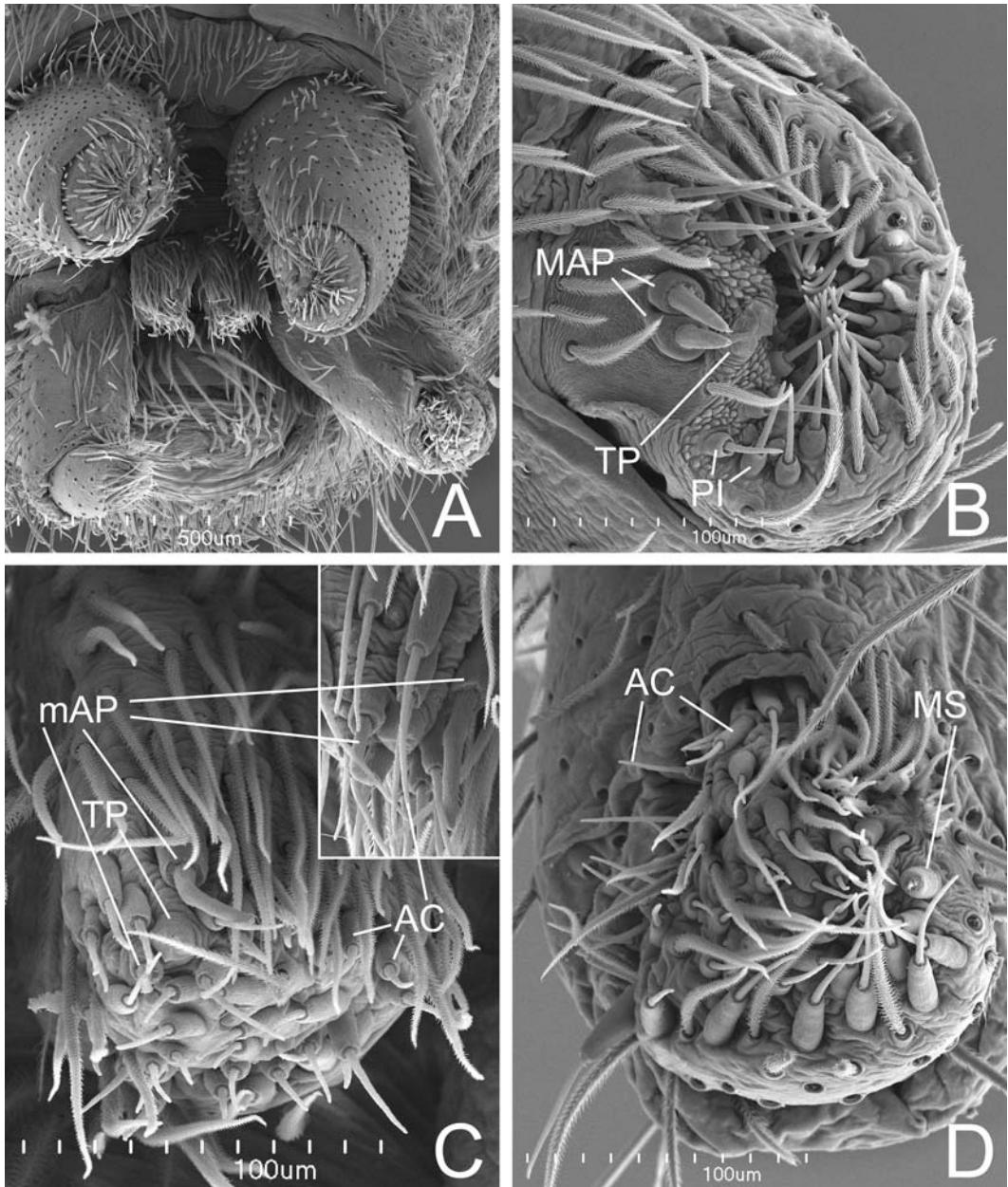


FIGURE 116. Spinnerets of male *Acanthoctenus* cf. *spinipes* from Loreto, Peru. A. Spinnerets, overview. B. Left ALS. C. Left PMS, inset of mAP, lateral. D. Right PLS (inverted). AC = aciniform gland spigots, MAP = major ampullate gland spigot(s), mAP = minor ampullate gland spigot(s), MS = PLS modified spigot nubbin, PI = piriform gland spigots, TP = tartipore(s). Scale bars: A = 500µm, B–D = 100µm.

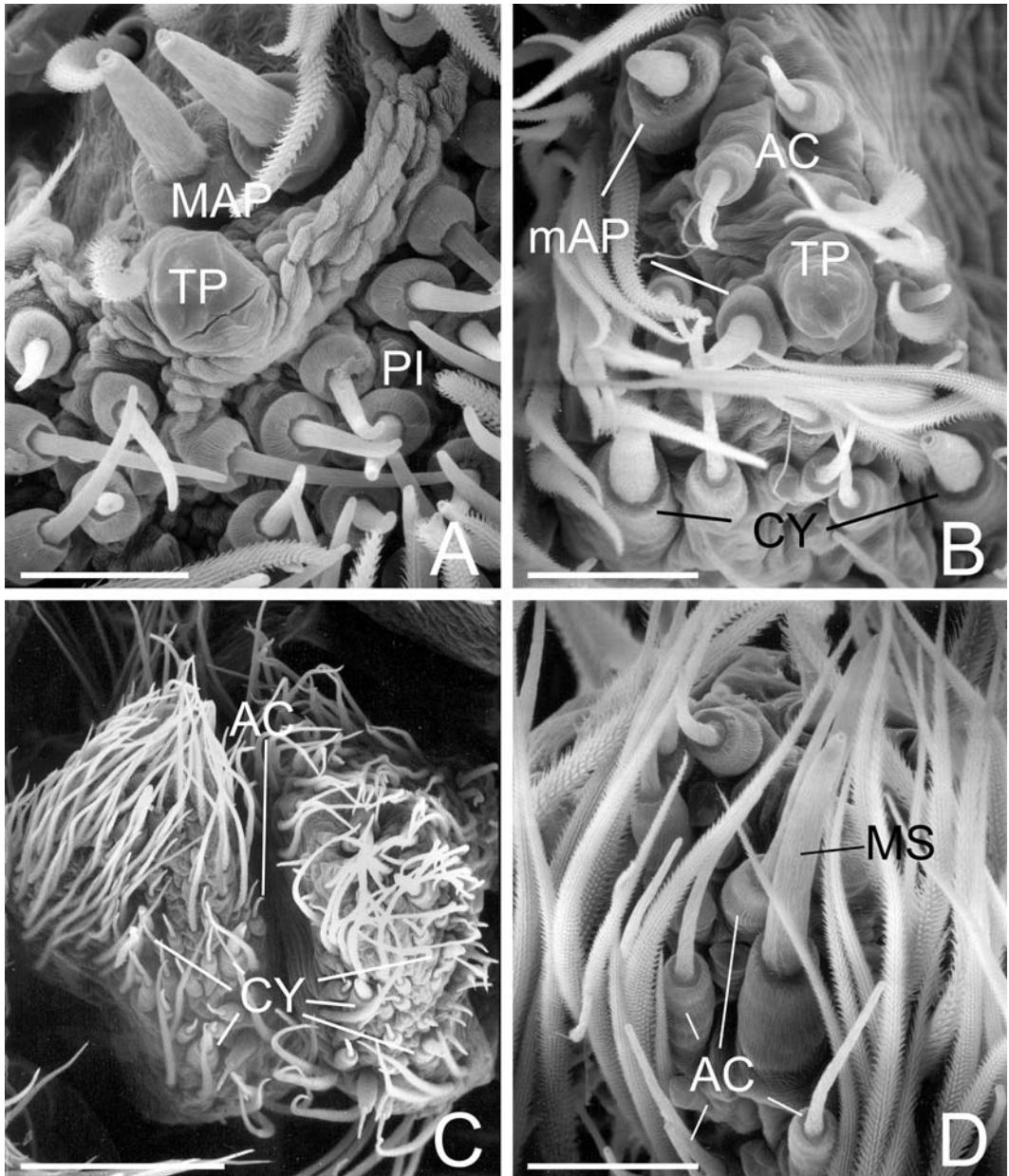


FIGURE 117. *Acanthoetus* female spinnerets. A, B, D. Changuinola, Panama. C. Ecuador. A. ALS. B. PMS. C. PMS. D. Right PLS apex. AC = aciniform gland spigot(s), CY = cylindrical gland spigot(s), MAP = major ampullate gland spigot(s), mAP = minor ampullate gland spigot(s), MS = PLS modified spigot, PI = piriform gland spigot(s), TP = tartipore(s). Scale bars: A, B, D = 25 μ m, C = 100 μ m.

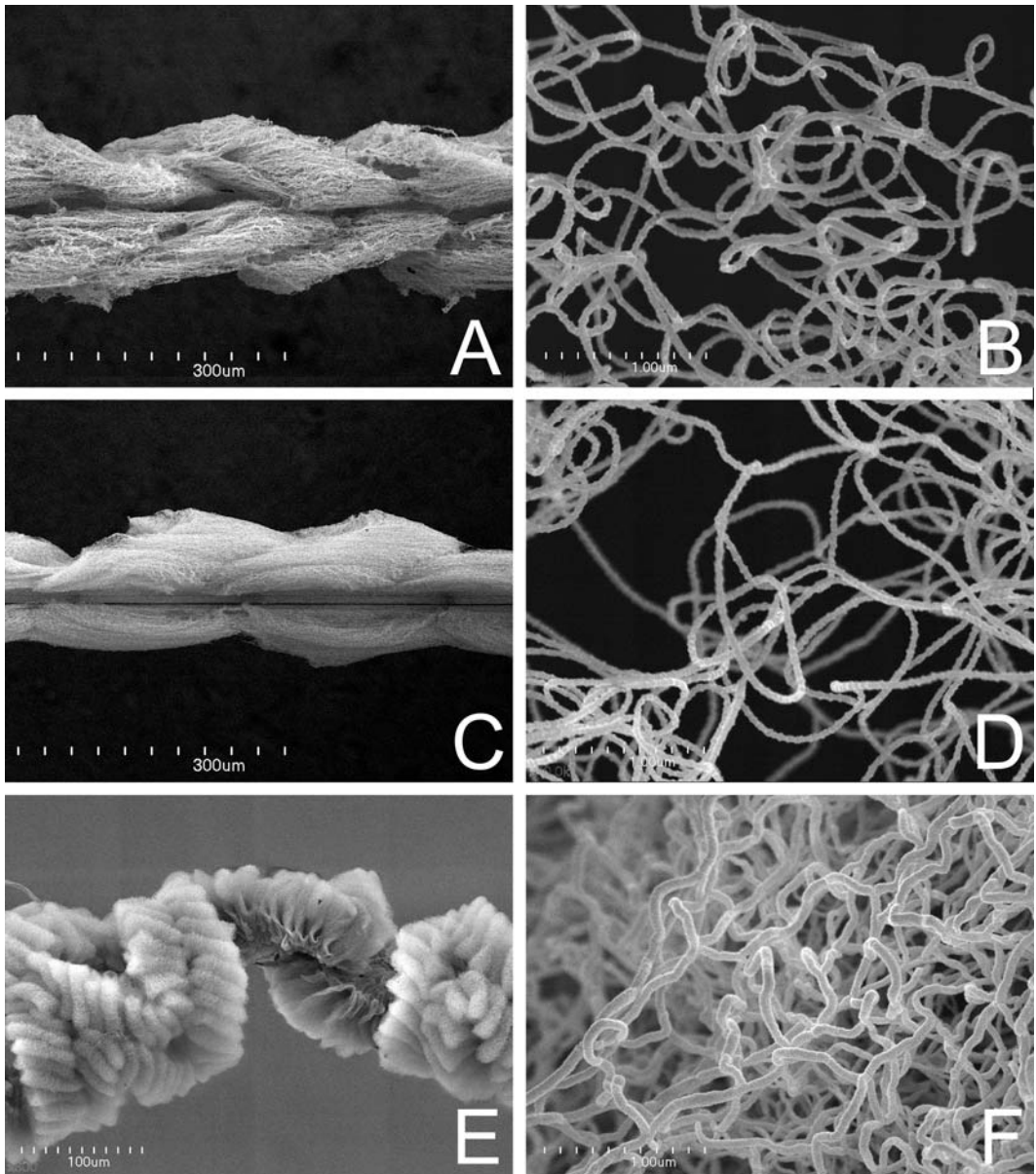


FIGURE 118. Cribellate silk, SEM images. A, B. *Hickmania troglodytes* from L. Trimmer Cave, Tasmania, Australia. C, D. *Thaida peculiaris* from Puerto Blest, Argentina. E, F. *Kukulcania* sp. from Buenos Aires, Argentina. A, C, E. Hacked band. B, D, F. Close up of cribellar fibrils. All appear to be round in cross section. Note nodules on fibrils of *Hickmania* and *Thaida*, and lack of nodules on *Kukulcania* fibrils. Scale bars: A, C = 300µm, B, D, F = 1.0µm, E = 100µm.

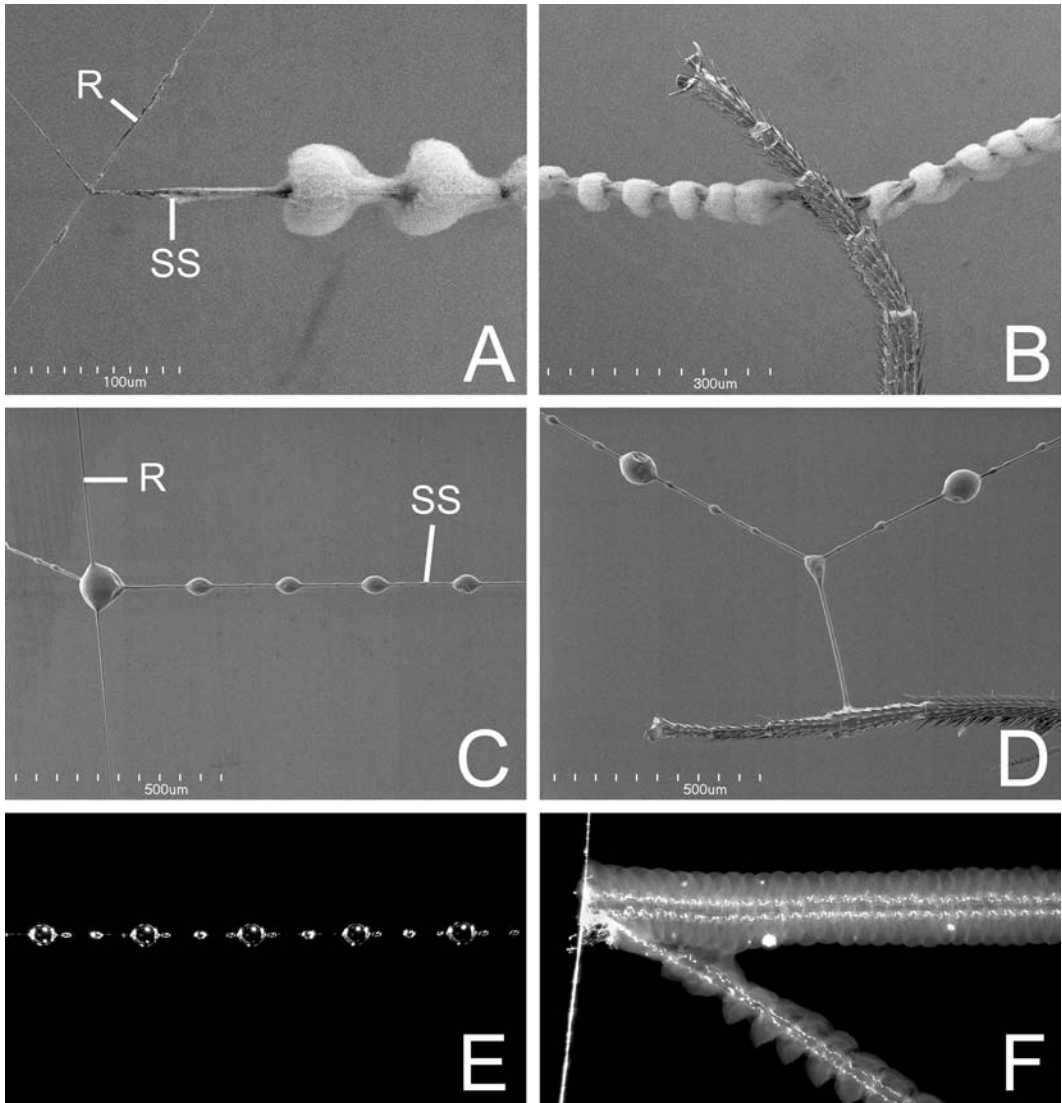


FIGURE 119. Sticky silk. A, B, F. Cribellate. C–E. Viscid. A–D. SEM. D, E. Photomicrographs. A, B. *Uloborus* sp. male subadult from Sodwana Bay, South Africa. A. SS and R. B. Insect leg attached to SS. C, D, E. *Nephila* sp. female from Sodwana Bay, South Africa. C. SS and R. D. Insect leg attached to SS. E. Close up of SS showing drops of glue. F. *Thaidia peculiaris* from Puerto Blest, Argentina, puffed cribellate band. R = radius, SS = sticky spiral. Scale bars: A = 100 μ m, B = 300 μ m, C, D = 500 μ m.

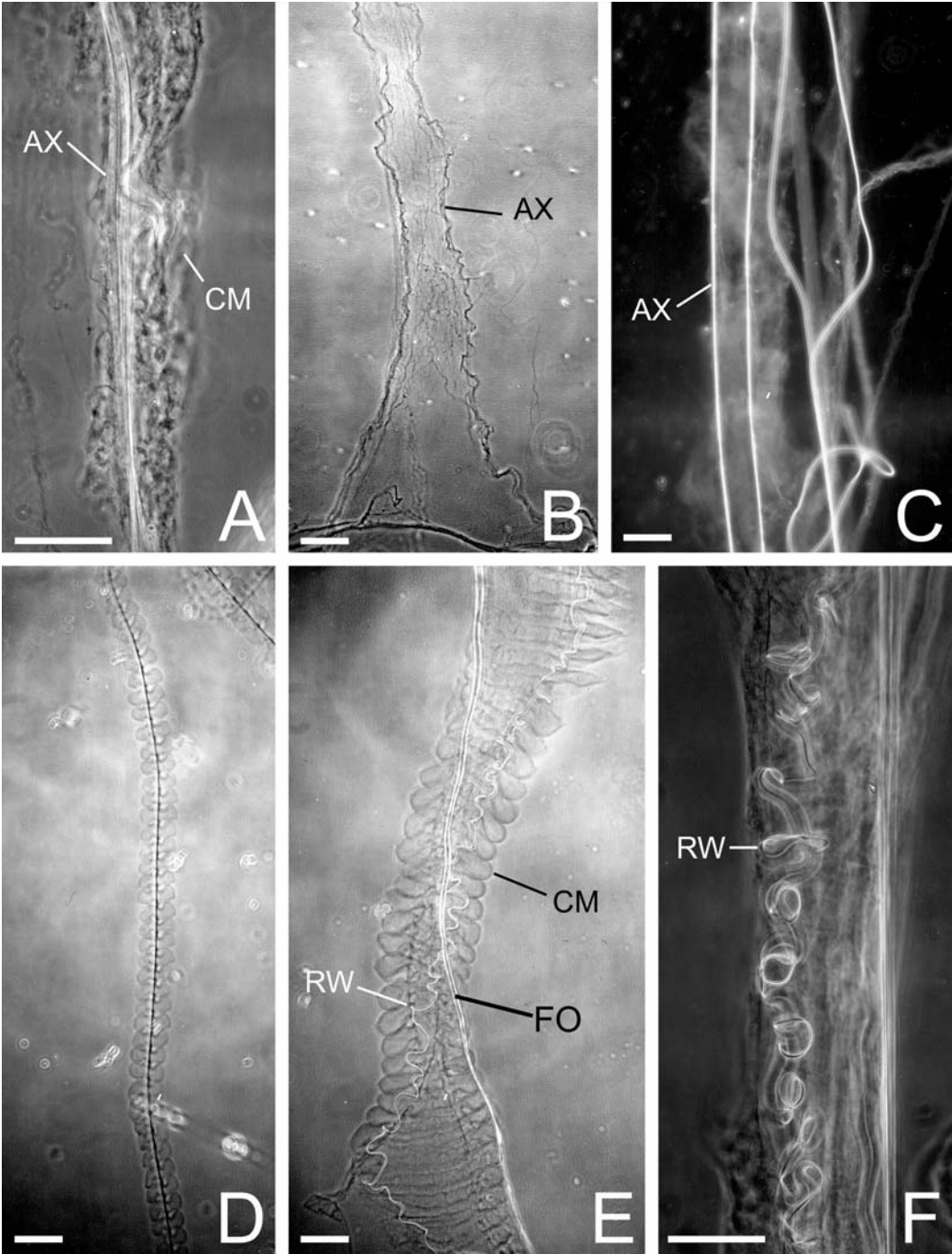


FIGURE 120. Cribellate silk. A–C. *Hickmania troglodytes* from Newdegate Cave, Tasmania, Australia. D. *Hyptiotes* sp. from Cazadero, California, USA, showing puffed cribellar band. E–F. *Mallos* sp. from Mt. Lemon, Arizona, USA, showing puffed cribellar band. AX = axial fibers, CM = cribellar fiber mass, FO = foundation line, RW = reserve warp. Scale bars: A, F = 100µm, B–E 50µm.

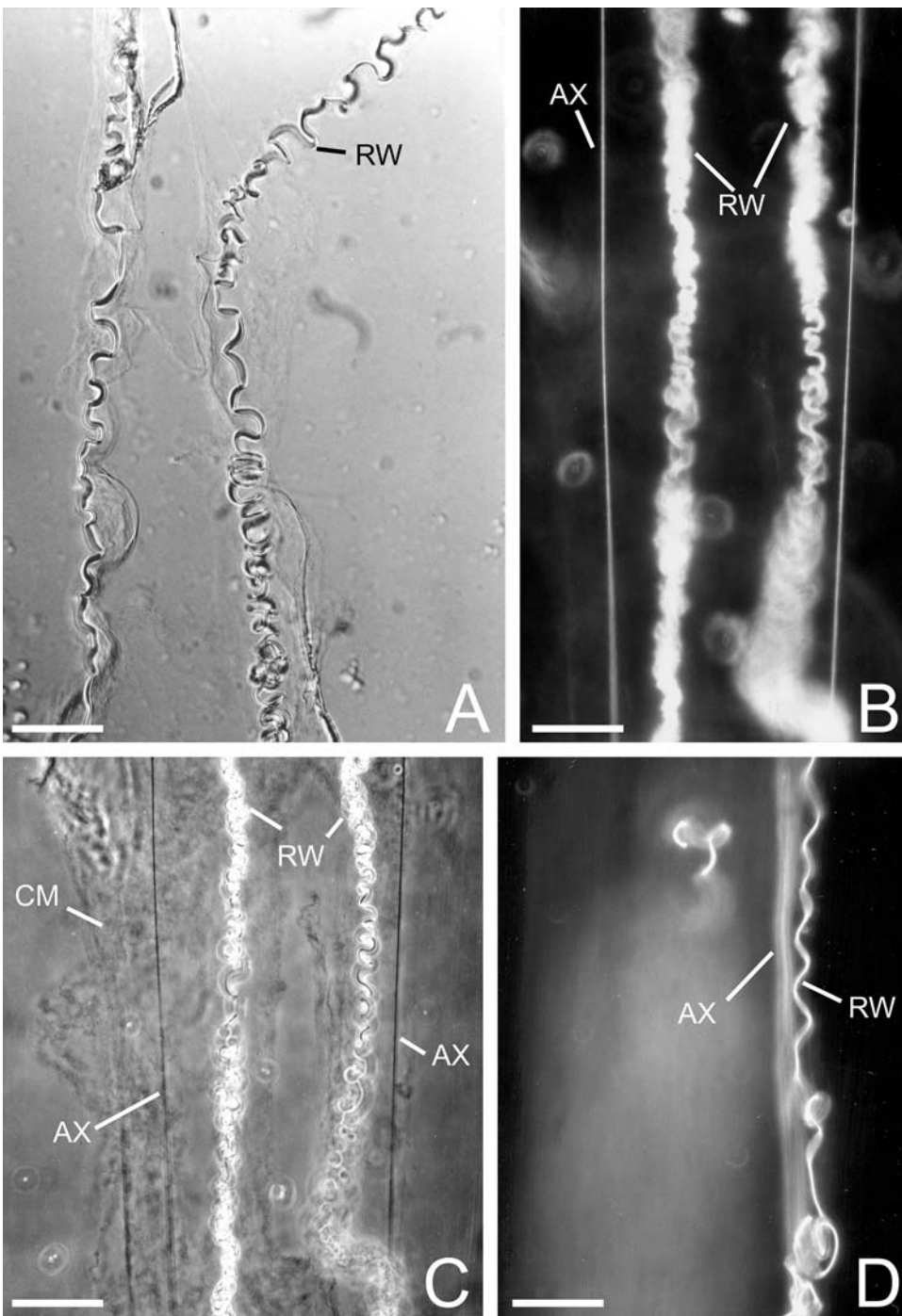


FIGURE 121. Cribellate silk. A–C. *Phyxelida tanganyensis* from Amani, Tanzania. D. *Titanoea nigrella* from Cave Creek, Arizona, USA. AX = axial fibers, CM = cribellar fiber mass, RW = reserve warp. Scale bars: A–D = 50 μ m.

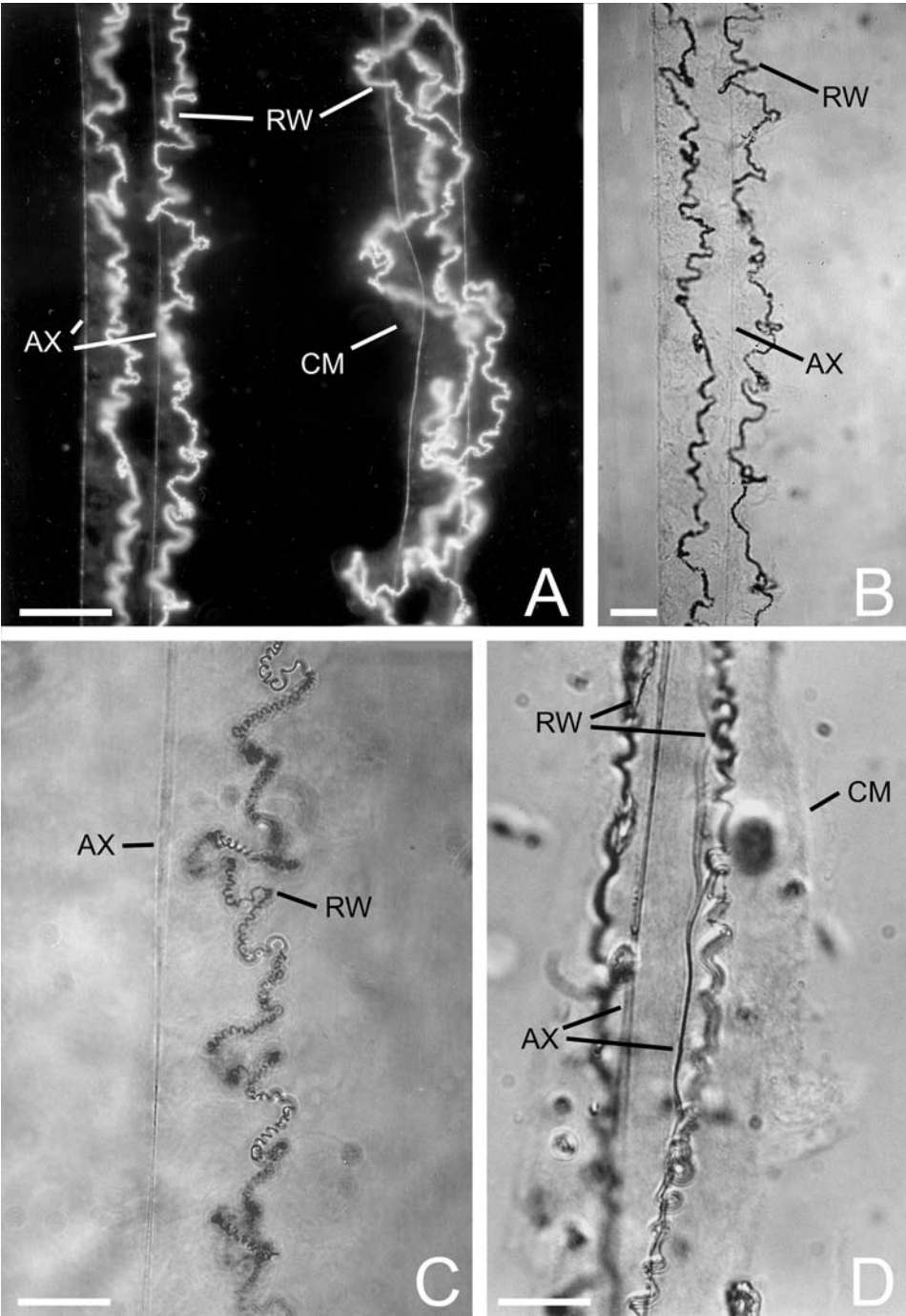


FIGURE 122. Cribellate silk. A–B. *Megadictyna thilenii* from Wellington, New Zealand. C. *Amaurobius* sp. from San Mateo, California, USA. D. *Badumna longinqua* from San Francisco, California, USA. AX = axial fibers, CM = cribellar fiber mass, RW = reserve warp. Scale bars: A, C, D = 50 μ m, B = 100 μ m.

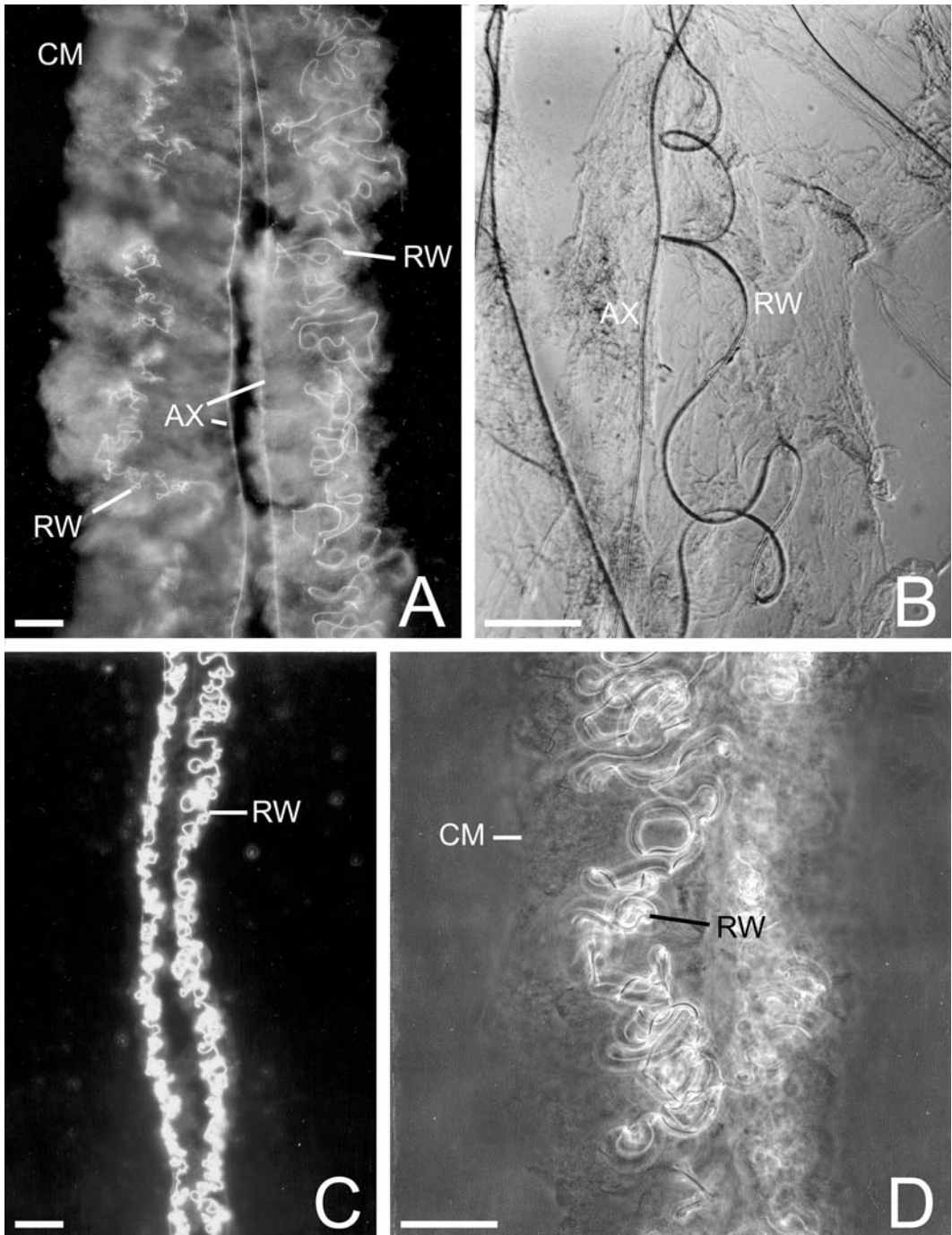


FIGURE 123. Cribellate silk. A–B. *Callobius gauchama* from San Bernardino Co., California, USA. C–D. *Pimus* sp. from San Mateo, California, USA. Axial line present but not visible in these views of *Pimus* silk. AX = axial fibers, CM = cribellar fiber mass, RW = reserve warp. Scale bars: A, C = 100 μ m, B, D = 50 μ m.

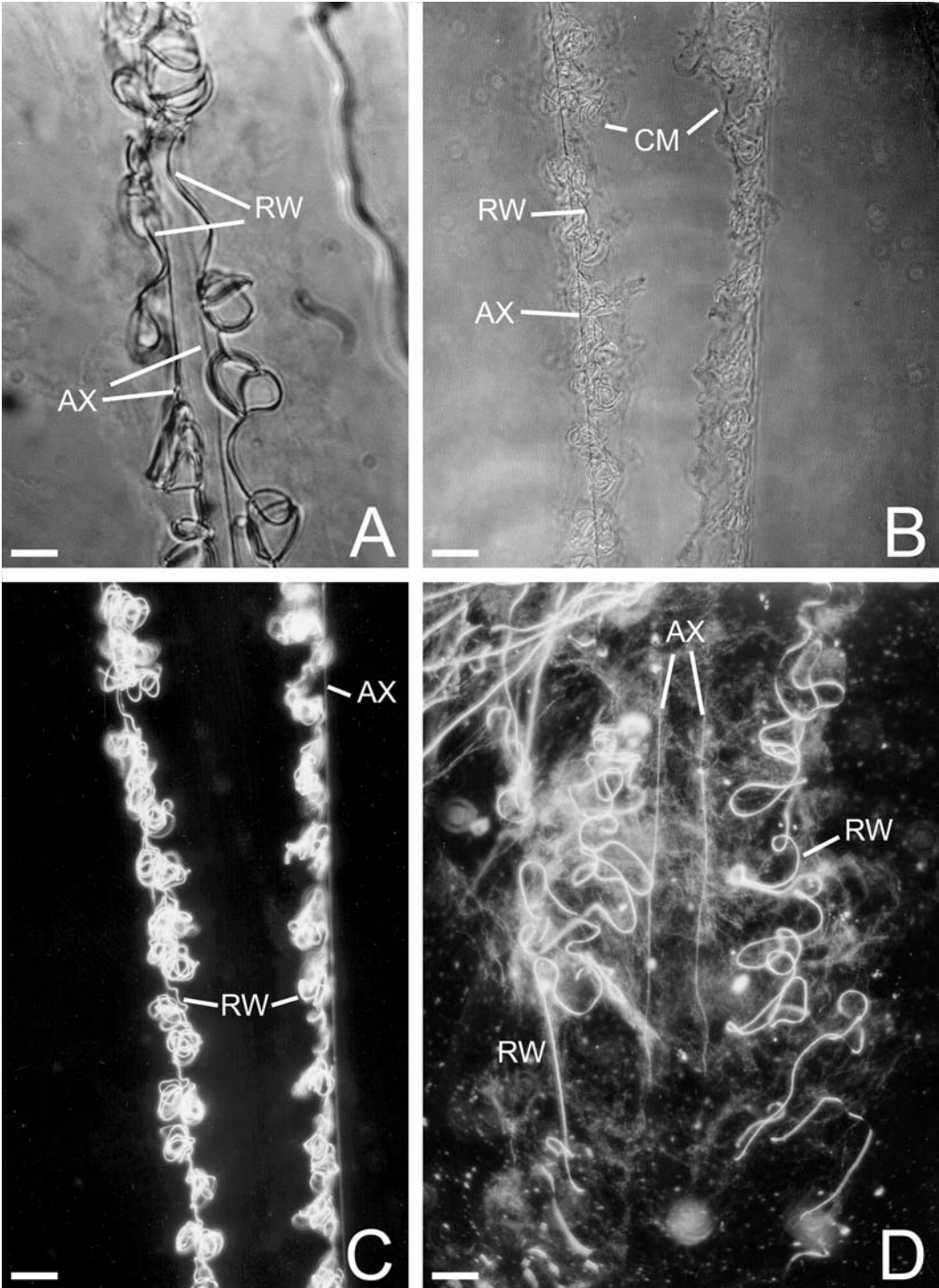


FIGURE 124. Cribellate silk. A–C. *Metaltella simoni* from Riverside, California, USA. D. *Raecius scharffi* juvenile from East Usambara, Tanzania. AX = axial fibers, CM = cribellar fiber mass, RW = reserve warp. Scale bars: A–D = 100µm.

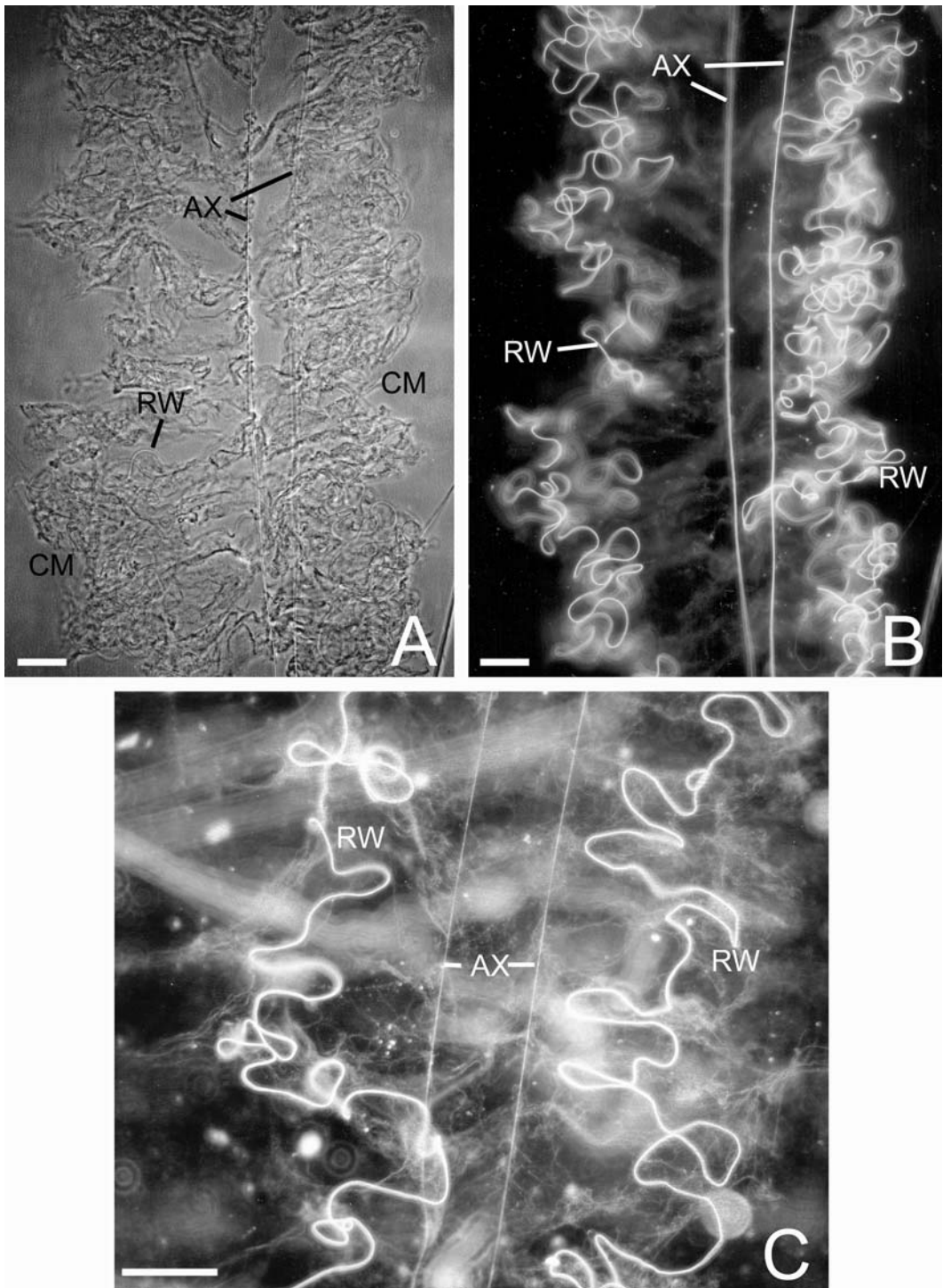


FIGURE 125. Cribellate silk. A–B. *Zoropsis spinimana* from Sunnyvale, California, USA. C. *Raecius scharffi*, juvenile from East Usambara, Tanzania. AX = axial fibers, CM = cribellar fiber mass, RW = reserve warp. Scale bars: A, B = 100 μ m, C = 50 μ m.

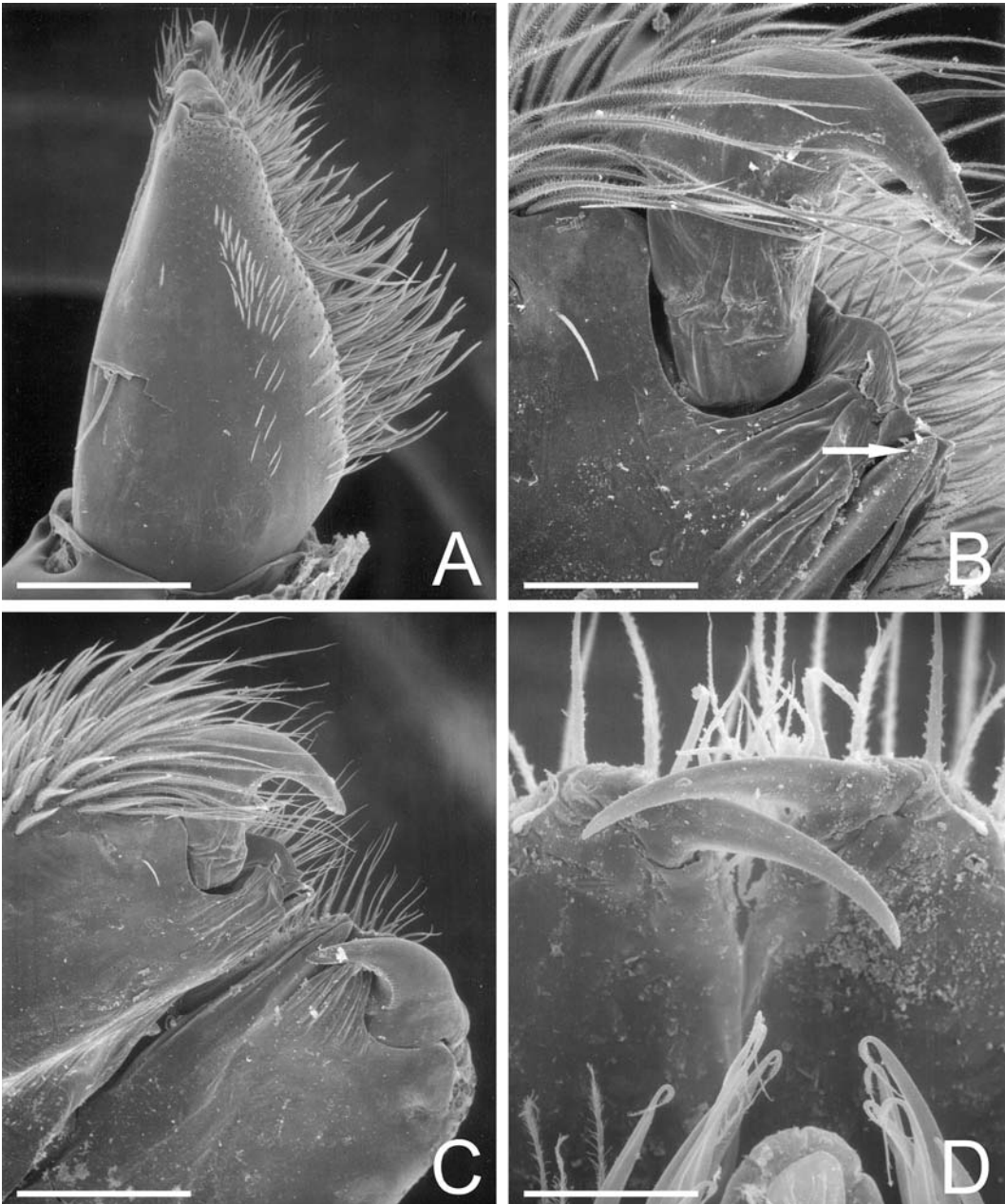


FIGURE 126. Chelicerae of Filistatidae and Oecobiidae. A–C. *Kukulcania hibernalis* female from Archibold Station, Florida, USA. D. *Oecobius* sp. juvenile from Novato, California, USA. A. Chelicera, retrolateral, note absence of boss. B. Paturon with fang, arrow to chela. C, D. Cheliceral apex and fangs; note lack of teeth. Scale bars: A = 750 μ m, B = 200 μ m, C = 430 μ m, D = 30 μ m.

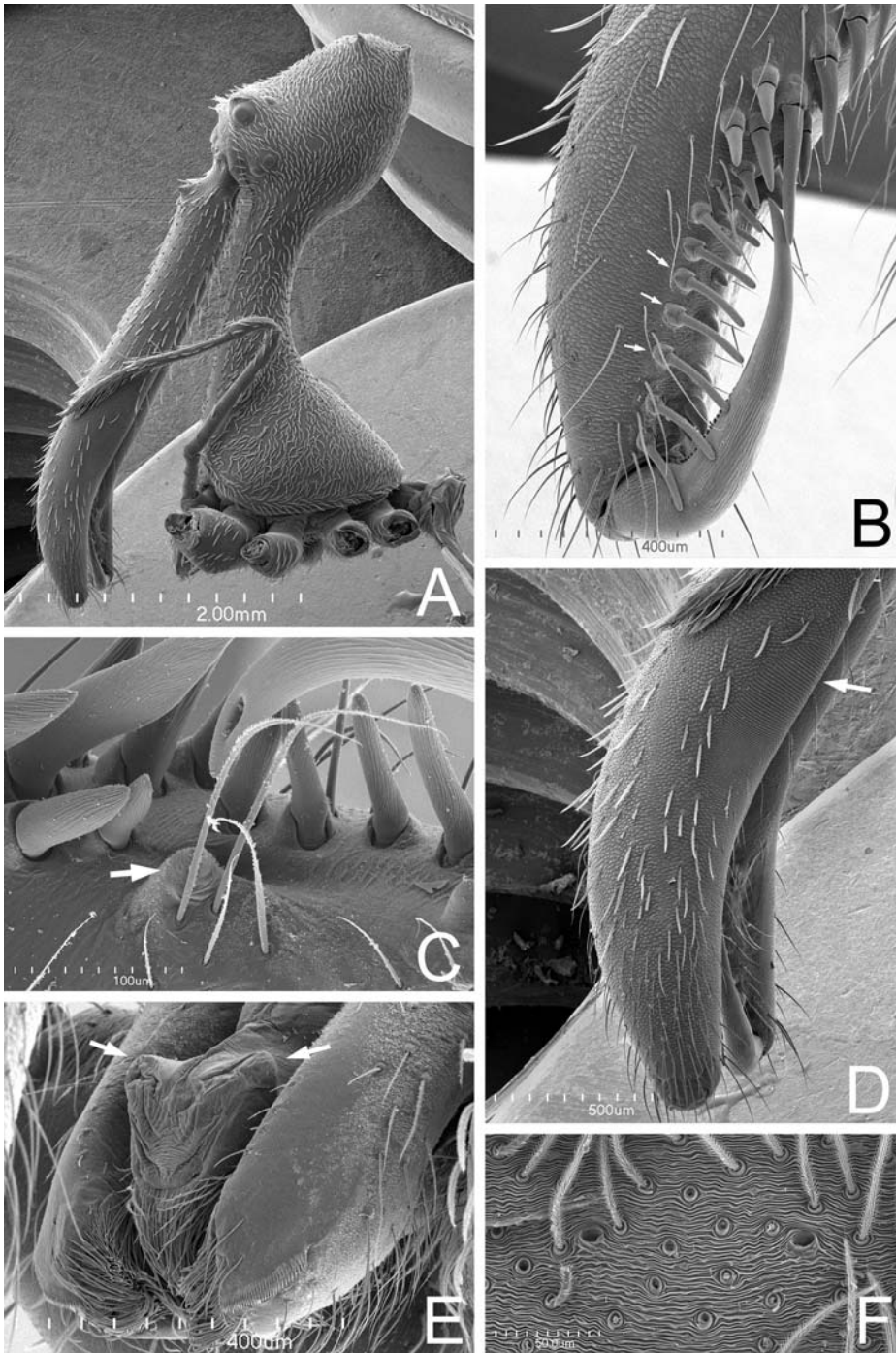


FIGURE 127. *Archaea workmani* female from Ranomafana, Madagascar. A. Cephalothorax, lateral. B. Right chelicera, anterior view, arrows to peg teeth. C. Left chelicera, showing gland mound (arrow). D. Left chelicera, retrolateral, showing stridulatory striae (arrow). E. Endites and labrum, anterolateral, arrows to lateral labral extensions. F. Tracheal spiracles. Scale bars: A = 2.0 mm, B, E = 400µm, C = 100µm, D = 500µm, F = 50µm.

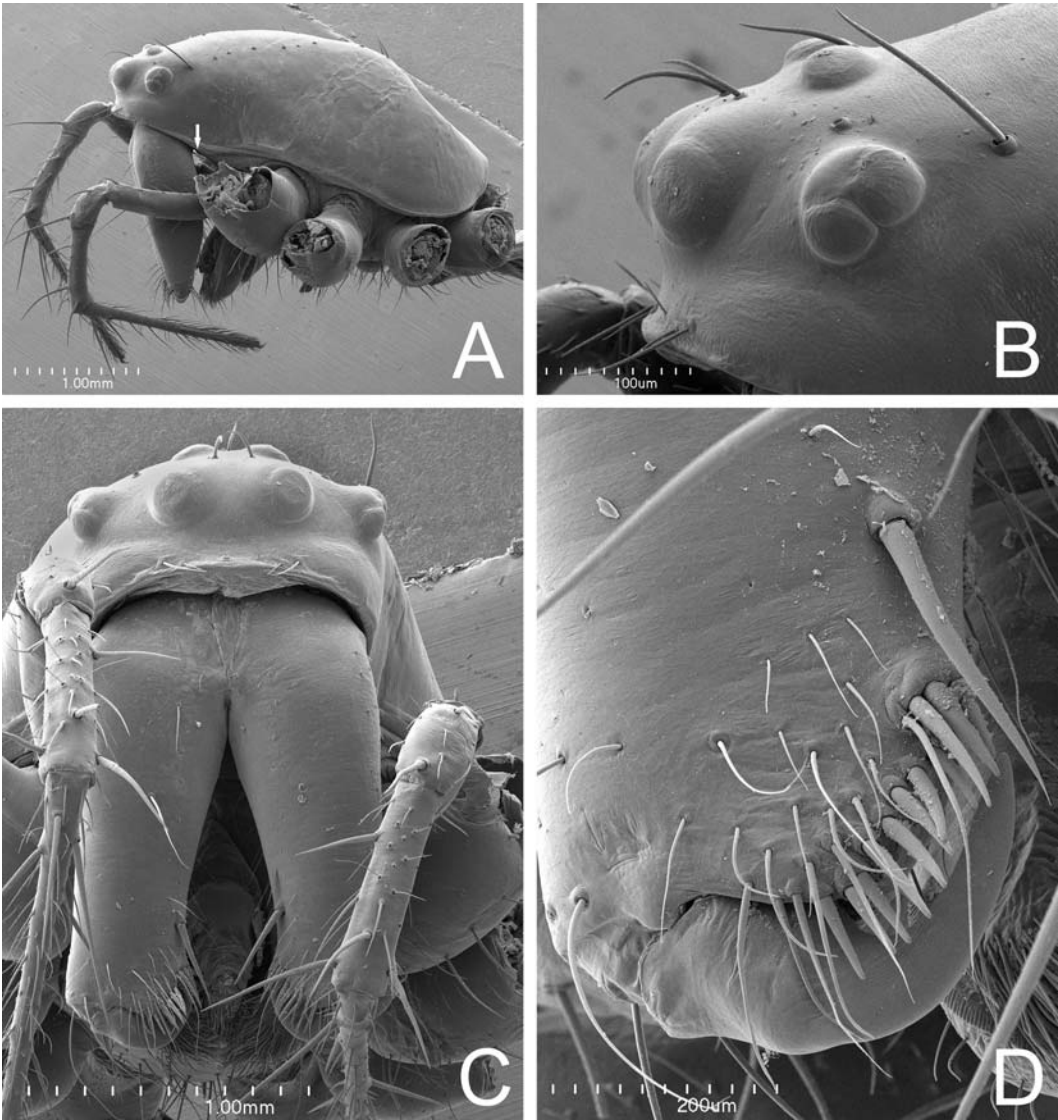


FIGURE 128. *Mimetus hesperus* female from Valles, Mexico, carapace and chelicerae. A. Carapace, lateral, note the chelicerae separated from the endites by a diastema (arrow). B. Carapace, lateral showing juxtapsed lateral eyes. C. Carapace, anterior, showing partially fused chelicerae. D. Right chelicera, anterior, showing peg teeth. Scale bars: A–C = 1.0mm, D = 200µm.

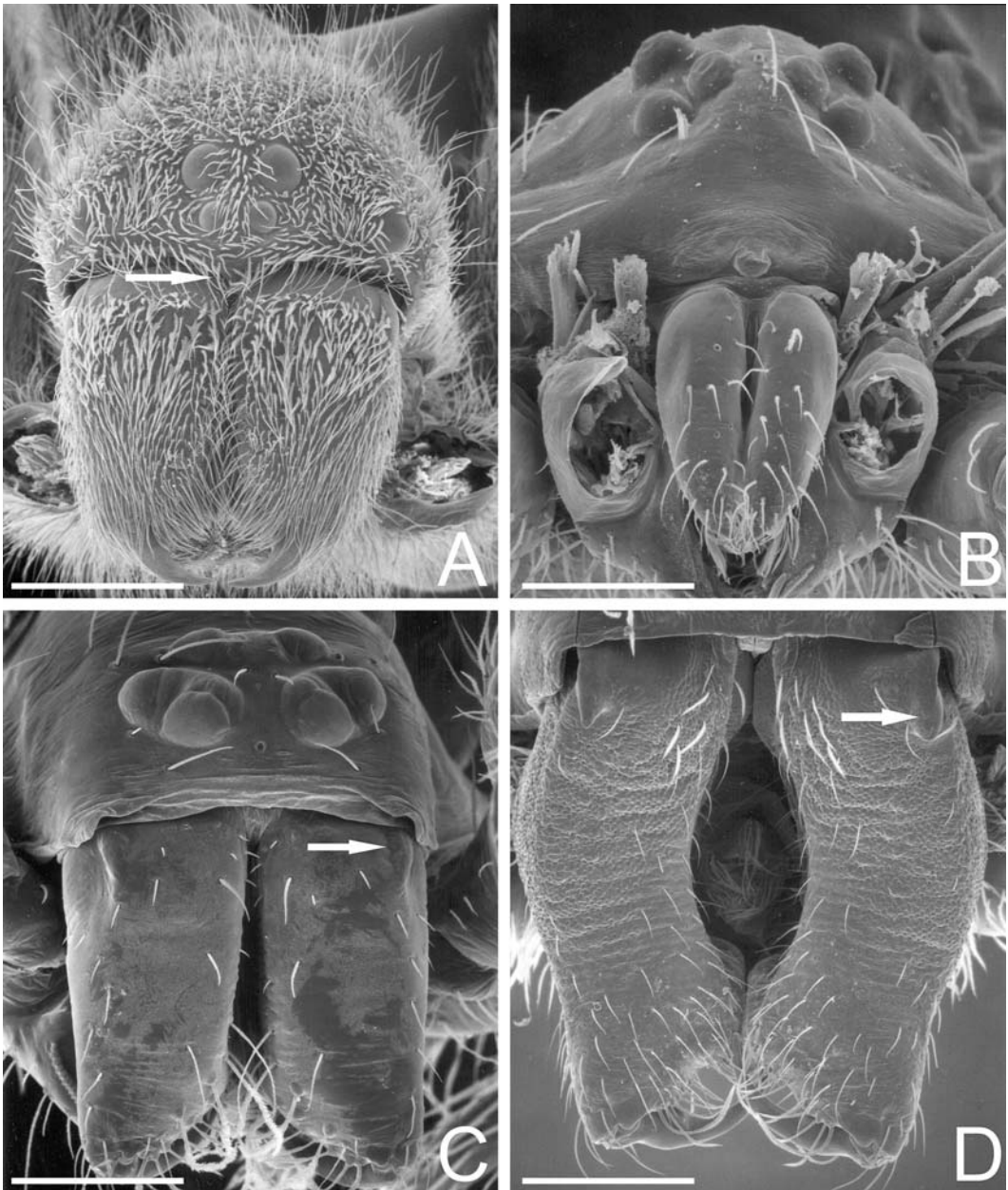


FIGURE 129. Faces and chelicerae. A. *Stegodyphus mimosarum* female from Fort Hill, Malawi, arrow to clypeal hood. B. *Oecobius* sp. juvenile from Novato, California, USA, showing small chelicerae. C. *Lathys immaculata* male from Bradley, Arkansas, USA, arrow to boss. D. *Dictyna arundinacea* male from Tuva, Russia, bowed chelicerae, arrow to boss. Scale bars: A = 750 μ m, B = 150 μ m, C = 100 μ m, D = 250 μ m.

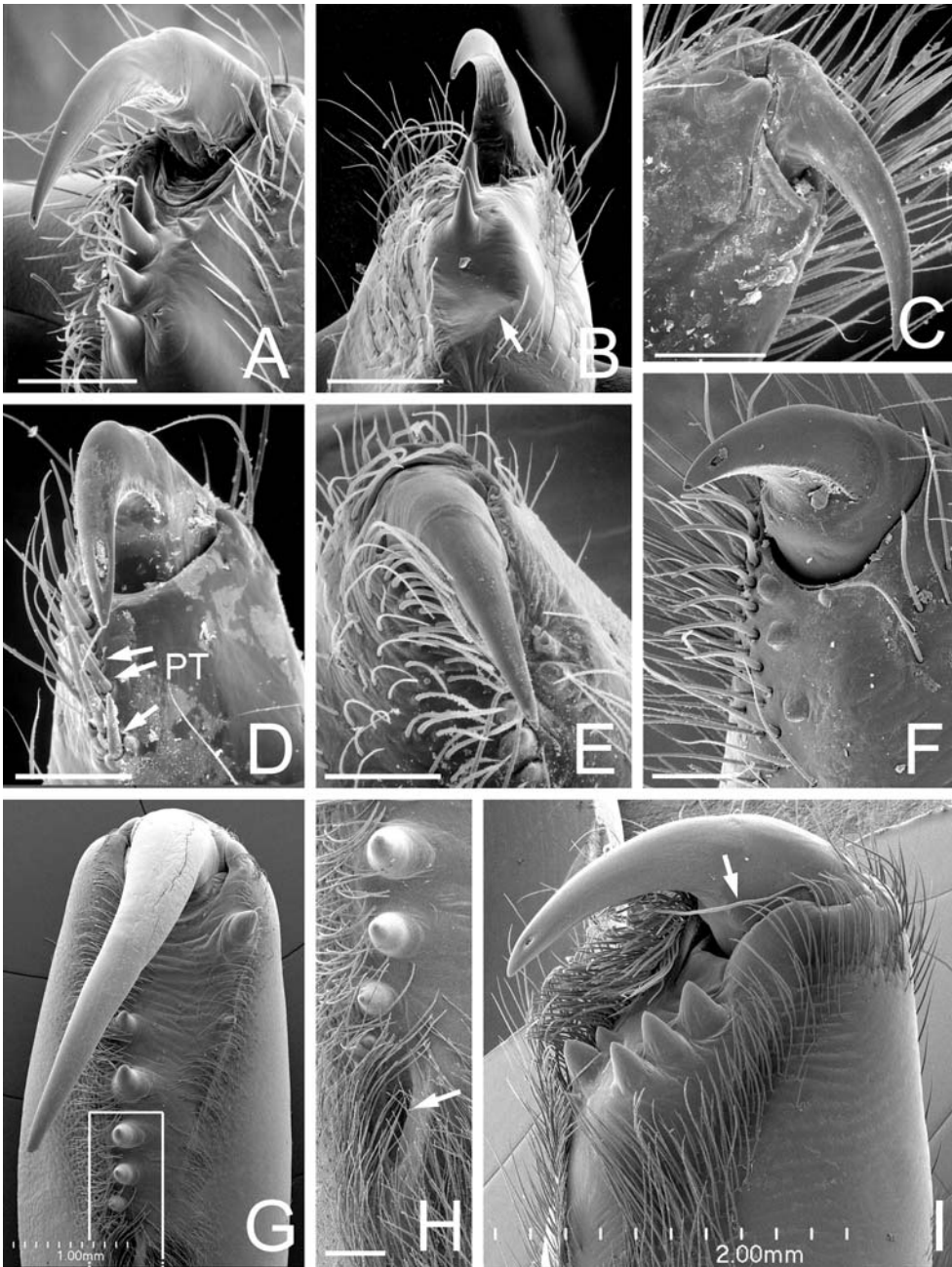


FIGURE 130. Chelicerae. A, B. Chelicerae of juvenile *Hypochilus sheari* from Crabtree Meadows, North Carolina, USA. A. Retromedian view. B. Median view, arrow to cheliceral concavity. C. *Uroctea* sp. juvenile from Julwania, India, chelicera, retrolateral. D. *Mimetus hesperus* female from Tampico, Mexico, paturon and fang, retromesal view, arrows to peg teeth (PT). E. *Aebutina binotata*, female from Río Cuyabeno, Ecuador, paturon and fang, mesal view. F. *Ariadna boesenbergii*, female from Buenos Aires, Argentina. G, H. *Desis formidabilis*, female from Cape Peninsula, South Africa. G. Left chelicera, marked area enlarged in H. H. Detail of promarginal teeth and excavated area (arrow). I. *Zorocrates* cf. *mistus*, female from Los Llanos, Chiapas, Mexico (arrow to stout retromarginal seta). Scale bars: A = 176 μ m, B = 231 μ m, C—F = 100 μ m, H = 250 μ m.

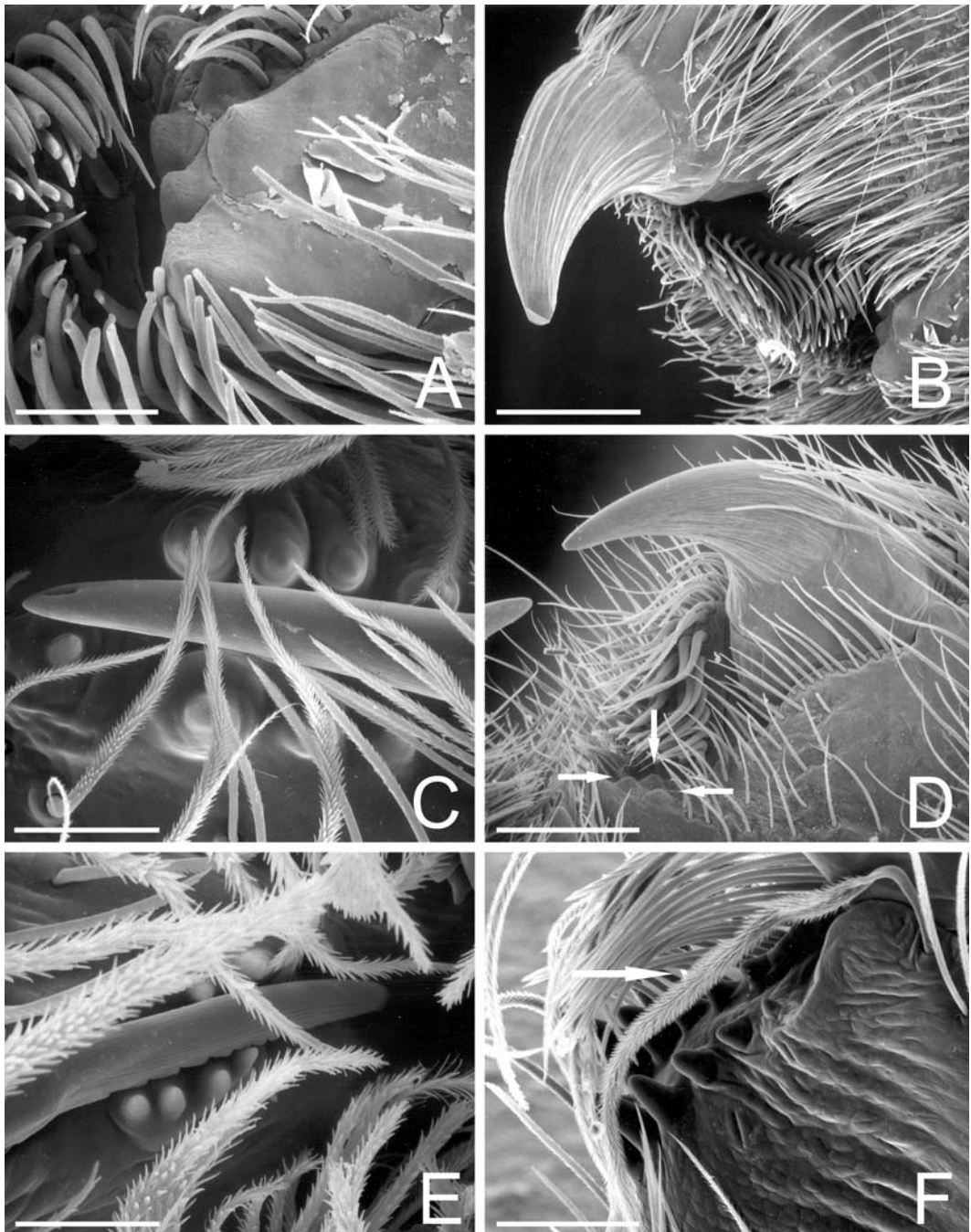


FIGURE 131. Fang region of chelicerae. A, B. *Eresus cinnaberinus* female from Fiesch Wallis, Switzerland. A. Teeth on fang furrow. B. Fang and teeth. C. *Tricholathys* sp. female from San Francisco, California, USA, fang and teeth. Note pore at tip of fang. D. *Stegodyphus mimosarum* female from Fort Hill, Malawi, fang and teeth (arrows). E. *Lathys immaculata* from Bradley, Arkansas, USA, male fang and teeth. F. *Xevioso amica* male from St. Lucia, South Africa, showing thickened setae (arrow to stout retromarginal seta). Scale bars: A, F = 100 μ m, B = 300 μ m, C = 43 μ m, D = 150 μ m, E = 20 μ m.

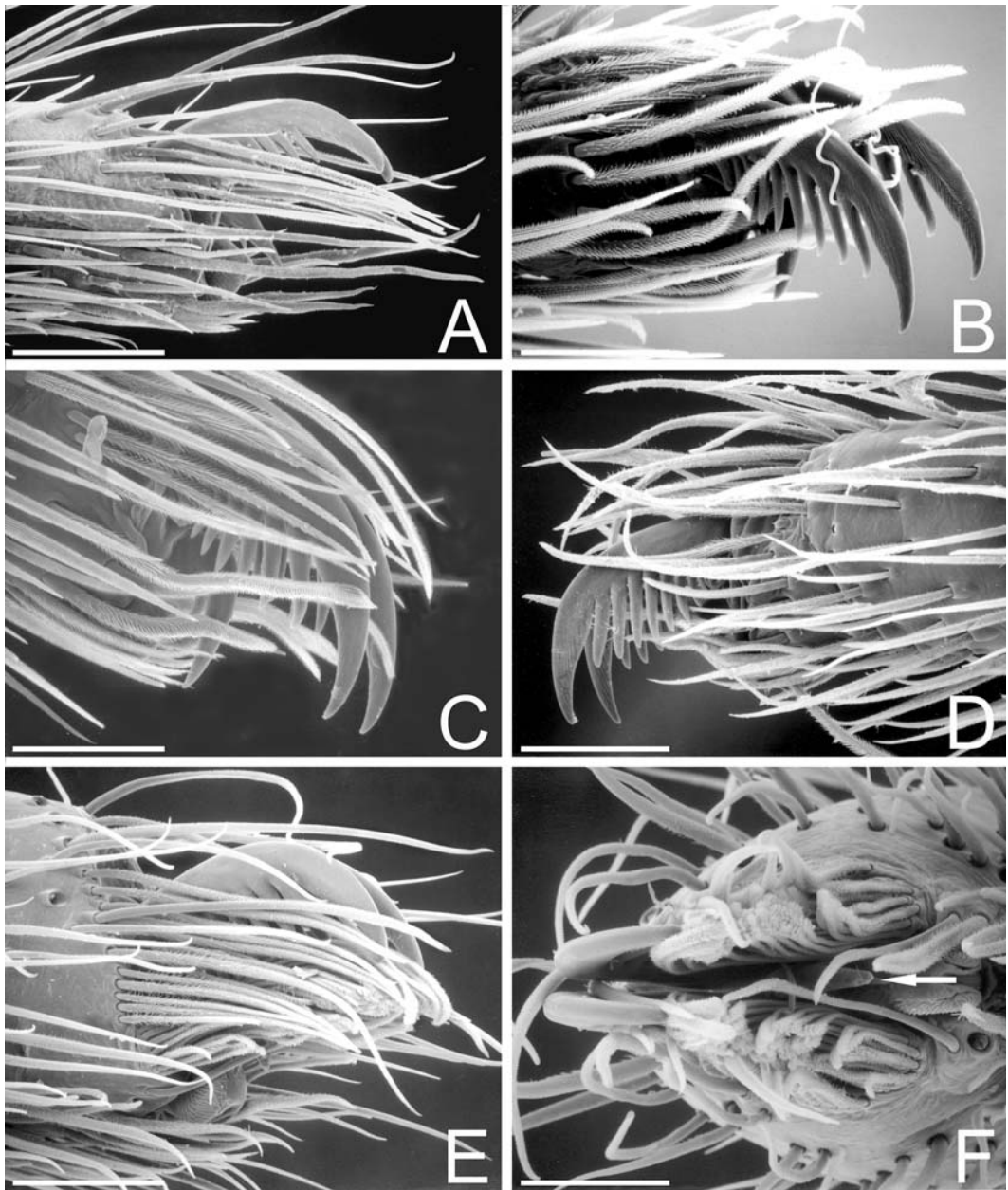


FIGURE 132. Tarsi of entelegyne spiders that hang beneath webs but lack serrate accessory setae. A. *Hypochilus pococki* female from Great Smokey Mts. N.P, Tennessee, USA, lateral, II. B. *Neolana dalmasi* female from Waipoua Forest, New Zealand, lateral, II. C, D. *Phyxelida tanganensis* female from Amani, Tanzania, lateral. C. IV. D. II. E, F. *Psechrus* sp. female from Tham Lot Cave, Thailand, II. E. Lateral. F. Ventral, showing lateral claw tufts and ITC (arrow). Scale bars: A = 136 μ m, B, C = 60 μ m, D, F = 86 μ m, E = 120 μ m.

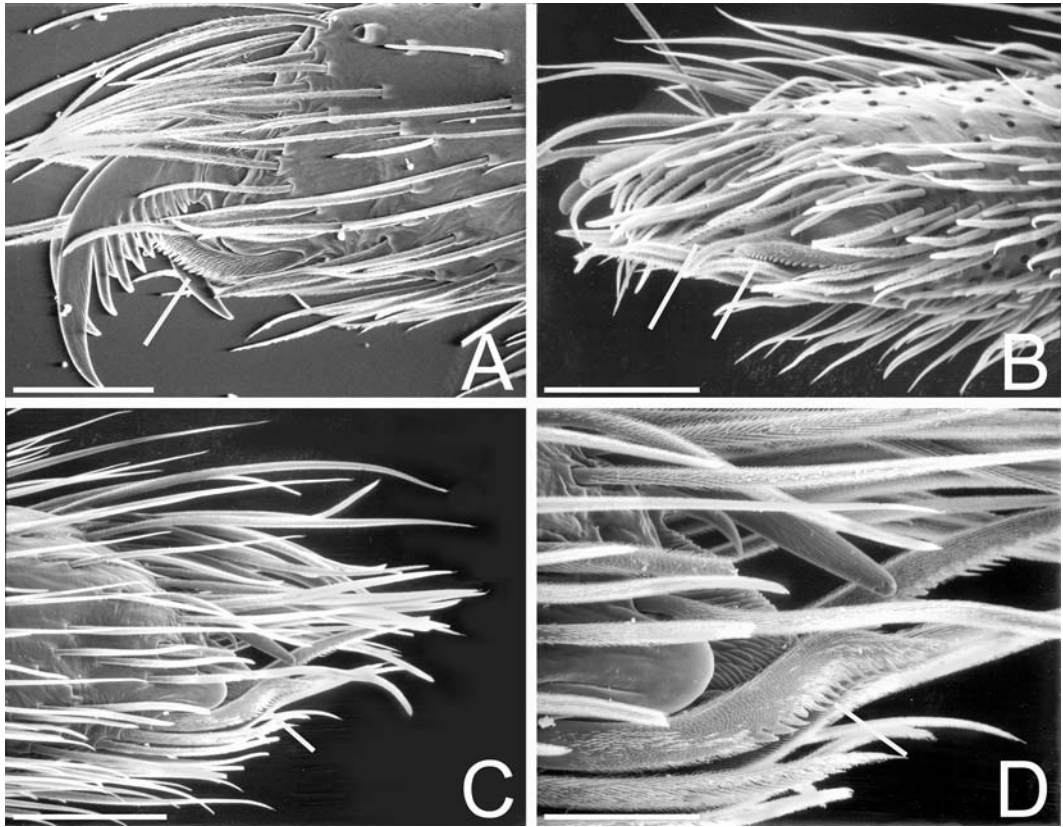


FIGURE 133. Tarsi of Austrochilidae, lateral views. Lines to serrate accessory setae. A. *Austrochilus melon* juvenile from Cuesta Pucalan, Chile, IV. B. *Thaida peculiaris* female from Lago Villarica, Chile, II. C, D. *Hickmania troglodytes* female from cave at Mole Creek, Tasmania, Australia. C. II. D. II close-up, showing ITC and serrate accessory setae. Scale bars: A = 100 μ m, B = 136 μ m, C = 200 μ m, D = 75 μ m.

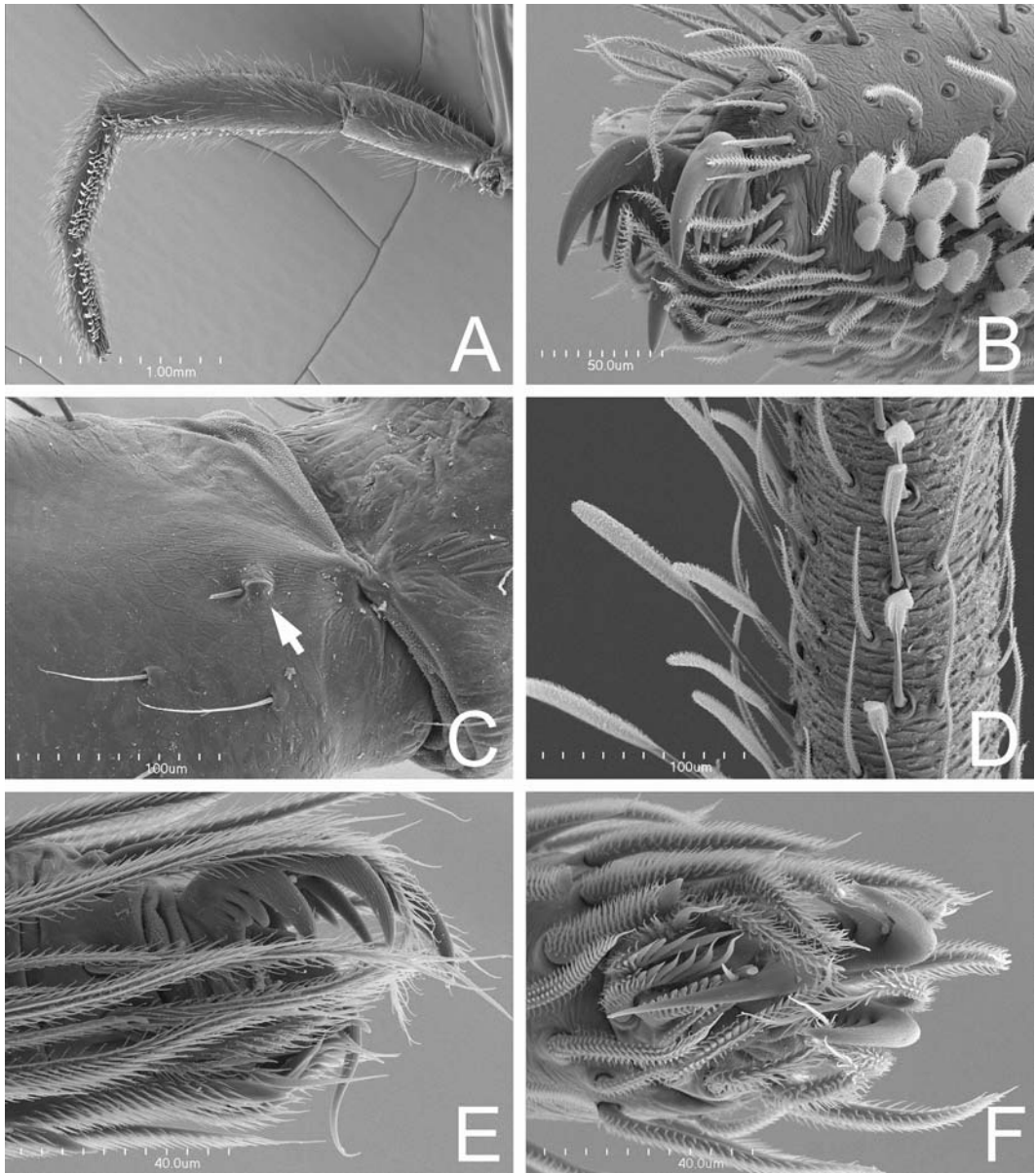


FIGURE 134. Appendages of Archaeidae and Huttoniidae. A–C. *Huttonia* sp. female from Orongorongo, New Zealand. A. Leg I, prolateral view, showing characteristic “palpimanoid” scopula on metatarsus and tarsus. B. Tarsus I, claws and scopula. C. Basal cusp on palpal femora (arrow). D–F. *Archaea workmani* female from Ranomafana, Madagascar. D. Left tibia I, scopula. E. Left tarsus I claws, lateral. F. Left tarsus I claws, ventral. Note serrate accessory setae. Scale bars: A = 1.0mm, B = 50µm, C, D = 100µm, E, F = 40µm.

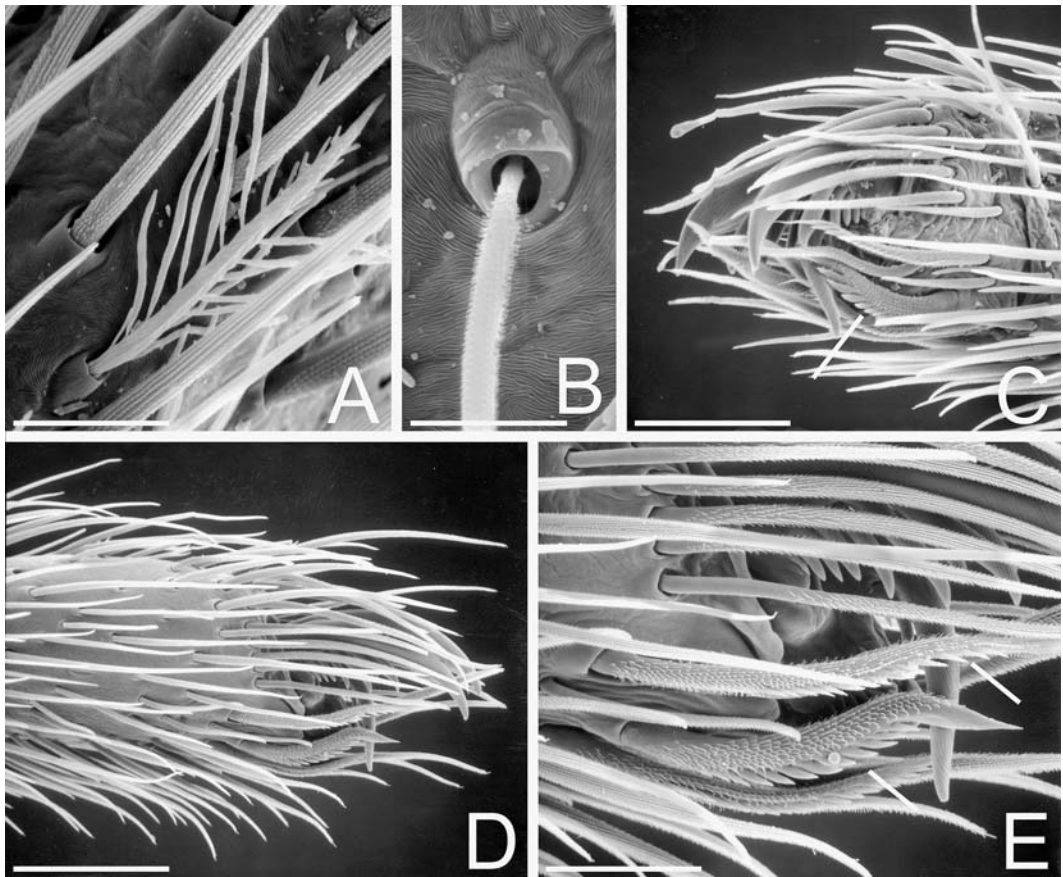
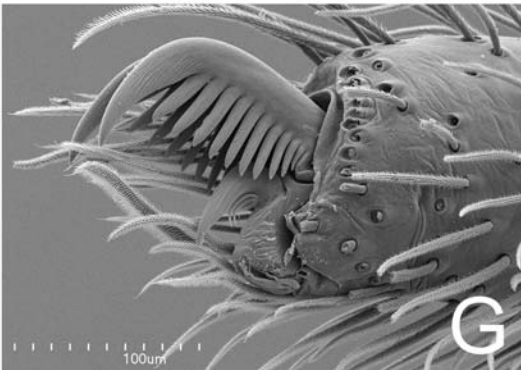
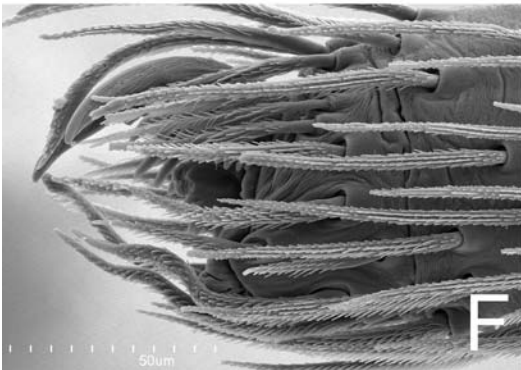
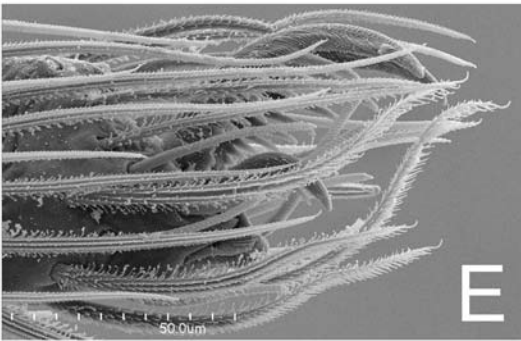
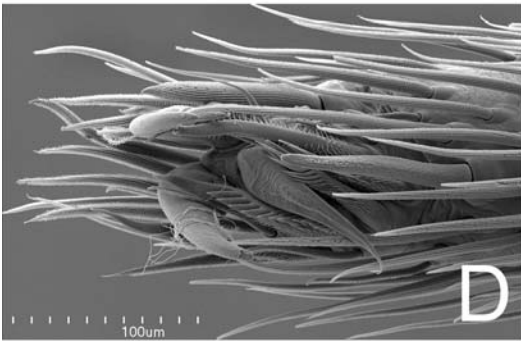
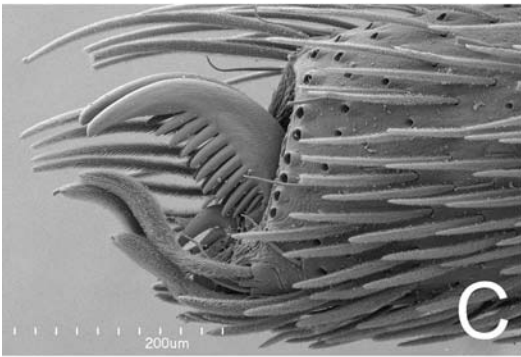
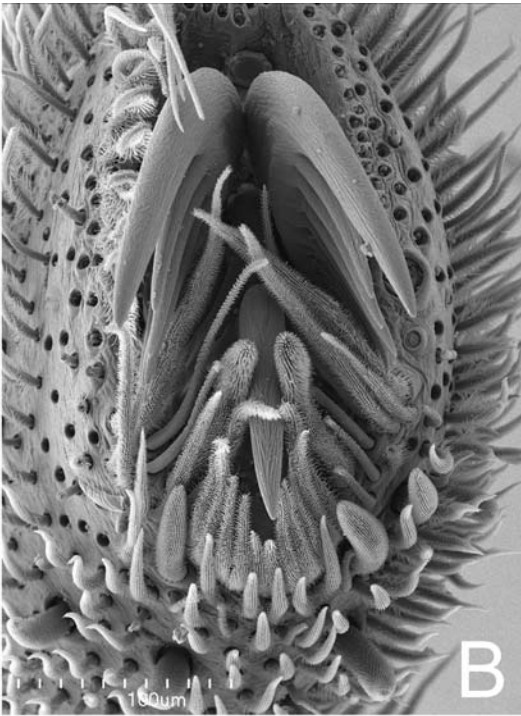
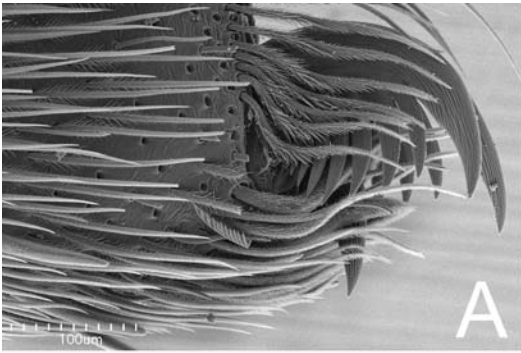


FIGURE 135 (above). Second legs of female Deinopidae. A–C. *Menneus camelus* from Songimvelo Nature Reserve, South Africa. A. Feathery hairs on metatarsus. B. Metatarsal trichobothrium base. C. Tarsus and claws, with line to serrate accessory setae. D–E. *Deinopis spinosus* from Gainesville, Florida, USA. D. Tarsus. E. Tarsus close-up, showing ITC and serrate accessory setae (lines). Scale bars: A = 27 μ m, B = 17.6 μ m, C = 86 μ m, D = 150 μ m, E = 60 μ m.

FIGURE 136 (right). Tarsi showing claws and setae. A, B. *Stegodyphus mimosarum*, female from Phinda Resource Reserve, South Africa, IV left. C. *Filistata insidiatrix* female from Siena, Italy, IV right. D. *Menneus* sp. female from Tembe Elephant Park, South Africa, IV right, note serrate accessory setae near ITC. E. *Oecobius navus* female from Sylvania, Georgia, USA, IV left. F. *Dictyna arundinacea* female from Dornoch, Scotland, IV right. G. *Pimus napa* female paratype from Oakville, California, USA, I left. Scale bars: A, B, D, G = 100 μ m, C = 200 μ m, E, F = 50 μ m.



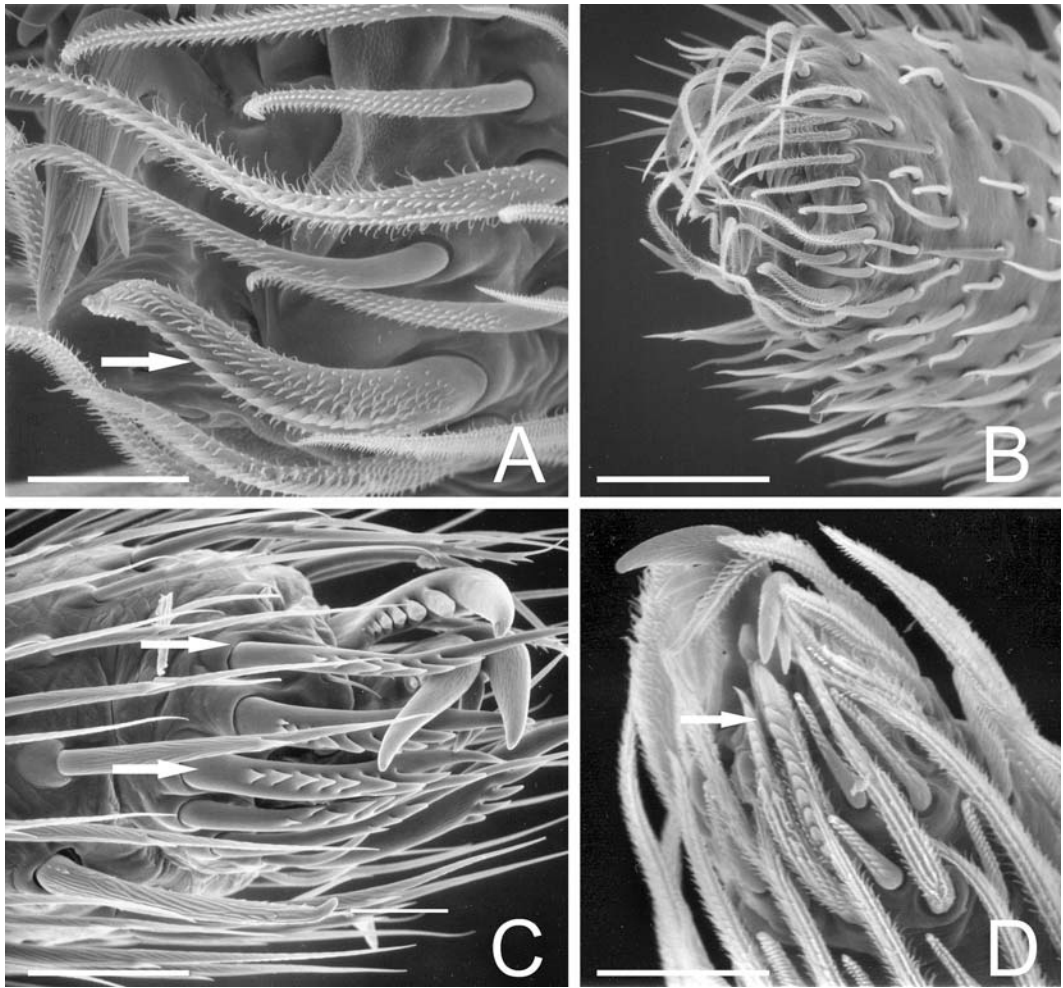


FIGURE 137. Tarsal apices, with claws and serrate setae. A, B. *Megadictyna thilenii* juvenile from, Cherry Bay, New Zealand, tarsus I. A. Close up of serrate hairs (arrow to largest). B. Apex of tarsus. C. *Metepeira* sp. female from Guanajuato, Mexico, tarsus IV showing serrate hairs (arrows) and sustentaculum (line). D. *Uloborus diversus* female from Napa Co., California, USA, tarsus I showing serrate hairs (arrow). Scale bars: A = 30 μ m, B = 100 μ m, C = 75 μ m, D = 20 μ m.

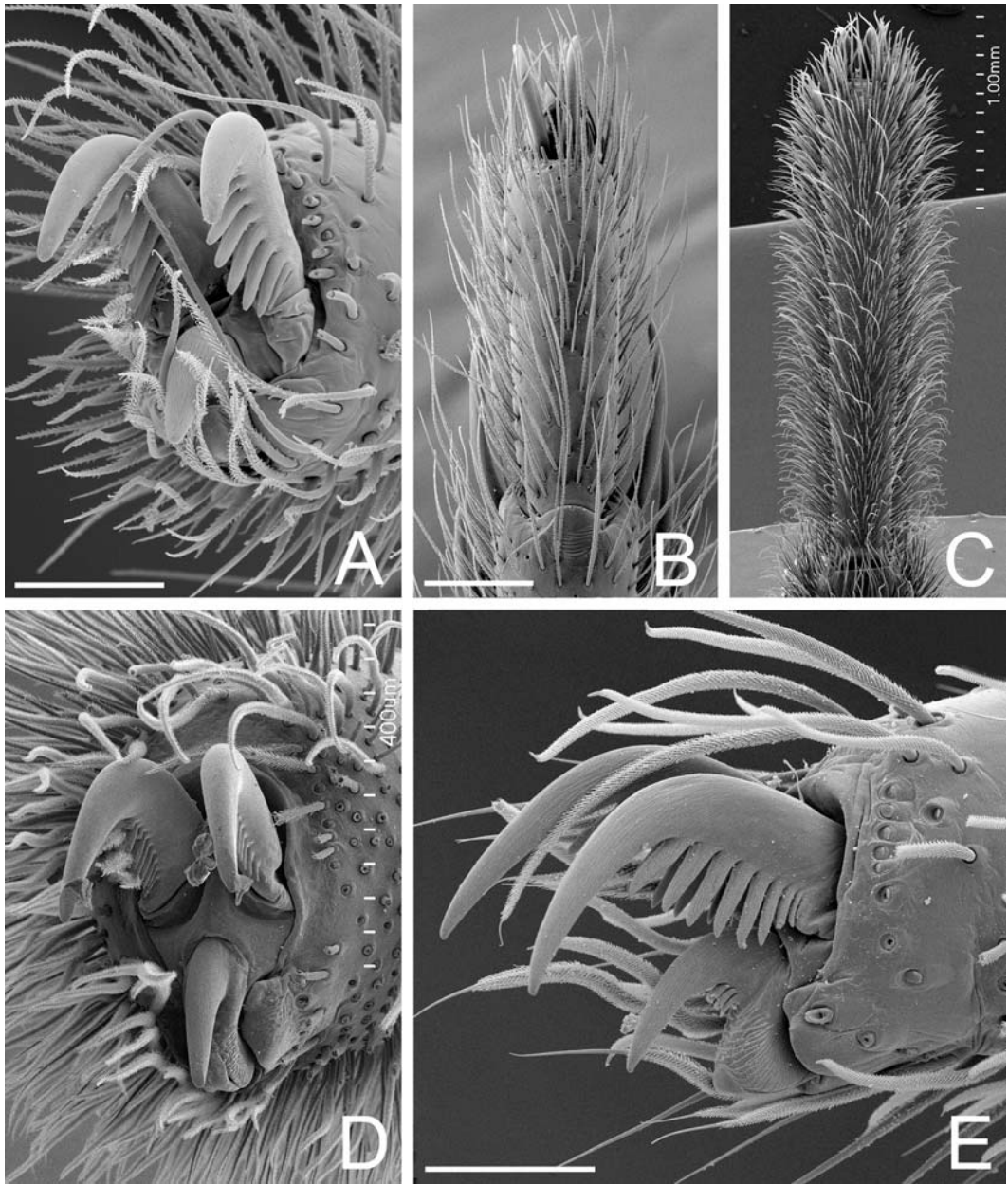


FIGURE 138. Left tarsi and claws I, female. A. Tarsal claws of *Ariadna boesenbergi* from Buenos Aires, Argentina. B. Same, tarsus, dorsal. C. Tarsus of *Desis formidabilis* from Cape Peninsula, South Africa, dorsal. D. Same, tarsal claws. E. Tarsal claws of *Macrobnus multidentatus* from Chiloé, Chile. Scale bars: A = 100 μm , B = 200 μm , C = 1.0mm, D = 400 μm , E = 100 μm .

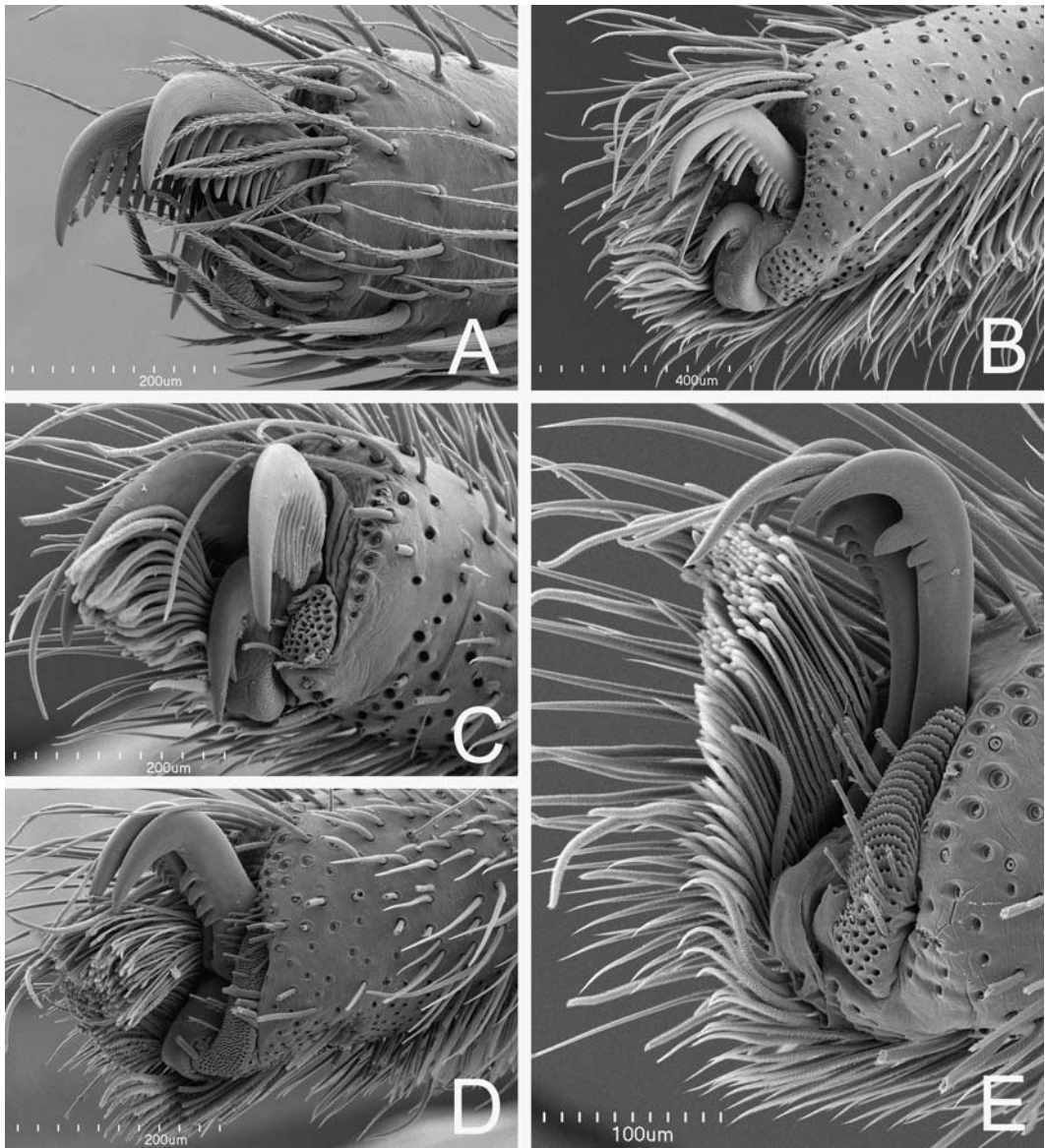


FIGURE 139. Female left tarsi I. Hairs of scopula or claw tuft on near side have been removed from B–E. A. *Nicodamus mainae* from Coalseam Park, Western Australia, Australia. B. *Tengella radiata* from Guanacaste, Costa Rica. C. *Psechrus argentatus* from Cape Vogel Peninsula, Papua New Guinea. D. *Zoropsis rufipes* from Tenerife, Canary Islands. E. *Acanthoctenus* cf. *spinipes* from Loreto, Peru. Scale bars: A, C, D = 200µm, B = 400µm, E = 100µm.

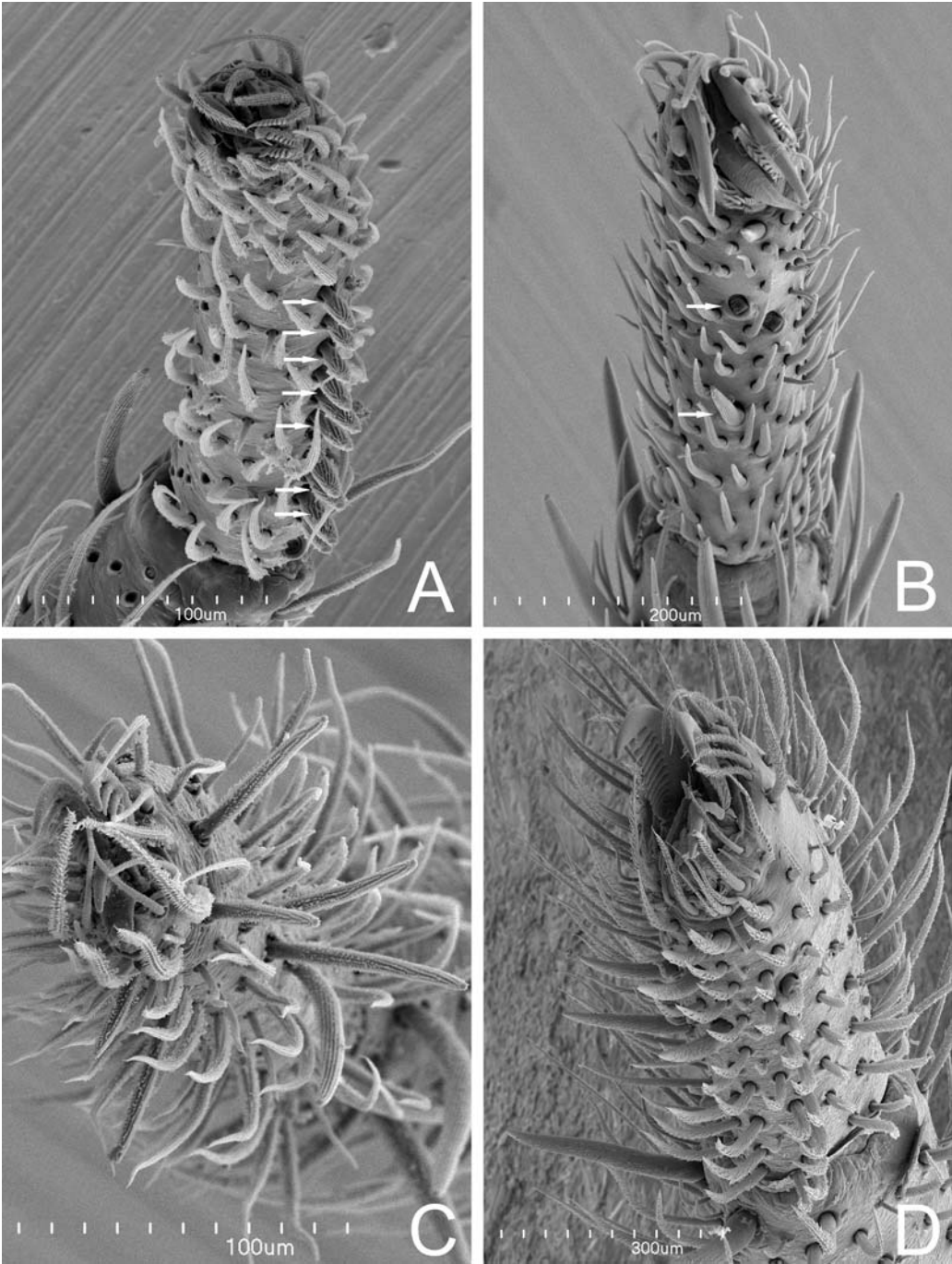


FIGURE 140. Female tarsi IV, ventral. A. *Uloborus glomosus* from Mast, North Carolina, USA, left, arrows to line of macrosetae forming deinopoid tarsal comb. B. *Menneus* sp. from Tembe Elephant Park, South Africa, right, arrows to scattered tarsal macrosetae or their bases. C. *Oecobius navus* from Sylvania, Georgia, USA, left. D. *Nicodamus mainae* from Coalseam Park, Western Australia, Australia, left, note numerous macrosetae. Scale bars: A, C = 100 μ m, B = 200 μ m, D = 300.

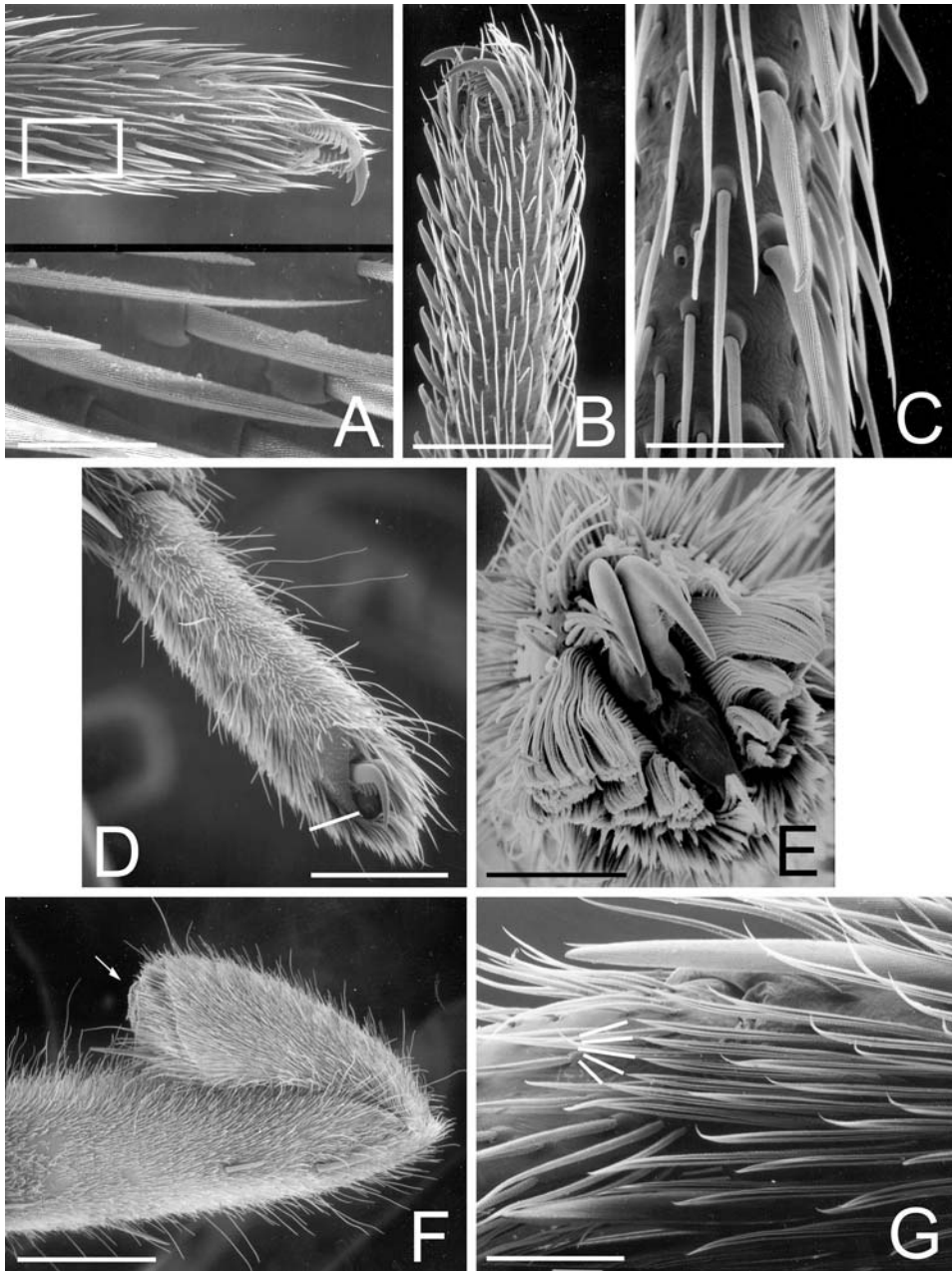


FIGURE 141. Legs of Entelegynae. A. *Megadictyna thilenii* female from Hicks Bay, New Zealand, tarsus IV showing macrosetae (detail below). B, C. *Deinopis spinosus* female from Gainesville, Florida, USA, tarsus IV. B. Deinopoid tarsal comb formed of line of macrosetae. C. Close-up of deinopoid tarsal comb. D. *Uduba* sp. female from Andohahela Madagascar, tarsus IV showing ventral scopula, STC and ITC (line), and multiple rows of dorsal trichobothria (the long dorsal setae extending out in all directions). E. *Zoropsis spinimana* female from Vernet-les-Bains, France, leg IV showing claw tufts, STC, and pretarsal plate lacking ITC. F. *Uduba* sp. male from Andohahela, Madagascar, femur to tibia base, tibia broken along tibial crack (arrow to broken face of tibia). G. *Xevioso amica* male from St. Lucia, South Africa, metatarsus III apex, showing preening comb (lines to comb setae). Scale bars: A = 250 μ m (refers to top image), B = 250 μ m, C = 75 μ m, D = 750 μ m, E = 200 μ m, F = 1.5mm, G = 40 μ m.

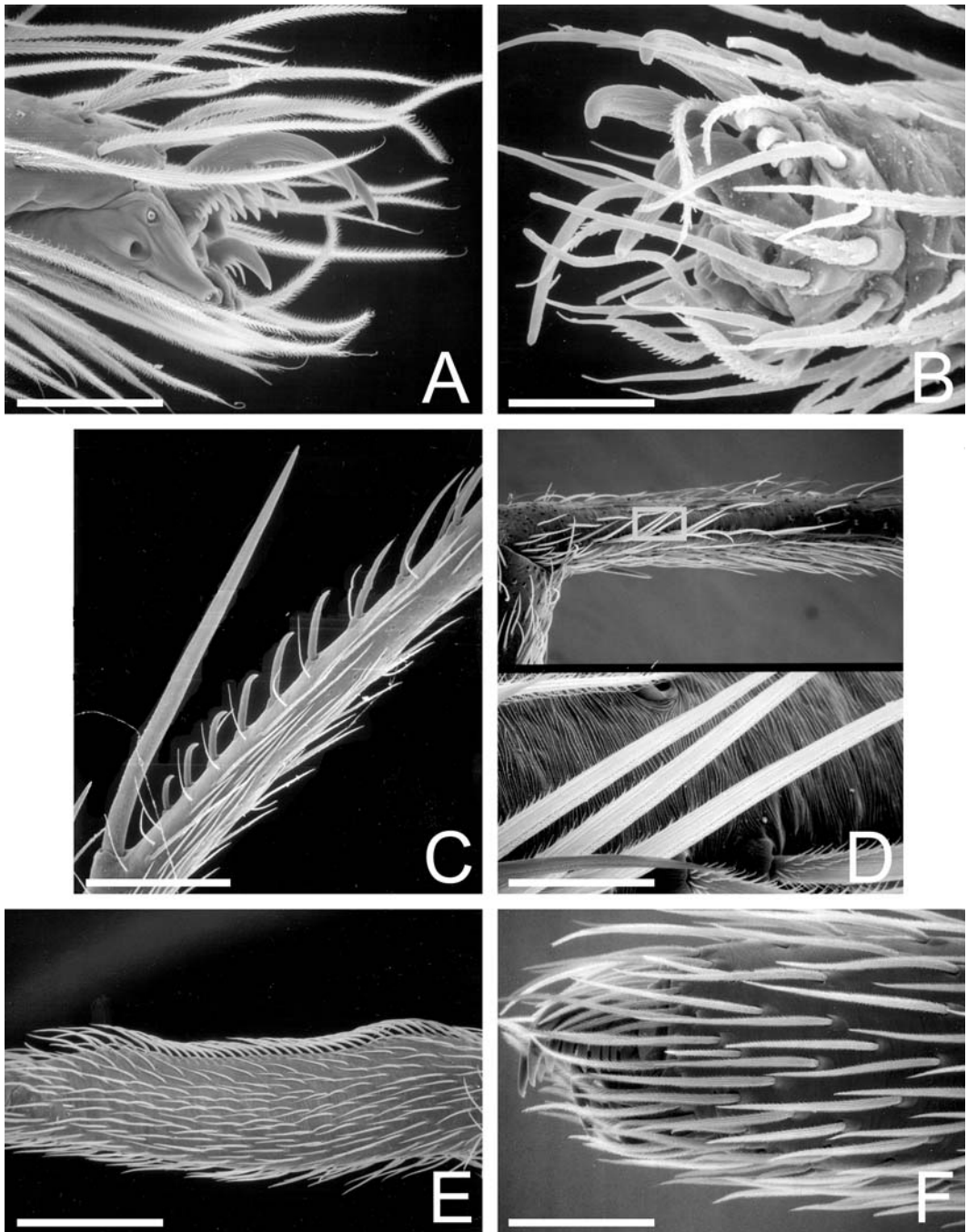


FIGURE 142. Leg morphology. A, D. *Poaka graminicola* female from Lincoln, New Zealand. B, C. *Mimetes hesperus* male from Baboquivari Mts., Arizona, USA. E, F. *Aebutina binotata* female from Rio Cuyabeno, Ecuador. A. Tarsus IV. B. Tarsus II. Note serrate accessory setae flanking ITC. C. Metatarsus II showing distally ascending series of spines characteristic of Mimetidae. D. Metatarsus IV, upper showing linear calamistrum, lower showing three calamistrual setae. E. Metatarsus IV showing calamistrum. F. Tarsus IV. Scale bars: A = 60 μ m, B = 30 μ m, C = 200 μ m, D = 300 μ m (refers to upper image), E = 250 μ m, F = 75 μ m.

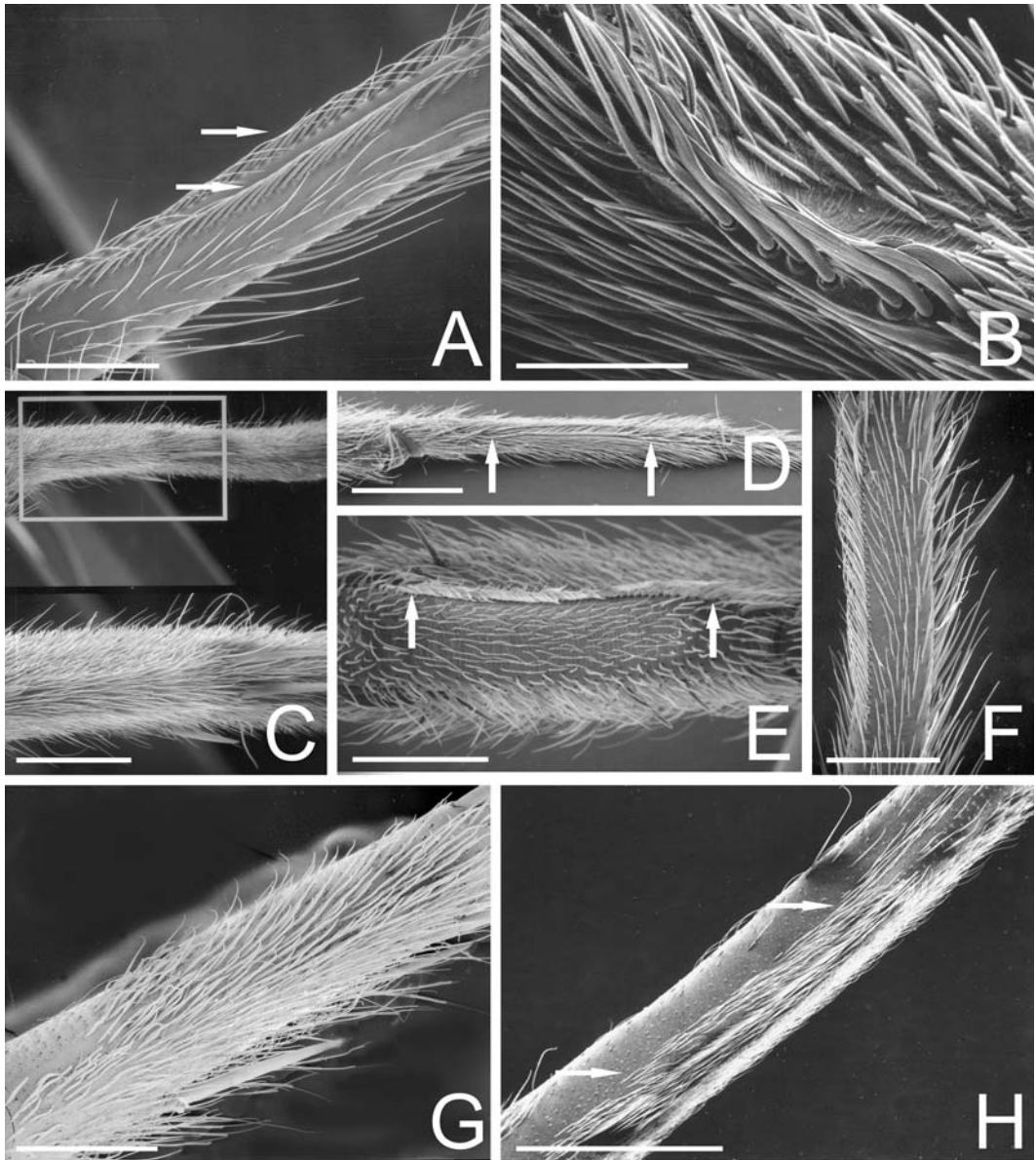


FIGURE 143. Female calamistra. A. *Hypochilus pococki* from Ramsey Cascade, Tennessee, USA, arrows to two calamistral rows. B. *Kukulcania hibernalis* from Alachua Co., Florida, USA, calamistral setae in three staggered rows. C. *Uduba* sp. from Andohahela, Madagascar, oval calamistrum, detail below. D. *Xevioso amica* from St. Lucia, South Africa, arrows to ends of median calamistrum. E. *Titanoeca americana* from Johnson Co., Missouri, USA, arrows to ends of basal calamistrum. F. *Phyxelida tanganensis* from Amani, Tanzania. G. *Zoropsis spinimana* from Vernet-les-Bains, France, oval calamistrum. H. *Psechrus himalayanus* from Gandaki Zone, Nepal, arrows to ends of elongate oval calamistrum. Scale bars: A = 430 μ m, B = 200 μ m, C = 1.5mm (upper), D = 1.0mm, E = 300 μ m, F = 250 μ m, G = 500 μ m, H = 1.0mm.

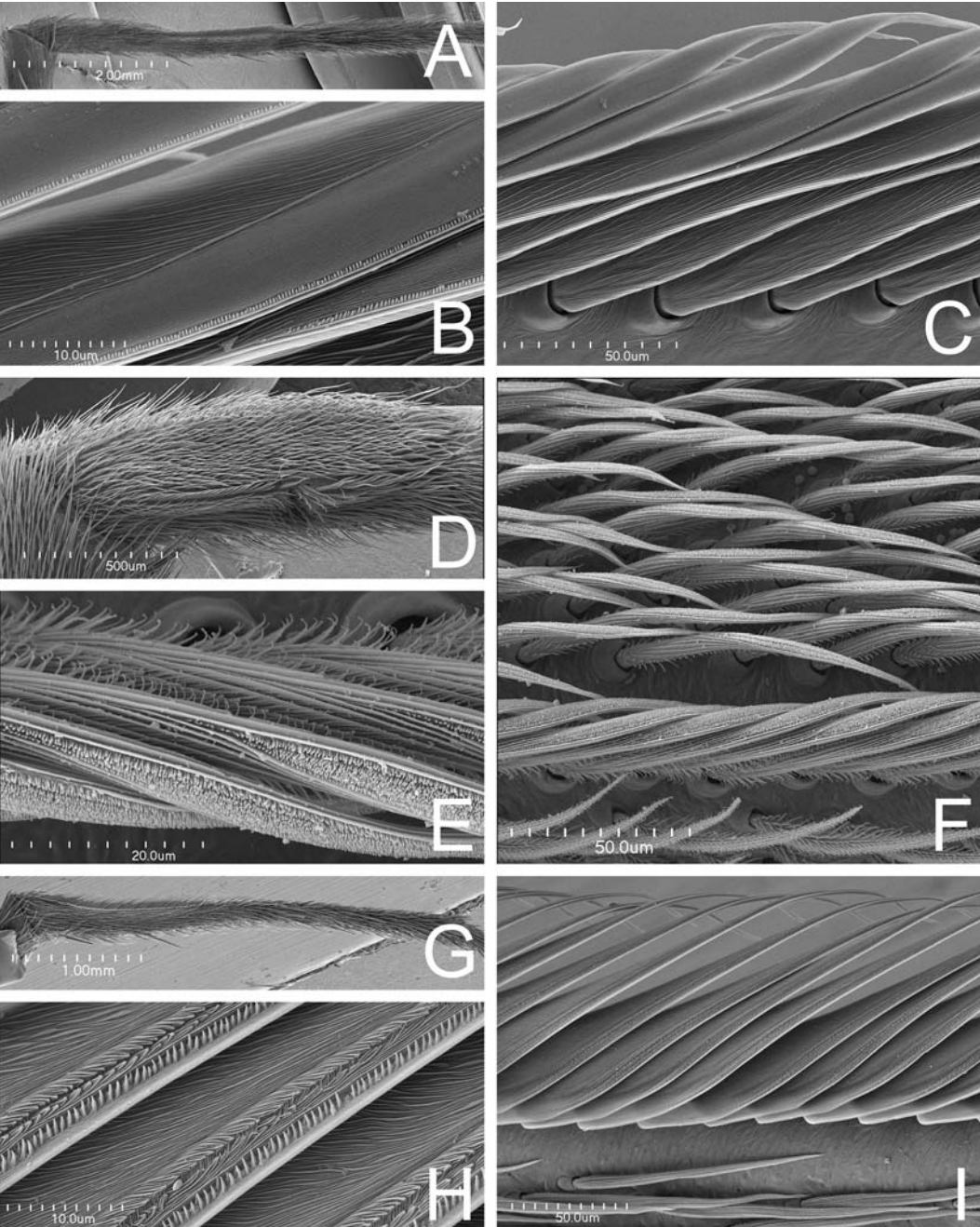


FIGURE 144. Female calamistra. A–C. *Thaida peculiaris* from Puerto Blest, Argentina, right. A. Metatarsus IV. B. Calamistrals setae, close up showing teeth. C. Base of calamistrals setae. D–F. *Stegodyphus mimosarum* from Phinda, South Africa, left, inverted. D. Metatarsus IV. E. Calamistrals setae, close up showing teeth. F. Calamistrals setae: row (below) and oval patch (above). G–I. *Menneus* sp. from Tembe Elephant Park, South Africa, right. G. Metatarsus IV. H. Calamistrals setae, close up showing teeth. I. Base of calamistrals setae. Scale bars: A = 2.0mm, B, H = 10µm, C, F, I = 50µm, D = 500µm, E = 20µm, G = 1.0mm.

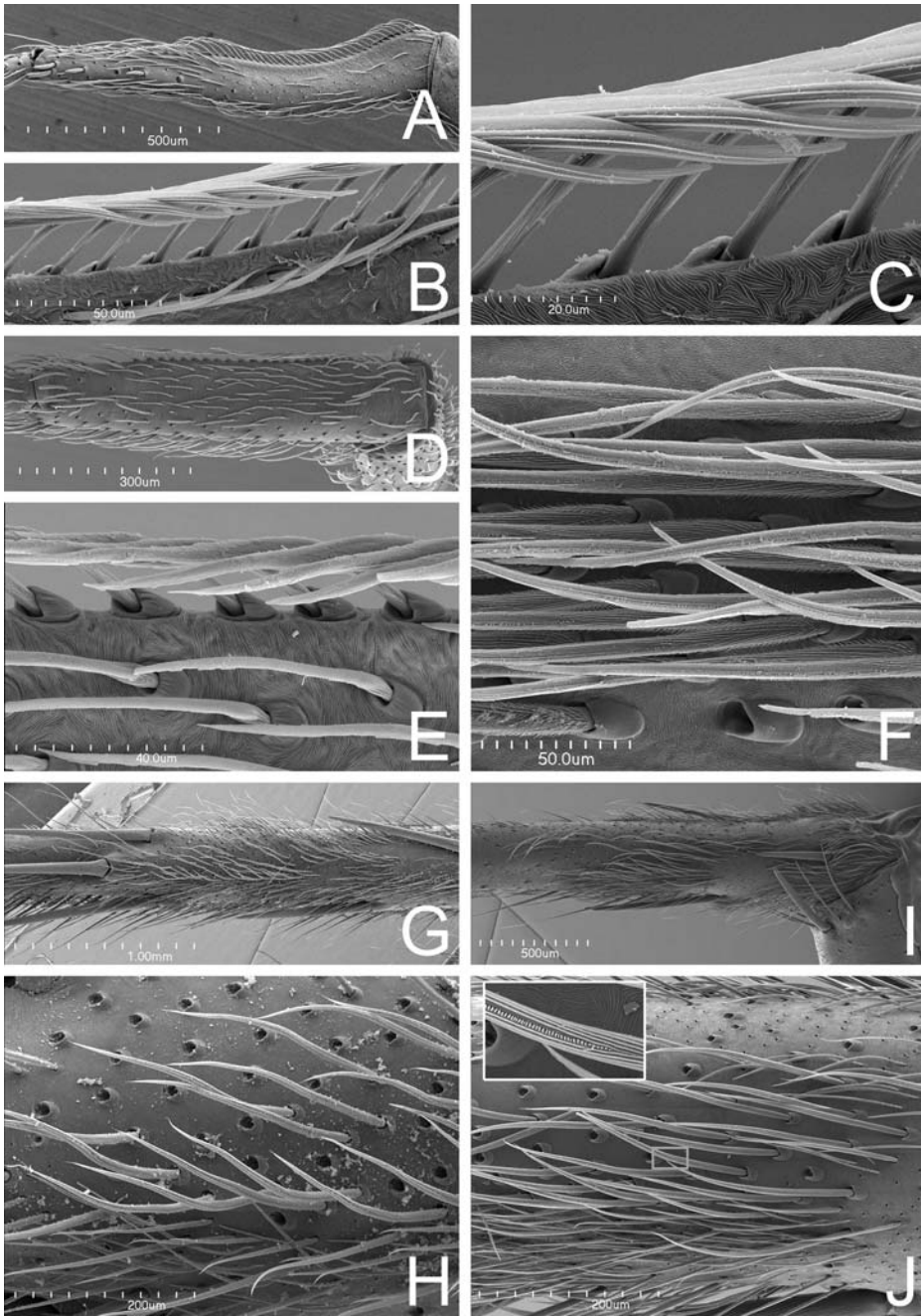


FIGURE 145. Female calamistra. A–C. *Uloborus glomusos* from Mast, North Carolina, USA, left. A. Metatarsus IV. B, C. Calamistras setae, close up, showing teeth. D, E. *Dictyna arundinacea* from Dornoch, Scotland, right. D. Metatarsus IV. E, F. Calamistras setae, close up, showing teeth. F. *Psechrus argentatus* from Cape Vogel Peninsula, Papua New Guinea, left metatarsus IV. G, H. *Zoropsis rufipes* from Tenerife, Canary Islands, left. G. Metatarsus IV. H. Calamistras setae, close up, showing teeth. I, J. *Acanthoctenus* cf. *spinipes* from Loreto, Peru, left. I. Base of metatarsus IV. J. Calamistras setae, close up; inset shows teeth on setae. Scale bars: A, I = 500µm, B, F = 50µm, C = 20µm, D = 300µm, E = 40µm, G = 1.0mm, H, J = 200µm.

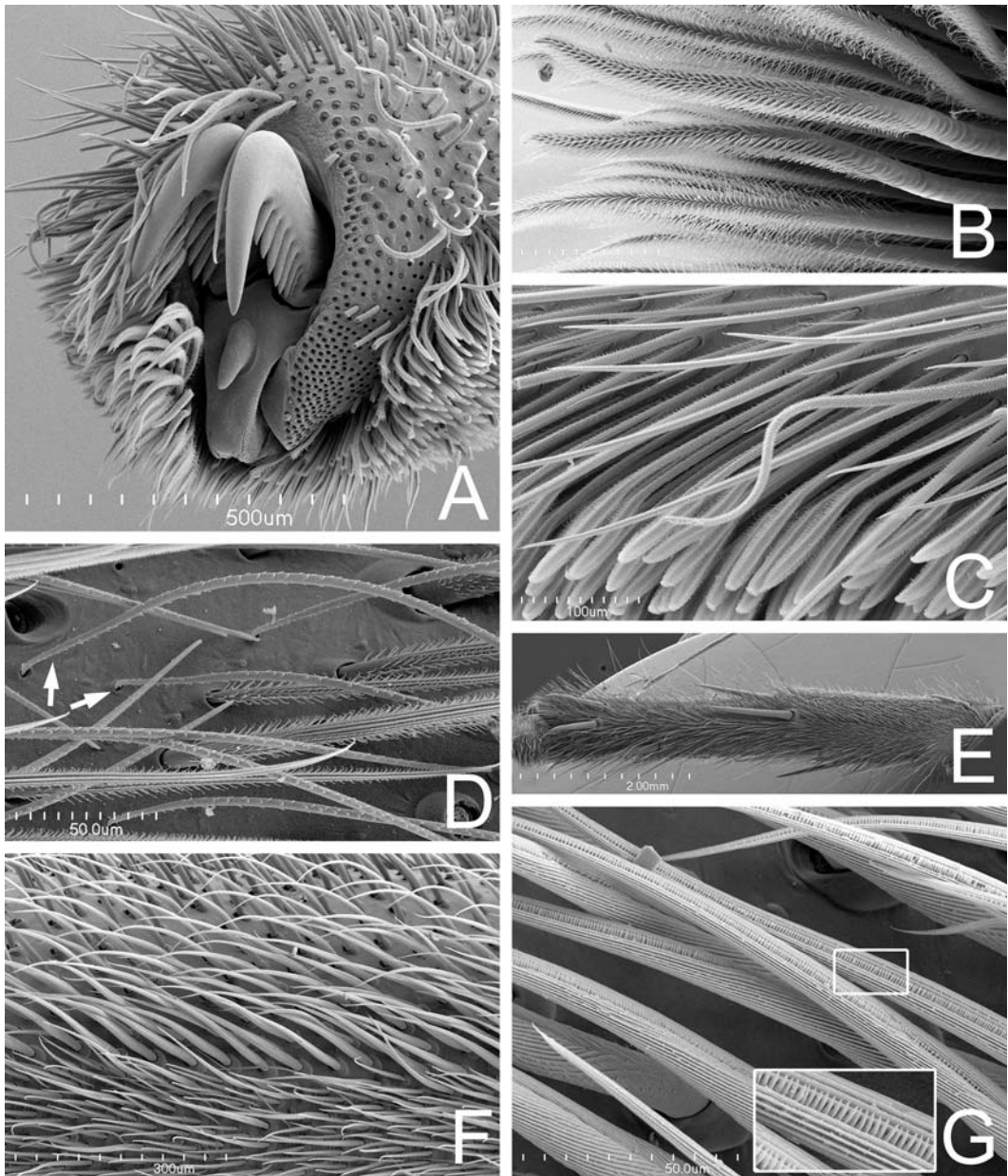


FIGURE 146. Legs of female *Zorocrates* cf. *mistus*, from Los Llanos, Chiapas, Mexico. A. Tarsal claws of left leg I, retrolateral scopula shaved. B. Same, detail of scopular setae close to claws. C. Tarsal scopula. D. Setae of metatarsus IV, showing cylindrical scales (arrows). E. Left metatarsus IV, retrolateral view, showing oval calamistrum. F. Same, detail of calamistrum. G. Same, detail of calamistrual setae, inset showing teeth on setae. Scale bars: A = 500µm, C = 100µm, B, D, G = 50µm, C = 100µm, E = 200µm, F = 300µm.

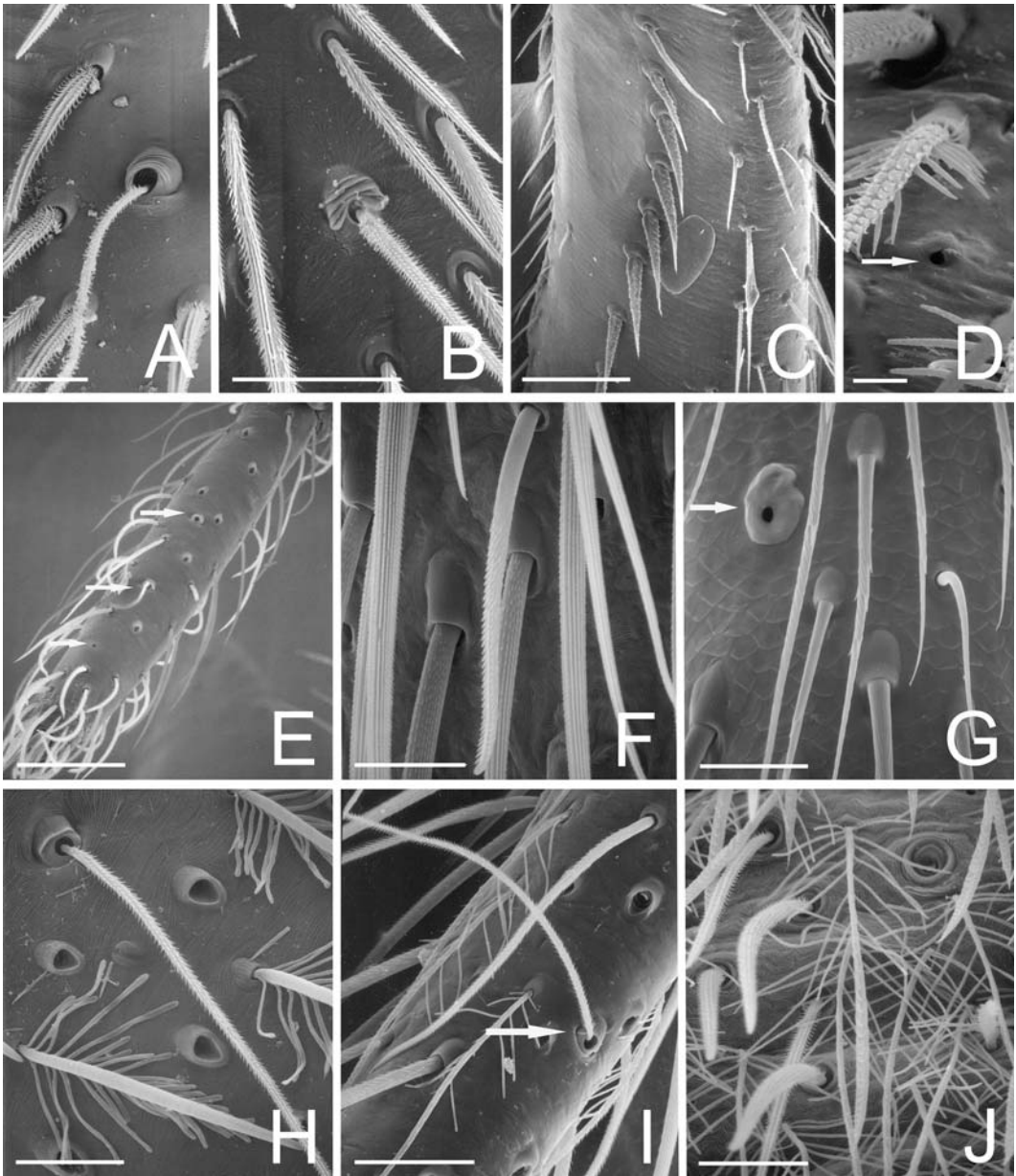


FIGURE 147. Body setae. A. *Xevioso amica* female from St. Lucia, South Africa, tibia III, plumose setae and trichobothrial base. B. *Callobius bennetti* female from Hampshire Co., West Virginia, USA, metatarsus I, plumose setae and trichobothrial base. C. *Pimus* sp. male from Mendocino Co., California, USA, right pedipalpal femur, prolatateral, showing thorns. D. *Maniho ngaitahu* female from Kaituna Valley, New Zealand, tarsus IV showing tarsal organ (arrow) and feathery hairs. E. *Lathys humilis* male from Kent, United Kingdom, tarsus I, arrows to tarsal organ and trichobothrial bases. F. *Deinopis spinosus* female from Gainesville, Florida, USA, tarsus IV. G. *Metepeira* sp. female from Guanajuato, Mexico, tarsus IV, tarsal organ (arrow), scaly cuticle and serrate hairs. H. *Octonoba octonaria* female from Washington Co., Arkansas, USA, tibia IV, trichobothrium and feathery hairs. I. *Stiphidion facetum* female from Royal National Park, New South Wales, Australia, tarsus I, trichobothrium (arrow) and feathery hairs. J. *Raecius jocquei* female from Apouesso, Côte d'Ivoire, venter of abdomen showing plumose and feathery hairs. Scale bars: A = 20 μ m, B = 50 μ m, C = 100 μ m, D = 15 μ m, E = 77 μ m, F, H = 25 μ m, G = 43 μ m, I = 40 μ m, J = 30 μ m.

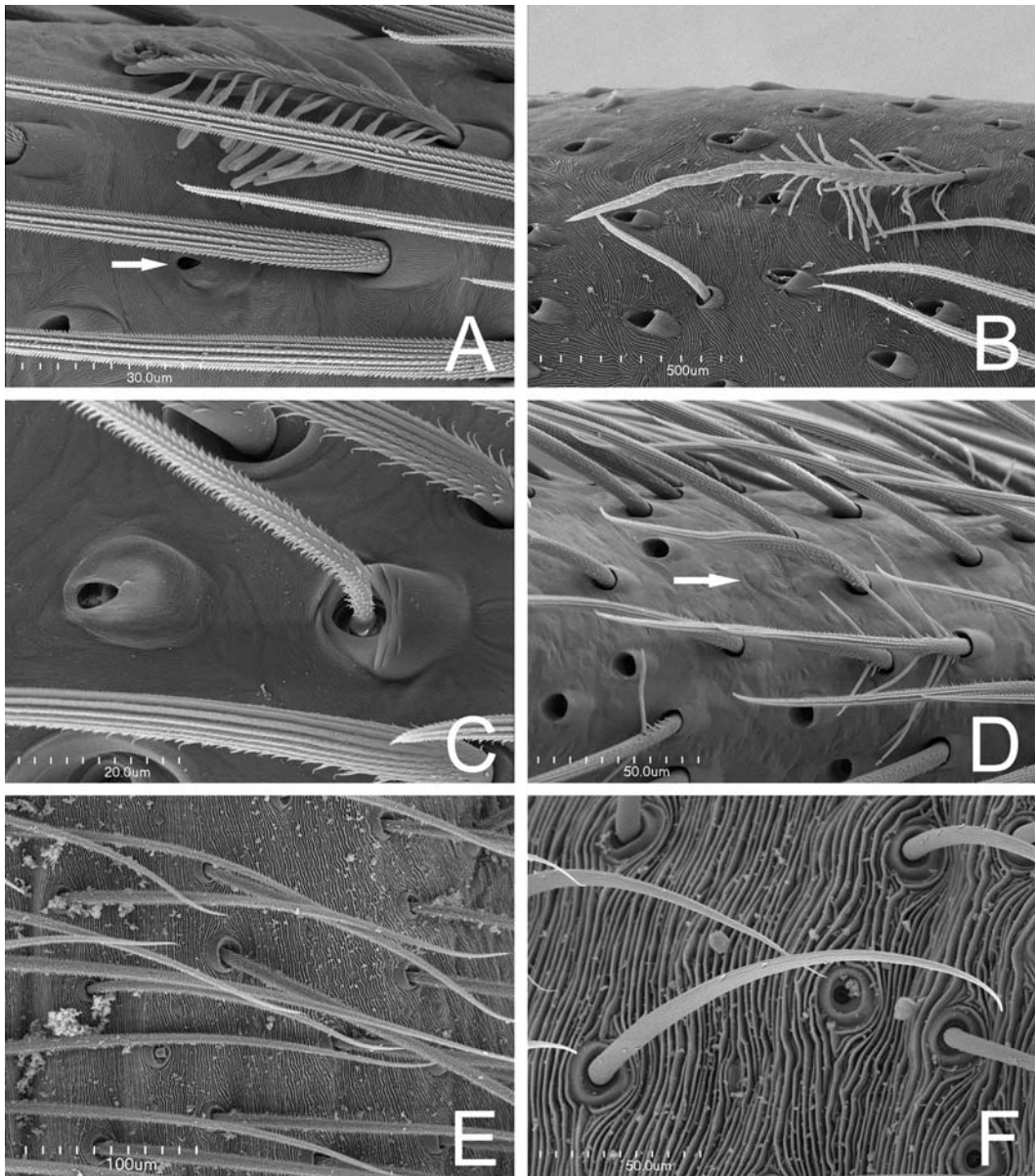


FIGURE 148. Setae of female spiders. A. *Menneus* sp. from Tembe Elephant Park, South Africa, tarsus IV, tarsal organ (arrow) and plumose and feathery setae. B. *Uloborus glomosus* from Mast, North Carolina, USA, tibia IV showing feathery and plumose setae. C. *Acanthoctenus* cf. *spinipes* from Loreto, Peru, tarsus I showing tarsal organ, trichobothrial base, and plumose setae. D. *Thaida peculiaris* from Puerto Blest, Argentina, tarsus IV showing exposed tarsal organ (arrow) and plumose and feathery setae. E. *Hickmania troglodytes* from Mole Creek Cave, Tasmania, Australia, abdomen. F. *Araneus diadematus* from Ontario, Canada, abdomen. Scale bars: A = 30µm, B, D, F = 50µm, C = 20µm, E = 100µm.

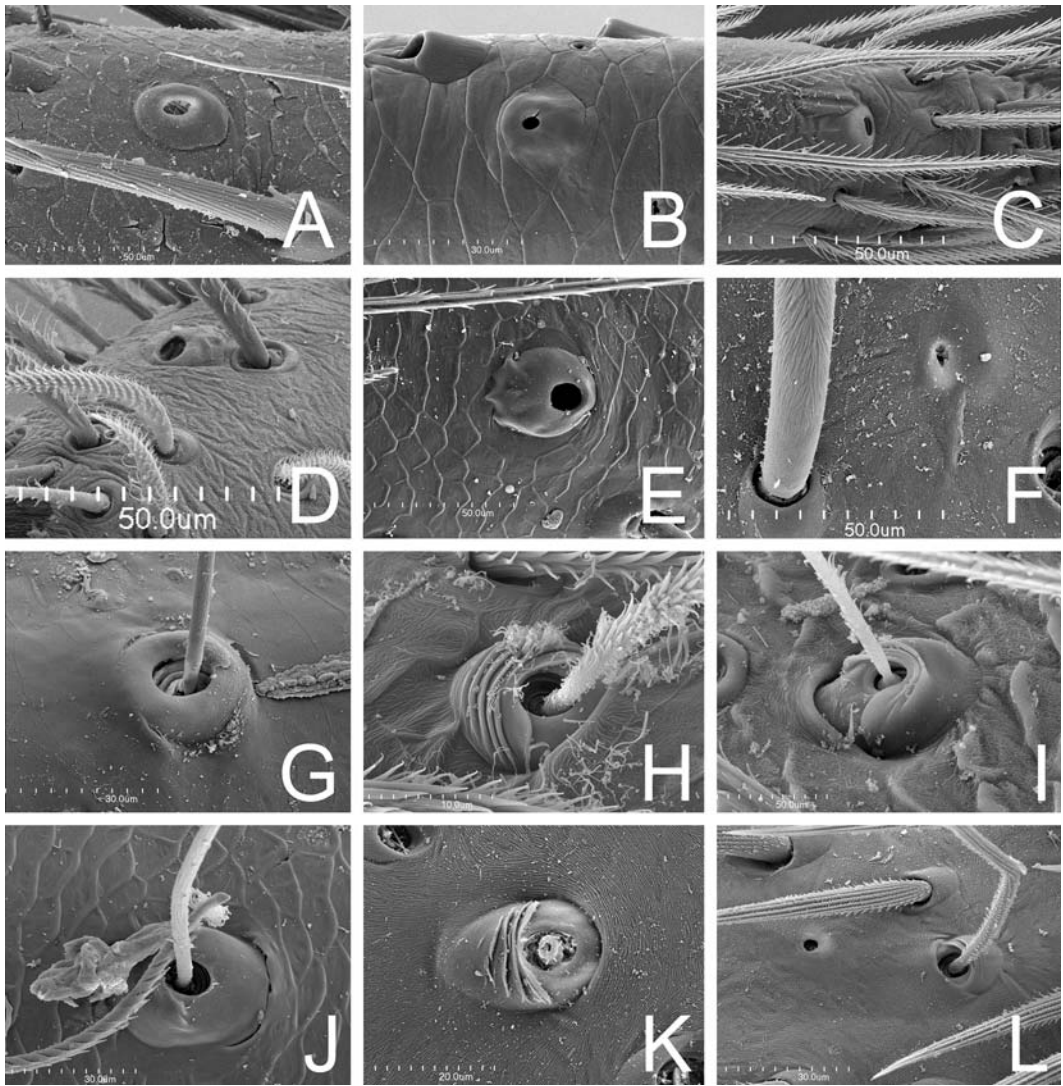


FIGURE 149. Tarsal organs and trichobothria of females. A. *Araneus diadematus* from Ontario, Canada, tarsal organ IV. B, G. *Mimetus hesperus* from Lander Co., Nevada, USA. B. Tarsal organ IV. G. Trichobothrial base, pedipalpal tibia. C, H. *Archaea workmani* from Ranomafana, Madagascar. C. Tarsal organ I. H. Trichobothrial base, metatarsus I. D, I. *Huttonia* sp. from Orongorongo, New Zealand. D. Tarsal organ I. I. Trichobothrial base, metatarsus I. E, J. *Nicodamus mainae* from Coalseam Park, Western Australia, Australia. E. Tarsal organ I. J. Trichobothrial base, metatarsus I. F, K. *Tengella radiata* from Guanacaste, Costa Rica. F. Tarsal organ I. K. Trichobothrial base, tarsus I. L. *Psechrus argentatus* from Cape Vogel Peninsula, Papua New Guinea, trichobothrial base and tarsal organ I. Scale bars: A, C, D, E, F = 50µm, B, G, I, J = 30µm, H = 10µm, K = 20µm.

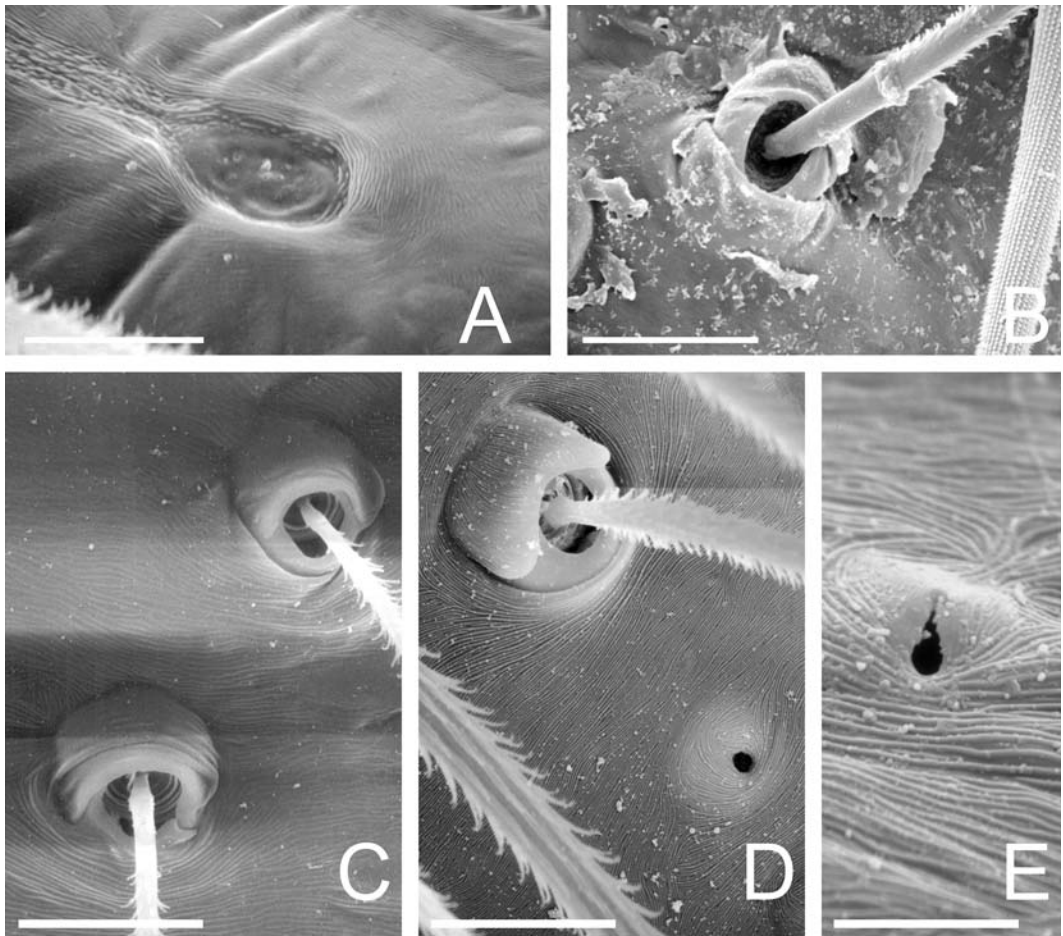
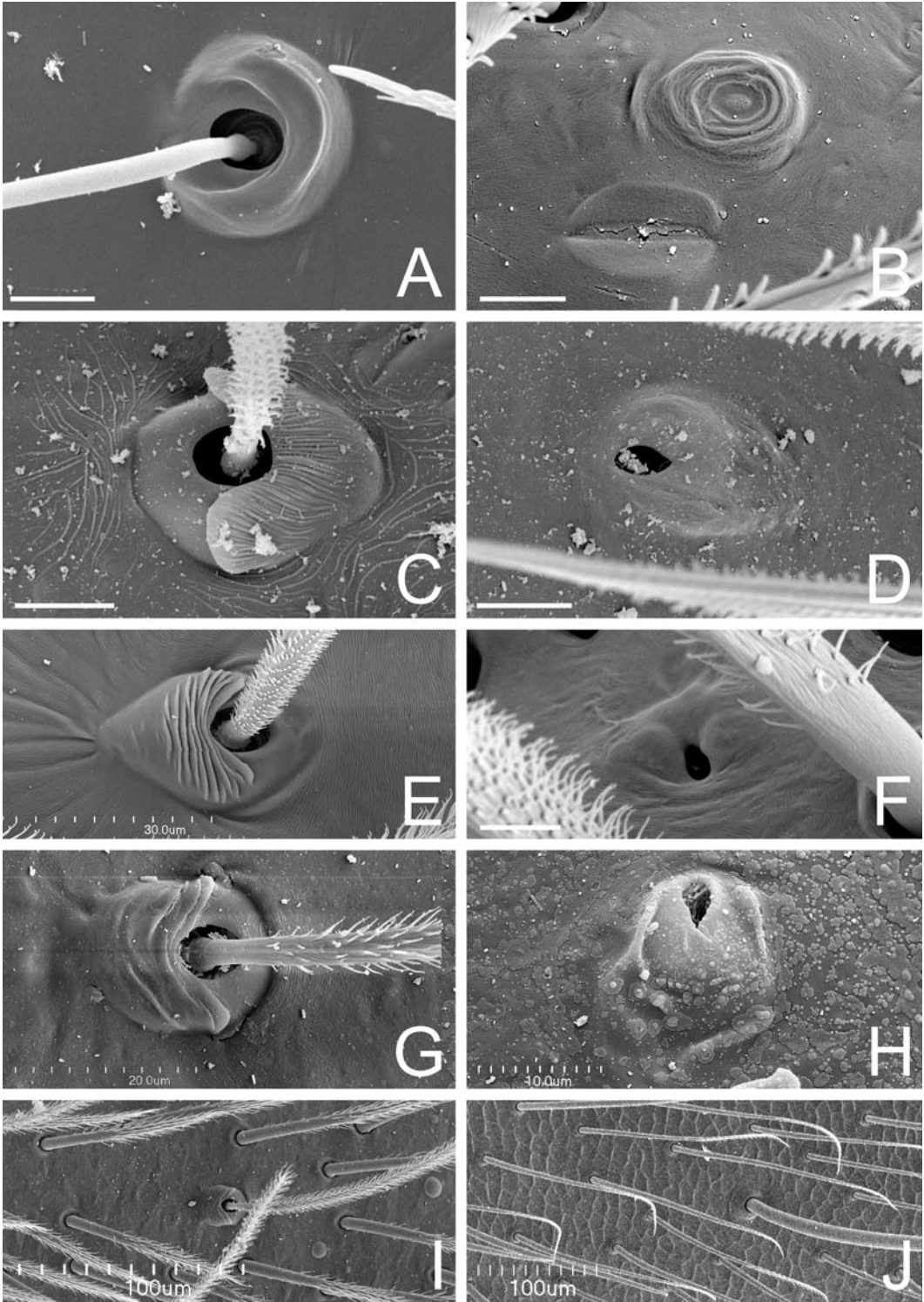


FIGURE 150. Tarsal organs and trichobothria. A. *Hickmania troglodytes* female from cave at Mole Creek, Tasmania, Australia, exposed tarsal organ II. B. *Hypochilus pococki* female from Great Smokey Mts., Tennessee, USA, metatarsus II trichobothrial base. C. *Aebutina binotata* male from near Tarapuy, Ecuador, trichobothria on pedipalpal tibia. D, E. *Poaka graminicola* from Lincoln, New Zealand. D. Female tarsus IV, trichobothrial base and tarsal organ. E. Tarsal organ on male pedipalpal cymbium. Scale bars: A = 176 μ m, B = 231 μ m, C, D = 15 μ m, E = 6 μ m.



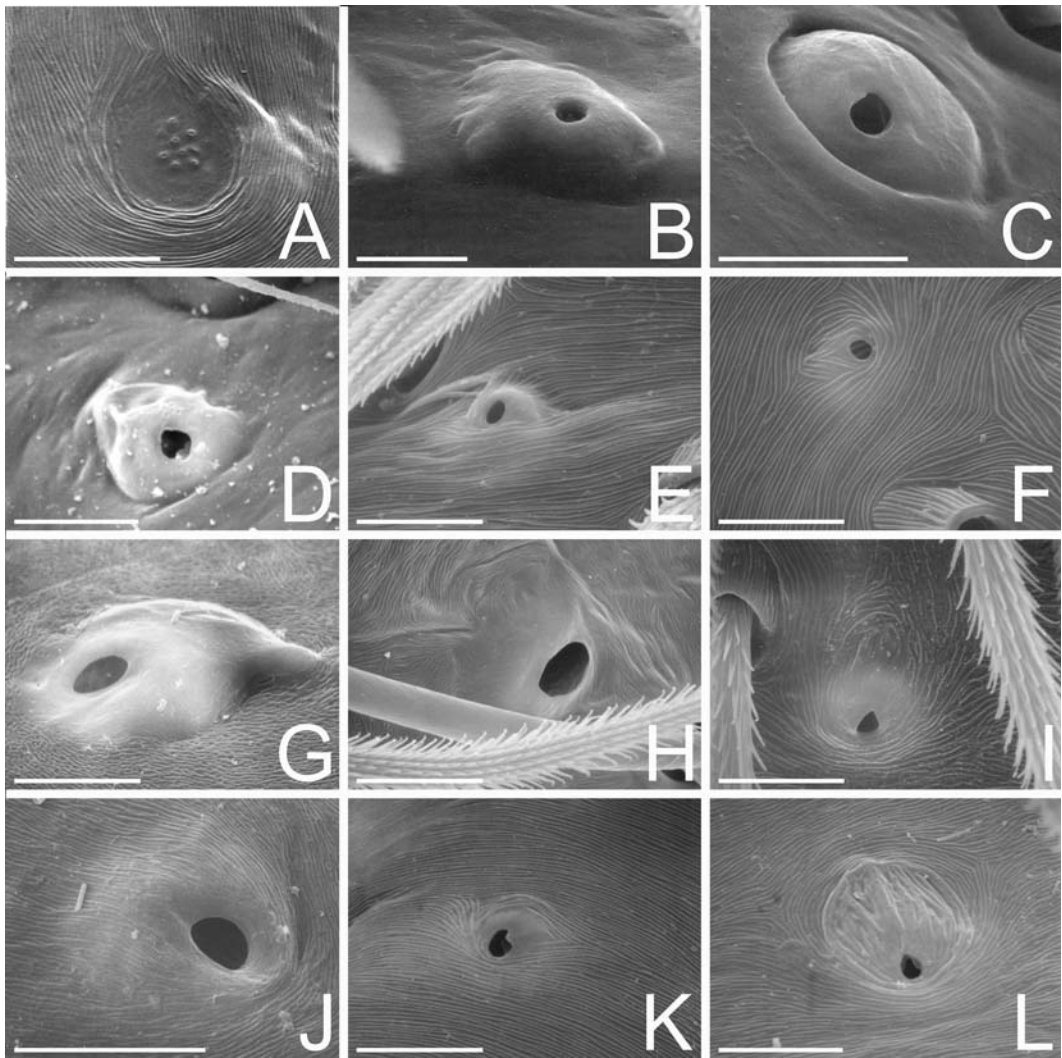


FIGURE 152 (above). Tarsal organs. A. *Austrochilus melon* from Cuesta Pucalan, Chile, juvenile IV. B. *Kukulcania hibernalis* from Alachua Co., Florida, USA, female IV. C. *Stegodyphus mimosarum* from Spioenkop, South Africa, female IV. D. *Uroctea* sp. from Julwania, India, juvenile I. E. *Octonoba octonaria*, from Washington Co., Arkansas, USA, female IV. F. *Uloborus diversus* from Napa Co., California, USA, female I. G. *Megadicctyna thilenii* from Hicks Bay, New Zealand, female IV. H. *Deinopis spinosus* from Gainesville, Florida, USA, male cymbium. I. *Titanoeca americana* from Johnson Co., Missouri, USA, female III. J. *Vytftua bedel* from Sumatra, Indonesia, female I. K. *Lathys humilis* from Kent, United Kingdom, male I. L. *Goeldia* sp. from Junin, Peru, female IV. Scale bars: A–C, G, I, J = 10 μ m, D, H = 15 μ m, E, F, K, L = 7.5 μ m.

FIGURE 151 (left). Tarsal organs, trichobothria, and cuticle sculpture from female leg I. A, B. *Ariadna boesenbergi* from Buenos Aires, Argentina. A. Trichobothrium. B. Tarsal organ. C, D. *Macrobunus multidentatus* from Chiloé, Chile. C. Trichobothrium. D. Tarsal organ. E, F. *Zorocrates* cf. *mistus* from Los Llanos, Chiapas, Mexico. E. Trichobothrium. F. Tarsal organ. G–J. *Desis formidabilis* from Cape Peninsula, South Africa. G. Trichobothrium. H. Tarsal organ. I. Tarsal trichobothrium and surrounding smooth cuticle. J. Tibial setae and surrounding squamate cuticle. Scale bars: A = 1 μ m, B, C, D, F = 10 μ m, E = 30 μ m.

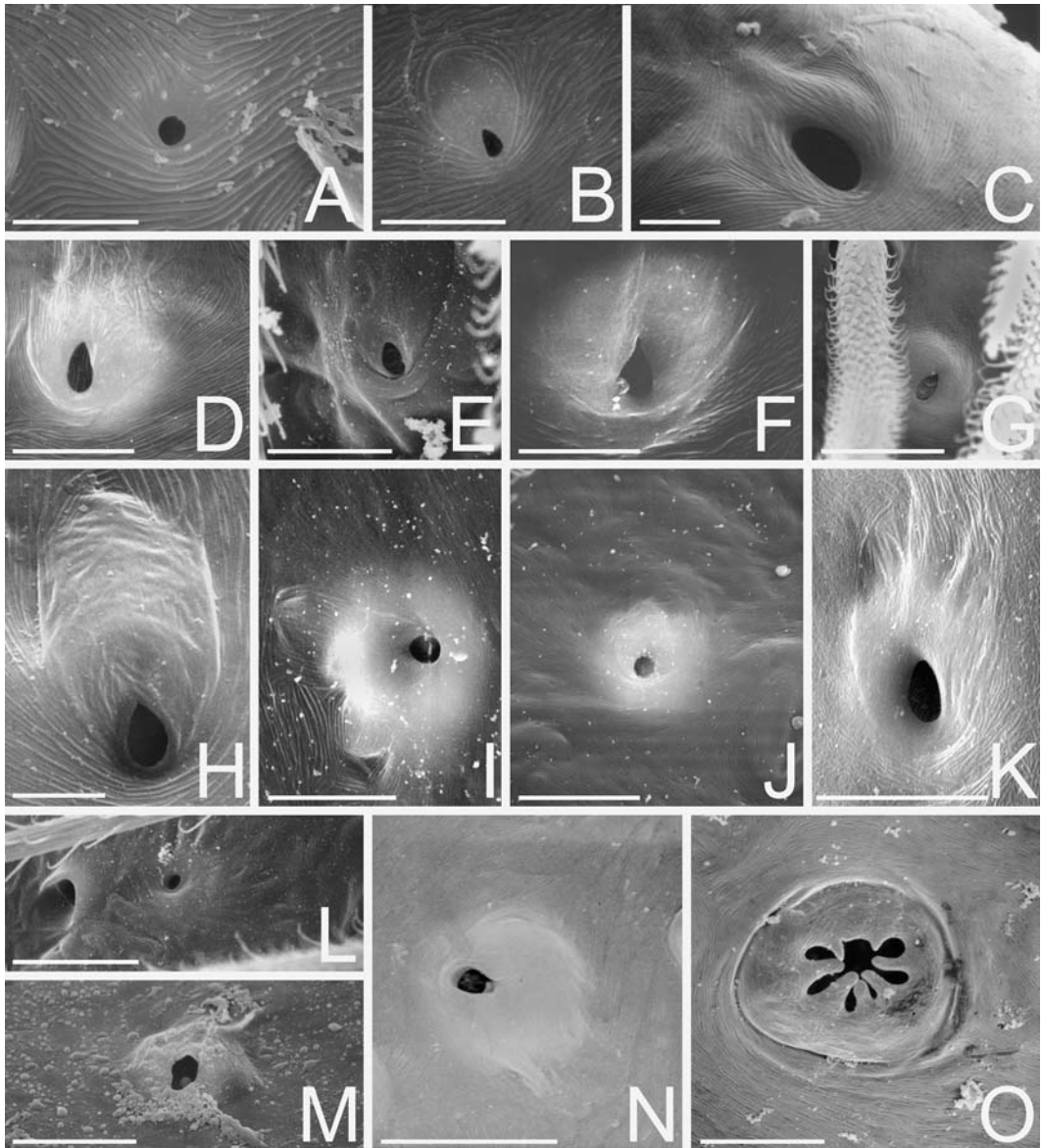


FIGURE 153. Tarsal organs. A. *Dictyna arundinacea* from Tuva, Russia, male I. B. *Tricholathys spiralis* from Lenore Lake, Washington, USA, female IV. C. *Stiphidion facetum* from Royal National Park, New South Wales, Australia, female I. D. *Neolana dalmasi* from Lake Okataina, New Zealand, male I. E. *Metaltella simoni* from Riverside, California, USA, cymbium. F. *Neoramia sana* from Dunedin, New Zealand, female I. G. *Matachia australis* from Dunedin, New Zealand, female pedipalpus. H. *Badumna longinqua* from Maui, Hawaii, USA, female III. I. *Retiro* sp. from Lima, Peru, female IV. J. *Pimus* sp. from Mendocino Co., California, USA, male cymbium. K. *Amaurobius fenestralis* from Tisvilde, Denmark, female II. L. *Raecius jocquei* from Appouesso, Côte d'Ivoire, male cymbium. M. *Acanthoctenus* sp. from Changuinola, Panama, female pedipalpus. N. *Zoropsis spinimana* from Barcelona, Spain, female IV. O. *Uduba* sp. from Anjozorobe, Madagascar, male cymbium. Scale bars: A = 6 μ m, B, D, E, J, K = 10 μ m, C, H = 4 μ m, F, I = 7.5 μ m, G, L, M, O = 15 μ m, N = 20 μ m.

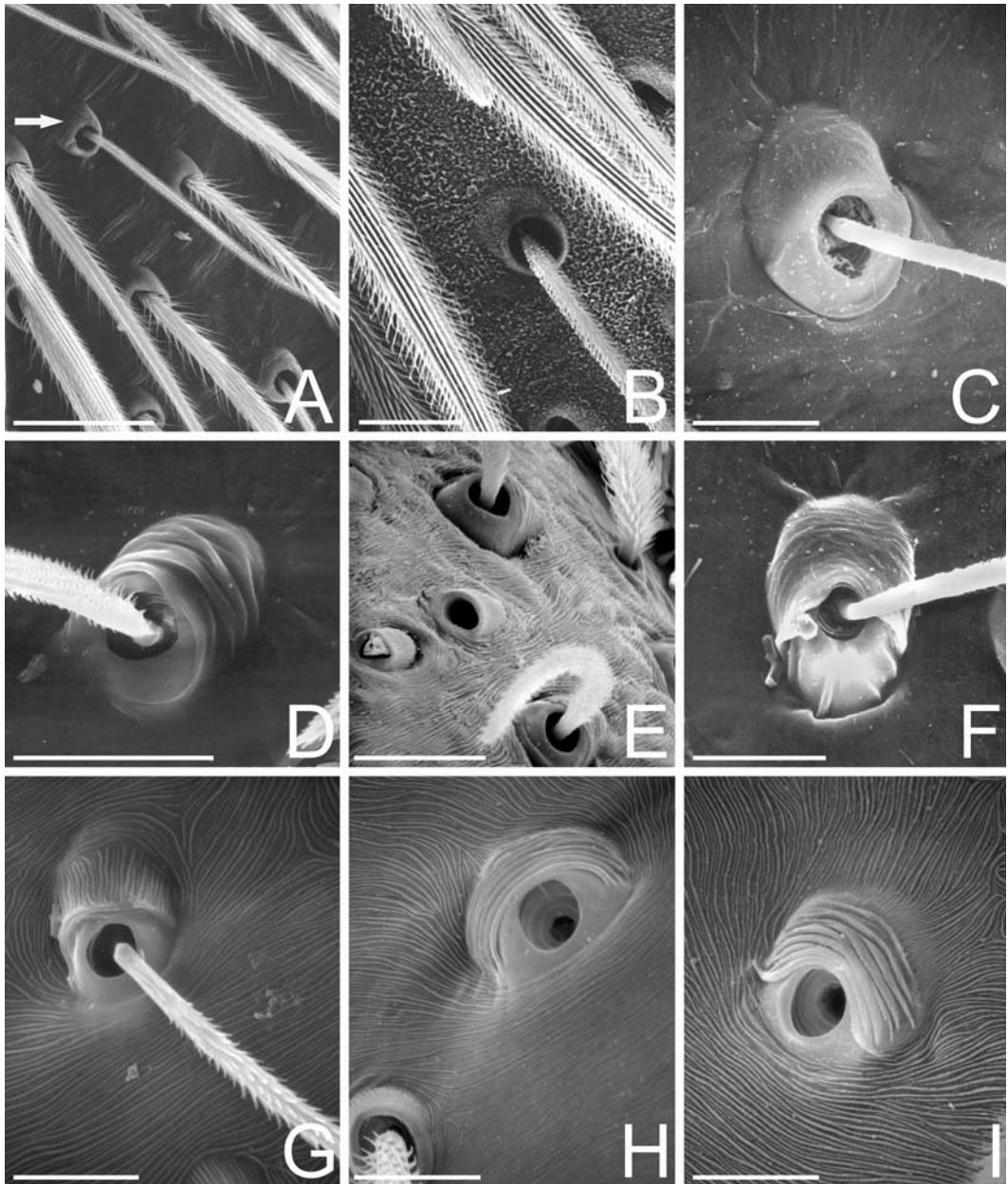


FIGURE 154. Trichobothrial bases. A. *Kukulcania hibernalis* from Alachua Co., Florida, USA, female metatarsus IV, trichobothrial base (arrow) and plumose setae. B. *Filistata insidiatrix* from Barcelona, Spain, female metatarsus I. C. *Uroctea* sp. from Julwania, India, juvenile metatarsus I. D. *Stegodyphus mimosarum* from Spioenkop, South Africa, female metatarsus I. E. *Deinopis spinosus* from Gainesville, Florida, USA, male pedipalpal tibia. F. *Megadictyna thilenii* from West Taupo District, New Zealand, female metatarsus I. G. *Uloborus diversus* from Napa Co., California, USA, female tibia I. H. *Goeldia* sp. from Junin, Peru, female metatarsus IV. I. *Titanoeca americana* from Johnson Co., Missouri, USA, female metatarsus III. Scale bars: A = 50 μ m, B, D, F = 20 μ m, C, E = 15 μ m, G—I = 10 μ m.

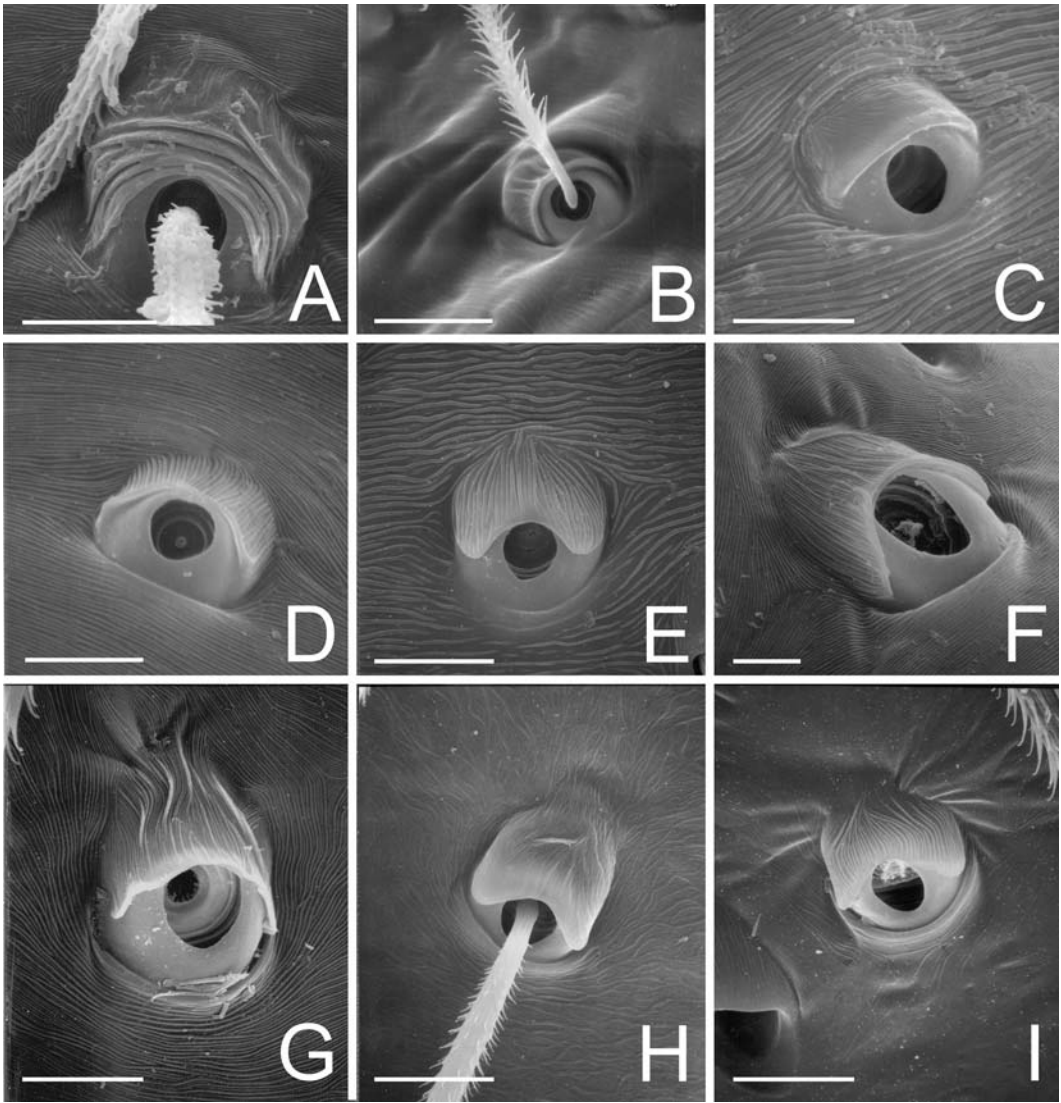


FIGURE 155. Trichobothrial bases. A. *Vytftia bedel* from Sumatra, Indonesia, female metatarsus I. B. *Nigma linsdalei* from San Francisco, California, USA, female pedipalpal tibia. C. *Dictyna arundinacea* from Tuva, Russia, male metatarsus I. D. *Lathys humilis* from Kent, United Kingdom, male tarsus I. E. *Tricholathys spiralis* from Lenore Lake, Washington, USA, female tarsus IV. F. *Stiphidion facetum* from Royal National Park, New South Wales, Australia, female tarsus I. G. *Neolana dalmasi* from Lake Okataina, New Zealand, male tibia I. H. *Neoramia sana* from Dunedin, New Zealand, male tarsus I. I. *Metaltella simoni* from Riverside, California, USA, female tarsus IV. Scale bars: A, B, E, G, I = 10 μ m, C, D = 6 μ m, F = 4 μ m, H = 15 μ m.

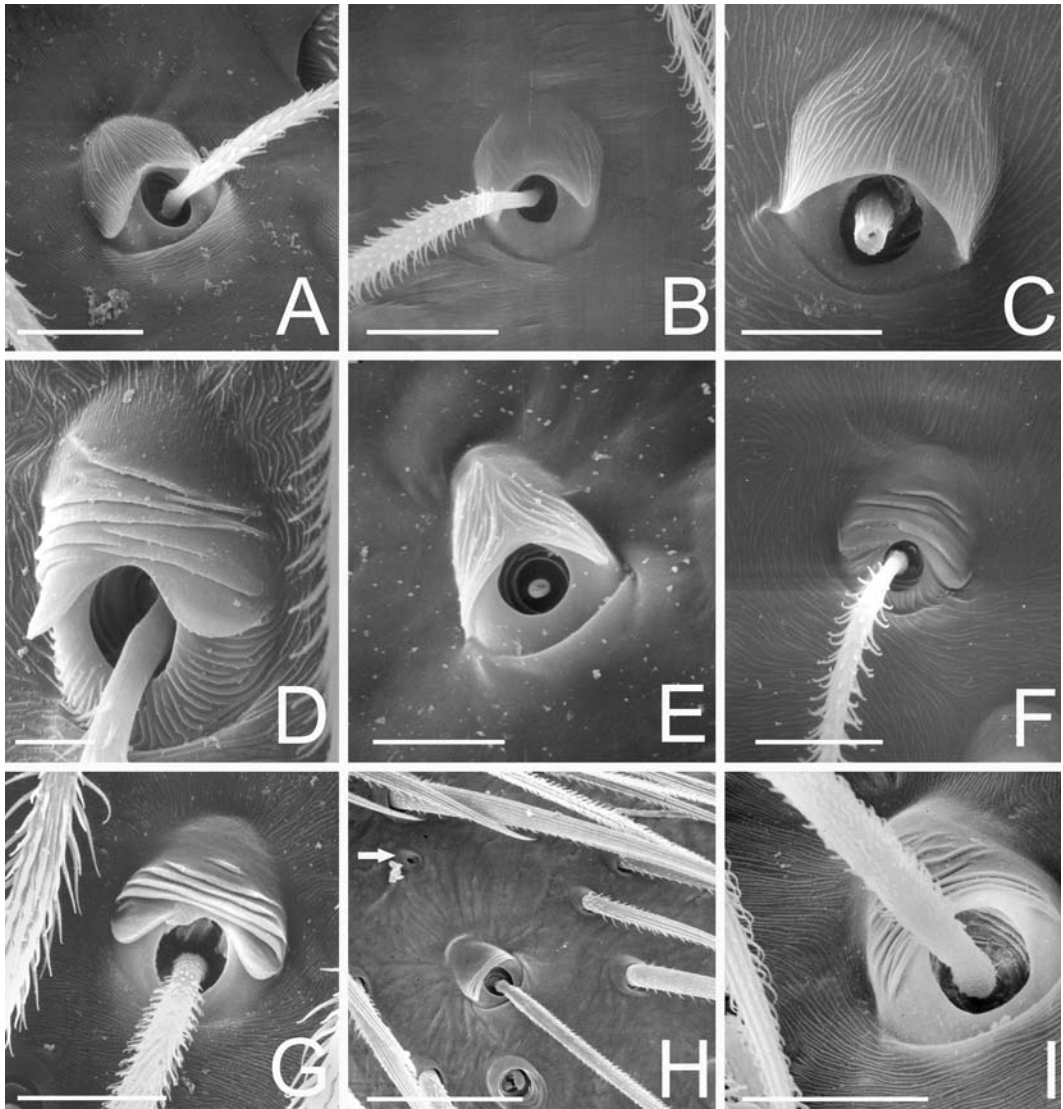


FIGURE 156. Trichobothrial bases. A. *Maniho ngaitahu* from Kaituna Valley, New Zealand, female tarsus IV. B. *Matachia australis* from Dunedin, New Zealand, female pedipalpal tibia. C. *Badumna longinqua* from Maui, Hawaii, USA, female tarsus III. D. *Amaurobius fenestralis* from Tisvilde, Denmark, female tarsus II. E. *Retiro* sp. from Lima, Peru, female tarsus IV. F. *Pimus* sp. from Mendocino Co., California, USA, male cymbium. G. *Uduba* sp. from Ranomafana, Madagascar, male tarsus I. H. *Acanthoctenus spiniger* from Changuinola, Panama, female tarsus I (arrow to tarsal organ). I. *Zoropsis spinimana* from Barcelona, Spain, female tarsus IV. Scale bars: A, C, F = 10 μ m, B = 15 μ m, D = 4 μ m, E = 7.5 μ m, G, I = 20 μ m, H = 50 μ m.

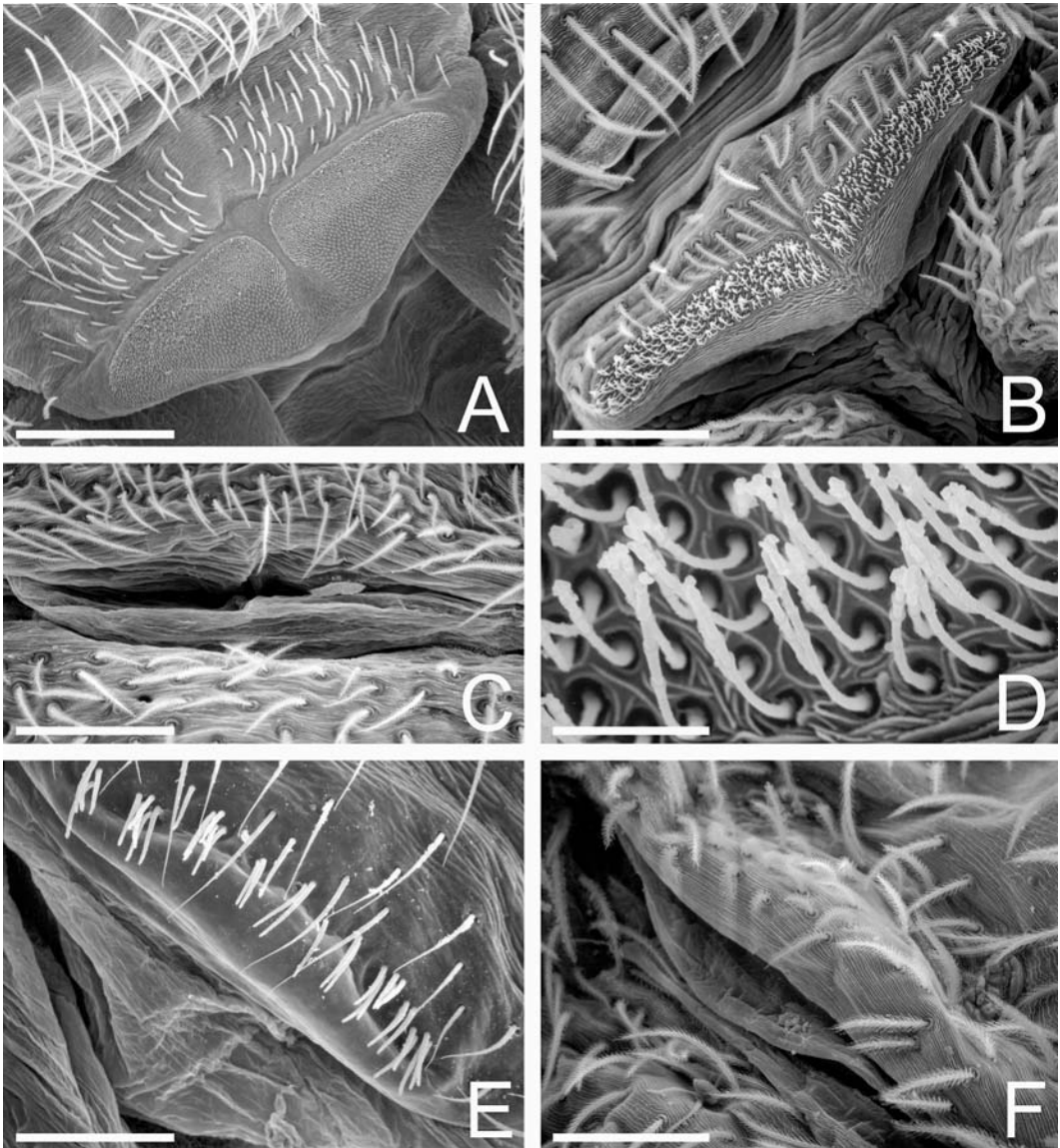


FIGURE 157. Cribellar and epiandrous regions. A, C. *Aebutina binotata* from Ecuador: female from Rio Cuyabeno, Sucumbos, male from near Tarapuy, Napo. B, D, F. *Poaka graminicola* from Lincoln, New Zealand. E. *Mimetus hesperus* male from Baboquivari Mts., Arizona, USA. A, B. Divided cribella. D. Close up of *Poaka* strobilate cribellar spigots. C, E, F. Male epiandrous regions. Note presence of spigots in *Mimetus* (E) and their absence in *Aebutina* (C) and *Poaka* (F). Scale bars: A = 150 μ m, B, E, F = 75 μ m, C = 100 μ m, D = 7.5 μ m.

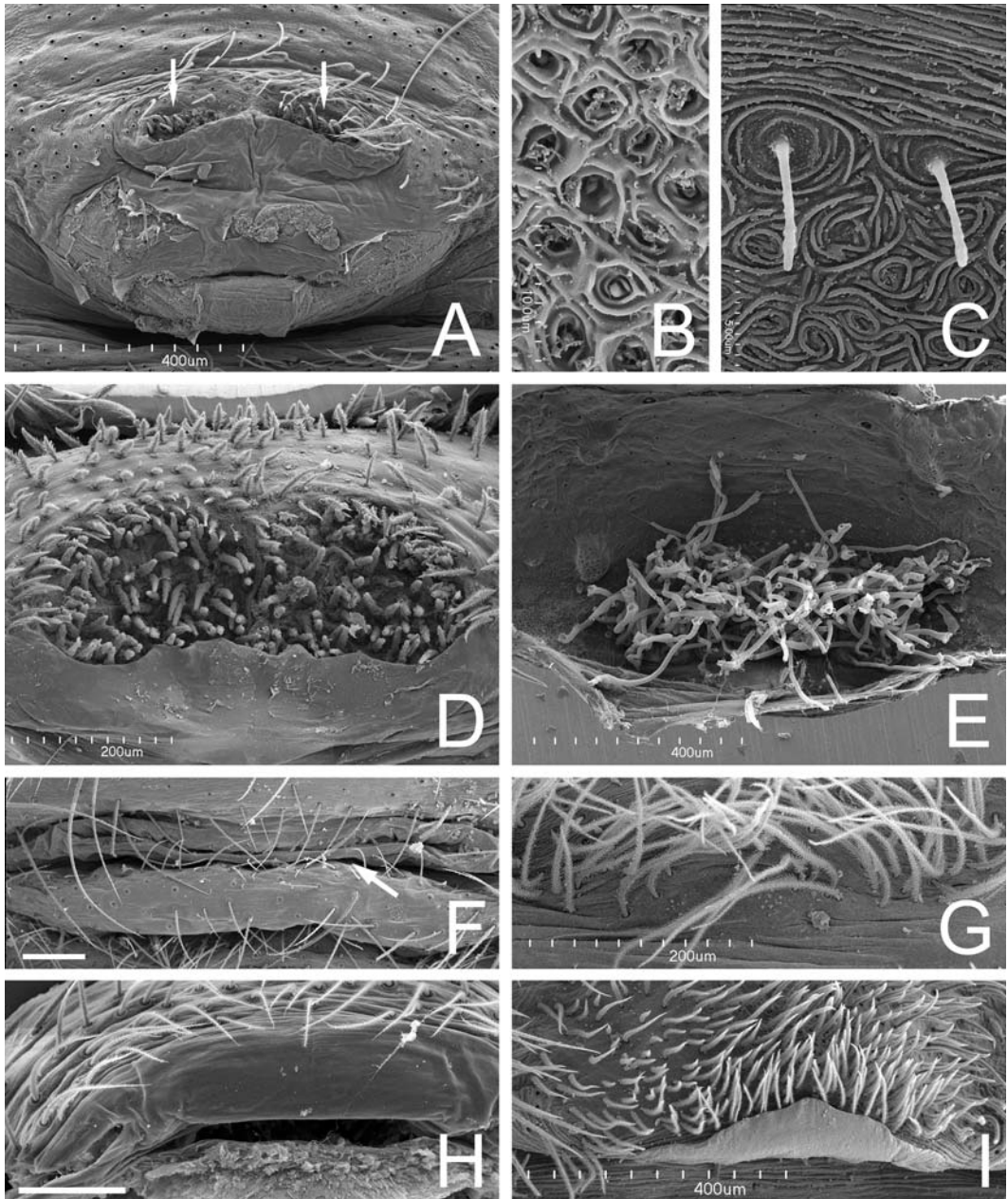


FIGURE 158. Male cribellar and epiandrous regions. A, B. *Thaidia peculiaris* from Cautin, Chile. A. Epiandrous spigots, note two bunches (arrows). B. Close up of remnant of male cribellum. C. *Pimus napa* from Oakville, California, USA, vestigial cribellar spigots. D, E. *Eresus* cf. *cinnaberinus* from Mistras, Greece. D. Epiandrous spigots. E. Internal view, KOH digested. F—I. Epiandrous regions lacking spigots. F. *Ariadna boesenbergi* from Buenos Aires, Argentina, arrow to epigastric furrow. G. *Desis formidabilis* from Cape Peninsula, South Africa. H. Epiandrous region of *Macrobnus multidentatus* from Chiloé, Chile. I. *Zorocrates* sp., from Big Bend Nat. Pk., Texas, USA. Scale bars: A, E, I = 400µm, B = 10µm, C = 5µm, D, G = 200µm, F, H = 100 µm.

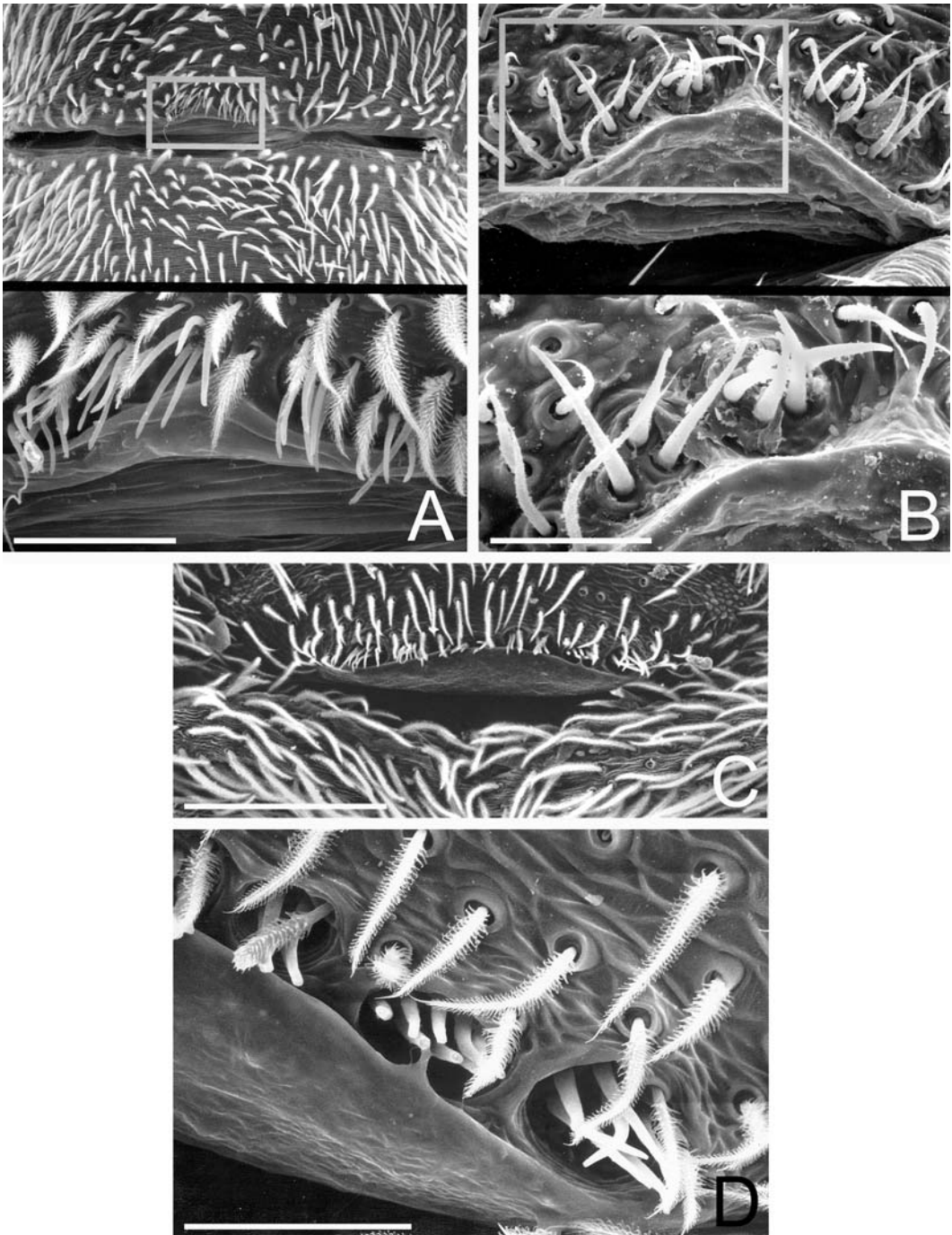


FIGURE 159. Male epiandrous region. A. *Stegodyphus mimosarum* from Malawi: overview (upper), close-up of spigots (lower). B. *Uroctea* sp. from Garies, South Africa: overview (upper), close-up of spigots (lower). C, D. *Deinopis spinosus* from Gainesville, Florida, USA. C. Overview. D. Close-up of spigots. Scale bars: A = 30 μ m (bottom), B = 100 μ m (upper), C = 200 μ m, D = 50 μ m.

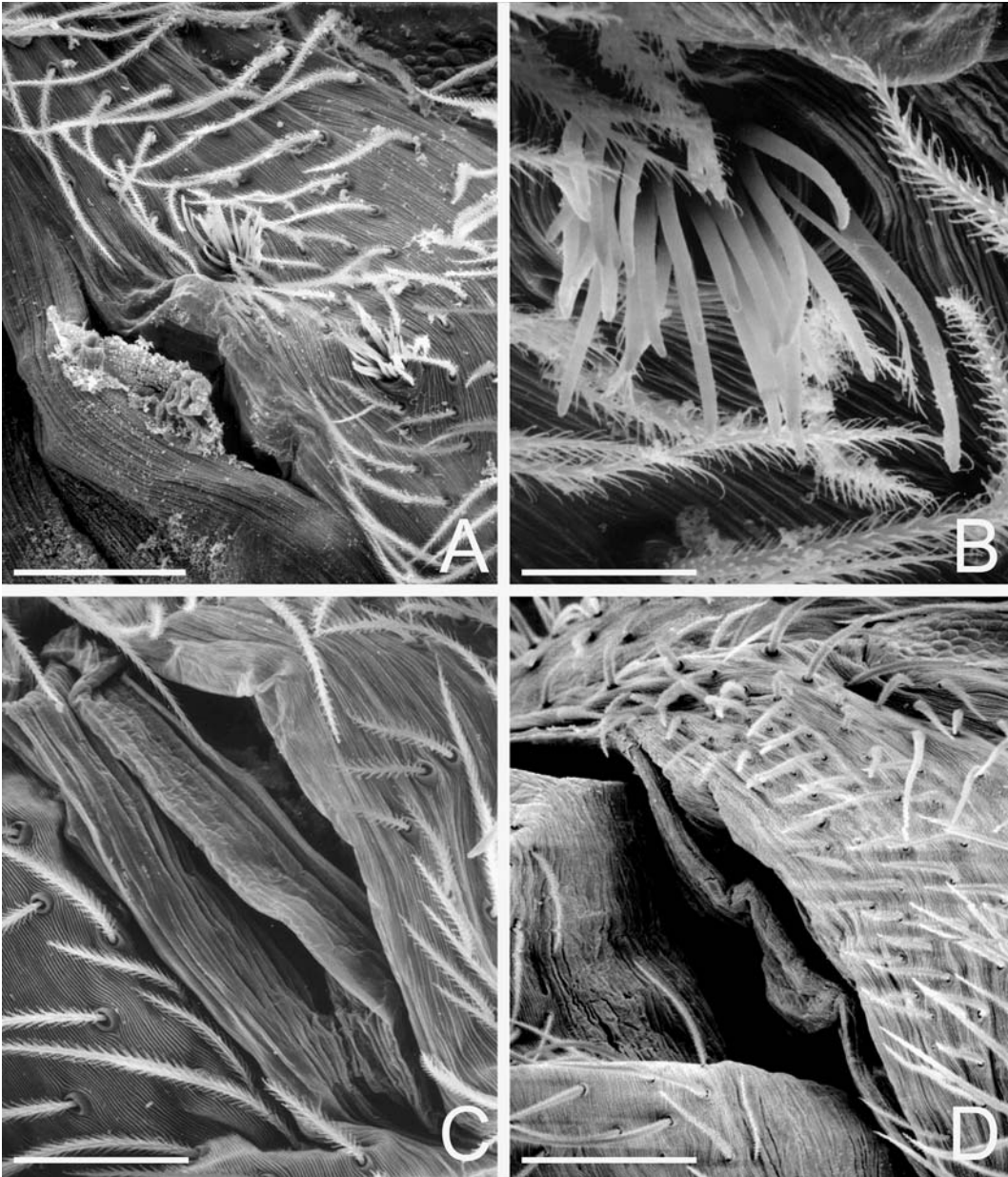


FIGURE 160. Male epiandrous region. A, B. *Phyxelida tanganensis* from Amani, Tanzania. A. Whole region showing two bundles of spigots. B. Close up of one spigot bundle. C. *Lathys humilis* from Kent, United Kingdom, lacking spigots. D. *Metaltella simoni* from Riverside, California, USA, lacking spigots. Scale bars: A = 100 μ m, B = 20 μ m, C = 43 μ m, D = 150 μ m.

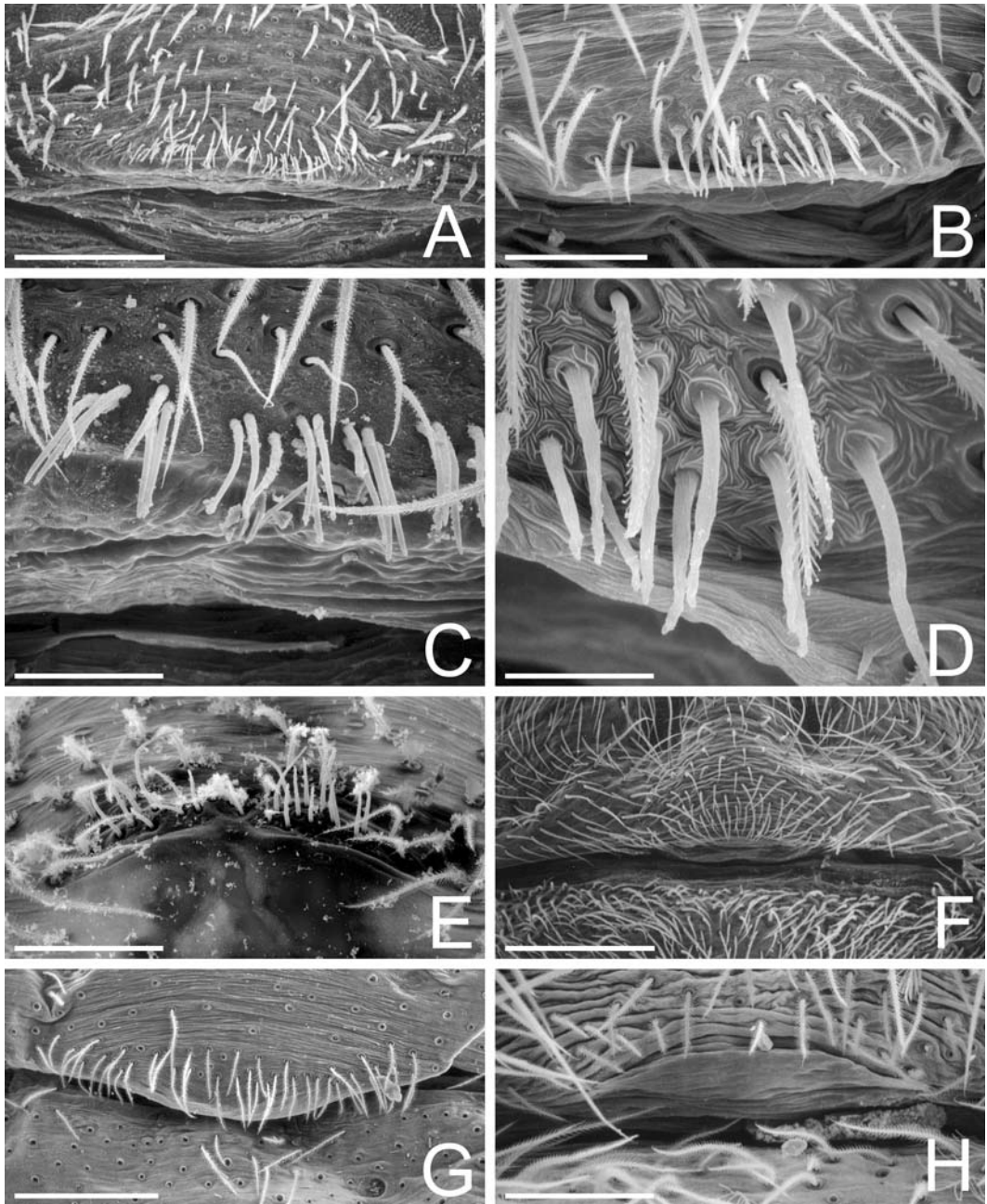


FIGURE 161. Male epiandrous region. A–E. Epiandrous spigots. F–H. Epigastric furrow lacking spigots. A, C. *Megadictyna thilenii* from Orongorongo, New Zealand. A. Epigastric furrow. C. Close-up of spigots. B, D. *Titanoeca americana* from Portle Springs, Missouri, USA. B. Epiandrous region. D. Close up of spigots. E. *Pimus* sp. from Mendocino Co., California, USA. F. *Neoramia sana* from Dunedin, New Zealand. G. *Vyffutia pallens* from Sarawak, Malaysia. H. *Raecius jocquei* from Apouesso, Côte d'Ivoire. Scale bars: A = 300 μ m, B, C = 60 μ m, D = 15 μ m, E, H = 75 μ m, F = 430 μ m, G = 150 μ m.

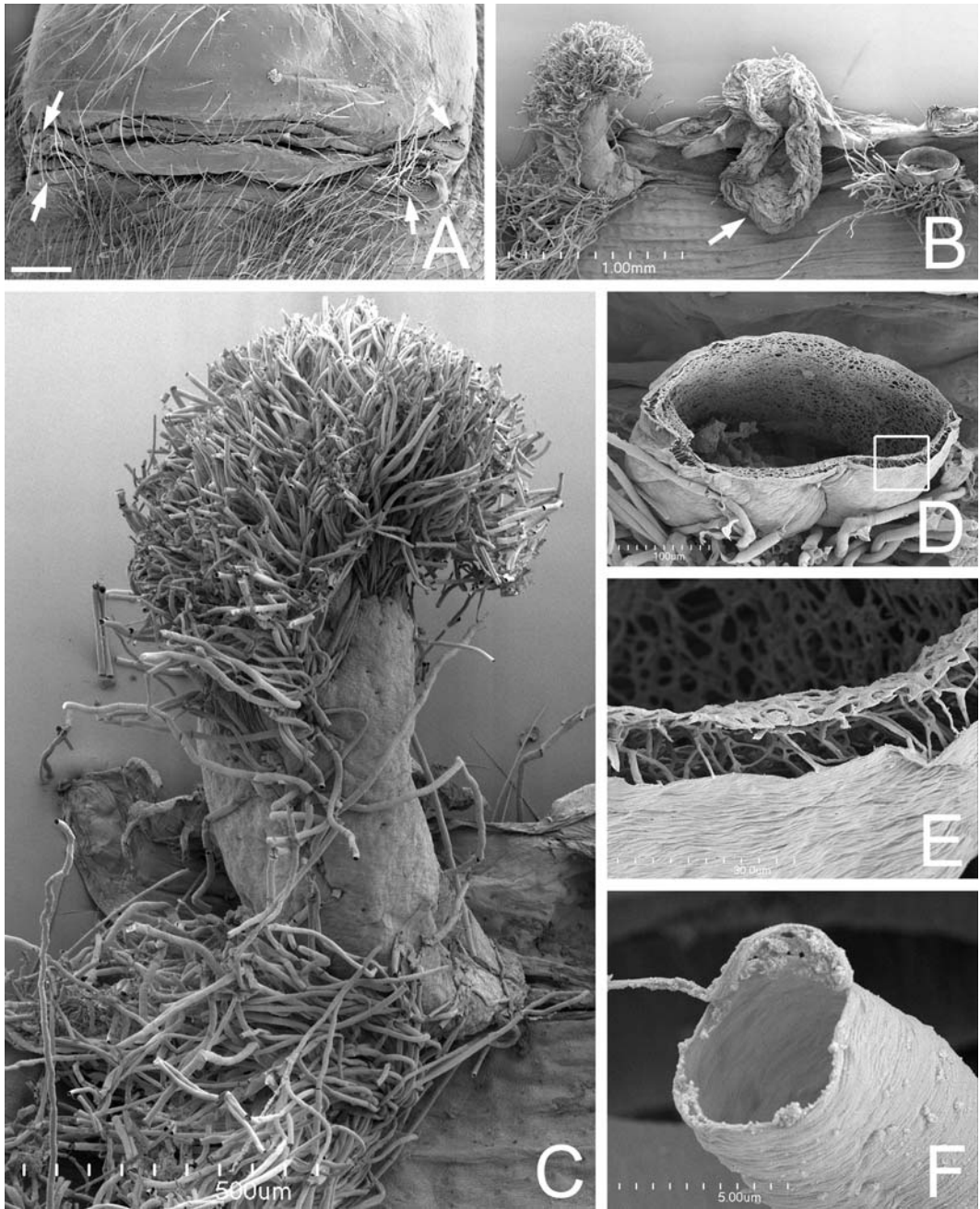


FIGURE 162. Tracheae of *Ariadna*. A. Booklung and tracheal spiracles (arrows) of male of *Ariadna boesenbergi* from Buenos Aires, Argentina. B–F. Tracheae of female *Ariadna maxima* from Cauquenes, Chile, KOH digested. B. Trunks of lateral tracheae, with bunches of tracheoles that were sectioned; the right tracheal trunk is sectioned near its base (arrow to posterior receptacle of spermatheca, collapsed during drying). C. Detail of left tracheal trunk. D. Right tracheal trunk sectioned, inset in E. E. Detail of wall of the right tracheal trunk. F. Detail of tracheole, sectioned. Scale bars: A = 200µm, B = 1.0mm, C = 500µm, D = 100µm, E = 30µm, F = 5µm.

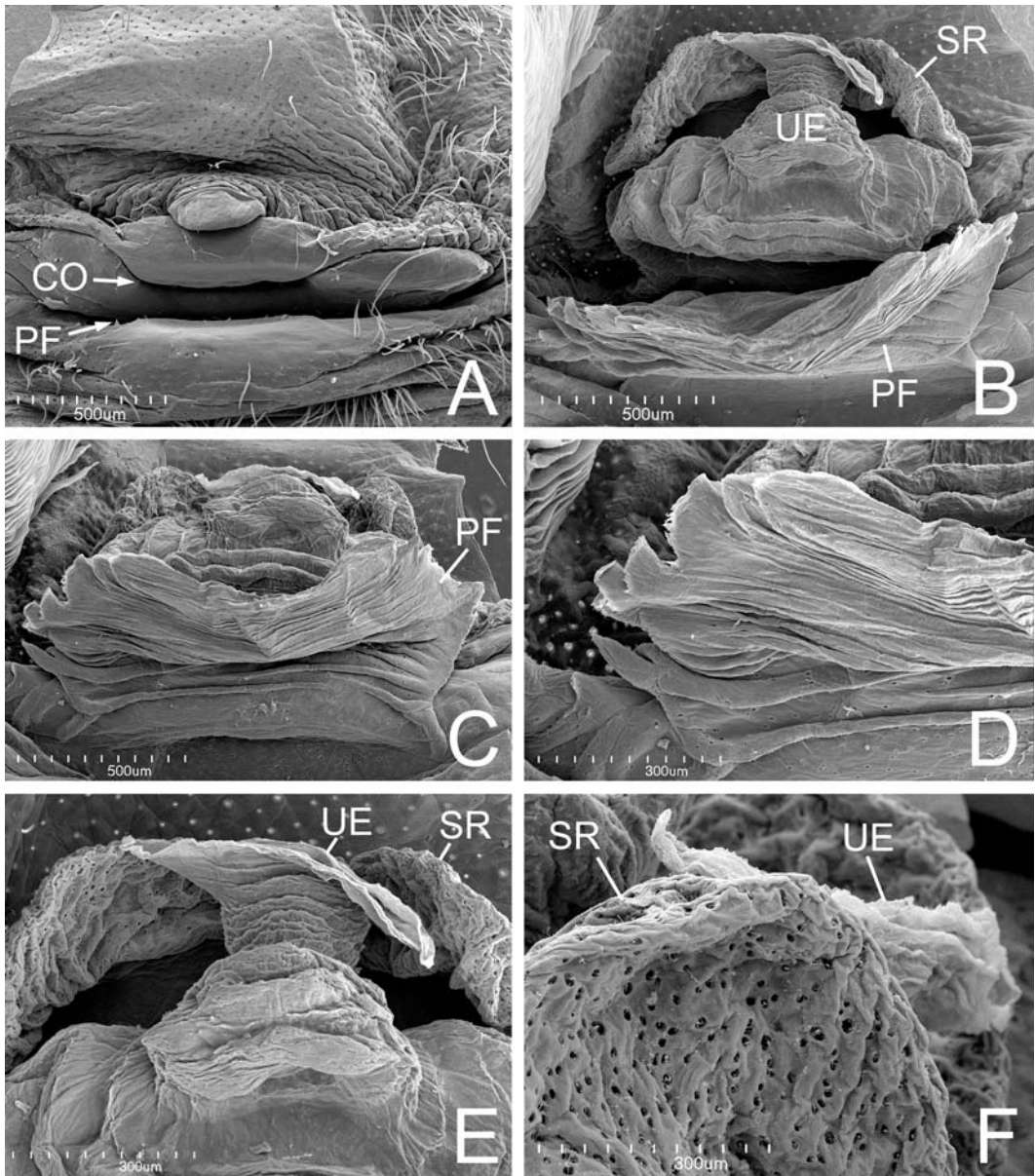


FIGURE 163. Female genitalia of *Thaida peculiaris* from Puerto Blest, Argentina. A. Epigynum. B. Vulva, dorsal. C. Vulva, posterior. D. Detail of posterior fold. E. Uterus externus. F. Pores on anterior receptacle. CO = copulatory opening (and gonopore), PF = postepigastric fold, SR = sperm receptacle, UE = uterus externus. Scale bars: A–C = 500µm, D–F = 300µm.

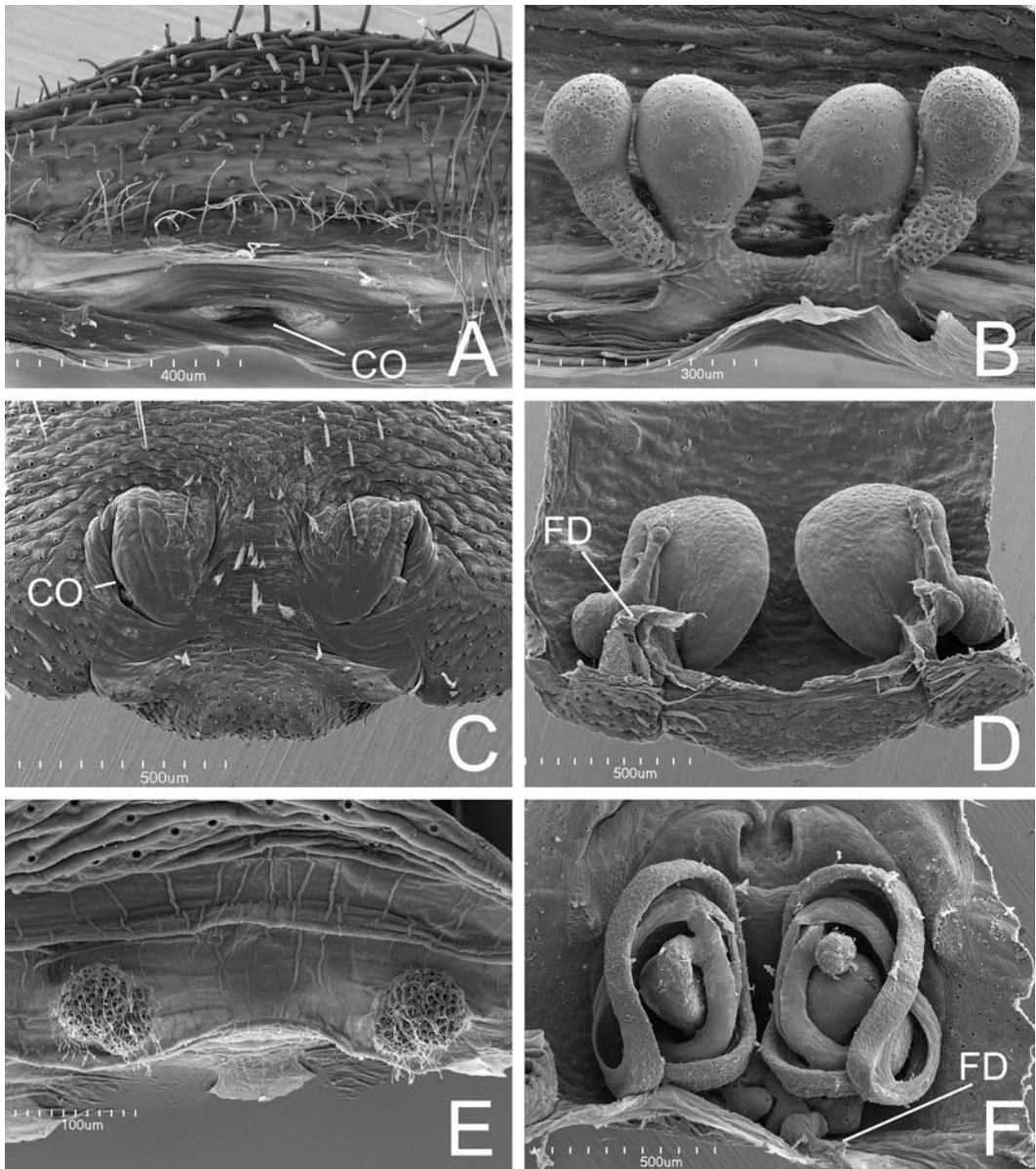


FIGURE 164. Female genitalia. A–B. *Hypochilus pococki* from Haywood Co., North Carolina, USA, haplogyne genitalia. A. Genital region, ventral. B. Spermathecae, dorsal. C–D. *Psechrus argentatus* from Cape Vogel Peninsula, Papua New Guinea, entelegyne genitalia. C. Epigynum, ventral. D. Vulva, dorsal. E. *Filistata insidiatrix* from Siena, Italy, haplogyne vulva, dorsal. F. *Metaltellinae* undet. sp. from Llanquihue, Chile, entelegyne vulva, dorsal. CO = copulatory openings, FD = fertilization ducts. Scale bars: A = 400µm, B = 300µm, C, D, F = 500µm, E = 100µm.

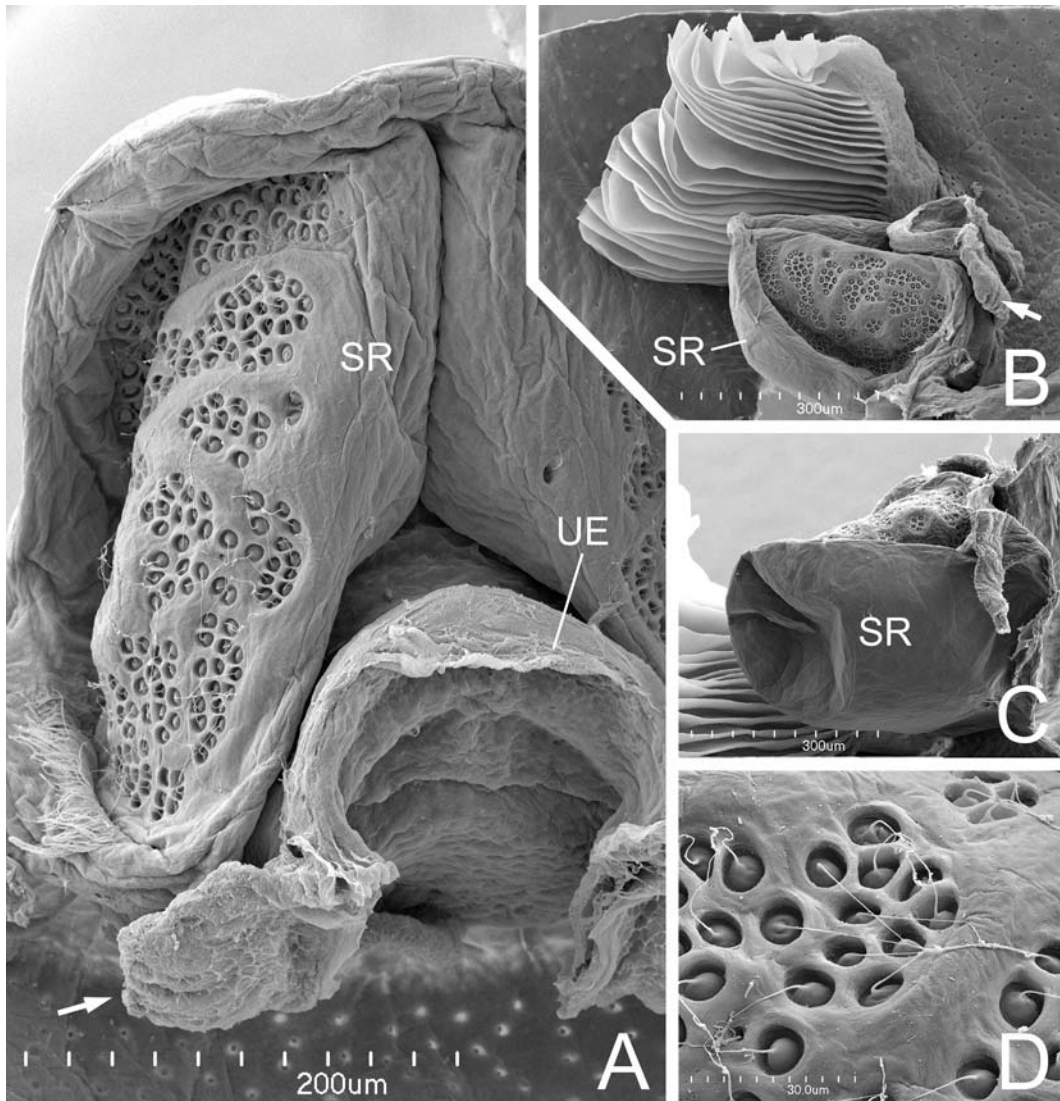


FIGURE 165. Female genitalia of *Archaea workmani* from Ranomafana, Madagascar, KOH digested. A. Dorsal view, arrow to muscle apodemes. B. Lateral view, spermatheca and left booklung, arrow to muscle apodeme. C. Seminal receptacle, lateral-ventral view showing ventral side devoid of gland ductules (epigastrium partially removed). D. Gland ductules on seminal receptacle. SR = seminal receptacle, UE = uterus externus. Scale bars: A = 200µm, B, C = 300µm, D = 30µm.

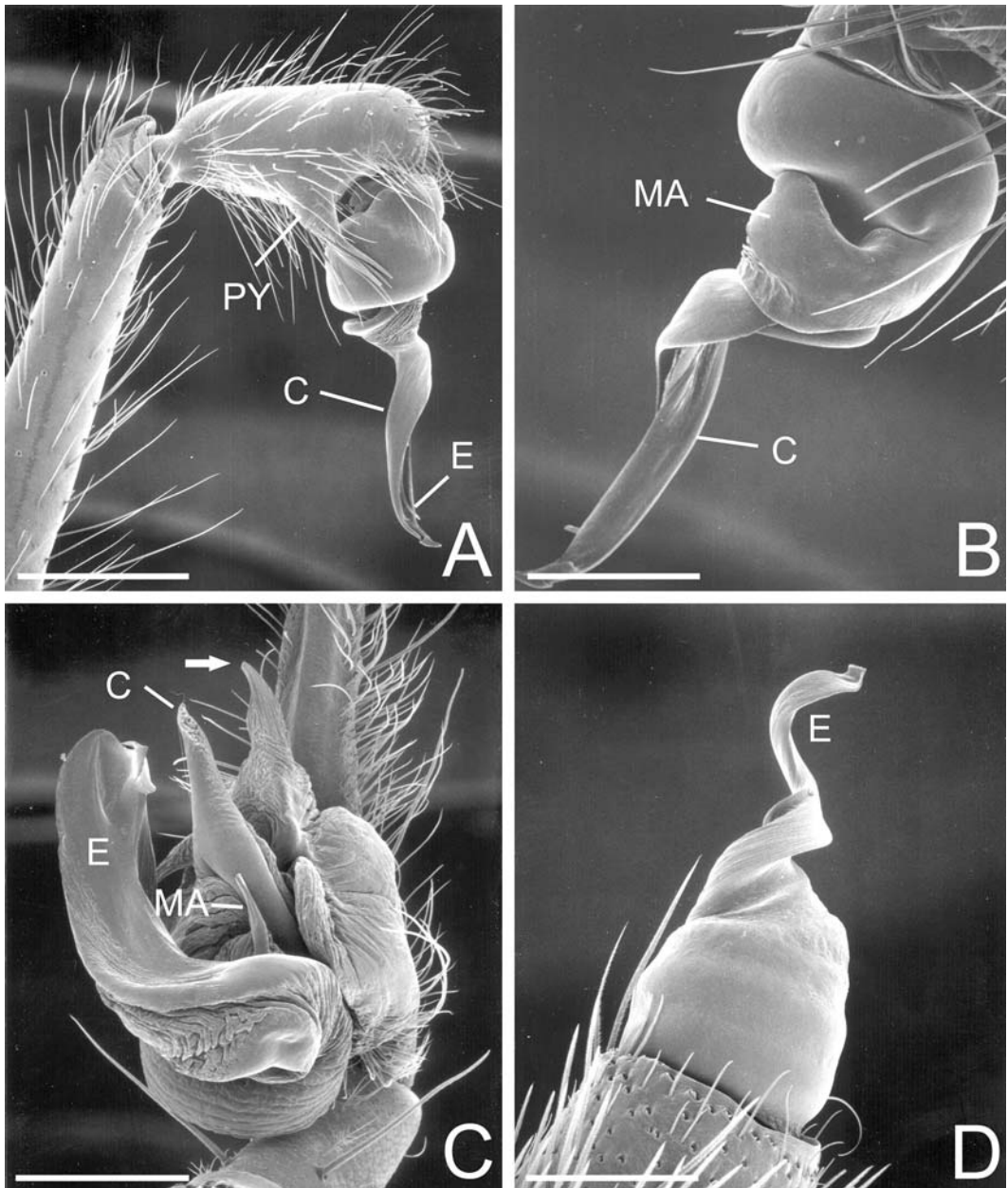


FIGURE 166. Right male pedipalpi of haplogyne spiders. A, B. *Hypochilus pococki* from Ramsey Cascade, Tennessee, USA. A. Tibia to tarsus, retrolateral. B. Bulb, prolateral. C. *Thaida peculiaris* from Lago Villarica, Chile, ventral. D. *Kukulcania hibernalis* from Clearwater, Florida, USA, bulb, prolateral. C = conductor, E = embolus, MA = median apophysis, PY = paracymbium. Arrow points to hook on *Thaida* subtegulum. Scale bars: A = 600 μ m, B = 300 μ m, C = 600 μ m, D = 250 μ m.

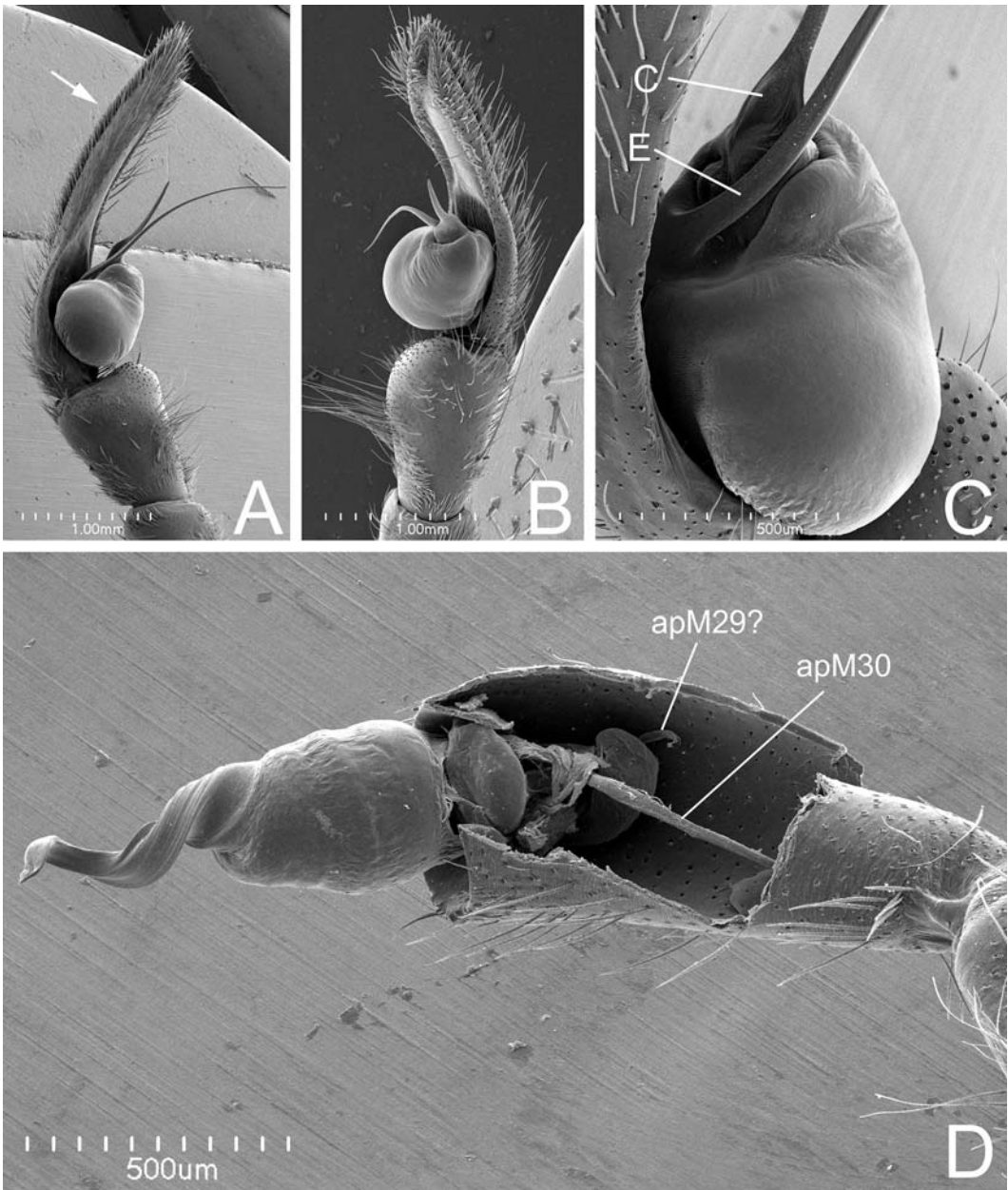


FIGURE 167. Right male pedipalpi. A–C. *Psechrus argentatus* from Cape Vogel Peninsula, Papua New Guinea. A, C. Retrolateral. Arrow in A points to scopula. B. Prolateral. D. *Kukulcania hibernalis* from Savannah, Georgia, USA, tarsus cut away and digested to show apodemes of M29 and M30 muscles. C = conductor, E = embolus, apM29 and apM30 = apodemes. Scale bars: A, B = 1.0mm, C, D = 500µm.

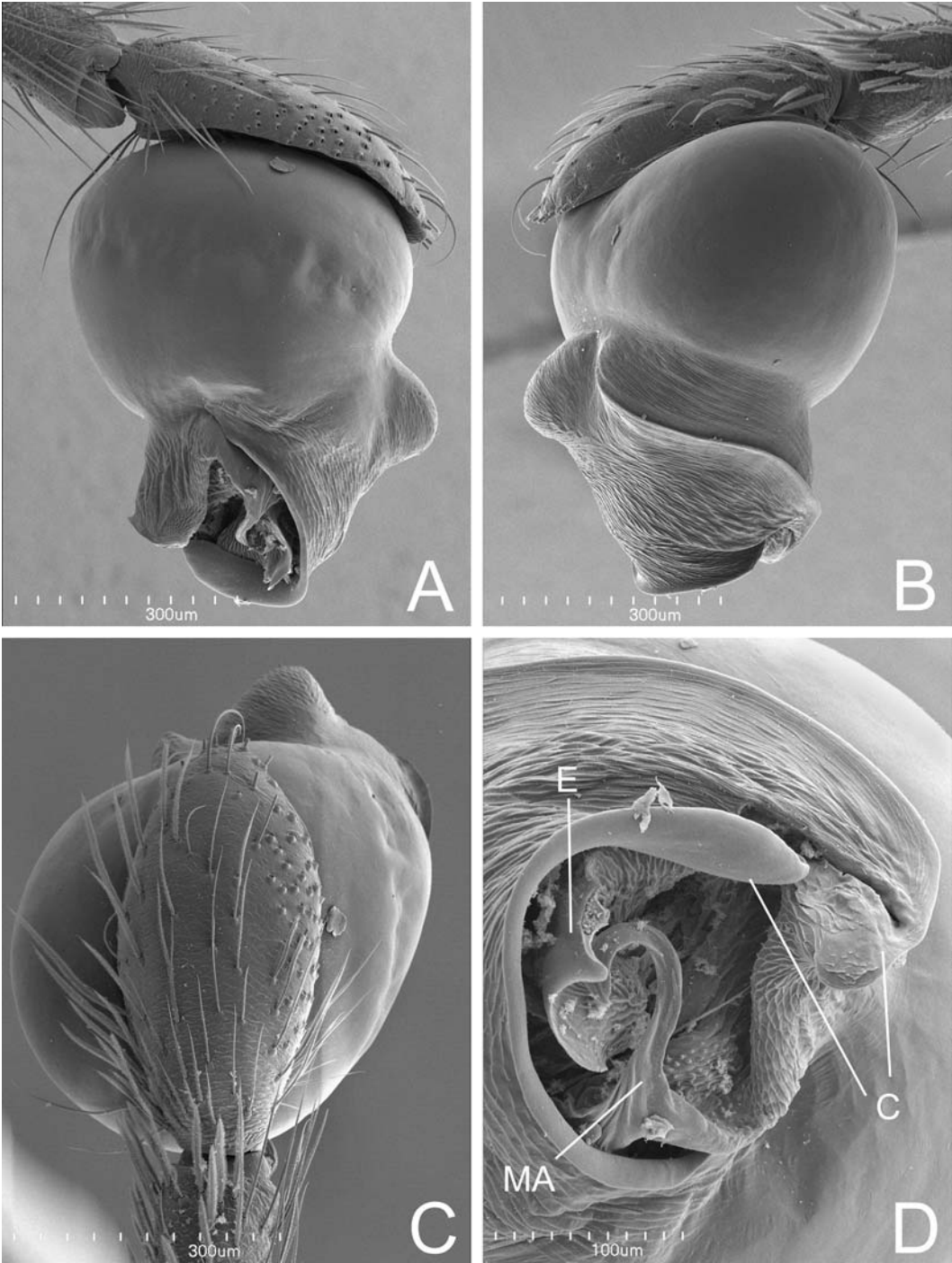


FIGURE 168. Left male pedipalpus of *Archaea workmani* from Ranomafana, Madagascar. A. Prolateral. B. Retrolateral. C. Dorsal. D. Detail, apical. C = conductor, E = embolus, MA = median apophysis. Scale bars: A–C = 300µm, D = 100µm.

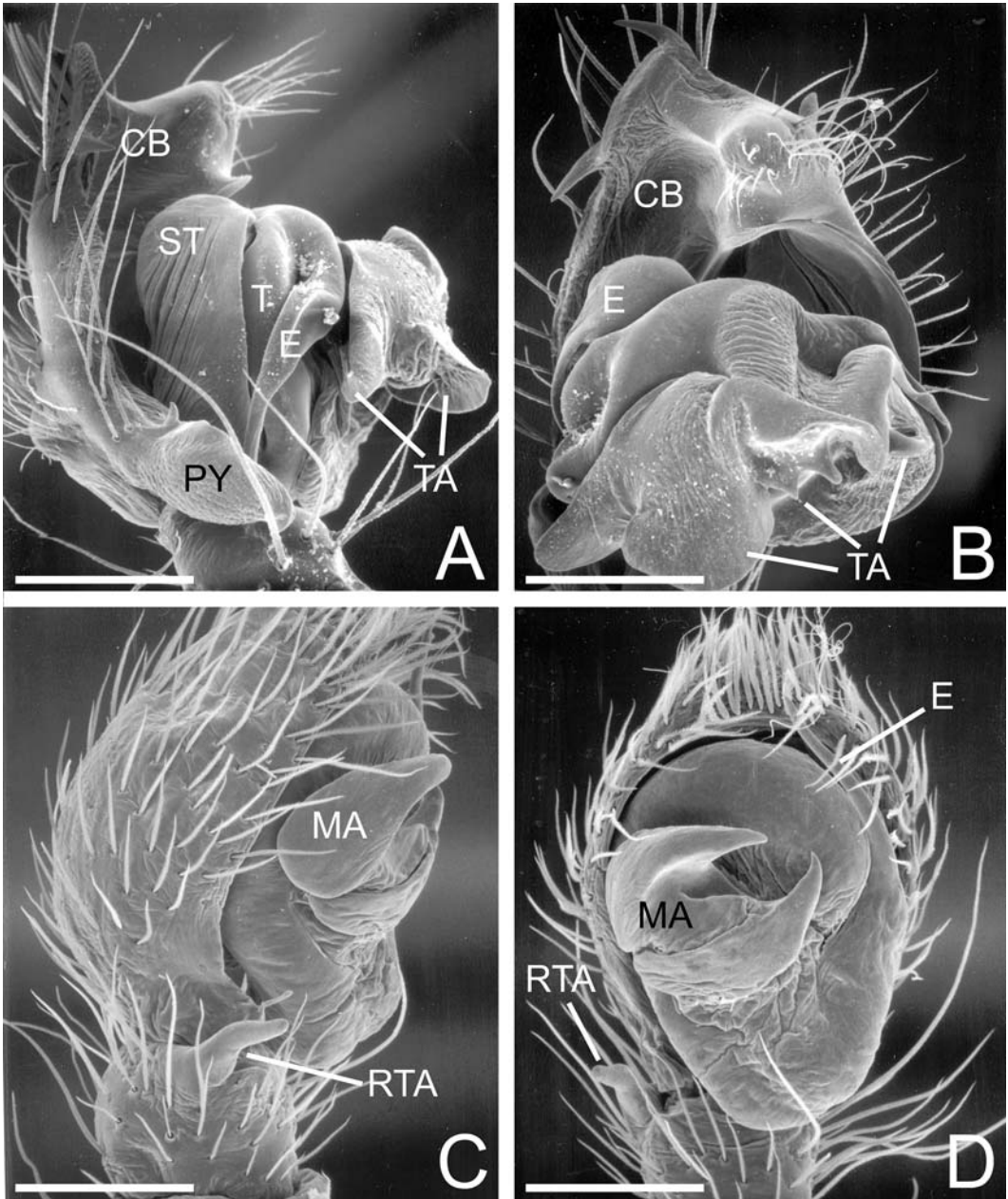


FIGURE 169. Right male pedipalpi. A, B. *Mimetus hesperus* from Baboquivari Mts., Arizona, USA. C, D. *Aebutina binotata* from Tarapuy, Ecuador. A, C. Retrolateral. B, D. Ventral. CB = cymbium, E = embolus, MA = median apophysis, PY = paracymbium, RTA = tibial retrolateral process, ST = subtegulum, T = tegulum, TA = tegular apophysis(es). Scale bars: A, B = 300 μ m, C, D = 150 μ m.

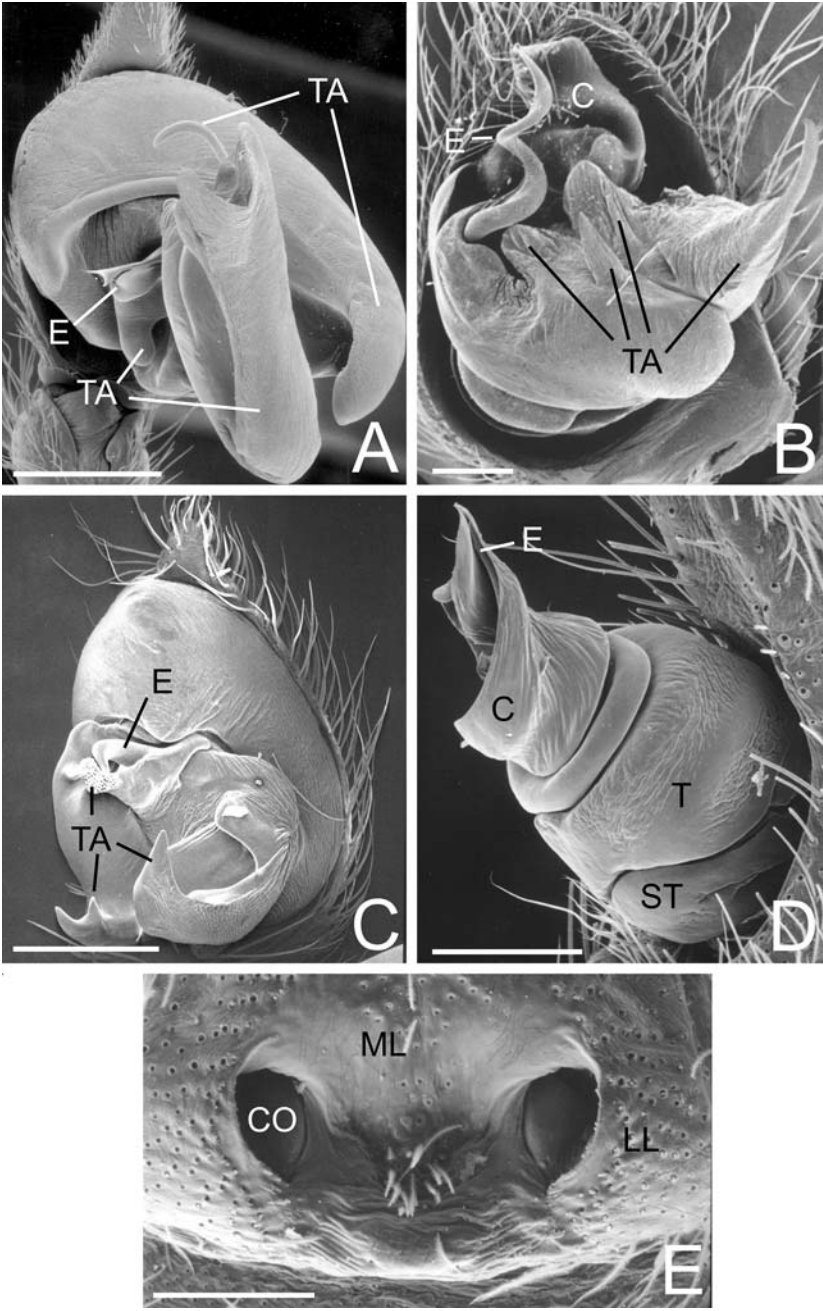


FIGURE 170. Genitalia. A–D. Male pedipalpi. A. *Uroctea* sp. from Garies, South Africa, right. It is not possible to determine which of the four TA is the C or MA. B. *Xevioso amica* from St. Lucia, South Africa, left. It is not possible to determine which of the four TA is the MA. C. *Oecobius navus* from Washington D.C., USA. It is not possible to determine which of the three TA is the C or MA. D. *Stegodyphus dumicola* from Spioenkop, South Africa, right. E. Epigynum of *Xevioso amica* from St. Lucia, South Africa. C = conductor, CO = copulatory openings of epigynum, E = embolus, LL = lateral lobes of epigynum, ML = median sector of epigynum, ST = subtegulum, T = tegulum, TA = tegular apophysis(es). Scale bars: A = 600µm, B–E = 200µm.

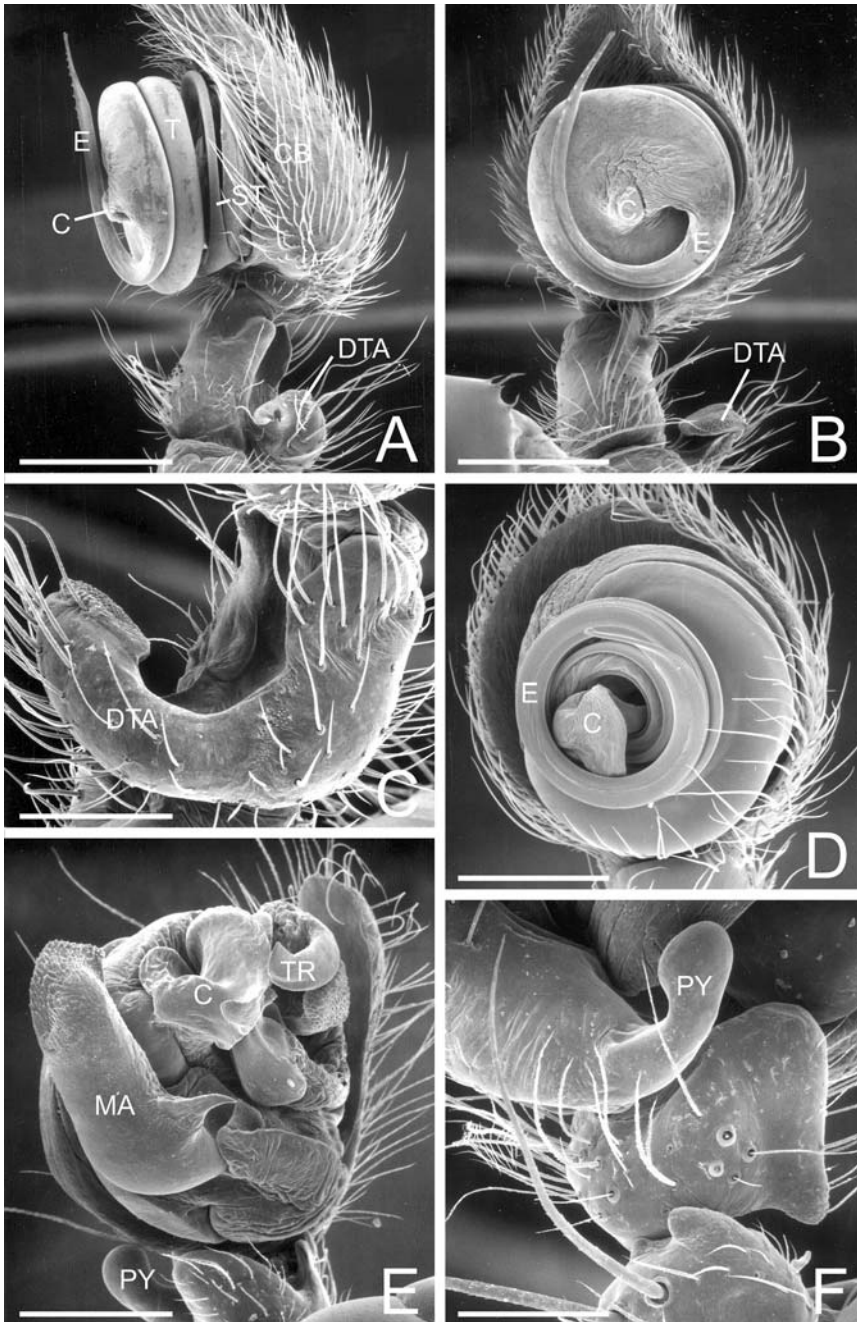


FIGURE 171. Male pedipalpi. A–C. *Megadicityna thilenii* from Orongorongo, New Zealand, left. A. Retrolateral. B. Ventral. C. Tibia, retrodorsal, showing proximal DTA. D. *Deinopis spinosus* from Gainesville, Florida, USA, right ventral. E, F. *Araneus diadematus* from Seattle, Washington, USA, right. E. Pedipalpal bulb, ventral. F. Tibia and paracymbium, retrolateral. C = conductor, CB = cymbium, DTA = tibial dorsal process, E = embolus, MA = median apophysis, PY = paracymbium, ST = subtegulum, T = tegulum, TR = terminal apophysis of embolic division. Scale bars: A, B = 600 μ m, C–E = 300 μ m, F = 200 μ m.

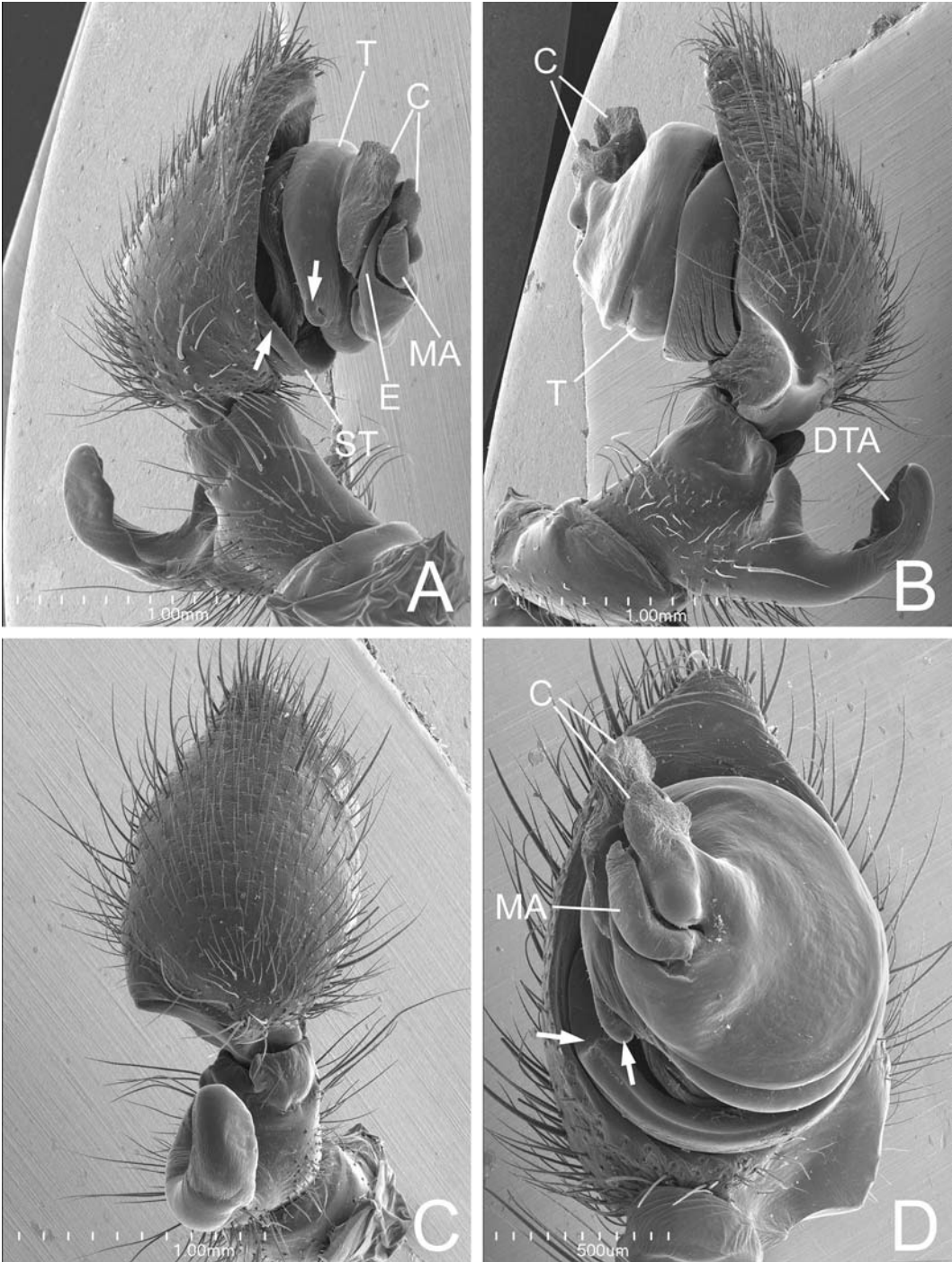


FIGURE 172. Left pedipalpus of *Nicodamus mainae* from Bush Bay, Western Australia, Australia. A. Prolateral. B. Retrolateral. C. Dorsal. D. Ventral. Arrows to subtegular and tegular locking lobes. C = conductor, DTA = dorsal tibial process, E = embolus, MA = median apophysis, ST= subtegulum, T = tegulum. Scale bars: A–C = 1.0mm, D = 500µm.

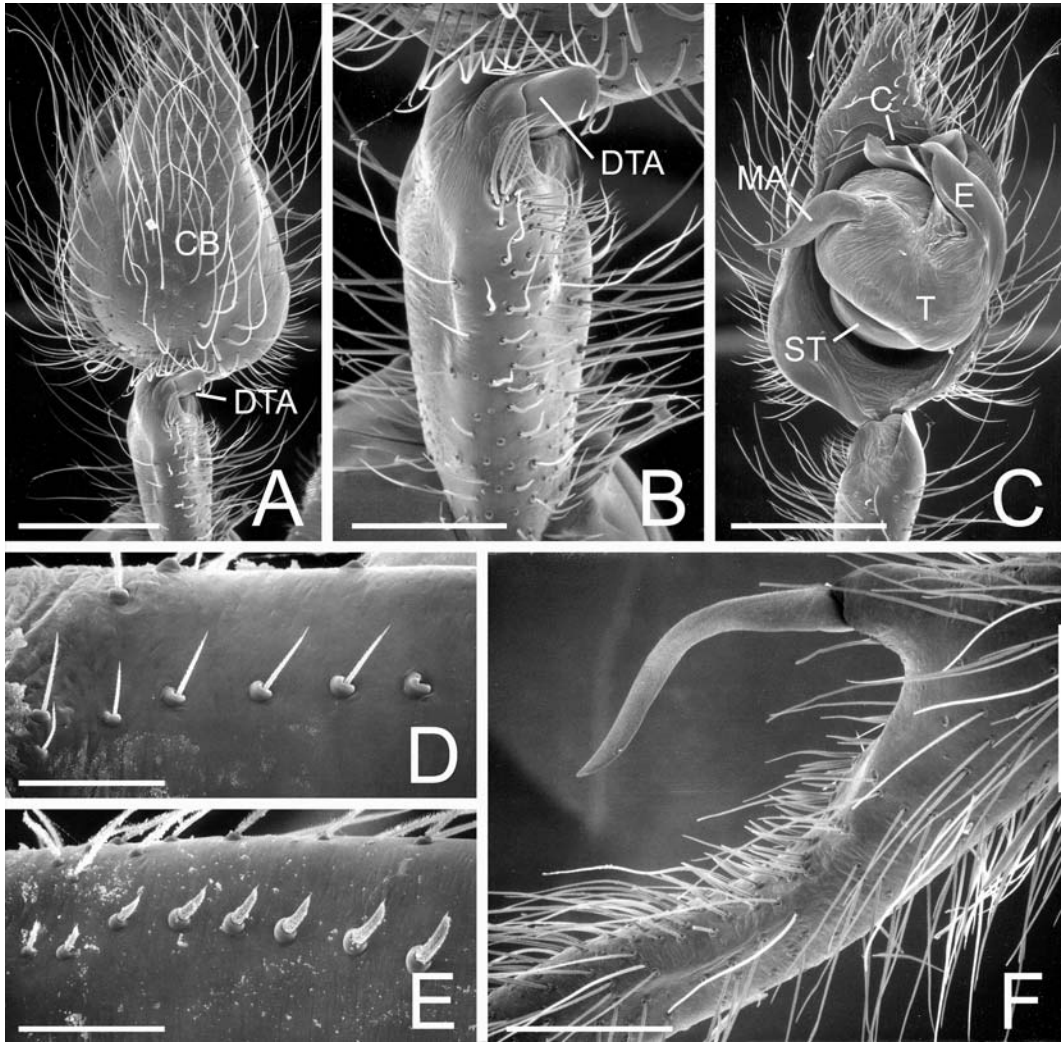


FIGURE 173. Male Phyxelididae. A–C. *Phyxelida bifoveata* from Mazumbai, Tanzania, pedipalpus. A. Tibia and tarsal cymbium, dorsal. B. Tibia, dorsal. C. Bulb, ventral. D, E. Inner base of pedipalpal femur showing thorns. D. Phyxelidid undet. sp from Périnet, Madagascar. E. Phyxelidid undet. sp from Ranomafana, Madagascar. F. *Phyxelida tangensis* from Amani, Tanzania, tibia I. C = conductor, CB = cymbium, DTA = dorsal tibial process, E = embolus, MA = median apophysis, ST = subtegulum, T = tegulum. Scale bars: A, C = 600 μ m, B, F = 250 μ m, D = 75 μ m, E = 100 μ m.

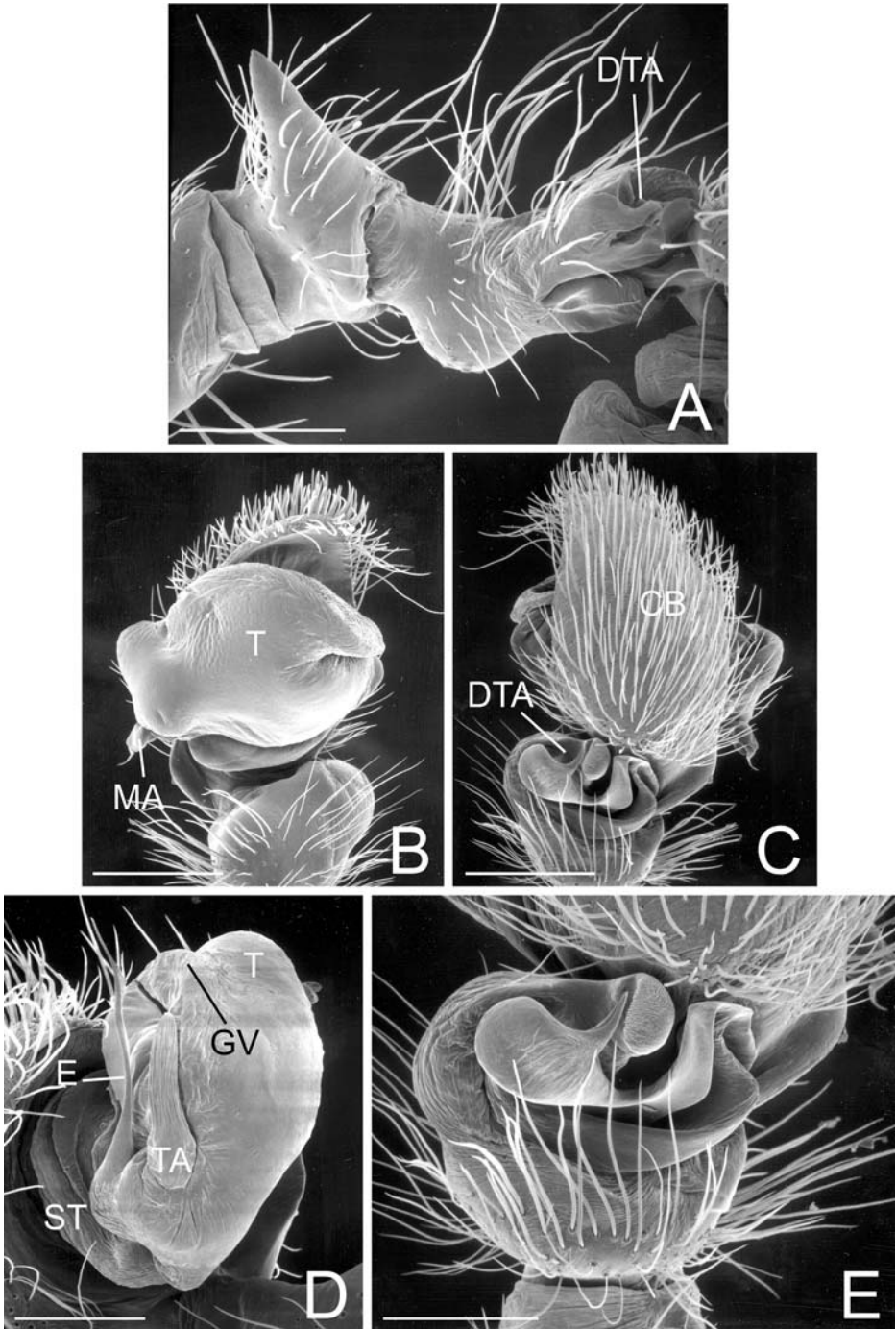


FIGURE 174. Right male pedipalpi of Titanoecidae. A, D. *Goeldia* sp. from Junin, Peru. B, C, E. *Titanoeca americana* from Johnson Co., Missouri, USA. A. Patella and tibia, dorsal. Note process on patella. B. Bulb ventral. C. Cymbium and tibia, dorsal. D. Bulb, ventral. GV points to tegular groove that serves as conductor. E. Tibia dorsal showing DTA. CB = cymbium, DTA = dorsal tibial process, E = embolus, GV = tegular groove, MA = median apophysis, ST = subtegulum, T = tegulum, TA = tegular apophysis. Scale bars: A, E = 250µm, B, C = 430µm, D = 200µm.

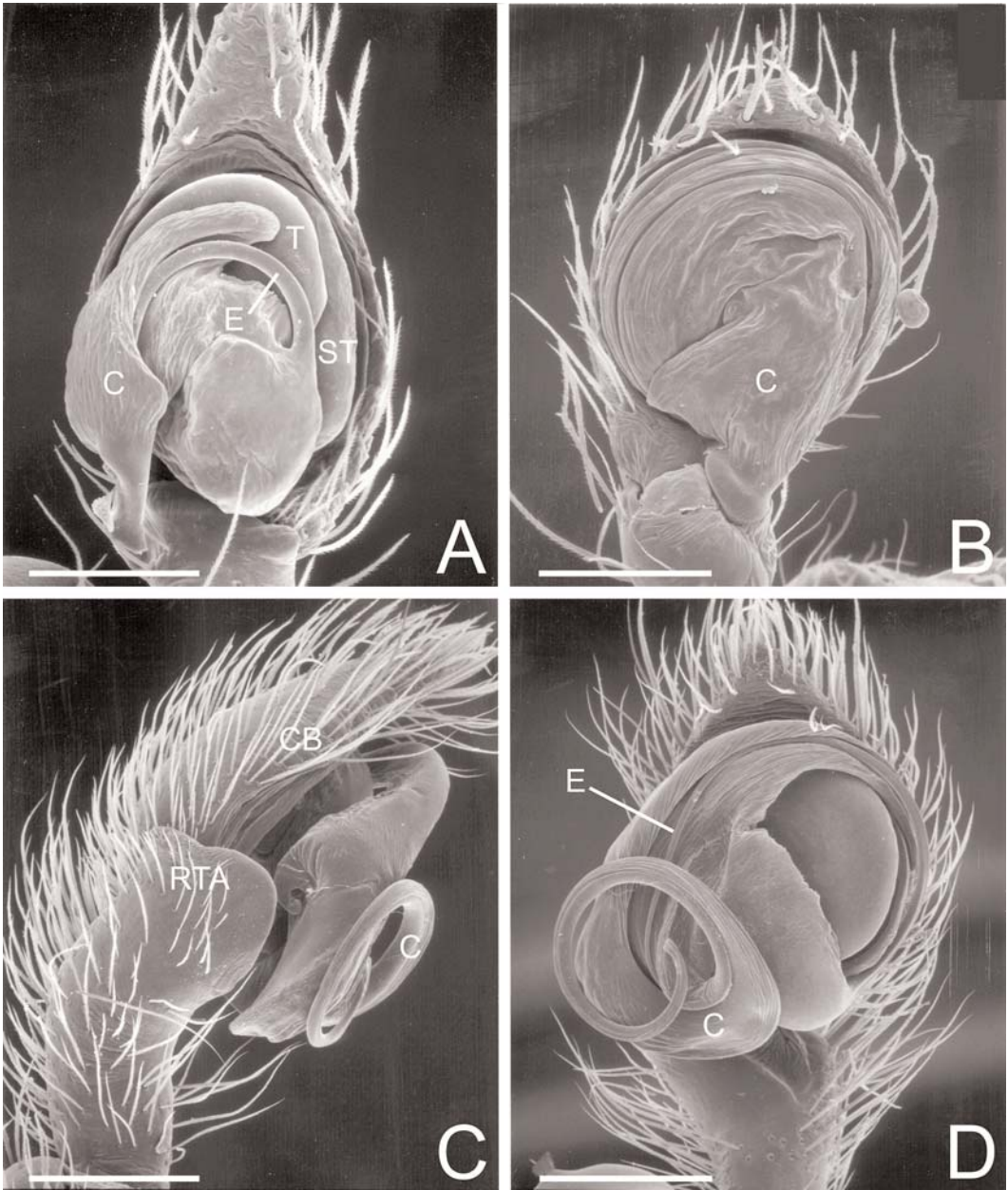


FIGURE 175. Left male pedipalpi of Dictynidae. A. *Dictyna bostoniensis* from Minnesota, USA, ventral. B. *Lathys immaculata* from Bradley, Arkansas, USA, ventral. C, D. *Tricholathys spiralis* from Lenore Lake, Washington, USA. C. Retrolateral. D. Ventral. C = conductor, CB = cymbium, E = embolus, RTA = retrolateral tibial apophysis, ST = subtegulum, T = tegulum. Scale bars: A, B = 100 μ m, C, D = 250 μ m.

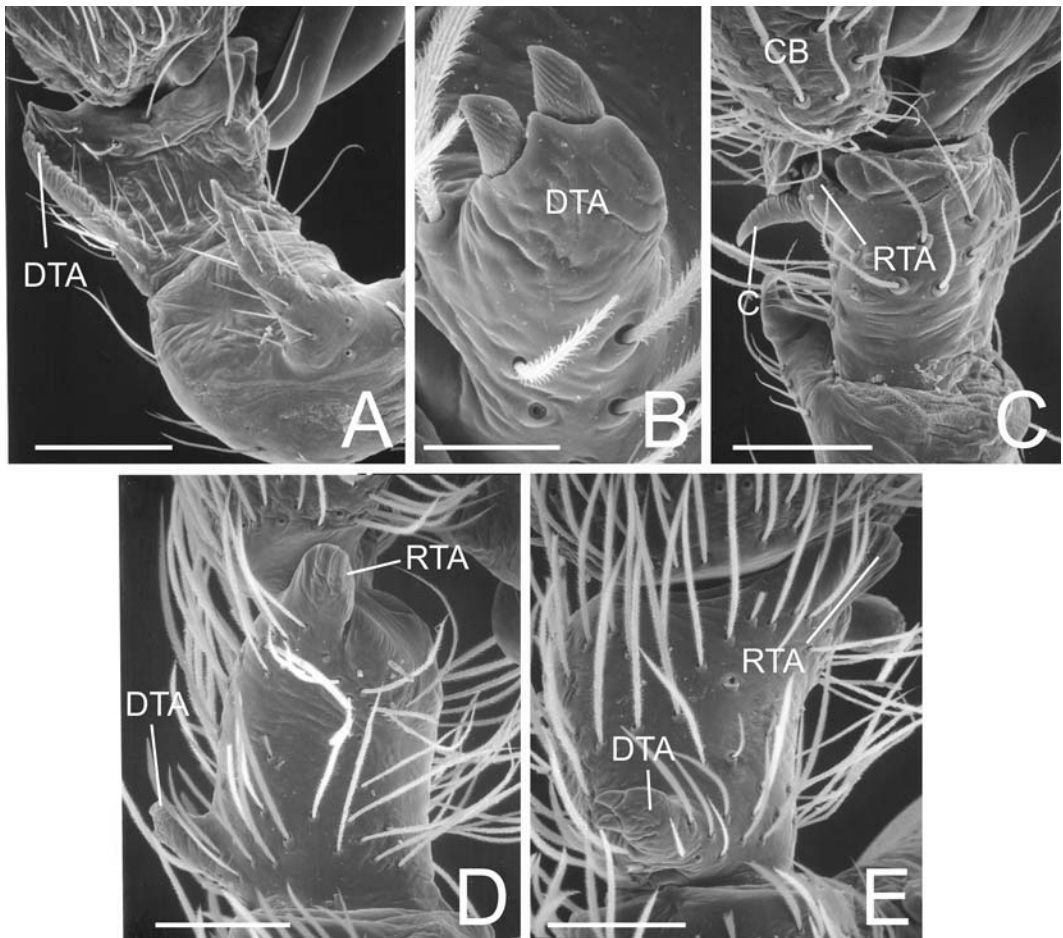


FIGURE 176. Right male pedipalpi of Dictynidae. A. *Nigma linsdalei* from San Francisco, California, USA, patella and tibia, retrolateral. Note process on patella. B, D, E. *Dictyna arundinacea* from Tuva, Russia. B. Tibia base, dorsal, showing DTA process with ctenidia. D. Tibia and base of cymbium, retrolateral. E. Tibia, dorsal. C. *Lathys humilis* from Kent, United Kingdom, patella and tibia, retrolateral. C = conductor, CB = cymbium, DTA = dorsal tibial apophysis, RTA = retrolateral tibial apophysis. Scale bars: A, D, E = 100 μ m, B = 30 μ m, C = 60 μ m.

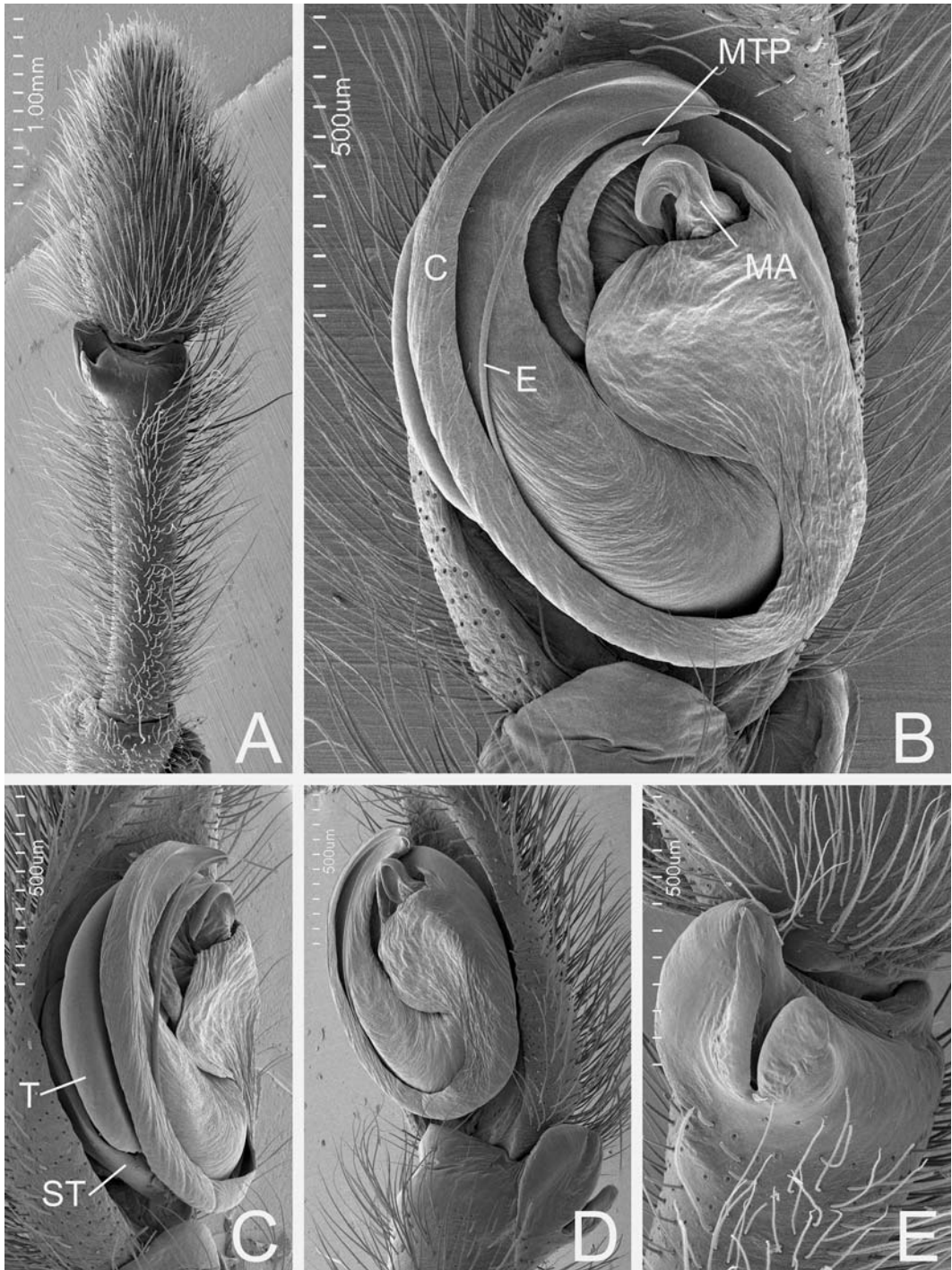


FIGURE 177. Left male pedipalpus and copulatory bulb of *Desis formidabilis* from Cape Peninsula, South Africa. A. Tibia and tarsus, dorsal. B. Bulb, ventral. C. Bulb, prolateral. C = conductor, DTA = dorsal tibial apophysis, E = embolus, MA = median apophysis, RTA = retrolateral tibial apophysis. Scale bars: A = 1.0mm. B–E = 500µm.

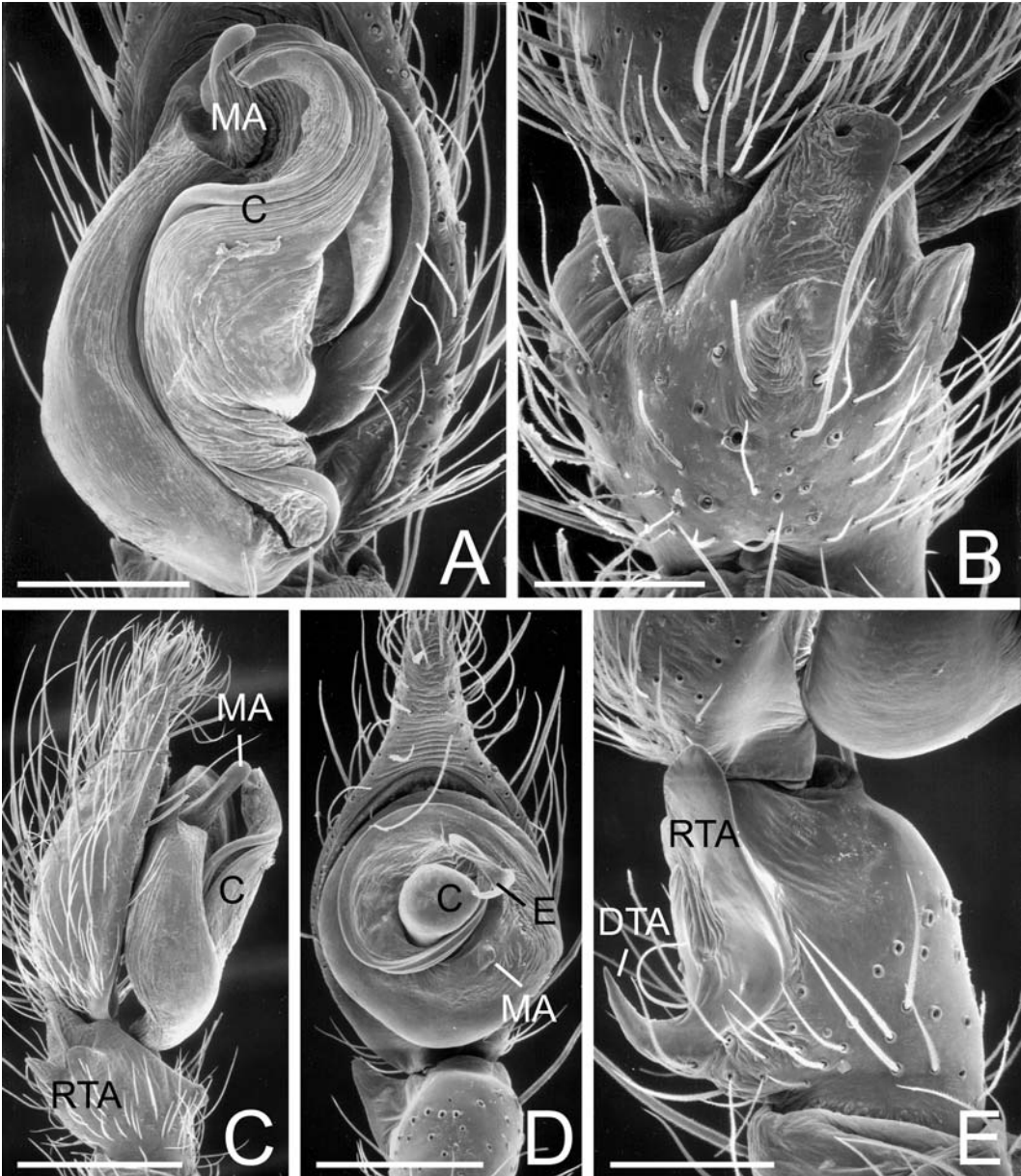


FIGURE 178. Right male pedipalpi. A–C. *Badumna longinqua* from Montevideo, Uruguay. A. Bulb, ventral. B. Tibia, retrolateral, showing complex RTA. C. Tibia and bulb, retrolateral. D, E. *Neolana dalmasi* from Lake Okataina, New Zealand. D. Bulb, ventral. E. Tibia, retrolateral. C = conductor, DTA = dorsal tibial apophysis, E = embolus, MA = median apophysis, RTA = retrolateral tibial apophysis. Scale bars: A, D = 300µm, B = 200µm, C = 600µm, E = 150µm.

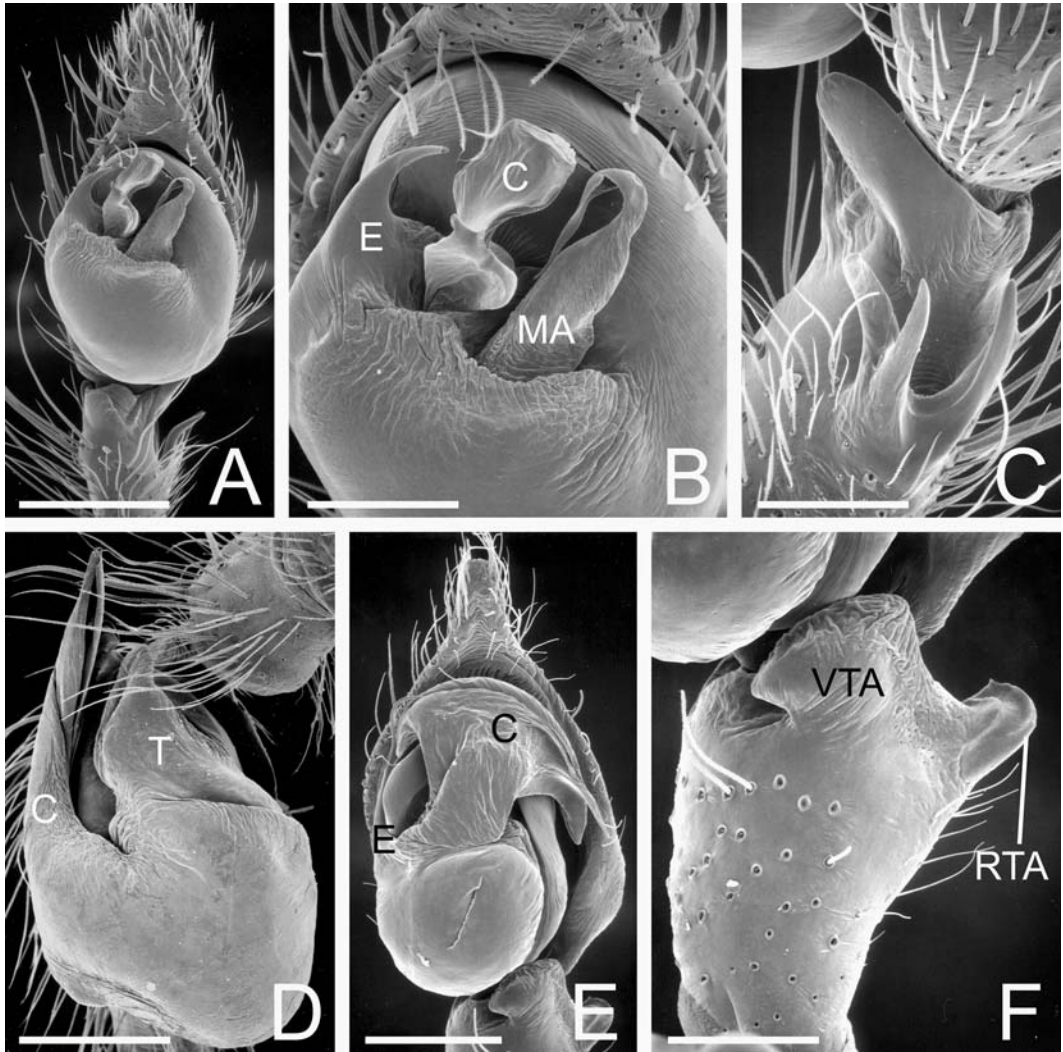


FIGURE 179. Right male pedipalpi. A–C. *Neoramia sana* from Dunedin, New Zealand. A. Tibia and bulb, ventral. B. Close up of bulb, ventral. C. Tibia, retrolateral, showing complex RTA. D. *Metaltella simoni* from Riverside, California, USA, partially expanded bulb, ventral. E, F. *Stiphidion facetum* from Lamington Plateau, Queensland, Australia. E. Bulb, ventral. F. Tibia, retrolateral. C = conductor, E = embolus, MA = median apophysis, RTA = retrolateral tibial apophysis, T = tegulum, VTA = ventral tibial apophysis. Scale bars: A = 600 μ m, B = 250 μ m, C = 200 μ m, D = 430 μ m, E = 300 μ m, F = 150 μ m.

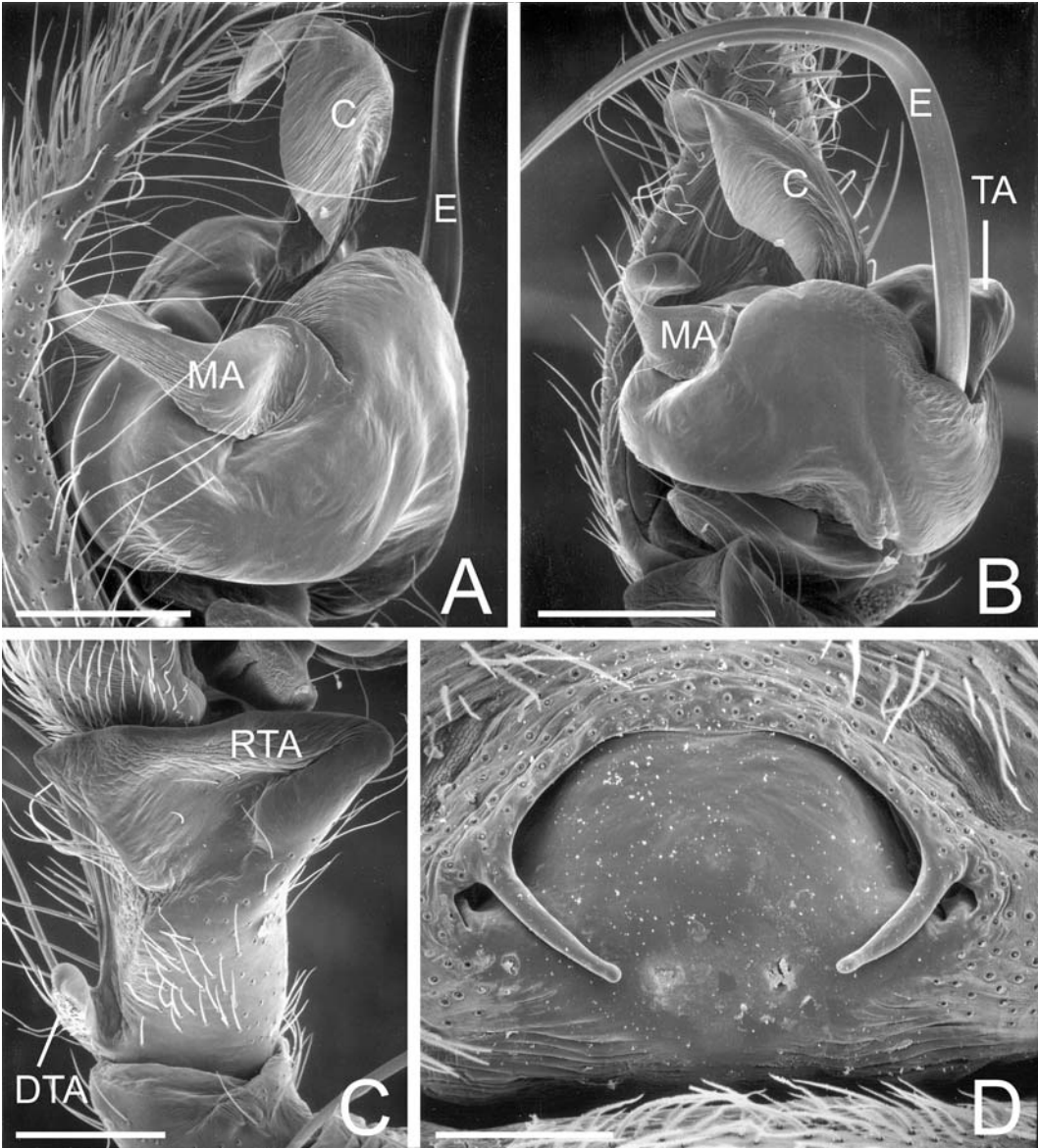


FIGURE 180. Genitalia of Amphinectidae. A–C. *Maniho ngaitahu* from Kaituna Valley, New Zealand, right male pedipalpus. A. Bulb, retrolateral. B. Bulb, ventral. C. Tibia, retrolateral, showing RTA and DTA. D. *Metaltella simoni* from Riverside, California, USA, female epigynum, ventral, showing lateral teeth. C = conductor, DTA = dorsal tibial apophysis, E = embolus, MA = median apophysis, RTA = retrolateral tibial apophysis, TA = tegular apophysis. Scale bars: A, C = 300 μ m, B = 430 μ m, D = 250 μ m.

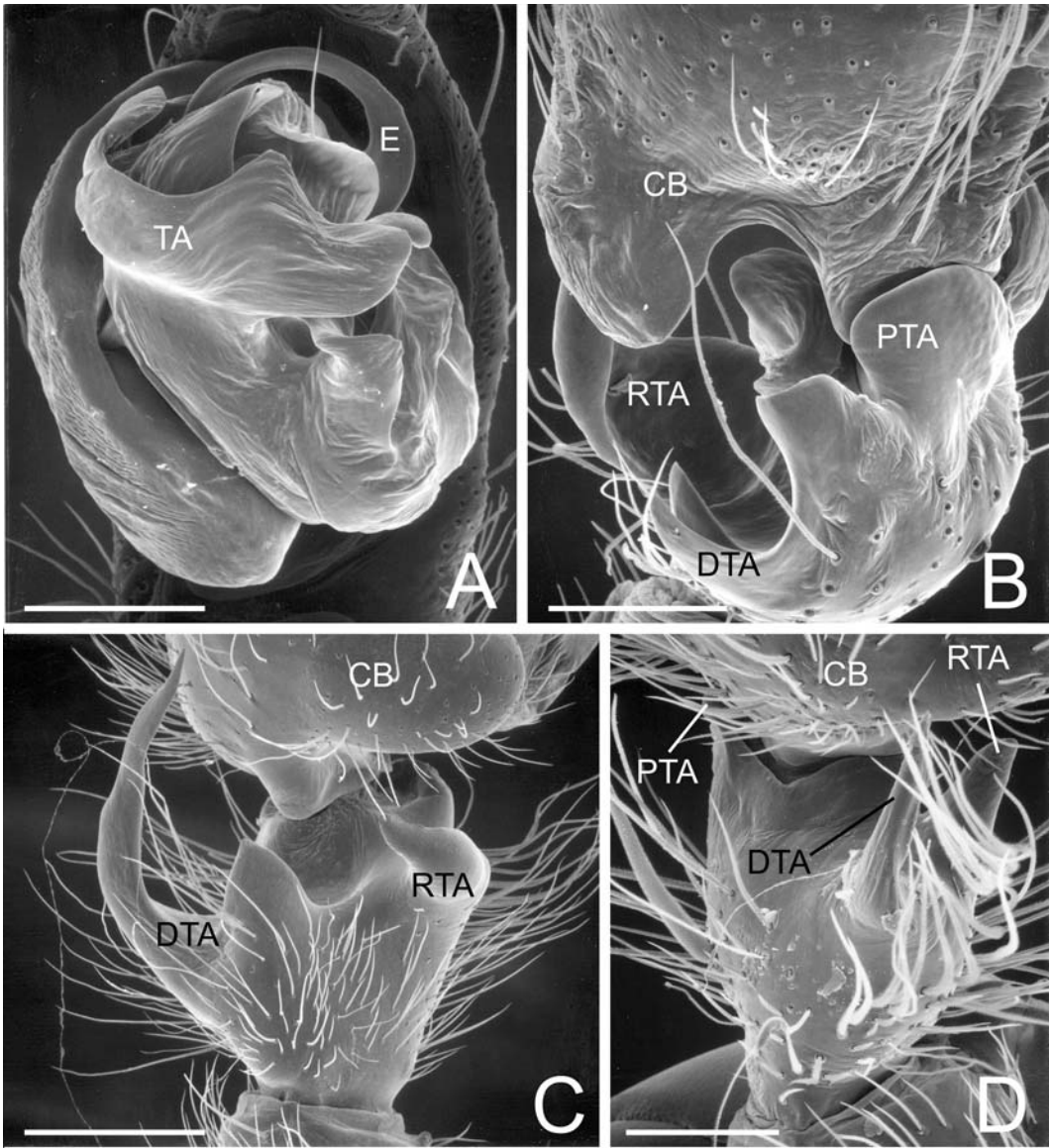


FIGURE 181. Right male pedipalpi. A, B. *Retiro* sp. from Lima, Peru. A. Bulb, ventral. B. Tibia and base of cymbium, dorsal. C. *Callobius bennetti* from Soubunge Mountain, Maine, USA, tibia, dorsal. D. *Pimus* sp. from Mendocino Co., California, USA, tibia, dorsal. CB = cymbium, DTA = dorsal tibial process, E = embolus, PTA = prolateral tibial process, RTA = retrolateral tibial apophysis, TA = tegular apophysis. Scale bars: A = 200 μ m, B, D = 150 μ m, C = 430 μ m.

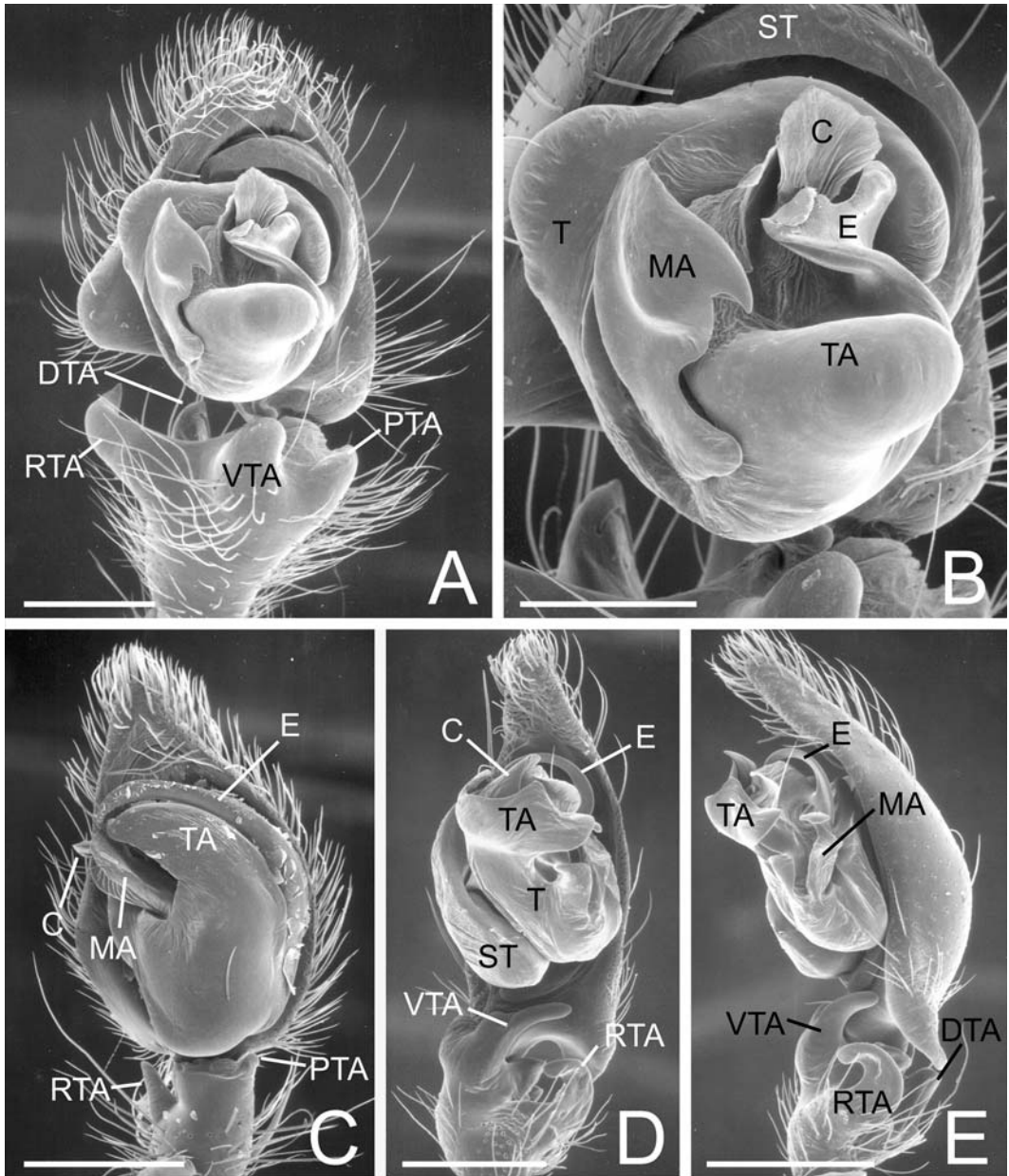


FIGURE 182. Right male pedipalpi. A, B. *Callobius bennetti* from Soubunge Mountain, Maine, USA, ventral. C. *Pimus* sp. from Mendocino Co., California, USA, ventral. D, E. *Retiro* sp. from Lima, Peru. D. Ventral. E. Retrolateral. C = conductor, DTA = dorsal tibial apophysis, E = embolus, MA = median apophysis, PTA = prolateral tibial process, RTA = retrolateral tibial apophysis, ST = subtegulum, T = tegulum, TA = tegular apophysis, VTA = ventral tibial process. Scale bars: A = 600 μ m, B = 300 μ m, C, E = 430 μ m, D = 420 μ m.

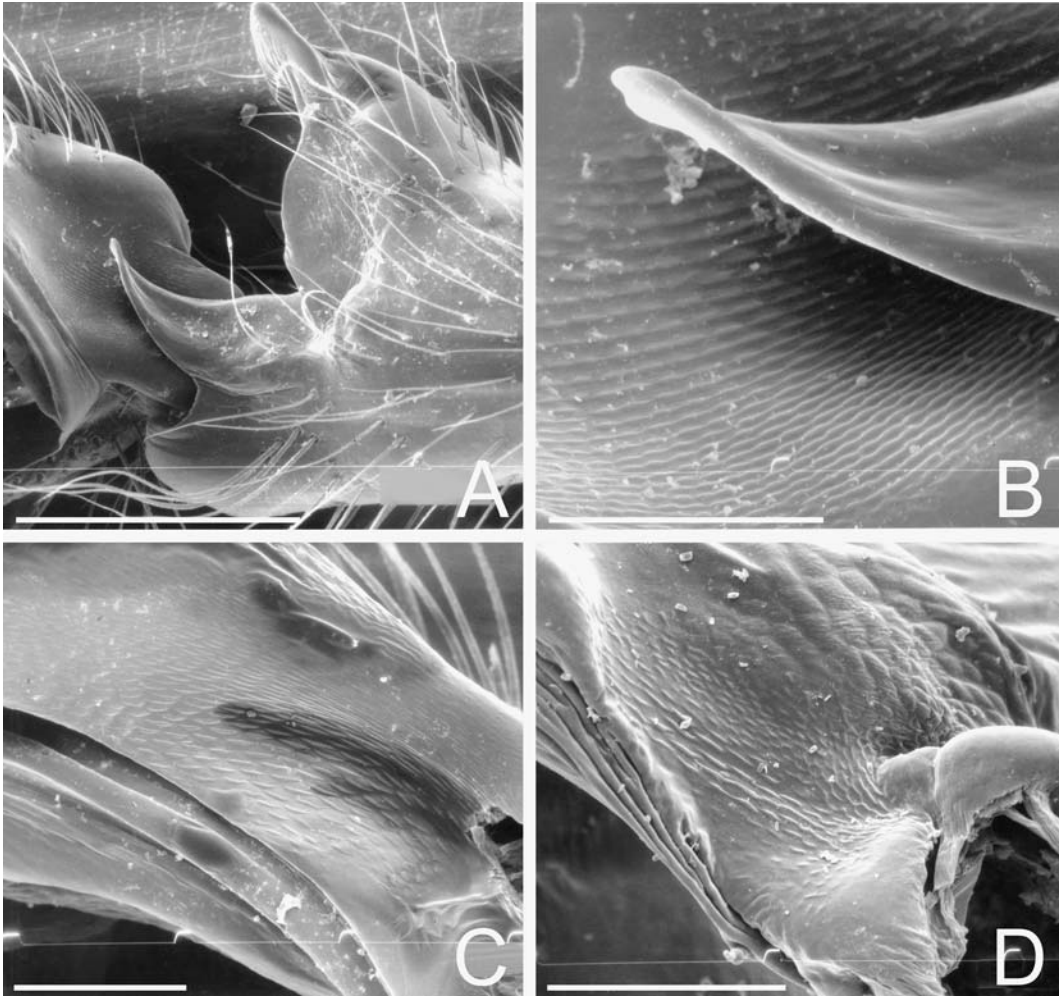


FIGURE 183. Left cymbium and RTA of Macrobininae, Amaurobiidae. A, B. *Macrobunus multidentatus* from Chiloé, Chile. A. Tibia and cymbium. B. Detail of RTA process and cymbial stridulatory area. C. *Rubrius antarcticus* from Tierra del Fuego, Argentina. D. *Emmenomma oculatum* from Tierra del Fuego, Argentina. C, D. Detail of cymbial stridulatory area. Scale bars: A = 500 μ m, B–D = 50 μ m.

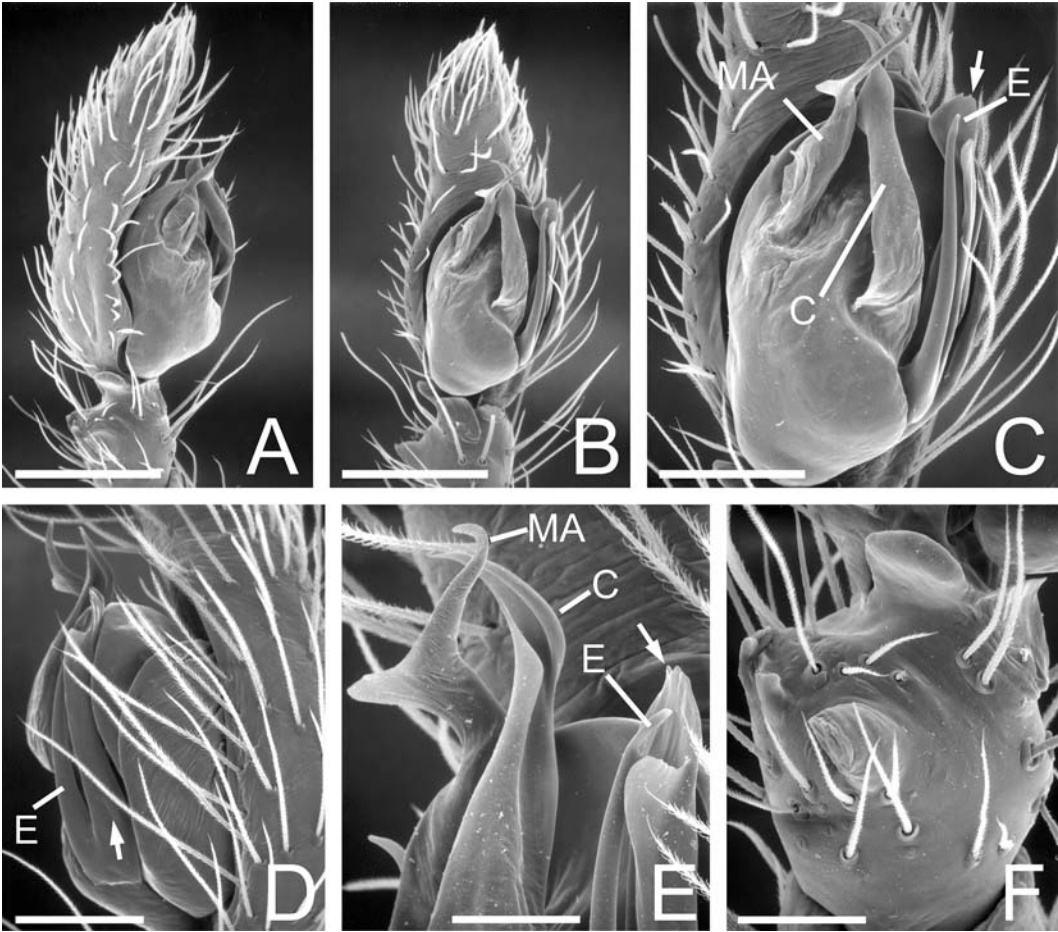
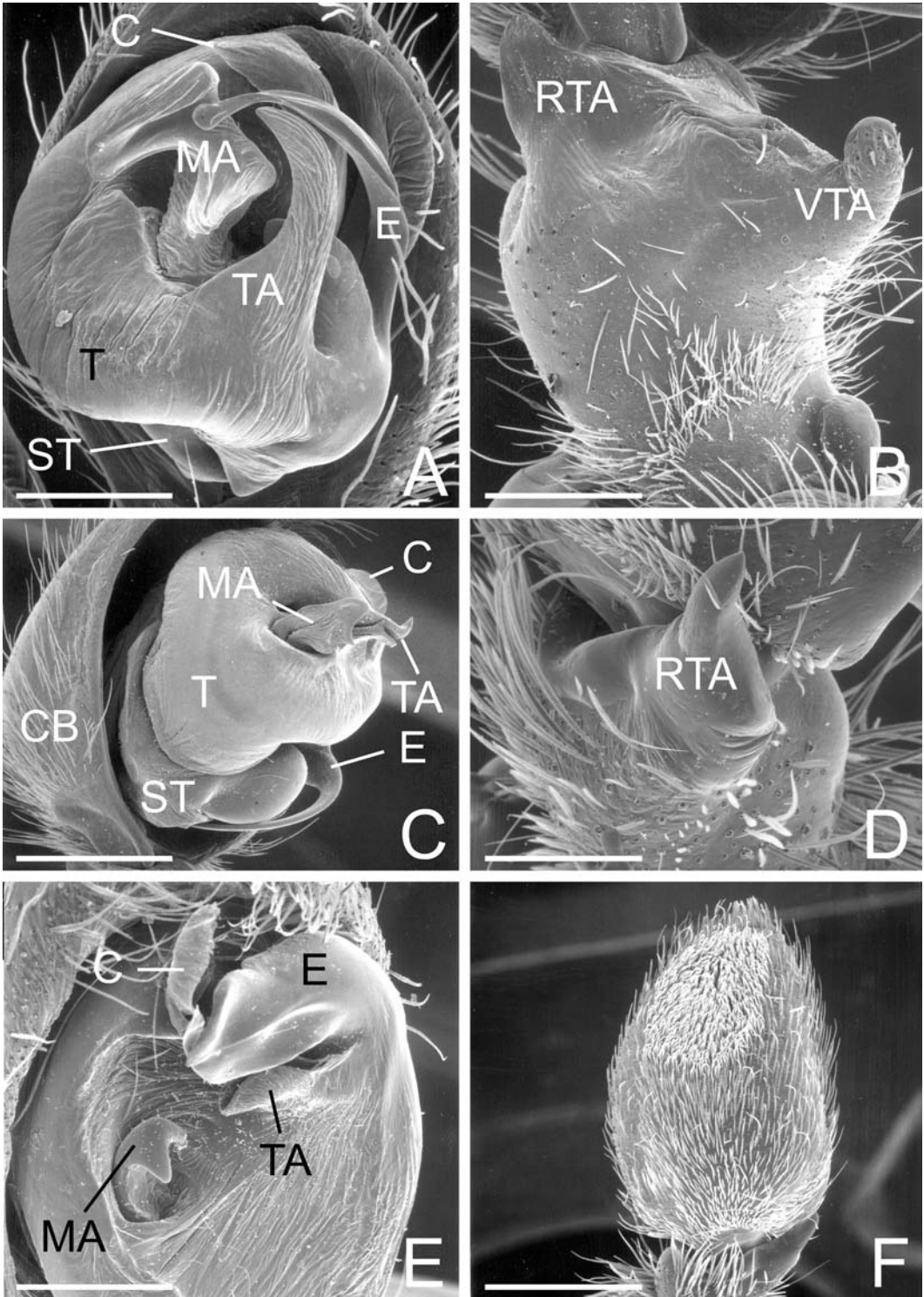


FIGURE 184. Right male pedipalpus of *Poaka graminicola* from Lincoln, New Zealand. A. Tibia and tarsus, retrolateral. B. Tibia and tarsus, ventral. C. Bulb, close up, ventral. D. Bulb, close up, prolateral. E. Apex of bulb. F. Tibia, retrolateral, showing complex RTA. C = conductor, E = embolus, MA = median apophysis, arrows = projecting embolar base. Scale bars: A, B = 200 μ m, C, D = 103 μ m, E = 43 μ m, F = 60 μ m.



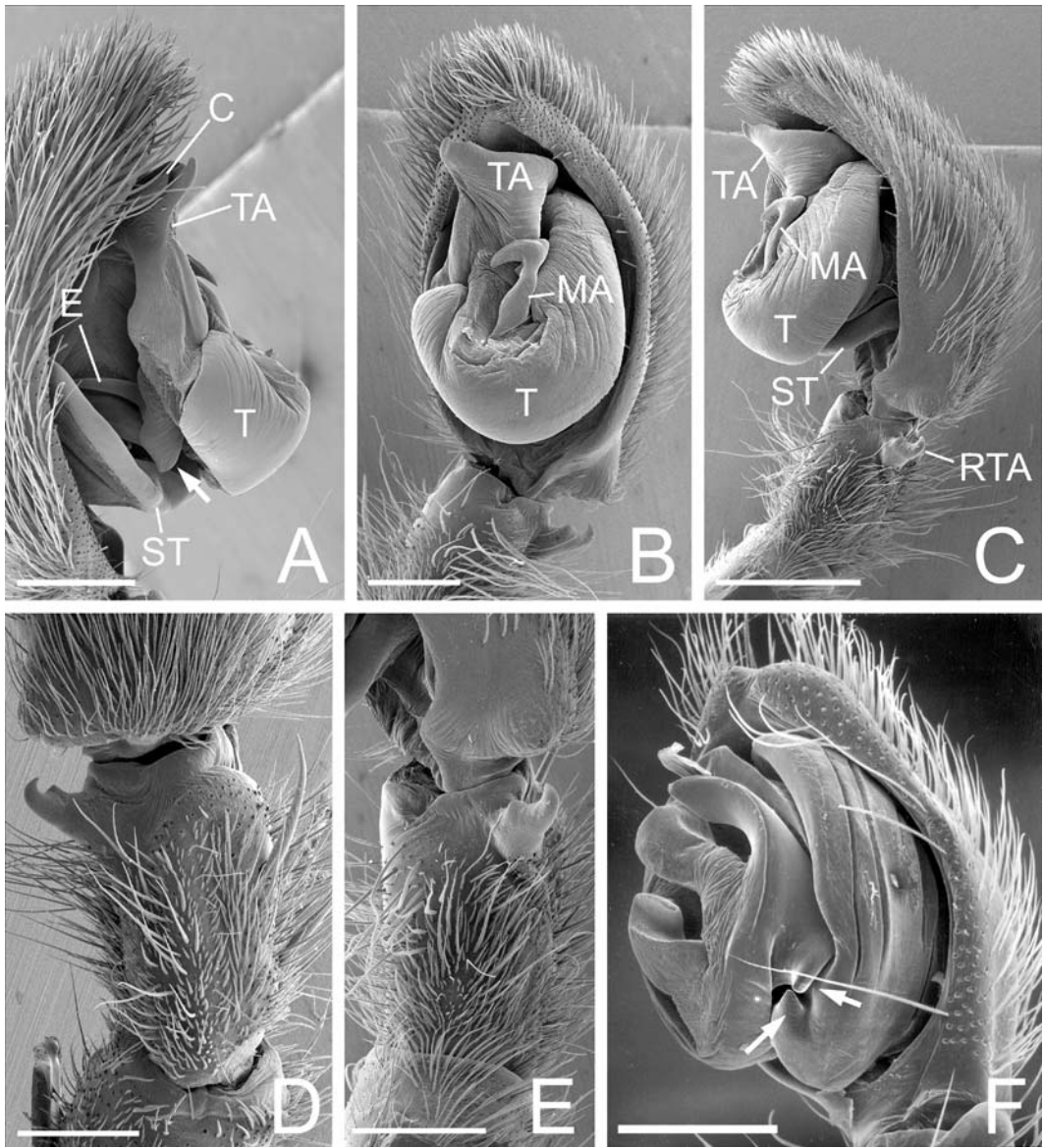


FIGURE 186 (above). Male pedipalpi of Zorocratidae. A–E. *Zorocrates* sp. from Big Bend National Park, Texas, USA, left. A. Prolateral view, arrow to tegular locking lobe formed by the embolar base. B. Ventral. C. Retrolateral. D. Tibia, dorsal. E. Tibia, retrolateral. F. Zorocratidae undet. sp. from English Camp, Madagascar, right, retrolateral, lines to T and ST locking lobes. C = conductor, E = embolus, MA = median apophysis, RTA = retrolateral tibial apophysis, ST = subtegulum, T = tegulum, TA = tegular apophysis. Scale bars: A, B = 500 μ m, C = 1.0mm, D, E = 500 μ m, F = 260 μ m.

FIGURE 185 (left). Right male pedipalpi. A. *Raecius jocquei* from Apouesso, Côte d'Ivoire, bulb, ventral. B. *Uduba madagascariensis* from Ambohimanga, Madagascar. B. Tibia, retrolateral. C. Tarsus, retrolateral. D–F. *Zoropsis spinimana* from Sunnyvale, California, USA. D. Tibia, retrolateral. E. Bulb, retroapical. F. Cymbium, dorsal, showing scopula. C = conductor, CB = cymbium, E = embolus, MA = median apophysis, RTA = retrolateral tibial apophysis, ST = subtegulum, T = tegulum, TA = tegular apophysis, VTA = ventral tibial apophysis. Scale bars: A = 200 μ m, B = 470 μ m, C, F = 1.0mm, D = 300 μ m, E = 430 μ m.

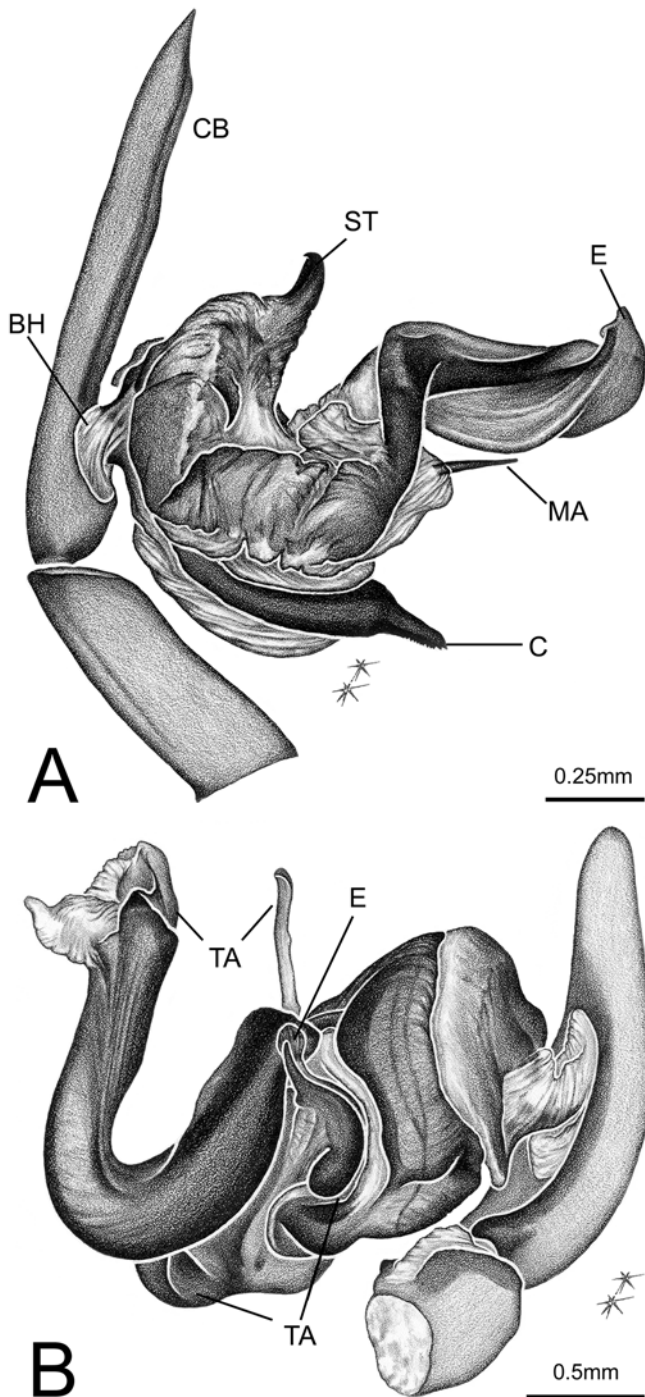


FIGURE 187. Expanded male pedipalpi, retrolateral. A. *Thaidia peculiaris* (Austrochilidae) from Neltume, Chile, right. B. *Uroctea* sp. (Oecobiidae) from Garies, South Africa, left. BH = basal haematodocha, C = conductor, CB = cymbium, E = embolus, MA = median apophysis, ST = hook on subtegulum, TA = tegular apophysis(es). Illustrations by Jenny Speckels.

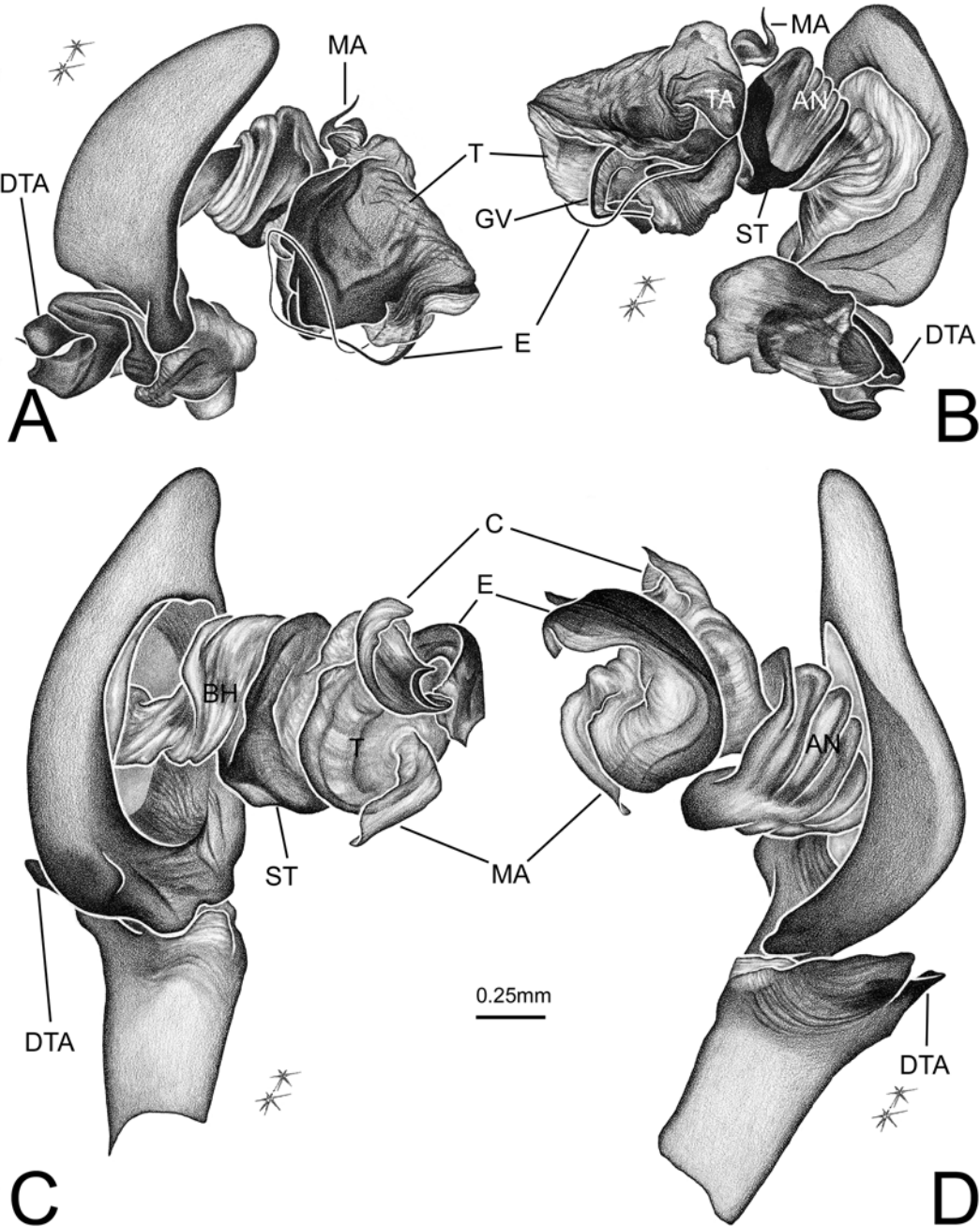


FIGURE 188. Expanded right male pedipalpi. A, B. *Titanoecca americana* (Titanoeceidae) from Johnson Co., Missouri, USA. C, D. *Phyxelida bifoveata* (Phyxelididae) from Mazumbai, Tanzania. A, C. Retrolateral. B, D. Prolateral. AN = annuli of subtegulum, BH = basal haematodocha, C = conductor, DTA = dorsal tibial apophysis, E = embolus, GV = tegular groove serving as titanoeceid conductor, MA = median apophysis, ST = subtegulum, T = tegulum, TA = tegular apophysis. Illustrations by Jenny Speckels.

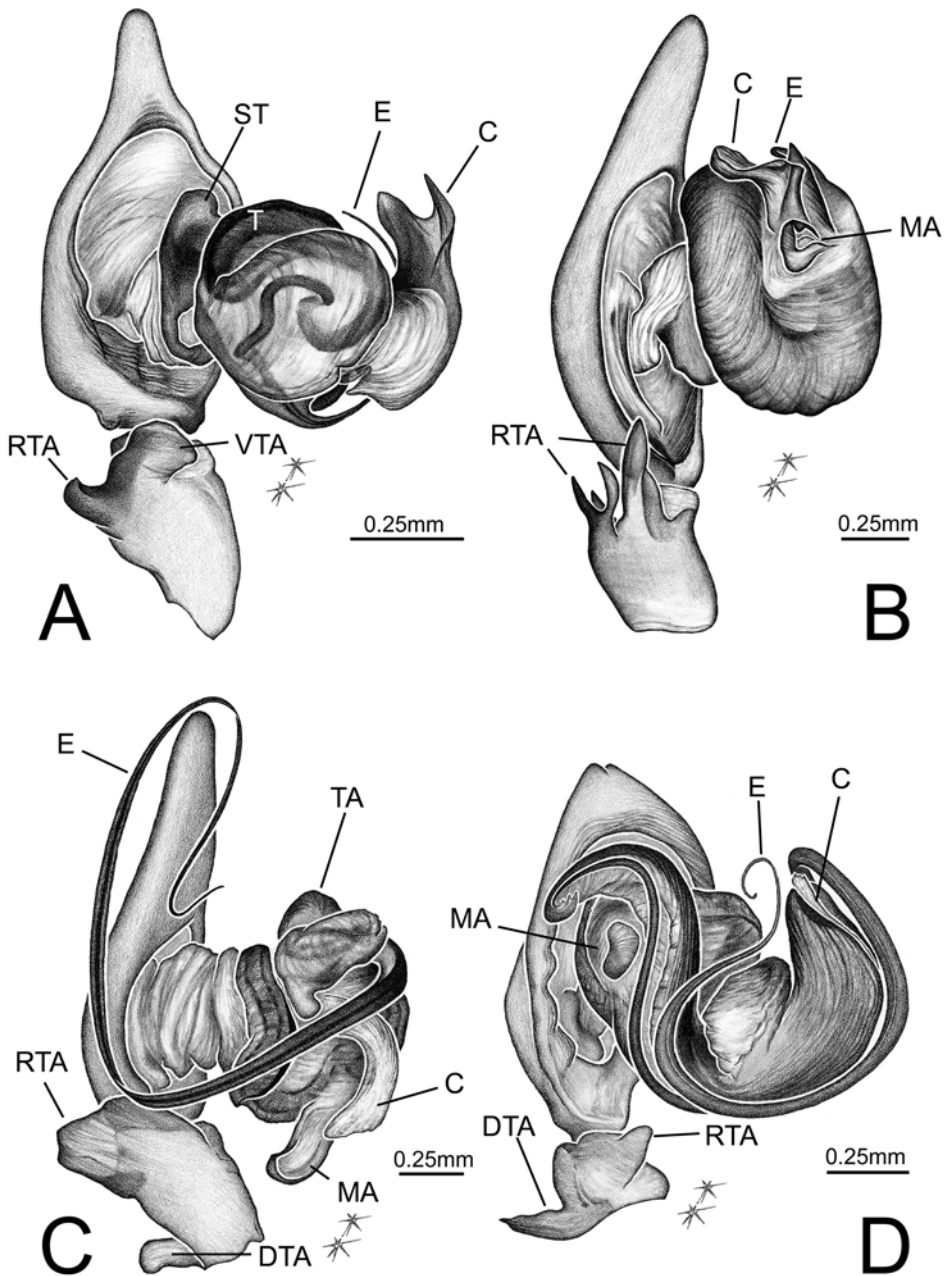


FIGURE 189. Expanded right pedipalpi, retrolateral. A. *Stiphidion facetum* (Stiphidiidae) from Binna Burra, Queensland, Australia. B. *Neoramia sana* (Agelenidae) from Dunedin, New Zealand. C. *Maniho ngaitahu* (Amphinectidae) from Kaituna Valley, New Zealand. D. *Phryganoporus candidus* (Desidae) from Canberra, Australia. C = conductor, DTA = dorsal tibial apophysis, E = embolus, MA = median apophysis, RTA = retrolateral tibial apophysis, ST = subtegulum, T = tegulum, TA = tegular apophysis, VTA = ventral tibial apophysis. Illustrations by Jenny Speckels.

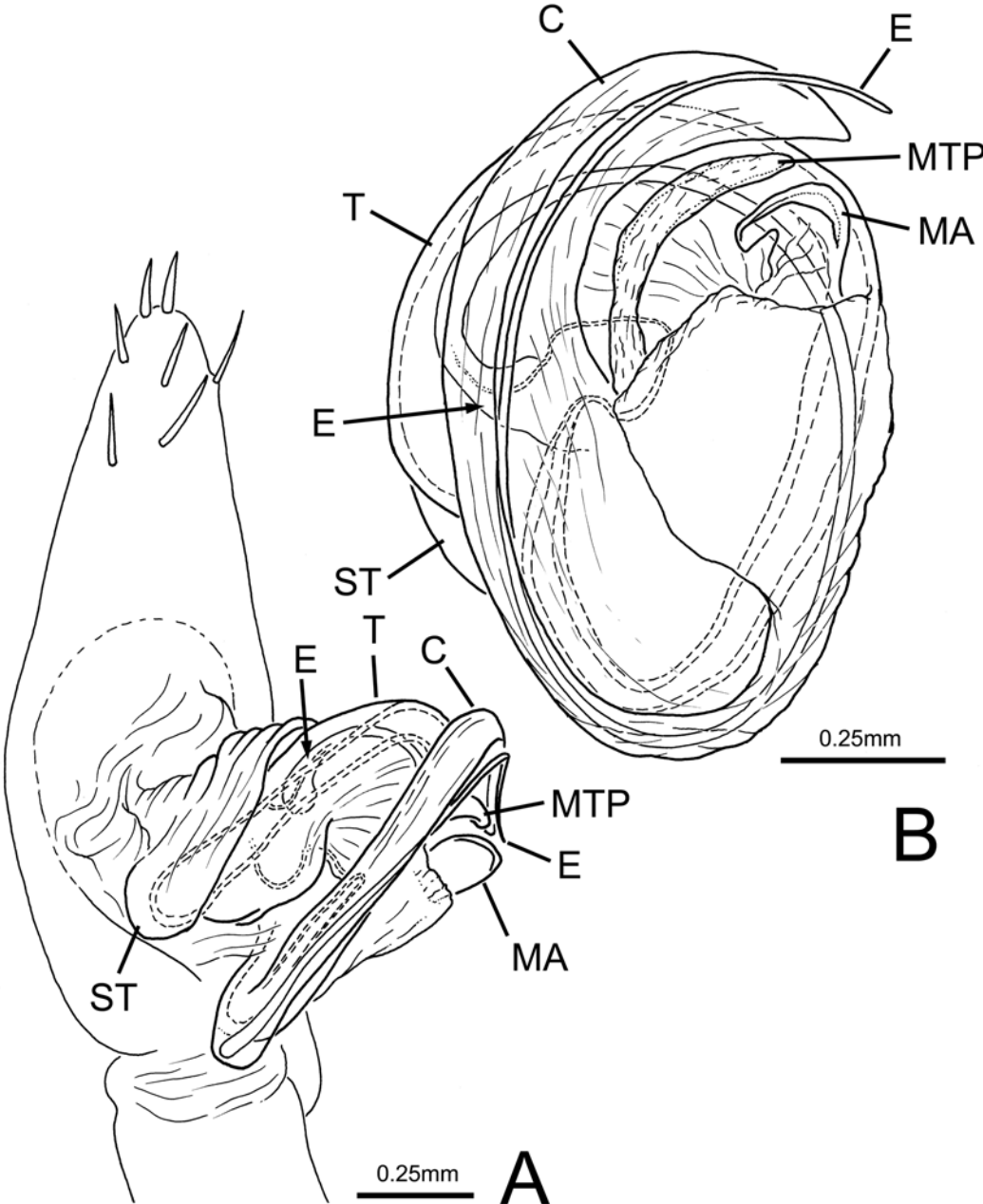


FIGURE 190. Partially expanded left male pedipalpus and copulatory bulb of *Desis formidabilis* from Cape Peninsula, South Africa. A. Prolateral. B. Bulb, ventral. C = conductor, E = embolus, MA = median apophysis, MTP = membranous tegular process, ST = subtegulum, T = tegulum. Illustrations by Martín Ramírez.

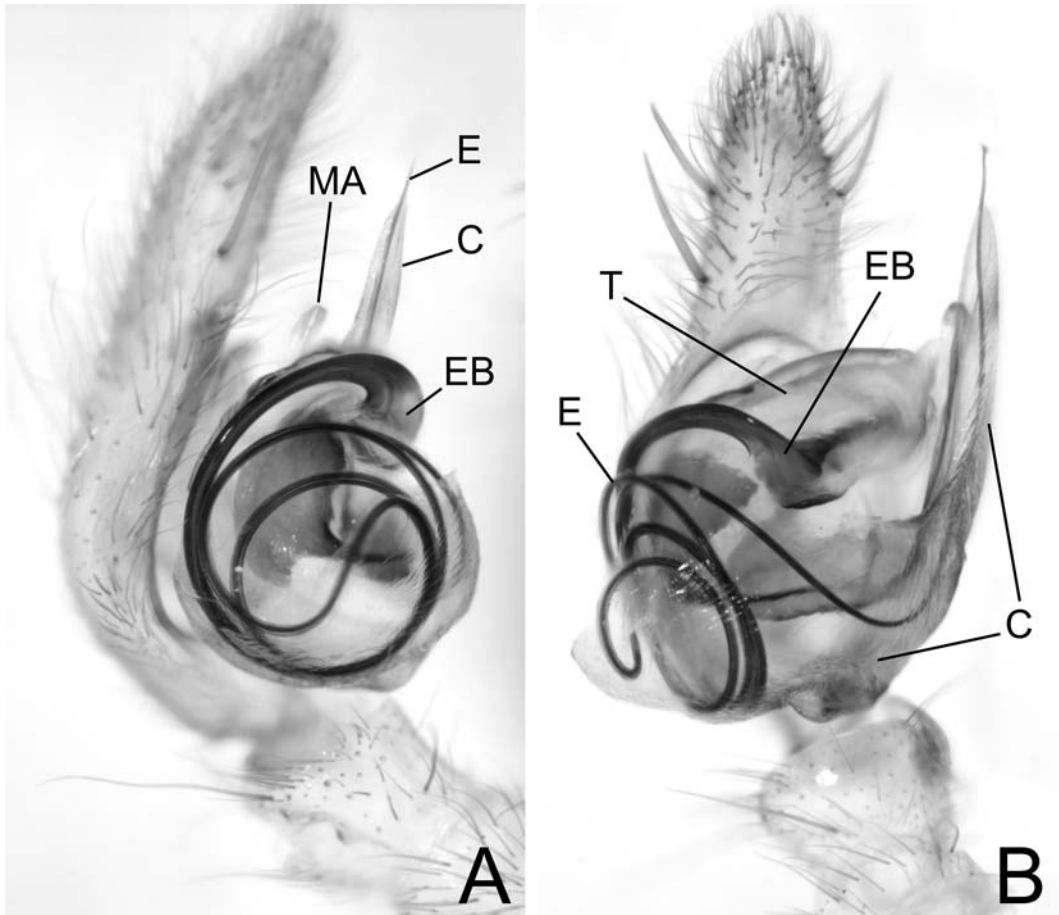


FIGURE 191. Left male pedipalpus of *Metaltella simoni* from Buenos Aires, Argentina, digested with KOH, part of conductor and tegulum removed. A. Prolateral. B. Ventral. C = conductor, E = embolus, EB = embolar base, MA = median apophysis, T = tegulum.

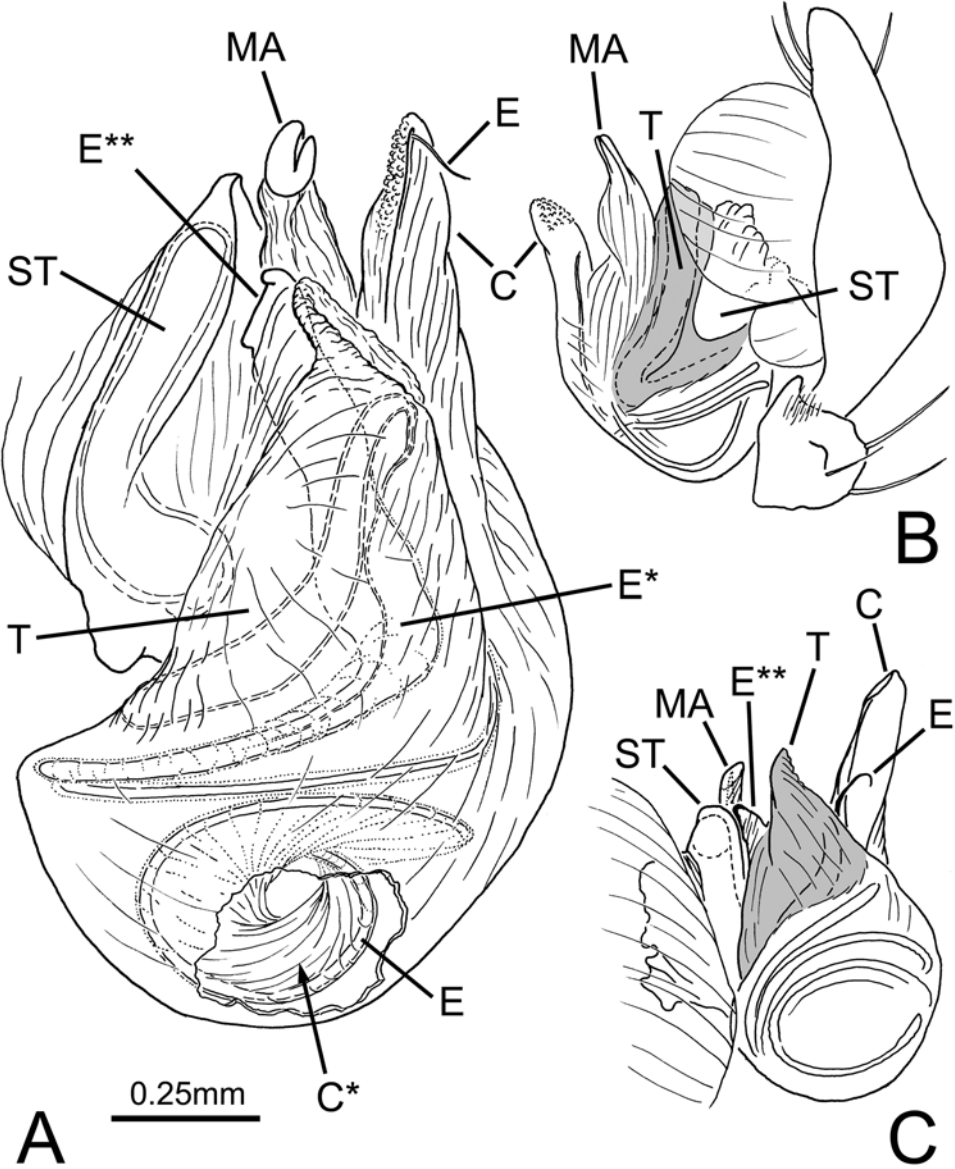


FIGURE 192. Left male pedipalpus of *Metaltella simoni* from Buenos Aires, Argentina. A. Bulb digested with KOH, part of conductor removed, prolateral. B, C. Expanded palp. B. Retrolateral, tegulum grayed. C. Prolateral, tegulum grayed. C = conductor, C* = internal foldings of conductor, E = embolus, E* = origin of embolus, E** = sclerotized process of the embolar base, MA = median apophysis, ST = subtegulum, T = tegulum. Illustrations by Martín Ramírez.

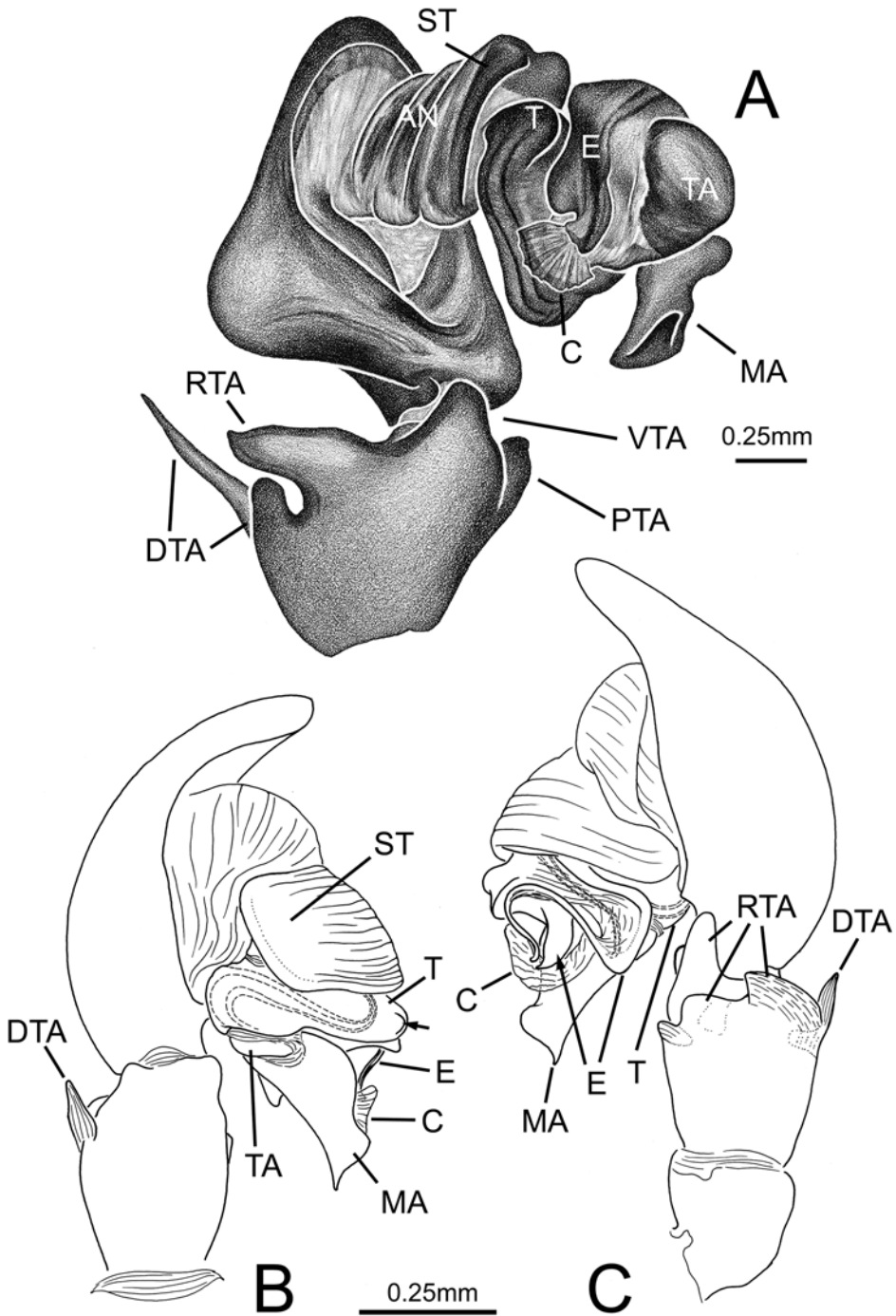


FIGURE 193. Expanded male pedipalpi of Amaurobiidae. A. *Callobius bennetti* from Piscataquis Co., Maine, USA, right, retrolateral. B, C. *Macrobnus* c.f. *multidentatus* from Chiloé, Chile. B. Prolateral. C. Retrolateral. AN = anneli of subtegulum, C = conductor, DTA = dorsal tibial apophysis, E = embolus, MA = median apophysis, PTA = prolateral tibial apophysis, RTA = retrolateral tibial apophysis, ST = subtegulum, T = tegulum, TA = tegular apophysis(es), VTA = ventral tibial apophysis(es). Illustration A by Jenny Speckels, B, C by Martín Ramírez.

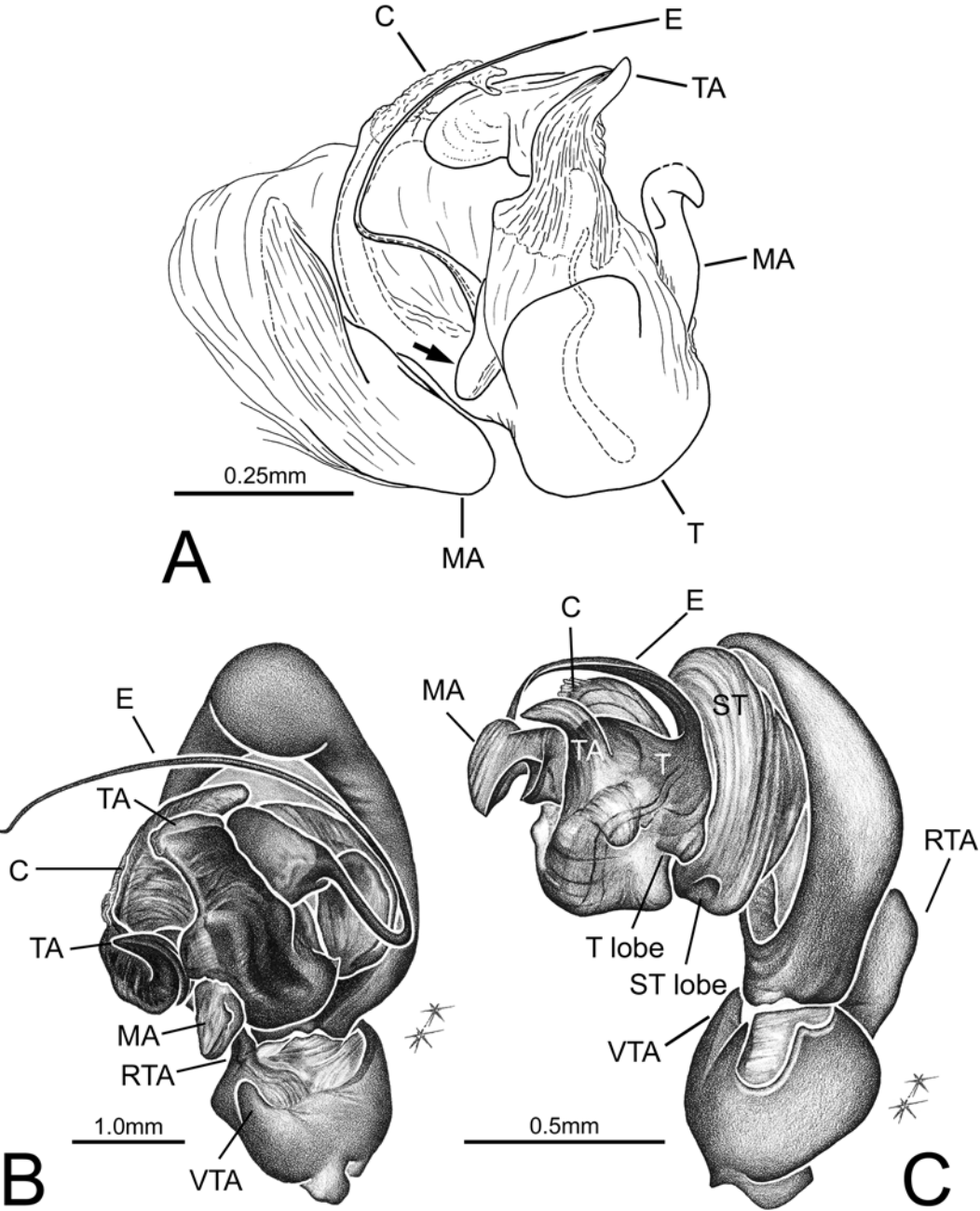


FIGURE 194. Expanded male pedipalpi of Zorocratidae. A. *Zorocrates* sp., male from Hidalgo, Mexico, left bulb prolateral. B. *Uduba dahli* from Ranomafana, Madagascar, right ventral. C. *Raecius jocquei* from Apouesso, Côte d'Ivoire, right prolateral. C = conductor, E = embolus, MA = median apophysis, RTA = retrolateral tibial apophysis, ST = subtegulum, T = tegulum, TA = tegular apophysis(es), VTA = ventral tibial apophysis(es). Illustration A by Martín Ramírez, B, C by Jenny Speckels.

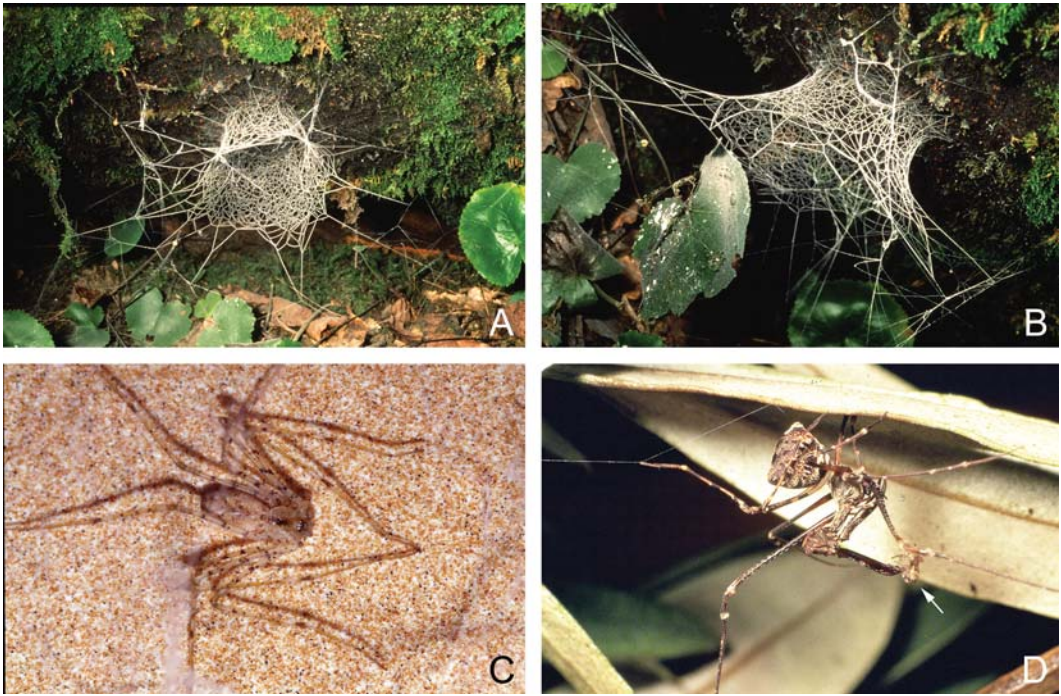


FIGURE 195. Webs and habitus of Hypochilidae and Archaeidae. A, B. *Hypochilus pococki* webs from North Carolina, USA. C. *Hypochilus kastoni* from Mount Shasta, California, USA. D. *Archaea workmani* from Ranomafana, Madagascar. Note theridiid spider prey held in left chelicera (arrow). Photos A, B by Jonathan Coddington, C by Joel Ledford, D by Rollin Coville.

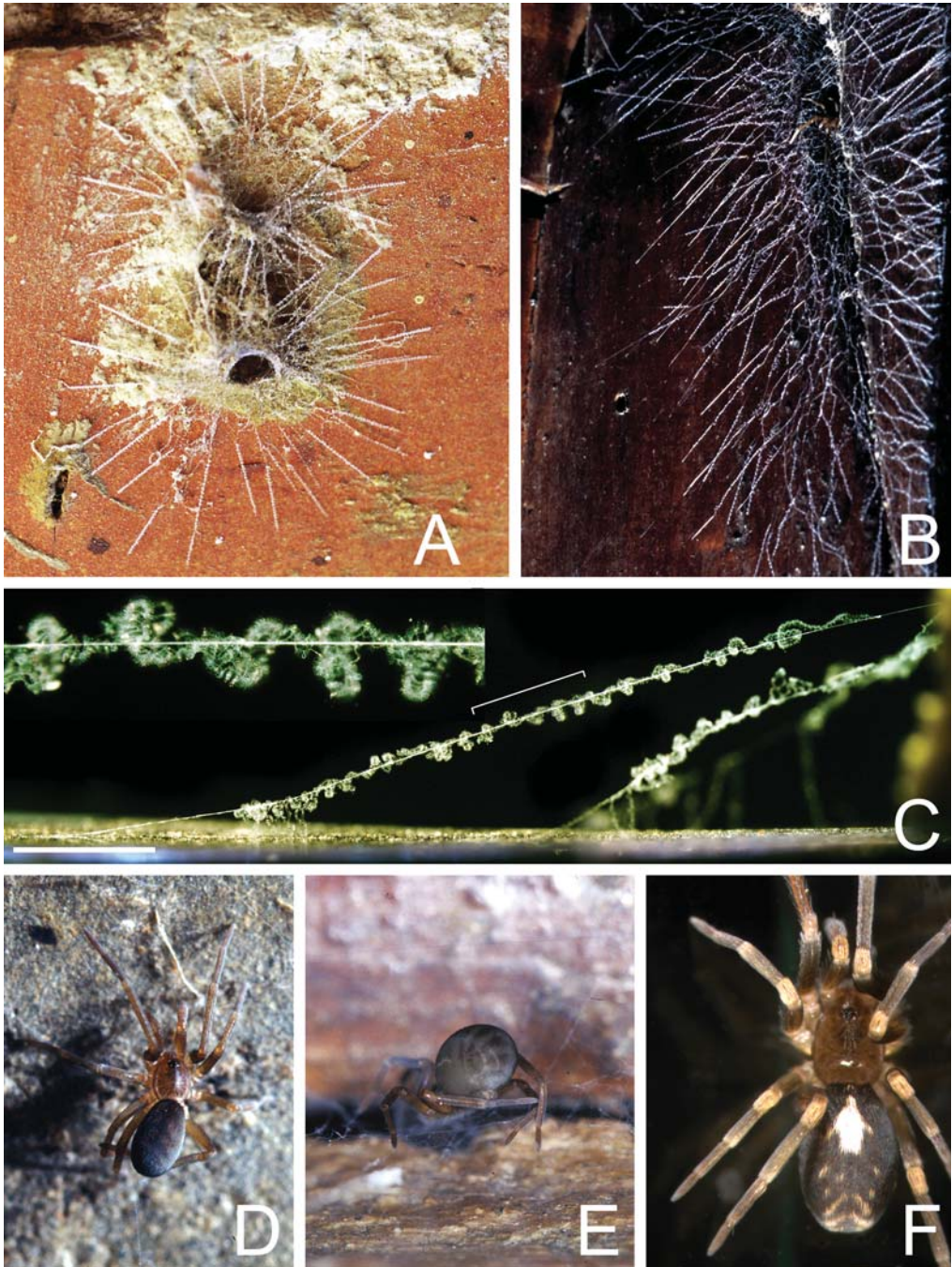


FIGURE 196. Webs and habitus of Filistatidae. A. *Filistata insidiatrix* (Filistatinae) from Siena, Italy, web of immature on a brick wall, note the radial lines with cribellar thread on their edges. B, C. *Kukulcania hibernalis* (Filistatinae) female from Buenos Aires, Argentina. B. Web. C. Cribellate capture threads (detail of a segment as marked). D, E. Female *Misionella mendensis* (Prithinae) from Misiones, Argentina, combing a cribellate segment: note the right combing leg IV resting on the left supporting leg III (stereotyped combing type 1). F. Female *Pritha nana* (Prithinae) from Bolzano, Italy. Photos by Martín Ramírez.

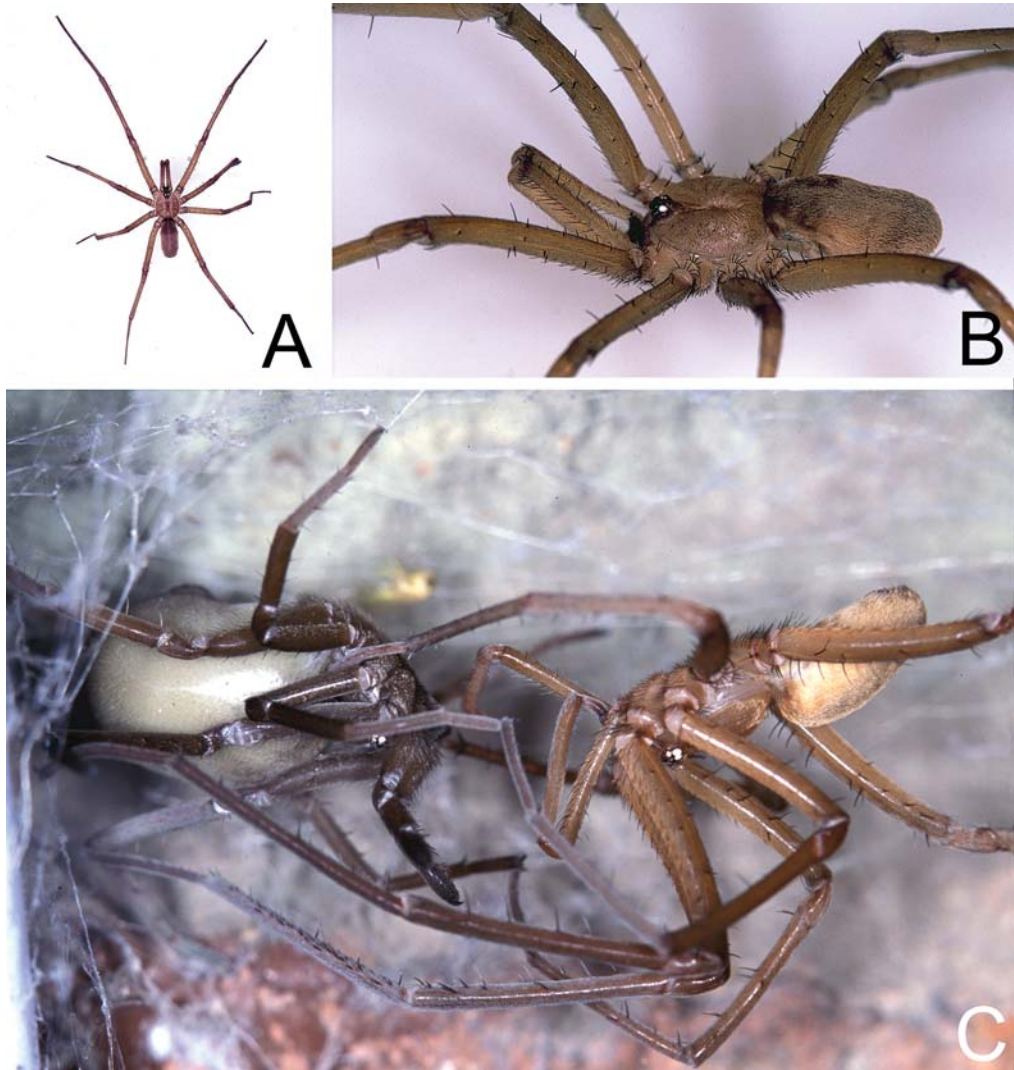


FIGURE 197. *Kukulcania hibernalis* (Filistatidae) from Buenos Aires, Argentina. A, B. Male. C. Male (right) and female mating. Photos by Martín Ramírez.

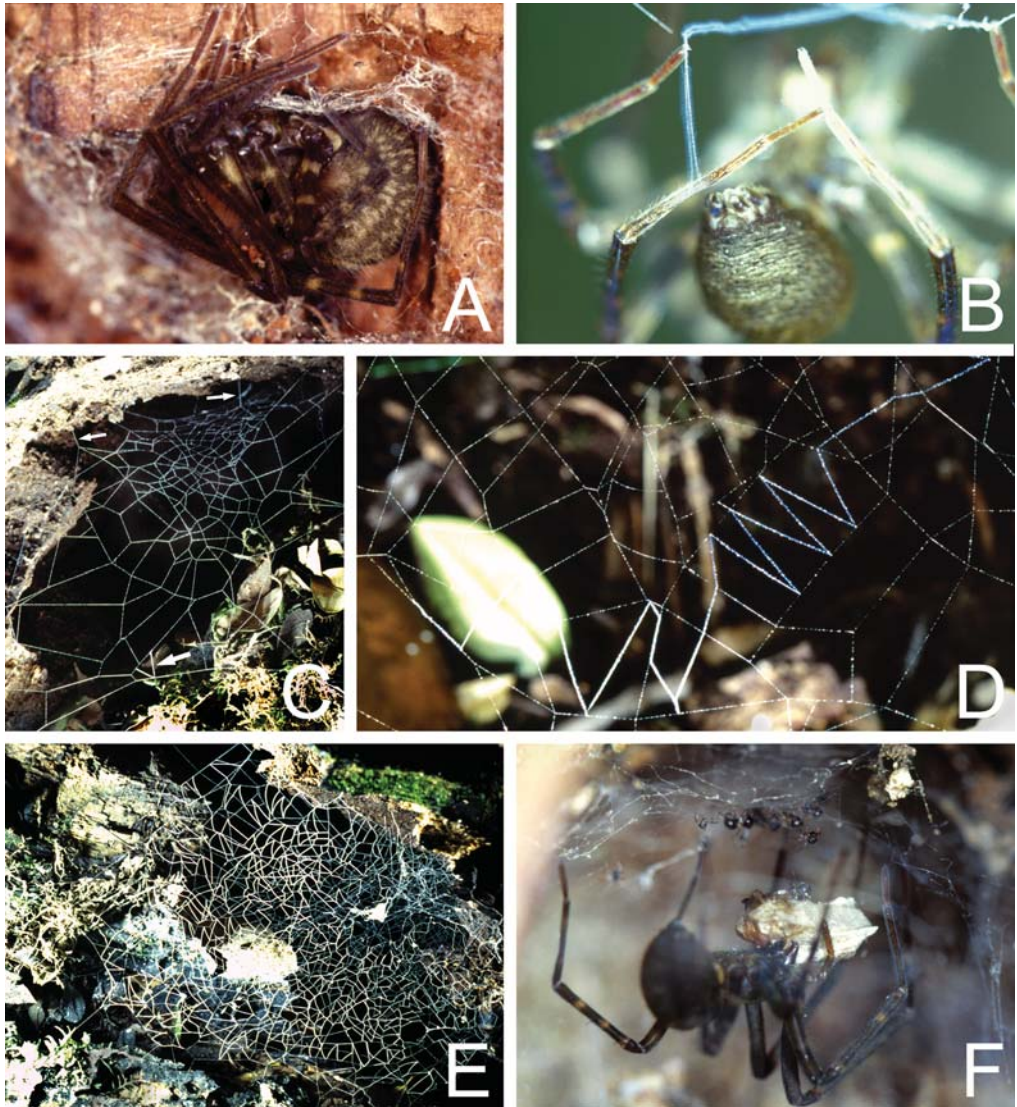


FIGURE 198. Webs and habitus of Austrochilinae, Austrochilidae. A, B. *Austrochilus forsteri* female from Contulmo, Chile. A. Cryptic posture after disturbance. B. Combing a cribellate thread. The right leg III is holding the last attachment position, the left leg III is testing threads where the next attachment will be made. C–F. *Thaida peculiaris* from Puyehue, Chile. C. Non-sticky scaffolding dusted with cornstarch, upper view. Thin arrows to the vertical supporting lines, thick arrow to first cribellate thread. D. Detail of sticky thread on non-sticky scaffolding. E. Non-sticky scaffolding and first cribellate threads, the cribellate threads laid on previous nights have been dusted with cornstarch. F. Spider feeding on a wrapped prey. Many kleptoparasitic *Sofanapis antillanca* (Anapidae) are around the prey, some are descending from the sheet to land on the prey. Photos by Martín Ramírez.

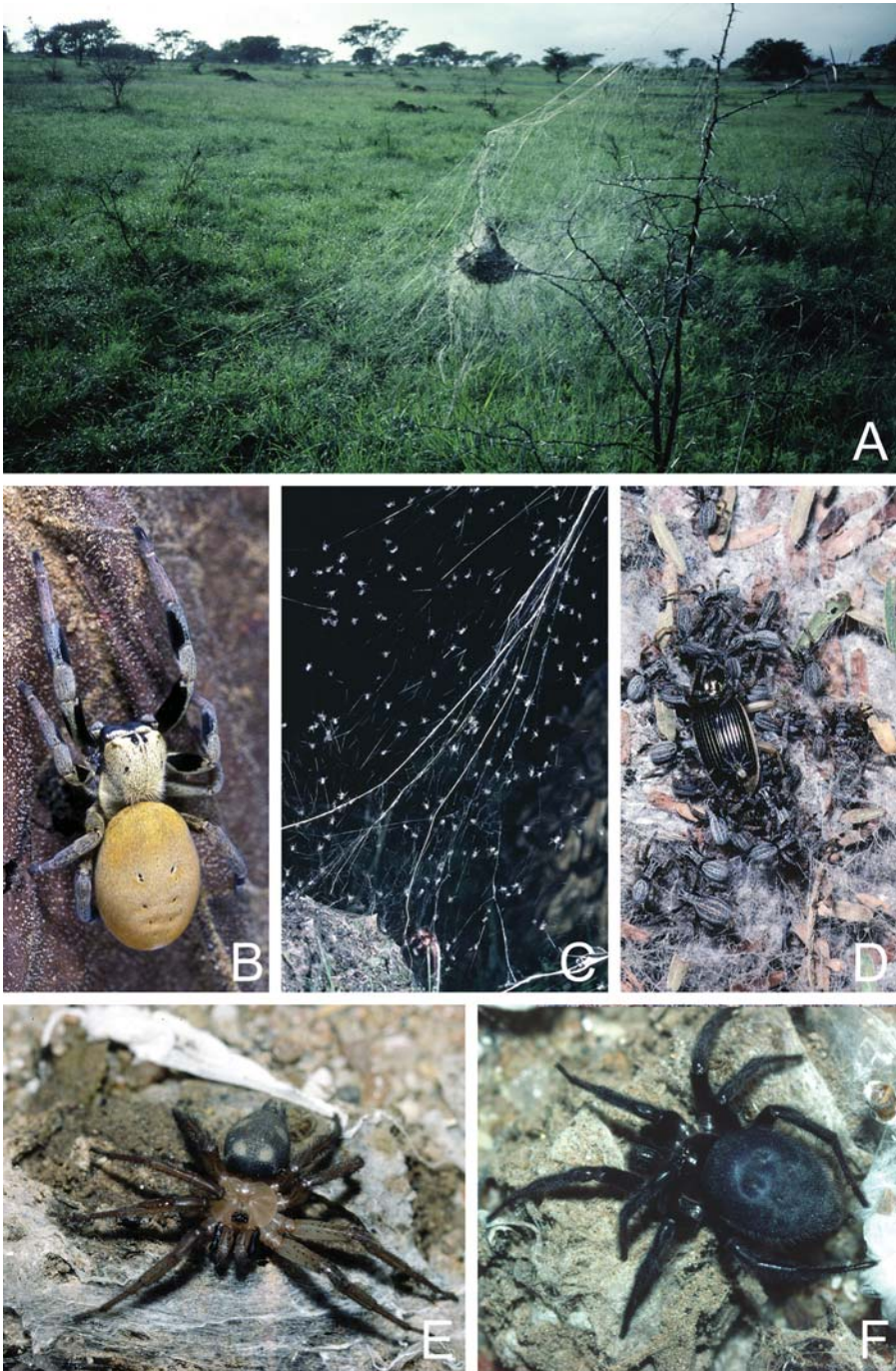


FIGURE 199. Webs and habitus of Eresoidea. A–D. *Stegodyphus* (Eresidae). A. Nest and trap web of social *Stegodyphus dumicola* in *Acacia* at Spioenkop, South Africa. Nest is approximately 30cm in longest dimension; foundation line of trap web is approximately 2m from top of bush to ground. B. *Stegodyphus* sp., female, Shwesattaw, Myanmar. C. Mass of *Stegodyphus dumicola* on trap web just after sunset, Spioenkop, South Africa. D. Mass attack on carabid beetle by *Stegodyphus mimosarum*, Spioenkop, South Africa. E, F. *Uroctea* (Oecobiidae), Noordoewer, Namibia. E. Male. F. Female. Photos A, C—F by Teresa Meikle, B by Dong Lin.

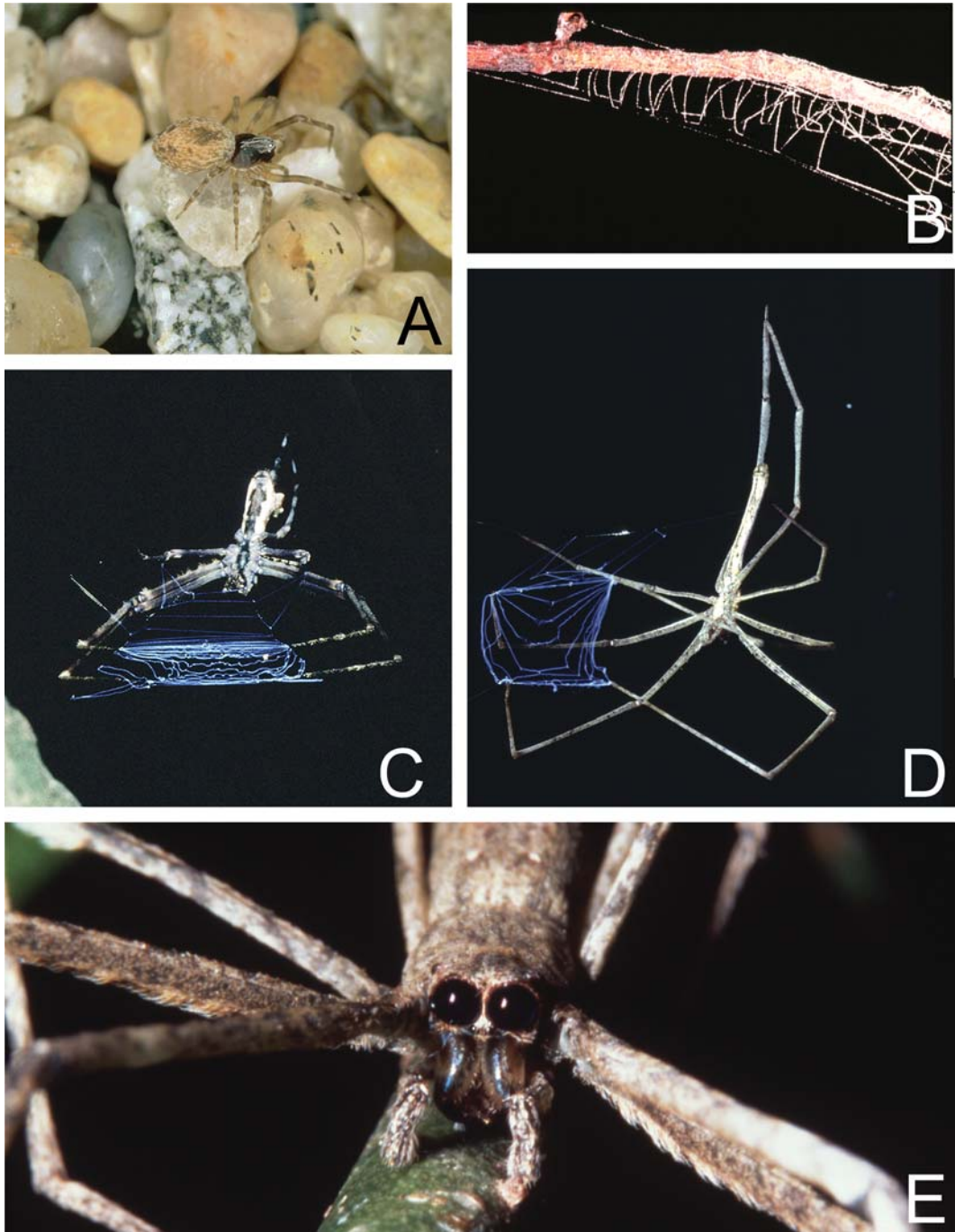


FIGURE 200. Webs and habitus of Deinopidae and Dictynidae. Dictynidae (A, B). Deinopidae (C–E). A. *Dictyna* from Whittier, California, USA. B. Web of dictynid from the USA. C. *Menneus camelus* with web, from Saint Lucia, South Africa. D. *Deinopis spinosus* with web from La Selva, Costa Rica. E. Close up of *Deinopis spinosus* from La Selva, Costa Rica, showing enlarged PME. Photo A by Leonard Vincent, B by Jon Coddington, C by Teresa Meikle, D by Rollin Coville, and E by Jonathan Coddington.

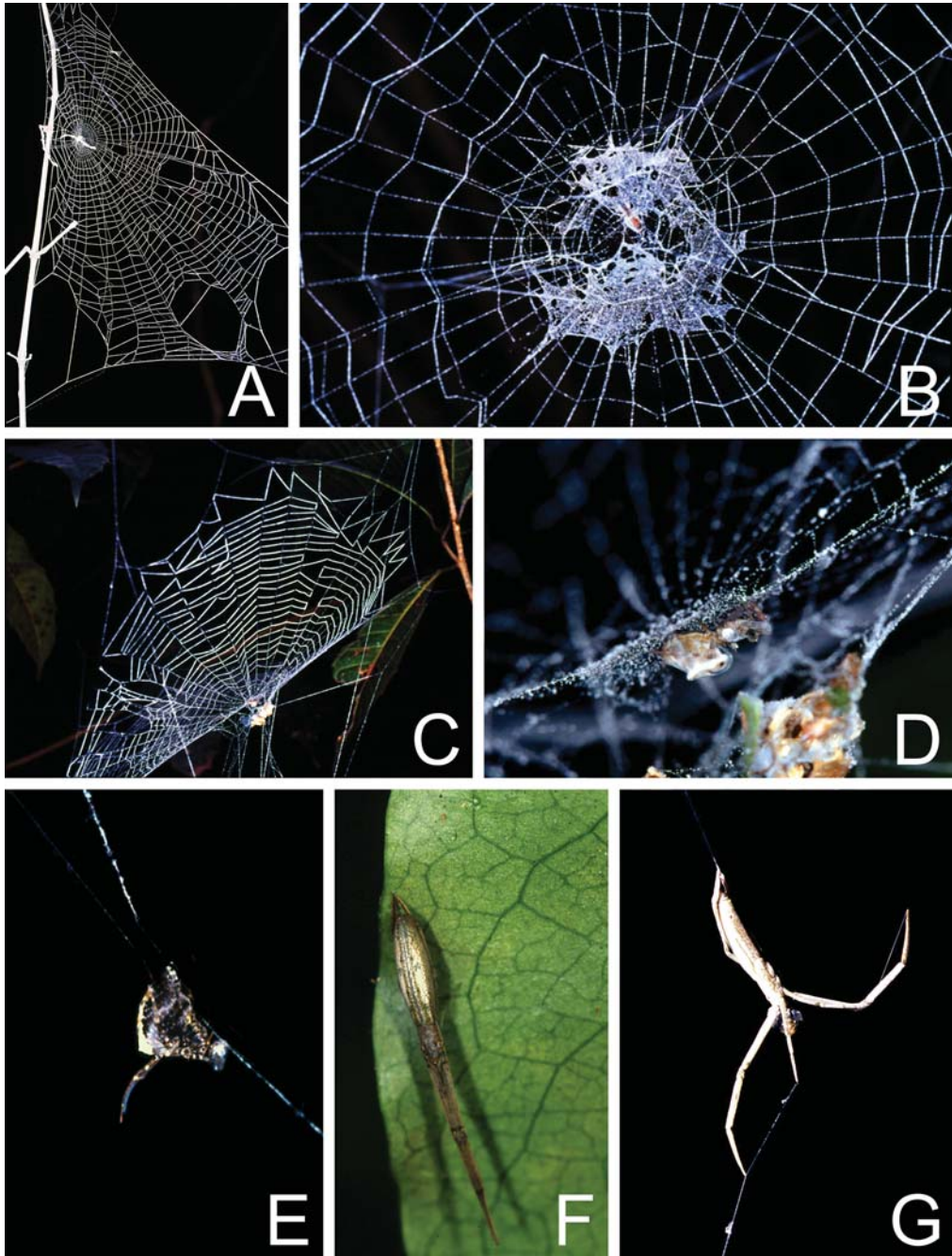


FIGURE 201. Webs and Habitus of Uloboridae. A. Web of female *Uloborus* sp. from Sodwana Bay, South Africa. B–D. Web of female *Conifaber guarani* from Parque Nacional Iguazú, Argentina. B. Hub and stabilimentum. C. Web. D. Detail of hub. E. *Philoponella* cf. *fasciata* from Parque Nacional Iguazú, Argentina, female in hub of an orb. F, G. *Miagrammopes zenzesi*. F. Female from Parc Nacional Iguazú, Argentina. G. Female from Parque Provincial Salto Encantado, Argentina, handling the unique cribellate line. Photos A–F by Martín Ramírez, G by Lara Lopardo.

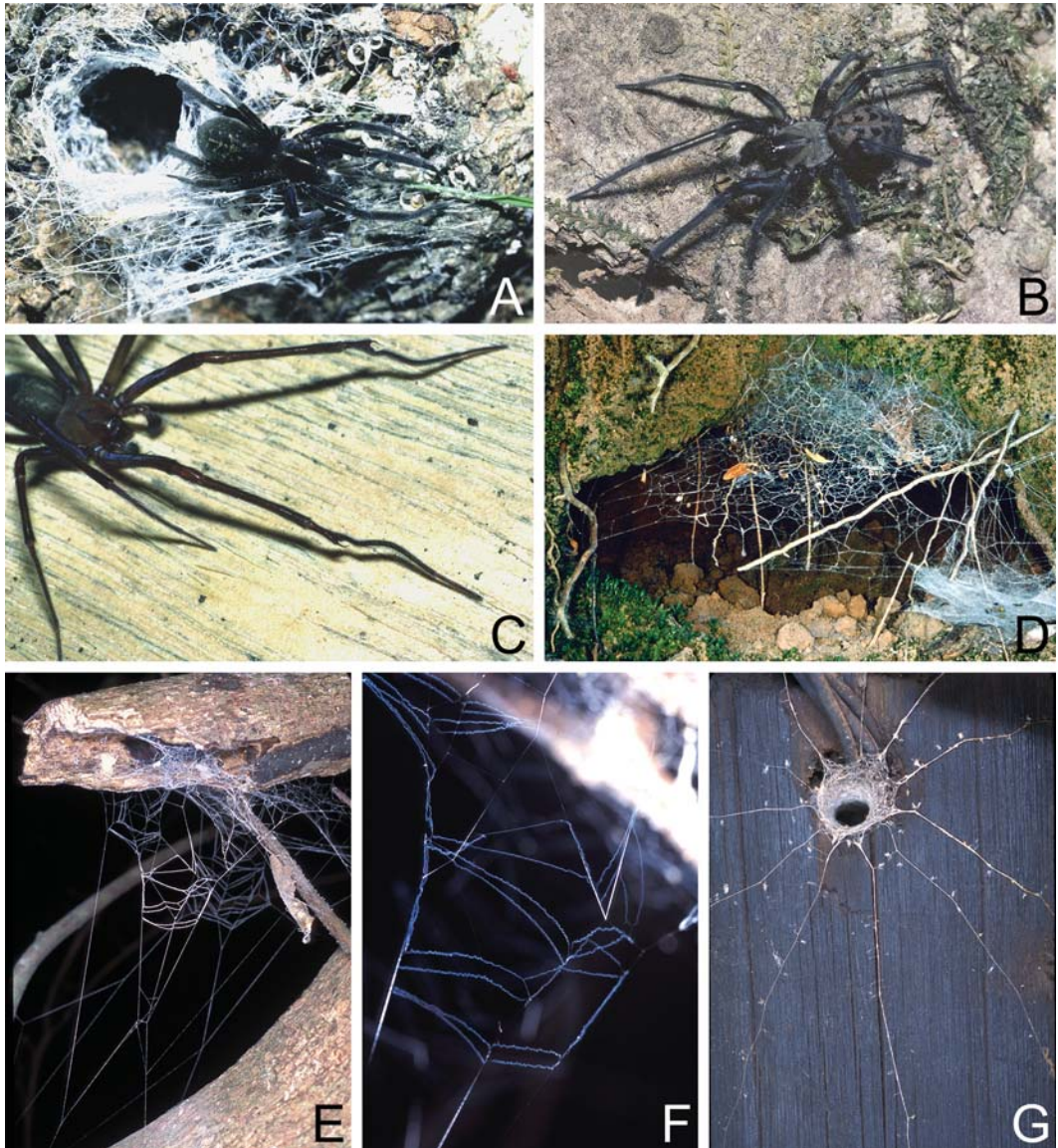


FIGURE 202. Webs and habitus of Phyxelididae and Segestriidae. Phyxelididae (A–F) and Segestriidae (G). A. *Vidole capensis* (Phyxelidinae, Vidoleini) female on appressed web surrounding cavity in tree trunk, Buffels Bay, South Africa. B. *Xevioso amica* (Phyxelidinae, Vidoleini) male from St. Lucia, South Africa. C. *Phyxelida tanganensis* (Phyxelidinae, Phyxelidini) male, Amani, Tanzania (note claspers on metatarsi I). D. Web of *Phyxelida tanganensis* (Phyxelididae, Phyxelidini) on earthen embankment, Amani, Tanzania. E, F. Web of *Xevioso orthomeles* (Phyxelidinae, Vidoleini) from Sodwana Bay, South Africa. E. Web and retreat. F. Detail of web. G. Web of *Ariadna* sp. from Phinda Resource Reserve, South Africa. Photos A, B by Teresa Meikle, C, D by Nikolaj Scharff, E–G by Gustavo Hormiga.

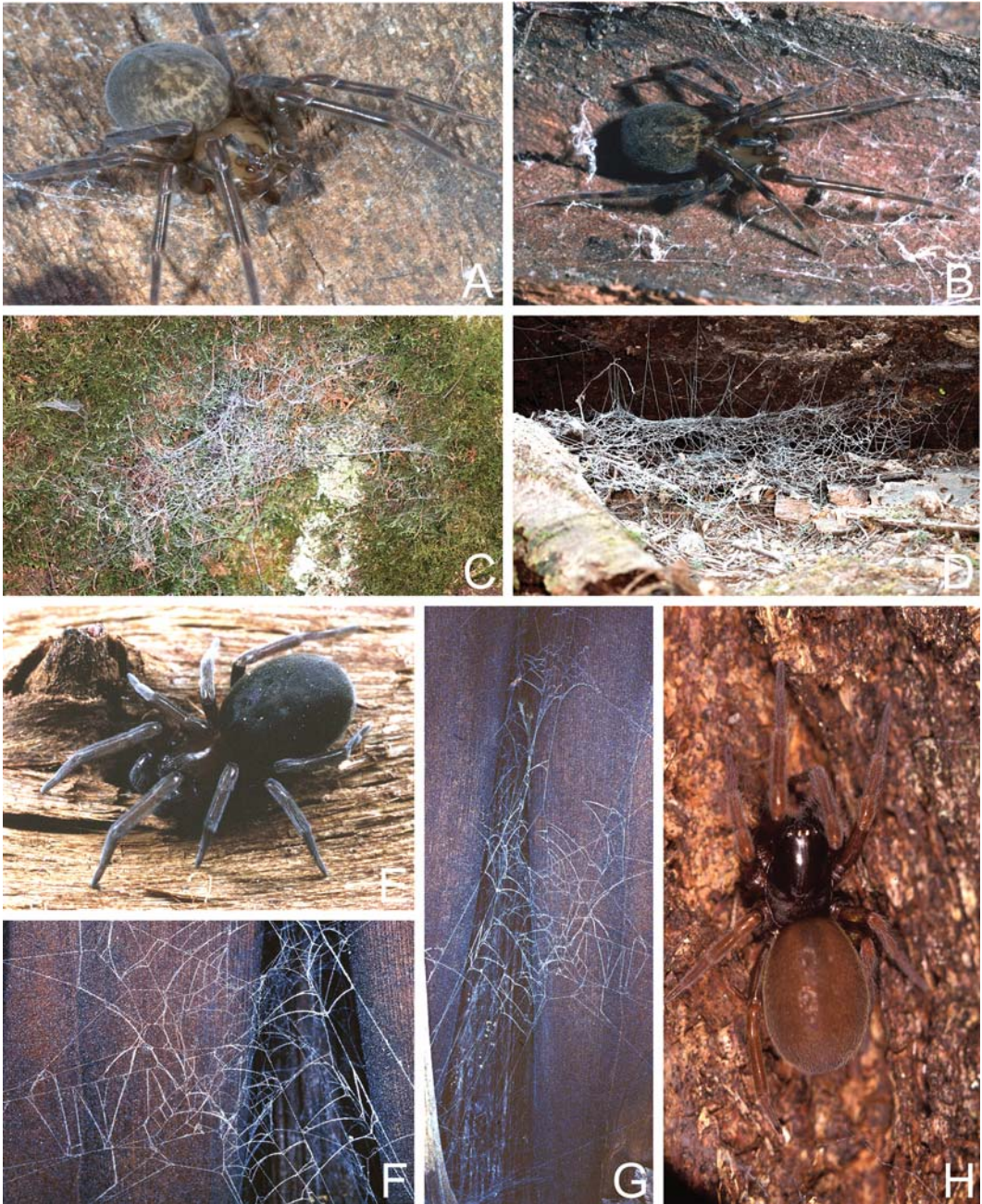


FIGURE 203. Webs and habitus of Nicodamidae and Titanocidae. Nicodamidae, *Megadictyna thilenii* (A–D) and Titanocidae (E–H). A. *Megadictyna* female from Onamalutu Scenic Reserve, South island, New Zealand. B. *Megadictyna* female from Queen Charlotte Sound, South Island, New Zealand. C, D. Webs of *Megadictyna* from Onamalutu Scenic Reserve, South Island, New Zealand. C. On tree trunk. D. Beneath fallen log. E. *Titanoeca nigrella* penultimate male from Cave Creek, Arizona, USA. F, G. Web of *Goeldia* sp. from Parque Nacional Iguazú, Argentina. F. Detail. G. Whole web. H. *Goeldia* sp. from Parque Nacional Pilcomayo, Argentina. Photos A by Charles Griswold, B, E by Rollin Coville, C, D by Hannah Wood, F, G, and H by Martín Ramírez.

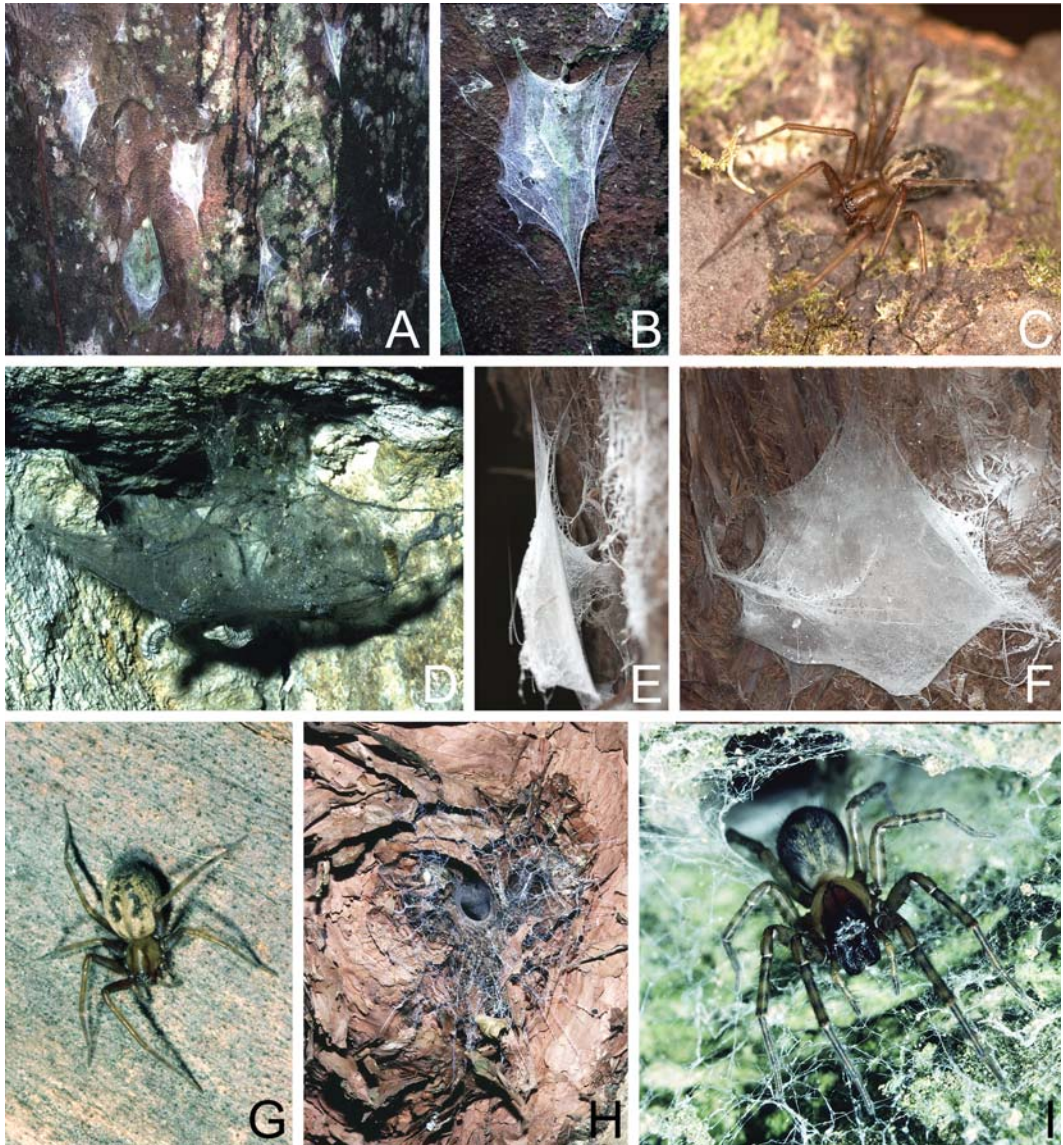


FIGURE 204. Webs and habitus of Agelenidae, Neolanidae and Stiphidiidae. Agelenidae (H–I), Neolanidae (A–C, G) and Stiphidiidae (D–F). A–C, G. *Neolana dalmasi* from Trounsons Kauri Park, North Island, New Zealand. A. Webs on Kauri (*Agathis australis*) trunk. B. Single, vertical web on tree trunk. C, G. Females on tree trunks. D–F. *Stiphidion facetum*. D. Lateral view of horizontal web beneath overhang on rock wall, Waitomo, North Island, New Zealand. E, F. Vertical web on redwood (*Sequoia sempervirens*) trunk, Waipoua, North Island, New Zealand. E. Lateral view, cribellate sheet torn away at side to reveal central funnel. F. Ventral view of sheet. H, I. *Neoramia sana*, Saddle Hill, Dunedin, South Island, New Zealand. H. Web on trunk of Kotukutuku (*Fuchsia excorticata*). I. Female at entrance to funnel retreat. Photos A, B, D, G–I by Teresa Meikle, C, E, and F by Hannah Wood.



FIGURE 205. Webs and habitus of Desidae. A. *Desis formidabilis* on intertidal rock, Lüderitz, Namibia. B, C. *Badumna*. D–G. *Matachia*. B. *Badumna* sp. From Waitomo, New Zealand, on web, carding cribellate silk with carding leg brached with mobile leg IV (stereotyped combing type 2). C. *B. longinqua* web from San Francisco, USA. D–F. *Matachia* sp. from Parakaunui Falls, New Zealand. D. Web. E. Close-up of retreat in hollow twig. F. Spider at retreat. G. *Matachia* web and retreat from Banks Peninsula, New Zealand. Photos A, B and G by Teresa Meikle, C by Patrick Craig, D–F by Hannah Wood.



FIGURE 206. Webs and habitus of Amphinectidae, Amaurobiidae and Tengellidae. Amphinectidae (A), Amaurobiidae (B, D, G), Tengellidae (C, E, F). A. *Metaltella simoni* juvenile from Whittier, California, USA. B, D, G. *Callobius* spp. from California, USA. B. *Callobius nevadensis* female eating fly, from Norden, California, USA. C, E, F. *Tengella radiata* from La Selva, Costa Rica. B. *Callobius nevadensis* female eating fly, from Norden, California, USA. C. Detail of *Tengella* sheet web and knock down strands. Note horizontal orb webs of *Philoponella vicina* (Uloboridae) strung between knock down strands. D. *Callobius* web on redwood (*Sequoia sempervirens*), Petaluma, California, USA. E. *Tengella* sheet web and knock down strands. F. Female *Tengella*. G. *Callobius* webs on redwood trunk (*Sequoia sempervirens*), Guerneville, California, USA. Photo A by Lenny Vincent, B by Tom Davies, C, E and F by Gustavo Hormiga and D, G by Charles Griswold.



FIGURE 207. Webs and habitus of Zorocratidae. A. *Uduba* sp. juvenile, Ranomafana, Madagascar. B. *Zorocrates* sp., female, Chiricahua Mts., Arizona, USA. C. Camouflaged silken tube above burrow of *Uduba* sp., Ranomafana, Madagascar. Tube is approximately 5 cm tall. D. *Uduba madagascariensis* male, Ambohimanga, Madagascar. E. Silken tube and funnel of cribellate silk above burrow of *Uduba* sp., Ranomafana, Madagascar. Tube is approximately 5 cm tall. F. Open, silk-lined burrow of *Uduba* sp., Ranomafana, Madagascar. Burrow is approximately 1.5 cm in diameter. G. Open, silk-lined burrow of *Raecius asper* in burned grassland on Mt. Cameroon, Cameroon. Burrow is approximately 1.0 cm in diameter. H. *Raecius asper* female from Mt. Cameroon, Cameroon. Photo A by Charles Griswold, B by Rollin Coville, C, E, F by Dong Lin, D by Nikolaj Scharff, and G, H by Gustavo Hormiga.

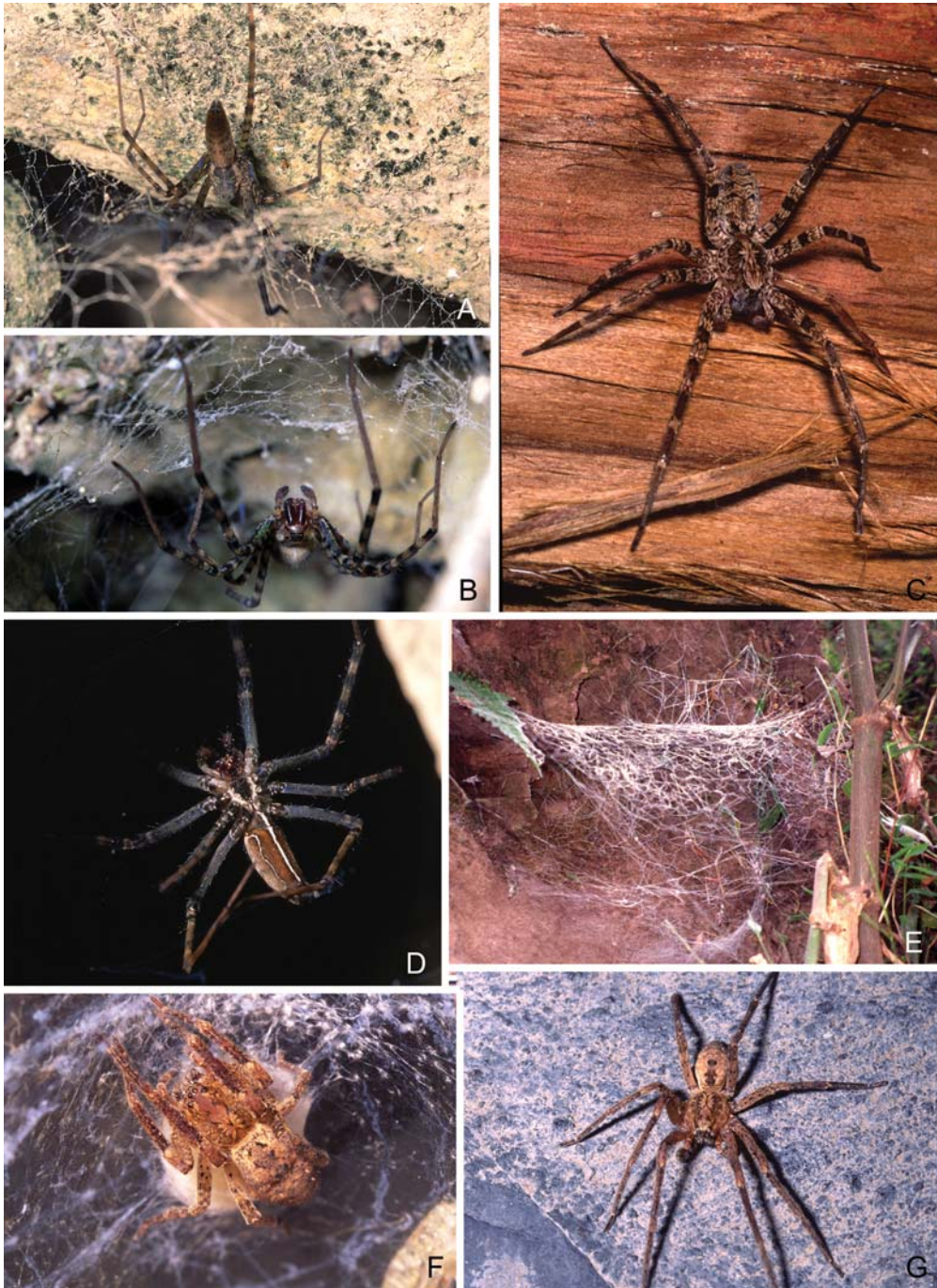


FIGURE 208. Webs and habitus of Ctenidae, Psechridae and Zoropsidae. A, B, D, E. *Psechrus* sp. (Psechridae) from Yunnan, China. A. On rock wall behind web. B. Hanging beneath web. D. Carding cribellate silk, carding leg braced with mobile leg IV (stereotyped combing type 2). E. Cribellate sheet web on rock wall. Web is approximately 0.75m across. C. *Acanthoctenus* sp. (Ctenidae) female from Formosa, Argentina. F, G. *Zoropsis spinimana* (Zoropsidae) from Sunnyvale, California, USA. F. Female on egg sac surrounded by curtain of cribellate silk. G. Male. Photos by Charles Griswold.

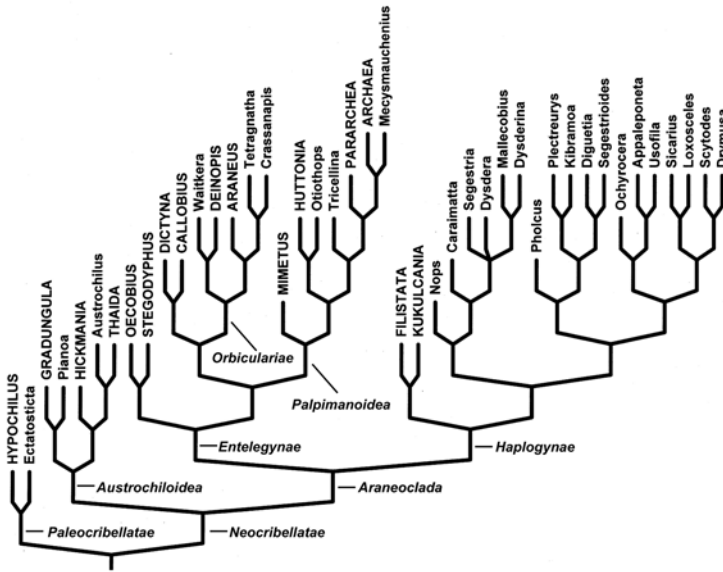


FIGURE 209. Cladogram from Platnick et al. 1991 (pg. 68, fig. 311) for Haplogynae exemplars and outgroups. Exemplars shared with our study are capitalized. Higher taxa listed next to nodes.

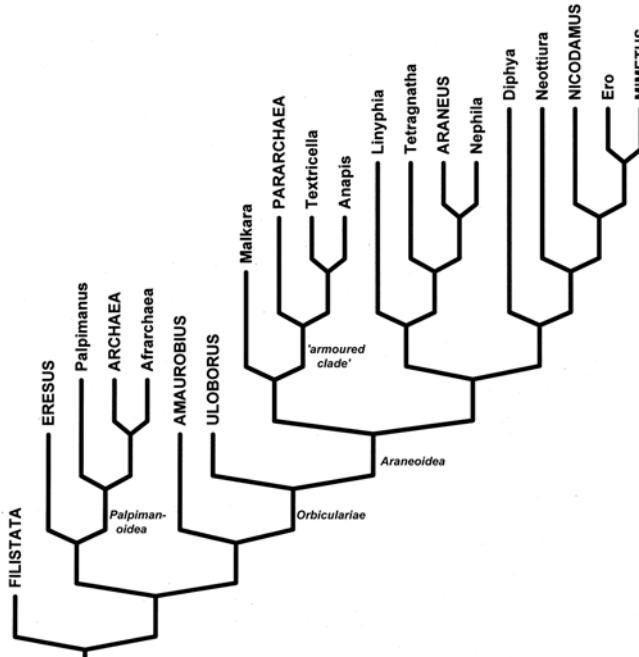


FIGURE 210 Cladogram from Schütt 2002 (pg. 97, fig. 2) for Orbiculariae, Palpimanoidea, and outgroups. Exemplars shared with our study are capitalized. Higher taxa listed next to nodes.

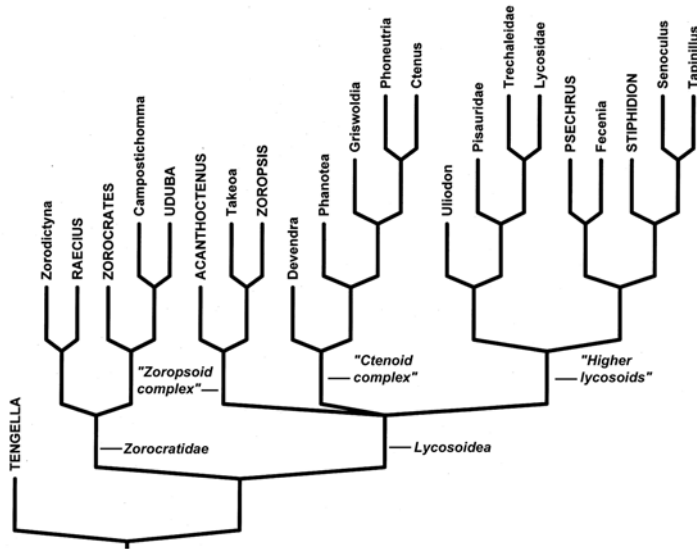


FIGURE 213. Simplified cladogram from Griswold 1993 (pp. 31–34, figs. 84–87) for Lycosoidea and their kin. Exemplars shared with our study are capitalized. Higher taxa listed next to nodes.

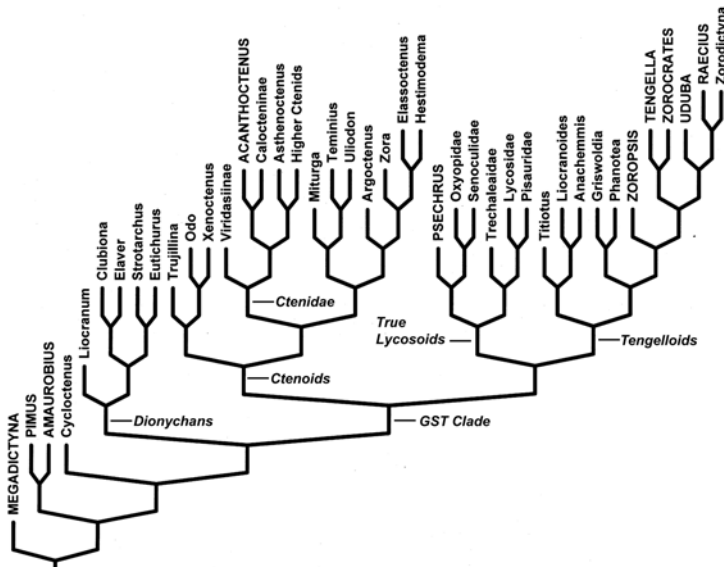


FIGURE 214. Simplified summary cladogram from Silva 2003 (pp. 18–24, figs. 3–9) for higher level relationships of ctenoids, tengeloids, lycosoids and various outgroups. Exemplars shared with our study are capitalized. Higher taxa listed next to nodes.

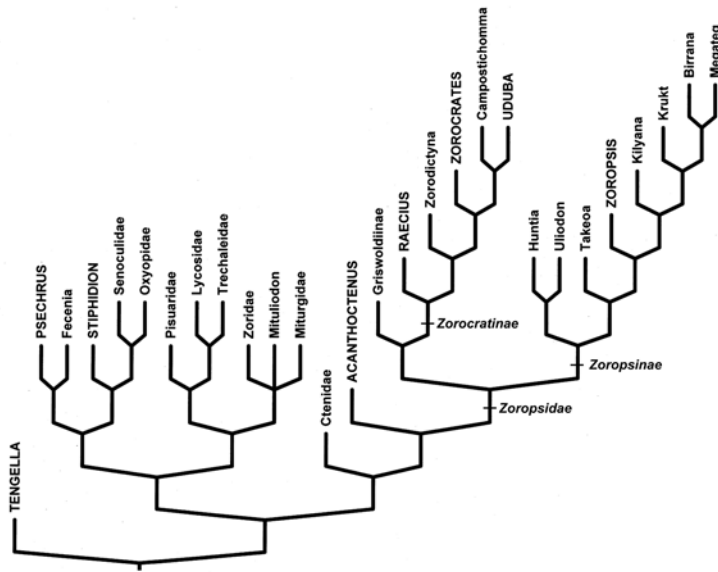


FIGURE 215. Simplified cladogram from Raven and Stumkat 2005 (pg. 354, fig. 2) for Zoropsidae and other lycosoids. Exemplars shared with our study are capitalized. Higher taxa listed next to nodes.

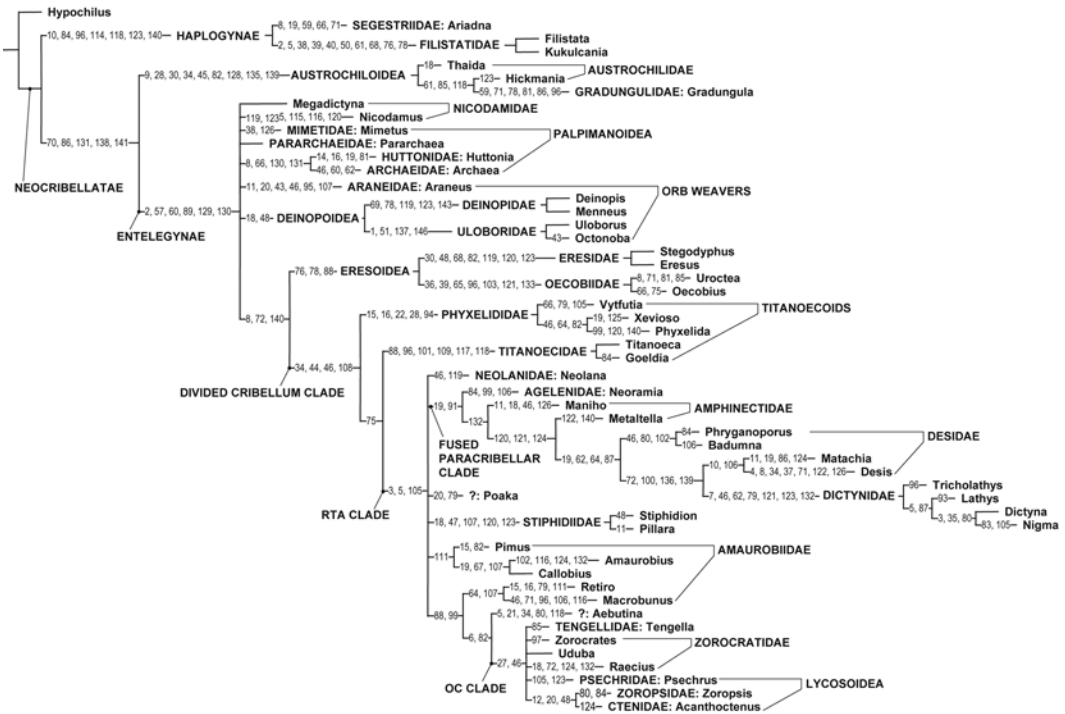


FIGURE 216. Consensus of 224 dichotomous trees (or 96 collapsed trees) obtained with equal weights (tree length = 483 steps). Unambiguous character changes common to all dichotomous trees are mapped on branches.

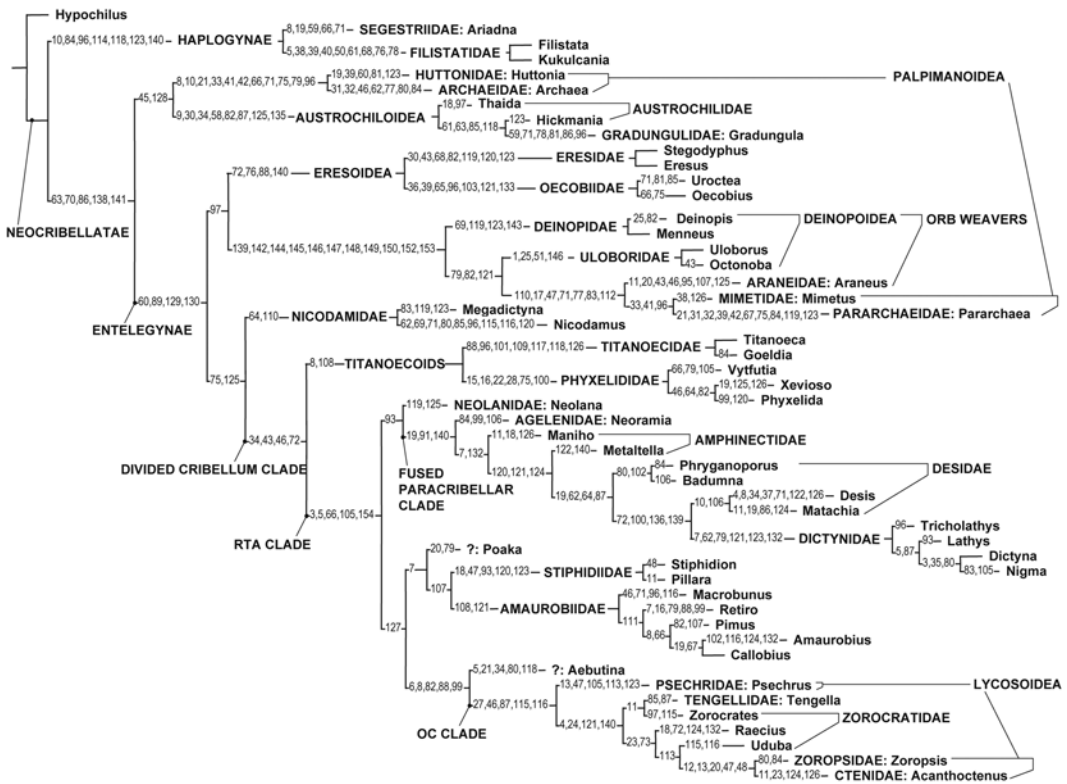


FIGURE 217. Optimal tree under implied weights for constant of concavity $K = 6$ (Fit = 115.93, length 488). Unambiguous character changes are mapped on branches.

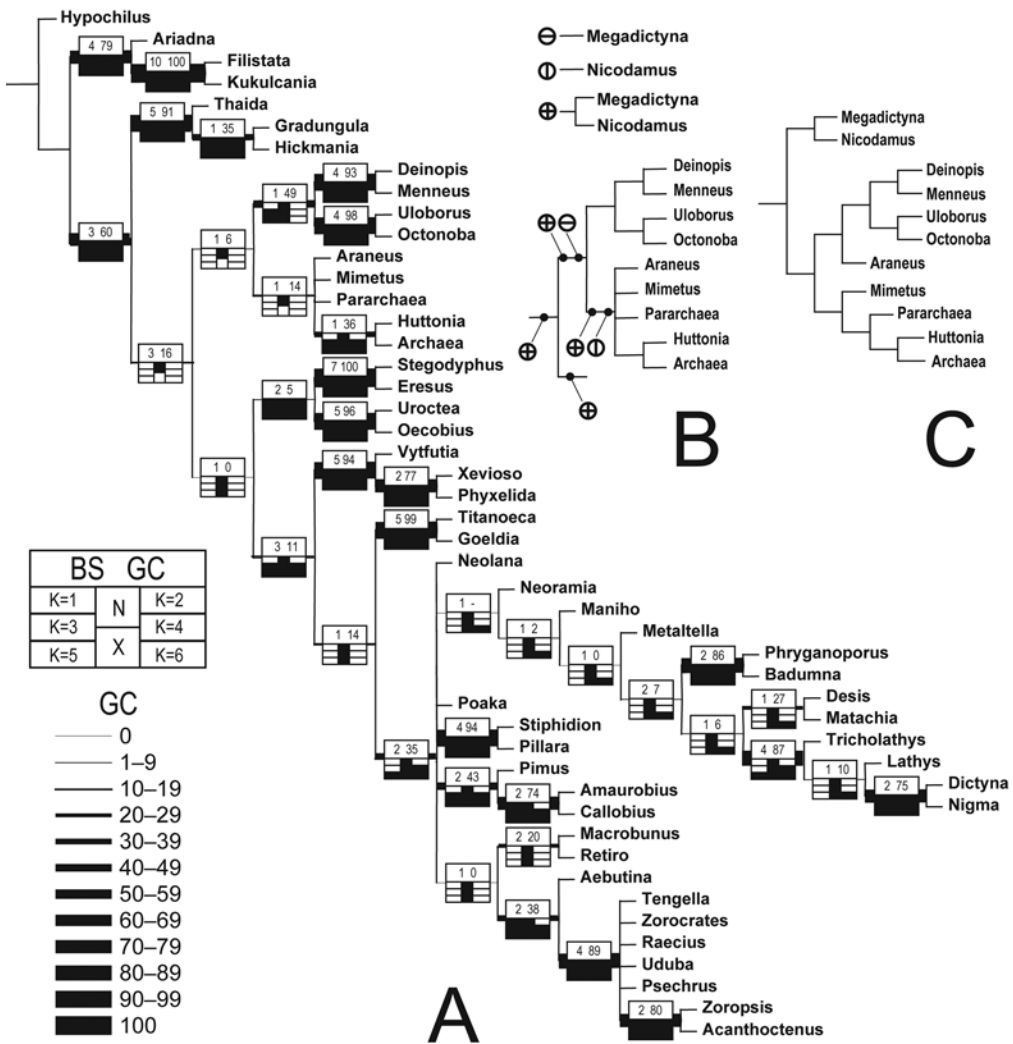


FIGURE 218. Results from equal weights. A. Group support under equal weights, shown on consensus of 224 dichotomous trees (or 96 collapsed trees). The consensus is represented excluding Nicodamidae (see resolutions in B and C). Boxes on each branch display Bremer support (BS), group-contradicted frequency (GC), and sensitivity of groups to parameters of weighting against homoplasy (K = 1-6 are concavities for implied weighting; N = equal weights; X = successive weighting; black box = present). B. The six resolutions including nicodamids. C. Resolution of orb weavers, palpimanoids and nicodamids obtained when inapplicable cells in characters for orb web details (142-153) are replaced by zeroes.

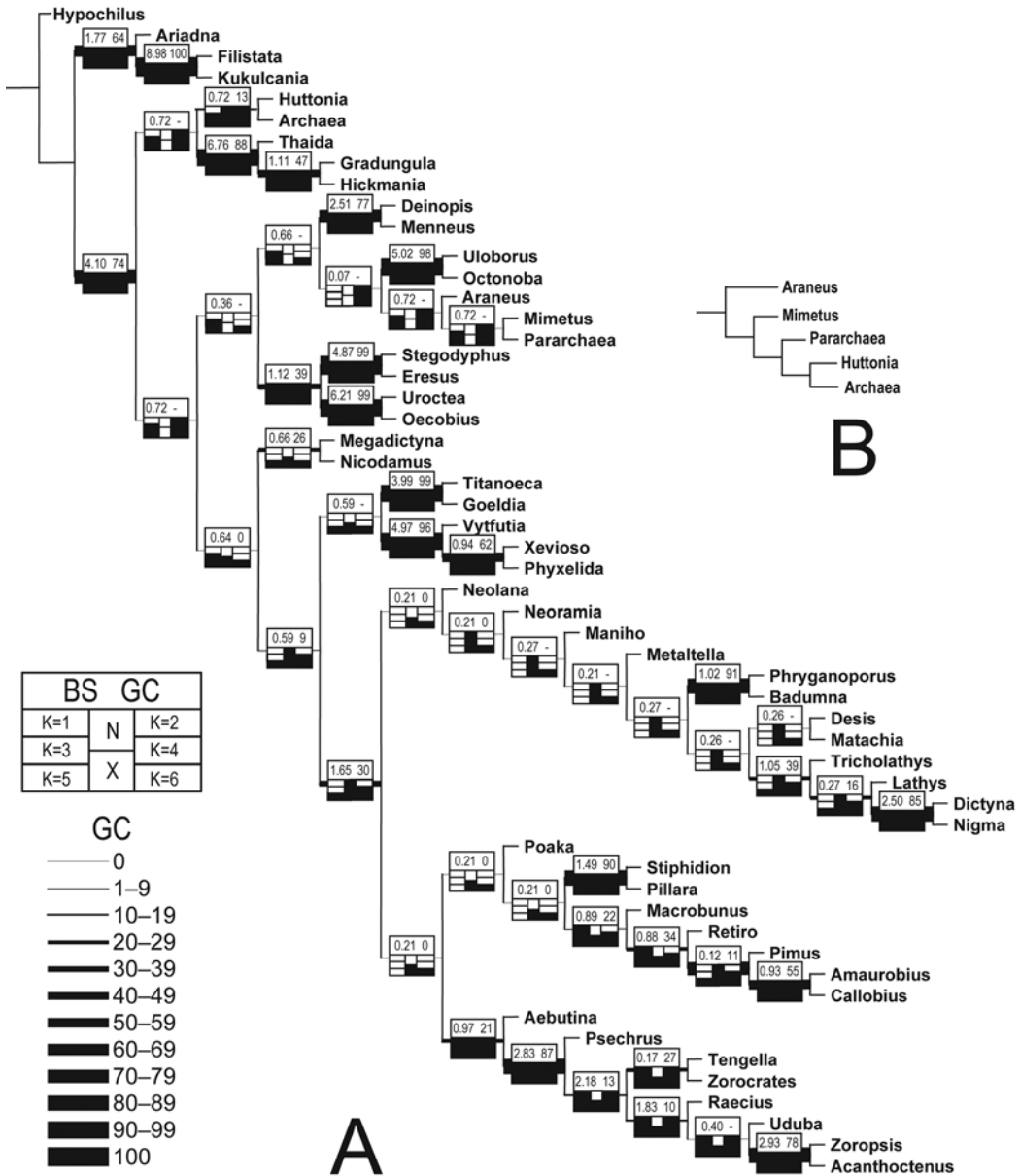
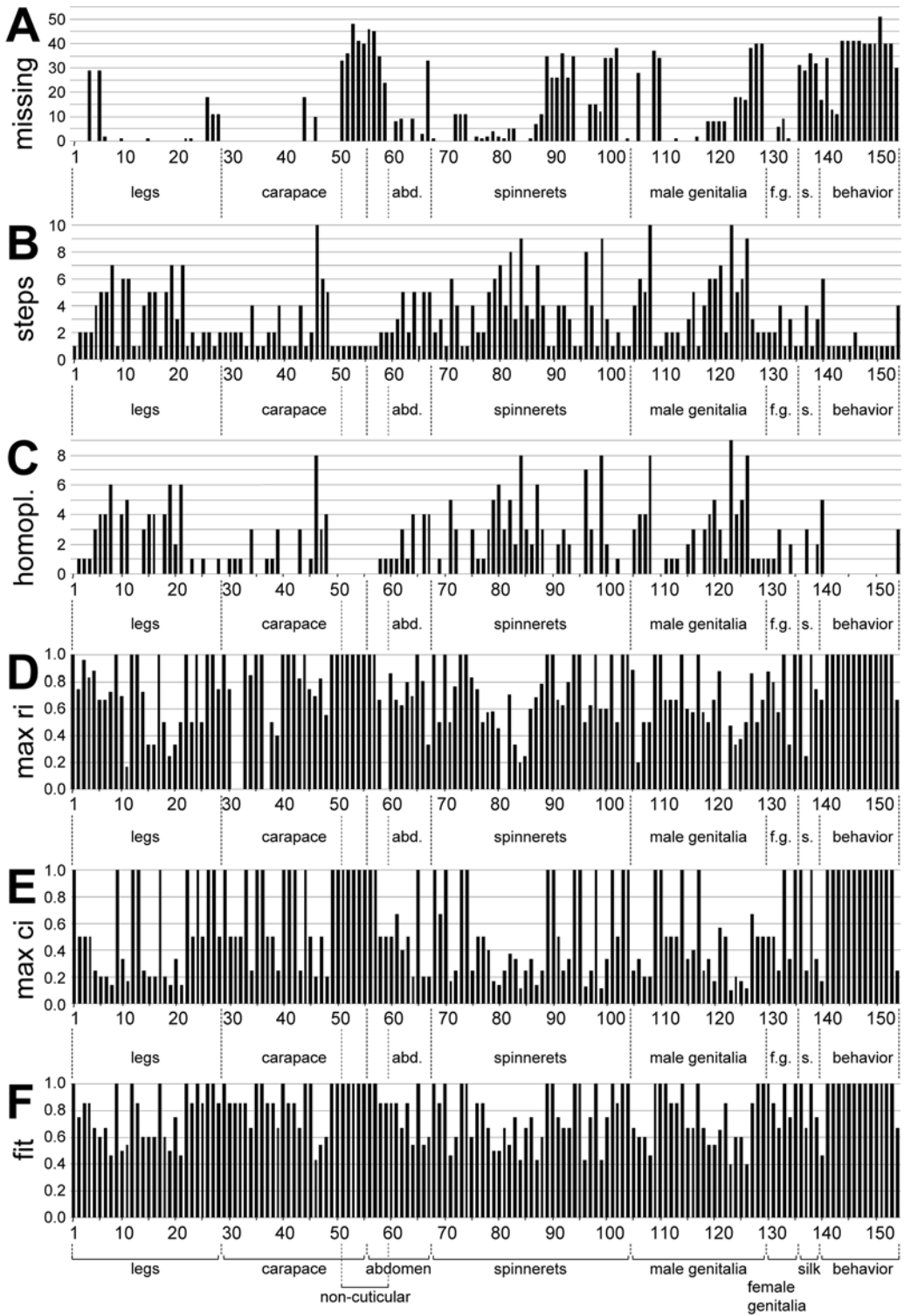


FIGURE 219 (above). Results from implied weights. A. Group support under implied weights; boxes on each branch display Bremer support (BS, multiplied by 10), group-contradicted frequency (GC), and sensitivity of groups to parameters of weighting against homoplasy (K = 1, . . . , 6 are concavities for implied weighting; N = equal weights; X = successive weighting; black box = present). B. The only difference in resolution for successive weighting, using the consistency index as weighting function (length = 484 steps).

FIGURE 220 (right). Summary indices from dataset and cladistic analysis. A. Number of missing cells by character. B-E. Character indices from equal weights analysis, based on the 224 most parsimonious dichotomous resolutions; best indices are reported when they differ among trees. B. Steps. C. Homoplasious steps. D. Retention index. E. Consistency index. F. Character fit = (K - steps) / (K - min steps), from implied weight analysis, one fittest tree for K = 6.



Index

Systematic and Geographic

A

- Acanthoctenus* 5, 17–18, 49, 53, 58, 60, 75, 86–87, 95–96, 198, 216–218, 240, 246, 249, 254, 257, 309; *A. cf. spinipes* 86, 216–217, 240, 246, 249; *A. spiniger* 86, 257
- Aebutina* 2, 5, 21, 23–24, 49, 56, 59, 62–63, 65, 75, 87, 95–96, 157–159, 231, 243, 251, 258, 270; *A. binotata* 23, 87, 157–159, 243, 251, 258, 270
- Africa 7–8, 14, 18–19, 24–26, 33–35, 42, 44, 87–88, 90–92, 130–131, 134, 138, 144–145, 147, 180–182, 220, 231–232, 236, 239, 241–242, 244–245, 248–249, 253, 255, 259–260, 271, 278, 288, 291, 300–303; Cameroon 7, 44–45, 92, 308; Côte d'Ivoire 45, 92, 198, 248, 254, 262, 287, 295; Equatorial Guinea 92 (Bioko Island 92); Kenya 18, 87–88; Malawi 26, 88, 135–137, 230, 232, 260; Morocco 26, 88, 132, 134; Namibia 33, 87, 90, 300, 306; South Africa 7–8, 18–19, 26, 33–34, 87–88, 90–92, 130–131, 134, 138, 144–145, 147, 180–182, 220, 231–232, 236, 239, 241–242, 244–245, 248–249, 253, 255, 259, 260, 271, 278, 288, 291, 300–303; Tanzania 7–8, 44, 88, 90, 93, 147, 150–151, 222, 225–226, 233, 244, 261, 274, 289, 303
- Agathis australis* 31, 305
- Agelenidae 1–2, 5, 8, 35, 74, 85, 290, 305
- agelenids 9, 47–48, 54–55
- agelenoids 3, 74
- Akamasia* 46
- Amaurobiidae 1–3, 5, 9–10, 35, 37–38, 49, 74, 85, 284, 294, 307
- amaurobiids 9–11, 47–49, 55, 61–62, 67, 75
- Amaurobiinae 5
- Amaurobioidea 3
- Amaurobioides* 21
- Amaurobius* 5, 9–11, 49, 56, 63–64, 74, 85, 94, 96, 189, 223, 254, 257; *A. fenestralis* 9–10, 85, 189, 254, 257
- Ambohima* 35–36, 50, 90; *A. sublima* 90
- Amphinecta* 12
- Amphinectidae 1–2, 5, 12, 21, 74, 85, 281, 290, 307
- amphinectids 12–13, 47–49, 61, 63, 67, 74
- Anapidae 14, 72, 86, 299
- Anisacate* 12, 74
- Araneidae 2, 4, 14, 86, 139
- araneids 31, 44, 50, 54–55, 65, 67, 70
- Araneoclada 2–3, 55, 71, 72
- Araneoidea 1, 3–4, 14, 32, 49, 58–59, 61, 64, 72–73, 121
- araneoids 14–15, 43, 53, 59, 62, 72–73
- Araneomorphae 1, 3, 27, 58, 60, 71
- Araneus* 4, 14, 48, 50, 54, 57, 64, 86, 94–95, 121, 249–250, 272; *A. diadematus* 86, 121, 249–250, 272
- Archaea* 5, 14–15, 32, 48–49, 51–53, 55–56, 58–59, 65–67, 72–73, 86, 95–96, 121–123, 228, 235, 250, 266, 269, 296; *A. workmani* 14–15, 86, 121–123, 228, 235, 250, 266, 269, 296
- Archaeidae 1–2, 5, 14, 72–73, 86, 121, 235, 296
- archaeids 67, 73
- Argentina 1, 15–16, 27, 39, 85–89, 91–92, 112, 115, 118, 120, 219–220, 231, 239, 245, 249, 253, 259, 263–264, 284, 292–293, 297–298, 302, 304, 309
- Argiope argentata* 86, 139
- Argyroneta* 21, 67; *A. aquatica* 21
- Ariadna* 4, 39, 56, 58, 91, 94, 95, 118, 120, 231, 239, 253, 259, 263, 303; *A. boesenbergi* 39, 91, 118, 120, 239, 253, 259, 263; *A. maxima* 39, 263
- Asia 19, 35, 37; China 29, 37, 89, 91, 103, 309; India 33, 37, 90–91, 231, 253, 255; Indonesia 90, 253, 256 (Sumatra 90, 253, 256); Malaysia 90, 147–149, 262 (Sarawak 90, 147–149, 262); Myanmar 88, 300; Nepal 37, 91, 244; Southeast Asia 19, 37; Thailand 37–38, 90, 157, 198, 212–213, 233
- Australia 5, 7, 12, 14, 19, 21, 24, 28, 32, 34, 37, 39–40, 86–87, 90–91, 108–111, 142–143, 169–170, 172–173, 185–186, 188, 219, 221, 234, 240–241, 248–251, 254, 256, 273, 280, 290; New South Wales 28, 40, 169, 170, 172–173, 248, 254, 256; Queensland 4, 7, 28, 91, 280, 290; Tasmania 15, 17, 86, 91, 108–111, 219, 221, 234, 249, 251; Victoria 28; Western Australia 90, 142–143, 240–241, 250, 273
- Austrochilidae 1–2, 4, 15, 32, 44, 71–73, 86, 234, 288, 299
- austrochilids 15–17, 28, 47–49, 52–54, 58–60, 68, 72, 115
- Austrochiloidea 2, 71–72, 76
- austrochiloids 49–51, 53–55, 60–61, 67–68, 71
- Austrochilus* 15–16, 72, 86, 234, 253, 299; *A. forsteri* 15, 86, 299; *A. melon* 16, 86, 234, 253

B

Badumna 5, 19–21, 56, 63, 87, 94, 96, 187–188, 223,

254, 257, 279, 306, 311; *B. candida* 19–20; *B. longinqua* 19–20, 87, 187–188, 223, 254, 257, 279, 306
Birrana 46

C

Calilena 9
Callobius 5, 9–10, 49, 56, 61, 74, 85, 94, 96, 190, 197, 224, 248, 282–283, 294, 307; *C. bennetti* 9, 85, 190, 197, 248, 282–283, 294; *C. gauchama* 85, 224; *C. nevadensis* 85, 307; *C. pictus* 9, 85
Cambridgea 41
Campostichomma 44–45; *C. manicatum* 44
Canada 86, 121, 249–250; Ontario 86, 121, 249–250
Canary Islands 93, 215, 240, 246
Canoe Tapetum Clade 3, 72
Central America 86; Costa Rica 7, 18, 41, 87, 91, 199–201, 240, 250, 301, 307; Honduras 86; Panama 18, 86, 92, 147, 198, 218, 254, 257
Cicurininae 5, 21
Conifaber 44, 92, 302; *C. guarani* 92, 302
Crassanapis chilensis 86, 121
Ctenidae 1–2, 5, 17, 75, 86, 309
ctenids 17, 48, 53–55, 64
Cyatholipidae 14

D

Deinopidae 2, 4, 18, 44, 72, 87, 236, 301
deinopids 18, 43, 49–50, 52–53, 55–58, 66–67, 69
Deinopis 4, 18–19, 54, 59, 62, 70, 87, 94–95, 147, 236, 242, 248, 253, 255, 260, 272, 301; *D. spinosus* 18, 87, 147, 236, 242, 248, 253, 255, 260, 272, 301
Deinopoidea 50, 60–61, 72–73, 145
Desidae 1, 2, 5, 19, 74–75, 87, 188, 290, 306
desids 21, 47–49, 55–56, 61, 63, 74
Desis 5, 13, 19–21, 48, 52, 56, 58, 65–66, 74, 79, 87, 94, 96, 180–182, 231, 239, 253, 259, 278, 291, 306; *D. formidabilis* 19–21, 79, 87, 180–182, 231, 239, 253, 259, 278, 291, 306
Devendra 46
Dictyna 5, 21–23, 47, 50, 52, 54, 56, 61, 64, 87, 94–95, 160–161, 167, 230, 236, 246, 254–256, 276–277, 301; *D. arundinacea* 87, 160–161, 167, 230, 236, 246, 254, 256, 277; *D. bostoniensis* 87, 276
Dictynidae 1–2, 5, 21, 23, 74–75, 87, 167, 276, 277, 301
dictynids 21–24, 47–49, 54–56, 58–59, 61–62, 66–68
Dictyninae 5, 21
Dictynoidea 3

Dionycha 3, 4
Divided Cribellum Clade 3, 73
Dresserus 26, 88; *D. subarmatus* 88
Dysderoidea 39

E

Ectatosticta 29–30, 54–55, 89, 103
Emmenomma 12, 74, 284
Entelegynae 1–3, 50, 55–56, 60, 70, 72, 76, 242
Eresidae 1–2, 4, 24, 50, 52, 72, 88, 134–135, 300
eresids 24–26, 47–53, 55, 57–62, 65–67, 73
Eresoidea 2–3, 70, 72–74, 76, 300
Eresus 4, 25–26, 50, 62, 88, 94–95, 132–135, 232, 259; *E. cf. cinnaberinus* 88, 132–134, 259; *E. cinnaberinus* 25, 88, 135, 232; *E. sandaliatus* 25–26, 88, 135
Eurasia 8, 24–25, 33, 42, 46
Europe 2; Denmark 9, 10, 26, 85, 87–88, 135, 160–161, 167, 189, 254, 257; Finland 87; France 46, 93, 242, 244; Greece 25, 88, 133–134, 259; Italy 27, 69, 88–89, 104, 106, 236, 265, 297; Spain 27, 88, 93, 105, 201, 215, 254–255, 257; Switzerland 26, 88, 135, 232

F

Fecenia 37–38, 63, 66
Filistata 4, 27–28, 50, 54–55, 60, 69, 88, 94–95, 104–106, 236, 255, 265, 297; *F. insidiatrix* 27, 69, 88, 104–106, 236, 255, 265, 297
Filistatidae 1–2, 4, 27, 50, 58, 64, 71, 74, 88, 227, 297, 298
filistatids 25, 27, 47–48, 50, 52–58, 60–62, 65–70, 115
Filistatinae 4, 297
Filistatinella sp. 115
Fused Paracribellar Clade 3, 5, 61, 74

G

Gippsicola 39
Goeldia 5, 42, 62, 91, 94, 96, 154–156, 253, 255, 275, 304
Gradungula 4, 28, 55–59, 63, 65–68, 72, 89, 94–95, 116–118; *G. sorenseni* 28, 89, 116–118
Gradungulidae 1–2, 4, 28, 71, 89
Griswoldia 46
Griswoldiinae 46

H

Haplogynae 2–3, 55, 60, 67, 71, 310
haplogynes 3, 25, 39, 57

- Hersilia* 67
Hickmania 4, 15–17, 28, 54–56, 59–60, 64–65, 67–68, 72, 86, 94–95, 108–111, 219, 221, 234, 249, 251; *H. troglodytes* 15–17, 86, 108–111, 219, 221, 234, 249, 251
Hickmaniidae 15
Holarchaeidae 73
Huntia 46
Huttonia 5, 28–29, 48–49, 51–53, 56, 58–59, 65, 67, 72–73, 89, 95–96, 124–125, 235, 250; *H. palpi-manoides* 28–29, 89
Huttoniidae 1–2, 5, 28–29, 73, 89, 235
huttoniids 29, 67
Hypochilidae 1–2, 4, 29, 89, 296
hypochilids 16, 29–30, 47–48, 52–55, 57, 60, 62, 67, 69
Hypochilus 4, 29–30, 49–50, 53–59, 62, 64–65, 68, 71, 89, 94–95, 102–103, 231, 233, 244, 251, 265, 267, 296; *H. kastoni* 89, 296; *H. pococki* 30, 89, 102–103, 233, 244, 251, 265, 267, 296; *H. sheari* 89, 231
Hyptiotes 43, 92, 221
- I**
- Ischalea* 40–41
Israel 42
- K**
- Kilyana* 46
Krukt 46
Kukulcania 4, 7, 27–28, 50, 54–55, 67, 76, 88, 94–95, 107, 115, 219, 227, 244, 253, 255, 267–268, 297–298; *K. hibernalis* 27, 67, 76, 88, 107, 115, 227, 244, 253, 255, 267–268, 297–298
- L**
- Lathys* 5, 21–23, 56, 87–88, 94, 96, 164–165, 167, 230, 232, 248, 253, 256, 261, 276–277; *L. humilis* 23, 88, 164–165, 167, 248, 253, 256, 261, 277; *L. immaculata* 88, 230, 232, 276
Linyphiidae 14, 72
Liocranoides 65, 91; *L. unicolor* 91
Liphistius 54–55, 67
Loxosceles 55
Lycosoidea 3, 37–38, 41, 46–48, 50–51, 60, 66, 75, 312
- M**
- Macrobininae 5, 74, 284
Macrobunus 5, 9–11, 64, 74, 75, 85, 94, 96, 195–196, 239, 253, 259, 284, 294; *M. cf. multidentatus* 9–10, 85; *M. multidentatus* 195–196, 239, 253, 259, 284
Macrogradungula 28, 72; *M. moonya* 28
Madagascar 7, 14–15, 35, 40, 42, 44–45, 86, 88, 90, 93, 121–123, 198, 205, 228, 235, 242, 244, 250, 254, 257, 266, 269, 274, 287, 295–296, 308
Malaika 35
Malkaridae 72–73
Mallos 21–22, 88, 221
Maniho 5, 12–13, 64, 68, 85, 94, 96, 176–177, 183, 248, 257, 281, 290; *M. ngaitahu* 12, 85, 176–177, 183, 248, 257, 281, 290; *M. pumilio* 85; *M. tigris* 85
Manjala 38
Matachia 5, 19–21, 48–49, 56, 60, 68, 74, 87, 94, 96, 184, 188, 254, 257, 306; *M. australis* 19, 87, 184, 188, 254, 257; *M. marplei* 87
Matachiinae 5
Mauritius 40
Mecysmaucheniidae 73
Mecysmauchenius 67
Megadictyna 5, 32, 33, 48, 50, 59–60, 62, 64, 66, 70, 73, 75, 89, 94–95, 139–141, 223, 238, 242, 253, 255, 262, 272, 304; *M. thilenii* 32, 89, 139–141, 223, 238, 242, 253, 255, 262, 272, 304
Megateg 46
Menneus 4, 18–19, 50, 87, 94–95, 144–145, 236, 241, 245, 249, 301; *M. camelus* 18, 87, 144–145, 236, 301
Mesothelae 54, 71
Metagonia 72
Metaltella 5, 12–13, 65, 68, 74, 85, 94, 96, 178–179, 183, 225, 254, 256, 261, 280–281, 292–293, 307; *M. rorulenta* 12, 85; *M. simoni* 12, 85, 178–179, 183, 225, 254, 256, 261, 280–281, 292–293, 307
Metaltellinae 66, 86, 265
Metepeira atascadero 86
Mexico 41, 44, 86, 89, 91, 93, 126, 139, 202–203, 229, 231, 238, 247–248, 253, 295; Baja California 86, 139; Chiapas 91, 93, 202–203, 231, 247, 253; Guanajuato 86, 238, 248; Hidalgo 93, 295; Tampico 89, 126, 231
Miagrammopes zenzezi 92, 302
Micropholcommatidae 14, 73
Mimetidae 1–2, 5, 30, 72–73, 89, 243
Mimetus 5, 30–31, 48–52, 58–59, 64, 66–67, 72, 89, 95–96, 126–127, 229, 231, 243, 250, 258, 270; *M. hesperus* 30, 89, 126–127, 229, 231, 243, 250, 258, 270
Misionella mendensis 89, 297
Miturgidae 46

Mygalomorphae 67, 71, 78
Mysmenidae 14

N

Namaquarachne 36, 90, 147; *N. tropata* 36, 90, 147
Neocribellatae 60, 62, 68, 71
Neocribellate 28, 71
Neolana 5, 31, 49, 62, 89, 94, 96, 168–169, 233, 254–256, 279, 305; *N. dalmasi* 31, 89, 168–169, 233, 254, 256, 279, 305
Neolanidae 1–2, 5, 31, 74, 89, 169, 305
neolanids 47–48, 61, 67
Neoramia 5, 9, 49, 60–61, 74, 85, 94, 96, 174–175, 183, 254, 256, 262, 280, 290, 305; *N. sana* 9, 85, 174–175, 183, 254, 256, 262, 280, 290, 305
Nephila 79, 91, 220
Nesticidae 14, 72
New Caledonia 19
New Guinea 32, 37, 42, 91, 210–211, 213, 240, 246, 250, 265, 268
New Zealand 4, 7–9, 12, 18–19, 24, 27–29, 31–32, 34, 37–38, 40, 85, 87, 89–91, 93, 116–118, 124–125, 139–141, 168–169, 171, 174–177, 183–184, 188, 208–209, 223, 233, 235, 238, 242–243, 248, 250–251, 253–258, 262, 272, 279–281, 285, 290, 304–306
Nicodamidae 1–3, 5, 32, 71, 73–74, 89, 139, 304, 315
nicodamids 32–33, 47–49, 64, 71, 73, 315
Nicodamus 5, 32–33, 48, 50, 56–57, 59, 64–65, 73, 90, 94–95, 142–143, 240–241, 250, 273; *N. mainae* 32, 90, 142–143, 240–241, 250, 273
Nigma 5, 21–23, 47–48, 52, 56, 88, 94–95, 162–163, 167, 256, 277; *N. linsdalei* 88, 162–163, 167, 256, 277
North America 8, 29–30, 44–46

O

Octonoba 4, 43–44, 92, 94–95, 145, 248, 253; *O. octonarius* 43; *O. octonaria* 43, 92, 145, 248, 253
Oecobiidae 1–2, 4, 33, 67, 72, 90, 227, 288, 300
oecobiids 33–34, 47–48, 51–53, 55–56, 58, 62–63, 65–68
Oecobius 4, 33–34, 50, 53, 58–59, 66–68, 70, 72, 90, 94–95, 128, 227, 230, 236, 241, 271; *O. navus* 33, 90, 128, 236, 241, 271
Oonops 67
Orbiculariae 2–4, 18, 30, 32, 47–49, 58, 62, 69–70, 72–73, 76, 147, 310–311
Oval Calamistrum clade (OC clade) 2, 75–76

P

Palaeocribellatae 2
Palpimanidae 29, 73
palpimanids 29, 73
Palpimanoidea 2–3, 5, 14, 29, 57, 71–73, 310
palpimanoids 47–49, 52, 62, 67, 72–73, 315
Palpimanus 67
Papua New Guinea 37, 91, 210–211, 213, 240, 246, 250, 265, 268
Paramatachia 20
Pararchaea 5, 34–35, 49, 51–53, 56, 58–59, 64–67, 72, 90, 95–96
Pararchaeidae 1–2, 5, 34, 72–73, 90
Phanotea 46
Philoponella cf. *fasciata* 92, 302
Phryganoporus 5, 19–21, 56, 63, 87, 94, 96, 185–186, 188, 290, 311; *P. candidus* 19–20, 87, 185–186, 188, 290
Physocyclus 55
Phyxelida 5, 35–36, 49–50, 64, 90, 94, 96, 147, 150–151, 222, 233, 244, 261, 274, 289, 303; *P. bifoveata* 90, 274, 289; *P. tanganiensis* 35–36, 50, 90, 147, 150–151, 222, 233, 244, 261, 274, 303
Phyxelididae 1–3, 5, 35, 50, 74, 90, 147, 274, 289, 303
phyxelidids 9, 35–36, 47–49, 59–61, 63, 70
Phyxelidinae 35, 303
Phyxelidini 63, 303
Pillara 5, 40–41, 91, 94, 96, 169, 172–173, 311; *P. griswoldi* 40, 91, 169, 172–173
Pimoidae 14
Pimus 5, 9–11, 49, 59, 74, 85, 94, 96, 191–192, 197, 224, 236, 248, 254, 257, 259, 262, 282–283; *P. napa* 85, 197, 236, 259; *P. pitus* 9, 85
Poaka 2, 5, 9–10, 37–38, 49, 75, 90, 95–96, 208–209, 243, 251, 258, 285; *P. graminicola* 37–38, 90, 208–209, 243, 251, 258, 285
Pritha nana 89, 297
Prithinae 50, 297
Progradungula 28; *P. carraiensis* 28
Psechridae 1–2, 5, 10, 37–38, 75, 90, 309
psechrids 37–38, 53, 55, 61, 63, 66
Psechrus 5, 37–38, 50, 60, 63, 66, 90–91, 95–96, 157, 198, 210–213, 233, 240, 244, 246, 250, 265, 268, 309; *P. argentatus* 91, 210–211, 213, 240, 246, 250, 265, 268

R

Raecius 5, 44–46, 58, 60, 64, 67, 92–93, 95–96, 198, 206–207, 225–226, 248, 254, 262, 287, 295, 308;

R. asper 45, 67, 92, 308; *R. congoensis* 46, 67, 92;
R. jocquei 45, 67, 92, 198, 206–207, 248, 254,
 262, 287, 295; *R. scharffi* 44, 93, 225–226
Retiro 5, 9–11, 48–49, 58, 74, 85, 94, 96, 193–194,
 197, 254, 257, 282–283
 RTA Clade 2–3, 74–75
Rubrius 12, 284
 Russia 87, 230, 254, 256, 277

S

Sahastata 50
Scytodes 55
Segestria 39
 Segestriidae 1, 2, 4, 39, 71, 91, 303
 South America 9, 12, 21, 42; Brazil 23–24; Chile 7–9,
 12, 15–16, 19, 39, 42, 85–86, 92, 113, 115, 121,
 154–156, 195–196, 234, 239, 253, 259, 263, 265,
 267, 284, 288, 294, 299; Colombia 92; Ecuador
 23, 86–87, 92, 157–159, 218, 231, 243, 251, 258,
 270; Peru 9, 18, 85–87, 91, 193–194, 197,
 216–217, 240, 246, 249, 253–255, 257, 275,
 282–283; Uruguay 19, 87, 279
Stegodyphus 4, 24–26, 62, 88, 94–95, 134–138, 230,
 232, 236, 245, 253, 255, 260, 271, 300; *S. dumico-*
la 88, 271, 300; *S. mimosarum* 25–26, 88,
 134–138, 230, 232, 236, 245, 253, 255, 260, 300
 Stenochilidae 28–29, 73
 Stiphidiidae 1–2, 5, 40–41, 74–75, 91, 169, 290, 305
 stiphidiids 40–41, 47–48, 53, 61–62, 66–67
 Stiphidioids 3, 74
Stiphidion 5, 40–41, 53, 91, 94, 96, 169–171, 248,
 254, 256, 280, 290, 305; *S. facetum* 40, 91, 169,
 170–171, 248, 254, 256, 280, 290, 305
 Symphytognathidae 14
 Symphytognathoidea 14
 Synaphridae 14
 Synotaxidae 14

T

Takeoa 46
Tama 67
Tegenaria domestica 9
Tengella 5, 41, 44, 59, 64, 69, 75, 91, 95–96,
 199–201, 240, 250, 307; *T. radiata* 41, 91,
 199–201, 240, 250, 307
 Tengellidae 1–2, 5, 37, 41, 65, 75, 91, 201, 307
 Tetragnathidae 14, 72, 91
 Textricellidae 73
Thaida 4, 15–17, 19, 28, 49–50, 53–56, 60, 62–63,
 67–70, 86, 94–95, 112–113, 115, 219–220,
 234–245, 249, 259, 264, 267, 288, 299; *T. pecu-*

liaris 15–16, 86, 112–113, 115, 219–220, 234,
 245, 249, 259, 264, 267, 288, 299

Thaididae 15

Theridiidae 14, 72

Theridiosomatidae 14

Titanoeca 5, 42–43, 62, 64, 92, 94, 96, 152–153, 156,
 222, 244, 253, 255, 262, 275, 289, 304; *T. albo-*
maculata 42, 82; *T. americana* 42, 92, 152–153,
 156, 244, 253, 255, 262, 275, 289; *T. nigrella* 42,
 92, 153, 156, 222, 304; *T. silvicola* 43

Titanoecidae 2, 5, 35, 42, 64, 74, 91, 156, 275, 289,
 304

titanoecids 42, 43, 47–48, 62–63, 65

titanoecoids 2–3, 5, 74

Tricholathys 5, 21, 22–23, 48, 56, 88, 94–95,
 166–167, 232, 254, 256, 276; *T. spiralis* 88, 167,
 254, 256, 276

Tricholathysinae 5, 21

U

Uduba 5, 44–46, 50, 58, 60, 93, 95–96, 198, 205, 242,
 244, 254, 257, 287, 295, 308; *U. dahli* 93, 295; *U.*
madagascariensis 93, 287, 308

Uliodon 46, 64, 93

Uloboridae 2, 4, 23, 43, 72, 92, 302, 307

uloborids 19, 43–44, 47, 49–50, 53–55, 59, 61, 65,
 67–70

Uloborus 4, 23, 43–44, 58, 92, 94–95, 147, 220, 238,
 241, 246, 249, 253, 255, 302; *U. diversus* 92, 238,
 253, 255; *U. glomosus* 92, 241, 246, 249; *U. trilin-*
eatus 92, 147

United Kingdom 88, 164–165, 167, 248, 253, 256,
 261, 277; Scotland 87, 236, 246

Uroctea 4, 33–34, 53, 57–59, 66–67, 90, 94–95,
 130–131, 231, 253, 255, 260, 271, 288, 300

Uroecobius 67

USA 1, 5, 9, 12, 18, 27, 33–34, 42–43, 85–93,
 102–103, 107, 115, 127–128, 145, 147, 152–153,
 156, 162–163, 166–167, 178–179, 183, 187–188,
 190–192, 197, 204, 221–227, 230–233, 236, 238,
 241–244, 246, 248–251, 253–262, 265, 267–268,
 270–272, 275–277, 280–283, 287, 289, 294, 296,
 301, 304, 306–309; Arizona 44, 87–89, 92–93,
 127, 153, 156, 221–222, 243, 258, 270, 304, 308;
 Arkansas 88, 92, 230, 232, 248, 253, 276;
 California 9–10, 12, 19, 27, 34, 43, 46, 85–90,
 92–93, 128, 162–163, 166–167, 178–179, 183,
 191–192, 197, 224–227, 230, 232, 236, 238, 248,
 253–254, 256–257, 259, 262, 277, 280–283, 287,
 296, 301, 307, 309; Florida 18, 27, 87–88, 107,
 115, 147, 227, 236, 242, 244, 248, 253, 255, 260,
 267, 272; Georgia 34, 88, 90, 236, 241, 268;

Hawaii 87, 187–188, 254, 257; Louisiana 85; Maine 85, 282–283, 294; Minnesota 87, 276; Missouri 92, 145, 152–153, 156, 244, 253, 255, 262, 275, 289; Nevada 89, 250; North Carolina 30, 88–89, 92, 102–103, 231, 241, 246, 249, 265, 296; South Carolina 92; Tennessee 89, 91, 233, 244, 251, 267; Texas 93, 204, 259, 287; Washington 167; Washington D.C 34, 90, 128, 271; West Virginia 85, 190, 197, 248

V

Vidole 35–36, 90, 303; *V. capensis* 90, 303
Vidoliini 36, 63
Vyffutia 5, 35–36, 60, 63, 90, 94, 96, 147–149, 253, 256, 262; *V. bedel* 90, 253, 256; *V. pallens* 36, 90, 147–149, 262

W

Waitkera 44
Wajane 25

X

Xenoctenus 65, 92

Xevioso 5, 9, 35–36, 49, 60, 62, 66, 90, 94, 96, 232, 242, 244, 248, 271, 303; *Xevioso amica* 36, 90, 232, 242, 244, 248, 271, 303; *X. orthomeles* 90, 303

Z

Zorocrates 5, 44–46, 64, 75, 93, 95–96, 202–204, 231, 247, 253, 259, 287, 295, 308; *Z. cf. mistus* 45, 93, 202–203, 231, 247, 253
Zorocratidae 2–3, 5, 44, 46, 50, 75, 92–93, 287, 295, 308
zorocratids 44, 48, 50, 58, 60, 64, 67, 75
Zorocratinae 44, 46
Zorodictyna 44
Zoropsidae 2, 5, 44, 46, 64, 75, 93, 201, 309, 313
zoropsids 48, 53, 55, 61, 64
Zoropsis 5, 44, 46–47, 49–50, 53, 58, 60, 64, 67, 75, 93, 95–96, 201, 215, 226, 240, 242, 244, 246, 254, 257, 287, 309; *Z. cyprogenia* 46; *Z. media* 93; *Z. nishimurai* 46; *Z. rufipes* 47, 93, 215, 240, 246; *Z. spinimana* 46–47, 93, 201, 215, 226, 242, 244, 254, 257, 287, 309
Zosis 92